

An Introduction to Climate Dynamics

Lecture notes for the undergraduate course in climate dynamics
(unfinished) version, May 24, 2022.



If you find any errors in this script or have suggestions of improvements, please correspond them to me. Thank you!

Dietmar Dommenges¹

¹Corresponding Author:
Dietmar Dommenges, Monash University, School of Earth, Atmosphere and Environment, Clayton, Victoria 3800,
Australia
email: dietmar.dommenges@monash.edu

Foreword to this course

These lecture notes should be the main reference for the undergraduate course EAE3111 'Climate dynamics'. The main aim of this unit is to give an introduction to the dynamics and processes that govern the large-scale climate of the atmosphere and oceans. It will introduce the students to the main concepts of the large-scale climate such as: the energy balances, the large-scale atmospheric and ocean circulations, the forces acting in the climate system. We will discuss some simple theoretical climate models, climate modelling on the more complex scales and important concepts for the climate and its variability.

The following questions are the main focus of this unit:

- What dynamics control the mean climate?
- How would the climate change if boundary conditions of the climate are changed?
- What are the characteristics and dynamics of natural climate variability?

These lectures notes are still under development and will be updated during this term. They will first of all focus to present all the figures and equations that are presented in the lectures. I will try to give some more discussion when time permits. So these lecture notes will grow over time.

Acknowledgements

These lecture notes have been developed on the basis of the lecture notes from Prof. Mojib Latif. Some material from the lecture notes of Richard Wardle have been used as well. Tess Parker helped to include the lecture slides into the lecture notes Latex files.

Best regards

Dietmar Dommenges, Melbourne, May 24, 2022

Contents

1	Introduction	9
1.1	Climate Mean State	9
1.1.1	Coordinate System	9
1.1.2	Map Projections	12
1.1.3	Some Climate Variables	14
1.1.3.1	Surface	14
1.1.3.2	Atmosphere	23
1.1.3.3	Oceans	32
2	Simple Climate Energy Balance Models	37
2.1	Basics	39
2.1.1	Energy conservation	39
2.1.2	Diagnostic equations	39
2.1.3	Prognostic equations	40
2.2	Zero order model (Radiation balance)	40
2.2.1	Greenhouse effect	43
2.2.2	Greenhouse Shield Model	46
2.2.3	Multi-layer Greenhouse Shield	48
2.3	Greenhouse model with ice-albedo feedback (Budyko, 1969)	51
2.3.1	The Ice-Albedo Feedback	52
2.4	Climate Sensitivity, Stability and Feedbacks	55
2.4.1	Stability and Climate Potential	55
2.4.2	Tipping points: The Climate Response to Forcing	58
2.4.3	Climate Sensitivity	62
2.4.4	Feedbacks	65
3	The Atmospheric and Ocean Circulation	73
3.1	Geofluid Dynamics	73
3.1.1	The Momentum Equation (Forces Acting in the Atmosphere and Oceans)	74
3.1.2	Gravitational force	75
3.1.3	Pressure Gradient Force	76
3.1.4	Hydrostatic Balance (Pressure)	77
3.1.5	Potential temperature	80
3.1.6	Buoyancy	82
3.1.7	Continuity and Convection	84
3.1.8	Coriolis Force (Earth rotation)	86
3.1.9	Geostrophic Balance	89
3.1.10	Thermal Wind Balance	94
3.1.11	Friction	97
3.1.12	Summary of GFD-theory	100

3.2	Atmospheric Circulation	101
3.2.1	The Large Scale Circulation	101
3.2.2	The Hadley Cell (the Direct Tropical Circulation)	105
3.2.3	The Ferrel Cell (the Indirect Extra-tropical Circulation)	106
3.3	The Oceans	108
3.3.1	Ocean stratification	110
3.3.2	Surface (wind driven) Circulation	117
3.3.3	Upwelling and Convection	118
3.3.4	Ocean Weather	124
3.3.5	Thermohaline (geostrophic) Circulation	125
3.3.6	Deep Ocean Time Scales	126
3.3.7	Sea Ice	127
3.4	Heat Transport in the Climate System	129
3.4.1	The Zonal Mean Heat Balance	130
3.4.2	The Heat Transport	132
3.4.3	The Advective and Turbulent Heat Transport	134
3.4.4	The Heat Transport between Seasons (from summer to winter)	137
4	Models of the Global Climate System	141
4.1	A Globally Resolved Energy Balance (GREB) model	142
4.1.1	Initial considerations	142
4.1.2	Solar radiation	144
4.1.3	Thermal radiation	149
4.1.4	Hydrological cycle	156
4.1.5	Sensible heat and atmospheric transport	163
4.1.6	Subsurface Ocean	166
4.1.7	Sea Ice	169
4.1.8	Estimating the equilibrium climate	170
4.1.9	The GREB climate simulation, limitations and correction terms	171
4.1.10	A short summary of the GREB model	173
4.2	A Conceptual Deconstruction of the Mean Climate with the GREB Model	176
4.2.1	The Mean Surface Temperature Structure	176
4.2.2	A Diagnostic Model for Precipitation	181
4.2.3	The Mean Precipitation Pattern	181
4.3	General Circulation Models (IPCC-type climate models)	184
4.3.1	The dynamical model	185
4.3.2	Radiation model	188
4.3.3	Precipitation model	188
4.3.4	Cloud model	190
4.3.5	Land/Surface model	191
4.3.6	Carbon cycle model	192
4.3.7	Numerical realisations of GCMs	193
5	Climate Change	195
5.1	Conceptual deconstruction of climate change	196
5.1.1	The GREB model response to CO_2 forcing	196
5.1.2	The Direct Local Forcing Effect - No Feedbacks (Exp. [1] to [4])	201
5.1.3	Ice/Snow-Albedo and Sea Ice Feedback	208
5.1.4	The Water Vapour Feedback	210
5.1.5	The Oceans Heat Up Take	212

5.1.6	Cautionary Note on the GREB model global warming	215
5.2	Anthropogenic climate change predictions	216
5.2.1	History of climate change predictions	216
5.2.2	IPCC CO ₂ scenarios	218
5.2.3	Prediction vs. Reality	221
5.2.4	Precipitation	225
5.2.5	Sea level	226
5.2.6	Extreme events	229
5.2.7	How significant is a 3°C global warming?	230
5.2.7.1	A comparison against natural climate variability	231
5.2.7.2	A comparison against regional climate differences	236
5.2.7.3	A comparison against seasonal climate differences	237
5.2.7.4	Summary of the significance of climate change	238
5.3	Climate change in the media	240
5.4	Summary: Evidence of anthropogenic climate change	245
6	Natural Climate Variability	247
6.1	Characteristics of climate variability	247
6.1.1	Some statistics background	247
6.1.2	Melbourne Temperature Variability	249
6.1.3	Observed global climate variability	252
6.1.4	Climate Variability Characteristics	255
6.1.5	Sources of climate variability	265
6.2	Chaos (The butterfly effect; The Lorenz Model (1963))	267
6.2.1	The Lorenz-Salzman model	268
6.2.2	Characteristics of the Lorenz-Salzman model	273
6.3	The Stochastic Climate Variability	281
6.3.1	The Power Spectrum	281
6.3.2	White Noise	287
6.3.3	The Stochastic Climate Model (Red Noise)	289
6.3.4	Extra-tropical time scales	300
6.4	Spatial patterns of climate variability	302
6.4.1	Statistical patterns of climate variability	303
6.4.2	A Null hypothesis for the spatial structure	308
6.5	Climate Modes	313
6.5.1	A Physical Climate Mode	314
6.5.2	The problem with defining climate modes based on statistical modes	316
6.5.3	Levels of Climate Modes	320
6.6	El Nino / Southern Oscillation	322
6.6.1	History	322
6.6.2	Phenomenon	323
6.6.3	ENSO teleconnections	330
6.6.4	Dynamics	332
6.6.4.1	Mean State	333
6.6.4.2	Bjerknes Feedbacks	343
6.6.4.3	Delayed Action Oscillator	347
6.6.4.4	The Recharge Oscillator Model	351
6.6.5	Predictability of ENSO	355
6.7	The Thermohaline Circulation (THC) Variability	357
6.7.1	Paleo climate variability of the THC	358

6.7.2	North Atlantic MOC circulation "breakdown"	361
6.7.3	The Stommel two box model	363
6.7.3.1	The ocean state in the North Atlantic	363
6.7.3.2	The two box THC model set up	367
6.7.3.3	Characteristics, stability and tipping points of the two box model	369
6.8	Paleo Climate Variability (Ice Ages)	375
6.8.1	Climate Proxy Data	375
6.8.2	The Climate History of the last 10,000 years	383
6.8.3	Ice Ages (The Milankovitch Cycles)	386
6.8.4	Orbital forcings (The Milankovitch Cycles)	393
6.8.5	The Climate History of the Past 500 Mill. Years	401

Chapter 1

Introduction

In this section we will introduce some important background information which we need for the further sections. We first discuss the coordinate system that we use in climate research. We will then focus on some of the characteristics of the mean state climate such as the global distribution of some of the most important climate variables and the main large-scale features of the atmospheric and ocean circulation. This information is somewhat important for the subsequent sections, as it helps to have some general idea about the values of some of the main climate variables. It is, for instance, helpful to know that the winds blow from the east to the west in the subtropics, but they mostly blow the other way around in the mid-latitudes.

1.1 Climate Mean State

1.1.1 Coordinate System

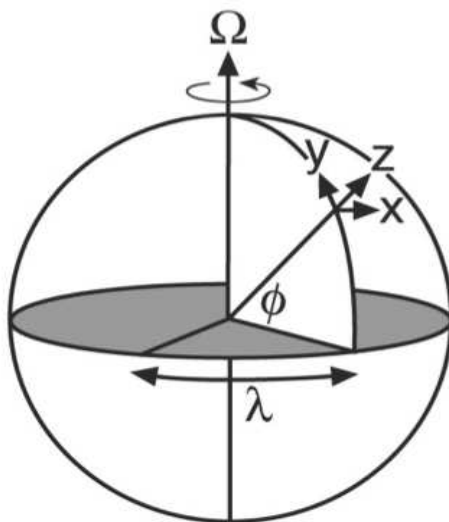


Figure 1.1: Spherical coordinates following the right-hand system (e.g. when x points right, then y points up).

The climate is usually described with a spherical coordinate system, see Fig. 1.1. The coordinates are usually two angles and a distance. The X -coordinate is the longitudes, which is an angle, λ (or sometimes ϕ). A positive longitude λ (X -coordinate) is a vector pointing from west to east. The

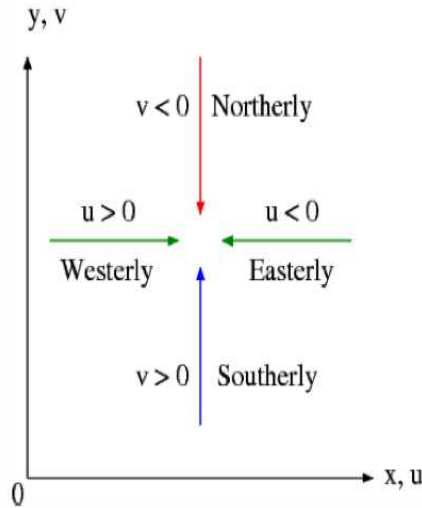


Figure 1.2: Coordinate system: Illustration of the directions of velocities in the spherical coordinate system of the climate.

origin of the longitude axis is at Greenwich, England and it increases to the east until the dateline at 180° or $180^\circ E$ (east). To the west it decrease until the dateline at -180° or $180^\circ W$ (west). Thus degrees east are positive values and degrees west are negative values.

Velocities (e.g. winds or currents) in the x-direction (longitude direction) are called zonal winds or currents. They are also often described by the direction from which they came from: e.g. westerlies are easterlies. Ocean current are often described by the direction to which they flow: e.g. westward or eastward currents. A positive zonal wind or current is from the west to the east, see Fig. 1.2. Although the longitude is an angle, velocities are usually given in m/s and distances are given in Metres.

The Y-coordinate is the latitude, which is also an angle ϕ (or sometimes θ). It is zero at the equator and increases to the north, thus a positive latitude vector is pointing towards north. Velocities in the north-south directions are called meridional winds or current. Lines of constant latitudes are called parallels, named after the latitude at which they are (e.g. $30^\circ N$ -parallel). As the latitude increases the length of the parallels (circles around the earth at constant latitudes) decreases. The length of a degree longitude is proportional to $\cos(2\pi\phi)$. Lines of constant longitudes are called meridians with the zero meridian crossing through Greenwich, see also Fig. 1.3.

The vertical coordinate points up and is often given as the distance relative to the mean sea level. Sometimes pressure coordinates are used as well, which point from low (often higher up) to high pressure (often down). So, pressure coordinates are point the wrong direction. In ocean and atmospheric dynamics such coordinates are popular.

The earth's radius ranges from 6,353 km at the poles to 6,384 km at the equator. The variations in the radius are small in relative values ($\pm 0.3\%$) but are large if compared to the topography.

The earth's rotation axis is tilted relative to the normal vector of the plain in which the earth circles around the sun by 23.5° . From this tilt, it follows that four different latitudes mark important lines: the polar circles at $66.5^\circ S$ and $66.5^\circ N$ and the tropic of Cancer at $23.5^\circ N$ and the tropic of Capricorn $23.5^\circ S$, see Fig. 1.4. Regions poleward of the polar circles have at least one day per year in which the sun does not set (24hrs of sunlight). The northern polar circle is roughly marked by Island, north of the Hudson Bay, northern Scandinavia and the Bering strait. The southern polar circle is roughly marked by the coast of Antarctica. Regions between the tropic of Cancer and the tropic of Capricorn have at least one day (usually two) in the year in which the sun is in

the zenith (maximal incoming radiation) at midday. The northern border is roughly marked by the Sahara desert and the Cuban island. The southern border goes through the middle of South America, South Africa and Queensland.

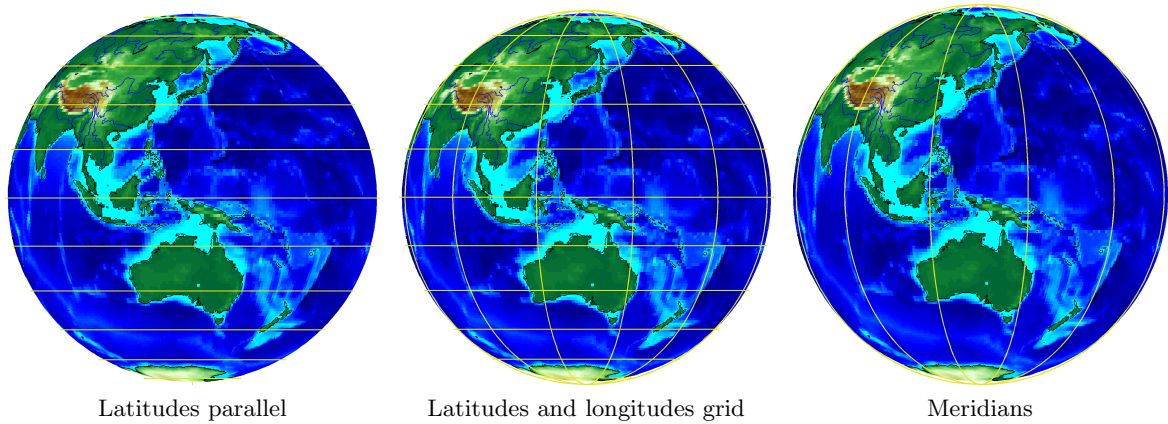


Figure 1.3: The coordinates grid: lines of constant latitude are called parallels and lines of constant longitudes are called meridians.

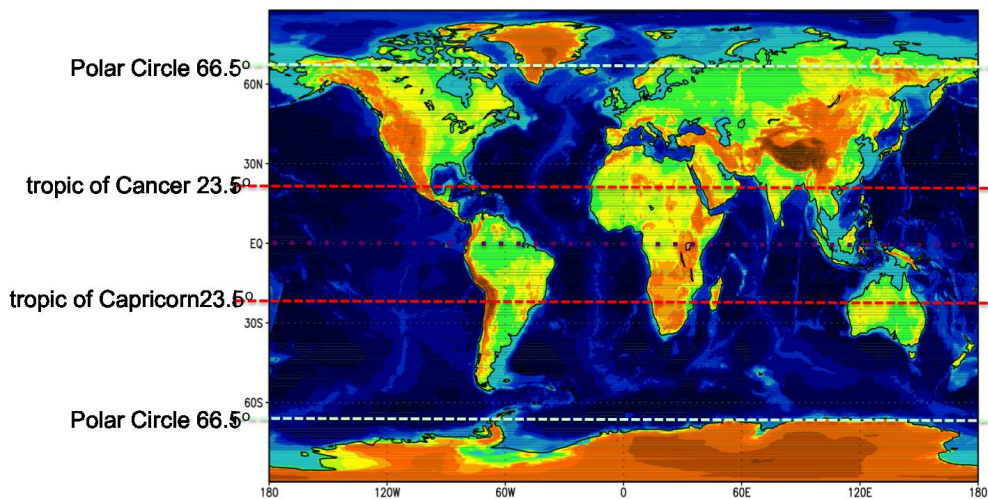


Figure 1.4: Important latitudes: Regions poleward of the polar circles have at least one day per year in which the sun does not set (24hrs of sunlight). Regions between the tropic of Cancer and the tropic of Capricorn have at least one day (usually two) in the year in which the sun is in the zenith (maximal incoming radiation) at midday.

1.1.2 Map Projections

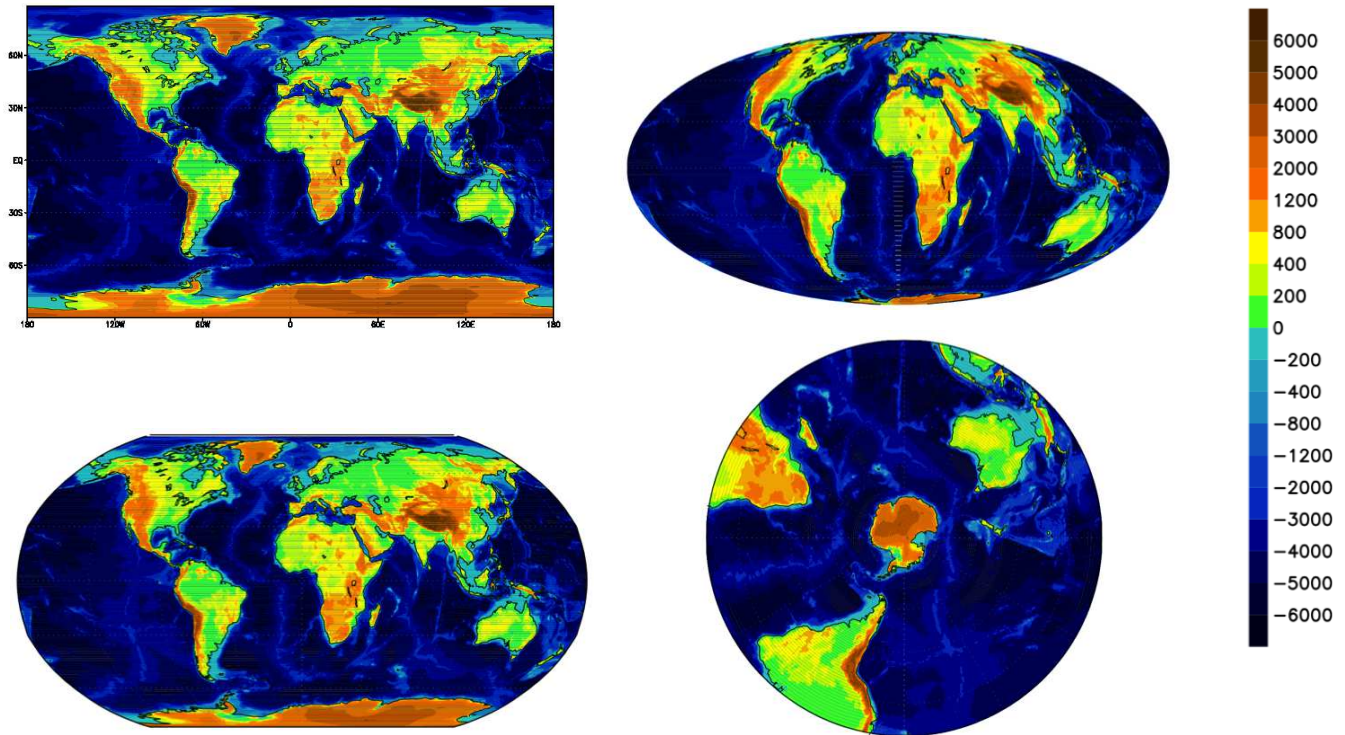


Figure 1.5: Map projections (1): Earth topography in four different projections: Upper left: lat-lon projection; upper right: Mollweide with relative area size conserved; lower left: Robinson projection as compromise between the upper two; lower right: The local perspective with view on the South Pole.

Mapping a sphere on a flat plane is never perfect. The Fig. 1.5 shows four common ways of projecting the earth surface on a flat plane. The lat-lon projection is the most commonly used projection, in which longitude and latitude angles are simply plotted as orthogonal vectors on the 2D-plane. This projection strongly skews the relative size of regions. Regions closer to the poles are strongly magnified relative to regions close to the equator. The Mollweide Projection conserves the relative size of regions, but skews the shape of regions. The Robinson is a compromise between the lat-lon and the Mollweide projection. The Azimuthal projection takes a local perspective by viewing down on one point of the earth (e.g. South Pole). This projection will skew the size of regions remote to this reference point.

In one way or the other every projection has some advantages and some disadvantages. However, in the context of climate dynamics we have to be aware of some of the drawbacks of the projections. Fig. 1.6 illustrates the scaling problem of the lat-lon projection with a comparison of the size of Greenland relative to the size of Africa. In the lat-lon projection it seems that Greenland is about half the size of Africa, but Africa actually is 15(!) times larger than Greenland. The lat-lon projection polar regions are largely over scaled and equatorial regions appear smaller than the actual are. Note, the area poleward of 45° latitude covers 50% of the area in the lat-lon projection but only 30% of the real earth surface. In turn the tropical regions between $45^\circ S - 45^\circ N$ cover 70% of the real earth surface. We have to keep this in mind when we think of the relative importance of

different regions for the earth climate dynamics.

As a rule of thumb: **Assume that the tropics are more important than the polar regions!!**

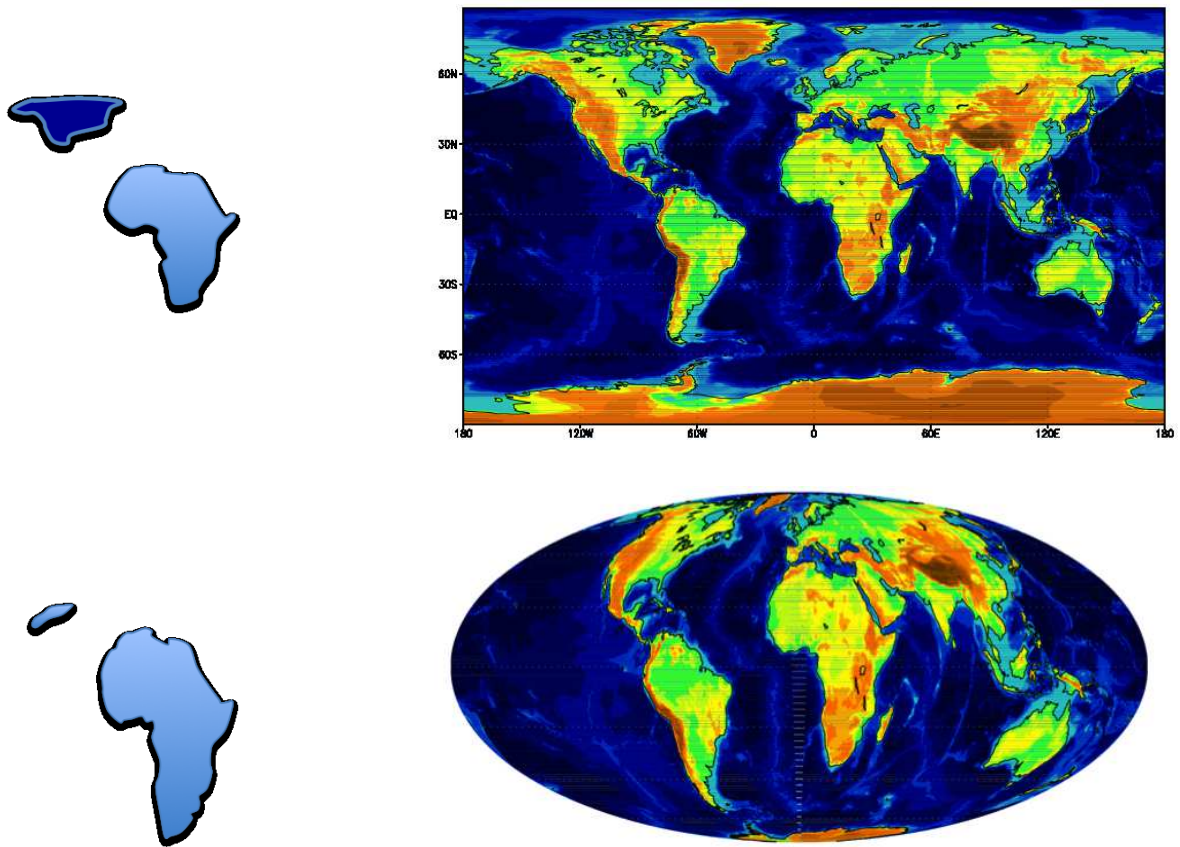


Figure 1.6: Map projections (2): A comparison of the relative size of Greenland versus Africa. In the upper projection the relative areas are skewed. In the lower 'Mollweide' projection the relative size of the areas is correct, but the shape of the areas is skewed.

1.1.3 Some Climate Variables

Some of the main climate characteristics of the surface, the atmosphere and oceans are important to know for the further discussions of the climate dynamics. We start with a short presentation of the main characteristics of the surface climate, followed by the main characteristics of the atmosphere and oceans.

1.1.3.1 Surface

Some of the main features of the surface climate are:

- Topography:
- Temperature
- Precipitation
- Snow / ice cover

Topography

Topography determines not only the landscape in terms of mountains or plains, but it first of all splits the earth into land and oceans. Furthermore, topography has a significant impact on the climate by affecting the winds in the atmosphere and currents in the oceans. It further leads to vertical motion of the air (lifting), which is one of the main processes that creates precipitation. Higher topography also goes along with lower atmospheric air pressure and therefore has a strong impact on the surface temperatures, because an ideal gas expands with lower pressure and subsequently cools with lower pressure. High altitudes also go along with drier climate, as water vapor decreases faster with height than the air pressure.

Some of the most important features of the earth's topography in the context of this course are:

- **70% is oceans.** The oceans cover most of the earth in particular in the tropical regions and on the Southern Hemisphere. Therefore global mean climate values (e.g. global mean temperature or rainfall) mostly reflect the ocean values. The land mean values can often be quite different from the ocean or global means (e.g. mean rainfall over land is much less than over oceans; see further below).
- **Mean altitude \sim 800m.** A look at Fig.1.7 shows that large parts of the land area are above 1000m (e.g. in Africa, Asia and North America). The mean value of 800m is mostly from less dense populated areas. Most high population densities are found in near sea level altitudes.
- **Oceans mean depth \sim 4000m.** Most of the ocean is quite deep. Only the coastal regions and some smaller shelf seas (e.g. north of Australia, South China Sea or the North Sea in northern Europe) are shallow ($< 100m$).
- **Greenland and Antarctica are mostly ice.** Although Greenland and Antarctica are effectively land and high mountains, they are actually mostly made of ice. If we would remove the ice from the area that is Greenland or Antarctica today than that area would be oceans.
- The most important mountain ranges are: **Himalaya, Andes, Greenland and Antarctica.**

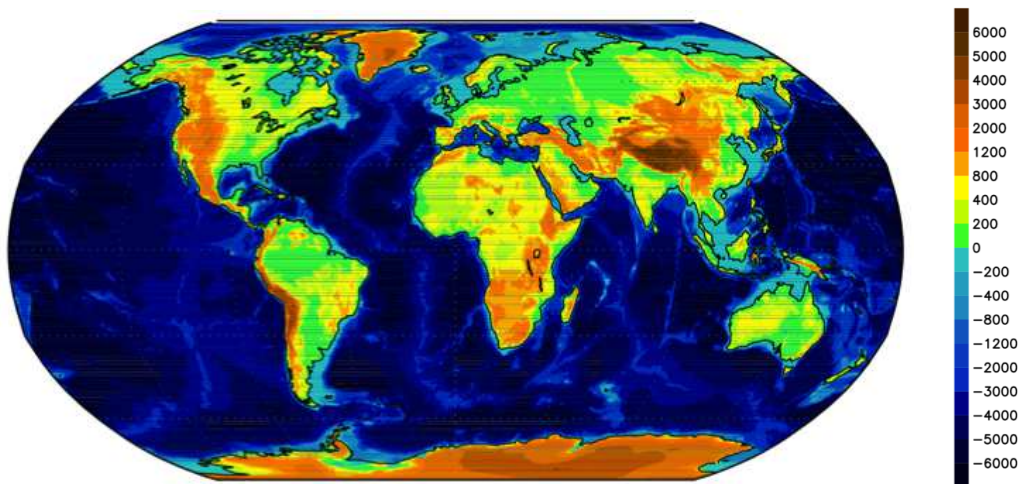


Figure 1.7: Topography in meter.

- Some important low level basins are: **Amazon Basin or India.**

Surface Temperature (2m height)

The surface, or near surface, temperature is probably the most commonly used physical variable to describe the climate. It is central in most discussions about climate and it is central in most simple and more complex climate models.

Figure 1.8 show the annual mean (over day and night), the winter and summer mean and the strength of the seasonal cycle. Some of the important characteristics are:

- **Global mean $\approx 15^\circ\text{C}$.** This is also roughly the annual mean temperatures in the midlatitudes (around 30 degrees). Note, that it may seem simple to state the global mean surface temperature, but it is actually very difficult to 'measure' the global mean surface temperature. It actually means that you have to measure the surface temperature at every location on earth and build the average. Today this is mostly done by satellites and a huge observation system of 10,000 measurement stations, most of them are drifting buoys in the oceans. In the past, 100 years ago, no such observation system existed and the global mean temperature was very difficult to estimate. This is important to know in the context of climate change. You can only know if the climate is changing, if you know how the climate was in the past. Unfortunately, we do not know this very well.
- **Zonal structure /Meridional gradients:** The mean temperatures gradients are in the meridional direction. Thus regions of the same latitudes tend to have similar mean temperatures. The annual temperatures range from -30°C in the polar regions (much colder in the Antarctic than in the Arctic) to $+25^\circ\text{C}$ in the tropics.
- **Annual cycle (strong in continental climate).** The amplitude of the annual cycle in the higher latitudes continental regions is about 20°C . It is mostly below 5°C over oceans and weaker in the tropics.
- **High altitudes have cooler climates.** High plateaus (e.g. Tibet, Colorado or Antarctica) have very cold climates, due to the reduced air pressure.

- **Land-Sea Contrast:** Due to the strong differences in the annual cycle, the land is much warmer in summer and much colder in winter than the nearby oceans.
- **Wind direction:** The mean wind direction often has a strong effect on the annual mean temperature. The subtropical oceans, for instance, have much colder temperatures at the eastern side of the ocean basins due to wind there coming from higher and colder latitudes; see Fig. 1.8. Similar the westerly winds in the higher northern latitudes warm the western sides of the continents mostly in winter due to the warmer oceans to the west; see Fig. 1.9. In particular notice the temperature difference between the western and eastern part of the northern continents. It is the other way around for the oceans, they get cold by the land.
- **Unusual climatologies:** Remarkable in India, for instance, where the mean temperatures in May and June decrease although the incoming solar radiation is still increasing, see Fig. 1.10. This is caused by the Monsoon winds which change directions during May/June, switching from dry continental clear sky to moist tropical cloudy climate. Fig. 1.10 shows the annual cycles of five different locations that are all on the same latitude. Thus they all get the exact same incoming sunlight, but still have very different climates. These differences are related to topography, mean wind directions, position relative to the oceans and the difference between land or oceans.

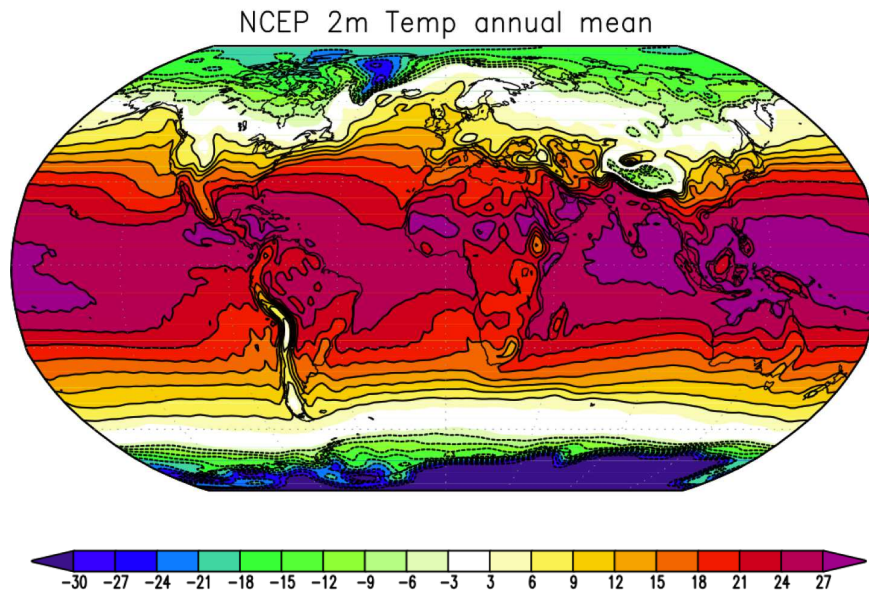


Figure 1.8: Annual mean temperatures in 2m height in the atmosphere from the NCEP data set over the period 1950-2000. Values in $^{\circ}C$.

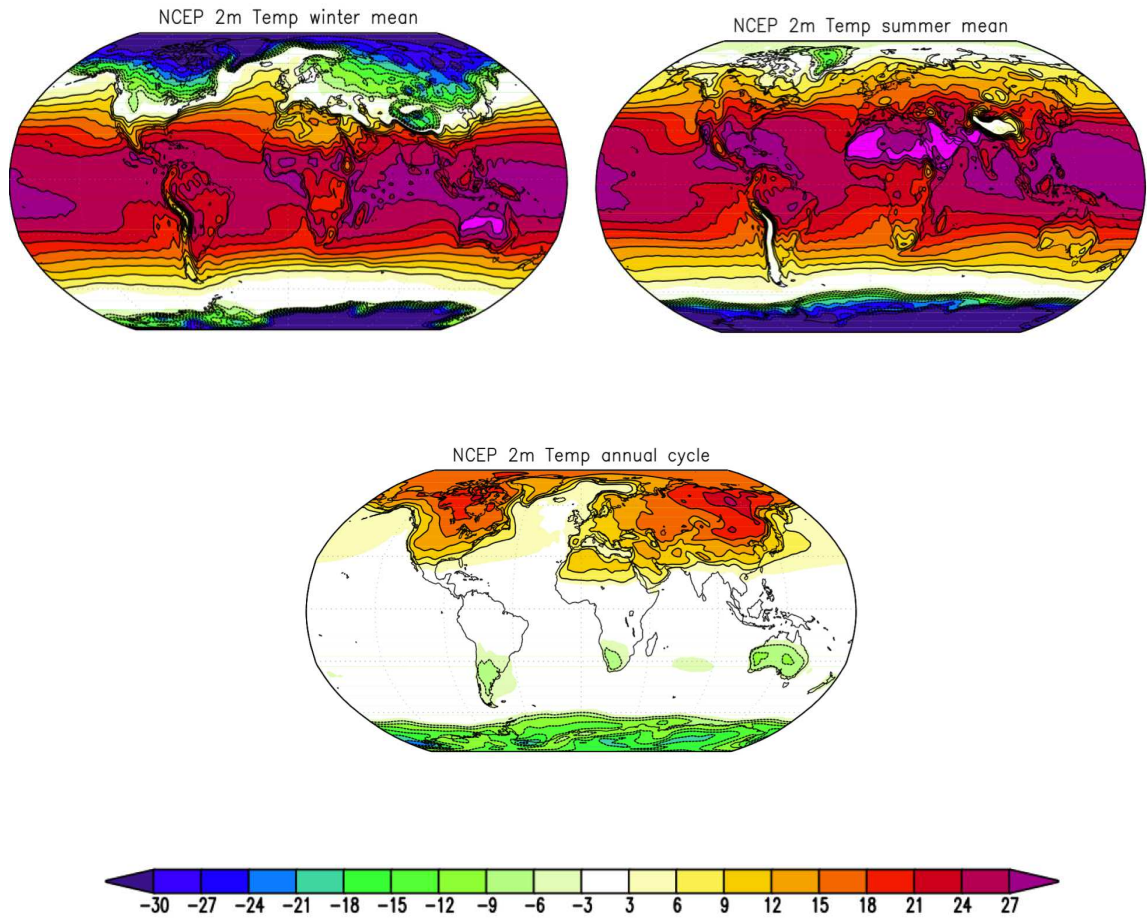


Figure 1.9: Annual cycle of temperature: Jan.-Mar. mean (upper left) and Jul.-Sep. mean (upper right) and the annual cycle amplitude (lower) defined as the difference between the two middle plots divided by two. Values in $^{\circ}C$.

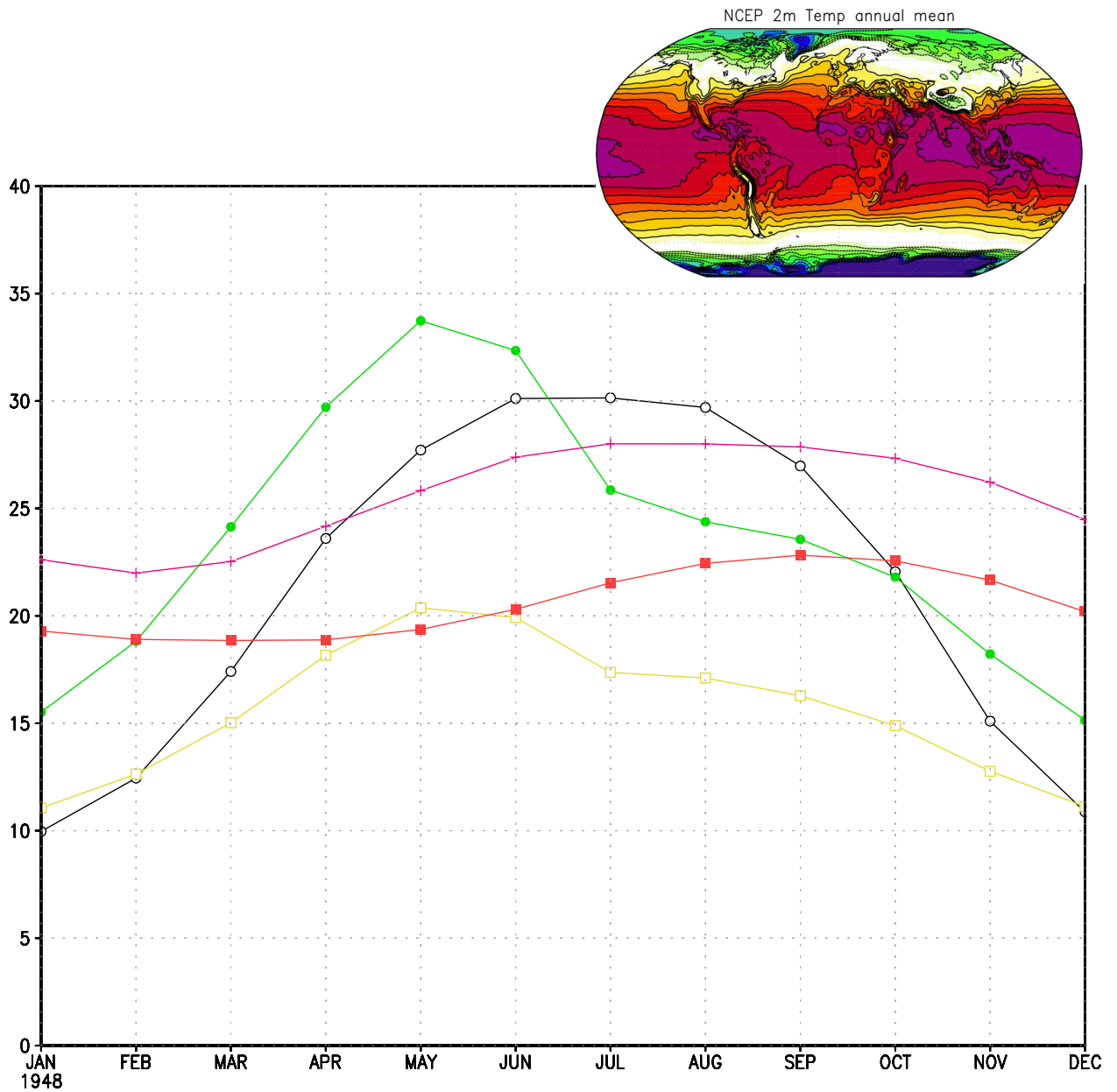


Figure 1.10: Climatologies along the 23rd parallel: Mexico (yellow), subtropical east Atlantic (red), Sahara (black), India (green), and the west subtropical Pacific (purple). Note, that all points receive the same incoming solar radiation at any given day of the year (on top of the atmosphere).

Precipitation

Precipitation is not only very important for life on earth, but is also has an important role in driving the atmospheric circulation. A few main features are:

- **Global mean of about 1-10mm/day:** Precipitation has very large regional differences. The regional differences are not only on the large scale (1000km), but also on very small regional scales (1km). It, for instance rains more in the South-eastern suburbs of Melbourne than in the northern suburbs.
- **Intertropical Convergence Zone (ITCZ):** The main band of precipitation follows a seasonal cycle around the equator, which is called the Intertropical Convergence Zone (ITCZ), see Fig. 1.11. This is where the heavy rain falls on almost every day. These seasonal changing rain band is often called 'monsoons', which means seasonally changing winds. They have different names in different parts of the world.
- **Stronger over warm and wet regions:** Precipitation is to zero order a function of how much moisture is in the air. Warm oceans are therefore the regions with the most rainfall.
- **Fronts:** Precipitation require mostly lifting of air masses. Regions in which cold and warm air hit in fronts are regions where air is lifted and it rains. These are marked in the midlatitudes over the oceans, see Fig. 1.11.
- **Deserts:** Regions where the large scale atmospheric circulations have mostly descending air masses have much less precipitation. These are mostly the subtropical deserts over land and over oceans (eastern side of the basins), but also Antarctica.

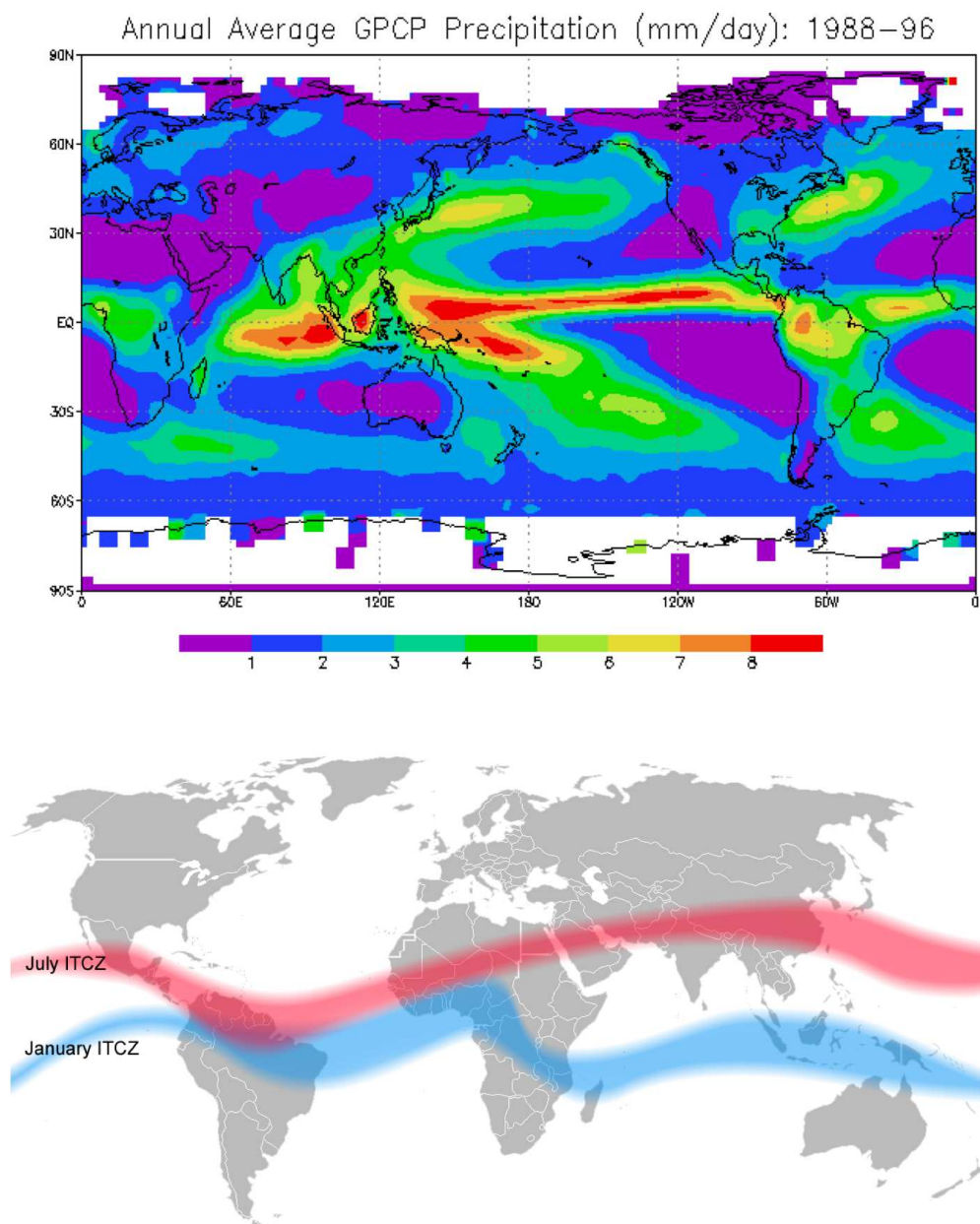


Figure 1.11: Annual average precipitation / Intertropical Convergence Zone (ITCZ)

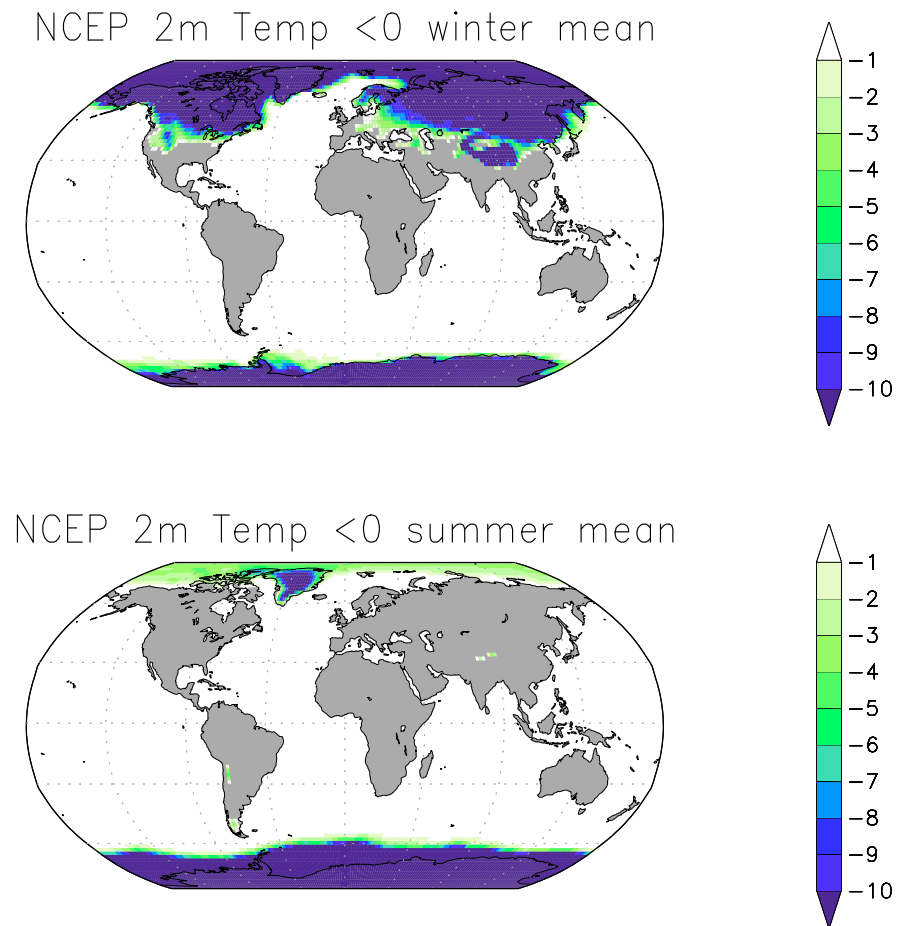
Ice : Glaciers, Snow Cover and Sea Ice

Ice is a very important element of the climate system. This is not just because it changes our outdoor activities, but it actually has very important impacts on the climate system. Some important effects the ice has in the climate system:

- **High Albedo of Ice:** Ice covered regions are usually much brighter (higher albedo) than the surface that they cover (e.g. oceans, vegetation or bare soil). This leads to increased reflection of incoming sunlight and therefore to cooling.
- **Insulation by sea ice:** Sea ice is a very effective insulation of the oceans from the very cold winter atmosphere. It effectively turns an ocean region into a land region in terms of its heat capacity.
- **Below freezing surface:** By definition an ice covered region has a surface temperature below freezing. Even if the atmosphere may become much warmer, the surface will not get above freezing temperature, as long as there is ice cover.
- **Latent heating:** The phase transitions of water from ice to liquid requires a large amount of heat. This is called latent heating (see later in the lecture). To melt a mass of ice is equivalent to heating the same mass of water by about 80 °C (assuming it would not evaporate).
- **Forming mountains:** Large land ice masses can form mountains of 4000m heights (Antarctica). These mountains change the atmospheric circulation substantially.

Here are some of the main characteristics of today's ice climatology:

- **Strong seasonal cycle:** Most of the ice covered regions have strong seasonal cycle, with no ice in the warm seasons; see Fig. 1.12. The largest ice covered regions are over the northern continents in winter and in the polar regions over the oceans.
- **Permanent land ice = glaciers:** Permanent ice cover is called a glacier. They exist in all major mountain regions (e.g. Himalaya, Andes, Alpes, etc.).
- **Sea ice is not permanent (it moves constantly):** Sea ice is constantly moving around mostly driven by winds. Even regions that have 100% ice cover of the year, will sometimes have openings for days due to the wind shifting the ice away.
- **Greenland :** up to 2000 m thickness (Total mass = 7 m global mean sea level equivalent)
- **Antarctica :** up to 4000 m thickness (total mass = 60 m global mean sea level equivalent)



25/Feb/11

Figure 1.12: The regions covered with ice or snow for the month Jan. to Mar. (upper) and for Jun. to Sep. (lower) as indicated by the mean surface temperature below zero. Color scale is mean temperature in °C

1.1.3.2 Atmosphere

Main features :

- Large scale circulation (winds)
- Pressure systems
- Vertical profile atmosphere
- Clouds
- Moisture

The large scale circulation

Main features:

- 2 x 3 zonal overturning cells:
 - Hadley cell: directly thermally driven
 - Ferrel cell: chaotic, indirectly driven
 - Polar cell: directly thermally driven
- The cells define the surface mean wind directions

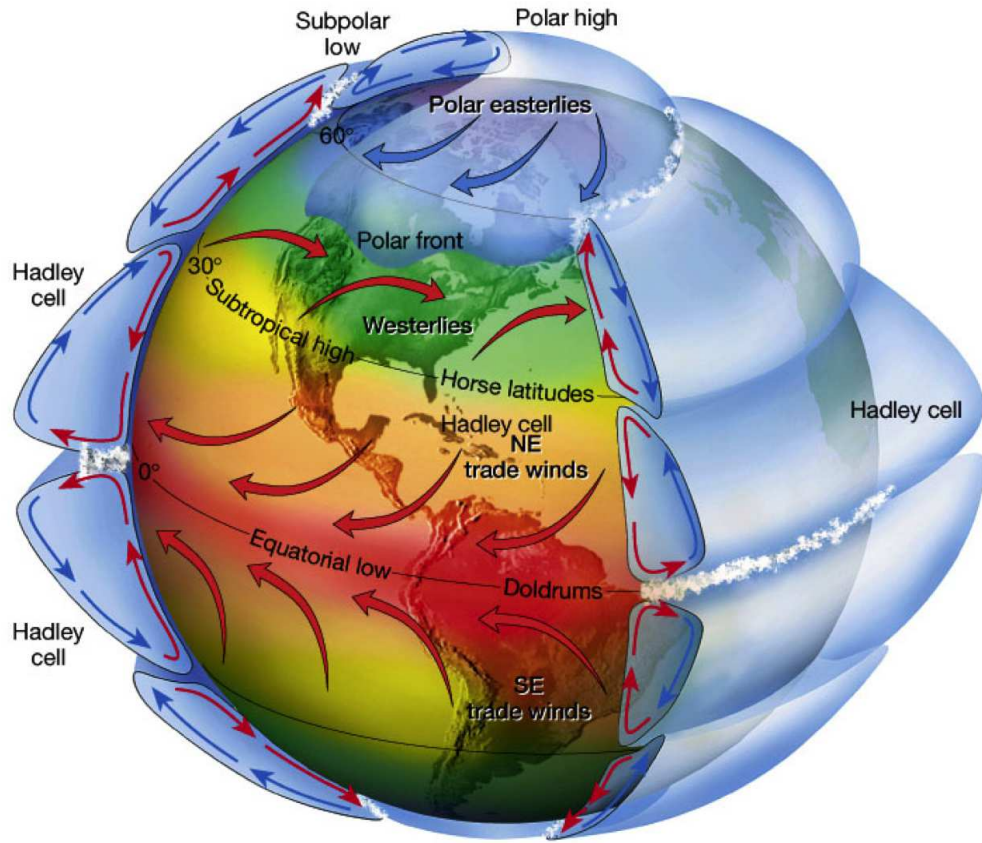


Figure 1.13: Sketch illustrating the main cells of the large scale circulations.

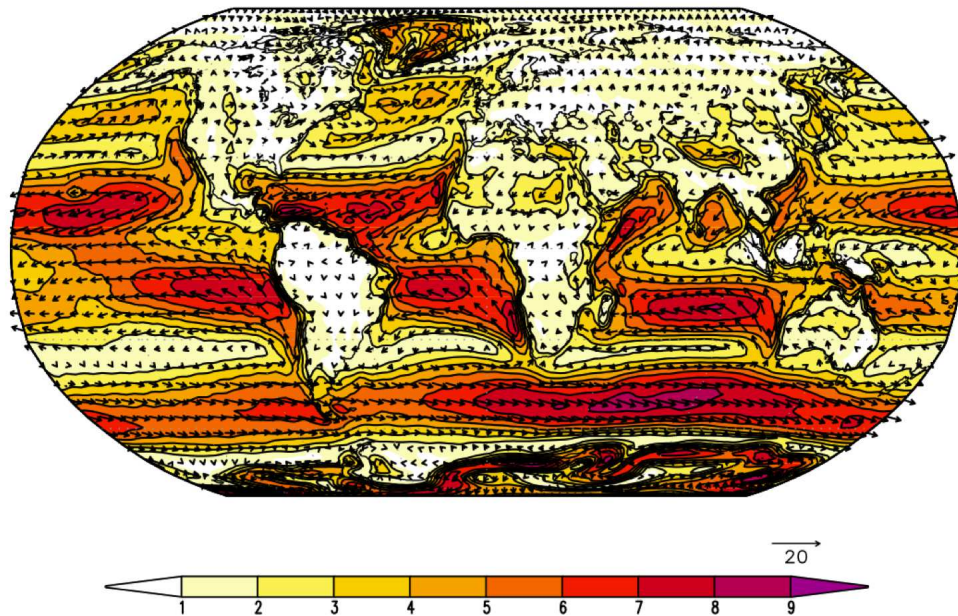


Figure 1.14: Mean winds in 10m height above the surface in m/s.

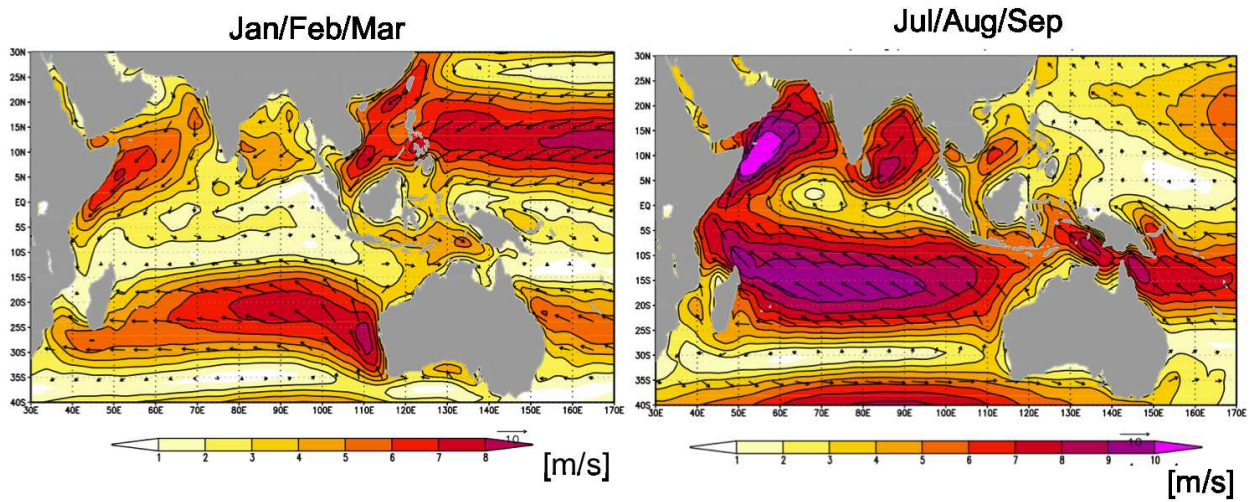


Figure 1.15: Indian Ocean Monsoon: An example of strong changes in the wind directions and magnitude over the seasonal cycle.

Pressure systems

Main features:

- Pressure = mass of air (hydrostatic balance)
 - pressure decreases with height
 - sea level pressure (SLP) instead of surface pressure
 - air mass : $10,000 \text{ kg/m}^2 \rightarrow \text{SLP} = 10^5 \text{ Pa} = 1000 \text{ hPa} = 1000 \text{ mb}$
- Tropical lows (ITCZ)
- Subtropical highs
- Subpolar lows (Icelandic low, Aleutian low)
- Polar high
- Low indicates rising air masses \rightarrow clouds / rain
- High indicates sinking air masses \rightarrow clear sky / deserts

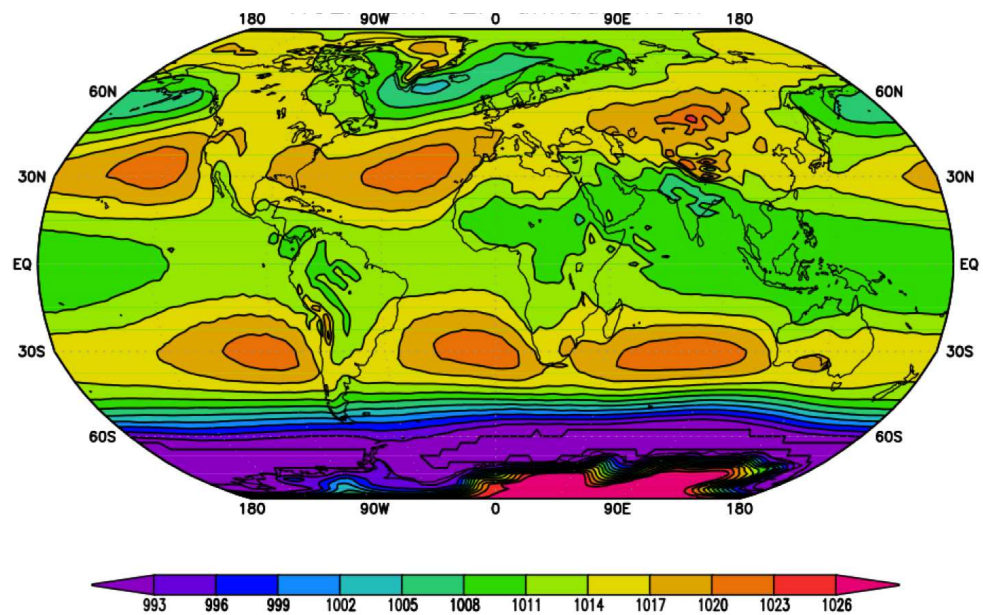


Figure 1.16: Mean Seal Level Pressure (SLP) in hPa.

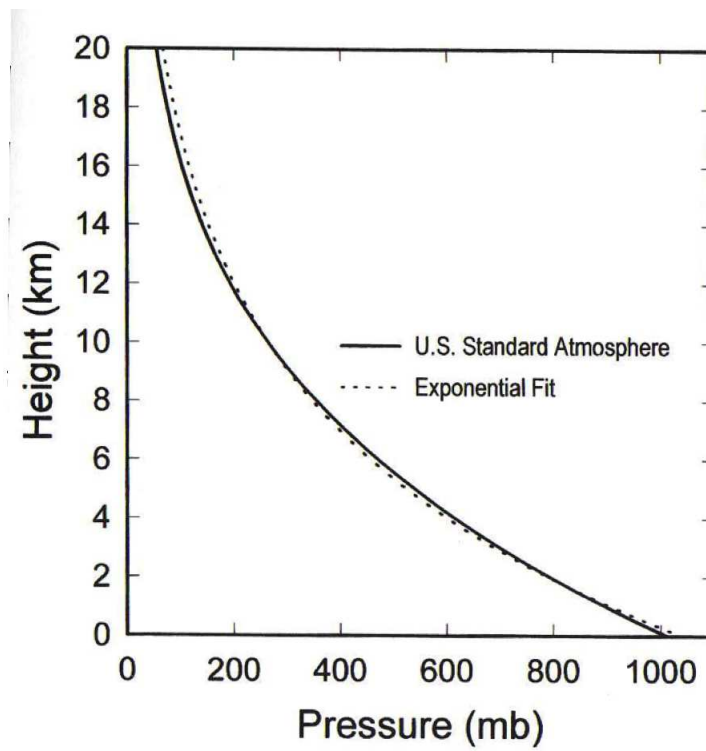


Figure 1.17: The standard air column profile of the air pressure. Roughly the same as an exponential function.

Vertical profile atmosphere

Main features :

- Troposphere : about 10 km high
- Troposphere : weather active part of atmosphere
- Troposphere : 75% of the atmosphere and 99% of the water vapor
- Stratosphere: about 10 km - 50 km
- Stratosphere : UV absorption
- Less than 0.1% of the air mass is above the stratosphere

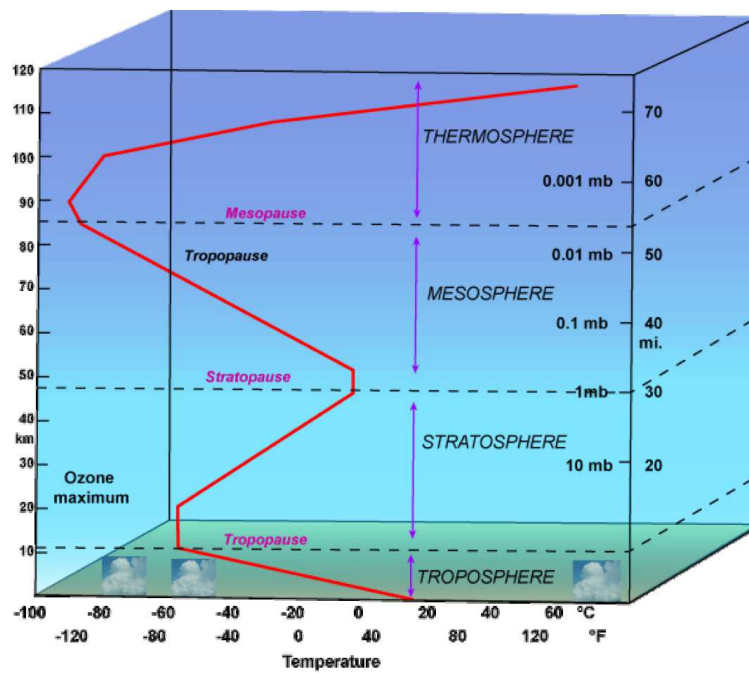


Figure 1.18: Sketch of the temperature profile of the whole atmosphere, illustrating the different layers of the atmosphere.

Clouds

Main features :

- Thickness : 100 m - 10,000 m
- Layers : low = warm, high = cold
- Clouds are sources for precipitation
- Reflect and absorb radiation
- Optical thickness 20% - 90% sunlight reflection
- Different regions have different types of clouds
- The global mean cloud cover is about 70%

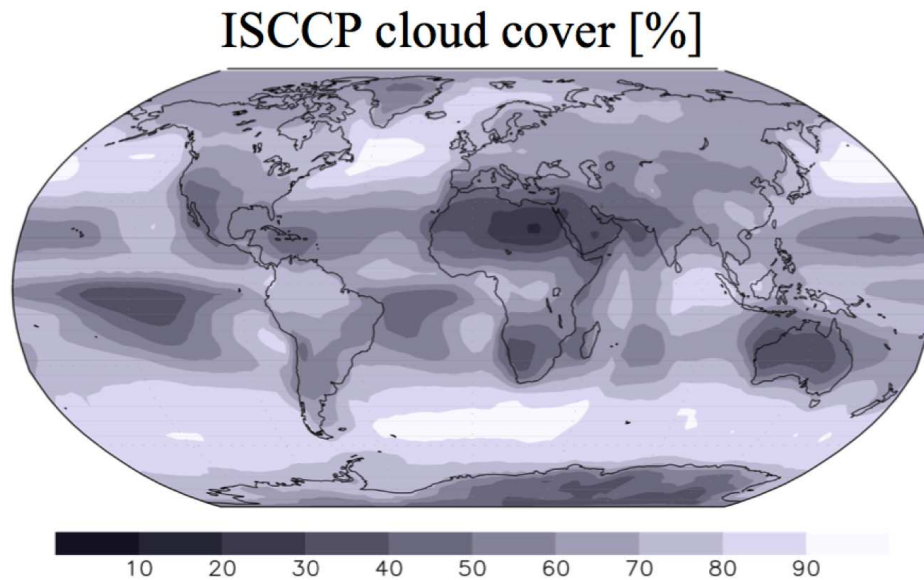


Figure 1.19: ISCCP mean cloud cover in percentage.

Moisture

Main features :

- Source for clouds and rain
- Condensation of moisture heats the atmosphere
- Condensation of moisture drives the atmospheric circulation
- Moisture content is highly variable and chaotic (weather)

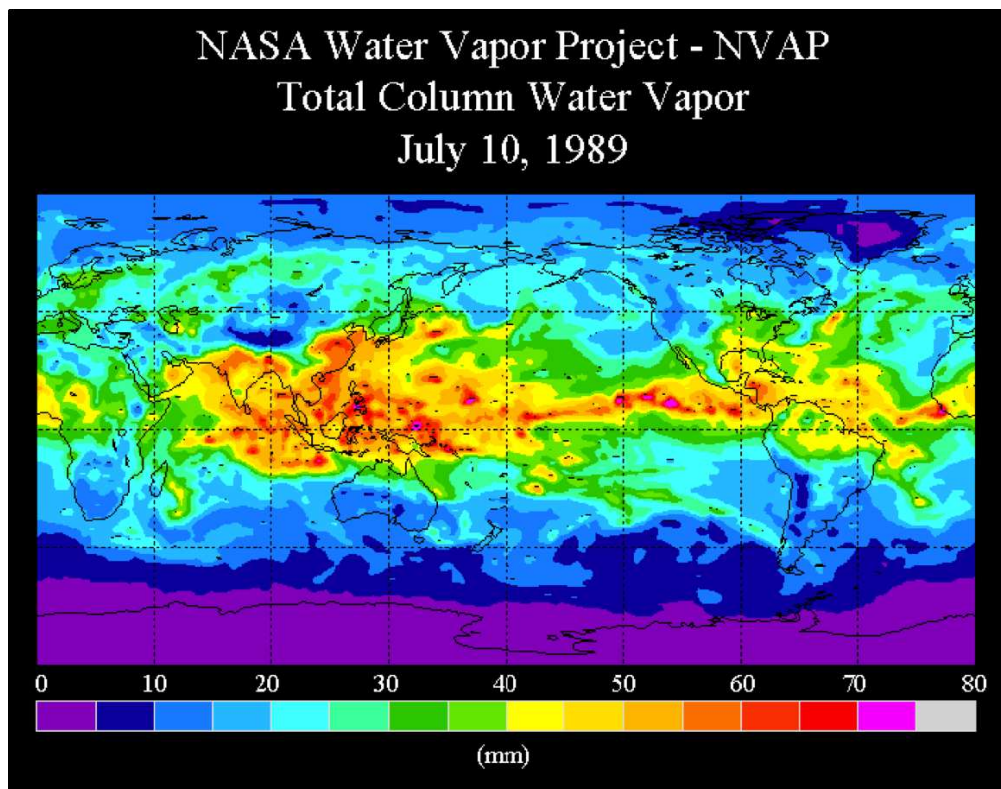
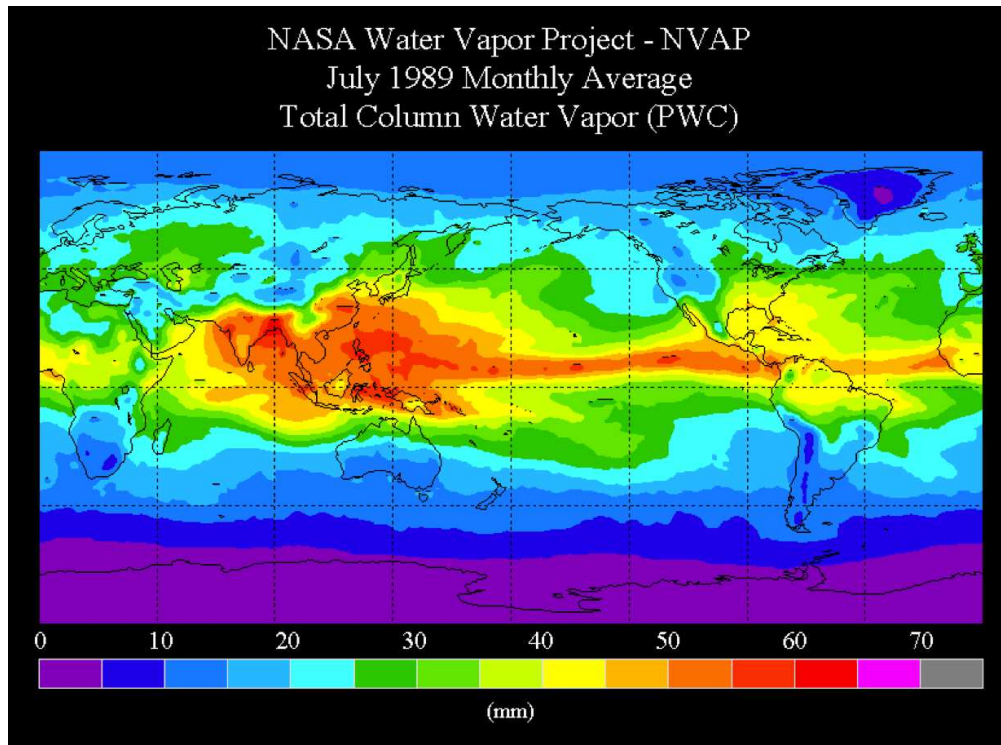


Figure 1.20: Water vapour distribution: Upper: The mean over one month. Lower: The mean over one day. Units are in liquid water column equivalent in mm (this is roughly the same as kg/m^2).

1.1.3.3 Oceans

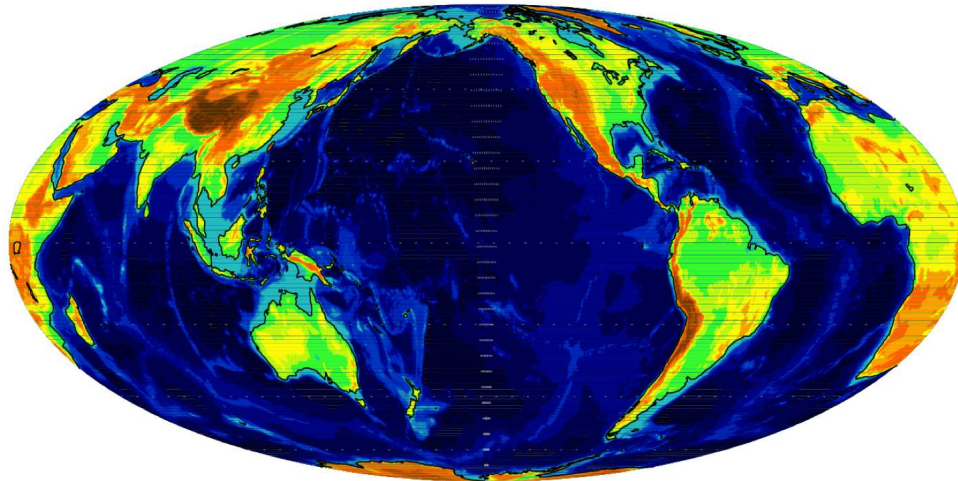


Figure 1.21: About 2/3 of the globe is oceans. This Mollweide projection with center on the North Pole illustrates the importance of the oceans. Most common projections of the earth focus on the land areas.

The oceans cover the largest part (70%) of the earth and are therefore one of the most important elements of the climate system. However, even for the land regions the oceans influence on the climate is quite important. Two main features of the oceans are important for the climate over land:

- **Heat capacity:** Most of the climate system's heat is stored in the oceans. The specific heat capacities are:
 - Oceans : 4,000,000 J/K/m water column. Thus to warm a one meter water column by 1 °K requires 4,000,000 J of energy.
 - Land : 1,000,000 J/K/m soil column
 - Atmosphere : 1,000 J/K/m air column

Further we need to consider that the ocean is 100m to 4000m deep, land conducts the heat only 1-5m into the soil and the atmosphere mixes the heat 1000m to 10,000m. Considering the size of columns and the specific heat capacities we find that the upper 5m of the oceans contain about the same amount of heat as the total atmosphere and land together.

- **Main source of Moisture:** Moisture in the atmosphere and rainfall over land comes from the oceans to the largest part. The oceans are central in understanding the hydrological cycle (precipitation, evaporation, etc.) of the atmosphere and land.
- **Transport of heat:** Ocean currents can transport heat from warmer to colder regions and vice versa. Further they store heat from the warm seasons and release the heat in the cold season.

Ocean circulation

The ocean circulation is very complex and much more chaotic than the atmospheric counterpart. The ocean circulation and the vertical mixing profiles are some of the main characteristics of the

oceans that are important in the context of the global climate dynamics.

Some of the main features of the oceans circulation :

- Circulation is complex, chaotic and on smaller scales than in the Atmosphere. Fig. 1.22 shows a snapshot of the ocean temperatures in the North Atlantic. It illustrates the complex motions in the surface oceans. You can see eddies that are much smaller than atmospheric cyclones, but you can also see currents meandering through the ocean (e.g. the Gulf Stream).
- Surface wind driven circulation: The surface currents are mostly directly forced by the winds above. They however, get deflected by coast lines and are mostly re-circle in large horizontal gyres.
- Large scale thermohaline deep circulation (thermohaline : temperature and salinity driven
 - salty \rightarrow denser
 - cold \rightarrow denser
- Formation of ice produces salty and cold water, which falls to the deep ocean : convection

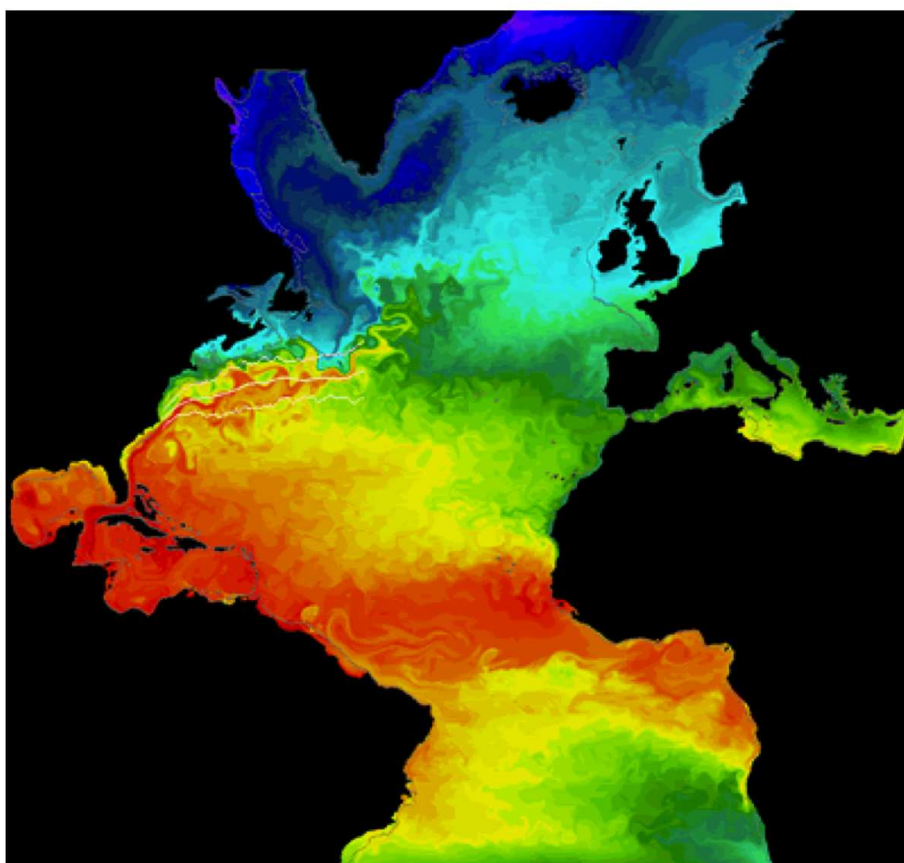


Figure 1.22: Snapshot of sea surface temperature illustrating the chaotic nature of the ocean surface currents. Messure with infrared (thermal) wavelength satellites from space.

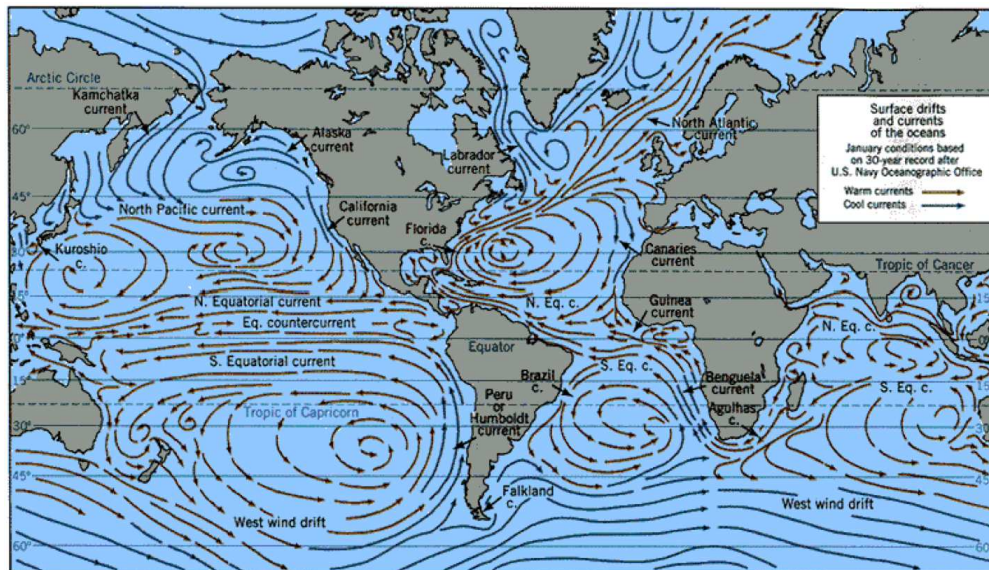


Figure 1.23: Sketch of the ocean surface currents; mostly forced by the atmospheric wind patterns.

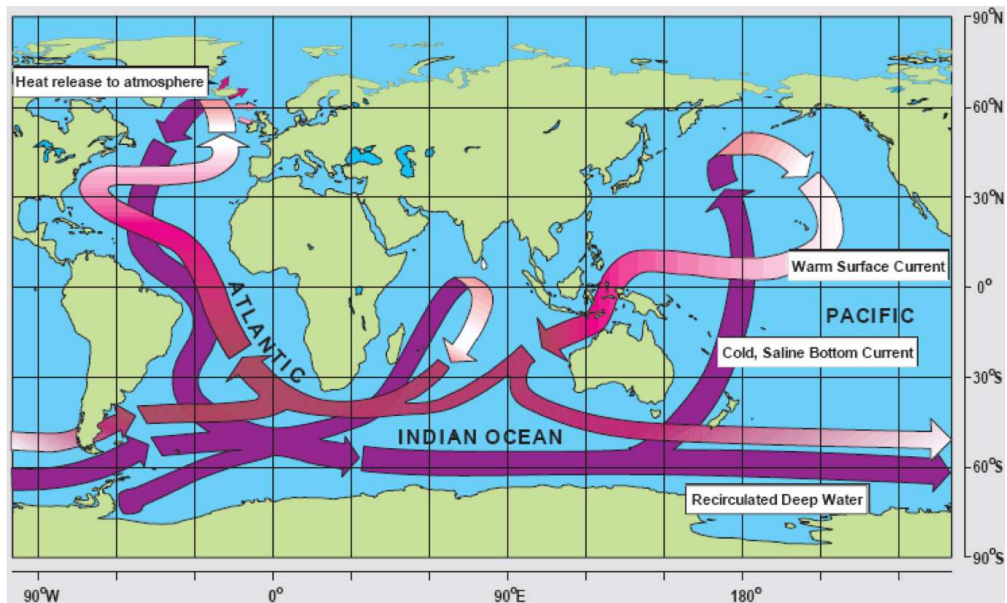


Figure 1.24: Ocean thermohaline circulation: The large-scale circulation into the deep ocean. This circulation is driven by density (temperature and salinity; called thermohaline) gradients.

Ocean mixing

Main features :

- The ocean is stratified by density: warm and fresh water is near the surface and cold and salty water is at the bottom.
- Vertical profile : mixed layer / thermocline / cold deep ocean
- Mixed layer depth :
 - mean ~ 50 m
 - range : 1 - 1000 m
- Only the well mixed upper ocean interacts with the atmosphere on time-scales of months to 10 years.
- The deep ocean (below the thermocline) is mostly inactive and only interacts with the atmosphere on time scales longer than a 100yrs. Thus most of the ocean is passive.

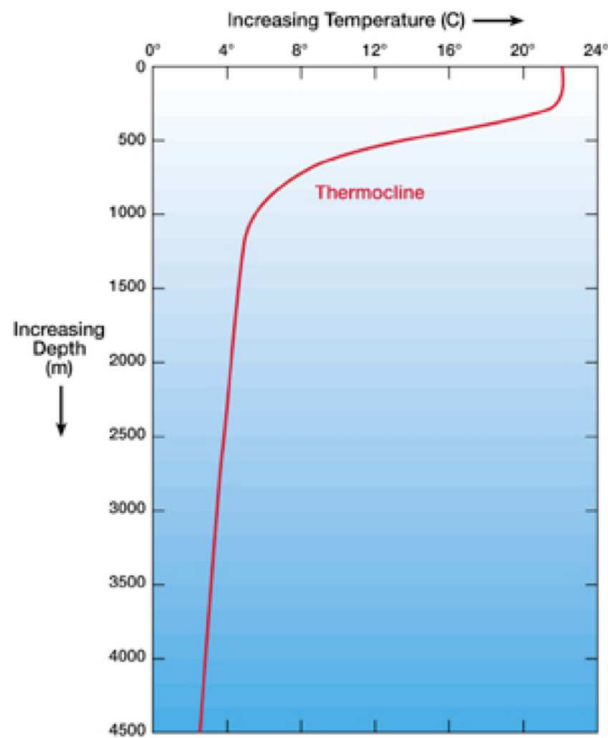


Figure 1.25: Sketch of the mean ocean column temperature profile.

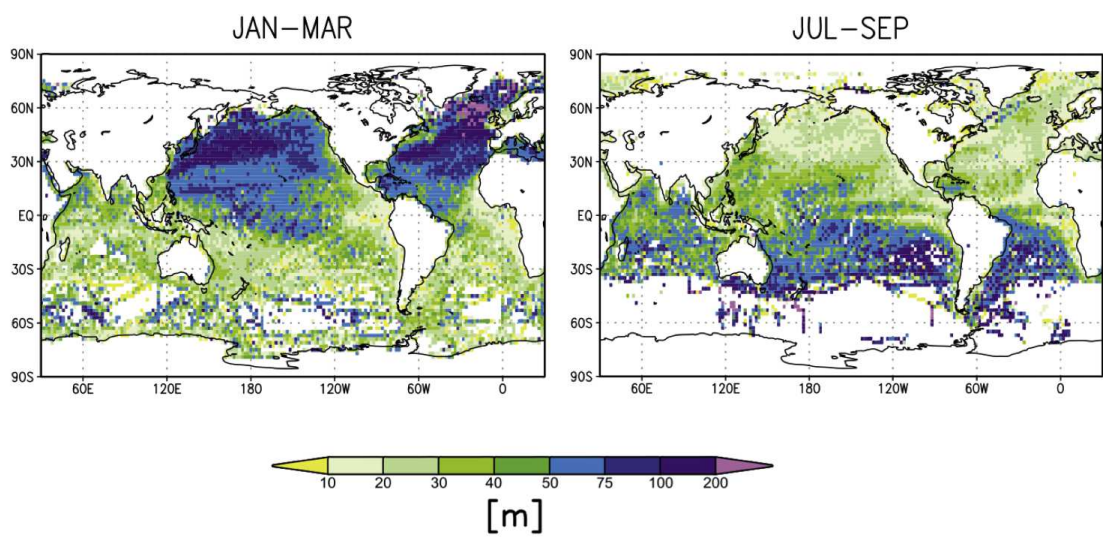


Figure 1.26: The mean ocean mixed layer depth; the depth of the well mixed surface layer of the ocean. For two different seasons. White oceanic regions mark regions with insufficient observational data to determine a mean mixed layer depth.

Chapter 2

Simple Climate Energy Balance Models

Greenhouse effect, Climate Sensitivity, Stability and Feedbacks

The energy balance of the earth climate system is a good starting point for understanding the dynamics of the climate. If we take the simple view of the earth as a mass that gains heat from the sun and loses heat by radiation into space we can get some idea of what the temperature of the earth would be. Starting from this simple view we can then add different elements of the climate system to get a more detailed understanding. These theoretical considerations are in general called energy balance models. In the following we will use these models to understand some of the basic principles for the climate, such as the Greenhouse effect, the Climate Sensitivity, Stability and Feedbacks.

An example from the 2007 IPCC report may illustrate how energy balance models may help to understand the climate dynamics: The IPCC report gives advice to policy makers, it addresses non-scientists. Most of the informations that the IPCC report provides are very difficult to understand if you are not familiar with the energy balance models of the climate system.

The Table in Fig. 2.1 is from the 2007 IPCC report. It provides informations of how different influences over the 20th century forced the climate system. These informations should summarise what influences over the 20th century had lead to changes in the climate system. The radiative forcings are given in W/m^2 , thus in terms of energy flux per surface area of the earth. A positive forcing leads to warming and a negative forcing leads to cooling of the earth mean climate. We can, for instance, see that increased CO_2 concentrations had the largest warming influence. Aerosols on the other hand had a cooling influence. A first question that comes to mind is: How do we know this? Another question that arises is: By how much would the surface temperature warm if this $+1.6W/m^2$ radiative forcing is added? It is helpful to put these numbers into perspective. The incoming solar radiation is $+1365W/m^2$. So one may wonder: How can the tiny $+1.6W/m^2$ (just 0.1 percent of the incoming solar radiation) lead to any significant climate change? The aim of the following discussions on energy balance models of the earth climate system is to understand how such questions are addressed.

We start this chapter with the introduction of the basic principle of conservation of energy which is the fundament for the energy balance climate models. We further introduce the concept of diagnostic prognostic equations. The first energy balance models we discuss are zero order climate models, which describe only the global mean climate as a radiation balance. In this model we introduce simple conceptual models of the greenhouse effect and a simple ice-albedo feedback of the climate system. The introduction of the feedback leads us to the discussion of multi equilibria, the stability of the climate equilibria and the definition of climate sensitivity. This discussion also involves the concept of a climate potential and the idea of tipping points in the climate system. We finish this

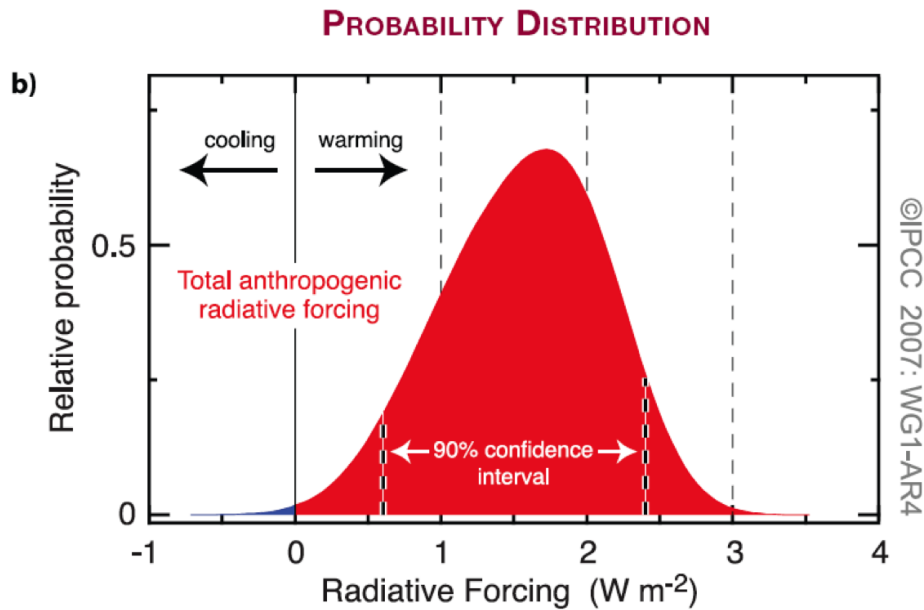
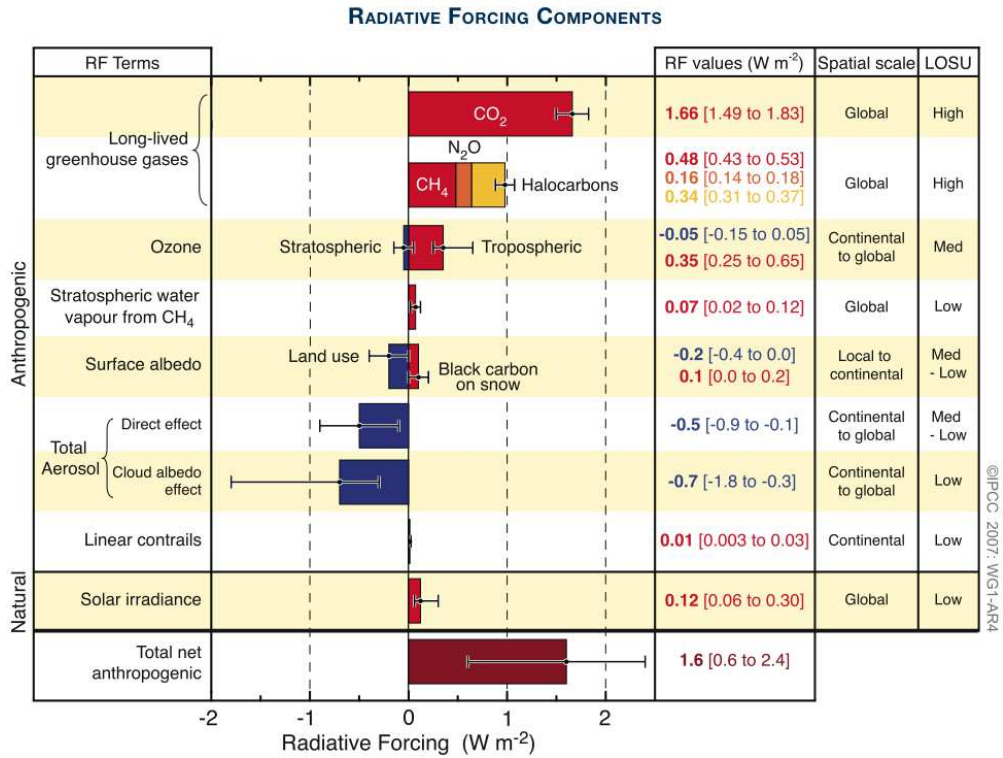


Figure 2.1: Upper: Table of global mean radiative forcing 1750 - 2005. The legend from left to right means: radiative forcing terms (RF terms); radiative forcing values (RF values); spatial scale refers to the area affect by the RF terms; level of scientific understanding (LOSU). LOSU basically reflects the size of the error bars relative to the mean signal. Lower: Anthropogenic radiative forcing probability distribution for the 20th century forcings.

chapter with a conceptual discussion of a number of different climate feedbacks and how feedbacks parameters can be defined.

2.1 Basics

Some basic considerations that we need for the further discussions:

2.1.1 Energy conservation

Climate energy balance models are based on the energy conservations laws. It simply states that the sum of all energy terms is constant:

$$E_{total} = \sum E_i = constant \quad (2.1)$$

Or alternatively we could say, that if the total energy is changing, then there must be a number of forcing terms that add up to the tendencies (derivative in time) in total energy:

$$\frac{dE_{total}}{dt} = \sum \frac{dE_i}{dt} \quad (2.2)$$

For the following discussions we make the simplification that we equate energy with heat and the heat of a system is proportional to the temperature of the system:

$$\frac{dE}{dt} \approx \frac{dH}{dt} = \frac{d(\gamma T)}{dt} = \gamma \frac{dT}{dt} \quad (2.3)$$

γ = heat capacity (constant)

Thus the conservation of energy and the energy balance equations leads us to a temperature tendency equation. The temperature tendency equation will, for all following discussions, be our energy balance equation. Thus our energy balance models are models of the temperature tendencies.

2.1.2 Diagnostic equations

In climate dynamics we often discuss tendency equations, even though we are not interested in the tendency of a variable, but we are actually interested in the absolute value of the variable itself. If, for instance, we are interested in the surface temperature of global mean climate we would like to write down an equation which equates the surface temperature to some function of other variables. However, such a function usually does not exist (with the exception of some simplified models; see later in the lecture notes). In complex systems or in chaotic systems, such as the climate, some state variables can not be written as a function of the other state variables, but we can only determine the tendency of the variables.

In climate dynamics (climate modelling) we therefore distinguish between diagnostic and prognostic variables. A climate variable, Φ , whose value we can determine as a function of other variables of the climate system at any time is called a diagnostic variable. We can write a diagnostic equation that defines the value of Φ by a function of other state variables:

$$\Phi = F(x, t) \quad (2.4)$$

So we can diagnose the values of Φ by knowing the state of the system (Examples: clouds diagnosed by water vapour saturation; snow cover by $T_{surf} < 0^\circ C$).

2.1.3 Prognostic equations

A climate variable that we can not determine by a diagnostic equation have to be determined by prognostic tendency equation:

$$\frac{d\Phi}{dt} = F(x, t) \quad (2.5)$$

To determine the value of Φ at any given time we have to integrate the prognostic tendency equation over a past time interval starting from some assumed initial value. Thus the current value of a prognostic variable may depend on the history of the climate system evolution. In turn this means that the climate, for a given boundary condition, can be in many different climate states, depending on the past evolutions. We will in later examples see that some simple climate models can have multiple climate states for the same fixed boundary conditions. More importantly, we will later discuss the Lorenz model introducing the chaotic nature of climate, which illustrates that the climate system will never be at rest or in equilibrium. So in a chaotic system a deterministic value of Φ does not really exist.

2.2 Zero order model (Radiation balance)

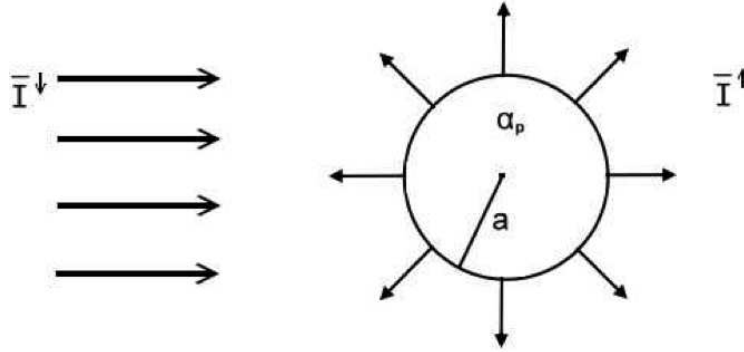


Figure 2.2: Sketch of the zero order climate model. The incoming solar radiation is balanced by the emission of thermal radiation from the earth.

We start our discussion of climate models with the simplest model, treating the global mean surface temperature, T_{surf} , as a zero dimensional (a single number, in contrast to a vector or field value) problem. Thus a zero order model. The total heat of the earth is balanced to the outer space by the incoming solar radiation, F_{solar} and the outgoing thermal radiation, $F_{thermal}$, see Fig. 2.2. This leads to the equation:

$$\gamma_{surf} \frac{dT_{surf}}{dt} = F_{solar} + F_{thermal} \quad (2.6)$$

γ_{surf} = heat capacity [$J/m^2/K$]

T_{surf} = surface temperature [K]

$F_{solar} + F_{thermal}$ = forcing terms [W/m^2]

Note that the eq. [2.6] has the same form as the energy conservation law in eq. [2.3]. On the left hand side we have a change in energy (heat) and on the right hand side we have a sum of forcing (energy flux) terms.

Note, that in the following discussions we will use the term '*forcing*' as a synonym for energy flux, but the term '*forcing*' can in general be used for any kind of driver leading to changes in the system. This could, for instance, be CO_2 -forcing, volcano forcing or land cover change forcing. These forcings are not necessarily energy fluxes, but are simply some changes to the climate system, that may lead to changes in the energy balance.

Further, climate models in general discuss the energy balance per surface area of the earth. So we will define the heat capacity and forcings per area. Thus γ_{surf} is given in units of $[J/m^2/K]$ and the forcings F_i are given in $[W/m^2]$. The heat capacity, γ_{surf} , is typically that of the surface layer over land (e.g. 2m soil layer) or oceans (e.g. a 50m water column), but for now we do not care about the heat capacity, as it will not be needed in the further discussion.

The incoming solar radiation on the global mean, F_{solar} , can be simplified to:

$$F_{solar} = \frac{1}{4}(1 - \alpha_p)S_0 \quad (2.7)$$

α_p =planetary albedo = 0.3

S_0 =solar constant = $1365W/m^2$

The solar constant, S_0 , is the amount of incoming solar energy per area facing towards the sun at the top of the atmosphere (before anything reflects or interacts with the sun light in any way). However, the earth surface in average only receives 1/4 of it, because one half of the earth is always facing away from the sun (night) and the day side of the earth is not all directly facing towards the sun. Or in a geometrical consideration: only the fraction of the earth surface perpendicular to the incoming sun light receives the sun light, which is the ratio of the area of a circle divided by surface of a sphere with the same radius, which is 1/4. This in summary leads to only 1/4 of S_0 being received by the earth surface in average over all regions over day and night.

A part of the incoming solar radiation is directly reflect back to space by the earth albedo. The albedo is the amount of reflectivity: a black body has the albedo=0 , absorbing all incoming sun light, and a white body has the albedo=1, reflecting all incoming sun light. The earth average albedo (the planetary albedo), $\alpha_p = 0.3$ (a dark grey). This reflection is mostly done by clouds and a little bit by snow/ice covered regions (we discuss the albedo in more detail in later parts of the lecture).

So the average over all regions over day and night absorbed solar radiation is about

$$F_{solar} = \frac{1}{4} \cdot (1 - 0.3) \cdot 1365W/m^2 \approx 240W/m^2 \quad (2.8)$$

To get an idea how much energy that is we can look at a view analogs for energy flux per m^2 :

- Lights (200 W; the traditional light bulbs) / living room = $200W/20m^2 = 10W/m^2$. Thus a 200W light bulb in a $20m^2$ living room is equivalent to a $10W/m^2$ energy flux.
- Heater (1000 W) / living room = $1000W/20m^2 = 50W/m^2$. Thus the heat flux through this living room is $50W/m^2$.
- The total energy consumption of all mankind per earth surface $\approx 0.024W/m^2$. This is tiny compared to the amount of heat coming from the sun.

The outgoing thermal radiation is the black body radiation of Stefan Boltzmann:

$$F_{thermal} = -\sigma T_{surf}^4 \quad (2.9)$$

σ =Stefan Boltzmann constant = $5.67 \cdot 10^{-8}[W/m^2/K^4]$

The thermal radiation is often referred to as the long wave radiation, since the radiation of the earth is on much longer wave length than the solar radiation, see Fig. 2.3. The solar and the earth thermal radiation are well separated in their wave length.

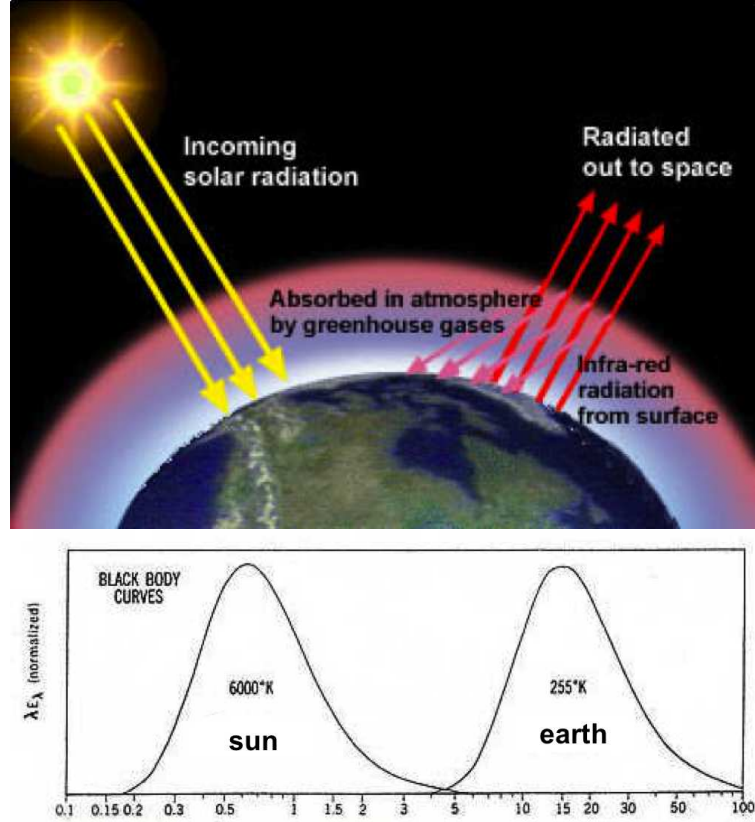


Figure 2.3: Black body radiation curves for the sun and the earth as function of wave length. The thermal radiation of the sun is on a much shorter wave length, therefore we refer to it as *short wave* radiation. The thermal radiation of the earth is on longer wave length, we therefore refer to it as *long wave* radiation.

We can now include eqs. [2.8] and [2.9] into eq. [2.6]:

$$\gamma_{surf} \frac{dT_{surf}}{dt} = \frac{1}{4}(1 - \alpha_p)S_0 - \sigma T_{surf}^4 \quad (2.10)$$

In equilibrium the tendencies are zero: $\frac{dT_{surf}}{dt} = 0$. It follows that the incoming solar radiation is in balance with the outgoing thermal radiation:

$$\rightarrow \frac{1}{4}(1 - \alpha_p)S_0 = \sigma T_{surf}^4 \quad (2.11)$$

We can solve this equation for the equilibrium T_{surf} :

$$\Rightarrow T_{surf} = \sqrt[4]{\frac{(1 - \alpha_p)}{4\sigma} S_0} = 255K = -18^\circ C = T_{rad} \quad (2.12)$$

Often this equilibrium temperature is called radiation balance temperature, T_{rad} , to indicate that it follows from the radiation balance in eq. [2.11]. In general (not just in climate dynamics) the

radiation temperature is defined as the temperature those black body radiation would balance a radiation Q :

$$\sigma T_{rad}^4 = Q \quad (2.13)$$

In the above equation $Q = 1/4 \cdot (1 - \alpha_p) \cdot S_0$.

The observed global mean $T_{surf} \approx 288^\circ K = 15^\circ C$. So we see that there is a mismatch of $+33^\circ C$ between our zero order model and the observed T_{surf} . First of all, this shows that the simple model is not so bad, as it gets to the real observed value with an error of 'just' about 10% (relative to $288^\circ K$). However, the mismatch indicates that we are missing something. The additional $+33^\circ C$ warming comes from the *greenhouse effect* of the atmosphere.

2.2.1 Greenhouse effect

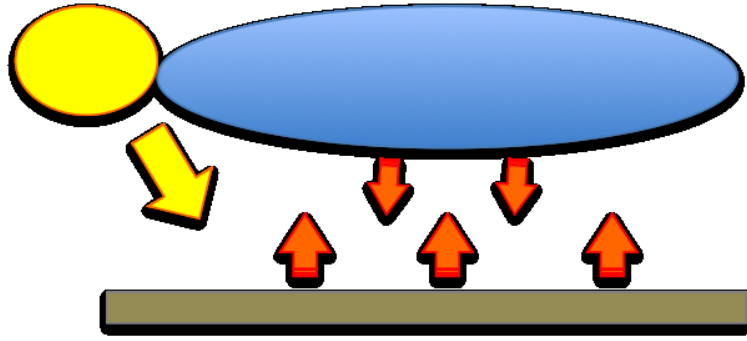


Figure 2.4: Sketch of Greenhouse effect.

In the above discussion we assumed that the surface radiates the thermal radiation directly into space (see Fig. 2.2). However, we need to consider that there is an atmosphere in between, which can absorb and emit thermal radiation. We can now add an atmosphere to the model, see Fig. 2.4. The atmosphere radiates thermal radiation to the surface. This is an additional heat forcing which we neglected in the previous section. The additional thermal heat coming from the atmosphere accounts for the missing $+33^\circ C$ warming. We can therefore define the *Greenhouse Effect*, G , by the ad hoc definition:

$$G = T_{surf} - T_{rad} = 33K \quad (2.14)$$

This is only an empirical definition to quantify the overall effect of the greenhouse. As a first zero order approach we can simplify the thermal radiation coming from the atmosphere as a partial reflection of the outgoing thermal radiation from the surface:

$$F_{atmos} = g_p \cdot \sigma T_{surf}^4 \quad (2.15)$$

The reflection parameter, g_p , determines how much the atmosphere radiates back to the surface and how much is left; going into space. We can include this term into eq. [2.10]:

$$\rightarrow \gamma_{surf} \frac{dT_{surf}}{dt} = \frac{1}{4}(1 - \alpha_p)S_0 - (1 - g_p)\sigma T_{surf}^4 \quad (2.16)$$

By knowing the observed T_{surf} we can solve this equation for g_p :

$$\Rightarrow g_p = 1 - \frac{(1 - \alpha_p)S_0}{4\sigma T_{surf}^4} = 0.38 \quad (2.17)$$

In this simple model 38% of the outgoing thermal radiation is directly reflected back to the surface and the residual of 62% goes into space. Note, that in more detailed energy balance models of the atmosphere, which resolve the processes in different vertical levels of the atmosphere, the budgets are quite different in numbers, but they results into the same net effect.

We can also solve the equation for T_{surf} to understand how it depends on the different elements:

$$\Rightarrow T_{surf}^4 = \frac{1}{4\sigma} \cdot \frac{(1 - \alpha_p)}{(1 - g_p)} \cdot S_0 \quad (2.18)$$

A few relations we want to point out here to get some understanding of this model:

- T_{surf} increases if S_0 increase. So simply it gets warmer if the sun is shining stronger.
- T_{surf} decreases if α_p increases. If the planetary albedo increase more sun light is reflected and subsequently less sun light is absorbed and it gets colder.
- T_{surf} increases if g_p increase. If the atmospheric greenhouse effect gets stronger, than it gets warmer. If g_p gets close to 1, T_{surf} would get to infinite.

The question arises: How close to 1 can g_p get? A good example in this respect is the planet Venus. The values for Venus are:

$$S_V = 2619W/m^2$$

$$\alpha_p = 0.7$$

$$T_{rad} = \sqrt[4]{\frac{(1-\alpha_p)}{4\sigma} S_V} = 242^\circ K$$

$$\text{Observed: } T_{surf} = 730K (!!)$$

From these values it follows for the atmospheric greenhouse effect:

$$\Rightarrow g_p = 1 - \frac{(1 - \alpha_p)S_p}{4\sigma T_{surf}^4} = 0.988 \quad (2.19)$$

So we see that for Venus g_p gets quite close to 1. Venus in comparison to earth has a much thicker atmosphere, which consist mostly of CO_2 (earth atmosphere has less than 1% CO_2 ; see later in the lecture). The overall greenhouse warming for Venus is $G = 730^\circ K - 242^\circ K = 388^\circ K$. So the greenhouse effect can lead to a quite substantial warming. In theory and in practise there is no upper limit.

Fig. 2.5 shows the radiation temperature, T_{rad} , and the true observed T_{surf} of Venus, Earth and Mars. We can see that the radiation temperature is usually below the theoretical curve of a black body absorbed, because the albedo of the planets are always reflecting some of the incoming sun light. Further, we see that the true surface temperature of Earth and in particular of Venus are much warmer due to there greenhouse effects of their atmospheres. Venus has the thickest atmosphere followed by that of Earth and Mars has a very thin atmosphere.

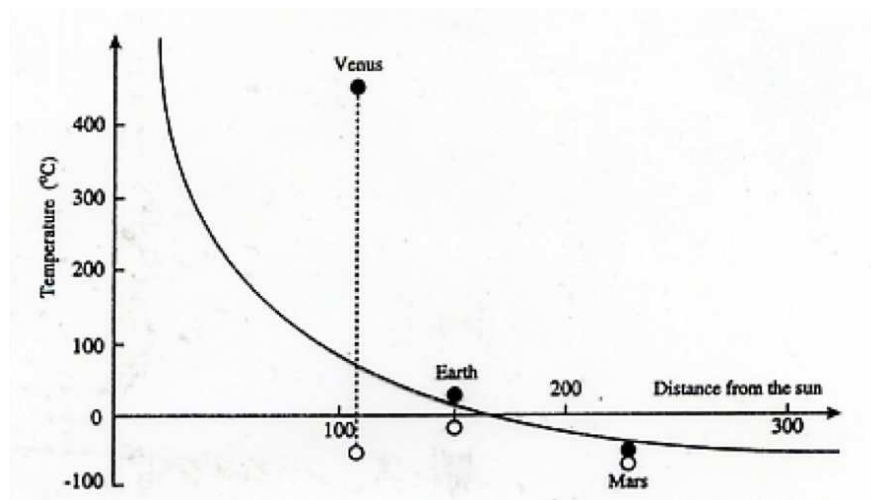


Figure 2.5: Distance from the Sun versus radiation temperature of a black body absorbing the incoming sun light (solid line). The black filled circles mark the observed T_{surf} of Venus, Earth and Mars and the black unfilled circles mark the radiation temperature of the planets according to their observed albedo.

2.2.2 Greenhouse Shield Model

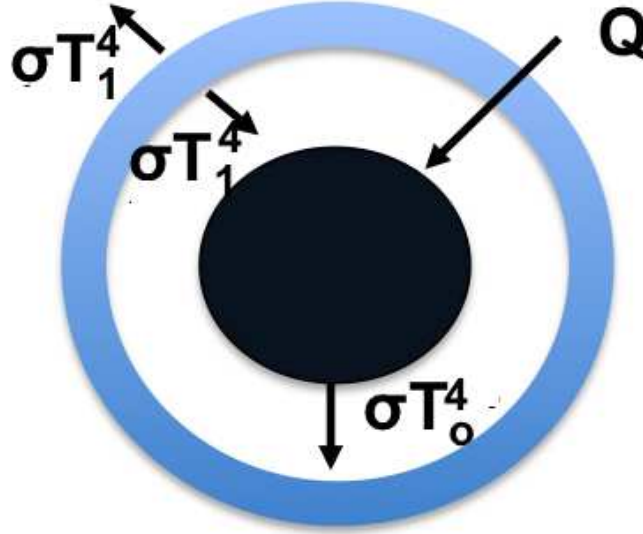


Figure 2.6: Sketch of the Greenhouse shield model.

We now like to refine our model for the atmospheric greenhouse, by assuming that the atmosphere itself is a black body radiator, see sketch 2.6. In this model the surface temperature $T_0 = T_{surf}$ and the atmospheric temperature, T_1 . To simplify the equations we represent the incoming solar radiation with the parameter, Q :

$$Q = \frac{1}{4}(1 - \alpha_p)S_0 \quad (2.20)$$

Thus we only consider the absorbed incoming solar radiation. The albedo effect is for the following discussion not important. Including the albedo effect would affect any of the results discussed in this section. So we assume all of Q is absorbed by the surface. Further we assume that the atmosphere is transparent to solar radiation. The thermal radiation of the surface is now not emitted to space but is fully absorbed by the atmospheric layer, shielding the earth surface from space. The atmosphere itself is heated only by the thermal radiation from the surface and radiates thermal radiation with its own temperature in both directions: back to the surface and out into the space.

The radiation balances for the earth surface in equilibrium ($\frac{dT_{surf}}{dt} = 0$) is now determined by three terms (see arrows pointing to or away from the earth surface in the sketch 2.6):

$$Q - \sigma T_0^4 + \sigma T_1^4 = 0 \quad (2.21)$$

In comparison to eq. [2.11] we now have the additional term from the atmosphere (σT_1^4). The radiation balances for the atmosphere in equilibrium is (see arrows pointing to or away from the atmosphere shield in the sketch 2.6):

$$+\sigma T_0^4 - 2\sigma T_1^4 = 0 \quad (2.22)$$

The radiation balance to space is (see arrows pointing to or away from the space in the sketch 2.6):

$$Q = \sigma T_1^4 \Rightarrow T_{rad} = T_1 \quad (2.23)$$

Note, that the space only sees the atmospheric temperatures, T_1 , as the atmosphere shields the surface from space. So we can not 'see' the surface from space in the thermal radiation wave lengths (we can see it in the visible wave length though, as the atmosphere is transparent to solar radiation). Therefore the radiation temperature (eq. [2.13]) of the earth in this model is the atmospheric temperature:

$$\Rightarrow T_{rad} = T_1 \quad (2.24)$$

Rearranging eq. [2.22] we find:

$$\frac{T_0^4}{T_1^4} = \frac{T_{surf}^4}{T_{rad}^4} = 2 \quad (2.25)$$

It follows assuming the same parameters as before:

$$\Rightarrow T_{surf} = 2^{\frac{1}{4}} \cdot T_{rad} = 303.3K \approx +30^\circ C \quad (2.26)$$

So we find that now the surface temperature is warmer than the radiation temperature by a factor of $2^{\frac{1}{4}}$. So in this model the greenhouse effect is scaling the surface temperature up to warmer temperatures. However, we also see that is it now too warm.

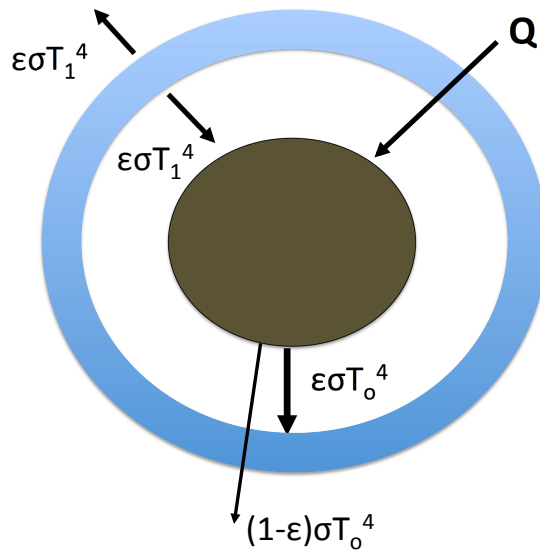


Figure 2.7: Sketch of the Greenhouse shield model with a partly transparent (emissivity, $\epsilon < 1$) atmosphere.

The unrealistic assumption we made was that we assumed that the atmosphere is absorbing all thermal radiation from the surface, but this is not true. Some of the surface thermal radiation goes into space through the so called 'window' of the atmosphere. This can actually be measured by satellites and is often used to measure the surface temperatures (see Fig. 1.22 for instance). So we have to refine our model to make the atmosphere partly transparent to thermal radiation.

We now assume that the atmosphere has an emissivity, ϵ , small than one, see sketch 2.7. The emissivity of a mass describes the ability to absorb and emit thermal radiation. A body that absorbs thermal radiation with an emissivity ϵ will also emit thermal radiation with the same emissivity ϵ .

The radiation balances for the earth surface in equilibrium is now:

$$Q - \sigma T_0^4 + \epsilon \sigma T_1^4 = 0 \quad (2.27)$$

The surface now receives less radiation from the atmosphere, since the emissivity $\epsilon < 1$. Note, that it will also receive less, because the atmospheric temperature, T_1 , will decrease. The radiation balances for the atmosphere is now:

$$+\epsilon \sigma T_0^4 - 2\epsilon \sigma T_1^4 = 0 \quad (2.28)$$

So the atmosphere now also receives less warming by thermal heating from the surface, since a fraction $1 - \epsilon$ is going directly into space. Subsequently the atmospheric temperature will be decreasing compared to the above model eq. [2.22] with $\epsilon = 1$.

The radiation temperature seen from space is now not equal to the atmospheric temperature T_1 anymore, but will depend on both T_1 and T_0 :

$$\sigma T_{rad}^4 = \epsilon \sigma T_1^4 + (1 - \epsilon) \sigma T_0^4 = Q \quad (2.29)$$

With the above eqs. it now follow for T_{surf} :

$$\Rightarrow T_{surf}^4 = \frac{1}{1 - \frac{1}{2}\epsilon} T_{rad}^4 \quad (2.30)$$

and for the emissivity we find:

$$\Rightarrow \epsilon = 2 \left(1 - \frac{T_{rad}^4}{T_{surf}^4} \right) = 0.77 \quad (2.31)$$

So the overall emissivity of the atmosphere is about 0.77.

2.2.3 Multi-layer Greenhouse Shield

It is also instructive to discuss the situation where the emissivity of the atmosphere is effectively larger than one. Thus if the atmosphere has several layers that absorb thermal radiation, so that the free transmission length of thermal radiation is shorter than the thickness of the atmosphere. A thermal radiation that is emitted from the surface, is absorb by some lower atmospheric layer, which than re-emites to space, but this radiation is than absorb by another high atmospheric layer, see Sketch 2.8. Such a model would, for instance, describe a planet with a very thick atmosphere like Venus. However, this model is also useful for the Earth, if we think of the thermal radiation at different wave length (see also later in the lecture). At some wave length the earth atmosphere is indeed thick enough to be modelled by a multi-layer greenhouse shield.

After some computations we can find, that the surface temperature in this model is now a function of the number of layers, N :

$$\Rightarrow \sigma T_{surf}^4 = (N + 1) \cdot Q \quad (2.32)$$

For $N = 0$ (no atmosphere) this eq. is identical to eq.[2.10] and for $N = 1$ it is identical to eq.[2.26]. The surface temperature increases with increasing numbers of atmospheric layers, but less than a linear function (power 1/4). The greenhouse parameter g_p as defined in eq. [2.15] is:

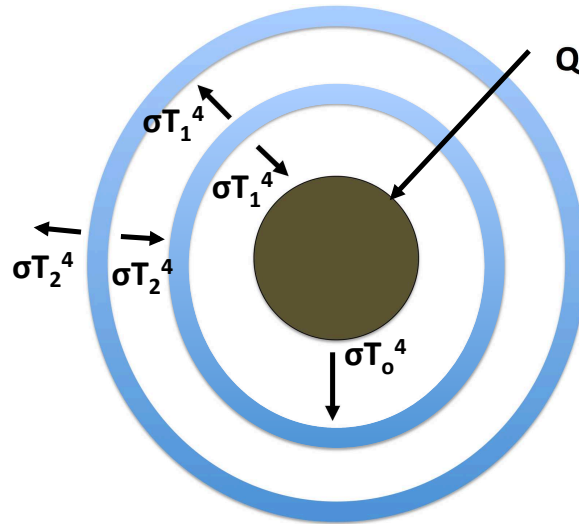


Figure 2.8: Sketch for the multi-layer greenhouse shield model.

$$\Rightarrow g_p = 1 - \frac{1}{(N+1)} \quad (2.33)$$

So for $N = 0$ the greenhouse effect is zero and for large N it converges towards $g_p = 1$, see Fig.2.9. The model can also be used for $N < 1$. We see that for $g_p = 0.38$, as in the above discussion of eqs. [2.15] and following, the atmospheric layer would be about 0.77, which is similar to the emissivity value we had in the above model (eq.2.31).

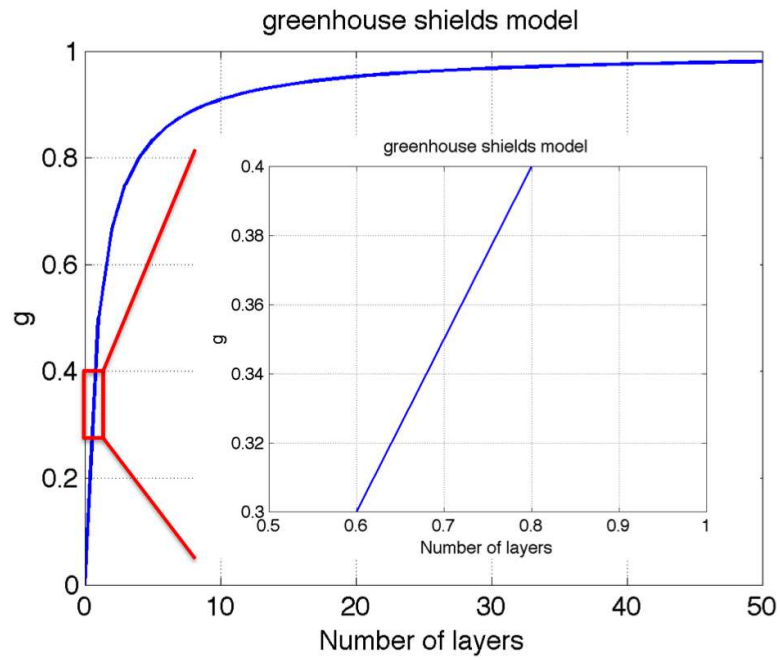


Figure 2.9: The greenhouse reflection parameter g_p as function of number of atmospheric layers N in the multi-layer greenhouse shield model. The inner graph is a zoom into the values of $N = 0.5$ to $N = 1.0$

2.3 Greenhouse model with ice-albedo feedback (Budyko, 1969)

The zero order energy balance model introduced the main concept that we like to use in the following to understand some simple climate dynamics. In the next step we want to analyse how the system may respond to some changes in the boundary conditions. One of the first scientist that address this problem with a simple zero order energy balance model was the russian Budyko (1969). The main idea that we like to explore now is that of climate feedbacks: when boundary conditions change the climate system may respond in a way that feeds back onto the energy balance. The simplest example to explore this concept of climate feedbacks is the ice-albedo feedback.

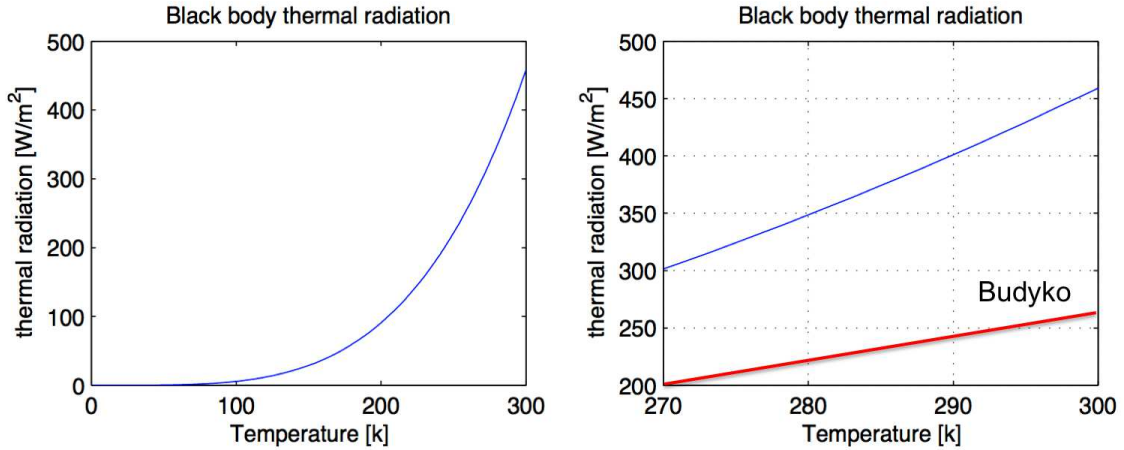


Figure 2.10: Black body thermal radiation: left: Black body thermal radiation for a wide range of temperatures. right: Black body thermal radiation (blue line) for a range of temperature closer to the earth climate in comparison to the Budyko linear model (red line).

In order to simplify the discussion Budyko simplified the thermal radiation of the earth to be a linear function. So originally the thermal radiation of the earth surface was:

$$F_{thermal} = \sigma T^4 \quad (2.34)$$

Solving equations with higher order power laws is complicated or even impossible. We therefore make an empirical parameterization (linearisation) of the thermal radiation:

$$-F_{thermal} = I(x) \uparrow = A + B \cdot (T_0(x) - 273.15) \quad (2.35)$$

$x = \sin(\phi) = \text{latitude}$

$T_0 = \text{zonal mean temperature}$

$A = 203.3 \text{ W/m}^2$

$B = 2.09 \text{ W/m}^2/\text{K}$

The empirical constants A and B are estimated from observed values. Budyko's model was initially formulated for zonal mean temperatures, but we will use it here only as a zero order global model. So we simplify this model to:

$$-F_{thermal} = A + B \cdot (T_{surf} - 273.15) \quad (2.36)$$

To understand the empirical parameters better we need to linearise the black body radiation with respect to T_{surf} for a mean $T_{surf} = 288\text{K}$ ($= 15^\circ\text{C}$):

$$\frac{dF_{thermal}(T_{surf} = 288K)}{dT_{surf}} = -4\sigma T_{surf}^3 \approx -5.4W/m^2/K \quad (2.37)$$

So the linear factor in the black body radiation is about $-5.4W/m^2/K$, which is about twice as much as the Budyko parameter $-B = -2.09W/m^2/K$, see Fig.2.10. This mismatch reflects the greenhouse effect that Budyko empirically already included in his model. So the Budyko model is effectively a linearisation of the last term right hand side of eq.[2.16]. We can also see in Fig.2.10 that a linearisation of $F_{thermal}$ is a good approximation, as the black body radiation is roughly linear in the temperature range of the earth climate.

2.3.1 The Ice-Albedo Feedback

The Ice-Albedo feedback is a simple example of the climate response to external changes. The albedo of the earth is not a constant but it depends on the climate itself. The ice covered regions are much brighter than the ice free regions and therefore reflect more incoming sun light back to space than the ice free regions. Thus the albedo of the earth is a function of the earth surface temperature itself.

So as a simple model we could assume that the planetary albedo of the earth is a function of the global mean surface temperature:

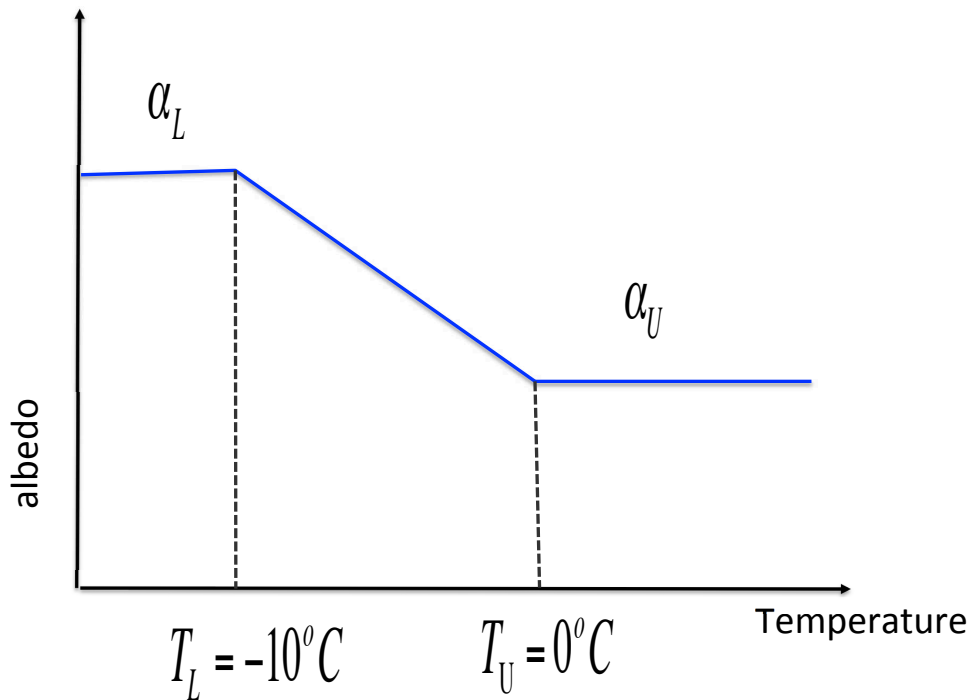


Figure 2.11: Albedo as a function of temperature

If the temperature is below T_L we assume the land is completely snow covered and the oceans would be covered with sea ice and snow on top of it. In that case the earth albedo is that of ice covered regions and it does not change if it gets colder as it is already fully ice covered. On the other side hand, if the temperatures are above T_U , then the land would be completely ice and snow free and if it warms further the albedo also does not change. Finally, there is a range where the earth is partly ice covered and the albedo changes as a function of temperature. This is the interesting range in which the climate feeds back on the energy balance via the albedo.

For simplicity we assume a simple linear function in a temperature range at which snow and ice cover vary and a fixed albedo outside this range:

$$\alpha_p = \alpha_L \quad \forall \quad T_{surf} < T_L \quad (2.39)$$

$$\alpha_p = \alpha_L + \frac{\Delta\alpha}{\Delta T}(T_{surf} - T_L) \quad \forall \quad T_L < T_{surf} < T_U \quad (2.40)$$

$$\alpha_p = \alpha_U \quad \forall \quad T_U < T_{surf} \quad (2.41)$$

with the parameter values:

$$\alpha_L = 0.62 \quad \alpha_U = 0.3$$

$$T_L = -10^\circ C \quad T_U = 0^\circ C$$

$$\Delta\alpha = \alpha_U - \alpha_L = -0.32$$

$$\Delta T = T_U - T_L = 10^\circ C$$

We can now write the Budyko model with the albedo function:

$$\gamma_{surf} \frac{dT_{surf}}{dt} = ((1 - \alpha_p(T_{surf})) \cdot Q - (A + B \cdot (T_{surf} - 273.15))) \quad (2.42)$$

Note, that the first term right hand side is the solar radiation ($((1 - \alpha_p(T_0))Q)$) and the second term is the thermal radiation ($(A + B \cdot (T_0 - 273.15))$). In equilibrium, the solar radiation balances the thermal radiation:

$$\rightarrow ((1 - \alpha_p(T_{surf})) \cdot Q = A + B \cdot (T_{surf} - 273.15) \quad (2.43)$$

Fig. 2.12 shows the terms on the left and right hand side of this equation as a function of T_{surf} . Note, that the solar radiation term is constant outside the temperature range in which the albedo is a function of the temperature. For $T_{surf} < T_L$ the larger albedo of the snow/ice covered earth leads to less absorbed solar radiation. For $T_{surf} > T_U$ the smaller albedo of the snow/ice-free earth leads to more absorbed incoming solar radiation. In between these two values the solar radiation is a linear increasing function of temperature, because the albedo is a linear function of temperature in this temperature range.

So the solar radiation has three regimes:

Fully ice covered:	less constant solar radiation absorbed
Partially ice covered:	increasing solar radiation absorbed with increasing surface temperature
No ice cover:	more constant solar radiation absorbed

The thermal radiation is a linear function through out the whole temperature range, but since it has smaller gradient it intersects with the solar radiation.

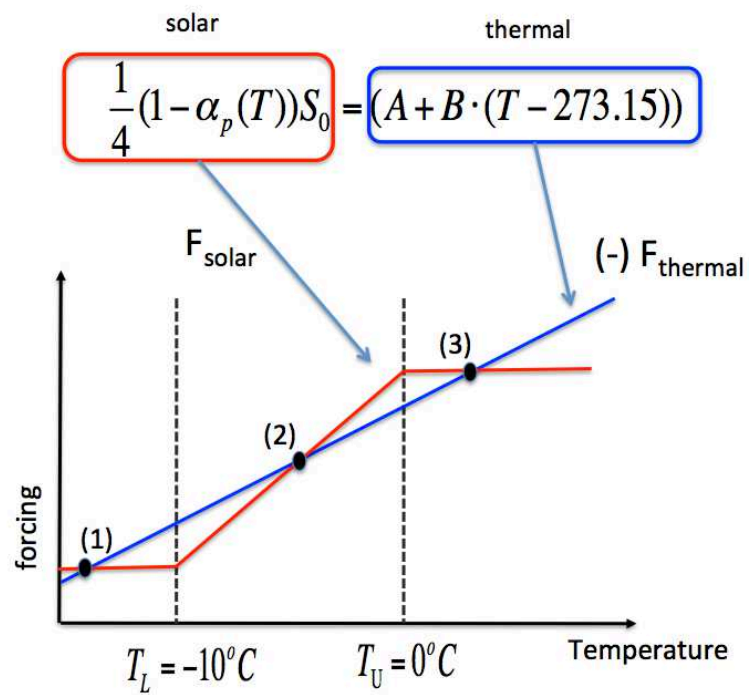


Figure 2.12: The terms solar radiation (blue) and thermal radiation (red) of the Budyko model in eq. [2.43].

Three equilibria states:

We can see that there are three points at which the two terms are the same (equal). At these three points the Budyko climate is in equilibrium, because thermal and solar radiation are balanced.

Solving eq. [2.43] for the three different solar radiation regimes we find the three equilibria:

$$\begin{aligned}
 (1) \text{ Totally ice covered earth} & \quad T_{surf}^{(1)} = \frac{(1-\alpha_L)Q-A}{B} = -35.2^\circ C \\
 (2) \text{ Partially ice covered earth (present day)} & \quad T_{surf}^{(2)} = \frac{Q(1-\alpha_L)\Delta T - A\Delta T + QT_L\Delta\alpha}{B\Delta T + Q\Delta\alpha} = -4.0^\circ C \\
 (3) \text{ Ice free world} & \quad T_{surf}^{(3)} = \frac{(1-\alpha_U)Q-A}{b} = +17/0^\circ C
 \end{aligned}$$

The next question that we need to address is: How stable are the equilibria of the Budyko model? In other words, what would happen if we would perturb the system with a small perturbation from its equilibria points. This leads us to the discussion of climate stability, sensitivity and feedbacks.

2.4 Climate Sensitivity, Stability and Feedbacks

In the previous section we found that the climate system can be in different equilibrium states given the same fixed boundary conditions. We now want to discuss the stability of these equilibria states. This involves also the question of how sensitive is the climate to changes in the forcing, which leads us to the definition of climate sensitivity. We will see that for the conceptual discussion of the stability and sensitive of the climate it is useful to introduce the a climate potential in analog to classical mechanics. The stability and sensitive of the climate is controlled by the strength of the different feedbacks acting in the climate system, which we will try estimate with simple linear feedback parameters. Finally, we also discuss the transition from one an unstable equilibrium state to a stable equilibrium state, which we call tipping points.

2.4.1 Stability and Climate Potential

In the Budyko model we found three equilibrium points for the climate. Equilibrium points of any dynamical system can be stable or unstable. A stable equilibrium would return to its equilibrium point if you perturb the system away from its equilibrium point by a small amount. An unstable equilibrium would drift away from its equilibrium point if you perturb the system a little bit.

An analog from classical mechanics helps to illustrate this point, see sketch 2.13. A ball in a gravity potential can rest at the equilibrium points in the valley (minima) and hill tops (maxima). If we give the ball a little kick to one side, it would only return to its resting point for the equilibrium points in the valley, because the gravity forces are always pointing against the direction of the little kick. If, for instance, we would have kicked the ball in the valley to the left, then the gravity force would point towards the right, bringing the ball back to its resting point. The ball on the hill top, on the other hand, would roll downhill, away from its resting point. In this case the gravity force would point into the same direction as the initial kick (e.g. a kick to the left would lead to a drift to left).

In the Budyko climate model we can, first of all, analyse the stability of the equilibrium points, by discussing how it would respond to a small perturbation from its equilibria points, T_{surf}^{eq} . The climate model near a stable equilibrium has to respond with a cooling forcing if we perturb the system to slightly warmer $T_{surf}^{eq} + \Delta T_{surf}$:

$$T_{surf}^{eq} + \Delta T_{surf} \Rightarrow F_{net} + \Delta F_{net} = +\Delta F_{net} < 0 \quad (2.44)$$

Analog: Mechanics <-> Climate

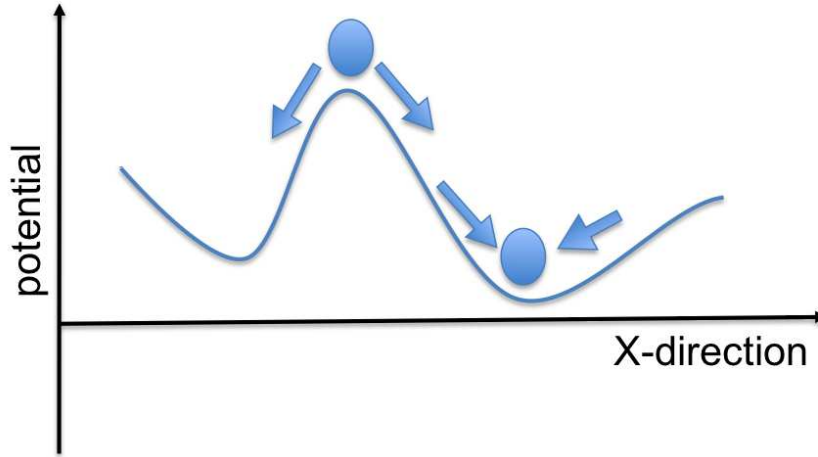


Figure 2.13: Analog for stability and potentials: A ball in a gravity potential can rest at the equilibrium points in the valley (minima) and hill tops (maxima). Only the valley are stable equilibria.

The net forcing, F_{net} , is the sum of the thermal and solar forcing terms, which at T_{surf}^{eq} is zero. So at $T_{surf}^{eq} + \Delta T_{surf}$ the net forcing is $+\Delta F_{net}$. In turn, if we perturb the system to slightly colder T_{surf} it has to respond with a warming forcing:

$$T_{surf}^{eq} - \Delta T_{surf} \Rightarrow -\Delta F_{net} > 0 \quad (2.45)$$

For an unstable equilibrium it is the other way around:

$$T_{surf}^{eq} + \Delta T_{surf} \Rightarrow +\Delta F_{net} > 0 \quad (2.46)$$

$$T_{surf}^{eq} - \Delta T_{surf} \Rightarrow +\Delta F_{net} < 0 \quad (2.47)$$

For infinitely small perturbations, this leads us to the derivatives:

For stable equilibrium:

$$\frac{dF_{net}}{dT}(T_{surf}^{eq}) < 0 \quad (2.48)$$

And for unstable equilibrium:

$$\frac{dF_{net}}{dT}(T_{surf}^{eq}) > 0 \quad (2.49)$$

So we can now use the Budyko tendency eq. [2.42] to estimate $\frac{dF_{net}}{dT}(T_{surf}^{eq})$. First of all F_{net} is just the right hand side:

$$F_{net} = ((1 - \alpha_p(T_{surf})) \cdot Q - (A + B \cdot (T_{surf} - 273.15))) \quad (2.50)$$

We can now evaluate this function at each equilibrium point using the right $\alpha_p(T_{surf})$ function. Fig. 2.14 shows the function. We can easily see that the gradient at the first equilibrium point is

negative, is positive at the second and negative again at the third. so from the above considerations we find:

- | | |
|---|------------|
| (1) Totally ice covered earth | → stable |
| (2) Partially ice covered earth (present day) | → unstable |
| (3) Ice free world | → stable |

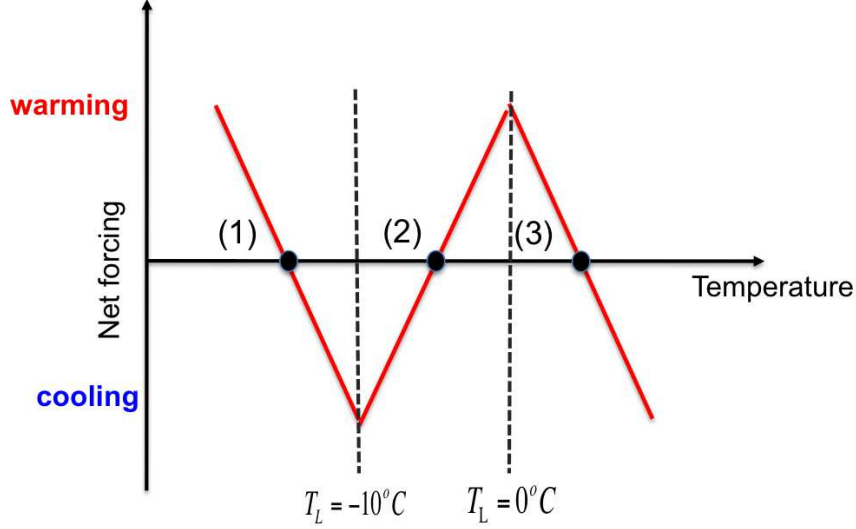


Figure 2.14: The net forcing in the Budyko model using eq. [2.50].

The above discussion of stability of the equilibrium points is very similar to the classical mechanics discussion of stable equilibrium points. The ball in Fig. 2.13 is in a gravity potential with the sum of all forces (net forcing, F_{net}) being zero at the equilibrium points (e.g. the valley and hill top). The net forcing is

$$F_{net} = -\frac{dP}{dx} \quad (2.51)$$

with the gravity potential, P . With rearranging we can write:

$$P = -\int F_{net} dx \quad (2.52)$$

We can use this define the climate potential, P , as function of T_{surf} :

$$P(T_{surf}) = -\int F_{net} dT_{surf} \quad (2.53)$$

The climate Potential of the Budyko model eq. [2.50] is:

$$P_{Budyko}(T_{surf}) = -\int (1 - \alpha_p(T_{surf}))Q - (A + BT'_{surf}) dT_{surf} \quad (2.54)$$

Solving the simple integrals gets us:

$$P_{Budyko}(T_{surf}) = AT_{surf} + \frac{1}{2}BT_{surf}^2 - Q \int (1 - \alpha_p(T_{surf})) dx \quad (2.55)$$

The climate potential of the Budyko model is shown in Fig. 2.15. We can see that the fully ice covered and totally ice free equilibria points are the two valley with the partially ice covered equilibria point has a hill top in between.

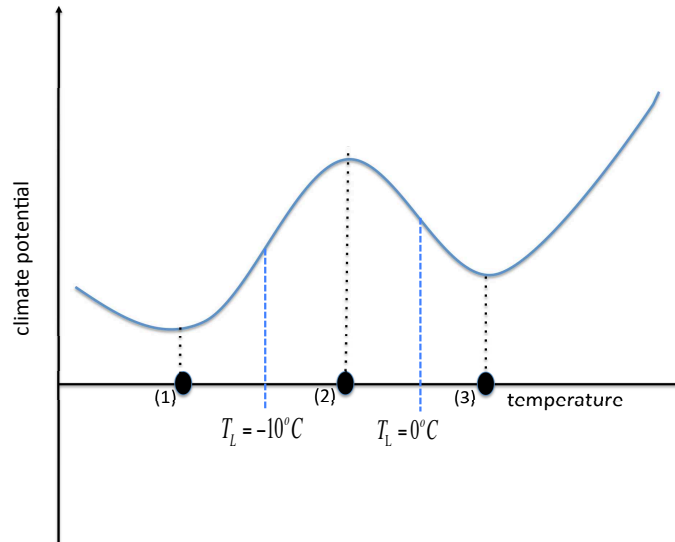


Figure 2.15: The climate Potential of the Budyko model eq. [2.50].

2.4.2 Tipping points: The Climate Response to Forcing

If we add some additional positive forcing to the right hand side of eq. [2.10] we could compute the new equilibrium temperature (eq.[2.12]) and it would be at higher values (more heat would lead to higher mean temperature obviously).

We can now use the concept of climate potentials to illustrate this increase in temperature for changes in the forcings or additional forcing. An additional positive constant forcing to the energy balance would, according to eq. [2.53], change the climate potential by adding a linear decreasing gradient (integral of a constant is a linear function). In other words the climate potential curve as function of temperature would be tilted more to the right, as illustrated in Fig. 2.16. The ball in the figure illustrates the equilibrium temperature, which is at the minimum of the curve. In the upper potential (without additional forcing) the equilibrium temperature (resting point of the ball) is at relatively low temperatures. Adding a positive constant forcing tilts the potential curve to the right (middle plot) and the ball, equilibrium temperature or minimum shifts to the right. If we further increase the additional forcing the ball shifts further to the right (lower plot). If take away the additional forcing the potential would tilt back to the original curve (upper plot).

The situation is much more interesting in the Budyko model with the ice-albedo feedback, where we have three equilibrium points, see Fig. 2.15. Lets assume the climate is at the fully ice-cover stable equilibrium, the ball in left valley in Fig. 2.17. If we now add a small positive forcing the equilibrium will increase by small amount (ball moves to the right). However, if we increase the forcing strong enough to get us above the little hill (the unstable partially ice cover equilibrium point) between the two valley, the climate temperature will make a big jump to the much warmer equilibrium points of the totally ice free world in the right valley. We say the climate has passed a **Tipping Point**. The Tipping Point in this case was the unstable equilibrium of partially ice cover world (the little hill) which separated the two stable equilibrium points. It is important to note in this example, that if we remove the additional forcing (going back to the original forcing in the upper plot of Fig. 2.17) after we passed the Tipping Point, the climate will not return to the old equilibrium point, but will stay at the equilibrium points of the totally ice free world in the right valley, see Fig. 2.18.

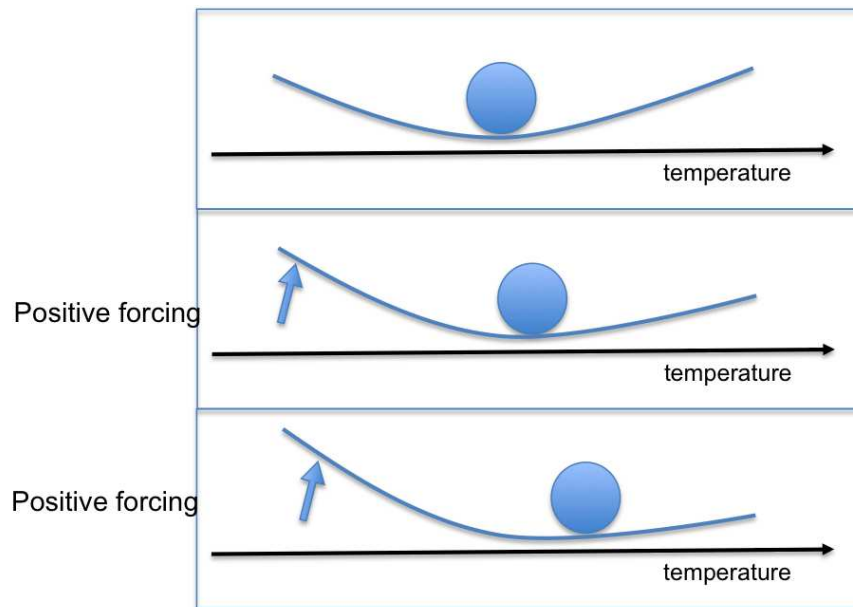


Figure 2.16: The climate potential of the zero order model (no feedbacks) as in eq. [2.10]. It is illustrated how an additional constant positive forcing would change the potential and the equilibrium temperature.

This may all seem quite theoretical, but it of course has really physical meaning. If start with the ice covered world and increase the heating, then the ice start to melt. The emerging ice free regions absorb more sun light, which again leads to further warming. Once the world is entirely ice free and we remove the additional heating, the world does not return to the fully ice covered world, because now the ice free world is absorbing more of the sun light due to its darker albedo. It will cool a little bit, but does not return to the ice covered equilibrium point, see Fig. 2.18.

Figure 2.19 illustrates the time evolution of the temperature in a hypothetical world where we increase the CO_2 concentration (add a heating) and pass over a Tipping Point.

How tipping points can be detected:

- note that the shape of the bowl is changing
- the feedbacks are different
- the interannual natural variability will change
- a climate close to a tipping point should behave erratically, the variability will increase compared to the preindustrial

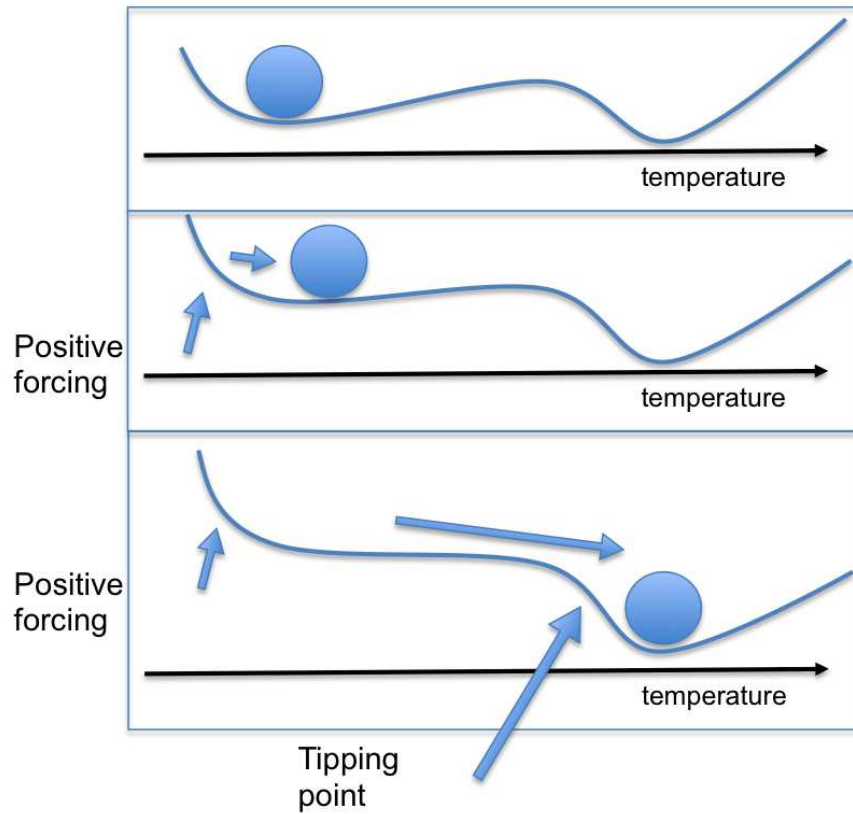
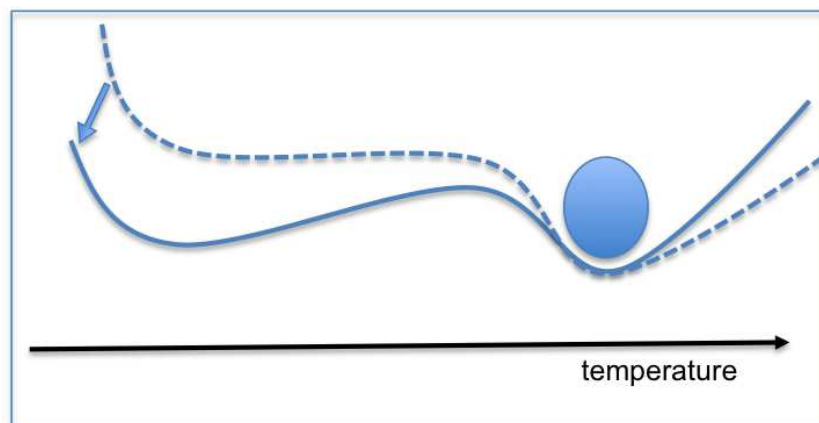


Figure 2.17: The climate potential of an example with feedbacks as in the Budyko model with the ice-albedo feedbacks or potentially in the real world.



Tipping point: climate change is irreversible

Figure 2.18: The climate potential as in 2.17. Returning the forcing back to the initial forcing does not let the ball (climate) return to the original equilibrium point.

Tipping point: climate change is irreversible

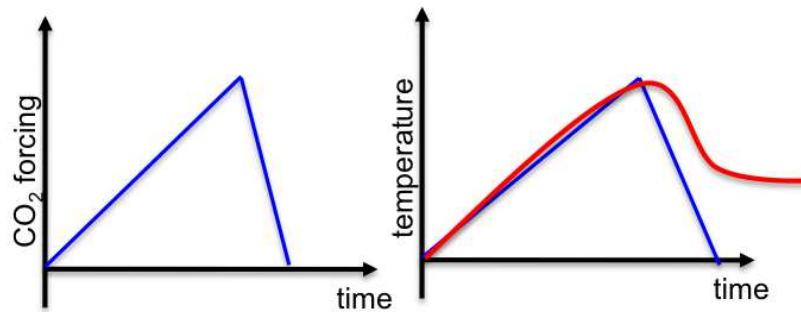


Figure 2.19: Tipping point: climate change is irreversible

Tipping Points in the Earth System

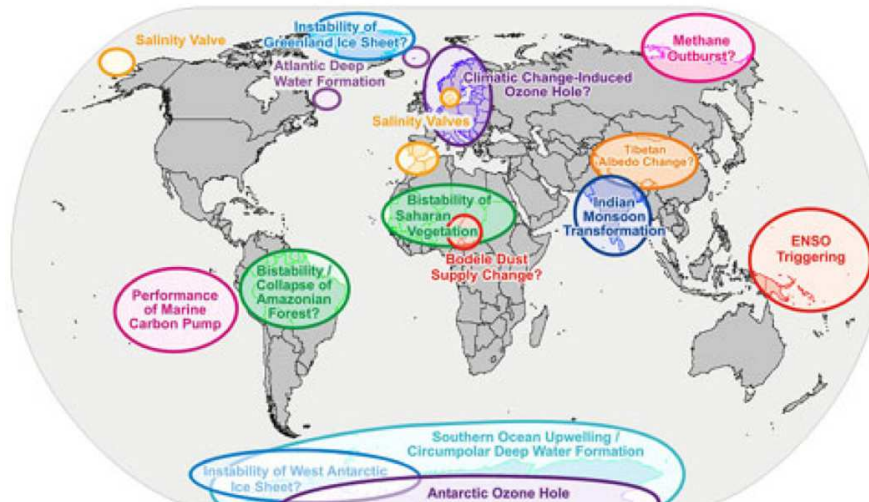


Figure 2.20: Tipping points in the Earth System

2.4.3 Climate Sensitivity

In the previous section we have seen that some climate equilibria are stable and others are unstable. The way the climate responds to a given forcing can be vastly different. Sometimes a small forcing gives a small climate response (Fig. 2.16), but sometimes the same small forcing gives a very strong climate response (Fig. 2.17). In other words the sensitivity of the climate to a given forcing can be very different.

The **Climate Sensitivity** can be defined as:

$$\lambda := \frac{\Delta T}{\Delta Q} \quad (2.56)$$

Thus the climate sensitivity, λ , gives the amount of temperature change (or any other climate variable of interest) per change in forcing, ΔQ . Here ΔQ is usually given as an energy flux forcing in W/m^2 , but it could also be any other kind of forcing (e.g. atmospheric CO_2 concentration change, land use change, earth axis tilt change in degrees, cloud cover change, etc.).

Thus the temperature change for a given climate sensitivity is

$$\Rightarrow \Delta T = \lambda \cdot \Delta Q \quad (2.57)$$

So the basic assumption here is that the climate will roughly respond in a linear way to any given forcing with the linear gradient of λ . So if you know the climate response ΔT for a given ΔQ , then you know λ and you can compute the climate response to any other ΔQ assuming it is just a linear scaling of it.

The definition of λ is essentially that of the derivative of the temperature to the forcing

$$\lambda = \frac{dT}{dQ} \quad (2.58)$$

However, in the real world and in complex climate models this derivative is not known. We can only compute it in simple climate models, such as those discussed in the previous sections.

In the following we will discuss a number of examples to illustrate the climate sensitivity values.

Example 1: IPCC - report

The IPCC report from 2007 states that the global mean surface temperature change is 3K until the year 2100 for one of the most likely anthropogenic CO_2 emissions (scenario A1B). This has been based on complex climate model simulations. The CO_2 concentration changes lead to an additional downward thermal radiation of about $+6W/m^2$ (see later sections for how to get to this number). So the climate sensitivity is

$$\rightarrow \lambda = \frac{\Delta T}{\Delta Q} = \frac{3.0K}{6W/m^2} = 0.5K / \left(\frac{W}{m^2} \right) \quad (2.59)$$

Example 2: Zero order model

For the zero order model discussed in section 2.2 we have eq. [2.12] that relates T to Q , so we can actually compute the derivative to get λ :

$$T = \left(\frac{1}{\sigma} \frac{(1 - \alpha_p)}{4} S_0 \right)^{\frac{1}{4}} = \left(\frac{Q}{\sigma} \right)^{\frac{1}{4}} \quad (2.60)$$

Here we assumed that $Q = \frac{(1 - \alpha_p)}{4} S_0$. So only the solar radiation that actually gets absorbed by the surface is considered to be the forcing. It follows

$$\lambda = \frac{dT}{dQ} = \frac{1}{\sigma} \frac{1}{4} \left(\frac{Q}{\sigma} \right)^{\frac{1}{4}-1} = \frac{1}{\sigma} \frac{1}{4} \frac{\left(\frac{Q}{\sigma} \right)^{\frac{1}{4}}}{\left(\frac{Q}{\sigma} \right)} = \frac{1}{4} \frac{\left(\frac{Q}{\sigma} \right)^{\frac{1}{4}}}{Q} = \frac{1}{4} \frac{T_{rad}}{Q} \approx \frac{1}{4} \frac{255K}{240W/m^2} = 0.27K / \left(\frac{W}{m^2} \right) \quad (2.61)$$

Note that this climate sensitivity is smaller than what the IPCC report finds with complex climate models. We will later see why that is.

Example 3: Budyko model (without ice-albedo feedback)

In the Budyko model without the ice albedo feedback we can use eq.[2.43] assuming that $\alpha_p = 0.3$ is a constant

$$\Rightarrow \lambda = \frac{(1 - \alpha_p)}{B} = 0.33K / \frac{W}{m^2} \quad (2.62)$$

This is larger than in the zero order model. In the zero order model we assumed that Q includes the albedo effect. We can do this here too:

$$\Rightarrow \lambda = \frac{1}{B} = 0.48K / \frac{W}{m^2} \quad (2.63)$$

This is even larger. It is related to the additional reflection of thermal radiation in the Budyko model.

Example 4: Budyko model (with ice-albedo feedback)

Including the ice-albedo feedback makes the albedo, α_p , a function of temperature. In the temperature range in which the albedo is a function of temperature, the Budyko model had one equilibrium point (the partially ice covered world). This equilibrium point was the unstable equilibrium point. The discussion of climate sensitivity λ at an unstable equilibrium point does not make much sense, as any tiny additional forcing ΔQ would lead to the climate moving away from the unstable equilibrium point until it reaches one of the two stable equilibrium points (e.g. the totally ice covered or the totally ice free). Thus λ would be

$$\Rightarrow \lambda = \frac{\Delta T}{\Delta Q} \approx \frac{\Delta T}{0} = \infty \quad (2.64)$$

Note, it also does not make much sense to discuss the climate sensitivity when the climate is not at an equilibrium, as in this case the climate would change without adding any forcing ΔQ .

We can alter the Budyko model to have a stable equilibrium point in the partially ice covered temperature range if we reduce the albedo gradient from the original

$$\frac{\Delta \alpha_p}{\Delta T} = -0.03K^{-1} \quad (2.65)$$

to a much smaller (in amplitude)

$$\frac{\Delta \alpha_p}{\Delta T} = -0.003K^{-1} \quad (2.66)$$

With the reduced albedo gradient the forcing balance changes and the equilibrium point in the partially ice covered temperature range is stable with positive net forcing at temperatures below the equilibrium and negative net forcing at temperatures above the equilibrium, see Fig. 2.21. The other two equilibrium points are gone.

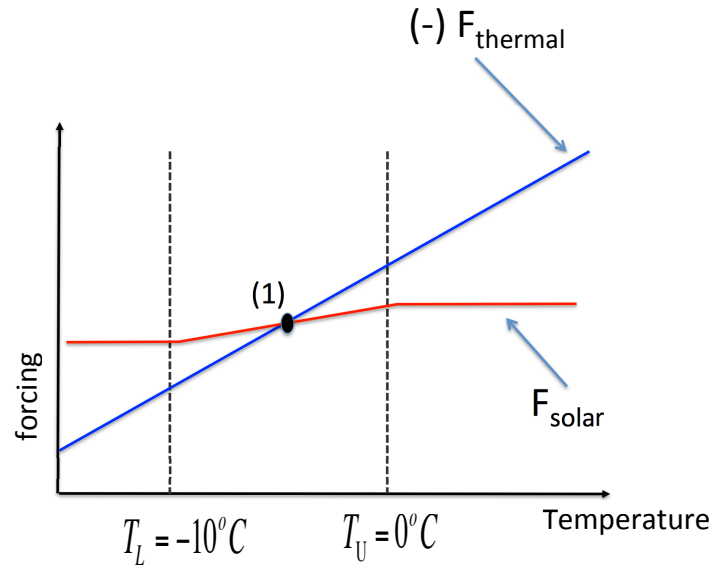


Figure 2.21: The terms solar radiation (blue) and thermal radiation (red) of the Budyko model in eq. [2.43] with the reduced albedo gradient as discussed in section 2.4.3.

The climate sensitivity at this equilibrium point is

$$\Rightarrow \lambda = 0.66K/\frac{W}{m^2} \quad (2.67)$$

So the introduction of the albedo feedback increases the climate sensitivity by about a factor of two relative to the Budyko model without the albedo feedback (eq. [2.62]).

2.4.4 Feedbacks

In previous section we seen that the introduction of the ice-albedo feedback in the Budyko model has changed the climate sensitivity by a factor of two. In general the feedbacks in the climate system determine the climate sensitivity.

A feedback is a response of the climate system to an initial forcing, tendency or perturbation, which affects the way the climate system response to the forcing, tendency or perturbation. Thus it is a feedback loop. This can be positive (amplifying) or negative (damping).

A **positive feedback** is illustrated in Figure 2.22 on the left on the basis of a ball in the gravity potential sketch. If we introduce a small forcing, tendency or perturbation to the ball at the equilibrium point it will start to move away from the equilibrium point. The increasing gravity force is a positive feedback, which will amplify the initial perturbation. If no negative feedbacks are present (as in the figure) the ball will drift away completely.

A **negative feedback** is illustrated in Figure 2.22 on the right. If we introduce a small forcing, tendency or perturbation to the ball at the equilibrium point it will move away from the equilibrium point a little bit. The increasing gravity force will force the ball back to equilibrium point. This is a negative feedback, which will act against the initial perturbation. It damps the initial forcing and makes system turn to its initial equilibrium point if the perturbation forcing is gone.

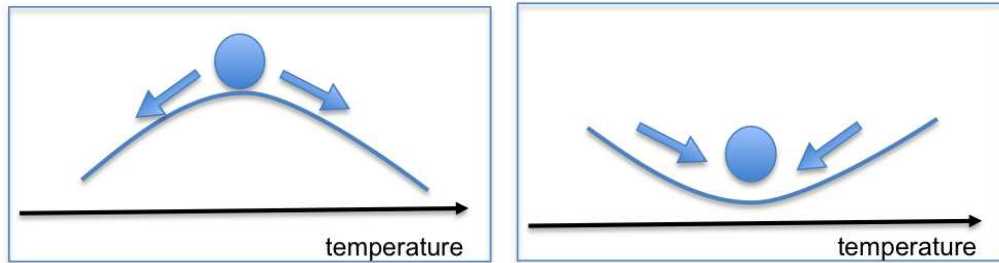


Figure 2.22: Positive (left) and negative (right) feedbacks illustrated on the basis of a ball in a gravity potential.

From the discussion of the climate potential and the stable or unstable equilibria we have seen that the positive feedback (unstable hill top) has a net forcing with

$$\frac{dF_{net}}{dT} > 0 \quad (2.68)$$

and the negative feedback (stable valley)

$$\frac{dF_{net}}{dT} < 0 \quad (2.69)$$

Thus the feedback is essentially the sensitivity of the net forcing to the temperature.

Definition of Feedback:

The linear feedback parameter of a forcing is defined as the sensitivity of the forcing relative to a variable of the dynamical system, Φ , (e.g. temperature):

$$\rightarrow C_f := \frac{dF}{d\Phi} \quad (2.70)$$

In our case we usually want to know the sensitivity of the forcing relative to changes in T_{surf} :

$$C_f := \frac{dF}{dT_{surf}} \quad (2.71)$$

So if we have a tendency equation with several terms, like

$$\gamma \frac{dT}{dt} = F_{solar} + F_{thermal} \quad (2.72)$$

The linear feedback parameter can be estimated for each term of the energy balance equation. In the simple zero order model the solar radiation did not depend on temperature, but for the thermal radiation it does. So we can discuss the thermal radiation as an example.

Example: Black body radiation:

The black body thermal radiation is

$$F_{thermal} = -\sigma T^4 \quad (2.73)$$

So the linear feedback parameter for $T = 300^\circ K$ (tropics) is

$$C_f = \frac{dF_{thermal}}{dT} = \frac{d}{dT} -\sigma T^4 = -4\sigma T^3 = -4 \cdot 5.6 \cdot 10^{-8} \frac{W}{m^2 K^4} \cdot (300K)^3 = -6 \frac{W}{m^2 K} \quad (2.74)$$

For polar regions it is $C_f(T = 250K) = -3.5 \frac{W}{m^2 K}$

So the feedback of thermal radiation is negative and it is different in strength (amplitude) for different temperatures. The different strength of feedbacks can again be illustrated with the help of a ball in the gravity potential, see sketch Fig. 2.23.

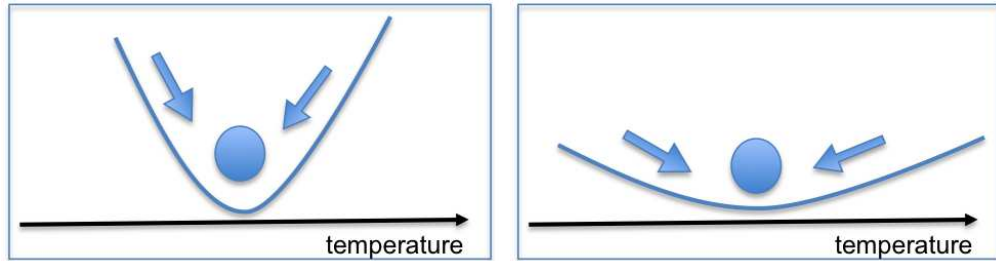


Figure 2.23: Strong (left) and weak (right) negative feedbacks illustrated on the basis of a ball in a gravity potential.

If we remember the definition of climate sensitivity, λ , (eq.[2.58]) we see that it is quite similar to the definition of the linear feedback parameter, C_f , (eq.[2.70]). To understand the relationship between the two we can discuss a simple linear climate model:

$$\gamma \frac{dT}{dt} = C_f \cdot T + Q \quad (2.75)$$

Here forcings in the tendency equation are a constant forcing, Q and a forcing that is a linear function of temperature, T with the linear (hence linear climate model) feedback parameter C_f .

In equilibrium we find:

$$\Rightarrow T_{eq} = \frac{Q}{-C_f} \quad (2.76)$$

The response of the system to a given external forcing Q depends on the strength of the feedback C_f . The climate sensitivity is:

$$\lambda = \frac{dT}{dQ} = \frac{1}{-C_f} \quad (2.77)$$

So the climate sensitivity is the negative inverse of the linear feedback parameter C_f . Lets discuss a few examples to see how large the net forcing feedback parameters are.

Example: IPCC:

$$\lambda = 0.5K / \left(\frac{W}{m^2}\right) \quad (2.78)$$

$$C_f = \frac{dF}{dT} = \frac{-1}{\lambda} = -2.0 \frac{W}{m^2} \frac{1}{K} \quad (2.79)$$

Example: Budyko model thermal forcing:

In the Budyko model without ice-albedo feedback the only feedback is from the thermal forcing. The solar forcing is not depending on T . The thermal forcing is:

$$F_{thermal} = -(A + B \cdot (T - 273.15))$$

It follows that:

$$C_f = \frac{dF}{dT} = -B = -2.09 \frac{W}{m^2} \frac{1}{K} \quad (2.80)$$

It is interesting to note here that the overall feedback parameter of the highly complex and comprehensive IPCC climate models results into roughly the same value as that of the very simple Budyko model. Here we have to remember that the Budyko thermal radiation model was estimated by empirical data. Thus it is based on observed weather and climate fluctuations. The fact that the IPCC model overall feedback parameter during climate change simulations comes down to the same value as those estimated from observed weather and climate fluctuations suggest that the feedback in both may be similar. However, this may also just be a coincident and one needs to be careful here.

Example: Budyko model ice-albedo feedback:

$$(1 - \alpha_p(T_0))Q \quad (2.81)$$

$$\frac{\Delta\alpha_p}{\Delta T} = -0.03K^{-1} \quad (2.82)$$

$$C_f = \frac{dF}{dT} = \frac{\Delta\alpha_p}{\Delta T} = 10.2 \frac{W}{m^2} \frac{1}{K} \quad (2.83)$$

Often feedbacks are illustrated by feedback loop diagrams; see example in Fig. 2.24. In the following we will illustrate a few of the main feedback loops in the physical climate system. We focus here on the main feedbacks on shorter time scales (days to weeks).

Ice-albedo: Colder than normal surface temperatures will lead to increased ice/snow cover. This is usually within days, but if glaciers are involved this can take years to 100yrs. More ice/snow cover leads (instantaneously) to increased surface albedo, which leads to less absorbed solar radiation. Less absorption of solar radiation leads to less warming and therefore to further cooling. Now we are back at the starting point of the feedback loop and can see that this feedback loop is a positive feedback loop, as it enhances the initial tendency. This feedback loop is fast all elements of the feedback loop respond very fast (unless glaciers are involved). This is something that typically happens on weather time scales or during the seasonal cycle, but also in natural climate variability on month to years.

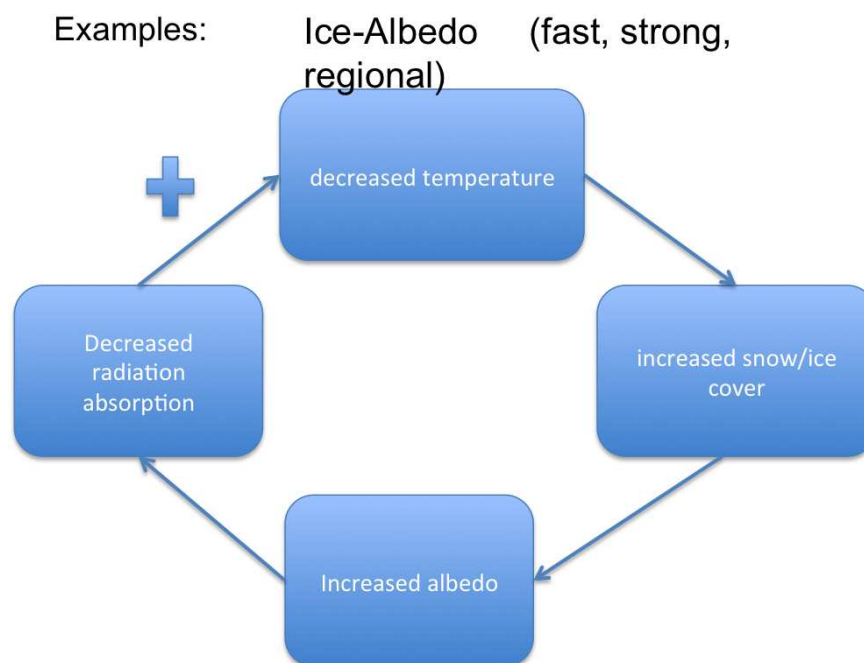


Figure 2.24: Ice-Albedo feedback

Black body radiation: The Black Body Thermal Radiation feedback is the most fundamental and most important feedback in the climate system. It acts global and immediately. The warmer a body gets the more heat it loses by thermal radiation. Thus it is a negative feedback. Since it acts over all temperature scales, on all material things and with T to the power of 4 it is the most powerful feedback in the climate system. Eventually it will overcome all other feedbacks and will therefore lead to an overall negative feedback. Thus it ultimately leads to a stable climate.

Water vapour greenhouse feedback:

Short wave cloud feedback:

Long wave cloud feedback:

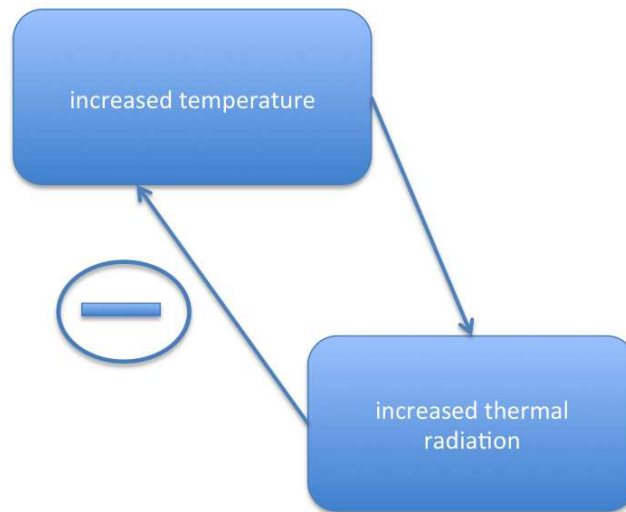
Black body radiation (fast, strong, global)

Figure 2.25: Black body radiation feedback

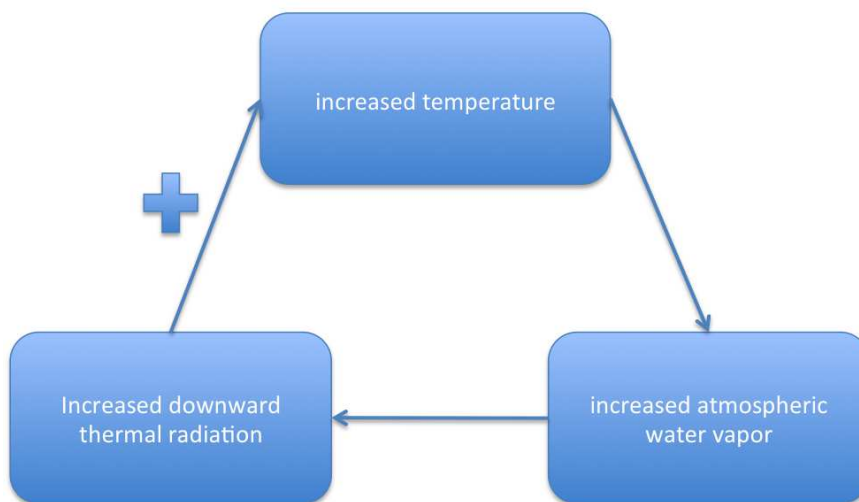
Water vapor greenhouse (fast, strong, global)

Figure 2.26: Water vapour greenhouse feedback

Clouds ***solar*** (fast, potentially strong, global)

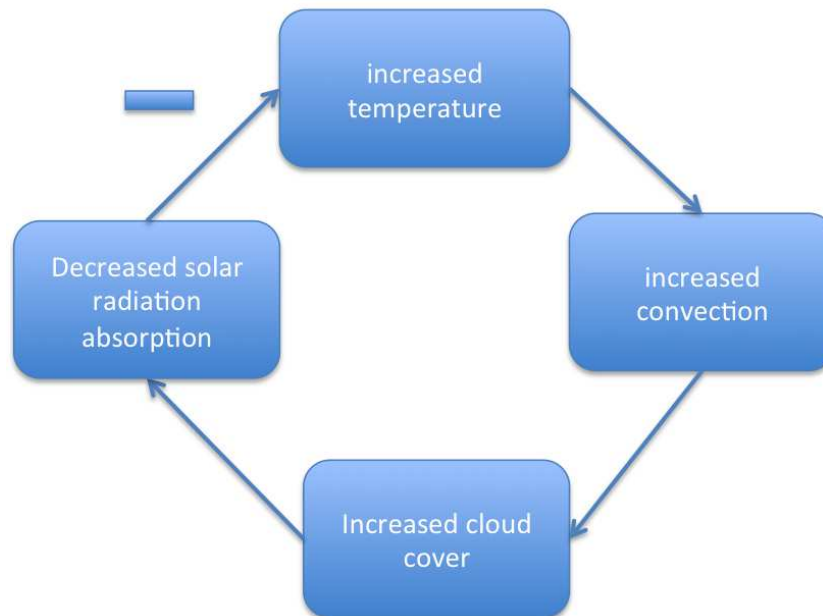


Figure 2.27: Clouds (solar) feedback

Clouds ***thermal*** (fast, potentially strong, global)

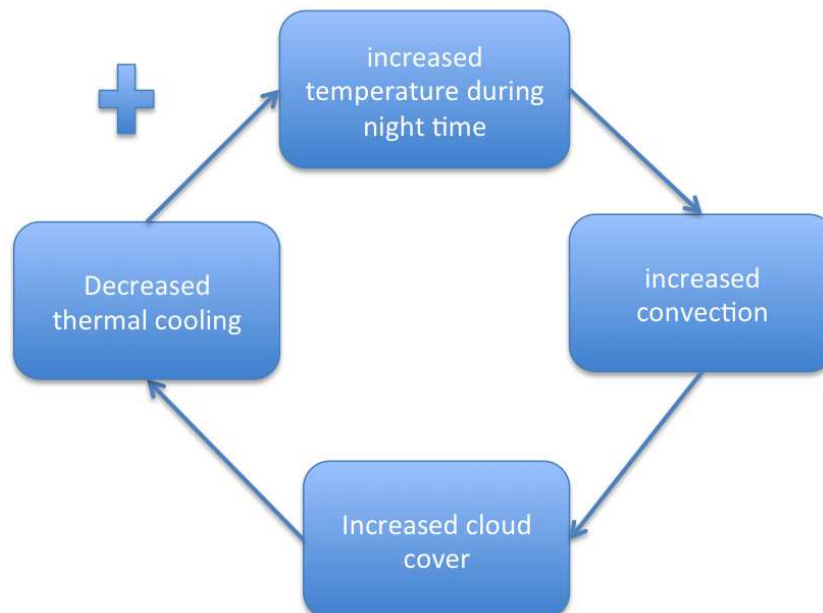


Figure 2.28: Clouds (thermal) feedback

The climate system has many many different feedback cycles. Some are more important than other, they can be local or global feedbacks and they act on short or very long time scales. Sometimes an element in the climate system has many different possible feedbacks that can counter act on each other or support each other. Clouds, for instance, can have different type of feedbacks depending on the type of clouds and the environment in which the are formed. When considering the climate system on different time scales you have to consider all important feedbacks that drive the climate system as a whole. Some examples of other feedbacks that can be important are listed below:

Feedback	Time scale	Scale/strength	Sign
Ocean-carbon	1000 yrs	Strong/global	Positive
Biosphere-vapour	10-100 yrs	Regional	Positive
Carbon sinks	1-100 kyrs	Global	Negative
Circulation	1-10 yrs	Regional, global	Negative

Ocean-carbon: The ocean capability to hold CO_2 depends on its temperature. The colder the oceans the more CO_2 can be stored in the deep carbon reservoir. This effectively defines a positive feedbacks loop: the colder the oceans the more CO_2 can be stored in the deep ocean this reduces the amount of CO_2 in the atmosphere, which in turn reduce the atmospheric greenhouse effect, which will then lead to further cooling. This is a global effect as CO_2 is well mixed and long leaved in the atmosphere. It is on time scales of 100-1000yrs, as the deep ocean circulation is fairly slow in taking up heat and CO_2 .

Biosphere-vapour: Rainforest increase the evaporation and therefore the humidity in the atmosphere over land. Since, water vapor is a greenhouse gas this increases the temperatures. So a rainforest-water-vapor feedback loop can be: increase temperatures lead to more rain and growth of the rainforest this lead to increased humidity which increases the greenhouse effect which then leads to further warming. This closes a positive feedback loop. However, you have to consider that rainforest have also other effect on the climate system (e.g. they have a darker albedo than desert, they also cool the surface). It also needs to be consider that rainforest may eventually die if it gets too warm and warming does not always mean more rainfall. The time scales of these feedbacks are set by the growth rates of the rainforest, which are typically in 1-100yrs.

Carbon sinks: On geological time-scales (mill. yrs.) the atmospheric carbon reservoir is in exchange with the sediments and volcanism. Rainfall, biological activities and erosion take out CO_2 from the atmosphere over time-scales of 10-100yrs. The carbon is fixed in sediments which end up on the ocean floor, which over geological time scales is resurfacing by the tectonic circulation of sediments through volcanic activities (e.g. exhaustion of gasses). This is on the time scales of mill. yrs. This cycle has an important atmospheric CO_2 regulation function and is considered a negative feedback on very long (100kyrs to mill. yrs.) time scales. It is assumed to explain the *The Faint Sun Paradox*. See also in the paleo section at the end of these lecture notes.

Circulation: Much of the atmosphere and ocean circulation is driven by temperature gradients (see also chapter 3). When the global temperature increases this often lead to more warming in the polar regions. This would reduce the meridional temperature gradients and this would reduce the atmospheric and ocean circulations. Since, these circulations do in average transport heat polewards a reduction in these circulation will reduce the poleward heat transport. This will lead to cooling in polar region and therefore counteract the warming. It thus would be a negative feedback. This is something happening on more regional scales and over time scales 1-10yrs related mostly to the adjustment time scales of the near surface ocean circulation. See also the global warming

section 5.2.

Table summarising some of the main feedbacks discussed; with simple equations:

Feedback	Forcing Q	Feedback
Black body radiation	$-\sigma T^4$	$-4\sigma T^3 = -5.4 \frac{W}{m^2} \frac{1}{K}$
Greenhouse	$+g\sigma T^4$	$+4\sigma T^3 = +2.0 \frac{W}{m^2} \frac{1}{K}$
Ice-albedo	$(1 - \alpha_p)Q \propto -\frac{\Delta\alpha}{\Delta T}QT$	$-\frac{\Delta\alpha}{\Delta T}Q = +10.0 \frac{W}{m^2} \frac{1}{K}$

Regional feedbacks: 10-100 W/m² 1/K

Global feedbacks: <5 W/m² 1/K (black body radiation)

Chapter 3

The Atmospheric and Ocean Circulation

In the previous chapter we treated the earth as on single point. In that case the discussion of the climate dynamics were relatively simple. The only thing that we needed to consider were the incoming and outgoing forcing to space or to the atmosphere on top. The climate energy balance at any given location on earth (e.g. Melbourne, South Pole, etc.) is not just a function of the local radiation balance, but strongly depends on the heat and mass (e.g. water vapor in the atmosphere or water in the oceans) exchange with neighbouring regions in the horizontal, but also with the subsurface deep ocean. The heat transport of the atmosphere and oceans has be discussed in the context of the circulations of both atmosphere and oceans.

The aim and objectives of this chapter are:

- Get an introduction to the basic dynamics of the large-scale atmospheric and ocean circulation.
- Introducing the forces and their characteristic interactions in the atmosphere and oceans.
- Get an introduction to the main large-scale characteristics of the atmosphere, oceans and the heat transport in the climate system.

We start this chapter with an introduction to the Geofluid Dynamics theory, which is the fundament for the dynamics of the atmospheric and oceans circulation. We will then discuss the most important characteristics of the large-scale atmosphere and the oceans. The chapter will be concluded with a discussion of the heat transport in the climate system.

3.1 Geofluid Dynamics

The dynamics of the atmospheric and ocean circulation follow the more general theory of Geofluid Dynamics. It describes the momentum equations of continuum fluids such as air or water. We will in the following discuss the forces acting on the air in the atmosphere and the water in the oceans and discuss some of the main characteristics that are relevant for the large scale climate, such as Hydrostatic balance, Buoyancy, Convection, Continuity, Geostrophic balance and the Thermal Wind balance.

3.1.1 The Momentum Equation (Forces Acting in the Atmosphere and Oceans)

The motion of the air in the atmosphere (winds) and the water in the oceans (currents) is controlled by the forces acting on the fluid. The central elements of the dynamics of the atmosphere and oceans are therefore the momentum equations.

The equation of motion (Momentum equation):

$$\rho \frac{D\vec{u}}{Dt} = -2\rho \cdot \Omega \times \vec{u} - \vec{\nabla} p + \rho \vec{\nabla} \Phi + F$$

The diagram shows the momentum equation with four terms on the right-hand side, each enclosed in a colored box. Arrows point from these boxes to descriptive labels below them:

- The first term, $-2\rho \cdot \Omega \times \vec{u}$, is in a blue box. An arrow points to a larger blue box labeled "Coriolis forcing due to the earth rotation".
- The second term, $-\vec{\nabla} p$, is in a purple box. An arrow points to a larger purple box labeled "Pressure gradient force".
- The third term, $\rho \vec{\nabla} \Phi$, is in a green box. An arrow points to a larger green box labeled "gravity".
- The fourth term, F , is in a red box. An arrow points to a larger red box labeled "friction".

Figure 3.1: Momentum equation: Left hand side is the tendency in momentum, assuming constant density. Right hand side are the acting forces: Coriolis, pressure gradient, gravity and friction.

ρ = density

\vec{u} = velocity (3-d vector)

Ω = earth angular velocity

p = pressure

Φ = geopotential

F = friction

Note, that this is a three dimensional vector equation. This equation describes all aspects of the dynamics of fluids from the very small scale to the global scale; from fast motions, like sound waves, to global motions of weather systems or ocean currents. A short discussion of the terms in the equation:

- **Momentum tendencies:** We know from mechanics, that a force leads to changes in the momentum (acceleration). The momentum here is given per unit volume (so density instead of mass on the right hand side) and the force are also per unit volume. In a fluid we have a continuum of particles moving around. To describe the motion of the fluid we can take the point of view of an observer resting at one location in space (Eulerian point of view) or we can flow with the particles (Lagrangian point of view). In the Eulerian point of view the momentum per unit volume can change due to acceleration of the fluid, $\frac{\partial \vec{u}}{\partial t}$, or due to the advection of momentum from other locations, $\vec{u} \vec{\nabla} \vec{u}$. So the total momentum change is:

$$\rho \frac{D\vec{u}}{Dt} = \rho \left(\frac{\partial \vec{u}}{\partial t} + \vec{u} \vec{\nabla} \vec{u} \right) \quad (3.1)$$

This is often called the material derivative, as it takes into the account the tendencies due to fluid continuum being advected.

- **Coriolis Force:** The earth rotation with the angular velocity, Ω , inserts a rotational force on any moving particle. The force acts perpendicular to the momentum of the fluid.

- **Pressure Gradient Force:** Pressure differences between two locations result into a force acting from the higher pressure region to the low pressure region. Thus the pressure gradient force acts against the pressure gradient, $\vec{\nabla}p$.
- **Gravity Force:** The gravity force acts into the direction of the geopotential. The earth zentrifugal force due to its rotation is usually included in the potential, $\vec{\nabla}\Phi$.
- **Friction:** Friction acts against the direction of the motion and usually it is only active at the boundaries of the atmosphere (surface) and the oceans (bottoms and coast lines).

The forces have horizontal and vertical components. We can divide the momentum equations into a horizontal and vertical part:

- **Horizontal:** The gravity force does not act in the horizontal, so the right hand side has only three terms:

$$\frac{Du}{Dt} = fv - \frac{1}{\rho} \frac{\partial p}{\partial x} + F_x \quad (3.2)$$

$$\frac{Dv}{Dt} = -fu - \frac{1}{\rho} \frac{\partial p}{\partial y} + F_y \quad (3.3)$$

The horizontal Coriolis parameter, f , vanishes at the equator.

- **Vertical:** Accelerations in the vertical are very small on the larger scales (several kilometers) and can be neglected (hydrostatic balance, see following sections). Friction only acts on the surfaces (in the horizontal) and the Coriolis force is negligible against the strength of the gravity force. Thus the vertical momentum equations simplifies a lot:

$$0 = -\frac{1}{\rho} \frac{\partial p}{\partial z} - g \quad (3.4)$$

3.1.2 Gravitational force

In the vertical, gravity is a very important force. In general we can write the gravity force as the gradient of the gravity potential:

$$\vec{\nabla}\Phi = \left(\frac{\partial\Phi}{\partial x}, \frac{\partial\Phi}{\partial y}, \frac{\partial\Phi}{\partial z} \right) \quad (3.5)$$

Which only has a vertical component:

$$\vec{\nabla}\Phi = (0, 0, -g) \quad (3.6)$$

Although the graviational acceleration varies with latitude and height (see table 3.1), in general we will assume it is constant.

Altitude	Latitude 0°	45°	90°
0	9.780	9.806	9.832
20	9.719	9.745	9.770
40	9.538	9.684	9.709

Table 3.1: Gravitational acceleration as it varies with height and latitude

The average value of the gravitational acceleration is 9.81 ms^{-2} . At any point on the Earth's surface, there is a downward force due to the weight of the air above it.

3.1.3 Pressure Gradient Force

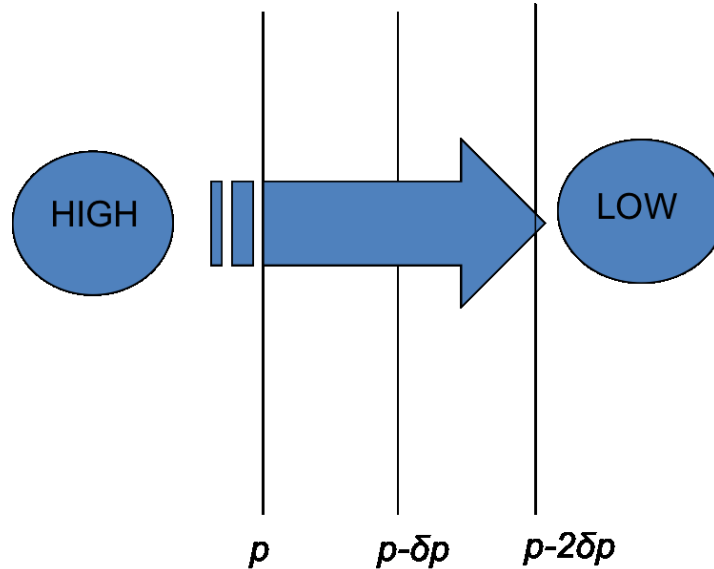


Figure 3.2

Pressure gradients between a high and low pressure creates a force that points against the pressure gradient from high to low pressure. In the horizontal we have high and low pressure regions, with pressure difference of a few hPa . The pressure gradient force of $1hPa$ is $100N$ per $1m^2$ is equivalent to the gravity force (weight) of $10kg$.

The horizontal pressure gradient force per fluid mass, PGF_h :

$$PGF_h = -\frac{1}{\rho} \nabla_h p \quad (3.7)$$

$$PGF_h = -\frac{1}{\rho} \left(\frac{\partial p}{\partial x}, \frac{\partial p}{\partial y} \right) \quad (3.8)$$

In nature we often see pressure gradients and may wonder why does the fluid does not flow into the low pressure even though the pressure gradient forces the fluid towards the low pressure. Although the air or water does flow into the low pressure, it does so much slower than one may think, because the momentum or some other forces act against this movement. In the horizontal and vertical we have different forces balancing the pressure gradient force:

- **Horizontal small scale:** On the small scale the pressure gradient force and the momentum of the fluid leads to rotations in cyclones (e.g. tornados). Here the pressure gradient and centrifugal force balance each other (*gradient wind balance* on the small scale).
- **Horizontal large scale:** On the large-scale (e.g. $1000km$) away from the equator the pressure gradient force is balanced by the Coriolis force (*gradient wind balance* on the large scale). This balance is called *Geostrophic Balance*.

- **Vertical:** In the vertical the pressure gradient force is balanced by gravity (the weight of the air or water column). This balance is called *Hydrostatic Balance*.

The gradient wind balance would not lead to any pressure changes (flow into the low pressure), but the air or water would move along lines of constant pressure. It is only the friction force that breaks this balance and leads to air flow into the low pressure. So note, without friction the water would never flow out of the bath tub!!!

3.1.4 Hydrostatic Balance (Pressure)

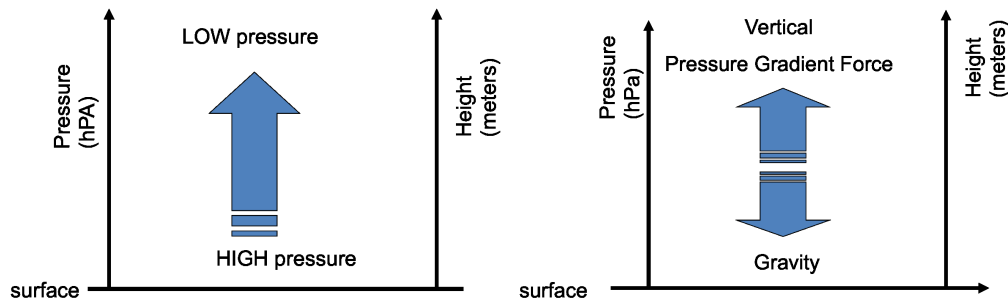


Figure 3.3: Left: Pressure is decreasing with, causing the pressure gradient force to point upwards. Right: Gravity force balances the pressure gradient force exactly on the large scale.

In both atmosphere and oceans the vertical forces are only the pressure gradient force and the gravity force, see Fig.3.3. The accelerations in the vertical are very small on the larger scales (several kilometers) and can be neglected. The upward pressure gradient force is balanced by the gravitational force (the weight of the air). Thus, as the pressure gradient attempts to move the air upwards (pressure times area results into a force), the weight is pushing downwards with the same amount of force per unit area (pressure). So we get to eq. [3.4], which we can rearrange for p :

$$\frac{\partial p}{\partial z} = -\rho g \quad (3.9)$$

So the change in pressure with height (the vertical pressure gradient) is caused by the gravity force, see sketch 3.4. We call this balance the *Hydrostatic Balance*. Thus, the weight of the atmosphere or ocean on top of it causes the pressure in this atmospheric or oceanic layer.

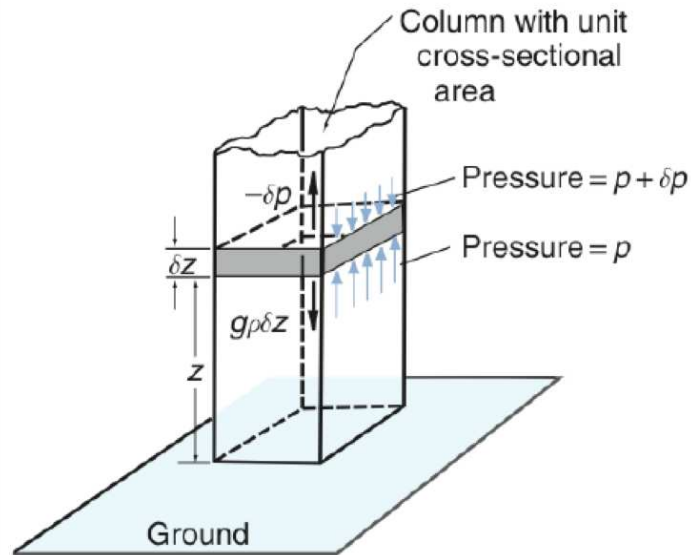


Figure 3.4

In the atmosphere the pressure and density are linearly related via the ideal gas law:

$$p = \rho RT \quad (3.10)$$

p is the pressure

ρ is the density

T is the temperature

R is the gas constant for air ($287 \text{ J kg}^{-1} \text{ K}^{-1}$)

So we can replace the density in eq. [3.9]:

$$\frac{\partial p}{\partial z} = -\frac{g}{RT} p \quad (3.11)$$

If we, for a first order guess, assume that temperature is roughly constant (it changes from 300K to 250K in 10km, this is roughly constant) we can see that:

$$\frac{\partial p}{\partial z} \approx -H p(z) \quad (3.12)$$

The solution of such a differential equation is the exponential function $p(z) \approx p(z=0)e^{-z/H}$. So the pressure as function of height is decreasing roughly exponentially, with the scaling height $H = \frac{g}{RT}$, see sketch ?? or Fig 1.17.

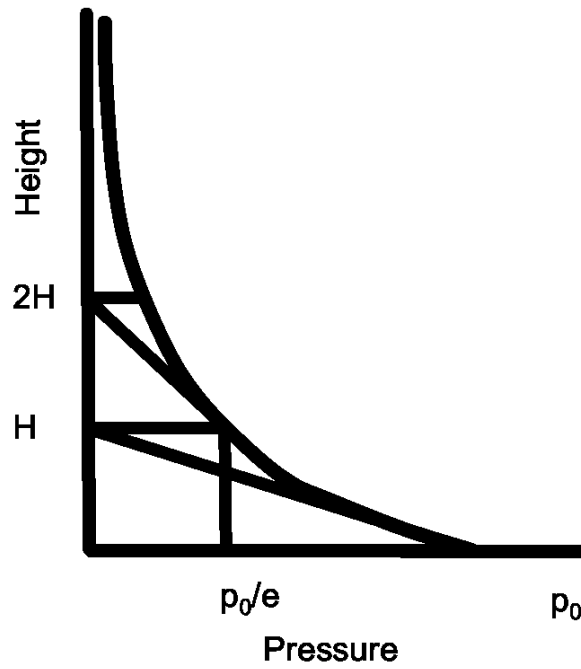


Figure 3.5: Illustration of the exponential pressure decrease and the scaling height H .

The hydrostatic balance can be used to calculate the thickness of the atmosphere:

$$\Delta z = \frac{RT}{g} \ln \left(\frac{p_0}{p_1} \right) \tag{3.13}$$

At upper levels, the pressure in the warmer air of the tropics is higher than in the cooler air of the high latitudes, creating a gradient of pressure which slopes downwards towards the poles, see Figs 3.6 and 3.8. So, when the temperature is higher, the atmosphere is deeper. Surfaces of constant pressure p slope down towards the poles.

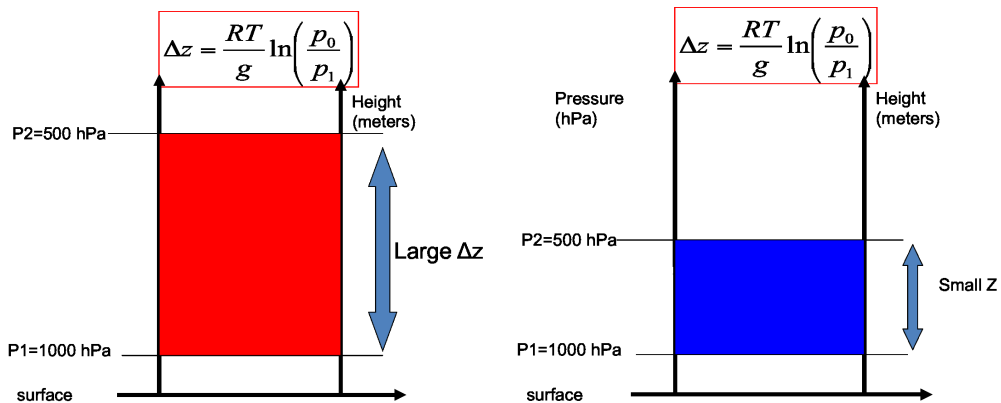


Figure 3.6: Left: Warm air is less dense and therefore reaches to higher levels. Right: Cold air is more dense and therefore does not reach to higher levels.

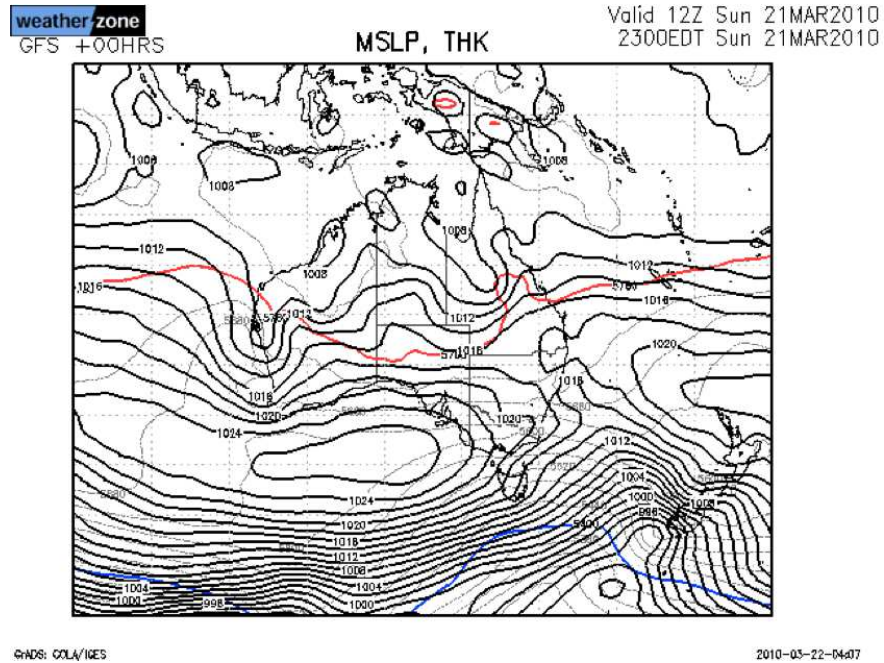


Figure 3.7: Mean sea level pressure (hPa) and thickness (meters, from 1000hPa to 500hPa)

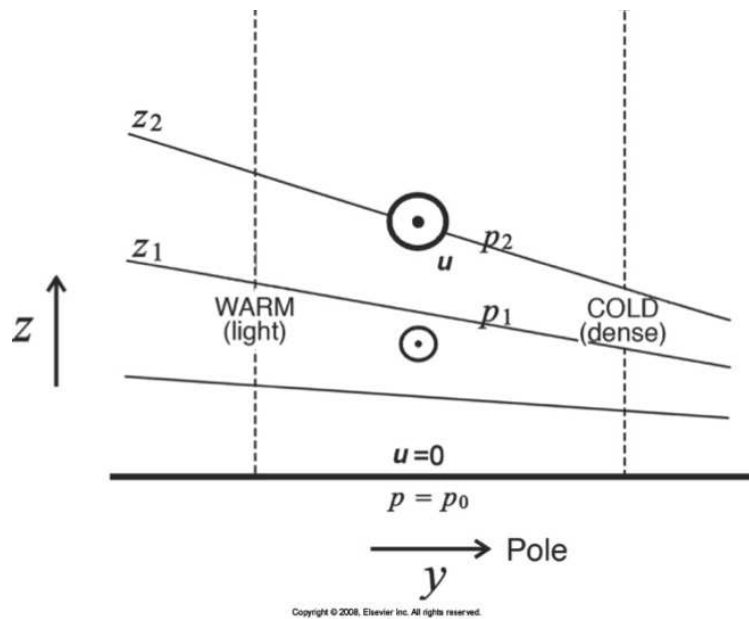


Figure 3.8: Pressure gradient at higher levels from tropics to pole due to the warm to cold density difference in the air. The circles mark the increasing winds with height. See also later for the thermal wind balance.

3.1.5 Potential temperature

We know that the temperature in the troposphere (surface to 10km) is decreasing with height (see Fig. 1.18). We also know that a hot air balloon would raise in cold air due to its Buoyancy (see next section). So why does the warm surface air does not raise above the colder air in higher levels?

From the point of view that warm fluid which is less dense should be above the cold fluid, which is more dense, the atmosphere seems upside down. This is due to the adiabatic temperature change with height due to pressure changes with height.

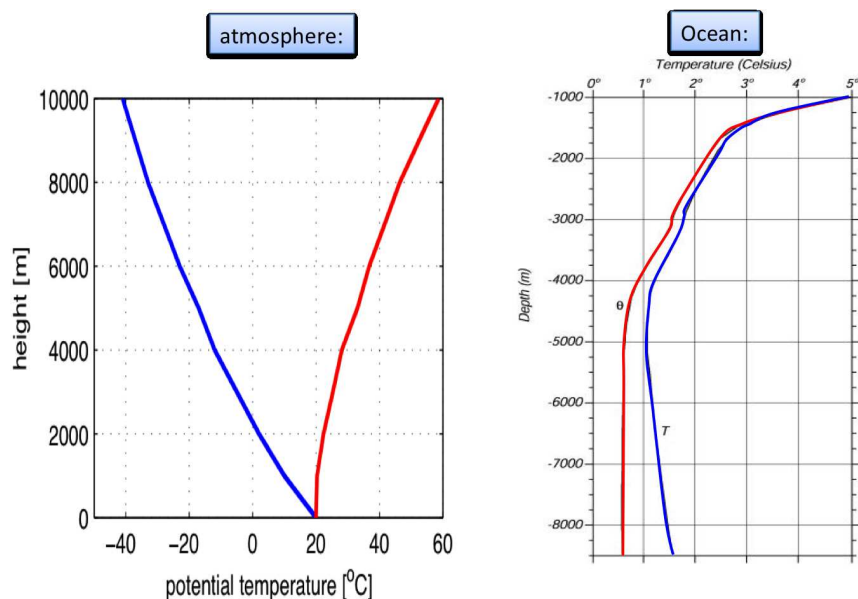


Figure 3.9: Temperature (blue) profile of the troposphere (left) and oceans (right) in comparison to the potential temperature (red) profile.

The first law of thermodynamics is the conservation of energy. In thermodynamics we have different types of energy: heat is one form of energy and work in form of pressure on the fluid is another form of energy. Without putting any energy into the system (fluid) the heat energy can be transformed into work energy. If, for instance, we would put some air from the surface at 1000hPa into a slack bag (it can expand or contract without any resistance) and bring it to a higher atmospheric level (about 5000m) at a pressure of 500hPa it would cool down up by about -50°C . The heat is turned into work by expanding the volume in the low pressure environment. This process is called adiabatic cooling. It also works the other way around, if we take an air mass from a higher atmospheric level at a pressure of 500hPa and bring it to the surface it would warm by about $+50^{\circ}\text{C}$ and the volume contracts.

This temperature gradient in the atmosphere that is entirely caused by the adiabatic cooling due to pressure changes is called *Dry Adiabatic Lapse Rate* $\approx 0.01^{\circ}\text{C}/\text{m} = 1^{\circ}\text{C}/100\text{m}$. So to understand if an upper layer atmospheric temperature is warmer or colder than a surface atmospheric layer if it were on the same pressure we can define a new variable: *The Potential Temperature θ* : The temperature that a fluid parcel would have if it is moved adiabatically (without adding energy) to a reference pressure.

The Reference level is different for the atmosphere and oceans:

Atmosphere: 1000hPa (roughly surface)

Ocean: usually 1000m depth (not the surface!)

Fig. 3.9 shows a temperature profile of the troposphere in comparison to the potential temperature profile. Although the 'in situ' (as measured at the spot) temperature is decreasing with height, the potential temperature is actually increasing with height. Now we can understand why the warmer

surface air layer would not raise: By raising into higher levels it would cool down faster by adiabatic cooling than its environment and therefore would fall down again. So in potential temperature the atmosphere is usually stratified in stable layers (warmer and less dense on top of colder and more dense air). This holds for both oceans and atmosphere, see Fig. 3.10. The difference between in situ and potential temperature in the oceans is much less, because in water the pressure effect on the density of the water is much smaller than on the air in the atmosphere. Subsequently water at different pressure levels will expand much less and therefore have also a much smaller change in temperature. Note, that the density of the oceans water also depend on the salinity. Therefore the potential temperature profile may seem unstable (Fig. 3.9), but the salinity effect on the density compensates for that.

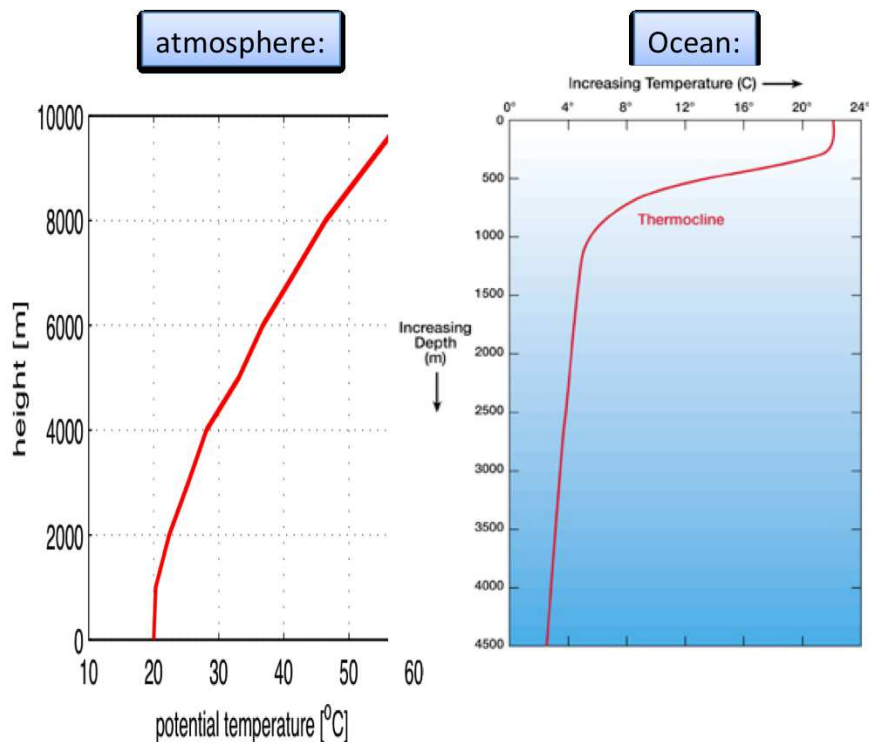


Figure 3.10: Potential temperature profiles for the atmosphere and oceans.

3.1.6 Buoyancy

In a fluid (air or water) a parcel that is warmer (and therefore less dense) than its surroundings will rise, assuming it overcomes the adiabatic cooling by pressure changes (see above section). A relative cold fluid parcel, which is more dense, will sink. This quality of a fluid parcel is called *Buoyancy*: A parcel that raises in a fluid due to its lesser density (warmer) is said to be buoyant.

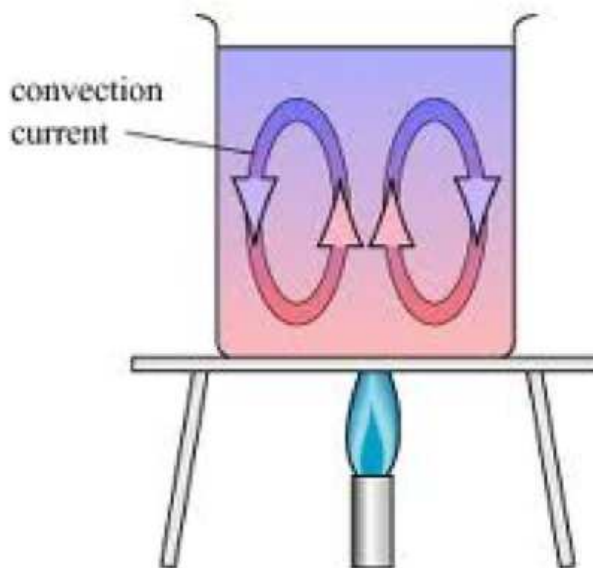


Figure 3.11: Buoyancy in a heated pot: The heated water rises from the bottom as it is less dense than the upper colder water. It builds up convection cells.

The incoming solar radiation is mostly absorbed at the surface. This is true for both the atmosphere and the oceans. This warms the surface, the air close to it becomes warmer than the surrounding air and becomes buoyant. If the air contains water vapour, this condenses within the air parcel as it rises, to form clouds and precipitation, see sketch 3.12.

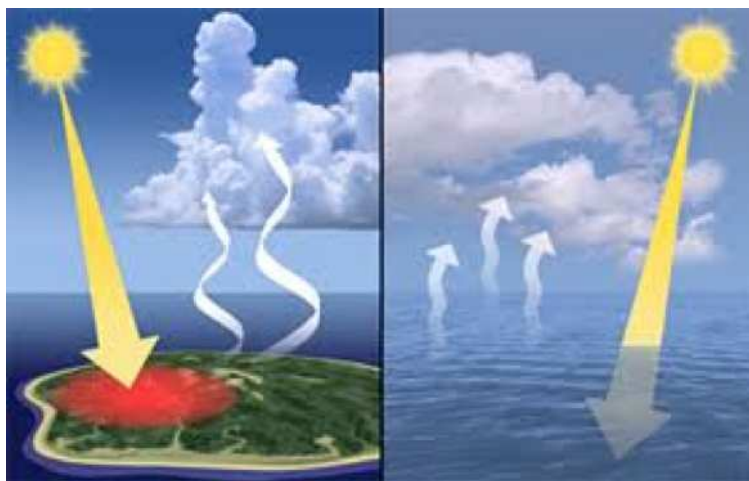


Figure 3.12: Illustration of the surface heating leading to convection in the atmosphere.

A few point should be noted here:

- The atmosphere is heated from below, which is very efficient in mixing the air by buoyancy, see sketch 3.13.
- Vertical temperature gradients indicate mixing throughout the profile (complete mixing would lead to constant potential temperature), see Fig. 3.10.

- The atmosphere is strongly mixed in the lower 10km.
- The oceans are heated from above, which is very inefficient in mixing the ocean, see sketch 3.13.
- The ocean is only well mixed in the upper 50-200m and some small mixing up to 1000m. This is mostly done by wind mixing and not by buoyancy. Below that the mixing is very weak, see Fig. 3.10.

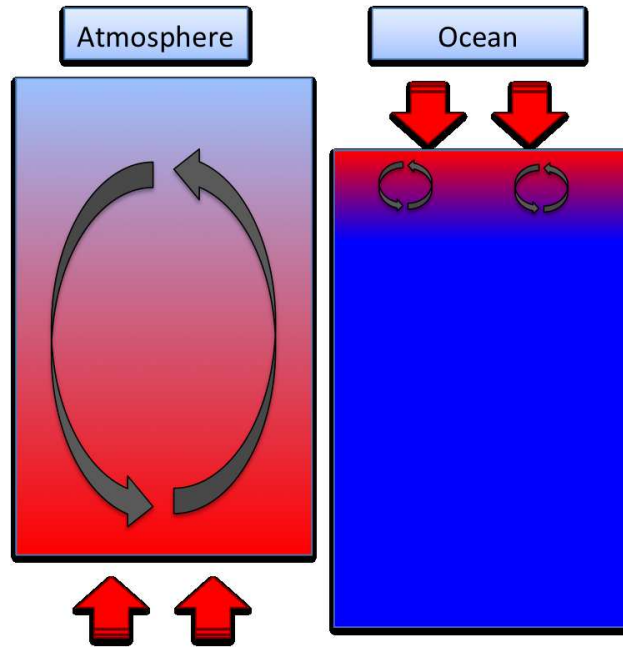


Figure 3.13: Sketch of the effect of heating and buoyancy in the atmosphere and the oceans. Atmosphere: is heat from below and mixed by the buoyancy of the heated air. Oceans: are heated from above and the buoyancy of the warmer surface waters block deeper mixing.

3.1.7 Continuity and Convection

The atmosphere and the oceans are continuum fluids. The mass does not get lost nor does mass gets created. So the mass of the fluid is conserved. This is called the *Continuity - conservation of mass*:

$$\frac{\partial \rho u}{\partial x} + \frac{\partial \rho v}{\partial y} + \frac{\partial \rho w}{\partial z} = \vec{\nabla} \cdot (\rho \vec{u}) = -\frac{\partial \rho}{\partial t} \quad (3.14)$$

Local changes in density, $-\frac{\partial \rho}{\partial t}$, must equate to the divergence of mass, as there are no mass sinks or sources. Thus

$$\implies \frac{\partial \rho}{\partial t} + \vec{\nabla} \cdot (\rho \vec{u}) = 0 \quad (3.15)$$

If density is assumed to be constant, then divergence must be zero.

$$\frac{\partial \rho}{\partial t} = 0 \implies \rho \cdot \vec{\nabla} \cdot \vec{u} = 0 \implies \vec{\nabla} \cdot \vec{u} = 0 \quad (3.16)$$

So the three dimensional flow has no divergence nor does it has convergence if the density is constant (good approximation for the oceans). Ocean circulation is mostly horizontal, due to the strong stratification:

$$\vec{u}_z = 0 \implies \vec{\nabla} \cdot \vec{u}_{xy} = 0 \quad (3.17)$$

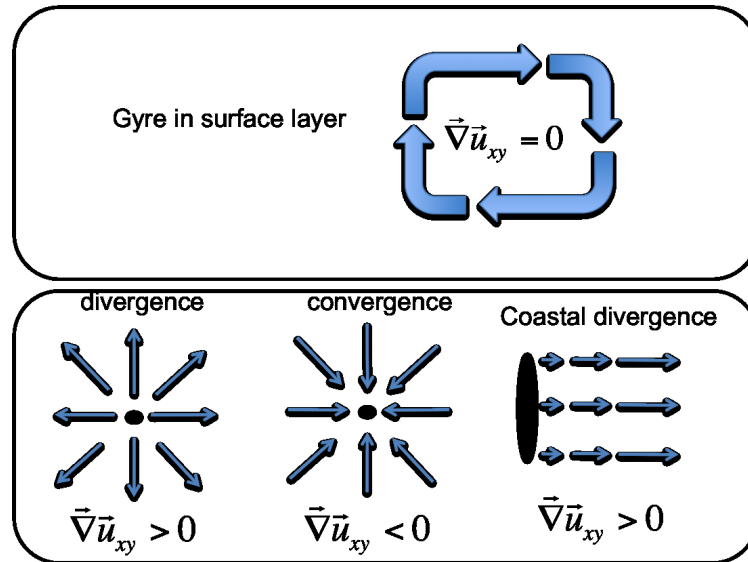


Figure 3.14

Most surface ocean currents recirculate horizontally, forming big gyres, see sketch 3.14. Note, that we will often see that the horizontal flow does converge or diverge, see sketch 3.14. If this is the case, then some vertical movement is implied, which it called *Convection* (vertical movement of the air in the atmosphere or water in the oceans) to maintain the mass conservation.

In the atmosphere horizontal convergence of air masses near the surface implies upward convection of air masses. In general, the heating at the surface causes convection of the air. Since the air is lifted it leaves a deficit of air at the surface (low pressure), which leads to surface air converging to the area of convection. On the large-scale we can see this along the equator with the InnerTropical Convergence Zone (ITCZ). The air converges towards the equator, because of the large-scale convection (lifting) of the air masses by heating.

In the oceans horizontal convergence of water masses implies downward convection of water masses. As water is much denser than air, these vertical motions (convection) are very rare and for most of the oceans this is suppressed (see later in the oceans section).

Moist convection

In the tropics, where there is a lot of heat and moisture, we see a lot of convective clouds. If the air contains water vapour, this condenses within the air parcel as it rises, to form clouds and precipitation. In turn the air that is lifted in the tropics must come down somewhere else. This is in the subtropics. The air that comes down is dry and heats up when it descends leading to very warm, clear sky and dry air at the surface, see sketch 3.15.

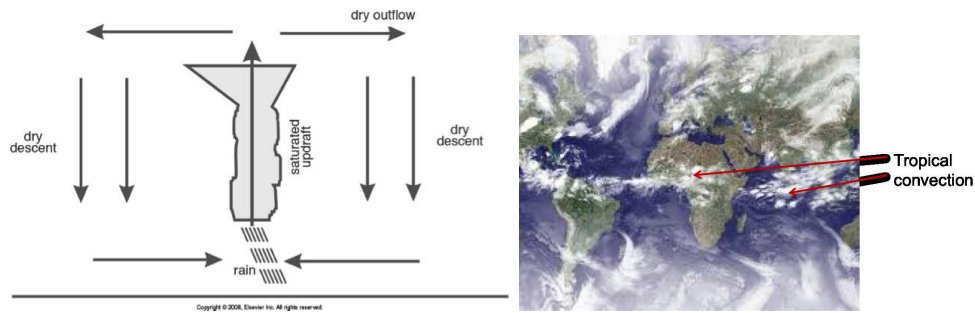


Figure 3.15

3.1.8 Coriolis Force (Earth rotation)

Coriolis acceleration

The earth is rotating with an angular speed of, $\Omega = 2\pi/24\text{hrs} = 7.292 \times 10^{-5}\text{s}^{-1}$. For an observer on the rotating sphere an object moving on a straight line appears to be moving in circles. In turn this means that any object (parcel) moving in a straight line on the earth will feel a force deflecting it into a curve movement.

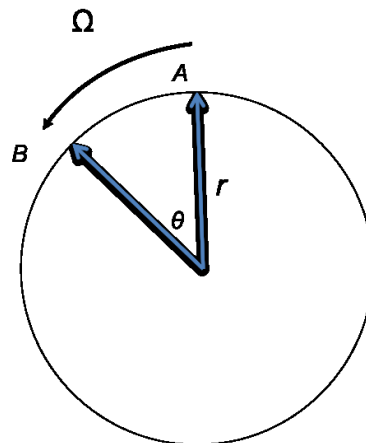


Figure 3.16: Sketch for understanding the Coriolis acceleration on a rotating plane: Parcel moving from A to B.

We can start with calculating the acceleration a parcel will feel due to the rotation, see sketch 3.16: The angle, θ , and distance, AB that it moves in time, t , due to the rotation by an angular speed of, Ω is:

$$\theta = \Omega t \quad (3.18)$$

$$r = vt \quad (3.19)$$

$$AB = r\theta = \Omega vt^2 = \frac{1}{2}at^2 \quad (3.20)$$

$$\Rightarrow a = 2\Omega v \quad (3.21)$$

So, the acceleration due to the rotation is two times the rate of rotation times the velocity of the parcel. In 3-dimensions, the direction of the Coriolis acceleration ($-2\Omega \times \vec{u}$) can be found using the component of the Earth's rotation in the z-direction and the y-direction as shown in Fig. 3.17.

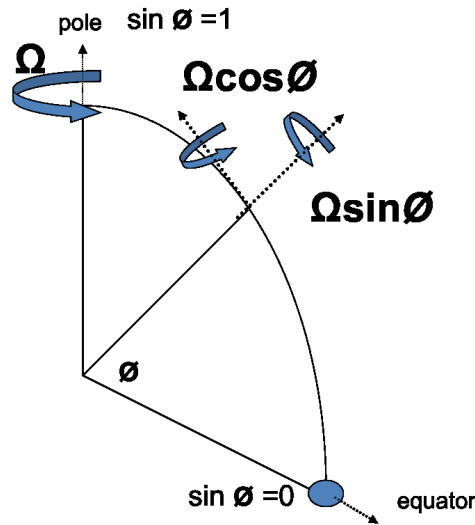


Figure 3.17: Sketch of the meridional and vertical component of the Earth's angular velocity as function of latitude, Φ . The zonal component is zero.

The vector product is

$$\Omega \times \vec{u} = \begin{vmatrix} \vec{i} & \vec{j} & \vec{k} \\ \Omega_x & \Omega_y & \Omega_z \\ u & v & w \end{vmatrix} = \begin{pmatrix} \Omega_y w - \Omega_z v \\ \Omega_z u - \Omega_x w \\ \Omega_x v - \Omega_y u \end{pmatrix} \quad (3.22)$$

From the sketch Fig. 3.17 we can get the three components of Ω

$$\Omega_x = 0, \quad \Omega_y = \Omega \cos \phi, \quad \Omega_z = \Omega \sin \phi \quad (3.23)$$

We can include these terms in the three components of the momentum tendency equations, see Fig. 3.18.

$$\begin{aligned} \frac{Du}{Dt} &= \cancel{2\Omega v \sin \phi - 2\Omega w \cos \phi} - \frac{1}{\rho} \frac{\partial p}{\partial x} + F_x \\ \frac{Dv}{Dt} &= \cancel{-2\Omega u \sin \phi} - \frac{1}{\rho} \frac{\partial p}{\partial y} + F_y \\ \frac{Dw}{Dt} &= \cancel{2\Omega v \cos \phi} - \frac{1}{\rho} \frac{\partial p}{\partial z} - g + F_z \end{aligned}$$

Figure 3.18: The three components of the momentum equation with some terms that can be neglected, as they are much smaller than the other terms.

We see here that there is a component of the Coriolis acceleration in the vertical direction, but this is so small compared to the gravitational acceleration and the vertical pressure gradient that we

can neglect it (hydrostatic approximation). We can also neglect the Coriolis term with the vertical velocity, w , as it is much smaller than the other term including the horizontal velocity. So we only need to consider the horizontal terms that are a function of the Coriolis parameter, f

$$f = 2\Omega \sin\phi \quad (3.24)$$

We can also neglect friction in the vertical, as it only acts at the surface. This gets us to the somewhat simpler equations for the horizontal momentum tendencies:

$$\frac{Du}{Dt} = fv - \frac{1}{\rho} \frac{\partial p}{\partial x} + F_x \quad (3.25)$$

$$\frac{Dv}{Dt} = -fu - \frac{1}{\rho} \frac{\partial p}{\partial y} + F_y \quad (3.26)$$

The f factor of the Coriolis force is a function of latitude, ϕ , see Fig. 3.19. It is zero at the equator and increases in magnitude the closer we get to the poles. The direction of the force is different on both hemispheres, see Figs. 3.19 and 3.20.

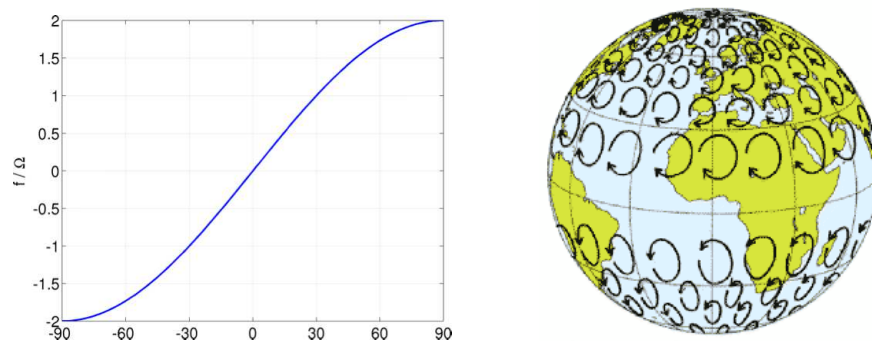


Figure 3.19: Coriolis parameter: left: .Right: Schematic representation of inertial circles of air masses in the absence of other forces, calculated for a wind speed of approximately 50 to 70m/s.

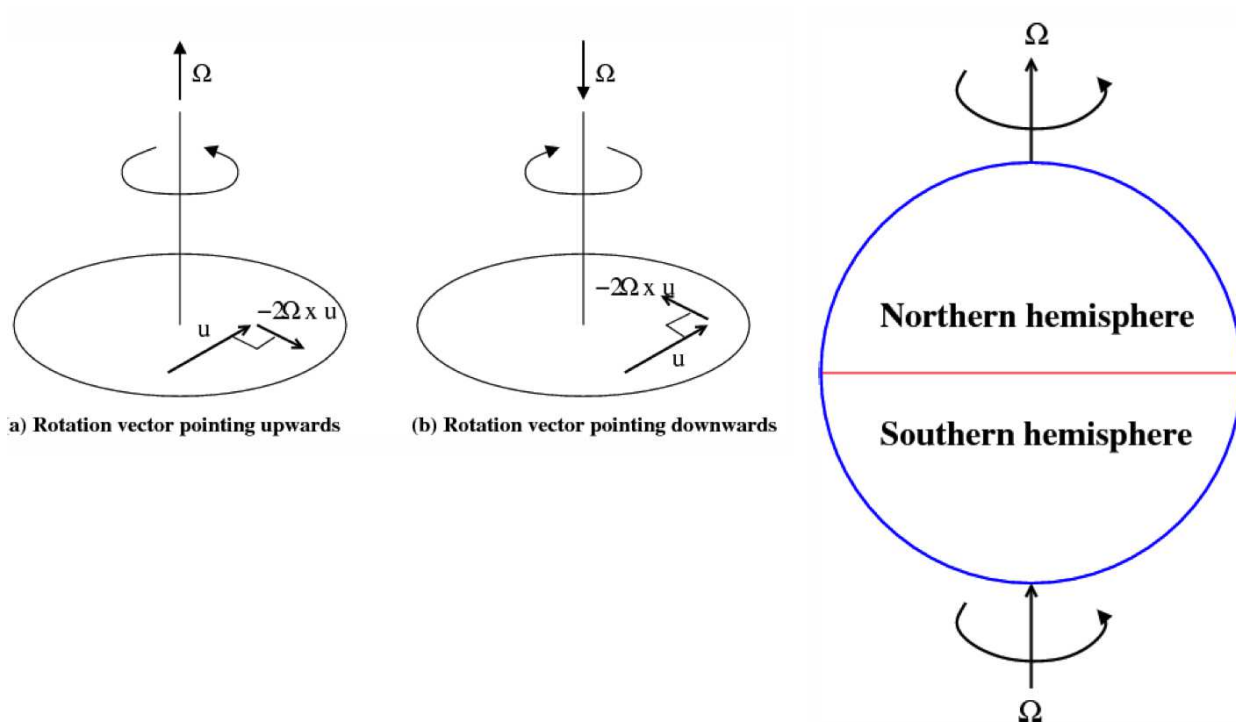


Figure 3.20: Left: Direction of the Coriolis force on a Northern Hemisphere plane. Middle: for a Southern Hemisphere plane. Right: Direction of the earth rotation for Northern and Southern Hemisphere.

Effect of Coriolis force in the Southern Hemisphere

Considering flow in the free atmosphere or ocean (away from the surface where the effects of friction are not important) we can discuss how the movement of parcel would change if it tries to move from high to low pressure in the Southern Hemisphere, see sketch 3.21. The parcel will be deflected to the left (right on Northern Hemisphere) and finally it will move parallel to the isobar lines.

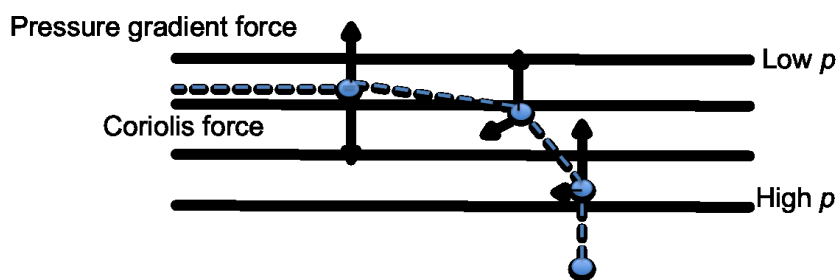


Figure 3.21: Coriolis force on a parcel moving from high to low pressure in the Southern Hemisphere. For the northern Hemisphere it is the mirror image.

3.1.9 Geostrophic Balance

Large-scale weather system (*Synoptic scale motion*) or ocean currents are essentially only balanced by the Coriolis and pressure gradient force. Friction does not matter within the free atmosphere or ocean, gravity does not act in horizontal motions and for large-scales the momentum changes

(accelerations) are small. Thus the only forces that balance the motion are Coriolis and pressure gradient force, see eq. [3.1]. This balance is called *Geostrophic Balance*.

The *Rossby number* is used to estimate whether or not a motion of a fluid can be considered to be in Geostrophic Balance. It is defined as the ratio of the total acceleration to the Coriolis acceleration:

$$R_o := \frac{U^2/L}{fU} = \frac{U}{fL} \quad (3.27)$$

The parameters that go into this equations are estimates of the scales of the velocity, U , the length, L and the Coriolis parameter, f of the motion. Using scale analysis for synoptic scale motion where the typical horizontal scale is 1000km and typical timescales are 1 day (10^5 s):

- $L \sim 10^6$
- $U \sim 10ms^{-1}$
- $f \sim 10^{-4} s^{-1}$
- $\Rightarrow R_o \sim 0.1$

So the Rossby number, $R_o \ll 1$. In other words, the Coriolis acceleration dominates over the total acceleration. The Coriolis force must be balanced (approximately) by the pressure gradient forces for these scales.

Geostrophic approximation

When the Rossby number is small, the Coriolis and pressure gradient forces balance. In the horizontal the momentum equations become:

$$fv_g = \frac{1}{\rho} \frac{\partial p}{\partial x} \quad fu_g = -\frac{1}{\rho} \frac{\partial p}{\partial y} \quad (3.28)$$

Geostrophic winds blow parallel to the isobars (lines of constant pressure). In the Southern Hemisphere the low pressure is on the right; in the Northern Hemisphere, the low pressure is on the left.

Geostrophic wind in Southern Hemisphere

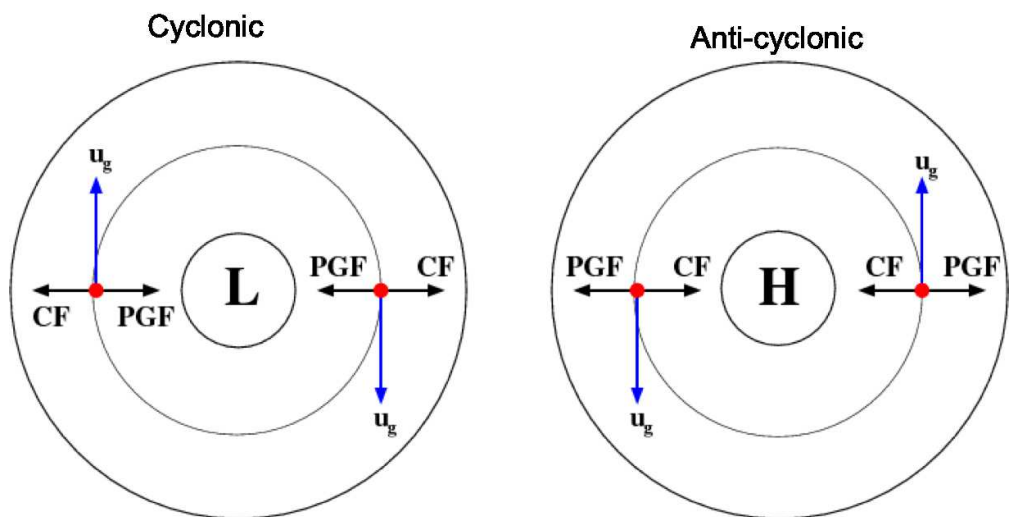
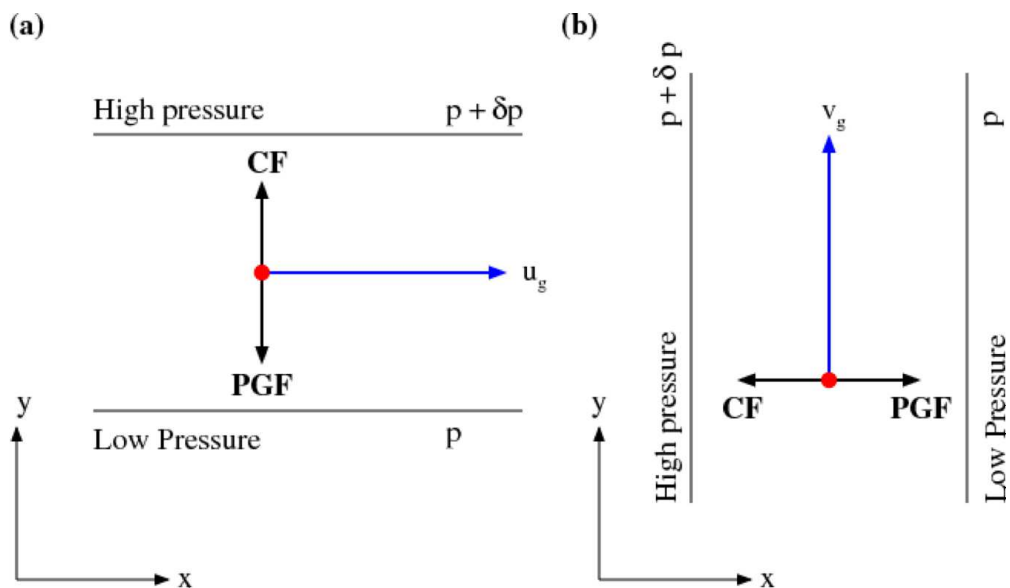


Figure 3.22: Geostrophic wind in the Southern Hemisphere for four different examples. Upper: meridional (left) and zonal (right) pressure gradients. Lower: Low- (left) and High-pressure (right) systems. CF: Coriolis force; PGF: pressure gradient force; u_g, v_g : geostrophic winds.

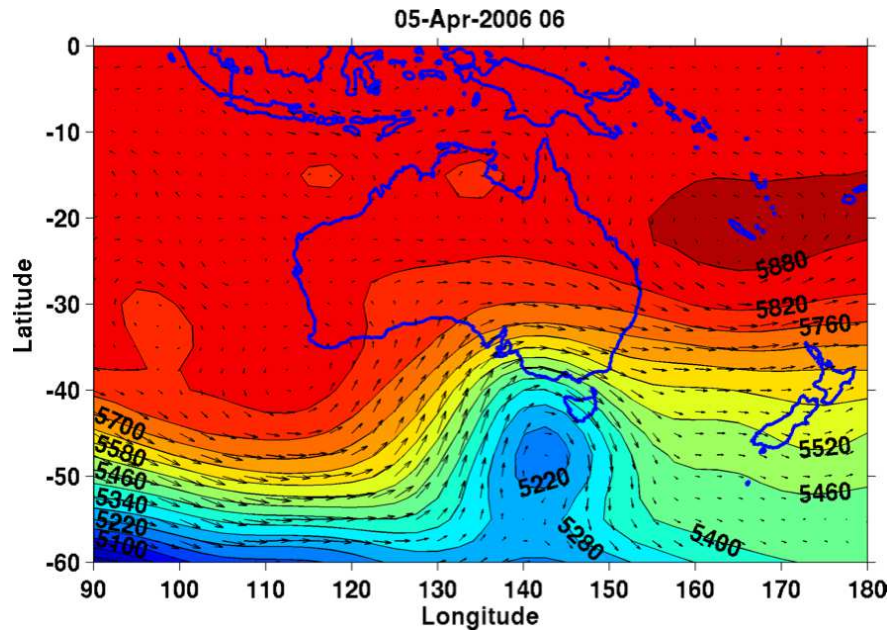


Figure 3.23: An example of geostrophic flow in the atmosphere. Colours are the 500 hPa geopotential height level in meter and vectors are wind barbs. We can see that the flow goes clockwise around the low pressure in the Southern Hemisphere.

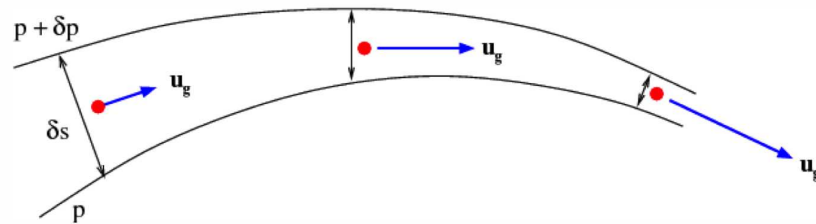


Figure 3.24: Illustration of the increase in geostrophic wind speed by increase in the pressure gradient (isobars are closer).

The geostrophic flow is parallel to the lines of constant pressure. The speed of the geostrophic wind is proportional to the pressure gradient, see eq. [3.28] and Fig.3.24. The curved lines show two isobars on which pressure is constant with values p and $p + \delta p$. Their separation is δs (a generic horizontal distance)

$$|u_g| = \frac{1}{f\rho} \left| \frac{\delta p}{\delta s} \right| \quad (3.29)$$

The flow is strongest when the isobars are closest together.

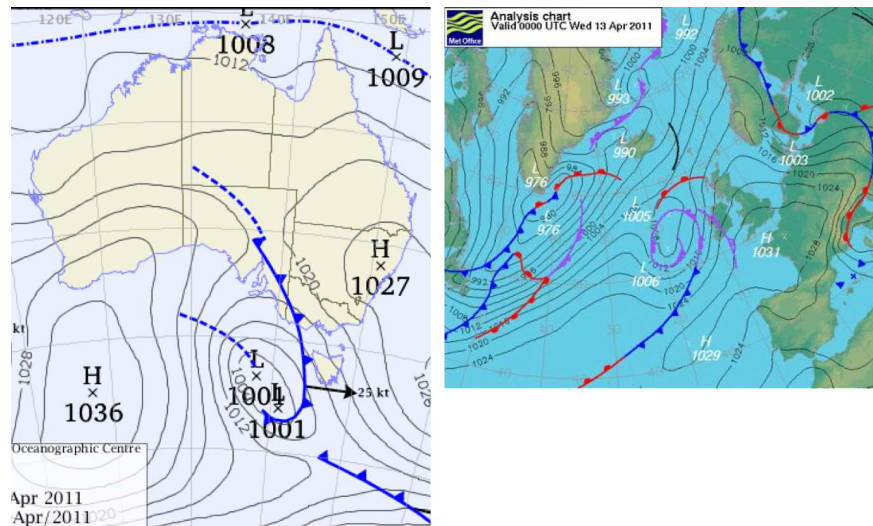


Figure 3.25: Flow parallel to isobars. In these maps the wind will always blow along the lines with the low pressure to right (Southern Hemisphere; left panel) and the low pressure to left (Northern Hemisphere; right panel). The closer the isobars to each other the stronger the winds (e.g. south of Australia, south of Greenland or North Italy).

The Geostrophic Balance is equally important for the Oceans. A few points to note here:

- As in the atmosphere most of the ocean circulation is in geostrophic balance. $2\rho\cdot\Omega\times\vec{u} = -\vec{\nabla}p$
- Low and high pressure in the oceans is related to difference in sea level height.
- As in the atmosphere stronger gradients in sea level (pressure) cause stronger currents (e.g. Antarctic Circumpolar Current (ACC) or Gulf Stream in the North Atlantic).
- Geostrophic balance holds for most of the oceans, but not along the equator or at coastal lines.

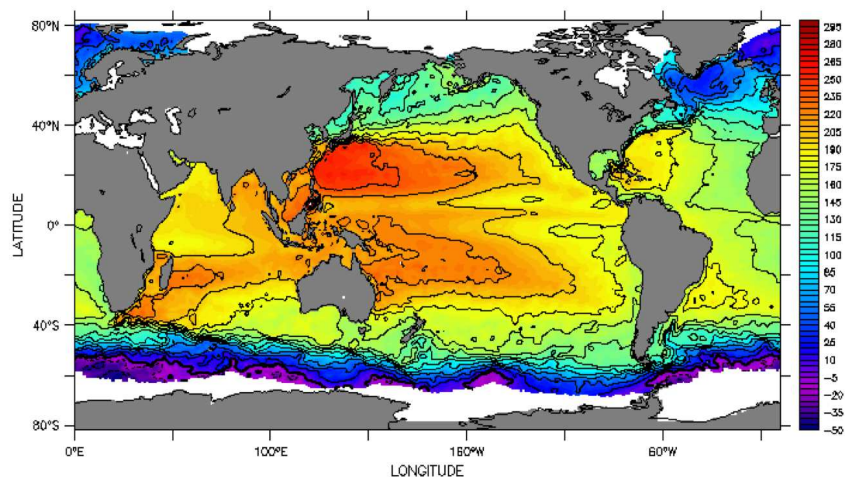


Figure 3.26: Snapshot of relative sea level (22 August 2001). Sea level is the oceans equivalent to atmospheric pressure and geostrophic flow will move along the lines of constant sea level with the low sea level to right (Southern Hemisphere) or to left (Northern Hemisphere).

3.1.10 Thermal Wind Balance

The thermal wind balance provides us with a relation between the change of geostrophic winds or ocean currents in height (du_g/dz) due to horizontal temperature gradients. It combines the hydrostatic balance, the geostrophic balance and in the atmosphere the ideal gas law.

Thermal wind relation in SH

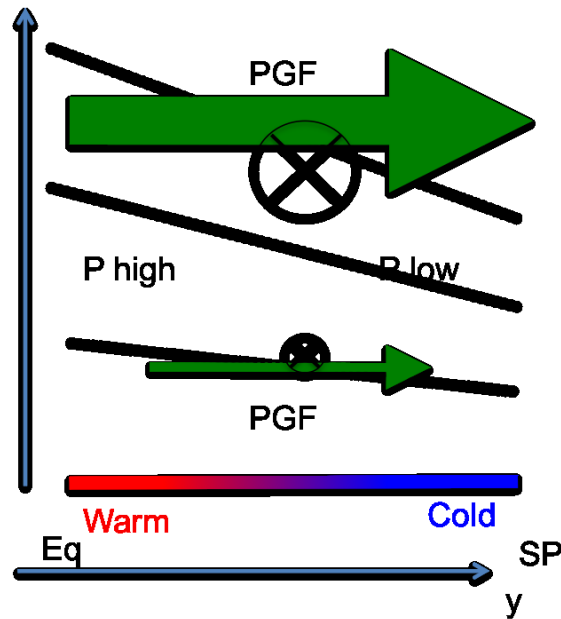


Figure 3.27: Illustration of the Thermal Wind Balance. the surface temperature gradient from the Equator to the pole, leads higher pressure at higher levels at the equatorial region relative to the polar region (Hydrostatic Balance). The pressure gradient is increasing with Height. The pressure gradient leads to geostrophic westerly winds that increase in strength with height (Geostrophic Balance).

The hydrostatic balance relates the thickness of an atmospheric layer to the temperature, see eq. [3.13]. So a relative warm air column will extend further up than a relative cold air column (see Fig. 3.6) and subsequently we will have a pressure gradient between the two air columns that increase with height, see Fig. 3.27. The geostrophic winds will blow perpendicular to the pressure gradient and proportional to the strength of the pressure gradient. Since the gradients are increasing with height, the geostrophic winds will also increase with height.

The combination of hydrostatic balance, the geostrophic balance, the ideal gas law and some approximations give us the *thermal wind balance* for the atmosphere:

$$\frac{\partial u_g}{\partial p} = \frac{R}{f_p} \frac{\partial T}{\partial y} \quad (3.30)$$

$$\frac{\partial v_g}{\partial p} = -\frac{R}{f_p} \frac{\partial T}{\partial x} \quad (3.31)$$

So the increase of the winds with heights ($\frac{\partial u_g}{\partial p}$) is proportional to the horizontal temperature gradient. So over the height of the troposphere the wind increase with height. Note, that near the surface on the smaller scales winds also increase with height due to the surface friction slowing the winds down. But the increase of the winds with heights due to the thermal wind balance goes in much higher atmospheric levels and acts on a much bigger scale.

The large scale winds as a result of the Thermal Wind Balance

In the Southern Hemisphere, the meridional temperature gradient is positive:

$$\frac{\partial T}{\partial y} > 0 \quad (3.32)$$

and in the Northern Hemisphere the meridional temperature gradient is negative:

$$\frac{\partial T}{\partial y} < 0 \quad (3.33)$$

The Coriolis parameter is also changing sign fro different hemispheres. Therefore in both hemispheres:

$$\frac{1}{f} \frac{\partial T}{\partial y} < 0 \quad (3.34)$$

and

$$\frac{\partial u_g}{\partial p} < 0 \quad (3.35)$$

Thus Winds become increasingly westerly (positive) with height or decreasing pressure (negative). This gives us the upper level westerlies wind jets in regions where the meridional temperature gradients are strongest (polar edge of subtropics).

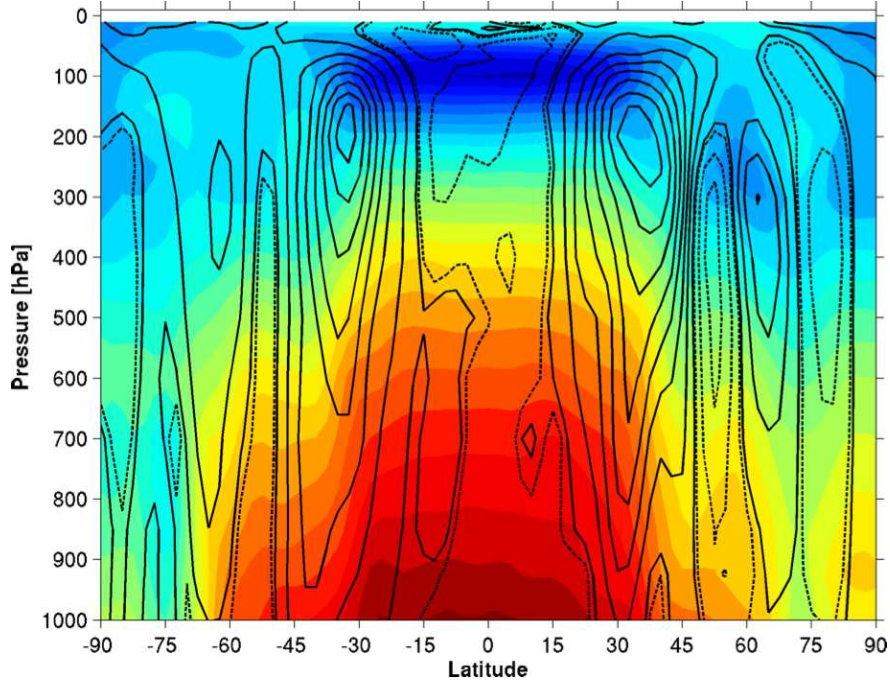


Figure 3.28: Meridional cross-section of zonal mean temperature, T and zonal wind u on April 5 2006.

The Thermal Wind Balance for the Oceans

- Hydrostatic and geostrophic balance lead to the thermal wind balance in oceans as well, but with some differences in the formulation of density.
- In the atmosphere the thermal wind balance is expressed in terms of a pressure coordinate system, while in the ocean we use the z -coordinate. $\frac{\partial p}{\partial z} = -\rho g \implies \partial p = -\rho g \partial z$
- Density in the atmosphere follows from the ideal gas law ($p = \rho RT$) and is a linear function of T . In the ocean it is a non-linear function of T, S . We therefore have horizontal gradients of density, σ , in the oceans (not gradients of T).
- Since geostrophic circulation is density driven and density in the ocean is controlled by T and S , the circulation is often called thermohaline circulation.

Ocean:

$$\frac{\partial u_g}{\partial z} = \frac{g}{f \rho_0} \frac{\partial \sigma}{\partial y} \quad (3.36)$$

$$\frac{\partial v_g}{\partial z} = -\frac{g}{f \rho_0} \frac{\partial \sigma}{\partial x} \quad (3.37)$$

The thermal wind balance can be used to estimate ocean currents by knowing T and S .

Example: Southern Ocean Antarctic Circumpolar Current (ACC)

Some physical constants:

$$g = 9.81 \frac{m}{s^2}$$

$$f = -10^{-4} \frac{1}{s}$$

$$\rho_0 = 1000 \frac{kg}{m^3}$$

Assumed values for the Southern Ocean:

$\Delta z = 1000m$ Depth of current (assumed level of no motion)

$\Delta\sigma = -1.5 \frac{kg}{m^3}$ Meridional density difference around 20-40°S

$\Delta y = 2000km$ Meridional width of the ACC

$$\frac{\partial u_g}{\partial z} = \frac{g}{f\rho_0} \frac{\partial\sigma}{\partial y} \implies u_g \approx \Delta z \frac{g}{f\rho_0} \frac{\Delta\sigma}{\Delta y} \approx 1000m \frac{9.81 \frac{m}{s^2}}{-10^{-4} \frac{1}{s} 1000 \frac{kg}{m^3}} \frac{-1.5 \frac{kg}{m^3}}{2 \cdot 10^6 m} = 0.07 m/s$$

- The ACC speeds at the surface are about 15cm/s getting weaker with depth.
- Despite the small speeds the mass transported is huge. $M_{ACC} = A \cdot u = 1000m \cdot 2 \cdot 10^6 m \cdot 0.07 m/s = 140 \cdot 10^6 m^3/s = 140 Sv$
- $1Sv \sim$ the sum of all gloval river run off into the ocean.

3.1.11 Friction

Friction

The large-scale flow in the free atmosphere (where the effect on the surface is negligible) is close to geostrophic and thermal wind balance. In boundary layers where fluid rubs over frictional boundaries (i.e. the rough surface of the Earth), the wind is no longer geostrophic due to the presence of friction. In the lowest 1km (approximately) of the atmosphere, the roughness of the surface generates turbulence which communicates the drag of the lower boundary to the free atmosphere.

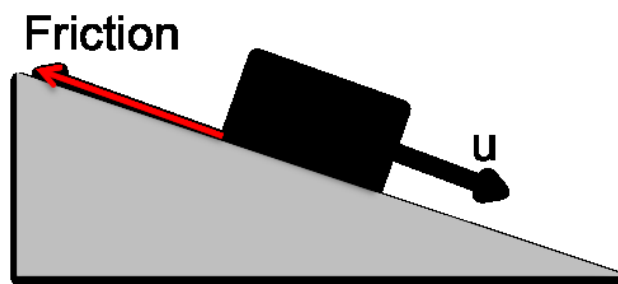


Figure 3.29: Frictional forces always act in a direction opposite to the direction of motion.

If we are considering synoptic scale motion where the Rossby number R_o is small, but we are close to the surface so that the effect of friction is now not negligible, then:

$$-fv + \frac{1}{\rho} \frac{\partial p}{\partial x} = F_x$$

$$fu + \frac{1}{\rho} \frac{\partial p}{\partial y} = F_y$$

Because of the effect of friction, the flow is no longer geostrophic. The horizontal wind now has a geostrophic component and an ageostrophic component:

$$v_{ag} = -\frac{1}{f} F_x$$

$$u_{ag} = \frac{1}{f} F_y$$

Friction - Southern Hemisphere

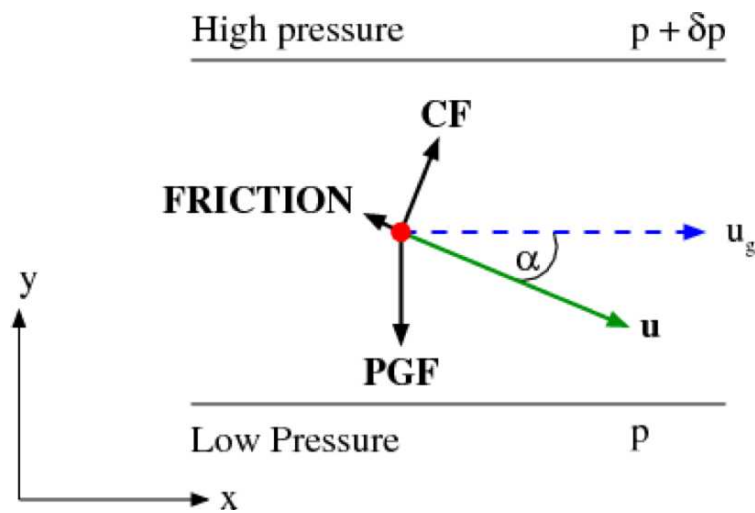


Figure 3.30

The Coriolis force acts to the left of the flow u . The friction force F acts as a drag in the opposite direction to the prevailing wind. The sum of these two forces must be balanced by the pressure gradient force, so the wind is no longer directed along the isobars. The flow still keeps the low pressure on its right, but it is now directed slightly towards the low pressure. There is now an ageostrophic component of the wind directed towards the low pressure.

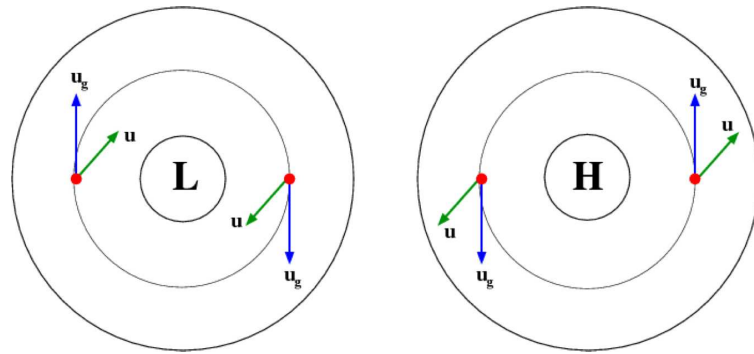


Figure 3.31: The effect of friction in high and low pressure systems in the Southern Hemisphere. The winds are now directed in towards the low pressure centre, and outwards away from the high pressure centre.

In the low pressure centre, there is now a build up of air, i.e. the flow is divergent.

$$\frac{\partial u}{\partial x} + \frac{\partial v}{\partial y} \neq 0$$

The continuity equation is concerned with the conservation of mass. The rate at which mass enters a system is equal to the rate at which mass leaves the system.

$$\frac{\partial}{\partial x}(\rho u) + \frac{\partial}{\partial y}(\rho v) = -\frac{\partial}{\partial z}(\rho w)$$

So, divergence of the horizontal winds implies a vertical motion.

Friction and the Ekman layer

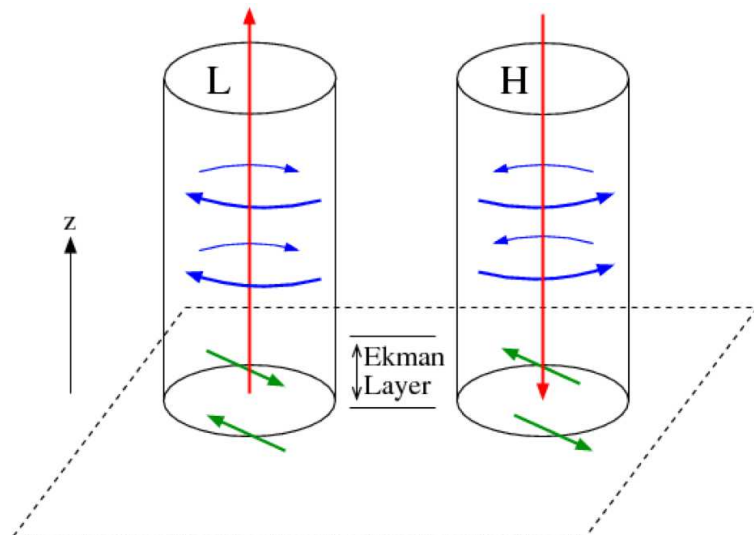


Figure 3.32: Schematic diagram showing the direction of frictionally-induced ageostrophic flow induced by low (L) pressure and high (H) pressure systems in the Southern Hemisphere.

In the low, a convergence of air induces rising motion (Ekman pumping), whereas in the high,

divergence of air out of the high in the Ekman layer induces sinking motion (Ekman suction), see Sketch 3.32.

Ageostrophic flow

In a low pressure system, Ekman pumping produces ascent, and in consequence, cooling, clouds and possibly precipitation. In a high, the divergence of the Ekman layer flow gives subsidence (through Ekman suction), which is dry, and is characterized by clear skies.

3.1.12 Summary of GFD-theory

- Generally the atmosphere and oceans are in **hydrostatic balance**.
- Horizontal differences in pressure lead to the **pressure gradient force**.
- Rotation of the Earth leads to the **Coriolis force**.
- Balance between Pressure Gradient Force (PFG) and Coriolis Force (CF) results in **geostrophic balance** - valid for large scale flow, at midlatitudes, away from the surface.
- Geostrophic winds are parallel to lines of constant pressure (isobars) and strength depends on pressure gradient.
- **Thermal wind** is the change in the winds or ocean currents strength with height and depends on the horizontal temperature gradient.
- Friction near the surface gives an ageostrophic flow which is towards the low pressure.
- This results in convergence and vertical motion.

Important equations

Momentum Equation

$$\frac{D\vec{u}}{Dt} = -2\Omega \times \vec{u} - \frac{1}{\rho} \vec{\nabla} p + \vec{\nabla} \Phi + F$$

Hydrostatic Equation

$$\frac{dp}{dz} = -\rho g$$

Horizontal components of acceleration

$$\frac{Du}{Dt} = fv - \frac{1}{\rho} \frac{\partial p}{\partial x} + F_x$$

$$\frac{Dv}{Dt} = -fu - \frac{1}{\rho} \frac{\partial p}{\partial y} + F_y$$

Coriolis parameter

$$f = 2\Omega \sin\phi$$

Rosby Number

$$R_o = \frac{U}{fL}$$

Geostrophic Winds

$$fv_g = \frac{1}{\rho} \frac{\partial p}{\partial x}$$

$$f u_g = -\frac{1}{\rho} \frac{\partial p}{\partial y}$$

Thermal Wind Relation

$$\frac{\partial u_g}{\partial p} = \frac{R}{f p} \frac{\partial T}{\partial y}$$

$$\frac{\partial v_g}{\partial p} = -\frac{R}{f p} \frac{\partial T}{\partial x}$$

Ageostrophic Winds

$$v_{ag} = -\frac{1}{f} F_x$$

$$u_{ag} = \frac{1}{f} F_y$$

3.2 Atmospheric Circulation

In this section we want to point out a few of the most important feature of the large scale atmospheric circulation

3.2.1 The Large Scale Circulation

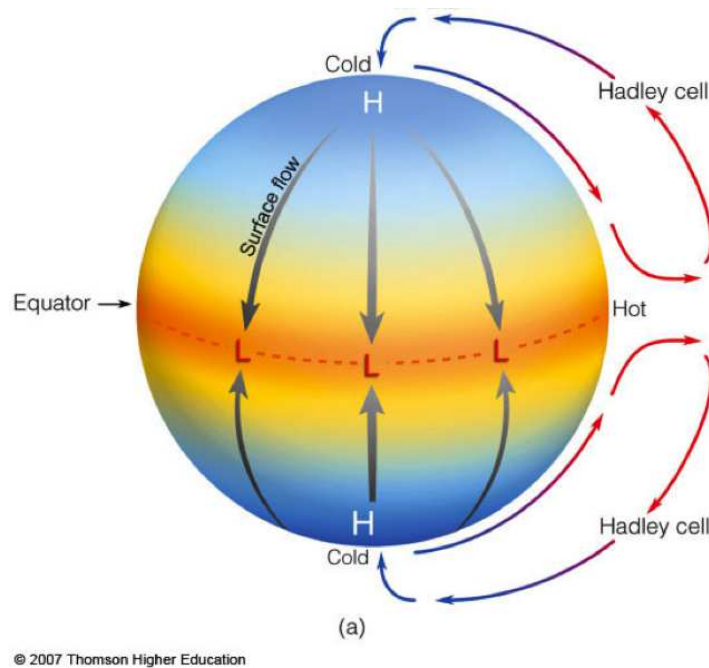


Figure 3.33: Simple sketch of the atmospheric circulation, if only the direct circulation would exist.

We can use the geofluid dynamics discussion from the previous section to get some basic understanding of how the large scale circulation should look like:

- **The Direct Circulation:** The heating by the incoming solar radiation makes the surface layer potentially buoyant. Thus the surface layer of the atmosphere would like to rise as the heated air comes less dense (*Buoyancy*). However, the air cannot rise everywhere at the time, as rising air has to come down at another place (*Conservation of Mass*). So the surface air

layer will rise where the heating is strongest and the air will come down where the heating is weakest. From this we would expect rising along the equator and sinking at the poles, see sketch 3.33. Such a cell is called a direct cell, as it is directly forced by heating and cooling.

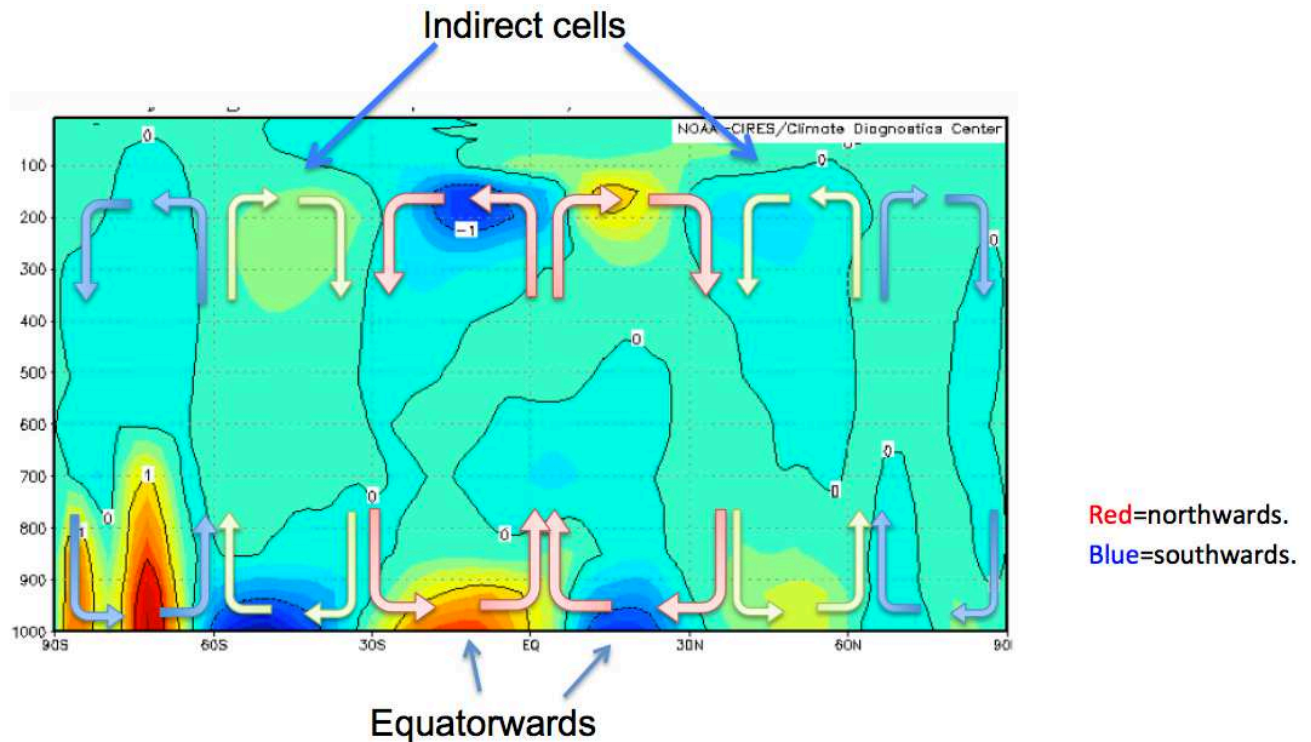


Figure 3.34: The zonally averaged annual mean meridional (North/South) wind. Red = northwards, blue = southwards. The polewards upper level winds only stretch from the equator to 30 degrees. The red vectors indicate the direct tropical cells, the blue vectors the direct polar cells and the green vectors the indirect extra-tropical cells.

- The Coriolis Effect:** The rotation of the earth does not allow for complete direct cells reaching from the equator to the poles. The air, that is set in motion by the direct forcing of the heating and cooling is starting to move poleward or equator-ward, but is then deflected by the Coriolis force, which leads to a breakdown of the direct cell after a certain distance. Fig. 3.34 illustrates that the poleward movement from the equator at higher levels stops at about 30° in both hemispheres. The return flow near the surface also starts at about 30°. Note, that the figure does not show a clear picture of a meridional circulation near the poles, but some indication of circulation cell from the poles to about 60° is visible in both hemispheres.

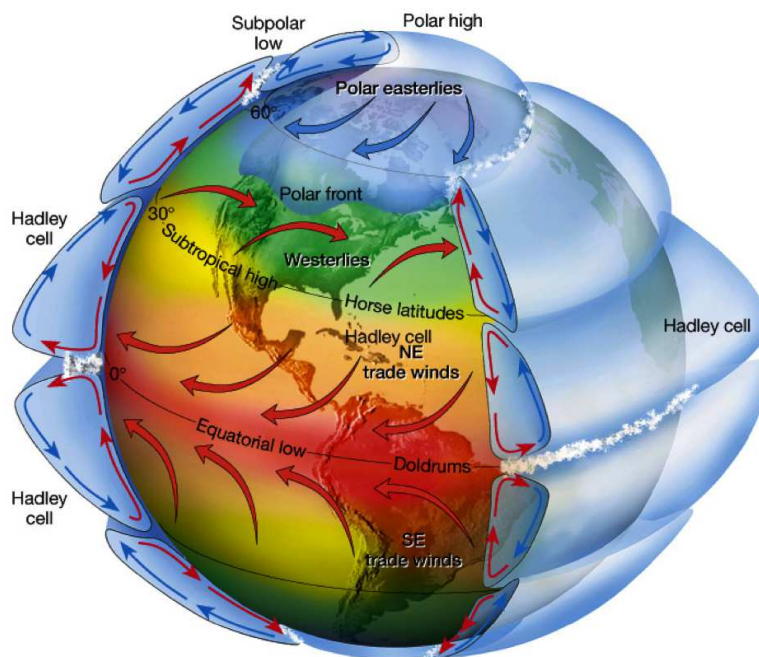


Figure 3.35: Sketch of the main cells of the general atmospheric circulation.

- The Indirect Circulation:** The upper poleward branch of the equatorial cells is deflected to the east and the surface equator-ward branch of the polar cells is deflected to the west. These two opposing wind directions lead to the indirect circulation cells between the equatorial and the polar cell, which rotate in the opposite direction to the direct cells, see Fig.3.35. These indirect cells are in the midlatitudes between 30° to 60° .

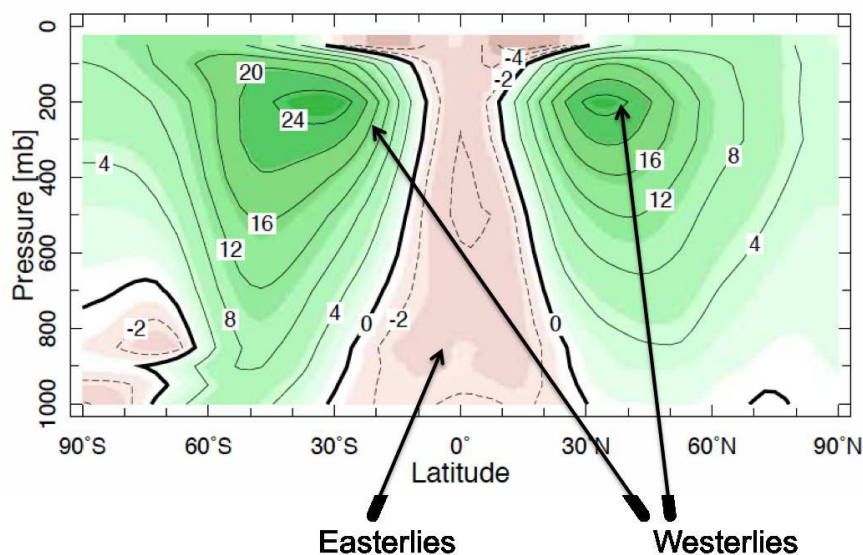


Figure 3.36: the mean zonal winds showing the upper levels subtropical Jets. In m/s; positive is westerly winds.

- The upper level Subtropical Jets:** From the Geofluid Dynamics section we know that the combination the meridional temperature gradient from the poles to the equator cause

upper level pressure gradients (*Hydrostatic balance*) and the pressure gradient and Coriolis force lead to the *geostrophic balance* winds. The zonal winds increase with height to form the upper level subtropical Jets as result of the *Thermal Wind Balance*.

- **The Turbulent and Chaotic Circulation:** Although some large scale structure exist with some mean flow directions, the atmospheric circulation has quite chaotic behavior. Waves, propagating weather systems and chaotic behavior are some of the main characteristics of the circulation. In particular in the indirect cells in the extra-tropics. The chaotic behaviour of the atmospheric circulation is a characteristic nature intrinsic to the atmospheric circulation and it not caused by changes in boundary conditions (see later in the variability chapter and the Lorenz model section).

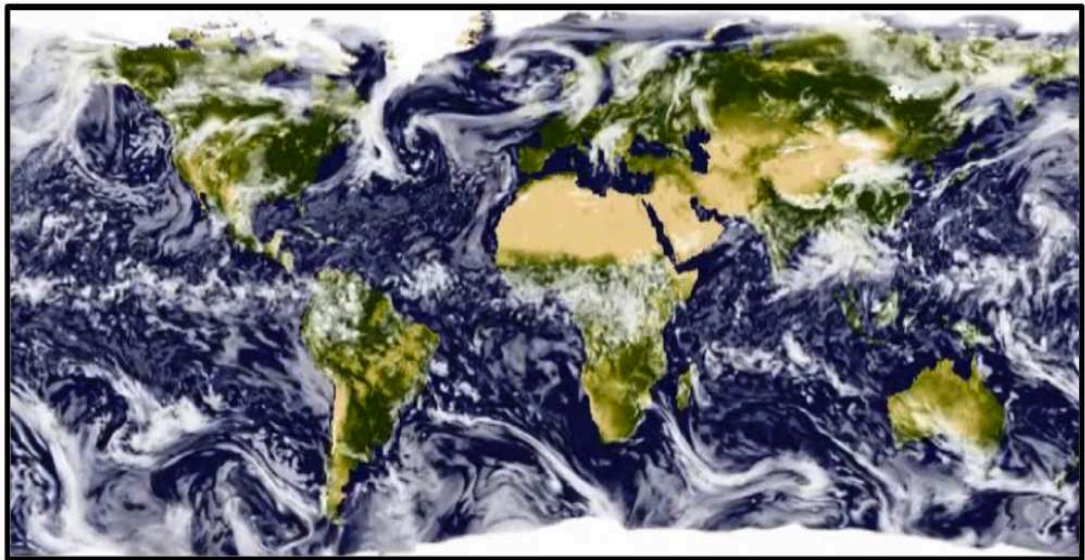


Figure 3.37: A snap shot of clouds in an atmospheric model simulations.

3.2.2 The Hadley Cell (the Direct Tropical Circulation)

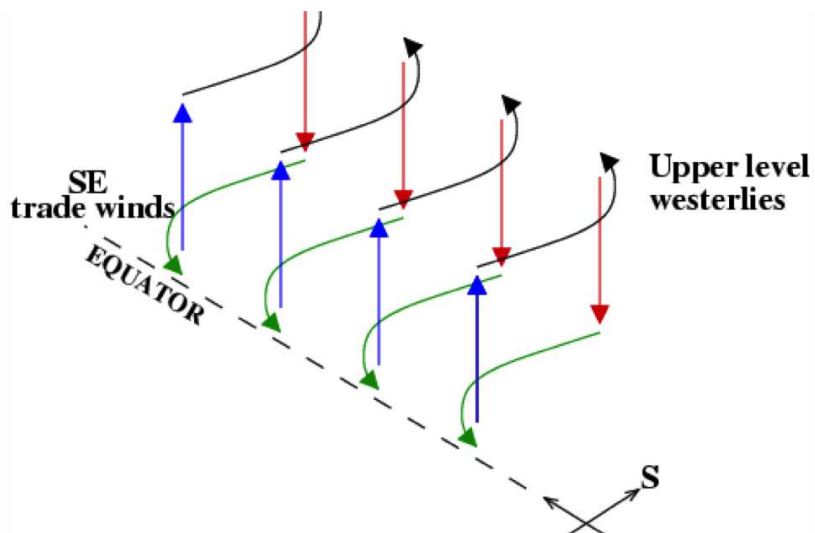


Figure 3.38: Schematic of the Hadley circulation (only the SH part; there is a mirror image circulation in the NH). Upper level poleward flow induces westerlies and low level equatorward flow is easterly.

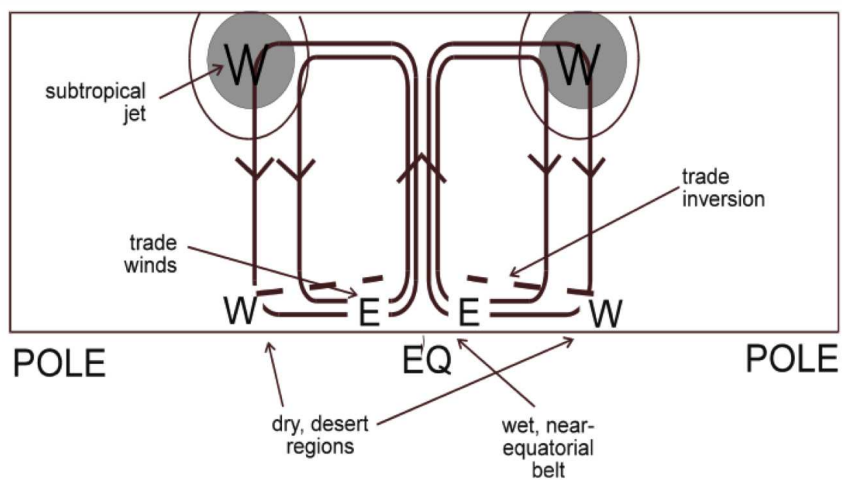


Figure 3.39: Schematic diagram of the Hadley circulation and its zonal flows and surface circulation.

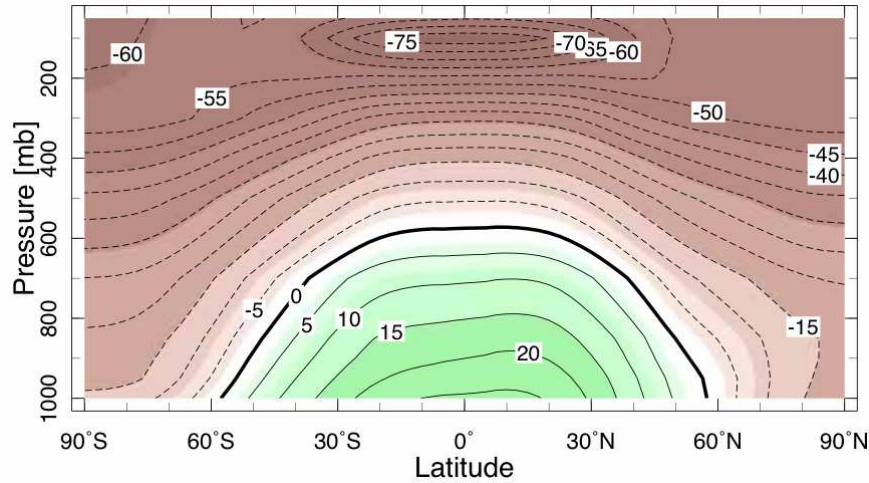


Figure 3.40: The zonal mean temperatures. Note that is meridional temperature gradient is relatively weak within the tropics, due to the very effective heat transport by the Hadley cell.

3.2.3 The Ferrel Cell (the Indirect Extra-tropical Circulation)

In the Geofluid Dynamics section we have seen that the effect of the Coriolis acceleration is very important for the flow of the atmosphere in the higher latitudes (see Coriolis force section). The strong meridional temperature gradient in the midlatitudes gives us, through thermal wind balance, the upper level jet. This jet is unstable to small perturbations and we get the generation of eddies (high and low pressure systems). These eddies dominate the circulation in the indirect Ferrel Cell and they transport heat polewards in the midlatitudes.

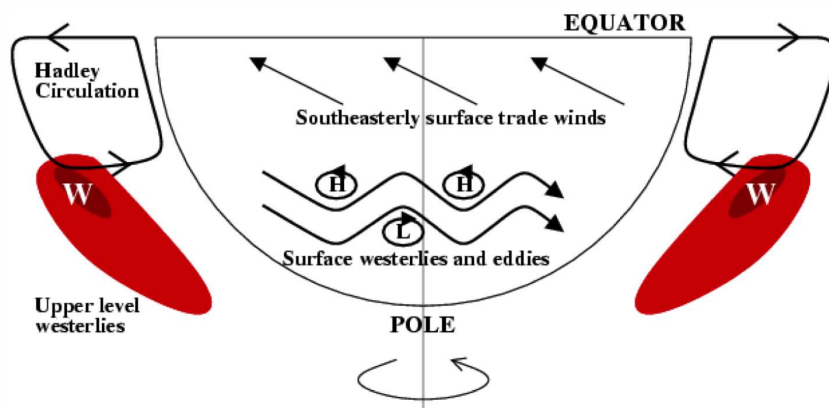


Figure 3.41: Schematic of the the circulation in the direct (Hadley) cell and the indirect (Ferrel) cell in the higher latitudes. The winds are steady and easterlies in the direct cell, and chaotic and westerlies in the indirect cell.

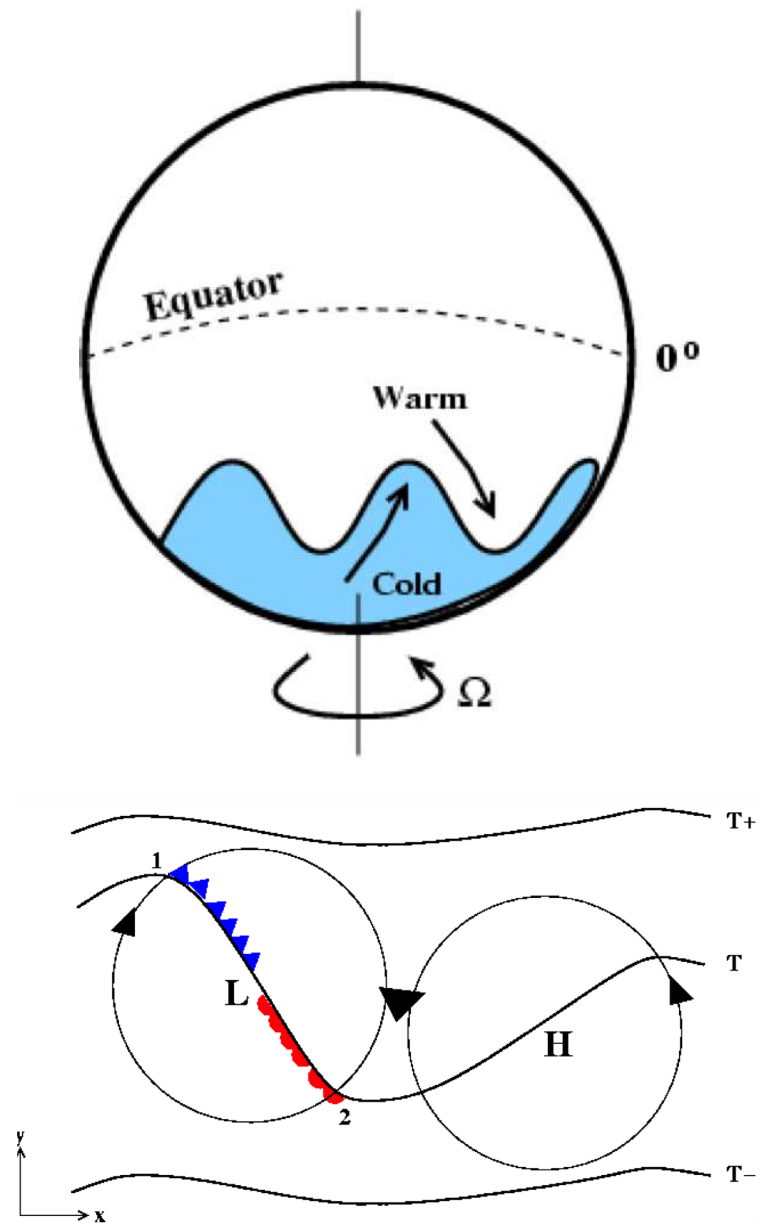


Figure 3.42: Illustration of the variability and waves in the extra-tropical Ferrel Cell. The waves and low- and high-pressure weather systems lead to exchange (mixing) of cold and warm air.

3.3 The Oceans

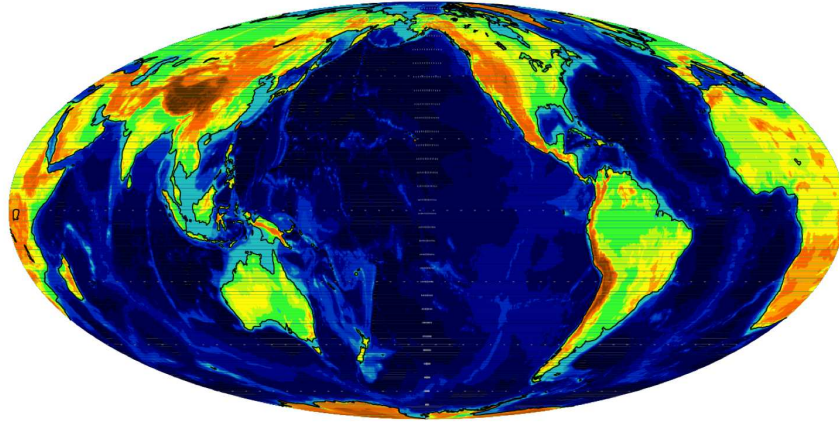


Figure 3.43: 2/3 of the globe is oceans

Two thirds of the earth surfaces are oceans and in terms of heat stored in the climate system, the oceans are the only thing that matters, as the oceans heat capacity is much larger than that of the atmosphere and land together. In addition to the heat storage the oceans are also the main source for atmospheric water vapour, which is the most important greenhouse gas and it is the source for rainfall globally. So in terms of the earth global climate the oceans are a central element.

The ocean dynamics follow the same geofluid dynamics as the atmospheric circulation, but the oceans have their own characteristics that are quite different from that of the atmosphere in many ways. In addition to the momentum equations the tendency equations for the density, temperature and salinity are important for the oceans, see eqs. in Fig. [3.44].

Ocean dynamics

Figure 3.44 displays four key equations for ocean dynamics, each with terms highlighted and labeled:

- Momentum:** $\rho \frac{D\vec{u}}{Dt} = -2\rho \cdot \Omega \times \vec{u} - \vec{\nabla} p + \rho \vec{\nabla} \Phi + F$. Labels: Coriolis forcing (blue), Pressure gradient force (purple), gravity (green), friction (red).
- Density:** $\frac{D\rho}{Dt} = -\rho \vec{\nabla} \cdot \vec{u}$. Label: Convergence of mass leads to a increase in mass (pressure) (black).
- Temperature:** $\rho \frac{D\Theta}{Dt} = -\vec{\nabla} \cdot J_{\Theta}^{iurb} - \vec{\nabla} \cdot \frac{J_{rad}}{c_p}$. Labels: Sensible heat (blue), radiation (purple).
- Salinity:** $\rho \frac{DS}{Dt} = \vec{\nabla} \cdot J_s^{iurb}$. Label: Turbulent transport (blue).

Figure 3.44: Equations important for the ocean dynamics. Tendency equations for the momentum, density, temperature and salinity

Some difference between the atmosphere and oceans should be pointed out for a start:

- The oceans are an incompressible liquid (not an ideal gas as is the atmosphere). Thus the density of the oceans water does not (not very much) depend on the pressure, as it does in the atmosphere.
- Water is about 1000 times denser than air: $\rho_{ocean} \approx 1000 \times \rho_{atmos}$.
- Water has a four times larger specific heat capacity ($J/K/kg$) than air. Combined with the much larger density, we have a much larger heat capacity per volumen (or column). Thus for the same amount of heat forcing the oceans will change much slower than the atmosphere.
- The oceans are forced from the top; the atmosphere is forced from the surface below. This has important implication for the mixing of the oceans.
- The oceans are forced by atmospheric winds. The oceans currents are mostly (at the surface) initiated by the atmospheric winds. In contrast, atmospheric winds are initiated by temperature contrast (e.g. heating at the surface or meridional temperature gradients).
- The oceans have lateral boundaries. we have essentially three major ocean basins, that are well separate. The gateways between the ocean basins are relatively small (e.g. Indonesian through flow or Drage passage.).
- The oceans do not have latent heating by water phase transitions (e.g. liquid to water vapor and vice versa). The latent heating in the atmosphere drives the atmospheric circulation to some part. This additional driver is missing in the oceans.
- The oceans have salinity affecting the density of the oceans. Salinity affects the water density and therefore affects the deep ocean circulation and the mixing at the surface.
- The oceans have floating sea ice. The sea ice over the oceans leads to a dramatic change in the heat and water vapor exchange between the atmosphere and the oceans.

In the following sections we will discuss the oceans *Stratification*, the characteristics of *Ocean Weather*, the *Surface Circulation* caused by wind stress, the vertical motions in the oceans by

Upwelling and Deep Convection. We further look at the deeper *Thermohaline Circulation*, the time scales of the *Deep Ocean* and finally we discuss the some characteristics of the *Sea Ice*. We will try to understand the main characteristics of the oceans by the dynamics controlling the state of the oceans.

3.3.1 Ocean stratification

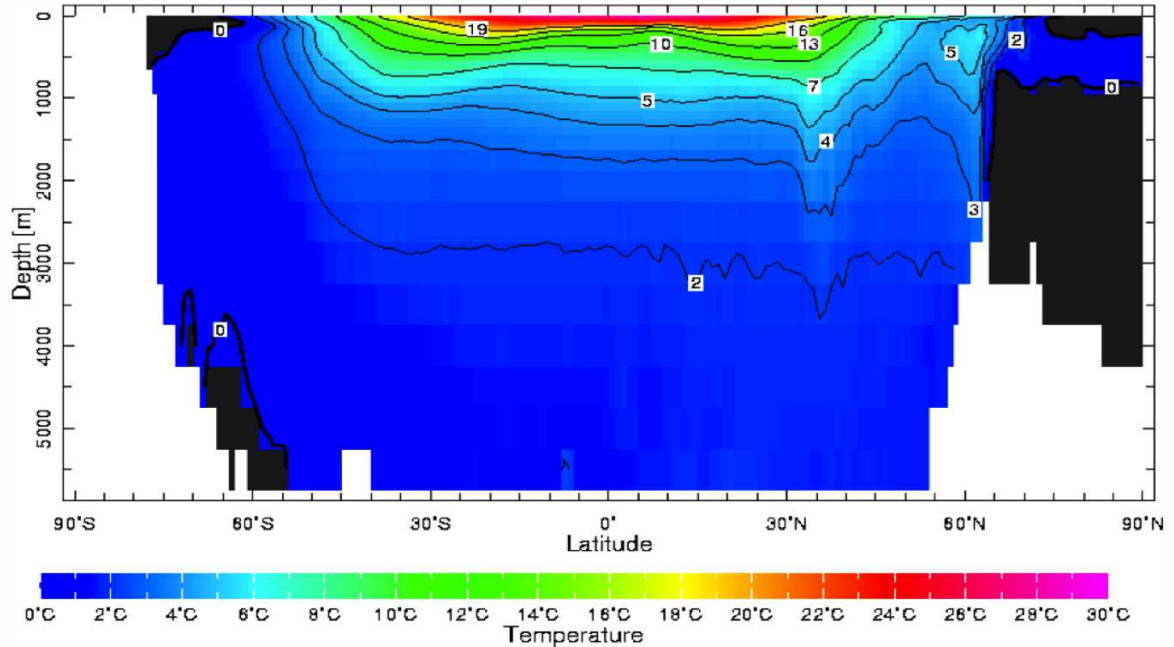


Figure 3.45: Annual-mean cross-section of zonal-average temperature [$^{\circ}\text{C}$] in the world's oceans - the whole water column. Data from the Levitus World Ocean Atlas 1994.

If we take a look at a vertical cut through the all oceans zonally average temperatures from the South Pole to the North Pole, we can see that most of the ocean are about $3 - 4^{\circ}\text{C}$ cold, see Fig. 3.45. The warm waters in the subtropics and tropics do not reach deep, but are swimming on top on the denser cold waters like a thin lens of warm waters. This is a signature of the oceans *Stratification*: Building layers, which lay on top of each other.

If we compare the atmospheric temperature profiles with those of the ocean (Fig. 3.46) we note some remarkable differences:

- The atmospheric temperature profile is dominated by the pressure effects (adiabatic cooling), see Fig.3.46. The temperature is decreasing with height due to expansion by decreasing pressure. This effect is not dominant in the oceans. In the oceans adiabatic cooling effect is weak and not visible in the temperature profile.
- A better way of understanding the dynamics (thermodynamics) of the vertical profile is by analysing the *potential temperature* profile. This excludes the pressure effect, see Fig. 3.10. Potential temperature in the atmosphere is very different from the in situ temperature, as the

atmosphere expands/contracts a lot by pressure changes. Potential and in situ temperature in the ocean are very similar, as ocean water does not expand/contract much by pressure changes.

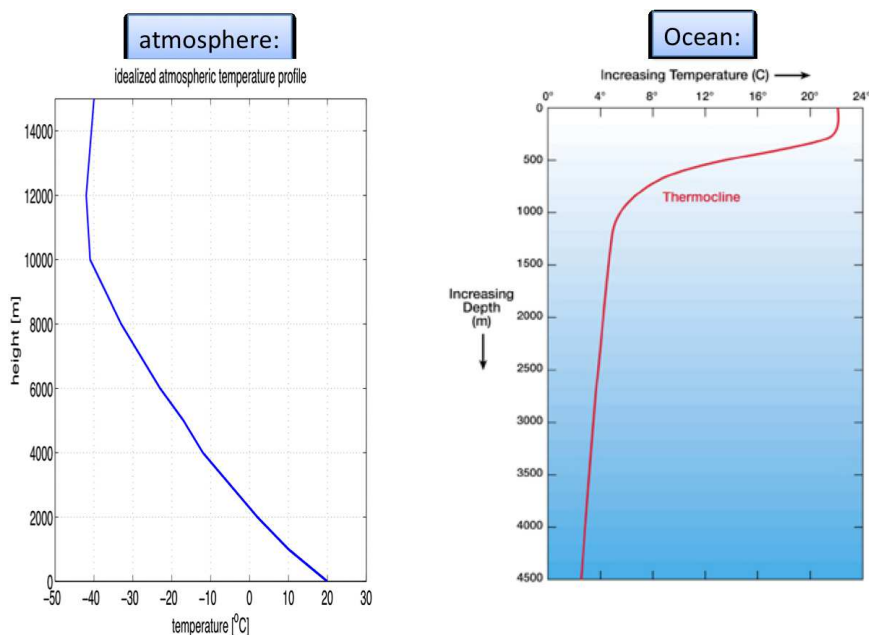


Figure 3.46: Typical temperature profiles of the atmosphere (left) and the oceans (right).

Seawater density: To understand what controls the stratification of the oceans it is important to understand how the density of sea water depends on state of the ocean (in general this is called the thermodynamic equation of state). A few points should be noted here.

- Seawater density is mostly a function of T and S. It does not depend much on pressure (incompressible) as it does for the atmosphere.
- The density function is non-linear in respect to T and S. This is different from the very simple ideal gas law for the atmosphere.
- Temperature increase decreases density. Figure 3.47 show how the density of sea water depends on temperature and salinity. Note, that the gradient of the density as function of temperature is changing. Note, also that the density has minimum that is depending on temperature and salinity. Fresh water (salinity=0) has the minimum at about $4^{\circ}C$, but salty sea water has the minimum at $-1.7^{\circ}C$. Thus sea water at the freezing point is the sea water with the highest density.
- Salinity increases density. Salty and cold water is the most dense sea water in the world oceans.
- In the linear approximation the density regression coefficient to salinity (in Practical Salinity Units (PSU) (β_S) is larger (in amplitude) than that of the regression coefficient to temperature (in K) (α_T), see example below. However, temperature variability dominates the density variability by about a factor of 2, because temperature values vary over a larger range ($dT \sim 20K$) than salinity ($dS \sim 2PSU$).

- A 20K warmer sea water, for instance, has a buoyancy force equivalent to about the weight of 4kg per m^3 relative to its surrounding colder water ($4^\circ C$).
- The ocean stratification follows mostly the temperature profile. In Figure 3.48 the surface density, temperature and salinity are shown. We can see that the density mostly follows (inverse) the temperature distribution. Low density regions typically warm regions (e.g. tropics) and high density regions are typically cold (polar) regions.
- The salinity profile is mostly destabilising the stratification.

The seawater density is a non-linear function of T and S: $\rho = \rho(T, S)$. We can have a look at an example in which we linearize the function. Linear approximation:

$$\rho \approx \rho_0 + \alpha_T \cdot (T - T_0) + \beta_S \cdot (S - S_0) \quad (3.38)$$

For example we can pick a reference point: $T_0 = 15^\circ C, S_0 = 35PSU$. This is near the point in the right panel of Figure 3.47. Here the linear gradients are:

$$\implies \alpha_T \approx -0.2kg/m^3 \cdot 1/K$$

$$\implies \beta_S \approx +0.8kg/m^3 \cdot 1/PSU$$

For a given $dT = 20^\circ K$ we can compute the change in density: $\rightarrow d\rho \approx \alpha_T \cdot dT = 4kg/m^3$

For $dS = 2PSU \rightarrow d\rho \approx \beta_S \cdot dS = 1.6kg/m^3$

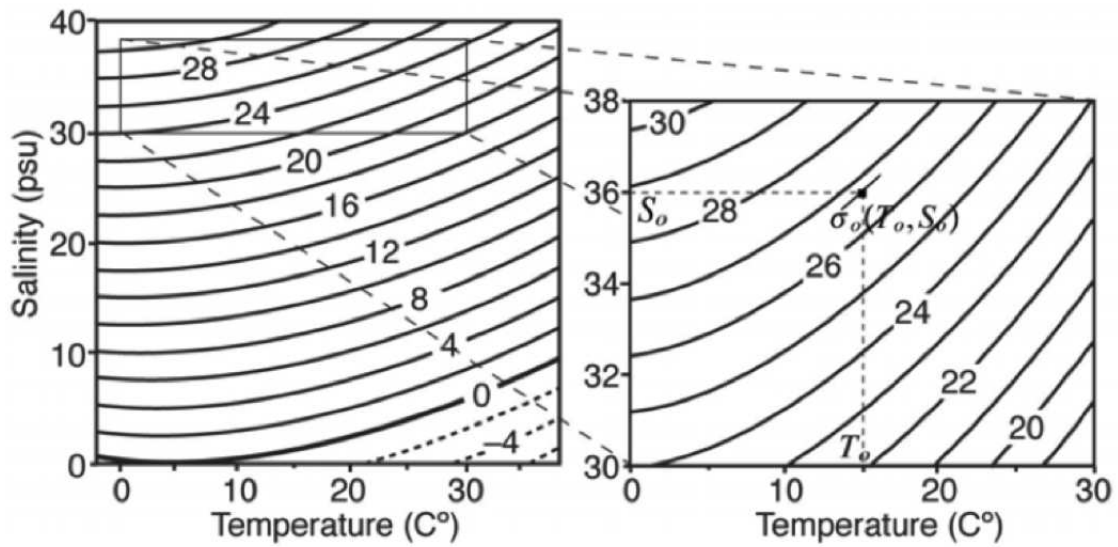


Figure 3.47: Contours of seawater density anomalies, $\sigma = \rho - \rho_0$ in kgm^{-3} , plotted against salinity ($\text{psu} = \text{gkg}^{-1}$) and temperature ($^{\circ}\text{C}$) at the sea surface. Note that sea water in the open ocean has a σ in the range 20 to 29 kgm^{-3} , a T in the range 0-30 $^{\circ}\text{C}$ and a S in the range 33-36 psu. The panel on the right zooms in on the region of oceanographic relevance. An approximation to the equation of state in the vicinity of the point $\sigma_0(T_0, S_0)$, is discussed in the text.

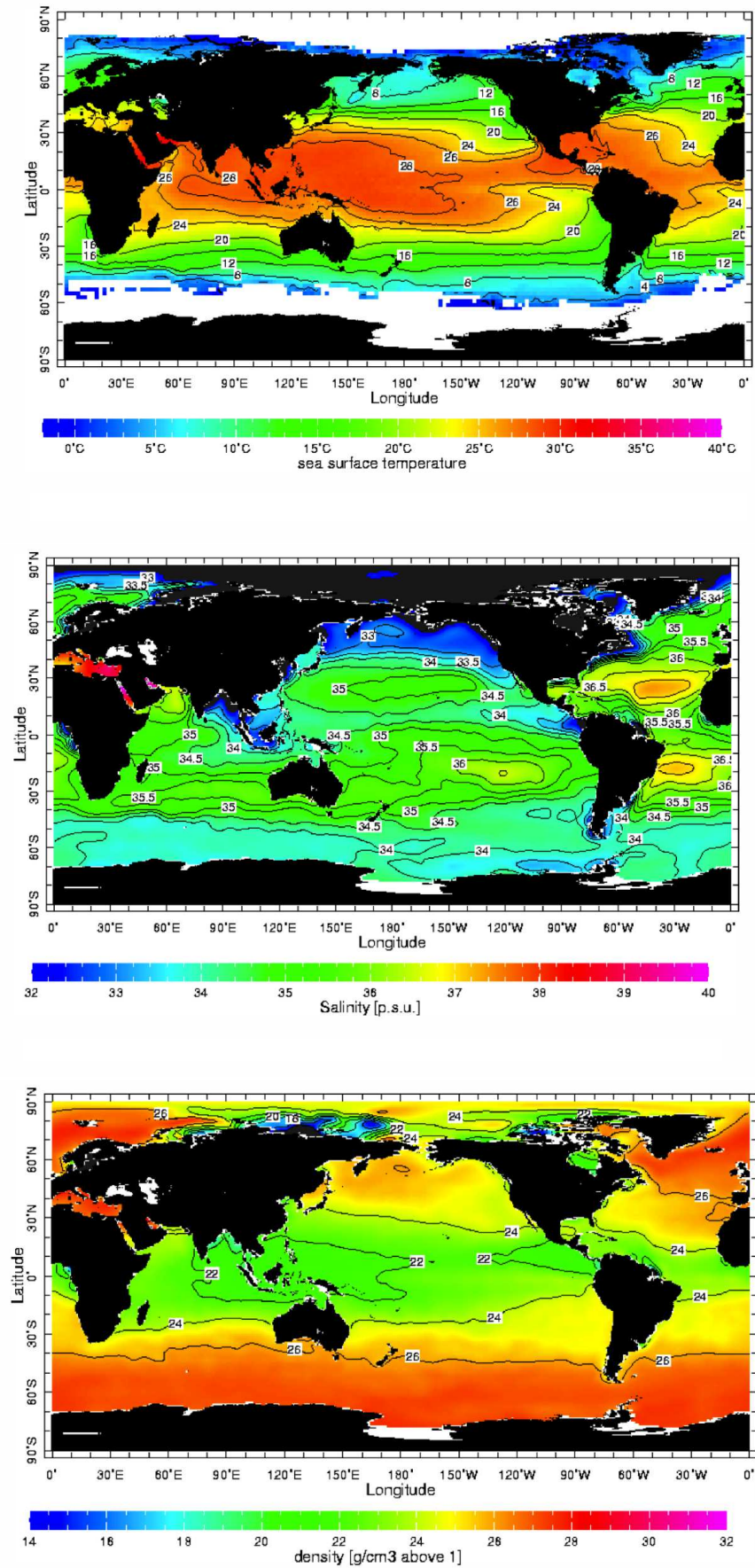


Figure 3.48: Upper: Jun./Jul./Aug. sea surface temperature (SST) from the Comprehensive Ocean-Atmosphere Data Set (COADS). Middle: The annual mean salinity in psu. From Levitus World Ocean Atlas, 1994. Lower: The annual mean density, σ . From Levitus World Ocean Atlas, 1994.

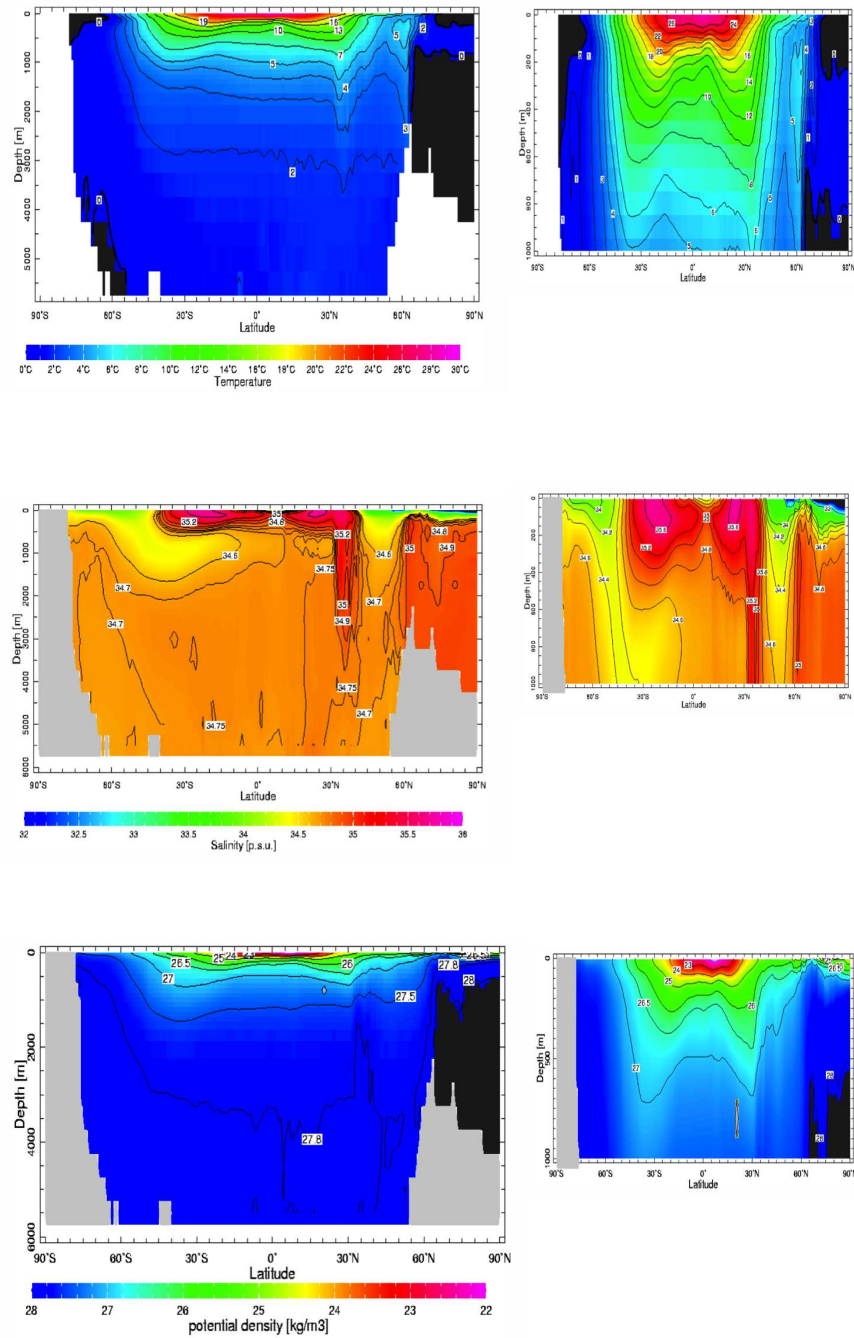


Figure 3.49: Upper: Annual mean cross-section of zonal average temperature [$^{\circ}\text{C}$] in the world's oceans - the whole water column. Note the different contour interval in the right-hand plot. Middle: Annual mean cross-section of zonal average salinity [psu] in the world's oceans - the whole water column. Note the different contour interval in the right-hand plot. Lower: Annual mean cross-section of zonal average $\sigma = \rho - \rho_0[\text{kgm}^{-3}]$ in the world's oceans - the whole water column. Note the different contour interval in the right-hand plot. All data from the Levitus World Ocean Atlas 1994.

Salinity Climatology

- Salinity is largest in regions with strong evaporation and weak precipitation (river inflow) (e.g. subtropics or Mediterranean Sea).
- Salinity in the deep ocean is smaller than at the surface, because these water masses come from regions with cold temperatures.
- The strong salinity at about 30°N comes from the Mediterranean Sea.
- The fresh water (small salinity) at 50-60°N is only in the Pacific.

Ocean mixed layer depth

- The depth of mixing from the surface layer depends on two factors: the strength of the mixing force (wind stress) and the strength of the buoyancy force of the lighter surface layer.
- Regions with strong winds have deeper mixed layer depth.
- Regions with cold or salty surface water have deeper mixed layer depth.
- Cold seasons have denser surface layers and stronger winds and therefore deeper mixed layer depths.

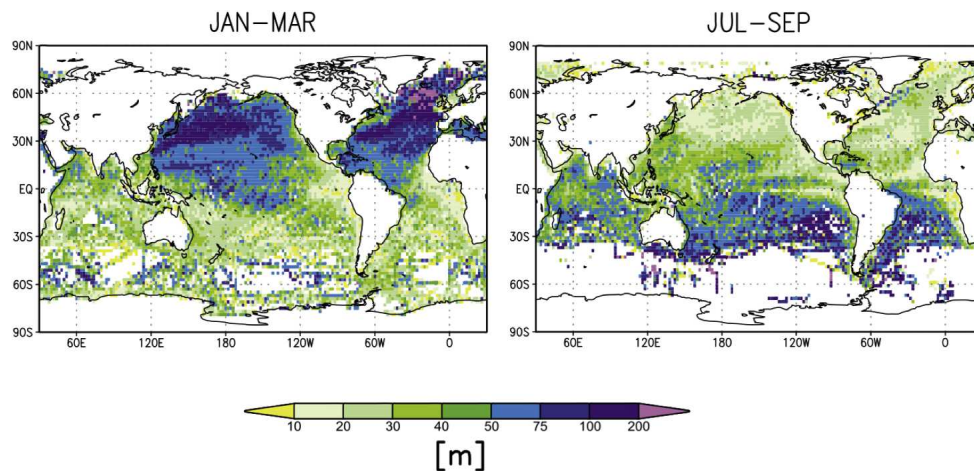


Figure 3.50

Ocean Stratification

Main cause:

- Buoyancy (gravity): Warm water float on top of the cold water. Cold waters sink underneath warm waters. See also later for deep ocean convection.

- Surface heating and cooling: Most of the surface water is much warmer than the most dense water. In cold polar regions dense cold water is formed that sinks to the ocean floors. See also later for deep ocean convection.

3.3.2 Surface (wind driven) Circulation

- Ocean circulations can be split into two parts: Wind driven and Thermohaline circulation.
- The two parts are not independent of each other and can not be totally separated from each other.
- Wind driven circulation is caused by atmospheric wind stress and is a surface circulation.
- The friction of the atmospheric winds (wind stress) causes the ocean surface to move, but not always in the same direction as the winds.
- Ocean currents are constrained by continuity, boundaries, gravity and coriolis forcings.
- The large scale surface ocean currents mostly follow the large scale atmospheric winds, as far as possible (e.g. boundaries and mass conversation).
- Ocean surface currents are in the order of 1cm/s to 1m/s.

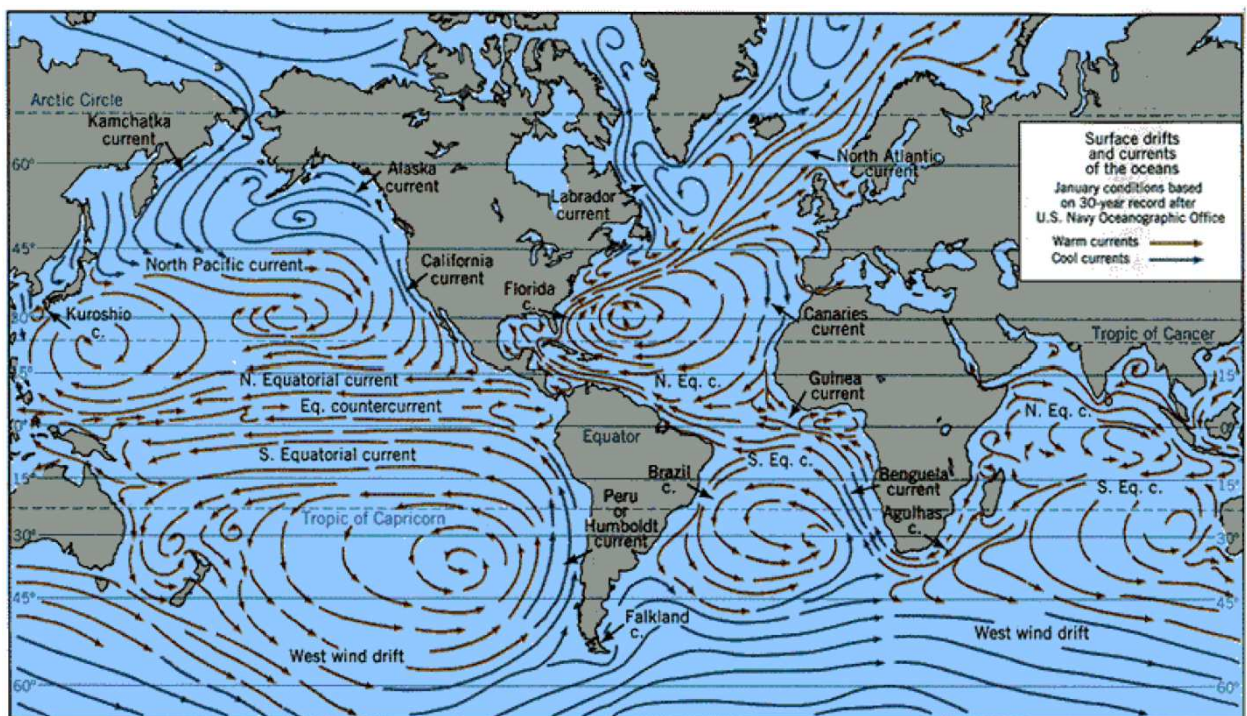


Figure 3.51: Ocean surface currents

Main cause:

- Friction by atmospheric winds: Unlike the atmosphere, which is set into motion by temperature (heating) differences, the oceans are set into motion by the friction force of the atmospheric wind stress. the ocean circulation caused by density differences is called thermohaline circulation.

- Continuity: Winds may blow the ocean waters against or away from barriers (coast lines). This causes the ocean surface currents to be deflected, mostly horizontally, but sometimes also vertically (downwards). Coriolis force also leads a deflection of the large scale surface currents from the the main wind direction.

3.3.3 Upwelling and Convection

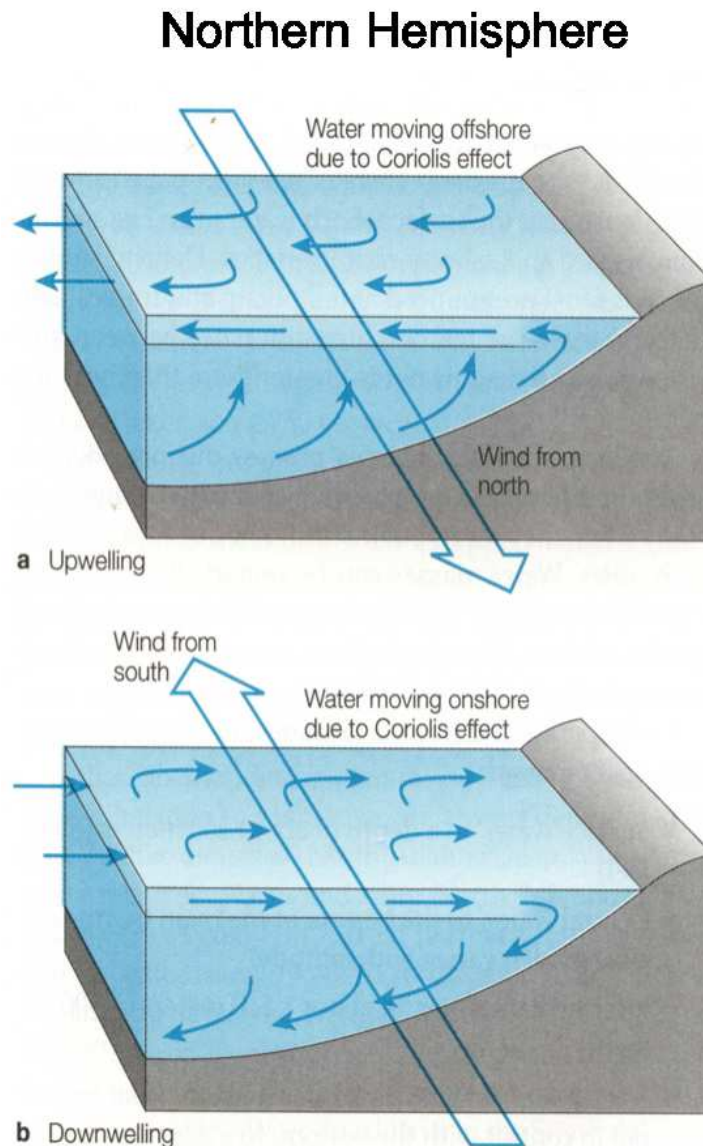


Figure 3.52: Upwelling in NH

Vertical motions in the oceans are the exceptions. Mostly the ocean water circulate horizontally. Some points:

- Continuity causes ocean circulation to recirculate in large gyres.
- Boundaries, strong divergence/convergence or weak stratification can sometimes cause vertical motions.

- Vertical motion caused by wind induced surface currents are called Upwelling/Downwelling.
- Vertical downward motion caused by buoyancy (weak stratification) by cold and salty waters is called deep convection. It is the oceanic equivalent to atmospheric convection, just the other way around.

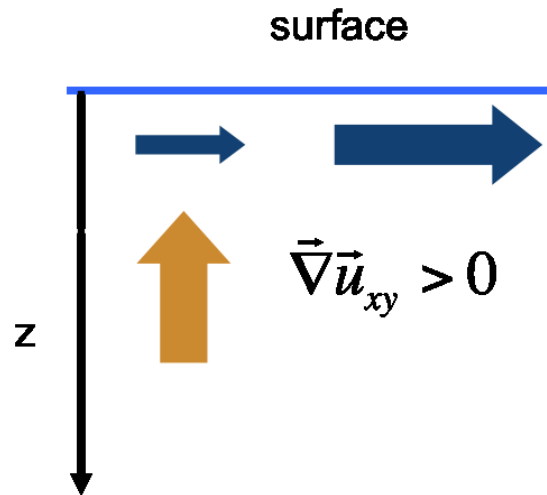


Figure 3.53: Upwelling along a coast line to left hand side.

- Winds parallel to coastlines force ocean surface currents perpendicular to the coast, due to the Coriolis forcing.
- Continuity forces vertical motion.
- Upwelling: surface currents moving away from the coast, cause subsurface water to rise.
- Downwelling: on shore currents force surface water to subduct.
- This vertical circulation is mostly constrained to the upper few hundred meters.
- Coastal upwelling exists on most coasts, in particular along the west coast of continents with deep coastal waters (e.g. America or Africa).
- Australia's west coast is something of an exception, due to a warm coastal current coming from the North.
- Wind forced upwelling can also exist along the equator, due to divergence of the Coriolis force along the equator, see Fig. 3.19.

Coastal upwelling

- Coastal upwelling brings subsurface waters to the surface that are often rich in nutrition.
- Upwelling regions are therefore rich in bioproductivity.
- Coastal upwelling brings cold subsurface waters to the surface that are often more than 10 degrees colder than the surface waters.

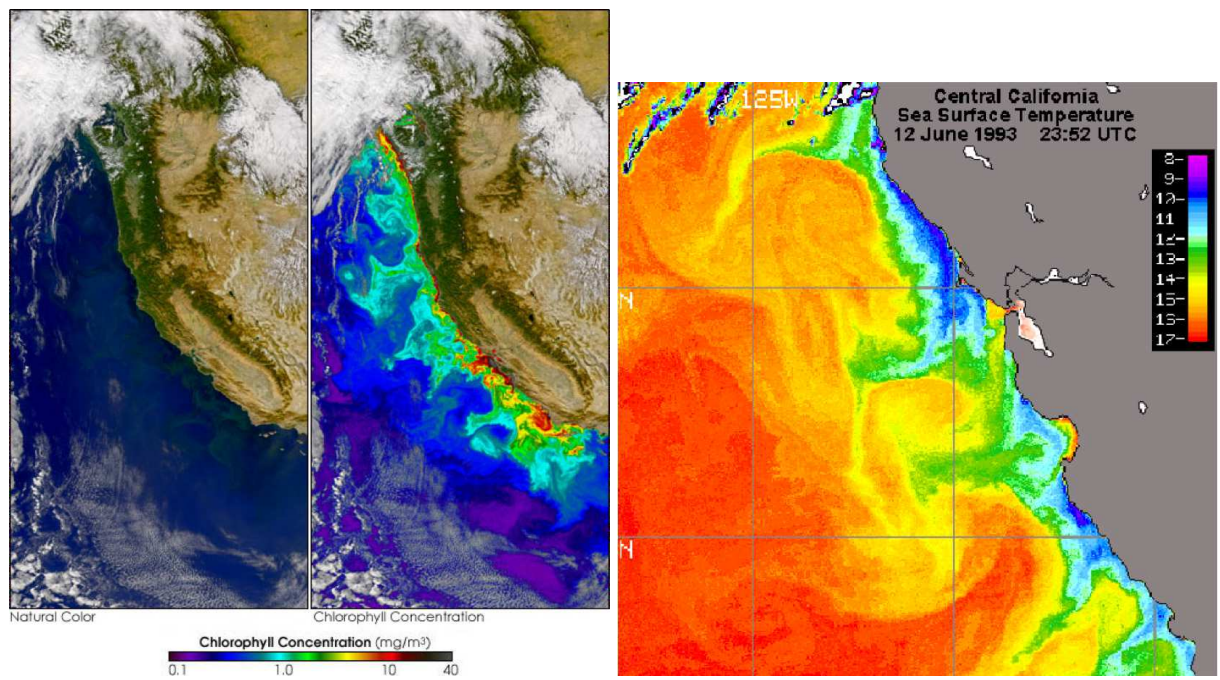


Figure 3.54: Coastal upwelling along the coast of California. Left: Chlorophyll as an indicator of bio production in the cold upwelling waters. Right: sea surface temperature.

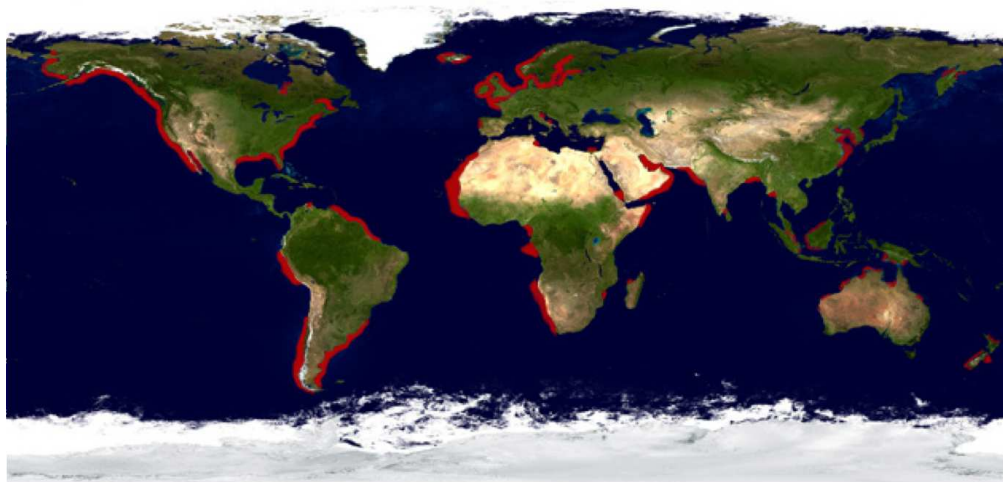


Figure 3.55: Coastal upwelling regions through out the global oceans.

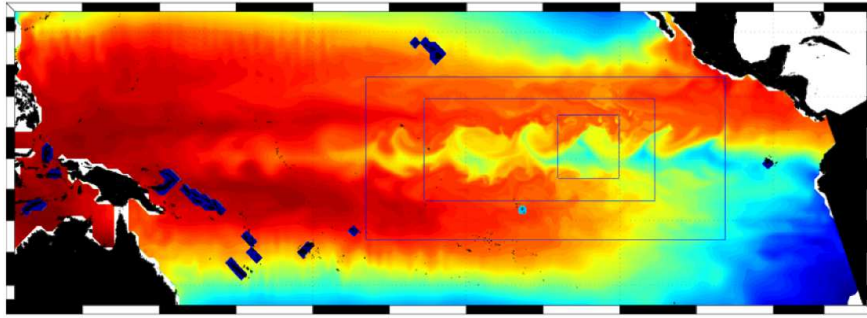


Figure 3.56: Equatorial upwelling, caused by the divergence of the Coriolis force along the equator, see Fig. 3.19. The figure shows sea surface temperatures.

Upwelling around Antarctica

Winds circling around Antarctica cause the Antarctic Circumpolar Current (ACC) and large scale upwelling that reaches more than 1000m deep.

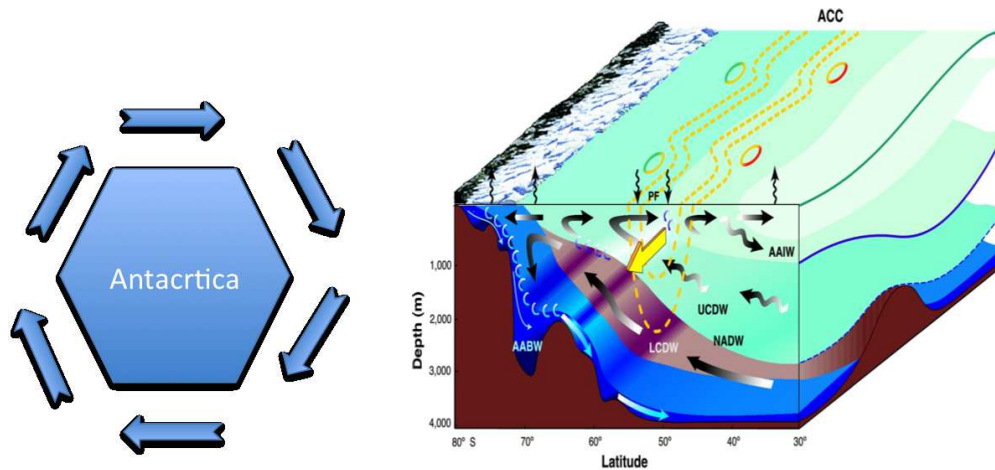


Figure 3.57: Upwelling around Antarctica

Deep ocean convection

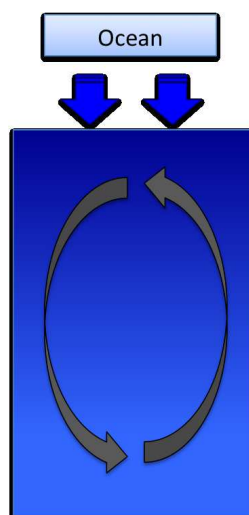


Figure 3.58: Deep ocean convection by cooling at the surface.

- Surface cooling is much more efficient in mixing the ocean to deeper levels.
- Polar regions are the regions where deep ocean mixing occurs, because ocean surface water is cooled here and the density differences between deep cold ocean waters and surface ocean waters are small.
- Deep ocean water comes from the polar regions. It is formed in the winter seasons, when surface waters are coldest.
- Formation of sea ice produces more salty surface water, as salt is not kept in ice crystals. This supports deep ocean mixing, as the water becomes denser by the salinity.
- The regions where deep ocean waters are formed are very small compared to the size of the global oceans.
- The regions where deep ocean waters resurface are not quite clear, but are probably more wide spread.

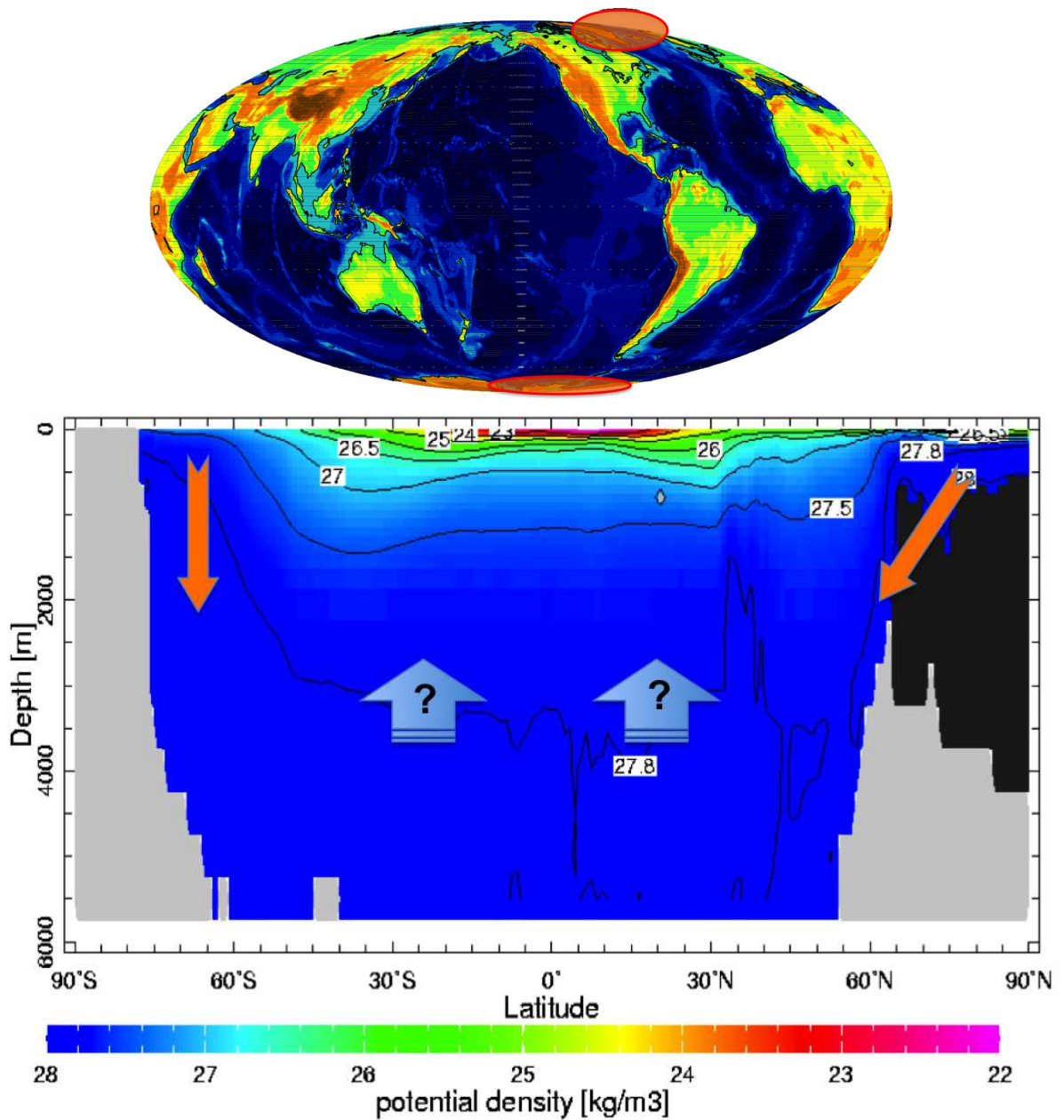


Figure 3.59: Deep ocean convection regions:

Upwelling

Main cause:

- Coastal winds
- Coriolis force
- Continuity

Deep convection

Main cause:

- Buoyancy
- Cooling
- Sea ice formation

3.3.4 Ocean Weather

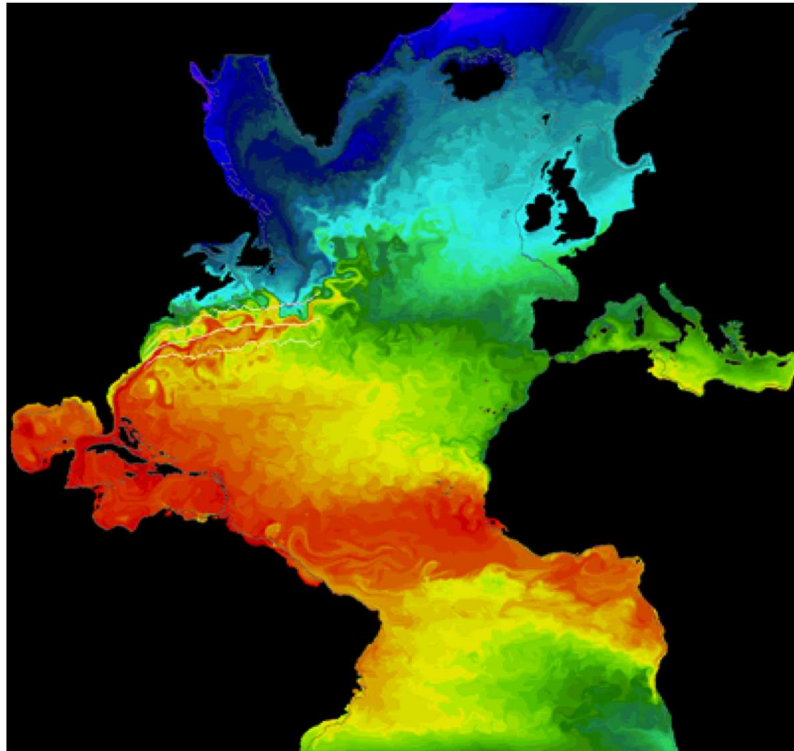


Figure 3.60: Snapshot of sea surface temperature

Momentum equations:

$\rho \frac{D\vec{u}}{Dt} = -2\rho \Omega \times \vec{u} - \vec{\nabla}p + \rho \vec{\nabla}\Phi + F$

Figure 3.61

- The relative strength of the forces in the momentum equations change compared to the atmosphere, due to the much larger density in the oceans.
- Coriolis, inertia and gravity are now more dominant.

- The lateral scale of geostrophic (weather) variability is decreasing significantly.
- Time scales are much longer (\sim months) due to larger density (inertia) and larger heat capacity.

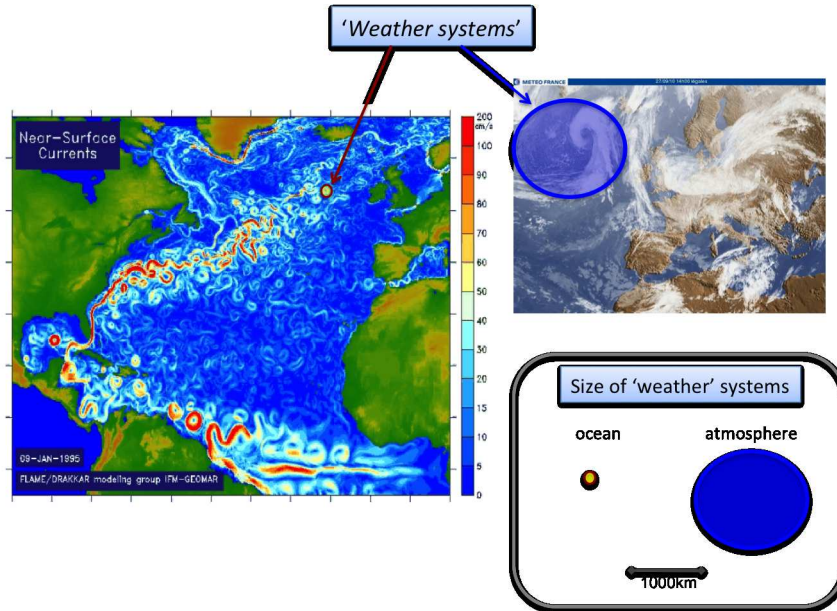


Figure 3.62: Weather systems

3.3.5 Thermohaline (geostrophic) Circulation

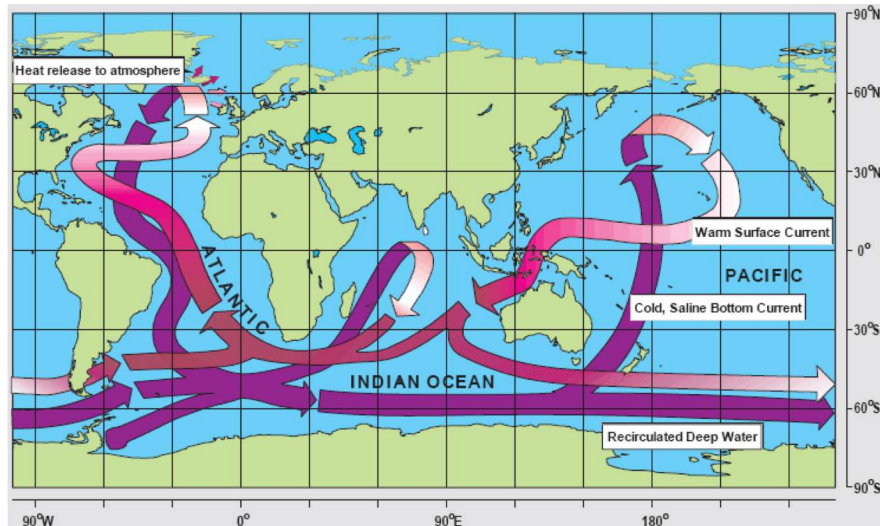
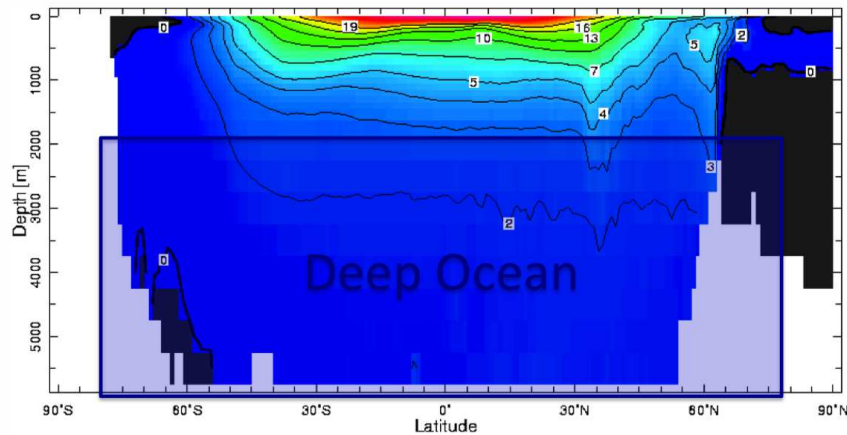


Figure 3.63: Sketch of the oceans thermohaline circulation.

- As in the atmosphere most of the oceans interior circulation is in geostrophic balance. $2\rho \cdot \Omega \times \vec{u} = -\vec{\nabla} p$

- The Rossby number (ratio inertia/coriolis) is $\ll 1$ for large scale ocean motions. $R_o = \frac{U}{fL} = \frac{0.01m/s}{5 \cdot 10^{-5} 1/s \cdot 10^6 m} = 10^{-3} \ll 1$
- Geostrophic circulation is due to the balance of coriolis and pressure gradients.
- Low and high pressure in the oceans is related to difference in sea level height.
- As in the atmosphere stronger gradients in sea level (pressure) cause stronger currents (e.g. Antarctic Circular Polar current (ACC) or Gulf Stream), see Fig. 3.26.
- Geostrophic balance holds for most of the oceans, but not along the equator or at coastal lines.
- In the climate context the thermohaline circulation is important for ventilating the deep oceans. It is the main cause for the mixing of the deep oceans. It transports heat and material (e.g. CO_2) into the deep ocean or brings deep ocean waters onto the surface and into contact with the atmosphere (e.g. outgassing of CO_2)

3.3.6 Deep Ocean Time Scales



Time scales - ACC circulation: Typical zonal surface currents in the ACC are ~ 15 cm/s and parcels thus circumnavigate the globe, a distance of some 23,000km at 55° S, in 4.9 years.

- The largest part of the oceans is passive, not interacting with the atmosphere on shorter (years to decades) time scales.
- This is due to the stratification and much weaker dynamics in the oceans.
- A surface warming by ΔT does not need to lead to a deep ocean warming by the same ΔT in equilibrium, because the deep ocean temperature is controlled by its density. As long as cold/dense waters are formed in the polar regions, the deep ocean temperature may not change much.
- Surface ocean dynamics are on the time scales of months to decades.
- Deep ocean dynamics are on time scales of 100 years to 10,000 years.
- The deep ocean interacts with the surface mostly in the polar regions.

- The deep ocean stores a large amount of CO_2 and other trace gases, that can be exchanged with the atmosphere during climate change.

Examples:

ACC circulation (the fastest large-scale ocean circulation)
 $\bar{u} \approx 0.15 \frac{m}{s} \implies \text{transport time} = \frac{\text{distance}}{\bar{u}} = \frac{23,000 km}{0.15 \frac{m}{s}} \approx 5 yrs$

Deep ocean circulation
 $\bar{u} \ll 0.001 \frac{m}{s} \implies \text{transport time} = \frac{\text{distance}}{\bar{u}} \gg \frac{20,000 km}{0.001 \frac{m}{s}} \approx 500 yrs$

3.3.7 Sea Ice



Figure 3.64

- Sea ice is highly variable, with large daily, seasonal and interannual variability.
- Sea ice is about 0.5-1.5m thick and typically forms and melts within one seasonal cycle.
- Some sea ice is older than one year and can be up to 2-5m thick.
- Sea ice is controlled by *thermodynamics*: heating/cooling by heat fluxes (sensible, radiation) from the atmosphere and also the ocean (currents). And by *fluid dynamics*: transport, friction and mechanical processes.
- Distribution of sea ice often depends more on the fluid dynamics than on the thermodynamics.
- Rotating winds (wind curls) of weather cyclones have strong impacts on sea ice cover, distribution and thickness.
- Sea ice has a strong impact on the local and larger-scale climate, as it changes the heat flux between the ocean and atmosphere dramatically.
- Sea ice formation influences the sea water density, as salinity is excluded from ice. This influences the thermohaline circulation.

Sea ice seasonal cycle

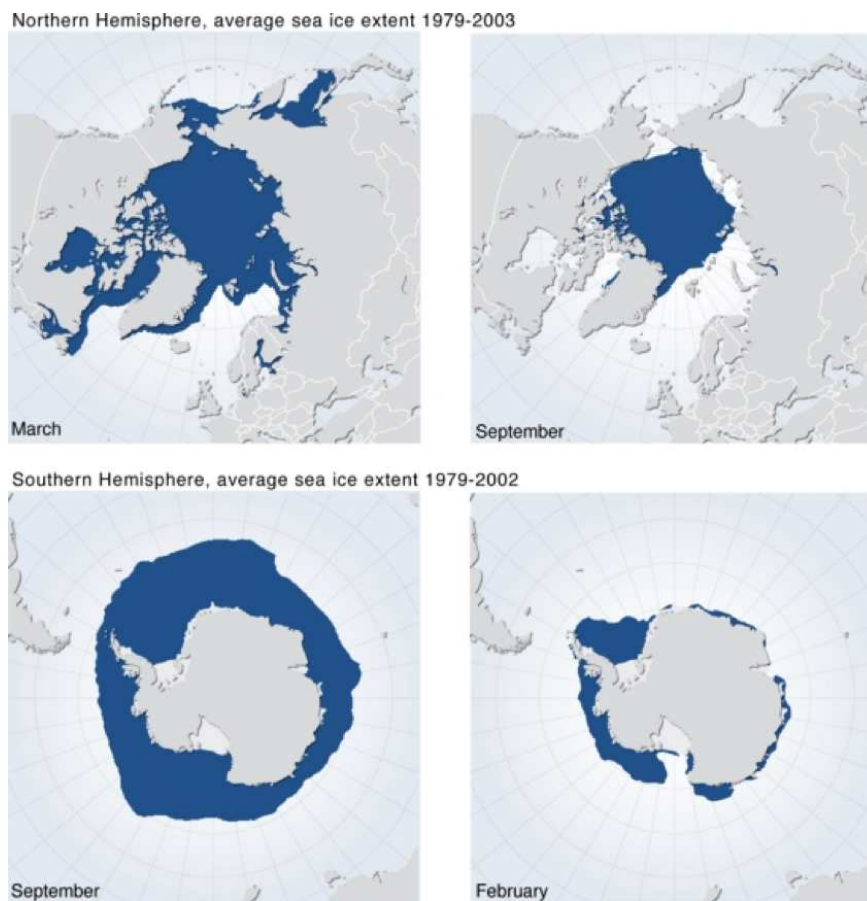


Figure 3.65: Sea ice seasonal cycle

Sea ice dynamics

Weather cyclones with rotating winds (wind curls) cause divergence in sea ice (also in ocean) due to the Coriolis force. This leads to gaps in sea ice and large-scale sea ice transport.

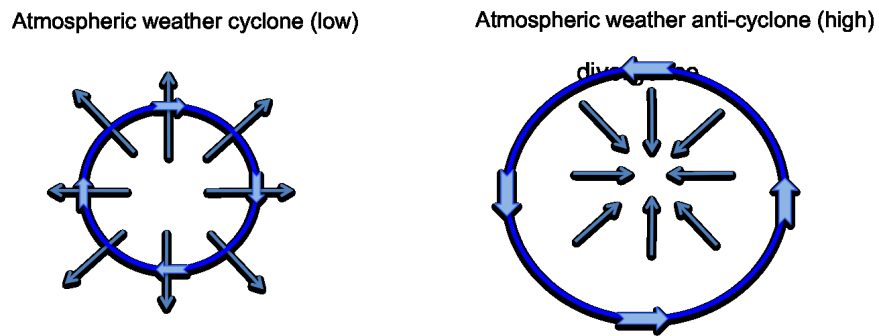


Figure 3.66: Sea ice divergence/convergence

Sea ice formation influence on deep ocean circulation.

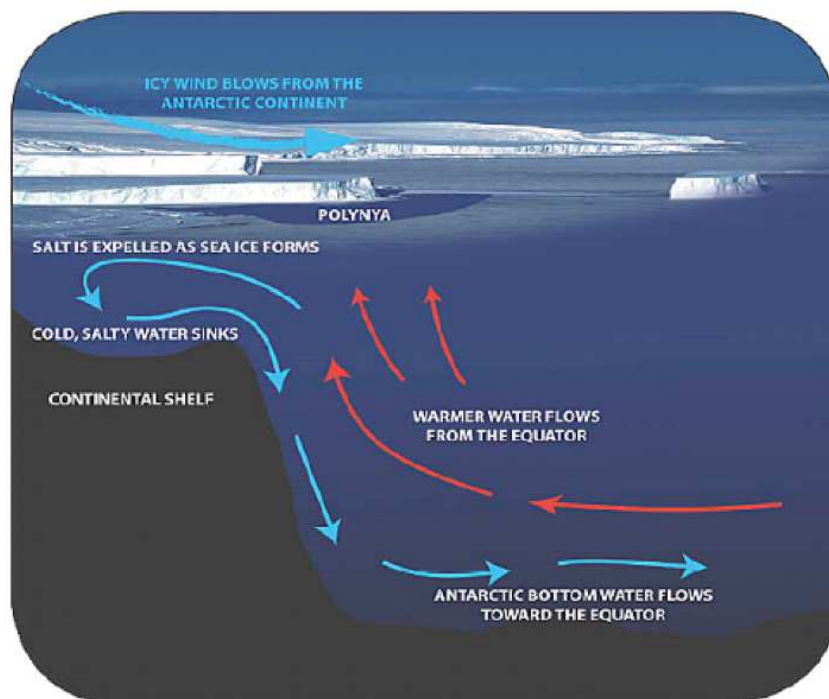


Figure 3.67: Sea ice

3.4 Heat Transport in the Climate System

The driving forces of the atmospheric and ocean circulation are the temperature gradient between warm and cool regions. Like in a heat engine the contrast between warm and cold air or water makes the air or water move. This circulation acts to reduce temperature gradients and subsequently transports a lot of heat. The transport of heat in the climate system eventually leads to heating to some locations and cooling at other locations. The atmospheric and ocean heat engines are so strong that in many regions and seasons the heating from the heat transported by the atmosphere

and oceans is larger than the radiation received by the sun.

In the first subsection we will illustrate the presents of significant heat transport in the climate system by some simple energy balance calculations. We will then define heat transport and heating resulting from the heat transport. In the next sections we will discuss the different kind of circulations that transport heat. We will distinguish here between the transport by the mean flow and the turbulent flow.

3.4.1 The Zonal Mean Heat Balance

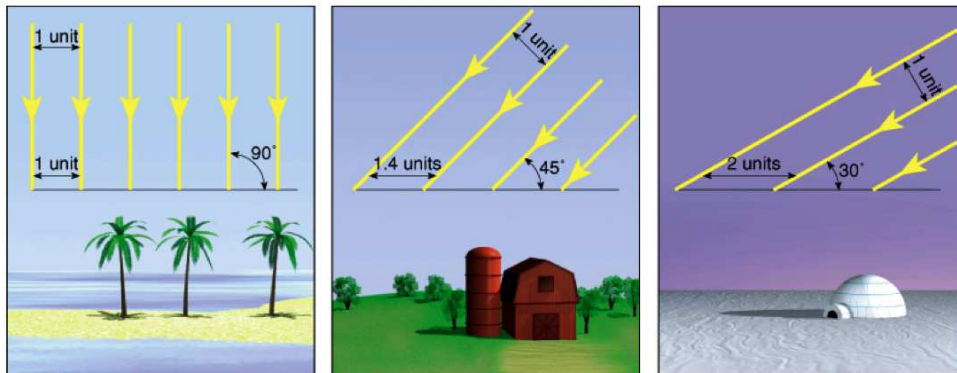
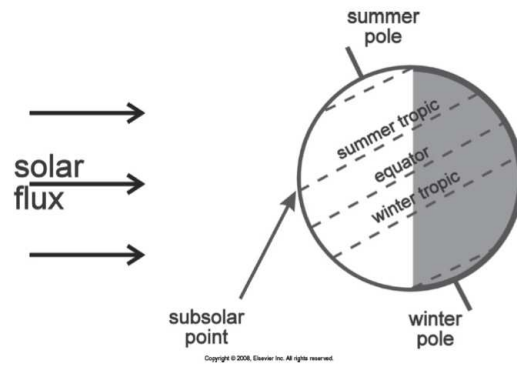


Figure 3.68: Incoming solar radiation: Due to the orientation of the Earth relative to the Sun, the poles receive very little solar radiation and the equatorial region receives a lot.

In the zero order energy balance we assumed a balance between incoming solar radiation and the out going thermal radiation (eq.[2.6]). So if there were no energy transports in the climate system, this energy balance would need to be closed at all locations.

Fig. 3.69 shows the balances of incoming solar radiation and the out going thermal radiation as function of latitudes. Between $\sim 40^\circ$ North and 40° South, there is more incoming than outgoing radiation. Polewards of 40° , there is more outgoing than incoming radiation. The energy that is

emitted at high latitudes has to have come from somewhere: the excess energy in the tropics is transported to higher latitudes.

The difference between the incoming and outgoing radiation is an indication of energy transport within the climate system. The net radiation in Fig. 3.69 is an indicator of energy transport. Positive values indicate that energy is transported away from that latitude and negative value indicate that energy is transported towards this latitude. In the tropics the climate gains more energy than it emits to space; roughly $50\text{W}/\text{m}^2$. This is transported to higher latitudes. Polewards of about 70° latitudes the energy gain by transport is larger than the mean incoming radiation. Thus, polar regions are mostly heated by lower latitudes rather than by sun light.

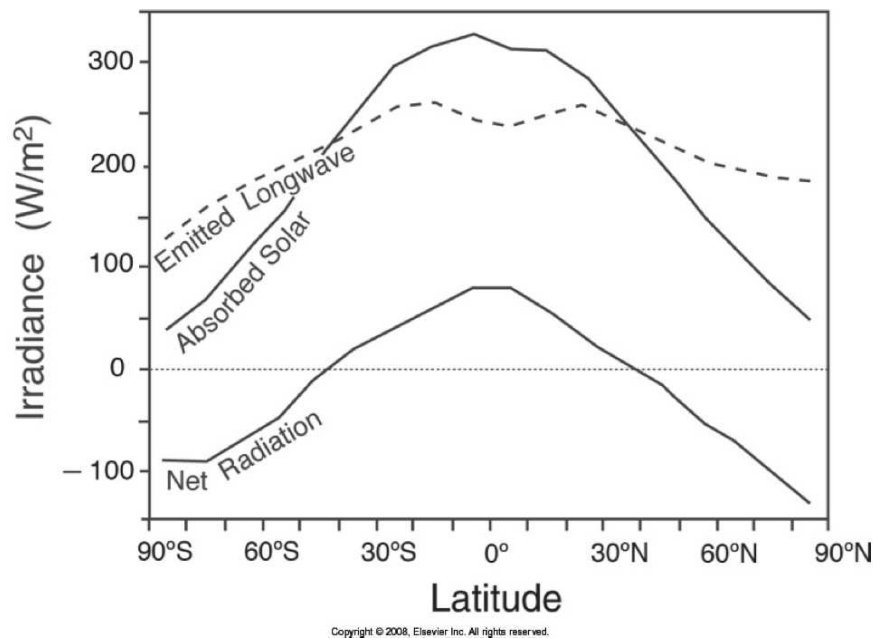


Figure 3.69: Incoming solar and outgoing terrestrial radiations: The zonal average of the incoming solar and outgoing thermal radiations as function of latitude. From satellite measurements.

Balancing the Energy

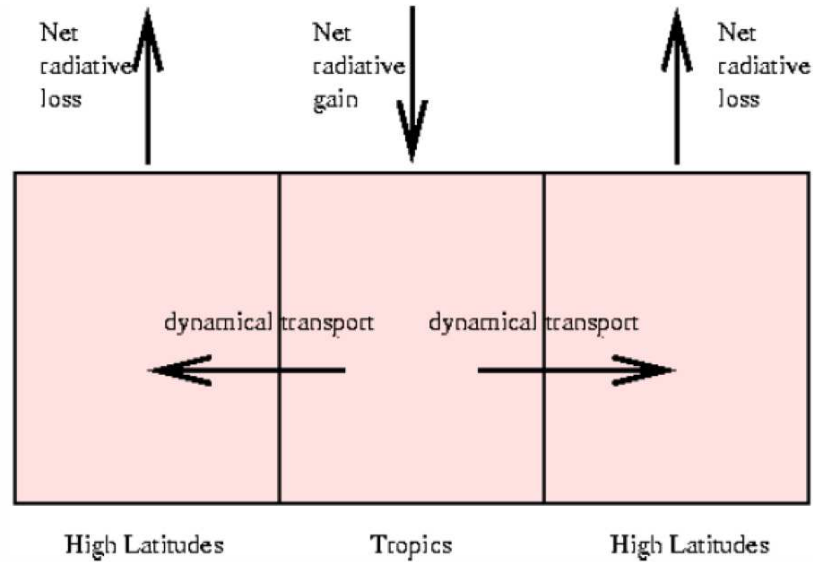


Figure 3.70: Dynamic energy transport

3.4.2 The Heat Transport

A transport of mass in the atmosphere or ocean implies a transport of heat. The heat transport, \vec{T}_H , is defined as:

$$\vec{T}_H = \vec{u} \cdot H \quad (3.39)$$

Here the heat, H , can be written as a specific heat capacity per mass, c_m , times the temperature,

$$\vec{T}_H = \vec{u} \cdot c_m \cdot T = c_m \cdot \vec{u} \cdot T \quad (3.40)$$

Since c_m can often be assumed to be a constant (e.g. within the whole column of the atmosphere or within in the ocean), the product of the winds/currents, \vec{u} , times the temperature is what is regionally changing. This heat transport \vec{T}_H is a vector with direction. If it is positive heat is transported northward. The units are in W/m^2 .

However, often we are interested in heat transport across an area, such as the heat transport across the area over whole circle around the earth at $30^\circ S$ latitude over the whole air column). Thus the area is height times circumference of the earth at $30^\circ S$ latitude. This integrated heat transport has then the unit of W . We can estimate this integrated heat transport across all latitudes from the zonal mean energy imbalance in Fig. 3.69 by integrating it from the south pole to north pole, see Fig. 3.71. Further calculations from atmosphere and ocean data can tell us how much energy is transported by each, see Fig. 3.71. We can see that in the Southern Hemisphere the heat transport is negative, indicating heat is transported southward and vice versa in the Northern Hemisphere. Before we go into further discussion, it is very important to note here that heat transport is not heating nor cooling. It just states how much heat is currently transported within the system (e.g. atmosphere or oceans). This is often misunderstood by students and is therefore important to point out here in more detail. Consider you are at a location and heat is being transported across your location. If the heat transport is not changing (e.g. no heat is leaving or entering the atmosphere or oceans), then your location will not be heated nor cooled. You will not feel any effect from the heat transport. If this is difficult to understand, consider the following analog: Lets assume you are at home and a pizza delivery transporter is passing by your home. If no pizza is leaving the pizza delivery transporter at your home, then you will not get any pizza.

How much heating or cooling is done by the heat transport is related to the change (convergences; negative of divergence) in heat transport:

$$Q = -c_m \cdot \vec{\nabla}(\vec{u} \cdot T) \quad (3.41)$$

We can simplify this if we assume that the winds/currents, \vec{u} , are not changing. Then the heating or cooling done by the heat transport is:

$$Q = -\vec{u} \cdot \vec{\nabla}(T) \quad (3.42)$$

An example: In the southern hemisphere it is cold at the poles and warm at the equator. Thus the temperature gradient $\vec{\nabla}T = \partial T/\partial y > 0$. If the winds blow from the south to north, $\vec{u} > 0$, then $\vec{Q} < 0$; it is cooling. So for the advection of heat the winds have to blow against the temperature gradient: They have to blow from warm to cold. Thus the change (gradient) in the heat transport shown in Fig. 3.71 is related to heating and cooling. An increase in heat transport implies cooling at this location and a decrease in heat transport implies heating at this location.

Starting at the equator the atmosphere and ocean gain heat in both hemispheres until about 40° North and 40° South and subsequently these regions are cooled by heat transport. At the peak the total heat transport by the climate system is $\sim 5.5PW = 5.5 \times 10^{15}W$. For comparison, the largest coal power station in Victoria has a capacity of $3.25GW = 3.25 \times 10^9W$. All of the nuclear power plants currently operational in the world have a capacity of $375GW = 3.75 \times 10^{11}W$. Polewards of 40° the total heat transport decreases, indicating that the climate is releasing the heat, heating these latitude bands. We can also see in fig. 3.71 that the atmosphere transports the largest part of the energy and that the oceans transport more heat in the Northern Hemisphere, which they also release at lower latitudes than the atmosphere.

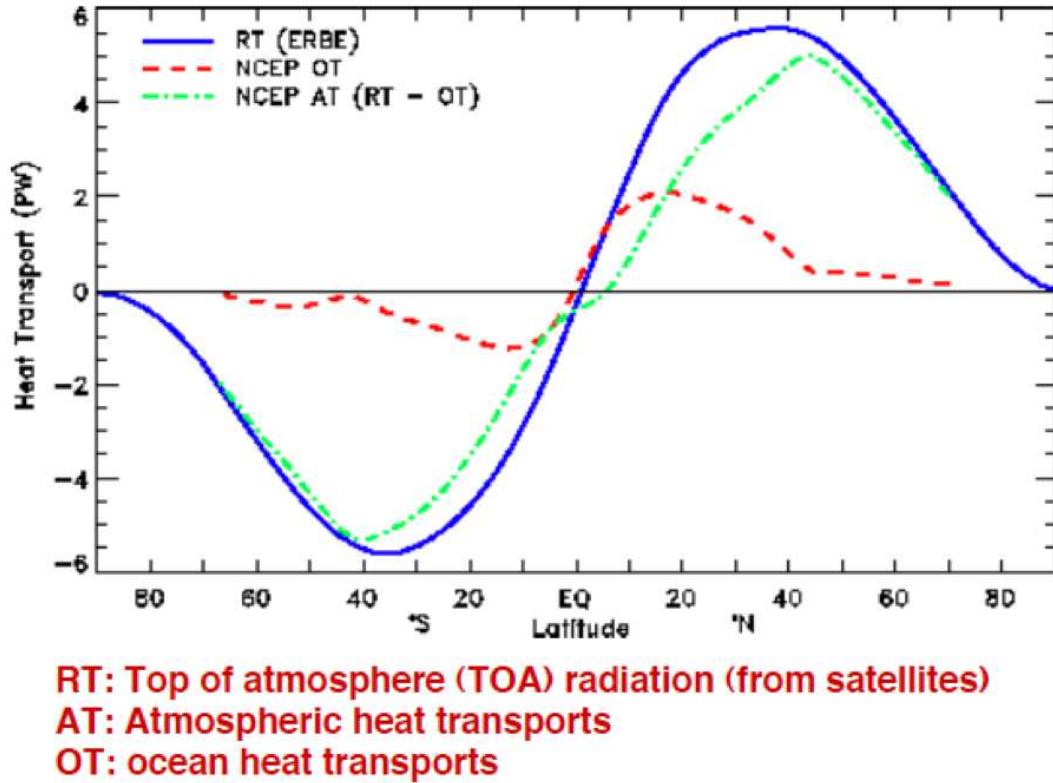


Figure 3.71: Positive values of heat transport correspond to Northward transport (defined as: $\vec{u} \cdot T$). The negative values in the Southern Hemisphere indicate that the transport is towards the South Pole. Note, that only the change in this total heat transport (derivative) leads to heating at a latitude band.

Example: Heating by ocean meridional heat transport

Heat flux per ocean surface:

$$Q = -\gamma_{ocean} \cdot \vec{u} \cdot \vec{\nabla} T \quad (3.43)$$

Example: Meridional transport in the North Atlantic

$$\gamma_{ocean} = 100m \cdot 4000J/kg/K \cdot 1000kg/m^3 = 4 \cdot 10^8 J/K/m^2$$

$$\vec{u} = 0.1m/s$$

$$\Delta T = -10K$$

$$\Delta y = 2 \cdot 10^6 m$$

$$Q_y = -\gamma_{ocean} \cdot \vec{u}_y \cdot \vec{\nabla}_y T = -\gamma_{ocean} \cdot \vec{u}_y \cdot \frac{\partial T}{\partial y} \approx -\gamma_{ocean} \cdot \vec{u}_y \cdot \frac{\Delta T}{\Delta y} \quad (3.44)$$

$$= -4 \cdot 10^8 J/K/m^2 \cdot 0.1m/s \cdot \frac{-10K}{2 \cdot 10^6 m} = 200W/m^2$$

3.4.3 The Advective and Turbulent Heat Transport

Heat transport in both the atmosphere and oceans is:

$$\overrightarrow{T_H} = c_m \cdot \vec{u} \cdot T \quad (3.45)$$

It is instructive to split the heat transport into a mean and a turbulent to illustrate the relative importance of each flow. First: Any time varying quantity can be written as a mean plus a fluctuation from the mean:

$$\overrightarrow{T_H}(t) = \hat{\overrightarrow{T_H}} + \overrightarrow{T_H}'(t) \quad (3.46)$$

With $\hat{\overrightarrow{T_H}}$ the time mean value:

$$\hat{\overrightarrow{T_H}} = \frac{1}{T} \int_0^T \overrightarrow{T_H}(t) dt \quad (3.47)$$

Here T is the length of the time period considered. The turbulent (fluctuating) part at any time, t :

$$\overrightarrow{T_H}'(t) = \overrightarrow{T_H}(t) - \hat{\overrightarrow{T_H}} \quad (3.48)$$

Note that:

$$\frac{1}{T} \int_0^T \overrightarrow{T_H}'(t) dt = 0 \quad (3.49)$$

From this it follows for the heat transport:

$$\hat{\overrightarrow{T_H}} = -c_m \cdot \widehat{\vec{u} \cdot T} = -(\widehat{\vec{u}} + \widehat{\vec{u}'}) \cdot (\widehat{T} + T') \quad (3.50)$$

Since averaging is building the integrals (eq.[??]) we can simplify the equation by using the integral rules:

$$\hat{\overrightarrow{T_H}} = -\widehat{\vec{u}} \cdot \widehat{T} - \widehat{\vec{u}} \cdot T' - \widehat{\vec{u}'} \cdot \widehat{T} - \widehat{\vec{u}'} \cdot T' = -\widehat{\vec{u}} \cdot \widehat{T} - \widehat{\vec{u}'} \cdot T' \quad (3.51)$$

The mean heat transport has two terms: A heat transport due to the mean flow times the mean temperature called the mean heat transport. The second term is the mean turbulent heat transport, which is due to variations in winds and temperature gradients at the same time. So the mean heat transport is not just a function of the mean wind and mean temperature. Actually we can have a mean heat transport even if the mean winds or the mean temperature are zero or if the scalar product of both is zero.

A non-zero mean turbulent transport requires that the fluctuation in wind and temperature co-vary in a way that the scalar product between both is in average not zero.

A few points for Figs. 3.72:

- Heat transport has a mean advection and a turbulent part, which is due to fluctuations (eddies).
- The turbulent part can be larger than the mean part.
- So heat transport can exist in zero mean winds.
- In the Hadley cell mean advection dominates.
- In the midlatitudes Ferrel cell the turbulent part by eddies dominates.

- Example: In Melbourne the mean winds are westerlies and the mean temperature gradient is from south to north. Thus the mean heat advection in eq.[3.45] is zero, since wind vector and temperature gradient vector are orthogonal to each other. But strong weather fluctuations (turbulent winds) in Melbourne transport a lot of heat from Melbourne to the south. It leads to a lot of cooling in Melbourne and heating of the southern ocean.

Observed atmospheric heat transport

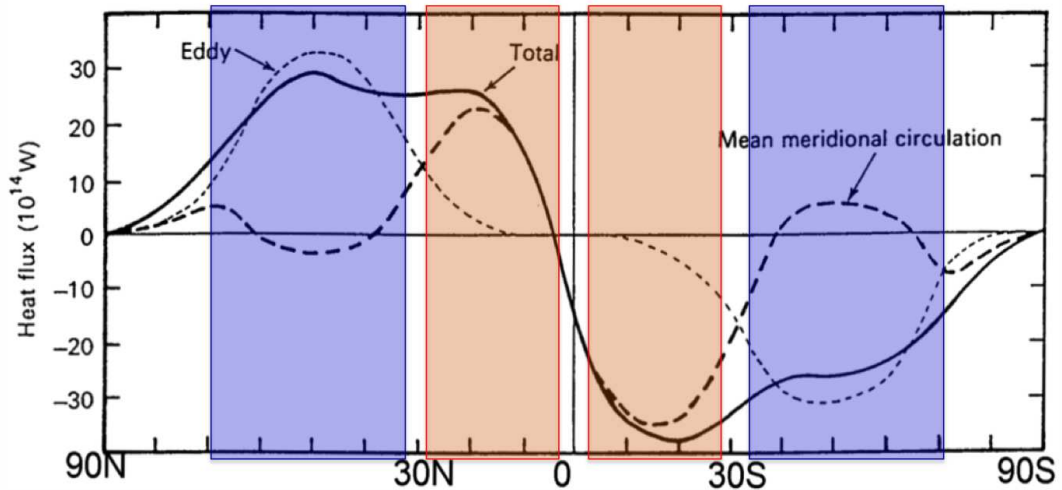


Figure 3.72: Annual mean zonal mean meridional heat transport in the atmosphere, showing the total transport (solid line), eddy (turbulent) transport (thin dashed line) and transport by the mean meridional circulation (thick dashed line). Note that positive transport is northward.

The total heat transport has strong seasonal cycle, see Fig. 3.73. Heat transport is stronger in the cold seasons, as the driving force for the circulation is the meridional temperature gradient, which is stronger in winter due to the cold polar regions.

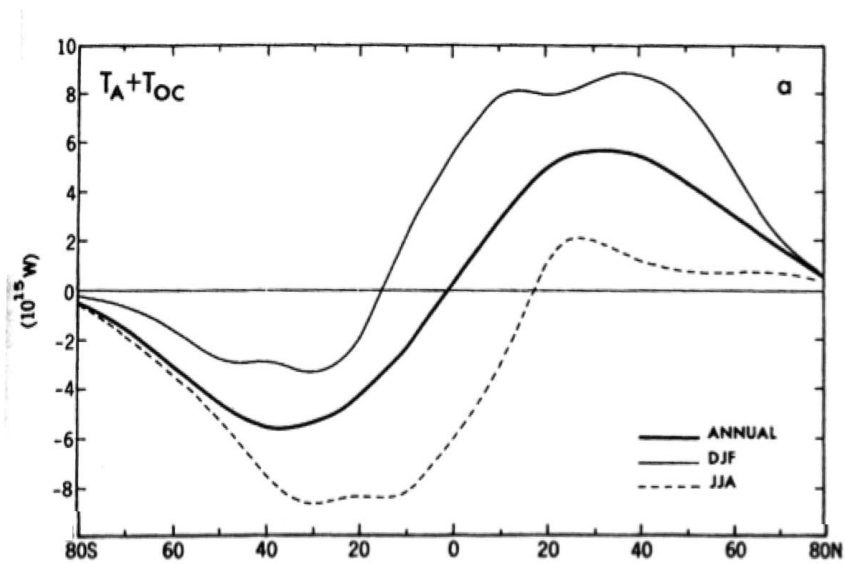


Figure 3.73: The total heat transport of Atmosphere and oceans for the annual mean (thick solid line), the DJF-season (thin solid line) and for the JJA-season (dash line).

3.4.4 The Heat Transport between Seasons (from summer to winter)

Heat transport is mostly discussed in the context of transport from one region (tropics) to another region (higher latitudes). However, the climate system can also transport heat from one point in time (summer) to another point in time (winter). The ocean is transporting heat from warm seasons to cold seasons by its large heat capacity. It takes up heat in summer from solar radiation and sensible heat exchange with the much warmer land and releases this heat in winter by sensible heat exchange with the much colder land, see Fig. 3.74.

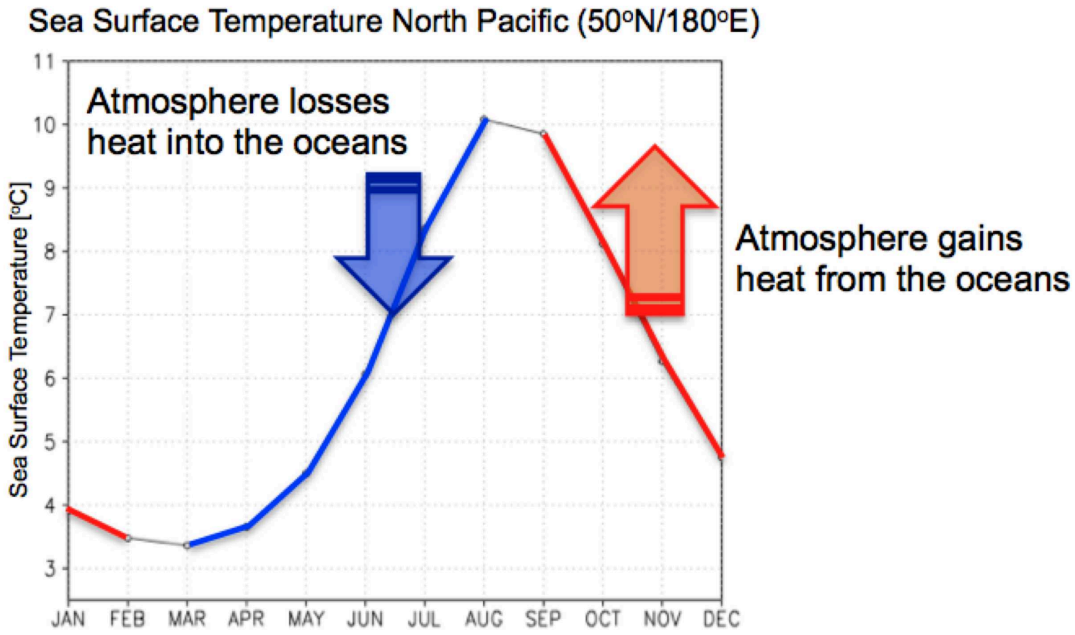


Figure 3.74: Mean sea surface temperature in the North Pacific. The ocean takes heat from the atmosphere when it warms and it returns heat to the atmosphere when it cools.

Example 1: Ocean-Atmospheric heat exchange in a simple model

We can use a simple energy balance consideration to get an idea of how much heat is being transported by the oceans heat capacity from summer to winter.

When the oceans cool, we can assume that most of the heat goes into the atmosphere, thus it heats the atmosphere. We can use the energy balance equation to compute the heat flux from the ocean into the atmosphere, F_{ocean} :

$$\gamma_{ocean} \frac{dT_{ocean}}{dt} \approx -F_{ocean} \quad (3.52)$$

Here we defined F_{ocean} as heat going into the atmosphere (therefore the minus). The heat capacity of the ocean γ_{ocean} is

$$\gamma_{ocean} = cp_{water} \cdot \rho_{water} \cdot h_{mixed-layer} \quad (3.53)$$

The specific heat capacity, $cp_{water} = 4 \cdot 10^3 J/Kg/K$, the density $\rho_{water} = 1000Kg$ and we assume a surface ocean layer thickness of $h_{mixed-layer} = 50m$. In Fig. 3.74 we can see that the mean sea surface temperature in the North Pacific cools by about $-6^\circ C$ in 4 month. Thus

$$\frac{dT_{ocean}}{dt} = \frac{\Delta T_{ocean}}{\Delta t} = \frac{-6^\circ C}{3600s \cdot 24 \cdot 30 \cdot 4} \quad (3.54)$$

If we include all these values in eq. [3.52] we get

$$F_{ocean} \approx 100W/m^2 \quad (3.55)$$

So the ocean heats the atmosphere in fall by about $+100W/m^2$, which is quite substantial, as it is as larger or larger than the incoming solar radiation in this season at this latitude. It is also comparable to the meridional heat transport that we computed in eq. [3.44].

Example 2: Ocean-Atmospheric heat exchange in a simple model

We can use a second approach to see how heat between nearby land and ocean may be exchanged in different seasons. A simple energy balance for the seasonal cycle at 37°S of incoming solar radiation and outgoing thermal radiation is:

$$\gamma_{surf} \frac{dT_{surf}}{dt} = \frac{1}{4}(1 - \alpha_p)S_0 - \sigma T_{surf}^4 \quad (3.56)$$

We can estimate the equilibrium temperature for this simple radiation balance for the seasonal cycle of the incoming solar radiation at 37°S and for γ_{surf} over land and oceans, see Fig. 3.75 (For more details on how to estimate the equilibrium temperature, the heat capacities and the seasonal cycle of incoming radiation see sections 4.1.8, 4.1.6 and 4.1.2).

We can first of all notice that the mean temperature for both land and ocean are much too warm, because we neglected any meridional heat transport. This is not important for the following discussion. Further we can notice that the land equilibrium has a huge seasonal cycle, but the ocean equilibrium has almost none. We can assume that nearby regions will exchange heat with each other by sensible heat transport. This heat transport between ocean-land is approximately proportional to the temperature difference between the two regions (see also section 4.1.5 for sensible heat flux). So we will have heat transport from the ocean to the land (via atmosphere) in winter and from land to the oceans in summer, see Fig. 3.75. Thus from the lands point of view we transport heat from the warm to cold season via the oceans heat storage. This leads to a much more moderate seasonal cycle, as we will see later in section 4.2.

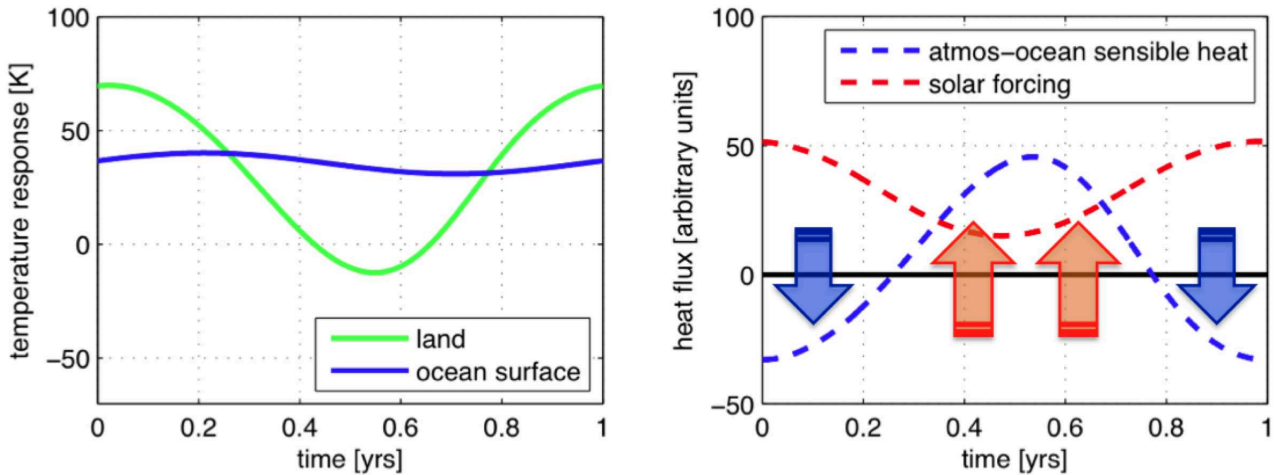


Figure 3.75: Seasonal heat transport: left: Equilibrium temperature for ocean and land following eq. [3.56]. right: incoming solar radiation and estimate of resulting sensible heat exchange between land (atmosphere) and oceans.

Chapter 4

Models of the Global Climate System

Climate models are the basis on which to understand the dynamics of the climate system. In the IPCC prediction of future climate change, climate models are the main tool to predict the future response of the climate. In this chapter we discuss how climate models simulate the global climate system. We will start this discussion with the development of a very simple climate model: The Globally Resolved Energy Balance (GREB) model. The aim of this model is to develop the simplest possible representation of the physical climate system, that can still simulate the main features in the regional (on the scale of about 500km) and seasonal different of T_{surf} . It further should also be capable to simulate the main features in the regional and seasonal different of the T_{surf} response to CO_2 forcing. So we aim for simplicity not for completeness.

The development of this model will help us to understand what processes are involved in building the mean climate and its regional and seasonal different. We also use the development of this model to point out aspects of the climate system which are much more complex than can be simulated by the simple GREB model. So we will see what aspects of the climate system would need more detailed and complex dynamics to be fully understood. At the end of the GREB model section will use the GREB model to deconstruct the regional and seasonal different in the earth mean climate. We will conceptually build up the climate components starting from a bare earth without the atmosphere or oceans (e.g. like our Moon) and ending at the full complexity of the earth regional and seasonal mean climate.

In the next step we will have a look at the state of the art climate models: The General Circulation Models (GCMs). These models are the most complex and most sophisticated model of the climate system. They are the basis for the IPCC climate change predictions, but are also the basis for weather forecasting.

4.1 A Globally Resolved Energy Balance (GREB) model

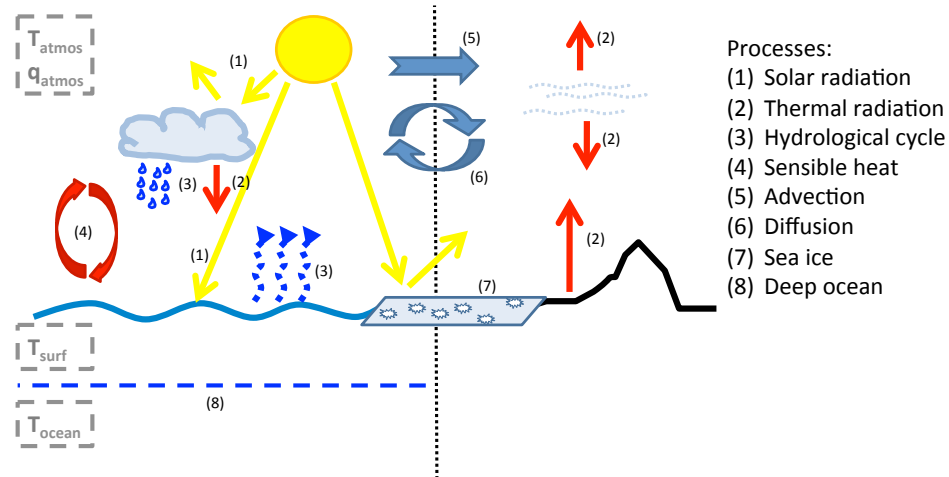


Figure 4.1: Sketch GREB model process:

In this section we want to develop a Globally Resolved Energy Balance (GREB) model. The aim of this model is to develop the simplest possible representation of the physical climate system, that can still simulate the main features in the regional and seasonal different of T_{surf} . It further should also be capable to simulate the T_{surf} response to CO_2 forcing. So we aim for simplicity not for completeness (see GCM models for the most sophisticated climate models).

The GREB model essentially tries to continue the simple energy balance model discussion by extending the global mean energy balance equation to regional and seasonal scale. By building the GREB model we will learn what is need to understand the mean climate. In the final part of this section we will conceptually build up the climate components starting from a bare earth without the atmosphere or oceans (e.g. like our Moon) and ending at the full complexity of the earth regional and seasonal mean climate.

4.1.1 Initial considerations

Some initial considerations:

The energy balance for the zero order global mean model is:

$$\gamma_{surf} \frac{dT_{surf}}{dt} = F_{solar} + F_{thermal}$$

So only radiation exchange with space (no heat or mass transport) is relevant.

The energy balance for regional model includes more terms, as we can exchange heat with other regions and transfer heat by phase transitions of water (latent heat), see sketch 4.2:

$$\gamma_{surf} \frac{dT_{surf}}{dt} = F_{solar} + F_{thermal} + F_{sense} + F_{latent} + F_{ocean}$$

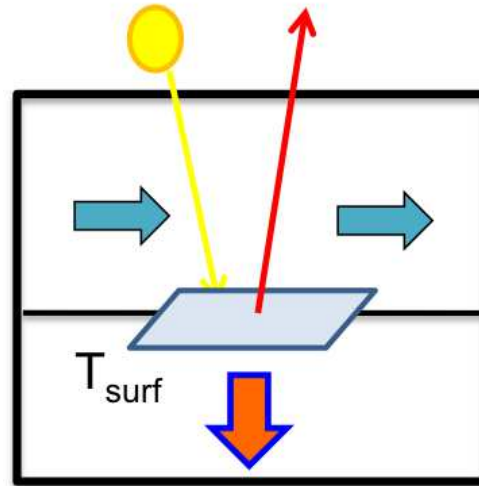


Figure 4.2: Simple sketch of regional heat balances.

F_{sense} = turbulent heat exchange with atmosphere.

F_{latent} = heat exchange by H_2O phase transitions (e.g. evaporation or condensation).

F_{ocean} = turbulent heat exchange of subsurface ocean with the surface.

The three terms $F_{sense} + F_{latent} + F_{ocean}$ are in general summarised as the **Turbulent Heat Fluxes**. They are a signature of the atmospheric and ocean circulation.

We want to resolve this equation on a global longitudes \times latitude model grid with points every $3.75^\circ \times 3.75^\circ$ (96×48 points), see map in Fig. 4.3 for an illustration of the model grid.

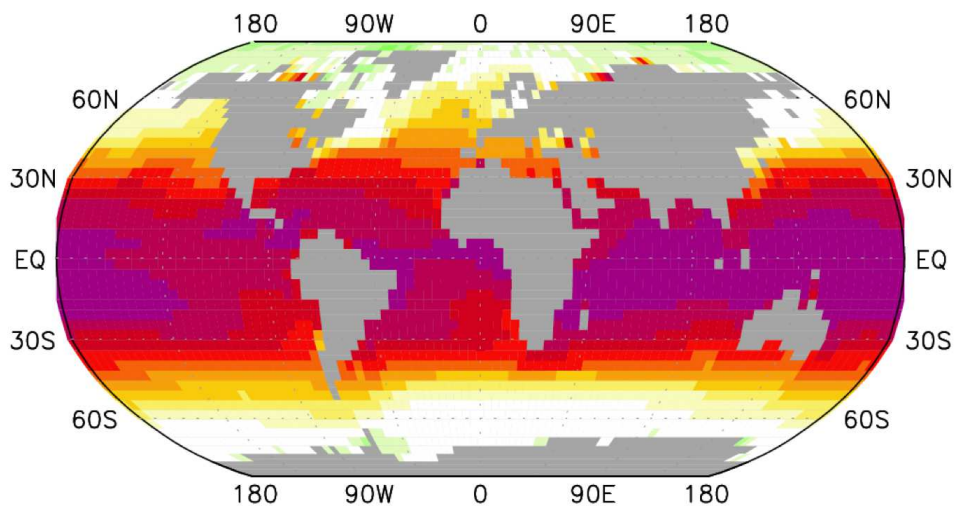


Figure 4.3: Map illustrating the GREB model resolution.

The heat transfer in the climate system is quite complex. It involves heat transport and exchange over many different levels in the atmosphere (see Fig. 4.4) and on very different spatial scales (from 1 few meters to 10,000km). For simplicity we will aim to present the atmosphere with just one layer, neglecting all vertical structure.

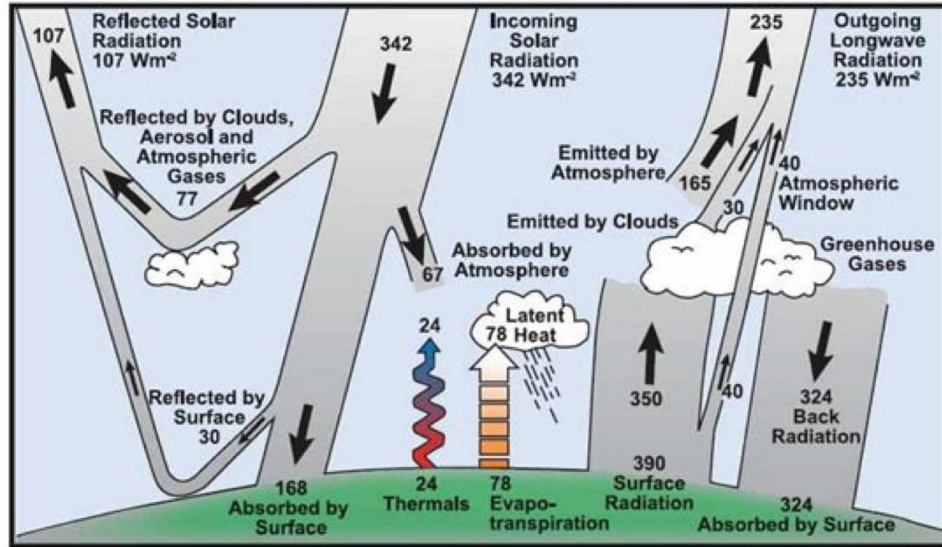


Figure 4.4: A simple sketch of the atmospheric radiation budget. It illustrates the heat exchange in different level in the atmosphere.

4.1.2 Solar radiation (F_{solar})

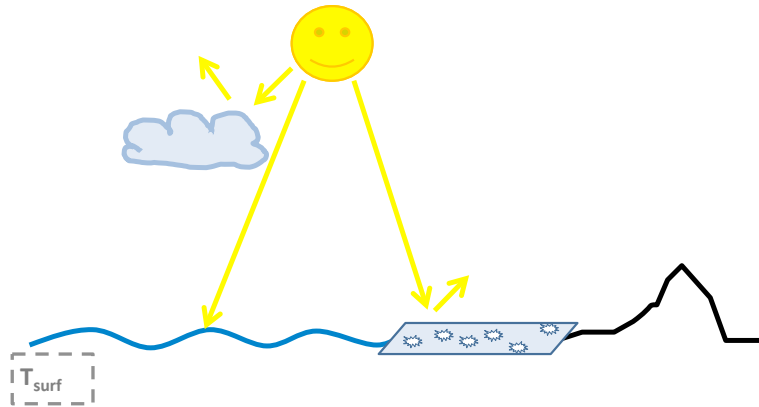


Figure 4.5: Sketch of the GREB solar radiation.

For the global zero order model (e.g. Budyko) the solar radiation was:

$$F_{solar} = \frac{1}{4}(1 - \alpha_p(T_{surf}))S_0 \quad (4.1)$$

For our regional GREB model we have to make it slightly more complex:

$$F_{solar} = (1 - \alpha_{clouds})(1 - \alpha_{surf})S_0 \cdot r(\phi, t_{julian}) \quad (4.2)$$

with $r(\phi, t_{julian})$ 24hrs mean incoming fraction of the solar constant S_0 as function of latitude, ϕ and calendar day of the year, t_{julian} . So in comparison to the zero order model we have included two more aspects in this equation: First, the incoming solar radiation is now given for each day of the year at each latitude and second the reflection of the incoming solar radiation by the albedo is

now split into two parts: one part is reflect in the atmosphere by the atmospheric albedo, α_{clouds} , and the remaining incoming radiation is reflected by the surface albedo, α_{surf} .

Incoming Solar Radiation: We make the simplification to assume a 24hrs mean solar radiation, and therefore do not simulate a daily cycle (no nights!). See Fig. 4.6 for the distribution of the 24hrs mean incoming solar radiation as function of latitude, ϕ and calendar day of the year, t_{julian} .

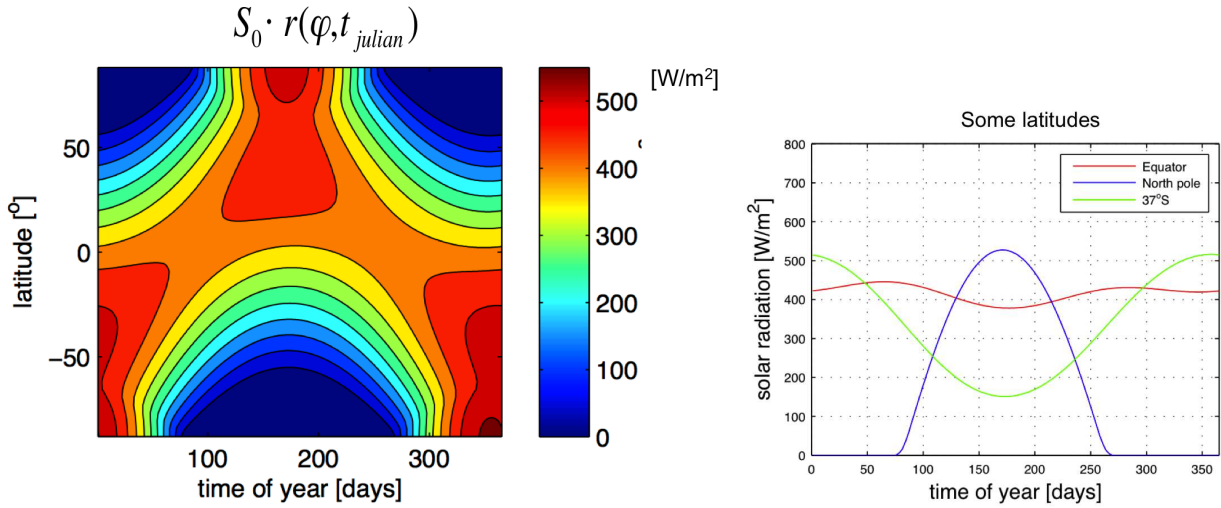


Figure 4.6: 24hrs mean incoming solar radiation as function of latitude, ϕ and calendar day of the year, t_{julian} . The 24hrs mean incoming solar radiation at three different latitudes (the lines are 'cut outs' from the left panel).

Albedo: The atmospheric albedo is

$$\alpha_{clouds} = 0.35 * a_{cloud} \quad (4.3)$$

$a_{cloud} =$ cloud cover

$a_{cloud} = 0 \rightarrow$ no clouds

$a_{cloud} = 1 \rightarrow$ complete cloud cover

So the atmospheric albedo is 0.35 if it is completely cloud covered. Thus it is assumed that 100% cloud cover ($a_{cloud} = 1.0$) reflects about 35% of the radiation $\alpha_{clouds} = 0.35$. We do not make any differentiation between different type of clouds (e.g. thickness or brightness). We further assume that the cloud cover distribution is a fixed, but seasonally varying, climatology, thus it is not responding to a changing climate (see Fig.4.7 for the annual mean). This simplification is not made, because it is realistic (it is probably not realistic). It is made because no simple physical model is known that would tell us how the cloud cover changes for given changes in the climate. In other words: The cloud response is complicated and we first of all do not know how to deal with it. So we assume to first order that there are no changes.

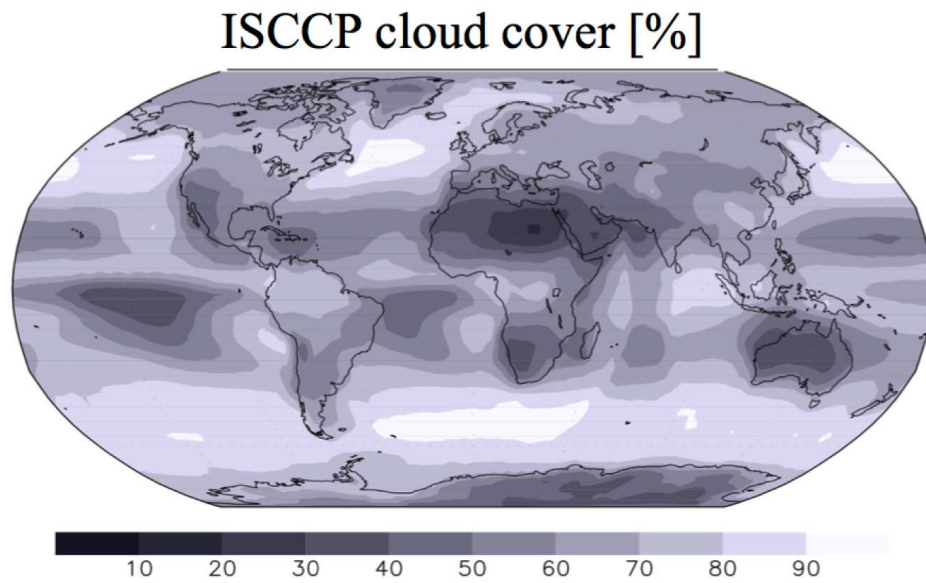


Figure 4.7: ISCCP cloud cover [%]

Surface albedo: The albedo of the earth surface varies with regions, due to different aspects: open ocean waters, snow, ice cover, trees, deserts, etc. See Table 4.1 and Fig. 4.8 for an overview.

Type of surface	Albedo (%)
Ocean	2 - 10
Forest	6 - 18
Cities	14 - 18
Vegetation	7 - 25
Soil	10 - 20
Grassland	16 - 20
Desert (sand)	35 - 45
Ice	20 - 70
Cloud (thin, thick stratus)	30, 60 - 70
Snow (old)	40 - 60
Snow (fresh)	75 - 95

Table 4.1: Albedos for different surfaces on Earth. Note that the albedo of clouds is highly variable and depends on the type and form [from Marshall and Plumb].

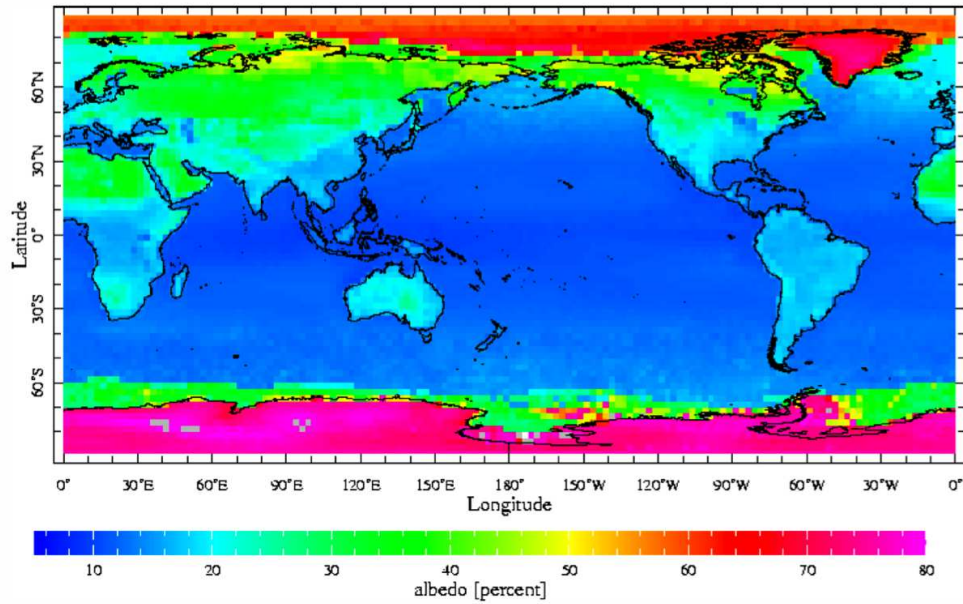


Figure 26: The annual mean surface albedo (%). Source: <http://iridl.ldeo.columbia.edu/SOURCES/.NASA/.ERBE>

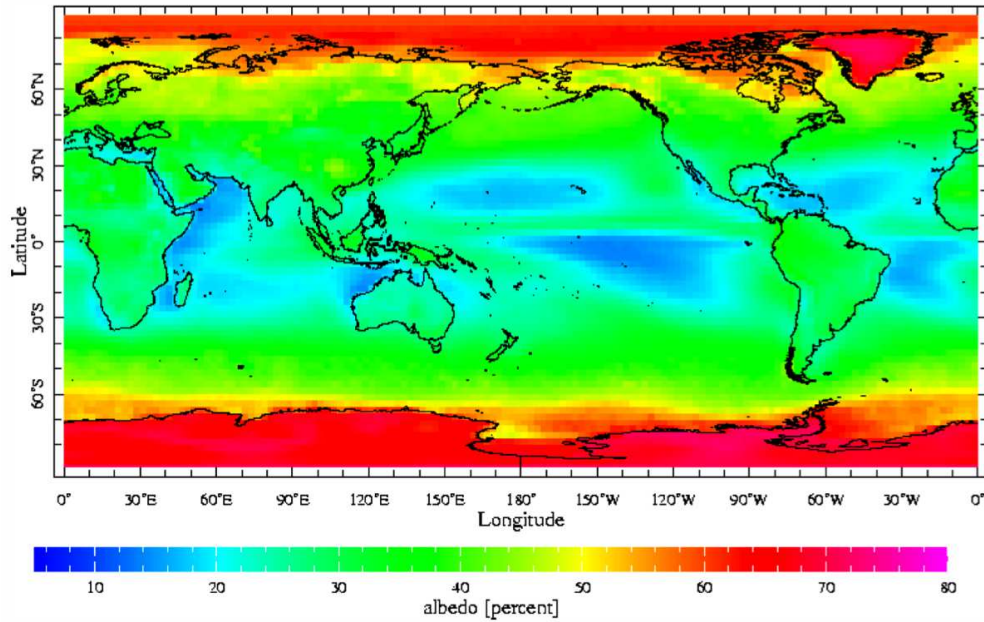


Figure 27: The annual mean surface + atmosphere albedo (%). Source: <http://iridl.ldeo.columbia.edu/SOURCES/.NASA/.ERBE>

Figure 4.8: Upper: Surface Albedo. Lower: Total albedo of the atmosphere (clouds) and the surface together.

For the surface albedo we assume the same kind of ice-albedo feedback as in the Budyko model (section 2.3). So we assume that the surface albedo is a function of T_{surf} :

$$\alpha_{surf} = \alpha_{surf}(T_{surf}) \quad (4.4)$$

As in the Budyko model we assume a constant albedo for very cold and warm temperatures and an albedo decreasing linearly with T_{surf} in a temperature range slightly below freezing, see Fig.

4.9. Note, that we make a difference between oceans and land temperature ranges. This reflects differences in spread of ice/snow cover response due to differences in freezing points (ocean water at -1.7°C), heat capacities and other influences, such as cloud cover, topography, land usage, vegetation, dust, etc.

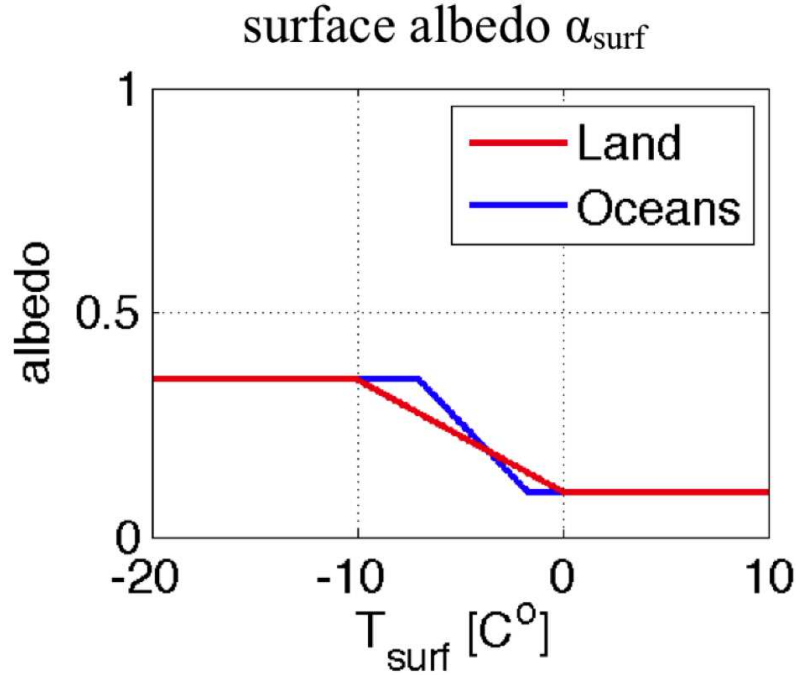


Figure 4.9: Ice-albedo function $\alpha_{surf} = \alpha_{surf}(T_{surf})$

Ice-Albedo feedback: In the temperature range where the albedo is a function of T_{surf} the solar radiation forcing is

$$F_{solar} = (1 - \alpha_{clouds})(1 - \alpha_{surf})S_0 \cdot r(\phi, t_{julian}) \quad (4.5)$$

with

$$\alpha_{surf} = \alpha_0 + \frac{\Delta\alpha}{\Delta T_{surf}} \cdot (T_{surf} - T_0) \quad (4.6)$$

with $\alpha_0 = 0.1$. Over land $\frac{\Delta\alpha}{\Delta T_{surf}} = -0.25/10^\circ\text{K} = -0.025\text{K}^{-1}$ and $T_0 = 273.15\text{K}$, See fig.4.9. We can now compute the strength of the ice-albedo feedback using the definition of the linear feedback parameter eq. [2.71]:

$$C_{ice-albedo} = \frac{dF_{solar}}{dT_{surf}} = (\alpha_{clouds} - 1) \cdot S_0 \cdot r(\alpha, t_{julian}) \cdot \frac{\Delta\alpha}{\Delta T} \quad (4.7)$$

for $T_{surf} \in [-10, 0]$

We can compute the value for a realistic T_{surf} and cloud cover climatology and the seasonal changing incoming solar radiation, see Fig. 4.10. A few points can be made about this Ice-Albedo feedback:

- It is only active for $T_{surf} \in [-10, 0]$. So regions and seasons where T_{surf} is mostly in this range will have a strong ice-albedo feedback,
- It is strong if solar radiation is strong. No sun light (polar winter) \rightarrow no ice-albedo feedback. So it is stronger at lower latitudes.

- It is weak if cloud cover is large, as it masks the surface.

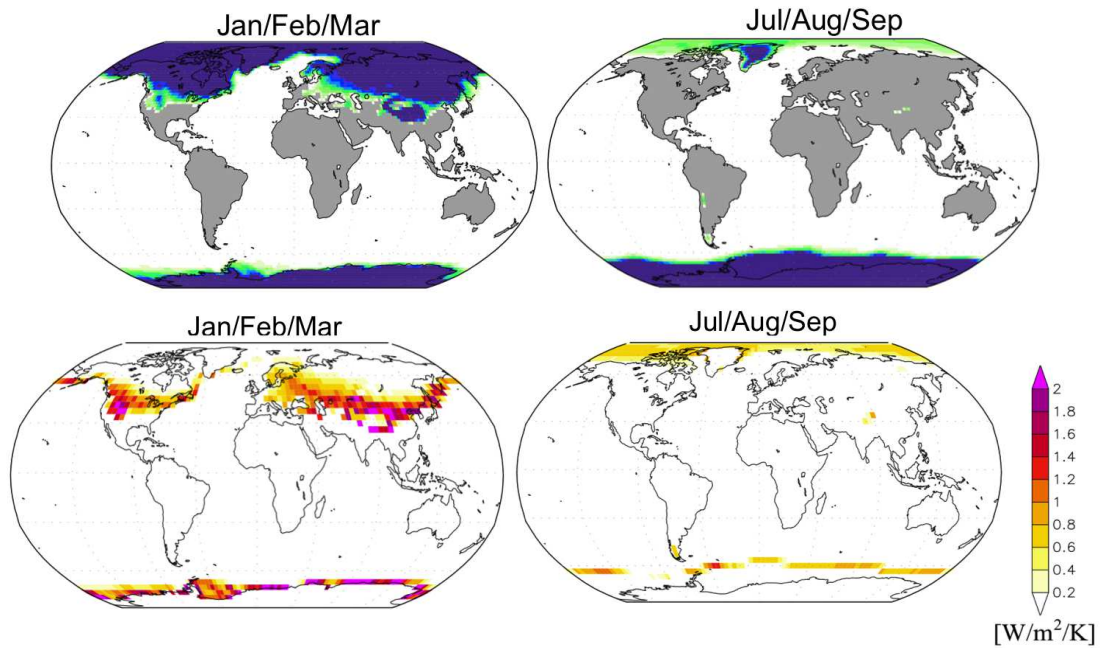


Figure 4.10: Upper: Typical Snow/Ice distribution. Lower: Ice-albedo feedback parameter strength in the GREB model for a given T_{surf} , cloud cover and incoming solar radiation climatology.

4.1.3 Thermal radiation ($F_{thermal}$)

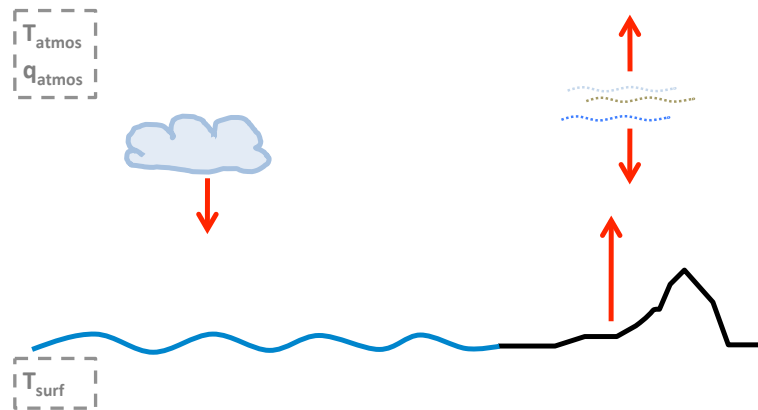


Figure 4.11: Sketch GREB thermal radiation

The thermal radiation of the atmosphere is the **only** way how the CO_2 or the other greenhouse gasses in general influence the climate. It is therefore central in understanding the climate response to anthropogenic forcing. Before we describe the GREB thermal radiation model it is instructive to have a view on a more detailed model of the thermal radiation balance in the atmosphere, see also sketches 4.12 and 4.13:

- Thermal radiation emitted from each layer is a function of emissivity, ϵ , and temperature, T at each layer.
- Thermal radiation absorbed from each layer is a function of the layer's emissivity and that of all other layers ϵ and T .
- Emissivity, ϵ , at each layer is a function of pressure, chemical composition (H_2O , CO_2) and cloud droplet density.
- Emissivity of chemical components is a function of wave length, see Fig. 4.14.
- Overall: it's complicated!

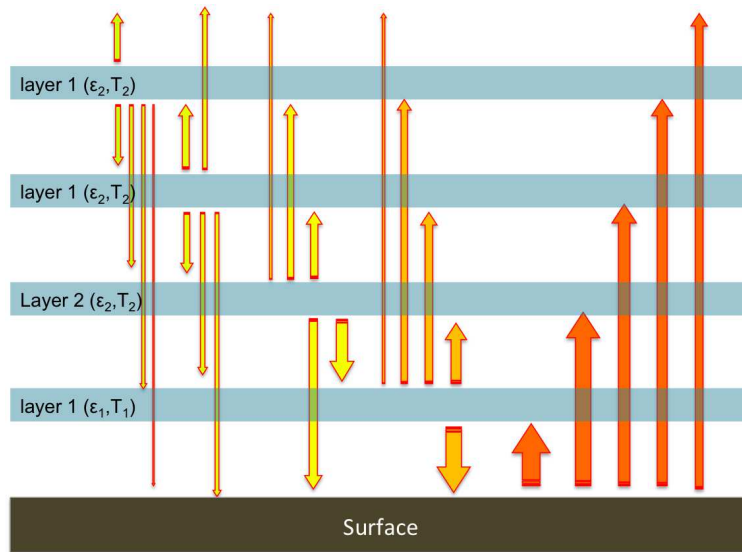


Figure 4.12: A more detailed model of thermal radiation. Each layer absorbs and emits thermal radiation as a function of its emissivity, ϵ_i , and temperature T_i .

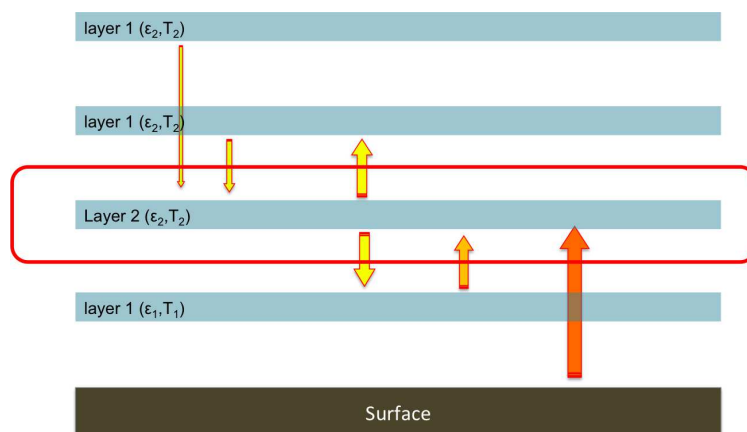


Figure 4.13: Thermal radiation balance for a single layer.

Chemical composition of the atmosphere

Air is a mixture of permanent gases (N_2 , O_2) in constant ratio with minor constituents and some non-permanent gases (e.g. water vapor or CO_2).

Chemical species	Molecular weight ($g\ mol^{-1}$)	Conc (% by vol)
N_2	28.01	78
O_2	32.00	21
Ar	39.95	0.93
H_2O (vap)	18.02	0.5
CO_2	44.01	385 ppm
Ne	20.18	19 ppm
He	4.00	5.2 ppm
CH_4	16.04	1.7 ppm
Kr	83.8	1.1 ppm
H_2	2.02	500 ppb
O_3	48.00	500 ppb
N_2O	44.01	310 ppb
CO	28.01	120 ppb
NH_3	17.03	100 ppb
NO_2	46.00	1 ppb
CCl_2F_2	120.91	480 ppt
CCl_3F	137.27	280 ppt
SO_2	64.06	200 ppt
H_2S	34.08	200 ppt
AIR	28.97	

Table 4.2: The major atmospheric constituents. The chlorofluorocarbons (CFCs) CCl_2F_2 and CCl_3F are also known as CFC-12 and CFC-11 respectively. (ppm, ppb, ppt) = parts per (million, billion, trillion). Source: Marshall and Plumb (2008).

GREB-model: For the GREB model we use the "greenhouse shield" / "slab atmosphere" model as in the previous Sect. 2.2.2. We simplify the atmosphere to just one layer, see sketch 4.15:

Surface:

$$F_{thermal} = -\sigma T_{surf}^4 + \epsilon\sigma T_{atmos-rad}^4 \quad (4.8)$$

Atmosphere:

$$F_{thermal} = -2\epsilon\sigma T_{atmos-rad}^4 + \epsilon\sigma T_{surf}^4 \quad (4.9)$$

Note, that the thermal radiation is a function of the atmospheric radiation temperature, $T_{atmos-rad}$, which is different from the atmospheric temperature, T_{atmos} , as we will discuss later in the sensible heat flux discussion. The temperature with which the earth radiates to space is that of the upper (about 4km height) level atmosphere.

GREB emissivity function: We simplify the emissivity of the atmosphere as

$$\epsilon_{atmos} = F(CO_2, H_2O_{vapour}, \text{cloud cover})$$

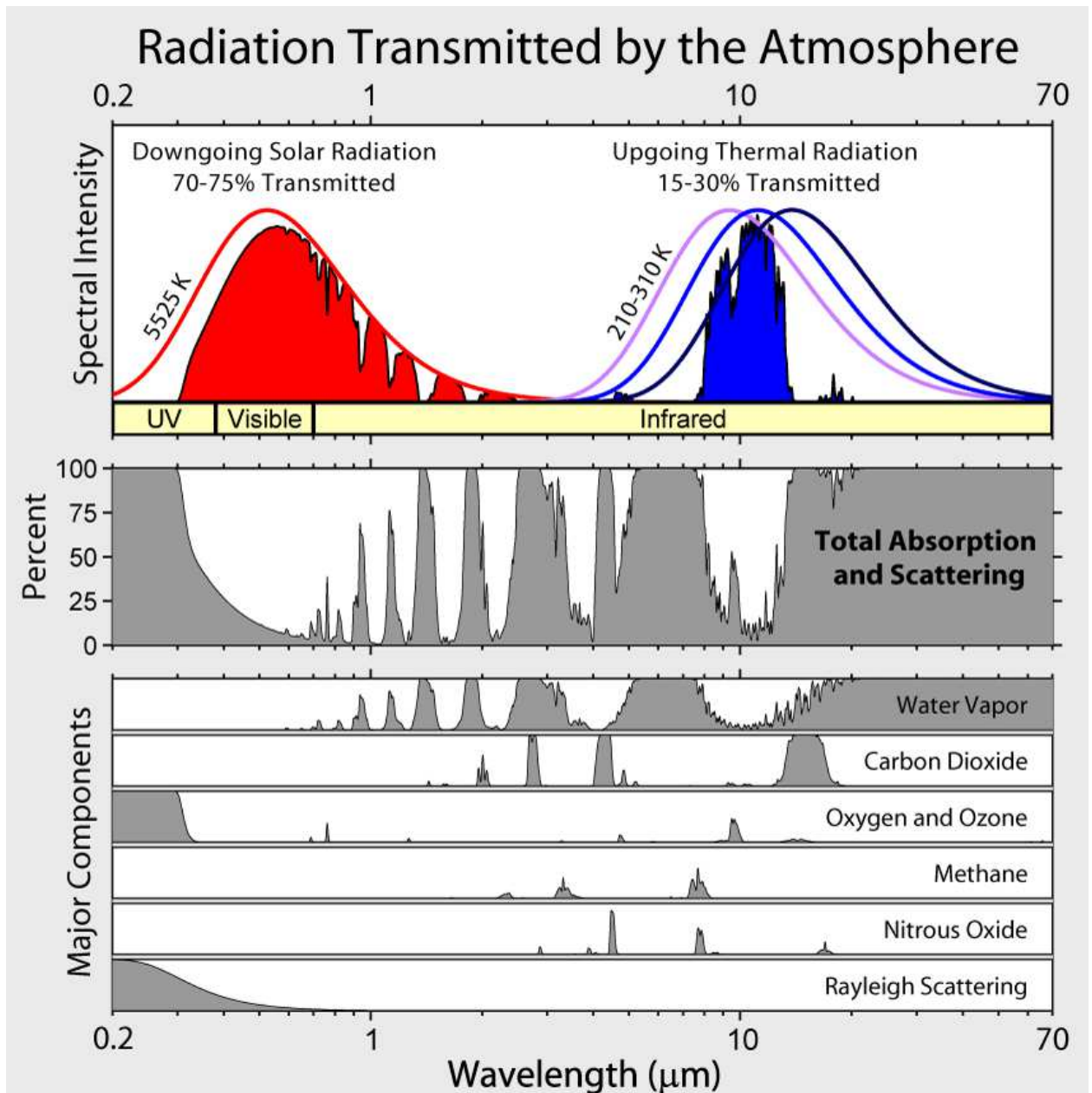


Figure 4.14: Radiation transmitted by the atmosphere. The lower panels: The amount of radiation absorption for the most important chemical components of the atmosphere as function of wave length. Middle: total absorption of the atmosphere as the sum of all components in percentage. Upper: Incoming Solar and outgoing terrestrial radiation power spectra.

Thus, we assume that only CO_2 , H_2O_{vapour} and cloud cover influence the emissivity of the atmosphere. Note, that take CO_2 as an estimate of all long lived greenhouse gasse (e.g. N_2O or CH_4); this is often referred to as **Equivalent CO_2 concentration**.

Approach for the emissivity function ϵ_{atmos} :

- Assume saturation effect: A doubling of greenhouse gases does not double the emissivity of the atmosphere as whole. This principle has been discussed in multi-layer greenhouse shield model.

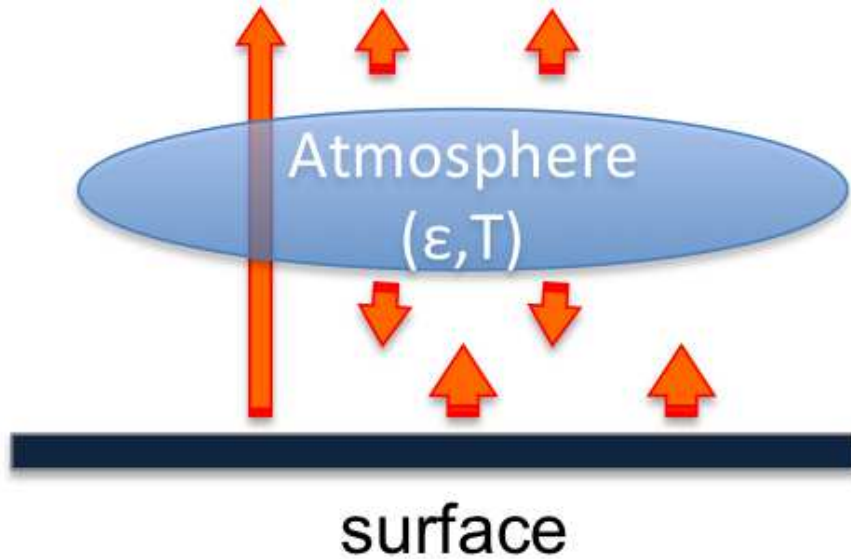


Figure 4.15: Sketch of GREB model thermal radiation: The Greenhouse Shield / Slab Atmosphere model.

- Log-function approximation: We try to model the saturation effect with a single layer model by a simple non-linear function: In this case the log-function. Note, there is no fundamental physical law behind this log-function (any non-linear function that mimics the saturation effect may do). This approach has been used in a number of studies before and is therefore somewhat established.
- 3 spectral bands: In Figure 4.14 see can see that CO_2 and H_2O are absorbing at different wave length and that at some wavelength both of them absorb. To simulate the overlap of absorption bands in CO_2 and H_2O we need three bands: Two bands in which each component absorbs independent of the other component and one band in which both absorb.
- Fit function to data: The log-function that we aim for will have 12 parameters that need to be determined. The simplest way to estimate these parameters is fit the values of these parameters to the observed characteristics of the emissivity function as see in Fig. 4.14, for instance, and from more sophisticated radiation models (GCM, IPCC-type models).

Saturation of the greenhouse effect: From the Multi layer greenhouse shield model in Sect. 2.2.2:

$$\rightarrow \sigma T_{surf}^4 = (N + 1) \cdot (1 - \alpha_p) Q \quad (4.10)$$

$$\rightarrow g = 1 - \frac{1}{N + 1} \quad (4.11)$$

From these equation we see that a doubling of concentrations (N) does not double the greenhouse effect. There is a saturation effect.

GREB emissivity function: The emissivity of the atmospheric layer is:

$$\epsilon_{atmos} = F(CO_2, H_2O_{vapour}, \text{cloud cover})$$

With:

$$\epsilon_{clear-sky} = \underbrace{p_4 \cdot \log[p_1 \cdot CO_2^{topo} + p_2 \cdot H_2O_{vapor} + p_3]}_{\text{CO}_2 \text{ and H}_2\text{O absorb}} + \underbrace{p_5 \cdot \log[p_1 \cdot CO_2^{topo} + p_3]}_{\text{only CO}_2 \text{ absorbs}} + \underbrace{p_6 \cdot \log[p_2 \cdot H_2O_{vapor} + p_3]}_{\text{only H}_2\text{O absorbs}} + p_7$$

Figure 4.16: The GREB model clear sky (no cloud effect) emissivity function. The three term represent the three spectral bands.

$\epsilon_{clear-sky}$ = clear sky emissivity (no clouds)

H_2O = total water vapour concentration in air column

CO_2^{topo} = concentration in air column

z_{topo} = altitude [m]

h_{atmos} = 8400 m = scaling height

a_{cloud} = cloud cover

Although CO_2 concentration is globally uniform, we need to consider that higher altitudes have less of an atmosphere above:

$$CO_2^{topo} = CO_2 \cdot e^{-\frac{z_{topo}}{h_{atmos}}} \quad (4.12)$$

Cloud cover scales the effective emissivity of ϵ_{atmos} by shifting it up or down and by diluting the effects of the trace gases:

$$\epsilon_{atmos} = \frac{p_8 - a_{cloud}}{p_9} (\epsilon_{clear-sky} - p_{10}) + p_{10}$$

So the 10 parameters of this function are:

p_4, p_5, p_6 = relative importance of each spectral band

p_1, p_2 = greenhouse scaling concentration

p_3 = contribution to greenhouse effect by other gases

p_7 = artificial fitting constant

p_8, p_9, p_{10} = cloud scaling parameter

$p_1 > 0$ all parameters are positive

The GREB emissivity function is a simple parameterisation of a complex problem. To estimate the parameters of this function we need to have data on which to constrain the parameters. The basis for the estimation of these parameters are some known characteristics of the emissivity function.

Characteristics of the emissivity function, which we can mostly get from evaluating the radiation spectrum in Fig. 4.14:

1. Global mean emissivity $\epsilon = 0.8$
2. $\Delta\epsilon$ (water vapour $\rightarrow 0$) ≈ 0.5 . the largest part of emissivity is due to water vapour.
3. $\Delta\epsilon(CO_2 \rightarrow 0) \approx 0.18$
4. $\Delta\epsilon(\text{cloud cover} \rightarrow 0) \approx 0.16$
5. $\epsilon(CO_2 = H_2O = \text{cloud cover} = 0) \approx 0$ No greenhouse gases and no clouds \rightarrow no emissivity.
6. $\epsilon(H_2O = 70\text{kg}/\text{m}^2, \text{cloud cover} = 1) \approx 1$ A very humid and fully cloud covered atmosphere has emissivity of about 1.
7. % of the H_2 absorption is non-overlapping with the CO_2 absorption bands.
8. H_2O and CO_2 have about equal strength in spectral bands where they both absorb.
9. CO_2 absorbs about equally strongly in the two absorption bands.
10. Clear sky sensitivity to greenhouse gases is about twice as strong as for completely cloud covered sky.
11. $\Delta\epsilon(2 \times CO_2) \approx 0.02$ The change in emissivity due to doubling of CO_2 , which follows from the IPCC models $3.8\text{W}/\text{m}^2$ additional thermal downward radiation.
12. $\Delta\epsilon(\Delta \text{ water vapour}) \approx 0.02$ It follows from the IPCC models.

With these 12 characteristics of the emissivity we can determine the 10 parameters of the GREB emissivity function using a numerical optimisation scheme. The values of the 10 parameters are listed in Dommenget and Floeter [2011].

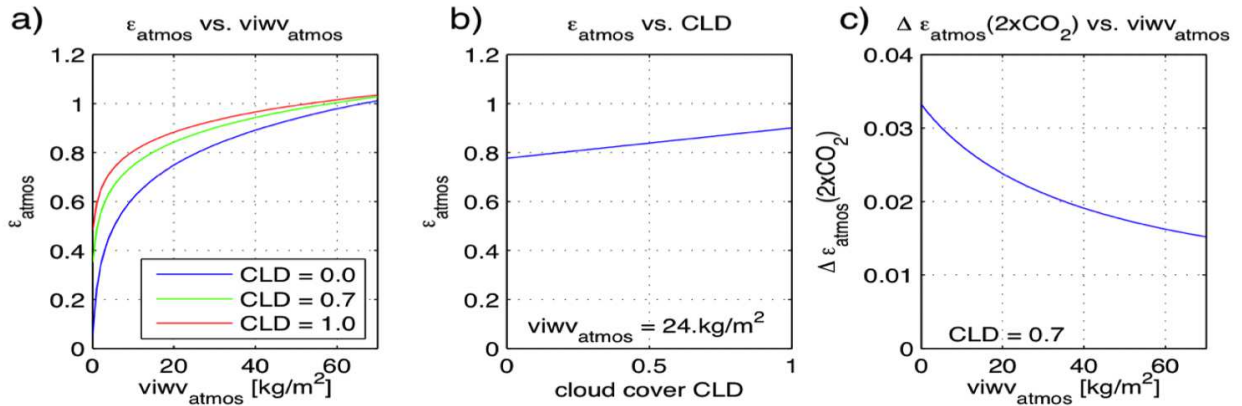


Figure 4.17: Some of the most important characteristics of the GREB emissivity function: (a) ϵ_{atmos} as function of H_2O for three different cloud covers. (b) ϵ_{atmos} as function of cloud covers for $H_2O = 24\text{kg}/\text{m}^3$. (c) $\Delta\epsilon_{\text{atmos}}$ for a doubling of CO_2 as function of H_2O . Note, the Vertically Integrated Water Vapor ($viwv_{\text{atmos}}$) is the same as H_2O in the GREB emissivity function.

Figure 4.17 shows some of the aim characteristics of the GREB emissivity function:

- Water vapour has a strong effect on ϵ .
- The effect of water vapour is non-linear.

- The sensitivity to change in water vapour (slope) is bigger for small amounts of water vapour.
- Clouds increase ϵ .
- Clouds dilute the effect of greenhouse gases.
- The sensitivity to CO_2 is bigger if water vapour is less.

The GREB model approach for the thermal radiation requires us to have an atmospheric temperature and atmospheric water vapor concentrations. So we need to extent the GREB model:

1. We need a prognostic equation for T_{atmos} :

$$\gamma_{atmos} \frac{dT_{atmos}}{dt} = F_{thermal} + \dots$$

2. We need a prognostic equation for q_{atmos} :

$$\frac{dq_{surf}}{dt} = \dots$$

4.1.4 Hydrological cycle

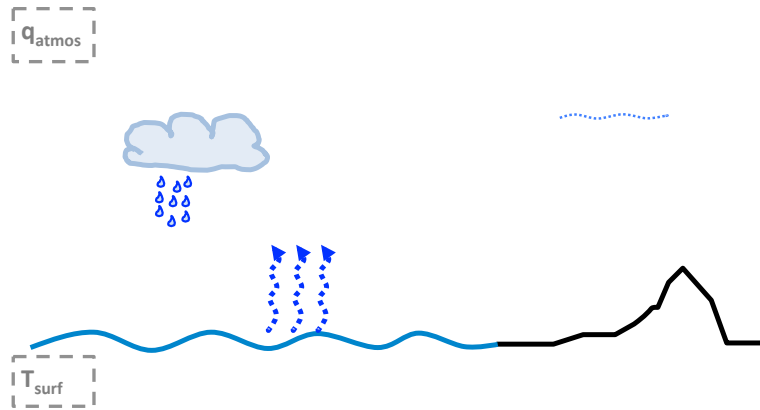


Figure 4.18: Sketch GREB model process: The hydrological cycle; evaporation, precipitation, latent cooling at the surface and heating in the atmosphere and the amount of water vapour in the atmosphere.

In the previous section we have seen that water vapour is the most important greenhouse gas. We therefore need to know the amount of water vapour in the atmosphere. Here it is important to note that CO_2 and water vapour have quite different characteristics in the atmosphere:

- Lifetime of CO_2 in atmosphere: 10 yrs - 10,000 yrs (different processes involved). Since it stays in the atmosphere for so long it is globally well mixed and therefore it is globally uniformly distributed; every point on the earth surface, that is on the same pressure level, has roughly the same amount of CO_2 in the air column above it.
- Lifetime of water vapour in atmosphere: 10 days (rain, weather). So it stays in the atmosphere only very shortly and is therefore not well mixed and has strong regional differences. This implies we need to simulate it with a prognostic equation:

$$\frac{dq_{surf}}{dt} = \Delta q_{eva} + \Delta Q_{precip} + \dots \quad (4.13)$$

Δq_{eva} = evaporation of water into the atmosphere

Δq_{precip} = condensation and precipitation of water out of the atmosphere

Complex weather: It rains if water vapour in the atmosphere condenses and the droplets get big enough to fall to the ground. Therefore the air must saturate with water vapour. Air typically saturates with water vapour if air is lifted (vertical motion) and therefore adiabatically (by reducing pressure) cooled. Thus many different processes are involved in precipitation and they are controlled by weather fluctuations.

→ Weather fluctuations can not be ‘*simulated*’ in the simple GREB model.

Precipitation:

How to estimate precipitation in GREB?

- Roughly: it rains if there is atmospheric water vapour.
- Atmospheric water vapour stays in the atmosphere for about 10 days

$$\Rightarrow \Delta q_{precip} = 0.1 \frac{1}{day} q_{atmos}$$

Thus we make the very strong simplification that it rains 10% of the water vapour in the air column every day.

Evaporation:

- Evaporation at the surface increases the relative humidity, q_{atmos} [%]
- Evaporation or any other phase change of water causes latent heat flux

An empirical bulk formula for the evaporation, Δq_{eva} :

$$\Delta q_{eva} = \frac{1}{r_{H_2O}} \cdot \rho_{air} \cdot C_w \cdot |\vec{u}_*| \cdot v_{soil} \cdot (q_{sat} - q_{atmos}) \quad (4.14)$$

r_{H_2O} = regression parameter

ρ_{air} = density of air at sea level

C_w = empirical transfer coefficient over oceans

$|\vec{u}_*|$ = effective wind speed

v_{soil} = surface moisture [%]

q_{sat} = saturated humidity [kg/kg]

q_{atmos} = atmospheric humidity [kg/kg]

Saturation

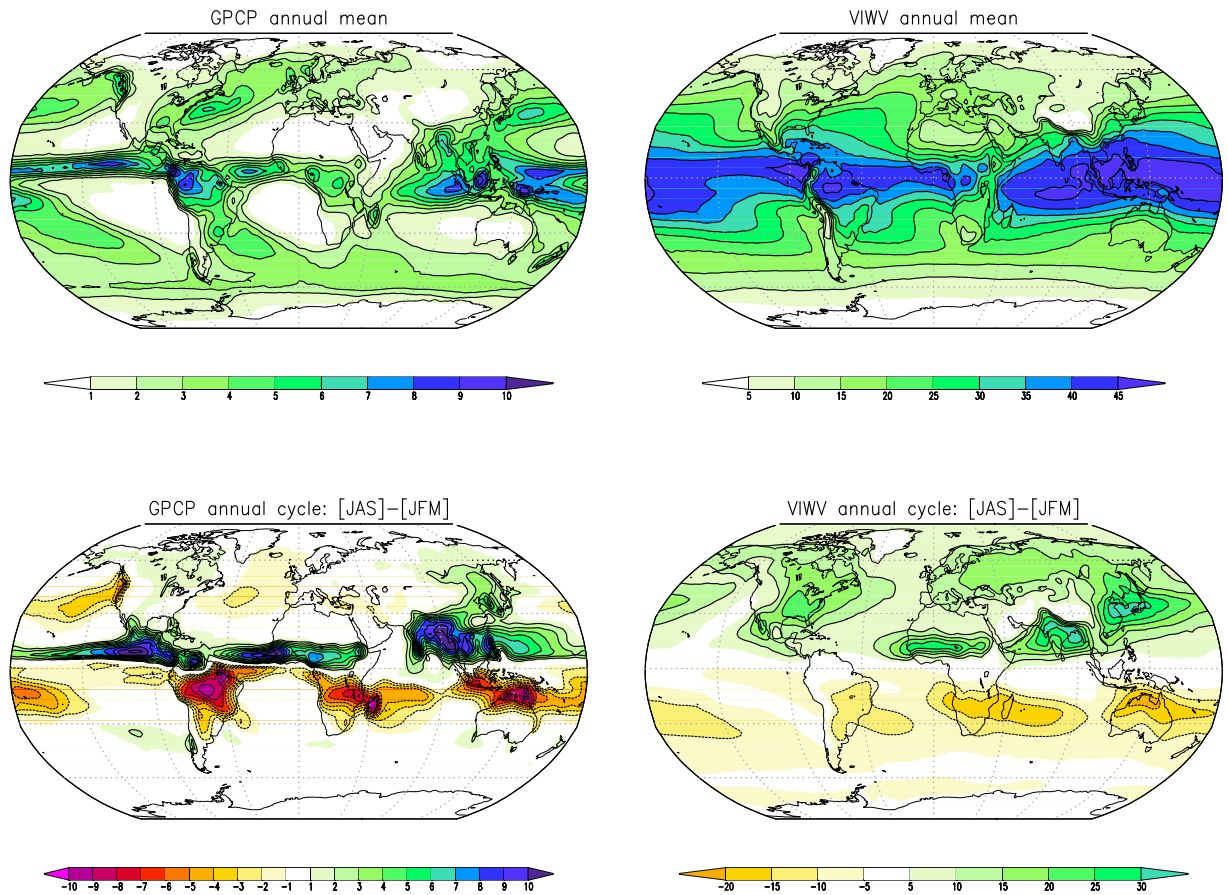


Figure 4.19: Left: annual mean precipitation (upper) and seasonal cycle estimated by the difference Jun./Jul./Aug. minus Jan./Feb./Mar. (lower). Right: same but for the vertically integrated water vapor. Note the similarity in the patterns suggests that rain is roughly proportional to the amount of water vapour in the air. However, you can also note that this similarity is not that strong.

A closed sample of air over a plane water surface in equilibrium between condensation and evaporation is said to be saturated.

Water Vapour Mixing Ratio

Typically r and q range from 20 g/kg at low levels in the tropics to very low values at high latitudes or at high elevations.

If neither evaporation nor condensation take place, the mixing ratio of an air parcel is constant.

20 g/kg $\approx \frac{1}{2}$ small glass of water per 1 m³
 20 g/kg \approx 10 litres per lecture room

Saturated water vapour: The amount of water vapour that the air can hold depends on the temperature; following from *Clausius-Clapeyron equation*:

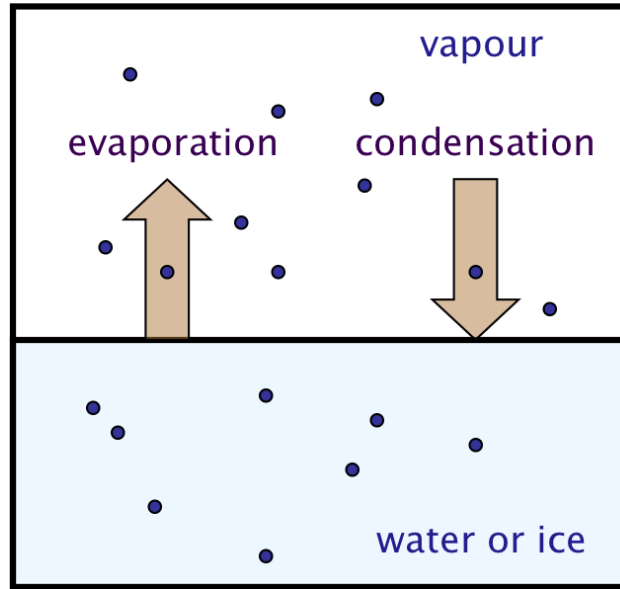


Figure 4.20: Sketch illustrating Saturation: Air over a moist surface is saturated if evaporation and condensation are in balance.

$$q_{sat} = e^{\frac{-z_{topo}}{h_{atmos}}} \cdot 3.75 \cdot 10^{-3} \cdot e^{17.1 \frac{T_{surf} - 273.15}{T_{surf} - 38.98}} \quad (4.15)$$

This equation also considers that the surface pressure decrease with altitude. The derivation of this equation (without the topography effect) and its solution is given in most texts on thermodynamics.

Note: if $dT = 3^\circ C \rightarrow q_{sat}$ changes by about 20%. Assuming relative humidity is not changing, global warming will most likely cause a significant change in q_{atmos} .

Over all we find that Evaporation is strong if:

- Winds are strong.
- Air is dry and warm.
- Surface is wet.

Surface Humidity vs. Total water vapour in air column: In the emissivity function for the thermal radiation we need to know the total amount of water vapour in the air column, H_2O . In the above hydrological cycle we discussed terms for the surface humidity change, q_{atmos} .

In the GREB model we make the simple approximation:

$$H_2O_{vapour} = e^{\frac{-z_{topo}}{h_{atmos}}} \cdot r_{H_2O} \cdot q_{atmos} = e^{\frac{-z_{topo}}{h_{atmos}}} \cdot 2.67 \cdot 10^3 \text{ kg/m}^2 \cdot q_{atmos} \quad (4.16)$$

The total amount of water vapour in an air column is proportional to the surface humidity and we assume some altitude effect, that reduces the total amount of water vapour in the air column for a given surface humidity.

Latent heat: F_{latent}

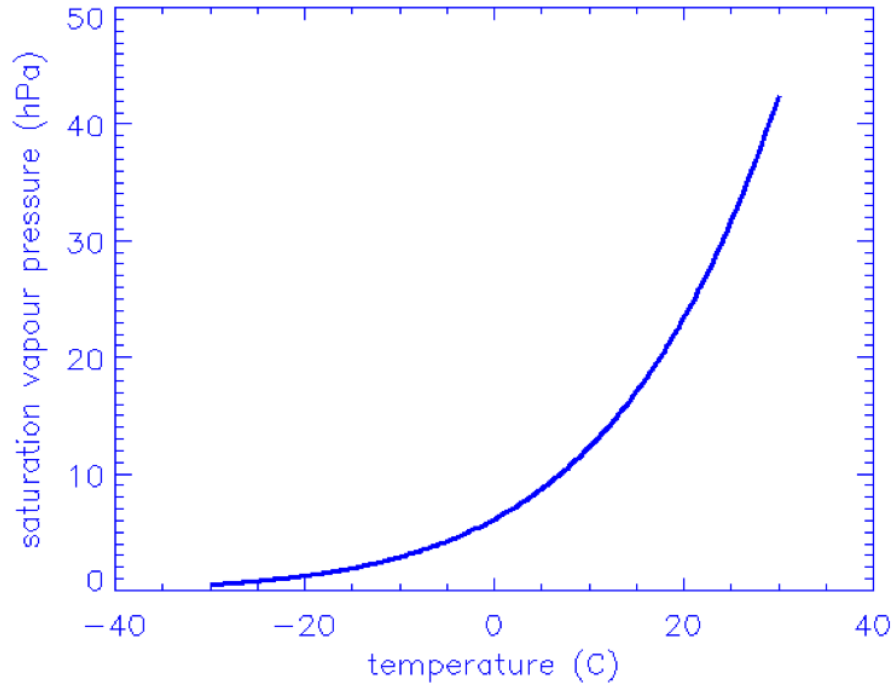


Figure 4.21: Saturation vapour pressure as function of temperature. The Clausius-Clapeyron relation.

$$F_{latent} = -L \cdot r_{H_2O} \cdot \Delta q_{eva}$$

$$L = 2.3 \cdot 10^6 J/kg = \text{latent heat of condensation}$$

$$c_{H_2O} \approx 4000 J/kg/K = \text{specific heat of water}$$

Note: this is a lot of heat if compared to the specific heat of water. Condensing water vapour to water (raining) releases more heat than is required to heat water by about 500 K!!

Latent heating implications for deep tropical convection: When air rises in convective thunderstorms, it loses all of its water vapour by raining or building clouds. This releases latent heat and heats the tropical atmosphere by about $+50^\circ C$ (see Fig.4.23). The vertical temperature gradient is much weaker than you would expect from the adiabatic cooling by expanding into the lower pressure high levels.

As a result of the hydrological cycle we have now extended our GREB model equations and added a prognostic equation for the surface humidity:

$$\gamma_{surf} \frac{dT_{surf}}{dt} = F_{solar} + F_{thermal} + F_{latent} + \dots$$

$$\gamma_{atmos} \frac{dT_{atmos}}{dt} = F_{thermal} + F_{atmos-latent} + \dots$$

$$\frac{dq_{surf}}{dt} = \Delta q_{eva} + \Delta q_{precip} + \dots$$

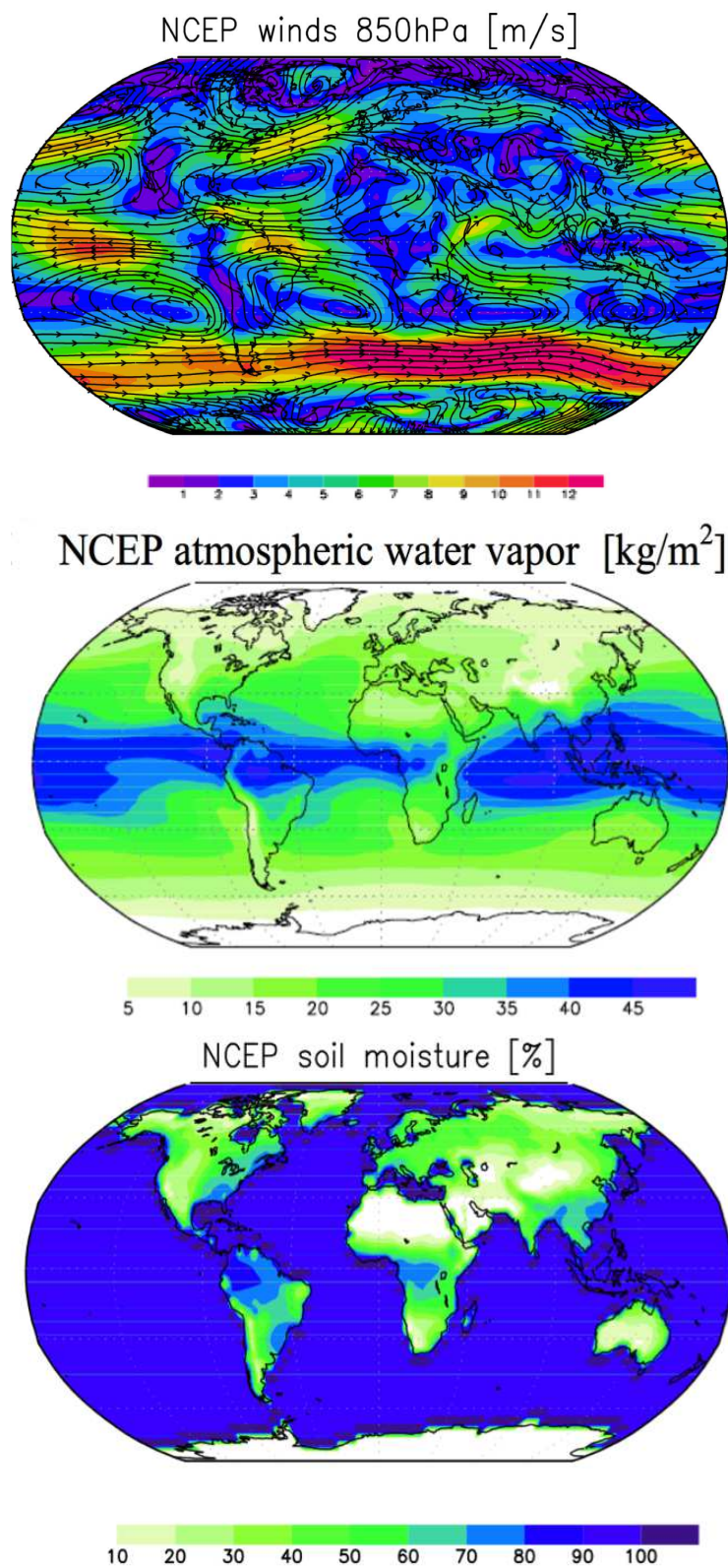


Figure 4.22: Climatic fields important for evaporation: Surface winds, soil moisture and atmospheric near surface humidity.

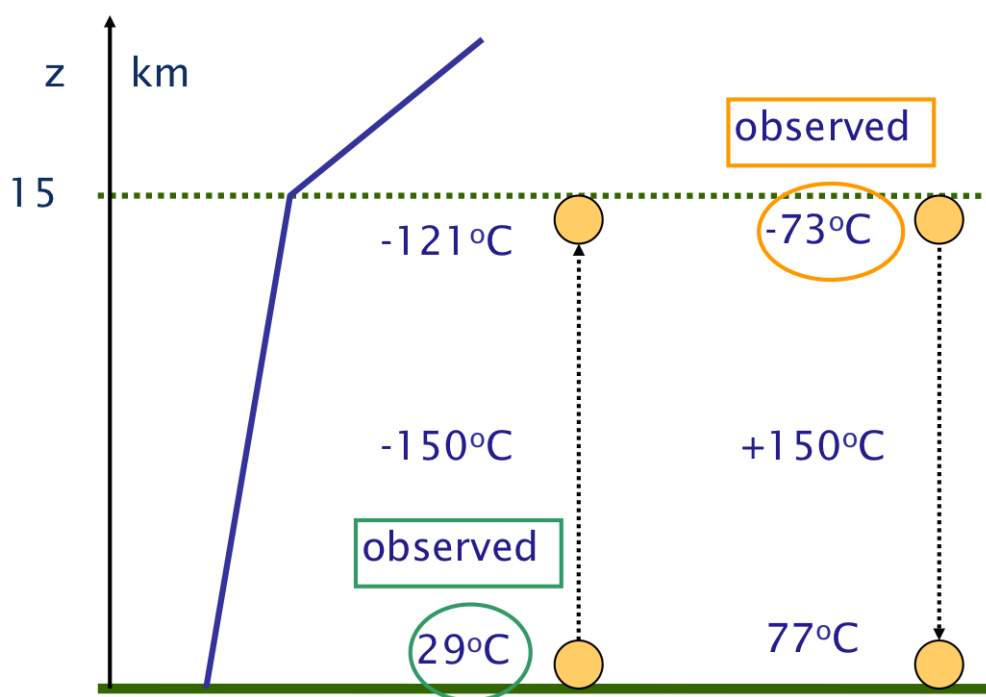


Figure 4.23: Illustration of tropical vertical temperature gradients. When air rises in convective thunderstorms, it loses all of its water vapour by raining or building clouds. This releases latent heat and heats the tropical atmosphere by about $+50^{\circ}\text{C}$. The vertical temperature gradient is much weaker than you would expect from the adiabatic cooling by expanding into the lower pressure high levels.

4.1.5 Sensible heat and atmospheric transport

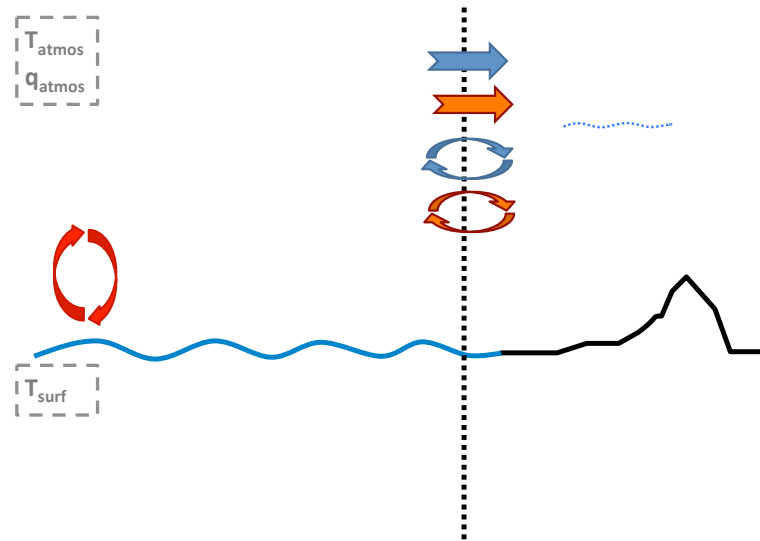


Figure 4.24: Sketch GREB model process: Sensible heating and transport of heat and moisture in the atmosphere.

The sensible heat flux is the heat exchange due to small scale turbulent heat transfer. In principle two objects in contact with each other will have the molecules hit each other and thereby exchanging heat. This molecular sensible heat exchange is however in general orders of magnitudes smaller than the total sensible heat exchange. The main sensible heat exchange is by turbulent transport. If, for instance, the ocean surface (or any atmospheric layer) is in contact with the above atmospheric layer, then small scale turbulence will transport the air close to the surface away from the surface taking with them the heat characteristics from the ocean surface. The air that replace the air taken away will have different heat characteristics (.e.g be warmer or colder), thus this air exchange at the surface is effectively a heat flux: the sensible heat flux.

Related to the sensible heat flux we can also discuss the transport of heat and water vapor from one region to another (lateral heat transport). This large scale transport is the only process that leads to interactions between different regions in the GREB model.

We can simplify the sensible heat flux and large-scale transport in the GREB to:

- Sensible heat flux is proportional to temperature differences: This is called *Newtonian damping*.
- Lateral transport is only in the atmosphere (not in ocean, not in surface layer).

Sensible heat flux

The Sensible heat flux between atmosphere and surface (land, ocean or sea ice) is:

$$F_{sense} = C_{A-S} \cdot (T_{atmos} - T_{surf})$$

The strength of this heat exchange coupling (damping) is

$$C_{A-S} = 22.5 \frac{W}{m^2 K}$$

The stronger the temperature difference the stronger the heat exchange. The coupling or damping strength C_{A-S} can also be interpreted as feedback parameter. Since is on the regional scale (e.g. one region being very different from neighbouring regions) a very strong feedback.

Note, that the atmospheric temperature in the real world, T_{atmos} , is in much colder than the surface temperature due to the adiabatic cooling by expanding to low air pressure. However, adiabatic effects due to pressure difference are not simulated in the GREB model. The absolute temperature is not important in the sensible heat flux, as only the temperature difference to T_{surf} matters, but it does matter for the thermal radiation of the atmosphere. The temperature with which the atmosphere radiates to space is that of the upper (about 4km height) level atmosphere. To consider the much colder atmospheric temperature we define the radiation temperature:

$$T_{atmos-rad} = T_{atmos} - \Delta T_{pressure} \quad (4.17)$$

with

$$\Delta T_{pressure} = 0.16 * T_0 + 5^\circ K \quad (4.18)$$

Here T_0 is the climatological mean T_{surf} . Thus $T_{atmos-rad}$ is assumed to be colder than T_{atmos} by $\Delta T_{pressure}$, which is proportional to the mean T_{surf} . This mimics the adiabatic cooling due to the reduced pressure effect.

The sensible heat flux from the subsurface ocean is:

$$F_{sense} = C_{O-S} \cdot (T_{ocean} - T_{surf}) \quad (4.19)$$

with a weaker coupling (feedback) constant $C_{O-S} = 5 \frac{W}{m^2 K}$. The turbulent heat exchange with subsurface ocean is much weaker due to the much weaker turbulence in the subsurface ocean.

Atmospheric transport of heat and water vapor

Simplification of transport:

- Assume a mean transport (advection)
- Assume a turbulent isotropic diffusion

Heat transport by advection is proportional to the scalar product between wind-vector and the direction of the temperature gradient:

$$F_{adv} \propto -\vec{u} \cdot \vec{\nabla} T$$

The amount of heat flux is depending on the amount of fluid heat, thus is depends on the heat capacity:

$$\Rightarrow \frac{F_{adv}}{\gamma_{atmos}} = -\vec{u} \cdot \vec{\nabla} T$$

Note, the temperature tendencies by advection do not depend on the heat capacity, but the heat flux does.

Isotropic diffusion (mixing by turbulent winds) heats or cools regions with extremes (minimas or maximas).

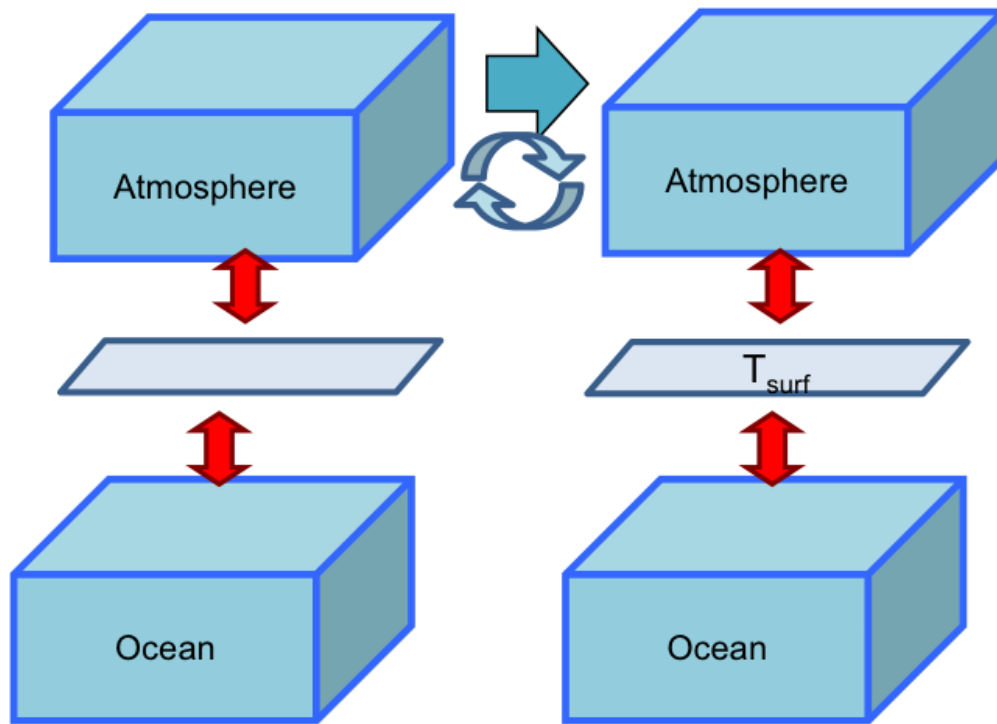


Figure 4.25: Sketch of the GREB sensible heat exchange. The surface exchanges sensible heat with the atmosphere and subsurface oceans. The heat is transported horizontally only in the atmospheric layer.

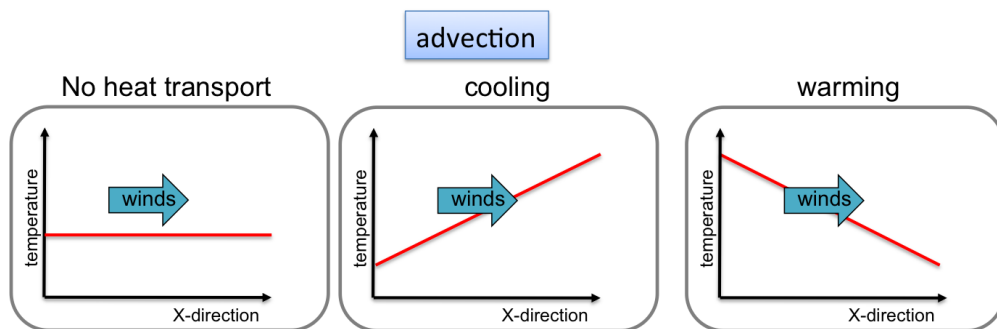


Figure 4.26: Advection with the mean winds transports heat across temperature gradients.

Diffusion transports heat away or to regions which are warmer or cooler than the neighbourhood, see Fig. 4.27. Heat transport by isotropic diffusion is strong if the 2nd derivative of the temperature field is strong and the turbulence of the winds (κ) is strong:

$$\frac{F_{diffuse}}{\gamma_{atmos}} = \kappa \cdot \nabla^2 T$$

with the effective diffusion coefficient:

$$\kappa = 2 \cdot 10^5 \frac{m^2}{s}$$

The value of κ defines the strength of turbulent winds (weather). The more turbulent the winds are (the more often they change direction and the stronger the winds are) the larger κ is. Here it assume that κ is a global constant, but in the real world the strength of the turbulent winds (weather) has significant regional differences. The heat transport by isotropic diffusion should erase any temperature maxima/minima in the atmosphere within days.

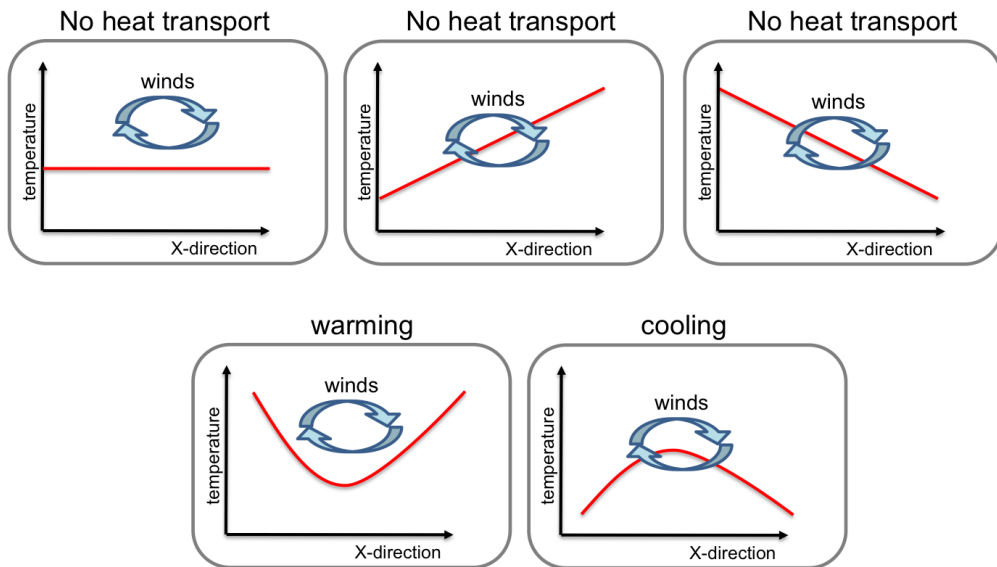


Figure 4.27: Heat flux by isotropic diffusion.

In the GREB model we make the simplification that transport only happens in the atmosphere, neglecting the ocean heat transport. In section 3.4 we illustrated that most of the transport is indeed in the atmosphere, however the oceans do contribute to the transport by about 20-30%. In some regions ocean heat transport is more important atmospheric heat transport. However, for a first order guess neglecting ocean heat transport is a decent approximation in the context of the large-scale global climate system.

4.1.6 Subsurface Ocean

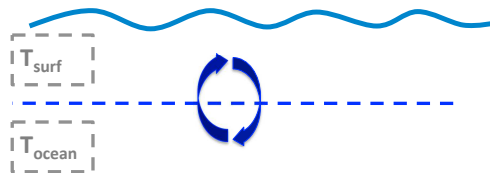


Figure 4.28: Sketch GREB model process subsurface heat exchange.

Most of the heat in the active climate system (those parts that interact with the atmosphere on time scales of month to decades) is stored in the upper ocean. The heat that goes in to the subsurface ocean is not just a function of the surface temperature change, but can be partly independent of the surface temperature. We therefore need to simulate a subsurface ocean temperature, T_{ocean} .

Here we do the following Simplifications:

- No lateral heat transport in ocean. We assume all heat is transported in the atmosphere.
- Sensible heat flux proportional to temperature differences (Newtonian damping).
- Entrainment by changes in mixed layer depth (MLD). The seasonal cycle in the thickness of the surface layer (mixed layer depth) does most of the heat exchange between the surface layer and the subsurface ocean.
- Effective ocean heat capacity is proportional to MLD. Regions that have a deeper surface layer (mixed layer depth) will also mix deeper into the ocean.

Sensible heat flux:

The sensible heat exchange between the surface layer of the ocean and the subsurface layers is assumed to be by Newtonian damping, as in the atmosphere-surface heat exchange:

Sensible heat flux from deeper ocean:

$$F_{O_{sense}} = C_{O-S} \cdot (T_{ocean} - T_{surf})$$

The strength of this heat exchange coupling (damping) is

$$C_{A-S} = 5 \frac{W}{m^2 K}$$

This is much weaker than in the atmosphere, because the turbulence in the ocean currents are much weaker than the turbulence in the atmospheric winds. However, the sensible heat flux is not the only process by which the surface and the subsurface ocean exchange heat in the GREB model. The total heat exchange has two terms:

$$F_{ocean} = F_{O_{sense}} + \Delta T_{entrain}$$

The second term is the heat exchange due to entrainment of water from one layer to the other. This $\Delta T_{entrain}$ term is in general much larger than the sensible heat flux $F_{O_{sense}}$.

Entrainment:

The sketch in Fig. 4.29 illustrates how heat is exchanged by entrainment. In spring, when the thickness of the surface layer (the mixed layer depth, h_{mix}) decreases, water from the surface layer goes into the subsurface layer. In turn, in fall, when the mixed layer depth increases subsurface water is entrained into the surface layer. If the subsurface layer has a different temperature than the surface layer, which is in general has, then this changes the surface layer temperature and thus effectively presents a heat transport into the surface layer. This heat transport by entrainment, $\Delta T_{entrain}$, is stronger if the seasonal cycle of the mixed layer depth is stronger. $\Delta T_{entrain}$ is a function of rate of change in h_{mix} and the temperature difference between the surface and the

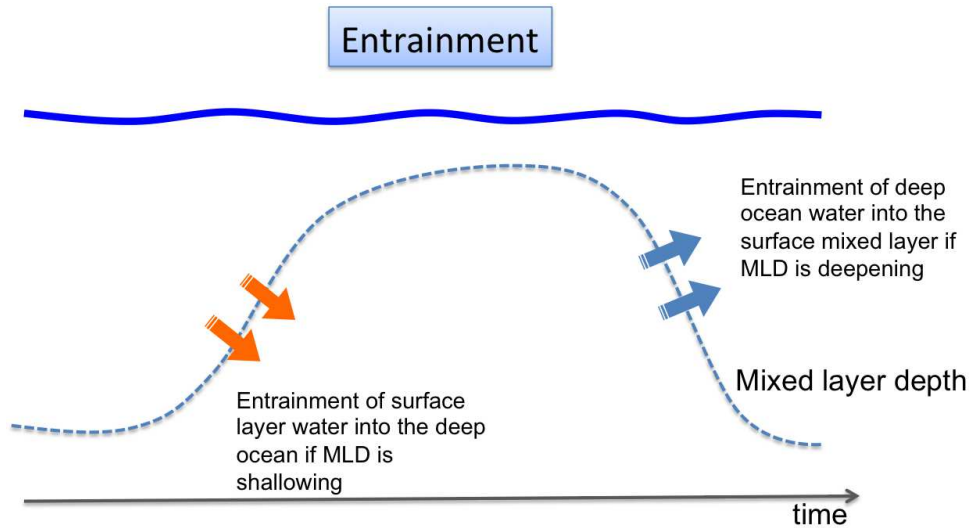


Figure 4.29: Entrainment: the seasonal cycle of the surface mixed layer depth causes most of the heat exchange between the surface and the subsurface oceans.

subsurface layer (Note, the detailed function of $\Delta T_{entrain}$ is not presented here as it would require too much space with too little information gained).

Subsurface ocean temperature tendencies

We can now formulate a subsurface ocean tendency equation:

$$\gamma_{ocean} \frac{dT_{ocean}}{dt} = \Delta T_{O_{entrain}} - F_{O_{sense}} \quad (4.20)$$

Ocean mixed layer depth

An important aspect in this equation is that the heat capacity, γ_{ocean} , is different at different location. For the surface layer the heat capacity, γ_{surf} , is proportional to h_{mix} , see Fig. 4.30.

The thickness of the subsurface layer in the GREB model is also a function of h_{mix} . Here it is assumed that the layers of the ocean that actively interact with the surface (atmosphere) are proportional to the annual mean strength of the entrainment rates, $\Delta T_{entrain}$. This is most strongly related to the maximum depth of h_{mix} during the year. Therefore the thickness of the subsurface ocean layer is chosen as three times the maximum h_{mix} minus the thickness of the surface layer. From Fig. 4.30 we can roughly see that the subsurface ocean layers are larger in higher latitudes (300m-800m) and thinner in near the equator (100m-200m). Thus most of the subsurface heat storage is at higher latitudes. We can also note that the GREB model neglects much of the deeper ocean (500m-5000m).

Heat capacity

The table below lists the different values of the heat capacities in the GREB model. We can clearly see that most of the heat is stored in the oceans.

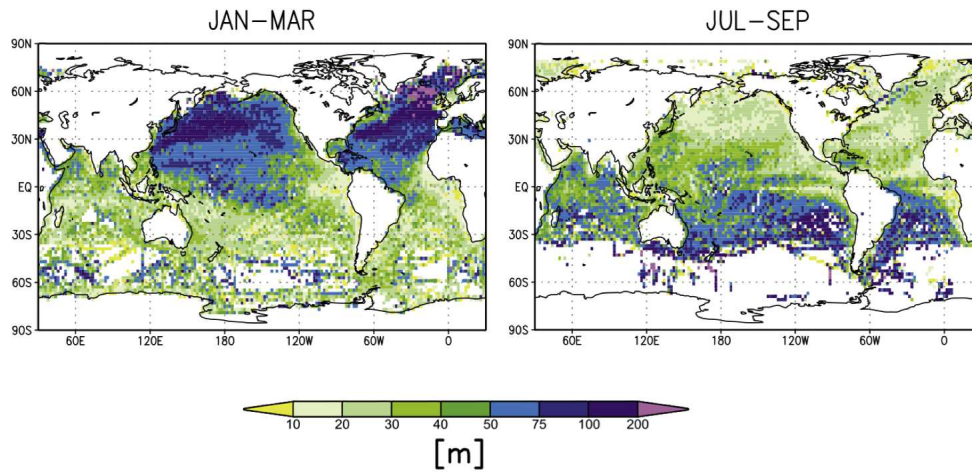


Figure 4.30: Ocean mixed layer depth. Regions with deep mixed layers are also regions in which a lot of heat is exchanged with the deeper oceans.

Atmosphere	$\gamma_{atmos} = 5 \cdot 10^6 \cdot J/m^2/K$	About 5000m air column
Land	$\gamma_{surf} = 4 \cdot 10^6 \cdot J/m^2/K$	About 2m soil column
Ocean surface	$\gamma_{surf} \approx 200 \cdot 10^6 \cdot J/m^2/K$	In average 50m water column; large regional and seasonal differences depending on mixed layer depth
Subsurface ocean	$\gamma_{ocean} \approx 1000 \cdot 10^6 \cdot J/m^2/K$	About three times the max. mixed layer depth; strong regional differences. Not the whole deep ocean is mixed.
Sea ice	$\gamma_{surf} = 4 \cdot 10^6 \cdot J/m^2/K$	As for ice-albedo feedback, some ocean points are sometimes ice covered. Sea ice insulates the ocean from the atmosphere very well. → heat capacity over ocean is function of temperature for below freezing values.

4.1.7 Sea Ice

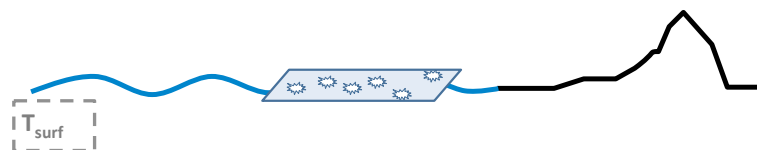


Figure 4.31: Sketch GREB model process sea ice.

An ocean area totally covered with sea ice is essentially like a land point covered with snow. It thus behaves like a land point in its heat exchange with the atmosphere. The sea ice main features in the large scale climate context and as simulated in the GREB model are:

- Changing heat capacity of oceans points to those of land points as function of temperature.
- Heat flux to the subsurface oceans due to entrainment is set to zero, as the sea ice will insulate the ocean from wind mixing.
- Change of albedo as function of temperature. Similar to land points, but with a different temperature range, see Fig. 4.9.

Sea ice heat capacity

The ocean heat capacity changes from that of a 30m water column to that of land if the temperature is below the freezing point of sea water. Thus in regions where sea ice accrues, the surface layer heat capacity is a function of temperature.

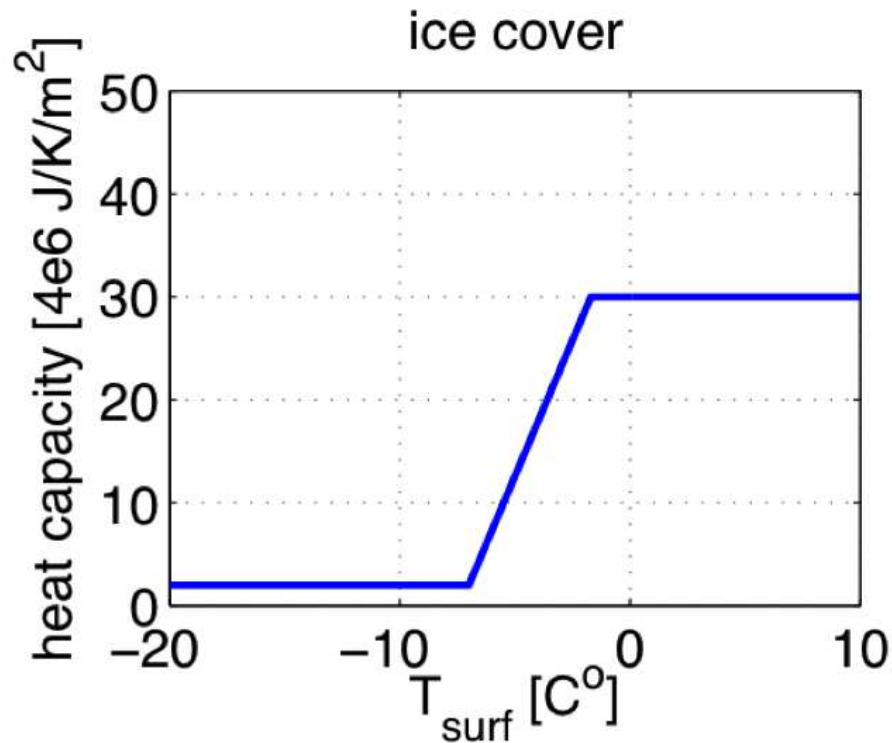


Figure 4.32: Sea ice heat capacity function for the GREB model.

4.1.8 Estimating the equilibrium climate

In the previous sections we have analysed simple climate models and calculated the equilibrium temperatures analytically. Although, the GREB model is still simple compared to state of the art climate models, it is complex enough that analytical solutions of the model do not exist. So we need to numerically solve the model to get an understanding of its equilibrium climate or sensitivity to

external forcings. We will first of all discuss how the GREB model equilibrium climate is estimated and then we will discuss the time scales that are involved in the climate model simulations.

Model integration

To estimate the equilibrium climate of a complex climate model (such as the GREB model) we need to integrate the model equations over a long time interval until the model has reach its equilibrium state. We can illustrate this with the T_{surf} tendency equation. The equilibrium T_{surf} is:

$$T_{surf}^{eq} = T_{surf}(t_0) + \int_{t=0}^{\infty} \frac{1}{\gamma_{surf}} F_{net}(t, T, q, \dots) dt \quad (4.21)$$

With F_{net} as the right hand side of the T_{surf} tendency equation. Thus, the equilibrium T_{surf} , T_{surf}^{eq} , can be calculated by starting with some initial condition (observed climate state) and then integrate the model tendencies for a very long time (theoretically infinit). Numerically the integral is approximated by a sum of very small integration steps:

$$T_{surf}^{eq} \approx T_{surf}(t_0) + \sum_{t=0}^{t_{eq}} \frac{1}{\gamma_{surf}} F_{net}(t, T, q, \dots) \Delta t \quad (4.22)$$

Figure 4.33 illustrates the integration. The time step $\Delta t = 12hrs$ for the GREB model. The time step has to be small enough that all tendencies of the model are small enough to be approximated by a linear gradient. Note, the tendencies are different in each time step as they depend on the climate state of the previous time step.

To estimate the equilibrium state we stop the integration at the time t_{eq} , for which:

$$\frac{dT_{surf}(t_{eq})}{dt} \approx 0 \quad (4.23)$$

This is the normal definition of the equilibrium.

Response time

How long does it take for the climate to respond to forcing? We can build a simple linear model to roughly estimate what the time scales are. Let's assume the simple tendency equation:

$$\gamma \frac{dT}{dt} = C_f \cdot T + Q \quad (4.24)$$

With a negative feedback of $C_f = -1 \frac{W}{m^2 K}$ and a constant forcing of $Q \approx 4 \frac{W}{m^2}$. We can again numerically integrate this simple equation and see how long it takes until T has reach its equilibrium ($\frac{dT_{surf}(t_{eq})}{dt} \approx 0$), see Fig. 4.34. It takes about 20-30 years for the surface ocean to respond, but the deep ocean will take much longer (1000 years).

4.1.9 The GREB climate simulation, limitations and correction terms

The GREB model set of equations is a very strong simplification of the climate. How good it presents the climate can be seen if we compute the equilibrium climate of this model and compare it with the observed mean state.

In Figure 4.35 we can see the winter and summer mean T_{surf} for both the GREB model and observations. The large scales features, such as land sea contrast, seasonal cycle and large scale zonal temperature gradients (e.g. subtropical east-west temperature gradient) are well represented by the GREB model. For most regions the GREB model can simulate the mean climate within a range of $\pm 5^\circ C$. However, in the polar regions the GREB model are much bigger. These extreme climates are not very well simulated by the simple GREB model.

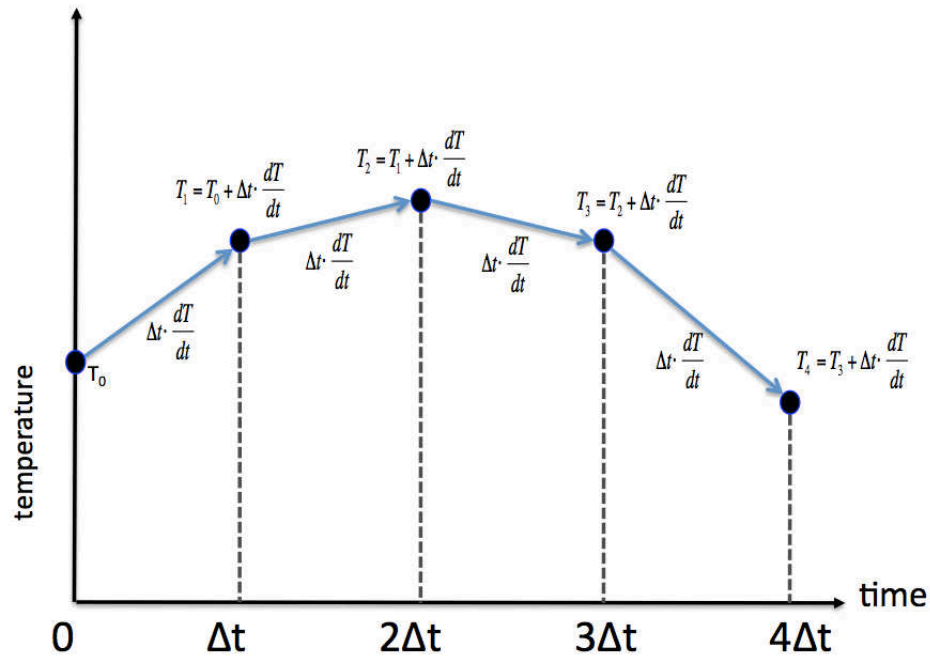


Figure 4.33: Numerical integration of tendency equations. Complex systems that can not be solved analytically, have to be integrated by small time steps Δt for the initial value T_0 to the future.

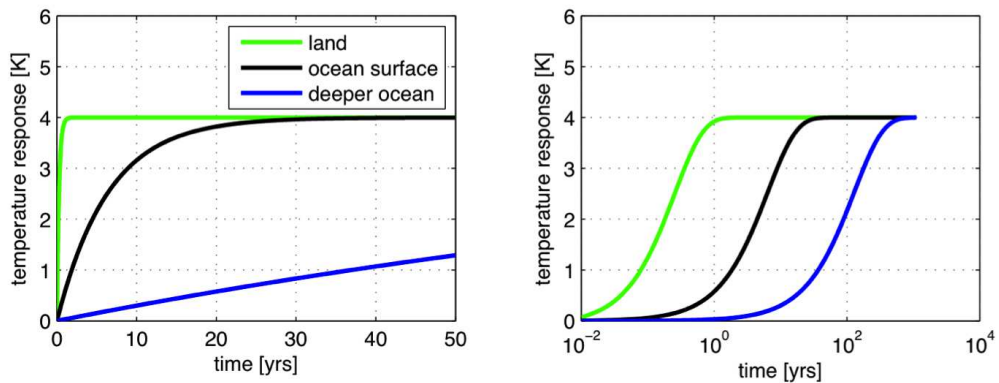


Figure 4.34: Response time to a fixed forcing in a simple linear response model. See text for details.

Note: The climate mean state has a range from -50°C to 40°C . So it is a $\Delta T \approx 100^\circ\text{C}$ for largely different forcings at different regions and seasons. So the errors of 5°C to 20°C are in relative terms, an error of about 10% to 20%. Thus the GREB model has for most regions an error of about 10%. Climate change is a $\Delta T \approx 5^\circ\text{C}$ for a small forcing, which is much smaller than the range in mean climate state. So a model which may have a 10-20% error in the tendencies will lead to a large error in the mean climate, but will have an 'OK' (0.5°C to 1°C) error for climate change.

In summary, we can see that the observed climate is decently represented by the GREB model. We therefore can use the GREB model to understand the basics of the large-scale mean climate interactions. However, before we take a closer look at the mean climate we have to discuss the GREB model errors and how to deal with them in more detail.

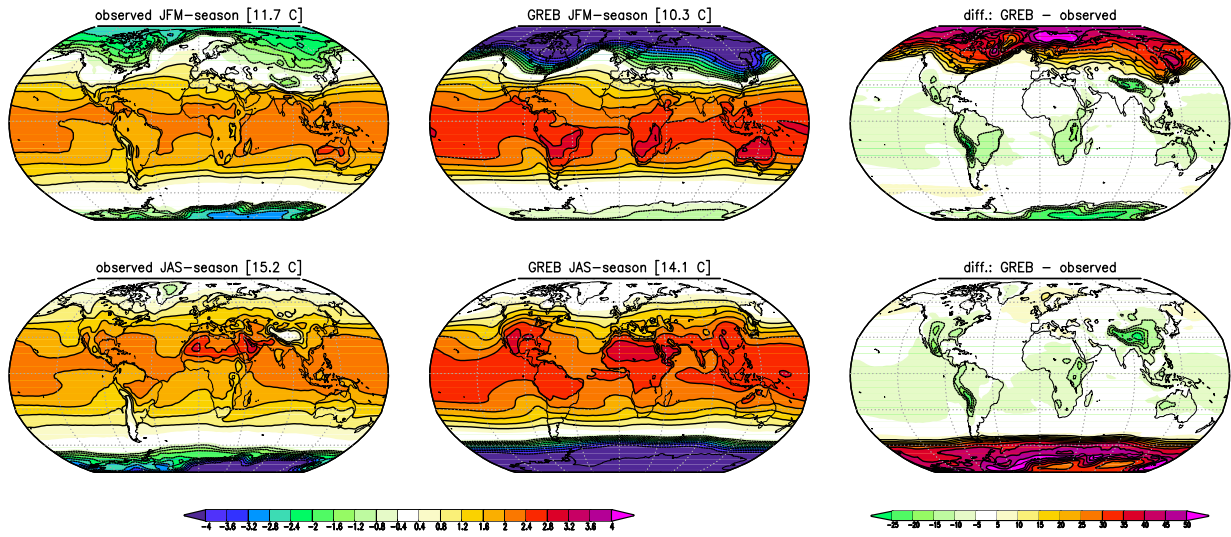


Figure 4.35: Comparison of the observed mean climate with the GREB model simulation for for two different seasons.

GREB model correction

As seen above: if we integrate the model from an observed climate initial condition it will drift into a climate state that is in some regions very different (10K or more) from the observed. To understand the climate response to external forcing, such as doubling of the CO_2 concentration, such large model simulation errors are not acceptable. We have to consider here that the response to external forcing will depend on climate feedbacks, which can be very different if the mean state is different by more than $10^\circ C$. The ice-albedo feedback, for instance, would be very different if the mean state climate is different. It is therefore important to keep the GREB model closer to the observed mean state.

Flux corrections

To keep GREB close to the observed climate state we need to introduce artificial heat fluxes to correct the tendencies. These correction terms in the tendency equations will force the GREB model to produce exactly the observed mean T_{surf} and mean q_{surf} .

4.1.10 A short summary of the GREB model

The GREB model has four prognostic equations:

$$\gamma_{surf} \frac{dT_{surf}}{dt} = F_{solar} + F_{thermal} + F_{sense} + F_{latent} + F_{ocean} + F_{correct} \quad (4.25)$$

$$\gamma_{atmos} \frac{dT_{atmos}}{dt} = +F_{atmos-thermal} - F_{sense} + F_{atmos-latent} \gamma_{atmos} (-\vec{u} \cdot \vec{\nabla} T + \kappa \cdot \nabla^2 T) \quad (4.26)$$

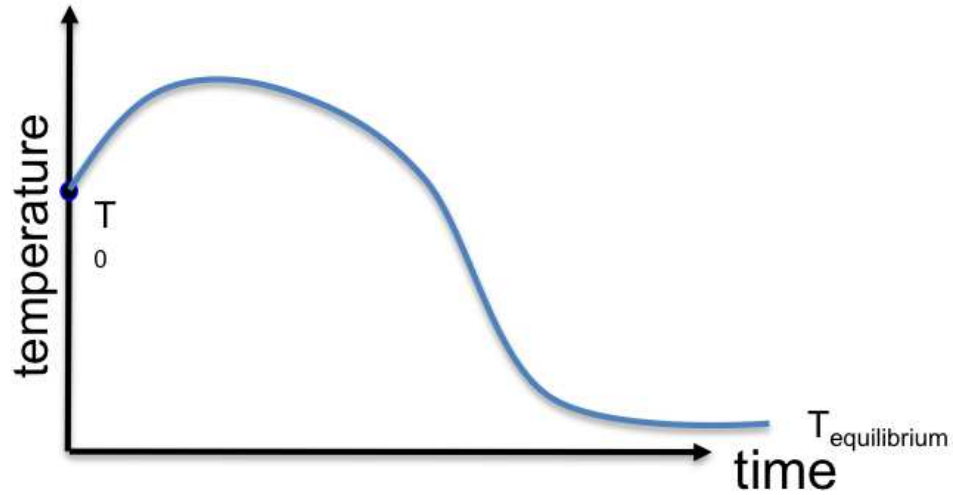


Figure 4.36: A imperfect climate model (all models are imperfect) will drift from an observed mean (equilibrium maybe?) climate state to another equilibrium climate state different from the observed if it is integrated over time from the mean observed climate state.

$$\frac{dq_{surf}}{dt} = \Delta q_{eva} + \Delta Q_{precip} + -\vec{u} \cdot \vec{\nabla} q_{surf} + \kappa \cdot \nabla^2 q_{surf} + \Delta q_{correct} \quad (4.27)$$

$$\gamma_{ocean} \frac{dT_{ocean}}{dt} = \Delta T_{O_{entrain}} - F_{O_{sense}} + F_{ocean-correct} \quad (4.28)$$

The individual terms of these four tendency equations are related to a number of equations that simulate the individual process.

GREB boundary conditions: *external*

IPCC models will have similar boundary condition.

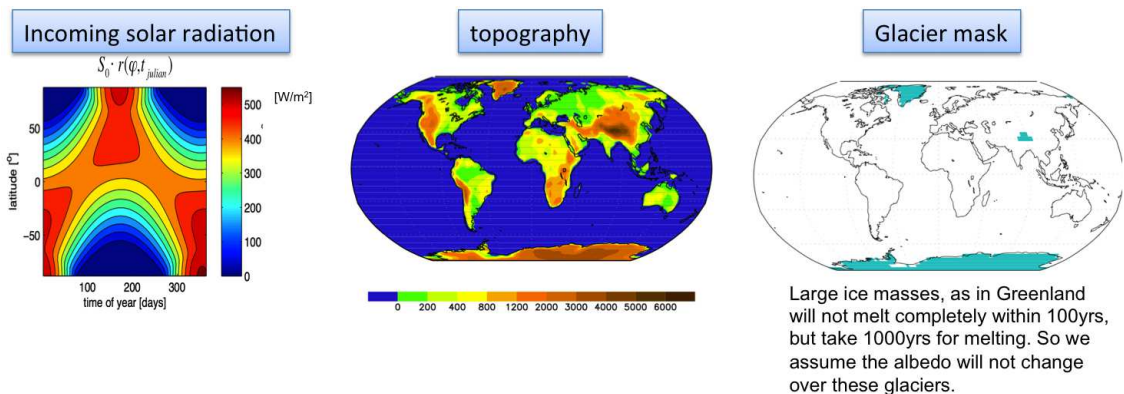


Figure 4.37: External boundary conditions for the GREB model.

Additionally there are some physical constants for the climate system: e.g. surface air pressure,

CO₂, concentration, etc.

GREB boundary conditions: *internal*

IPCC models will simulate these internal boundary conditions. So for an IPCC model these are not boundary conditions, but are computed by the state of the system with prognostic equations.

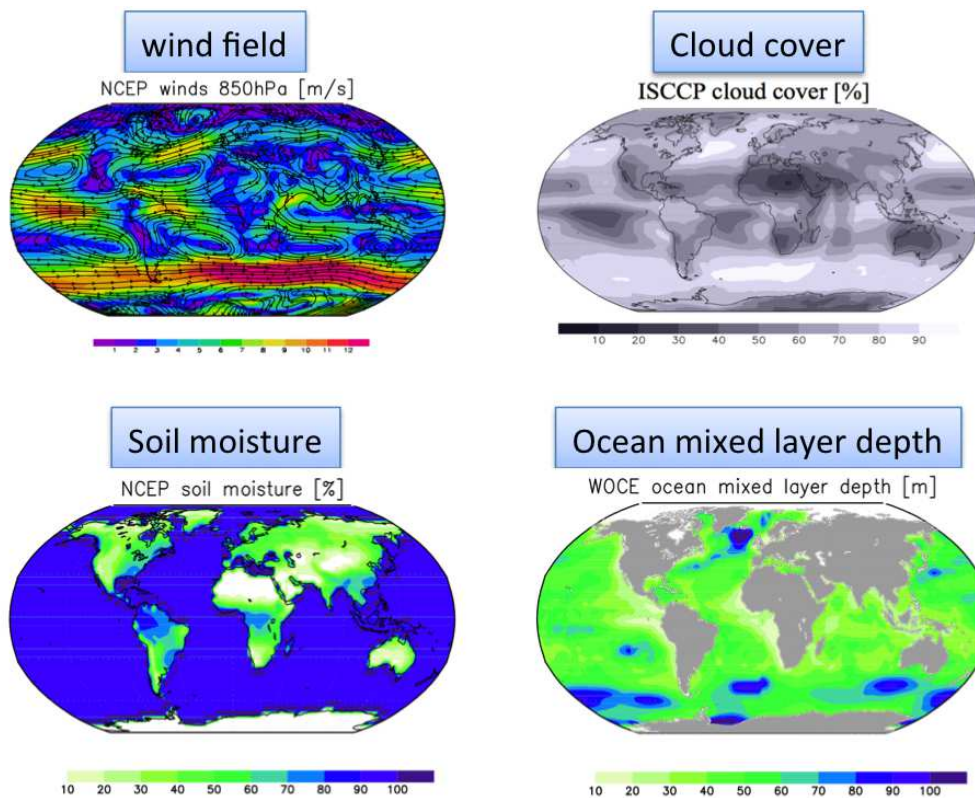


Figure 4.38: Internal boundary conditions for the GREB model. These are not really boundary conditions, but are parts of the climate system that the GREB model assumes to be given. In the real world these are variable and will change over time.

All given with seasonally changing climatology.

GREB constraints

IPCC models will simulate these variables without artificial constraints.

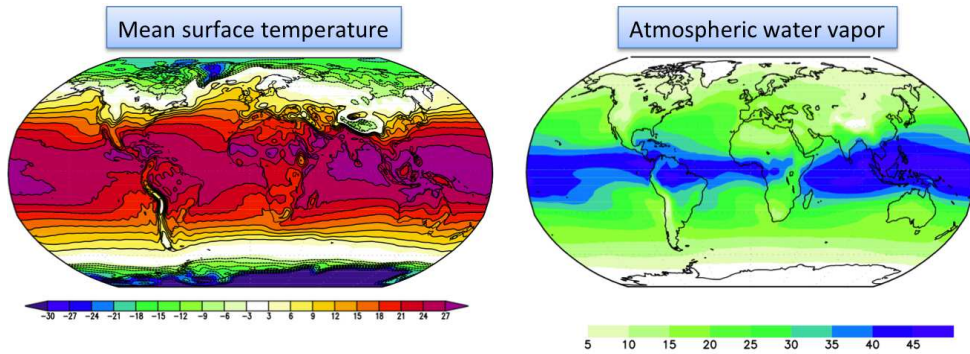


Figure 4.39: ExtConstraints for the GREB model. We artificially force the GREB model to have the mean observed surface temperature and atmospheric surface humidity by flux correction terms.

Enforced in GREB by flux correction terms in the T_{surf} and q_{surf} tendency equations.

4.2 A Conceptual Deconstruction of the Mean Climate with the GREB Model

We can now use the GREB model to deconstruct or construct the regional and seasonal mean climate of the earth. This will illustrate what processes are involved to build the mean climate at different locations and also how different process affect the climate. In the set of GREB model equations, we can conceptually define 10 processes that build the complete GREB model:

4.2.1 The Mean Surface Temperature Structure

We can now use the GREB model to deconstruct or construct the regional and seasonal mean climate of the earth. This will illustrate what processes are involved to build the mean climate at different locations and also how different process affect the climate. In the set of GREB model equations, we can conceptually define 10 processes that build the complete GREB model:

- **Ice/Snow cover:** The effect of the snow and sea ice cover on the albedo, heat capacity and insulation of the subsurface ocean from the atmosphere are simulated in the Monash simple climate model as a simple function of T_{surf} . If turned OFF albedo, heat capacity and interaction of the subsurface ocean with the atmosphere are that of ice-free conditions.
- **Clouds:** The solar and thermal radiation effect of the mean cloud cover. If turned OFF cloud cover is zero.
- **Oceans:** The large heat capacity of the two layer ocean. If turned OFF the ocean is a just a surface layer with the same heat capacity as the land.
- **Atmosphere:** In the absent of transport, CO_2 or water vapor, the atmosphere still has a heat capacity and a sensible heat exchange with the surface. It also has a small residual emissivity. If turned OFF no atmosphere exist, on all process related to it do not exist (e.g. transport, CO_2 or water vapor, etc.).

- **Diffusion of Heat:** This process exchanges heat between neighbouring points by isotropic diffusion. Note, that diffusion and advection of both heat and water vapor are the only way that points in the GREB climate interact. . If diffusion is turned OFF neighbouring points do not interact unless advection by mean winds is active.
- **Advection of Heat:** This process exchanges heat between neighbouring points in the direction of the mean winds. If advection is turned OFF heat is not transported along the mean winds.
- **CO₂:** The CO₂ concentration affects the emissivity of the atmosphere. If turned OFF CO₂ concentration is zero.
- **Hydrological Cycle:** Introduces water vapor into the atmosphere and therefore increases the atmospheric emissivity. It also introduce latent heating and cooling due to precipitation and evaporation. If turned OFF no water vapor is in the atmosphere and no latent heat flux.
- **Diffusion of Water Vapor:** This process exchanges water vapor between neighbouring points by isotropic diffusion. If diffusion is turned OFF neighbouring points do not exchange water vapor unless advection by mean winds is active.
- **Advection of Water Vapor:** This process exchanges water vapor between neighbouring points in the direction of the mean winds. If advection is turned OFF water vapor is not transported along the mean winds.

We have combined a few processes (equations) of the GREB model to simplify the discussion (e.g. Ice-albedo and sea heat capacity effect are combined).

It is interesting to see how the climate changes if one or several of the processes are neglected (e.g. terms are set to zero or are not considered). This illustrates what role each of the processes has in the mean climate. The Monash Simple Climate Model (MSCM) web-based interfaces allows you to look at the equilibrium model simulation results for all combinations ($2^{11} = 2048$) of the 10 conceptual processes with or without correction terms. The web-interface also provides a number of tutorials that discuss different combinations of the processes and model correction terms with the focus on different aspects (e.g. CO₂, clouds, etc.).

As a starting point we look at how the mean climate changes if one of the 10 processes is turned OFF, see figs. 4.40 and 4.41. This gives us some idea of how important a process is at different regions and in different seasons:

- **Ice/Snow cover;** Figs. 4.40a and 4.41a: the ice and snow cover has a strong cooling effect mostly the high latitudes in the cold season, which is due to the ice-albedo feedback. However, in the warm season the insulation effect of the sea ice actually leads to warming, as the ocean can not cool down as much during winter as it does without sea ice.
- **Clouds;** Figs. 4.40b and 4.41b: Clouds have a large net cooling effect globally. Thus the solar radiation reflection effect dominates over the thermal radiation warming effect. However, when can note the thermal radiation warming effect in the polar winter night, when the solar radiation is not important. To see this effect other climate processes need to be turn off as well (e.g. ice-albedo, hydro. cycle and CO₂). Is is also interesting to note that the the strongest cooling effect of cloud cover is over regions with fairly little cloud cover (e.g. deserts and mountain regions). This is due to the interaction with other climate feedbacks such as the water vapor feedback.
- **Oceans;** Figs. 4.40c and 4.41c: the large ocean heat capacity slows down the seasonal cycle. Subsequently, the seasons are more moderate than they would be without the ocean

transferring heat from warm to cold seasons. This is in particular important in the mid and higher latitudes. The effect of the ocean heat capacity is mostly a seasonal, however, the GREB model without flux corrections has also an annual mean warming effect by the ocean heat capacity, which is not that strong with the flux corrections. It is unclear to me (yet) why that is, however, we could expect some annual mean warming effect by the large ocean heat capacity due to the non-linear thermal radiation cooling. The non-linear black body negative radiation feedback is stronger for warmer temperatures, which are not reached in a moderated seasonal cycle with the larger ocean heat capacity.

- **Diffusion of Heat;** Figs. 4.40d and 4.41d: The diffusion of heat reduces temperature extremes. It therefore warms extremely cold regions (e.g. polar regions) and cools the most warmest regions (e.g. warm deserts). In global average this is mostly cancelling each other out.
- **Advection of Heat;** Figs. 4.40e and 4.41e: The advection of heat has strong effects where the mean winds blow across strong temperature gradients. This is mostly present in the Northern Hemisphere. The most prominent feature is the strong warming of the northern European and Asian continents in the cold season. In global average warming and cooling is mostly cancelling each other out.
- CO_2 ; Figs. 4.40f and 4.41f: The CO_2 leads to global warming of about 9 degrees. Even though it is the same CO_2 concentration everywhere, the warming effect is different at different locations. This will be discussed in much more details in the climate change section.
- **Hydrological Cycle;** Figs. 4.40g and 4.41g: The input of water vapour into the atmosphere by the hydrological cycle leads to a substantial amount of warming globally. It is amplified over the midlatitudes in the cold seasons.
- **Diffusion of Water Vapor;** Figs. 4.40h and 4.41h: The transport of water vapor away from warm and moist regions (e.g. tropical oceans) to cold and dry regions (e.g. high latitudes and continents) leads to additional warming in the regions that gain water vapour and cooling to those that lose water vapor. The effect similar on both hemispheres.
- **Advection of Water Vapor;** Figs. 4.40i and 4.41i: The transport of water vapor along the mean wind directions has stronger effects on the Northern Hemisphere than on the southern Hemisphere, since here the mean winds have more of a meridional component, which creates advection across water vapor gradients. This effect is most pronounced in the cold seasons.

As an alternative way of understanding the role of the different processes we build up the complete climate by introducing one process after the other, see Figs. 4.42 and 4.43. We start with the bare earth (e.g. like our Moon) and then introduce one process after the other. The order in which the processes are introduced is mostly motivated by giving a good representation for each of the 10 processes. However, it can also be interpreted as a build up the Earth climate in a somewhat historical way: We assume that initially the earth was a bare planet and then the atmosphere, ocean and all the other aspects build up over time:

The Bare Earth, Fig.4.42a: At the start we have all switches OFF, which is essentially a planet without atmosphere, ocean or ice. Just like our Moon. It has an extremely strong seasonal cycle and is much colder than our current climate. It also has no regional structure other than meridional temperature gradients. The combination of processes we will introduce will create most of the regional and seasonal differences that make our current climate.

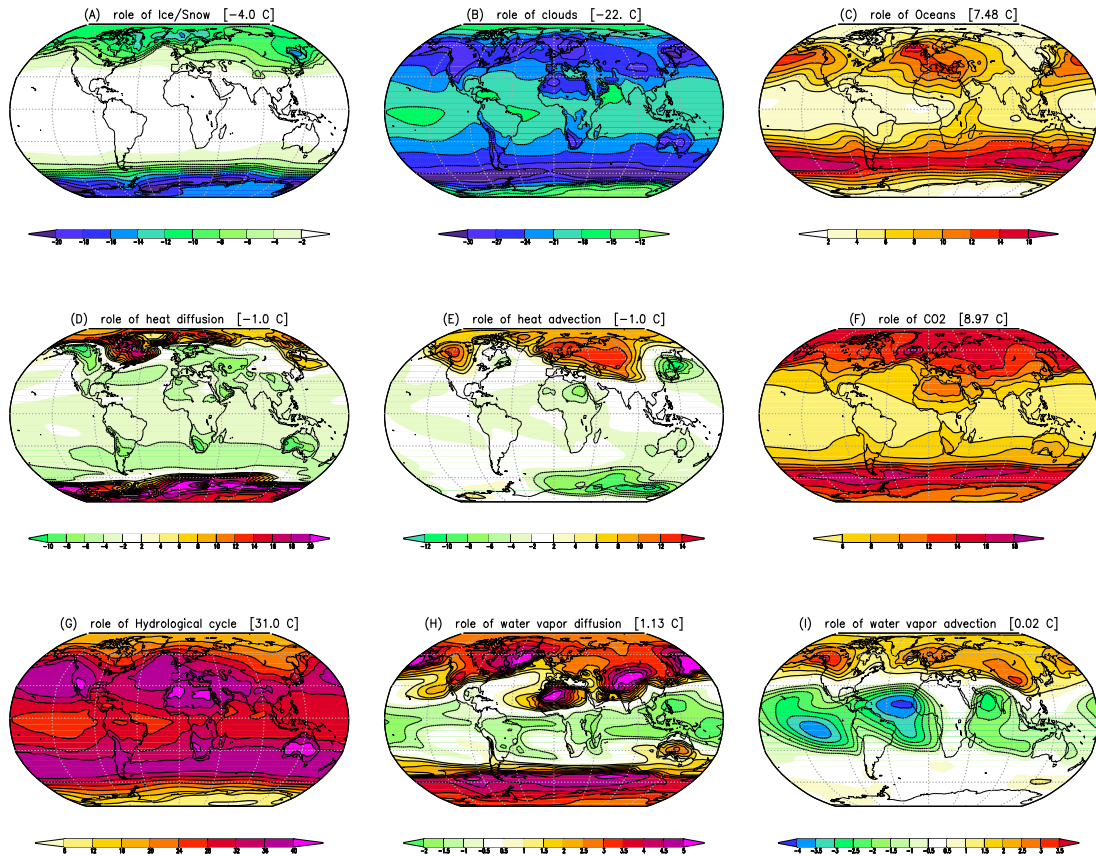


Figure 4.40: The role of different processes on the annual mean climate of the GREB model. In each panel we see the difference between the annual mean T_{surf} of the complete GREB model without flux correction terms minus the annual mean T_{surf} of the GREB model without flux correction terms and one process missing (noted in the heading of each panel). The number in the headings is the global mean difference. Note, the colorbars are different for different panels.

Atmosphere, Fig.4.42b: In the GREB model the atmospheric layer simulates two processes, if all other processes are turned off: a turbulent sensible heat exchange with the surface and thermal radiation due to residual trace gasses other than CO_2 or water vapor. The sensible heat exchange cools the surface, because the atmospheric layer is in average colder than the surface. This effect dominates for most regions. The thermal radiation effect warms the surface, which, in the absence of CO_2 and water vapor, is very weak and only dominating in the very cold polar regions in winter time. We can also note some small topographic effects.

CO_2 , Fig.4.42d: The warming effect is nearly uniform, if all other processes are turned OFF. It accounts for a warming of about $9^\circ C$. In the following climate change sections we will focus on how the different processes in the climate system interact to create the well known pattern of anthropogenic global warming. You can also have a look at the MSCM tutorial CO_2 concentrations to get some better idea on how the CO_2 concentration affects the climate.

Oceans, Fig.4.42f: The oceans slow down the seasonal cycle by their large heat capacity. The effective heat capacity of the oceans is proportional to the observed mixed layer in the GREB model, which causes some structure (differences from the zonal means) we can see in the seasonal

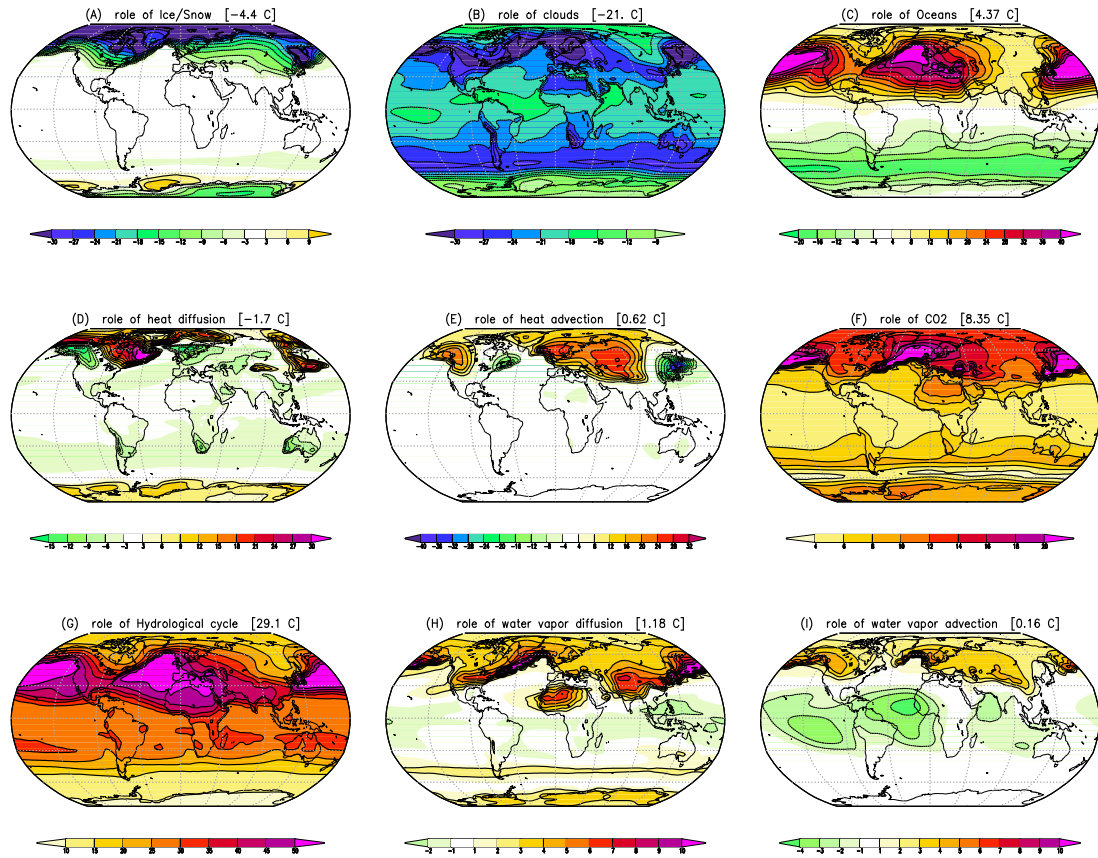


Figure 4.41: As Fig. 4.40, for the mean of the JFM-season to highlight seasonal differences in the processes. Note the colorbars are different from Fig. 4.40 and different for different panels.

cycle of the oceans. Land points are not affected, since no atmospheric transport exist (advection and diffusion turned OFF). The different heat capacity between oceans and land already make a significant element of the regional and seasonal climate differences.

Diffusion of Heat, Fig.4.42h: We now turn on some interaction between points by introducing turbulent diffusion of heat in the atmosphere. This has the strongest effects along coastlines. It reduces the land-sea contrast and has strong warming effects in winter over land and cooling in summer over land. The extreme climates of the winter polar region are most strongly effect by the turbulent heat exchange with lower latitudes. The turbulent heat exchange makes the regional climate difference again a bit more realistic.

Advection of Heat, Fig.4.43h: The advection of heat is strongly depending on temperature gradient along the mean wind field directions. This has strong seasonal changes that are most pronounced over Europe, Russia and North America. It provides substantial heating during the winter season for Europe, Russia and western North America. The structure (differences from the zonal mean) created by this process is mostly caused by the prescribed mean wind climatology. In particular the milder climate in Europe compared to the northeastern Asia on the same latitudes are create by wind blowing form the ocean onto land. The same is true for the differences between the west and east coast of the northern North America. The climate regional and seasonal structures are now already quite realistic, but the overall climate is much too cold. This will change if

we introduce water vapor into the atmosphere.

Ice-albedo, Fig.4.43l: This cools the climate in particular the polar regions. The difference illustrates that the ice-albedo feedback is primarily leading to cooling in higher latitudes and mostly in the winter season. However, we can also see a warming in the Arctic Sea in summer. This is due to the insulation effect of sea ice, which leaves the ocean waters just above freezing temperatures in winter, which would without sea ice get much colder in winter and therefore would remain colder in summer.

Hydrological Cycle, Fig.4.43n: Introducing the hydrological cycle brings the most important greenhouse gas into the atmosphere: water vapor. This has an enormous warming effect globally. It warms by more than $30^{\circ}C$.

Clouds, Fig.4.43p: This cools the climate substantially. However, with all interactions (feedbacks) with the other processes it is not easily seen where the clouds are strong or weak. See also the MSCM clouds tutorial for more details on the clouds.

Diffusion and Advection of Water Vapor, Fig.4.43r: The turbulent transport (diffusion) of water vapor brings water vapor from relative moist regions to relatively dry regions. This lead to enhanced warming in the dry and cold regions (e.g. Sahara desert or polar regions) by the water vapor thermal radiation (greenhouse) effect and cooling in the regions where it came from (e.g. tropical oceans). The advection of water vapor has a similar effect as the transport by diffusion. It brings water vapor from relative moist regions (e.g. subtropical oceans) to relatively dry regions (e.g. northern continents) along the mean wind streamlines. The heating effect is similar to the heat transport by advection and has also a strong seasonal cycle.

4.2.2 A Diagnostic Model for Precipitation

4.2.3 The Mean Precipitation Pattern

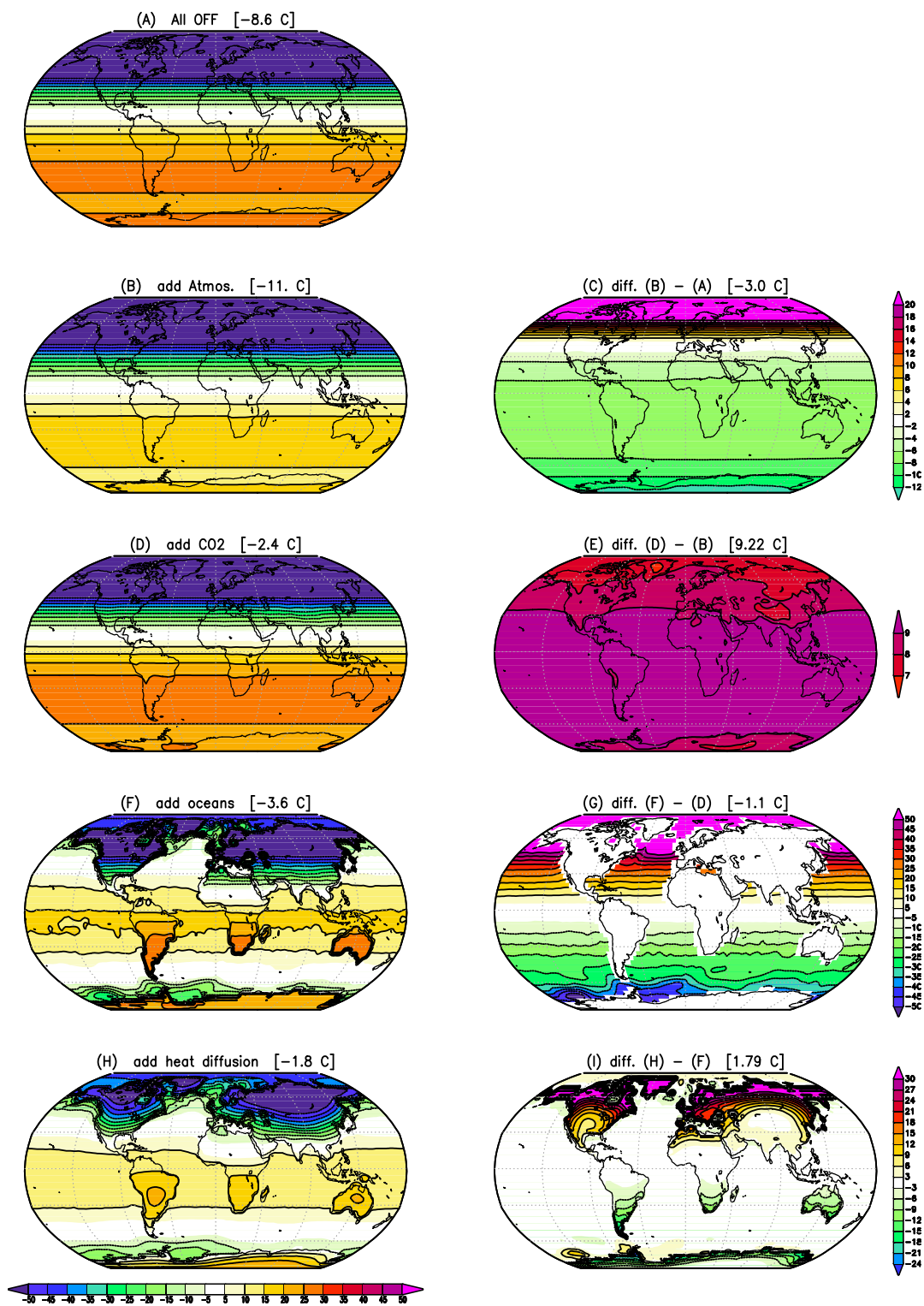


Figure 4.42: A deconstruction of the mean climate with the GREB model.

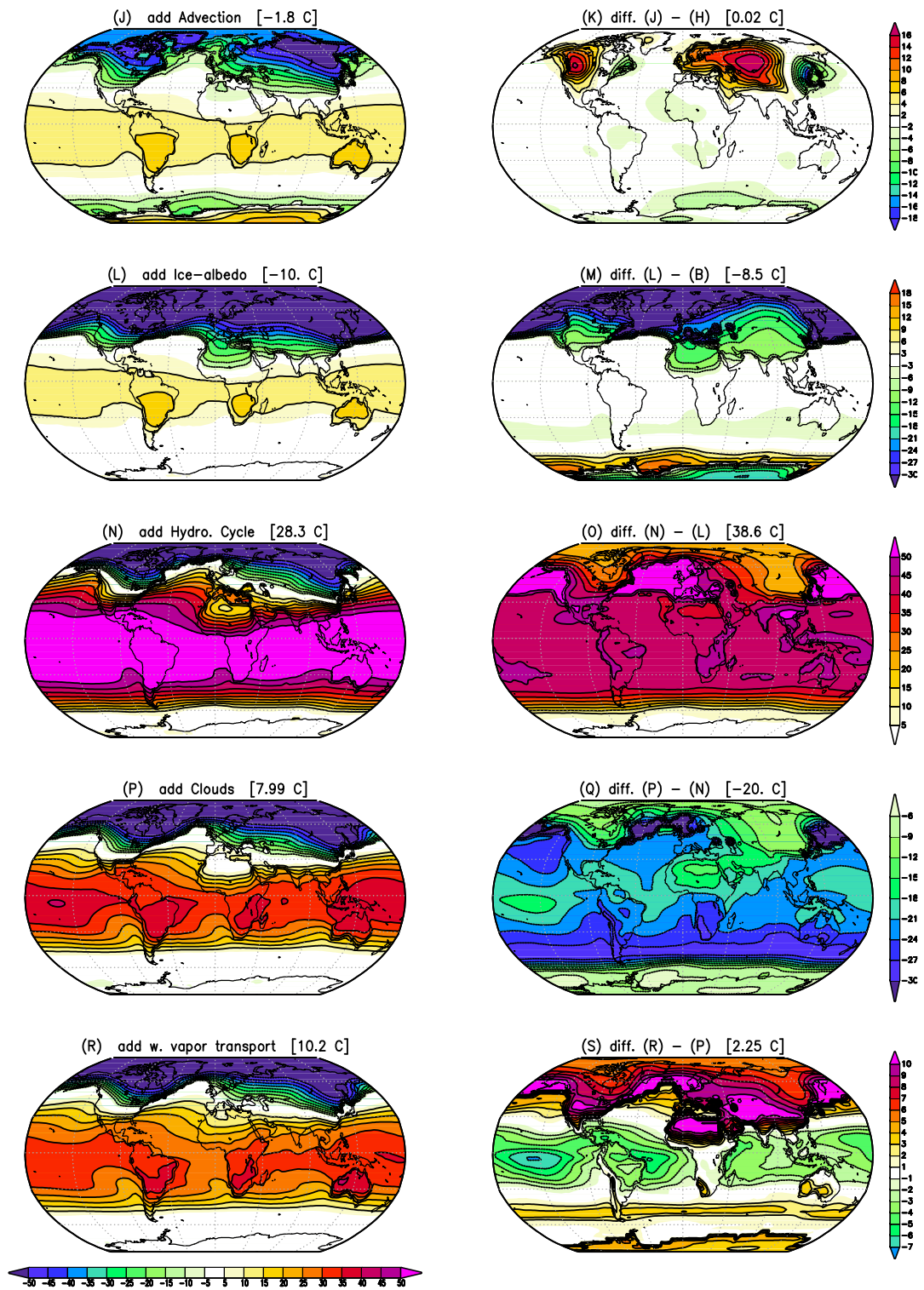


Figure 4.43: A deconstruction of the mean climate with the GREB model continued.

4.3 General Circulation Models (IPCC-type climate models)

State of the art climate models are called General circulation models (GCMs). They are the basis for the IPCC climate change predictions. The GCMs are based on weather forecast models. A GCMs is often a simplified version of a real weather forecasting model. Main features simulated by a weather/climate model:

- Circulation of the atmosphere/ocean (dynamical core)
- Radiation
- Clouds
- Land/Surface processes
- Precipitation
- Sea ice

Each of these features is basically and in most often in reality a model (computer code/program) of their own. The core element of a weather/climate models is the dynamics of the atmospheric circulation: The development of low/high pressure system and their movement in the atmosphere. So unlike our discussion of the energy balance equations, which has the temperature tendencies as the central element, the GCMs have the tendencies of the atmospheric pressure and momentum as the central element. Hence they are called General Circulation models and not energy balance models. The energy balances are of cause also part of these models, but they do not play the central part. Models simulating the general circulation exist for the atmosphere and the oceans. Since they are two independent models, the combined model including both a GCM of the atmosphere and the oceans are called a coupled GCM (CGCM). So keep in mind, GCM does not stand for: Global Climate Model!!

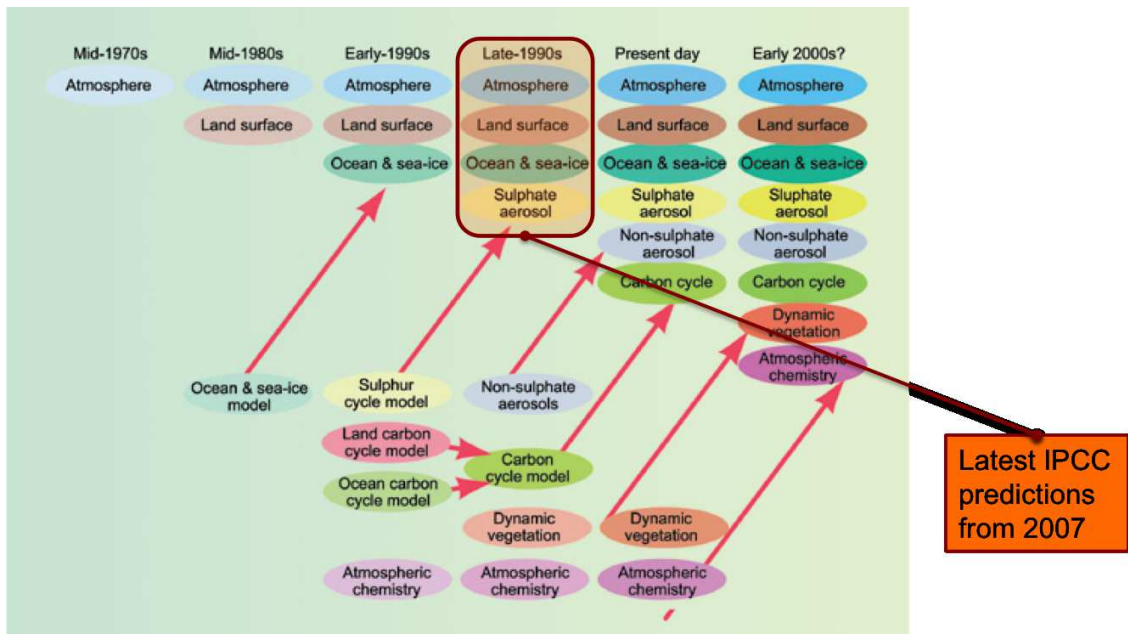


Figure 4.44: History of development of GCMs: the diagram illustrates how the complexity of climate models has increased over time.

4.3.1 The dynamical model

Simulation of the atmosphere/ocean dynamics:

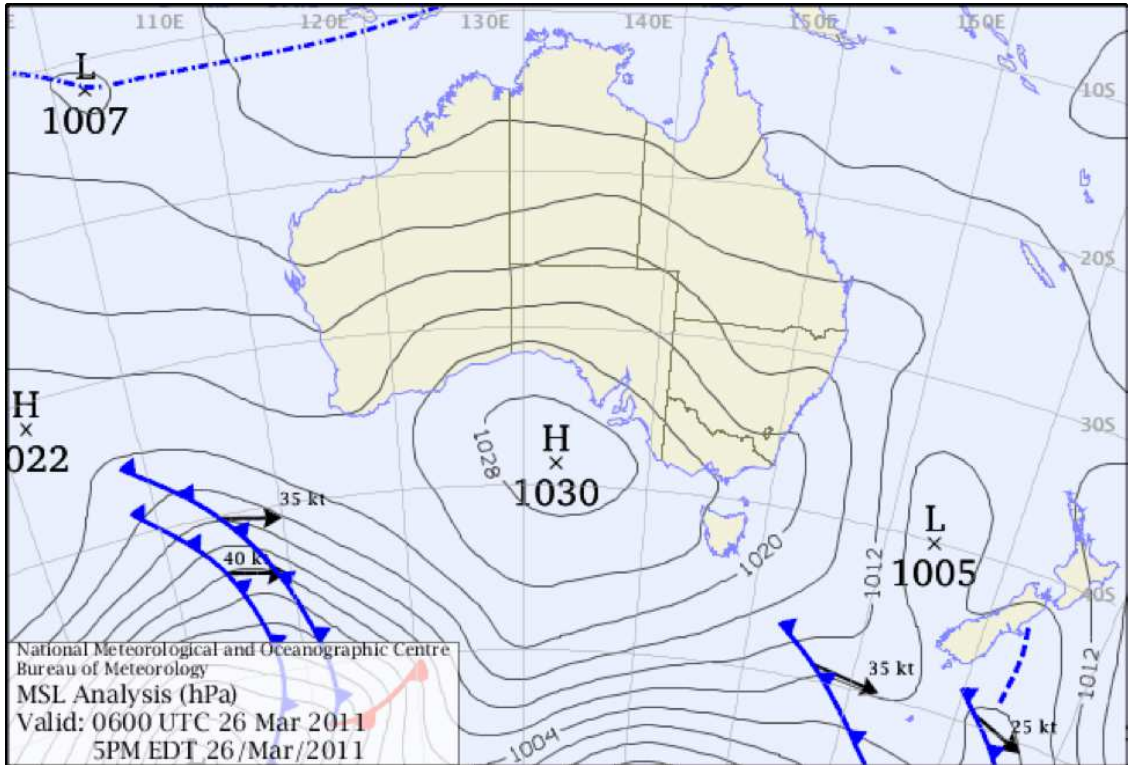


Figure 4.45

A dynamical atmosphere model predicts how the low and high pressure systems evolve in time.

Momentum equations:

$$\rho \frac{D\vec{u}}{Dt} = -2\rho \cdot \Omega \times \vec{u} - \vec{\nabla}p + \rho \vec{\nabla}\Phi + F$$

Coriolis forcing due to the earth rotation

Pressure gradient force

gravity

friction

Figure 4.46

ρ = density

\vec{u} = velocity (3-d vector)

$$\frac{D\vec{u}}{Dt} = \frac{\partial \vec{u}}{\partial t} + \vec{u} \cdot \vec{\nabla} \vec{u}$$

Ω = earth angular velocity

p = pressure

Φ = geopotential

F = friction

Changes in momentum (acceleration) are caused by different forces. This set of equations is fundamental to geophysical fluid dynamics (the physics of the motions in gases and liquids).

Tendencies in density (pressure):

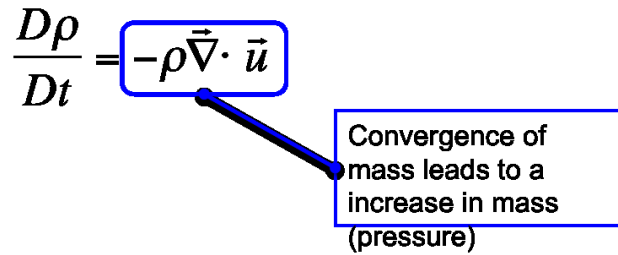
$$\frac{D\rho}{Dt} = -\rho \vec{\nabla} \cdot \vec{u}$$


Figure 4.47

ρ = density

\vec{u} = velocity (3-d vector)

The material derivative:

$$\frac{D\rho}{Dt} = \frac{\partial \rho}{\partial t} + \vec{u} \cdot \vec{\nabla} \rho$$

is the change of a fluid's (gas or liquid) characteristics, such as temperature or density, over time if you follow the fluid partical with the fluid flow. It has two components: one is the local rate of change, and the other the change due to flowing with the currents (winds).

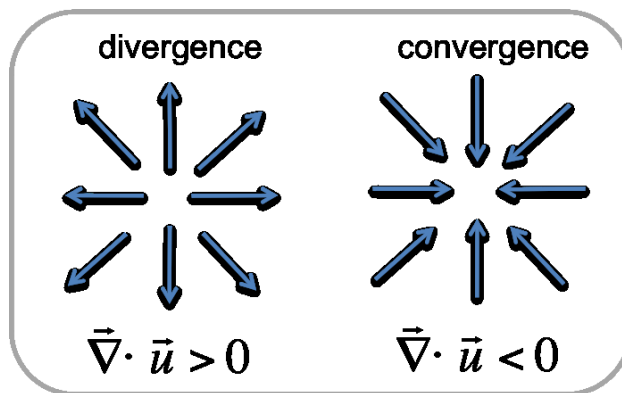


Figure 4.48

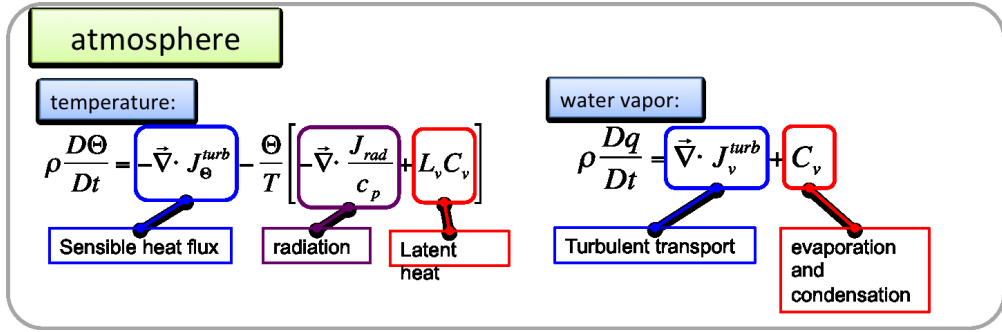


Figure 4.49

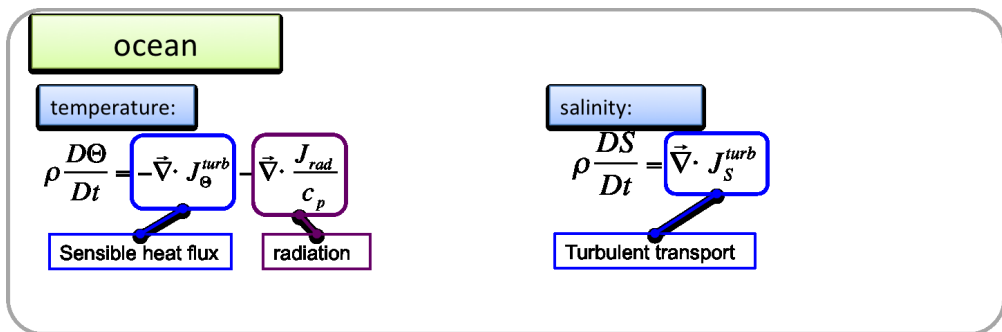


Figure 4.50

4.3.2 Radiation model

Solar and thermal radiation transfer through the atmosphere must be simulated on different spectral bands. It depends on the chemical composition of the atmosphere (H_2O , CO_2 , etc.) and on the particles in the atmosphere (cloud drops or aerosols).

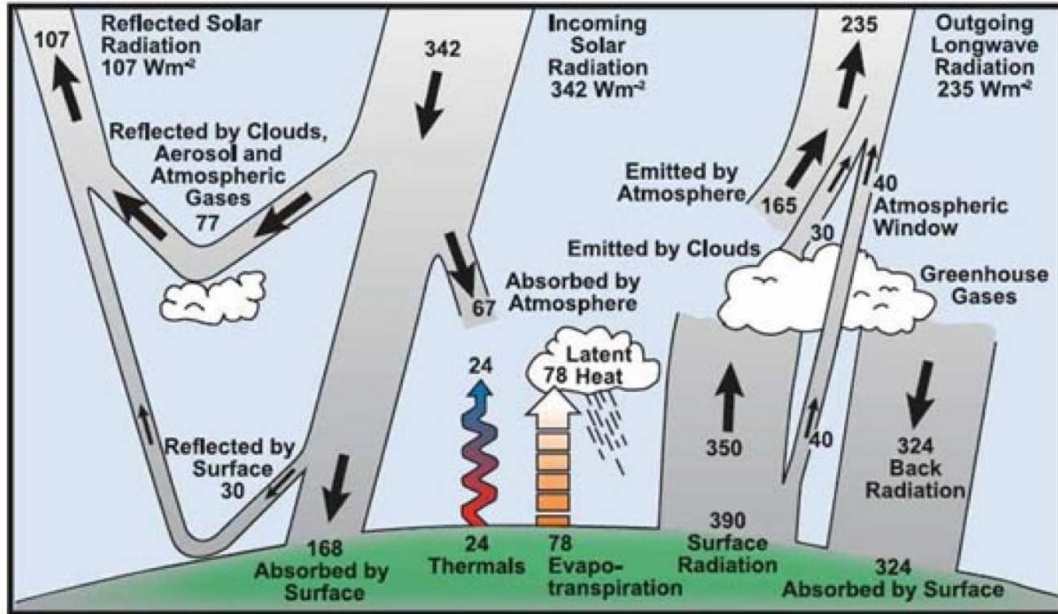


Figure 4.51: A simple sketch of the atmospheric radiation budget

4.3.3 Precipitation model

Precipitation is a very complex process. It involves the simulation of water vapour and its condensation and evaporation, small changes in vertical motion of the atmosphere, formation of droplets or ice crystals and their movement in the air. Precipitation can happen on a very small scale, too small to be resolved by climate models. Models have to find smart simplifications (parameterizations). Models simulate two types of rain: convective (small scale) and large scale precipitation.

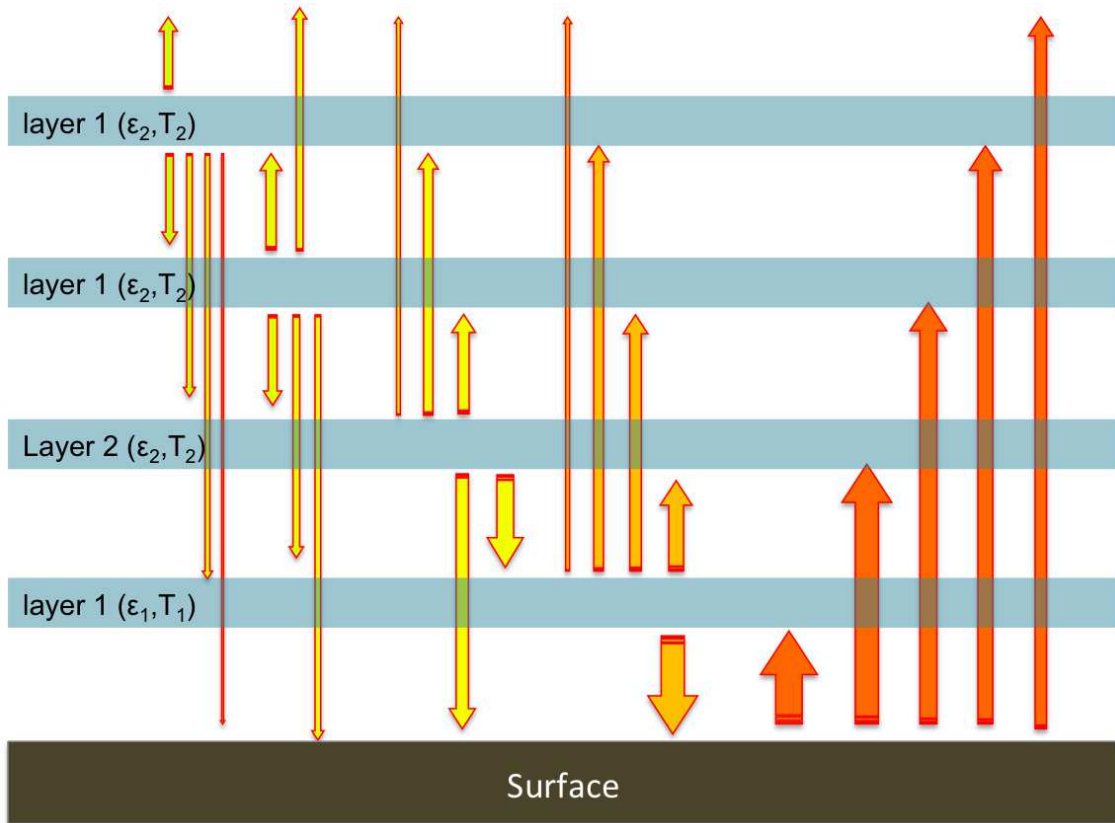


Figure 4.52: A more detailed model of thermal radiation

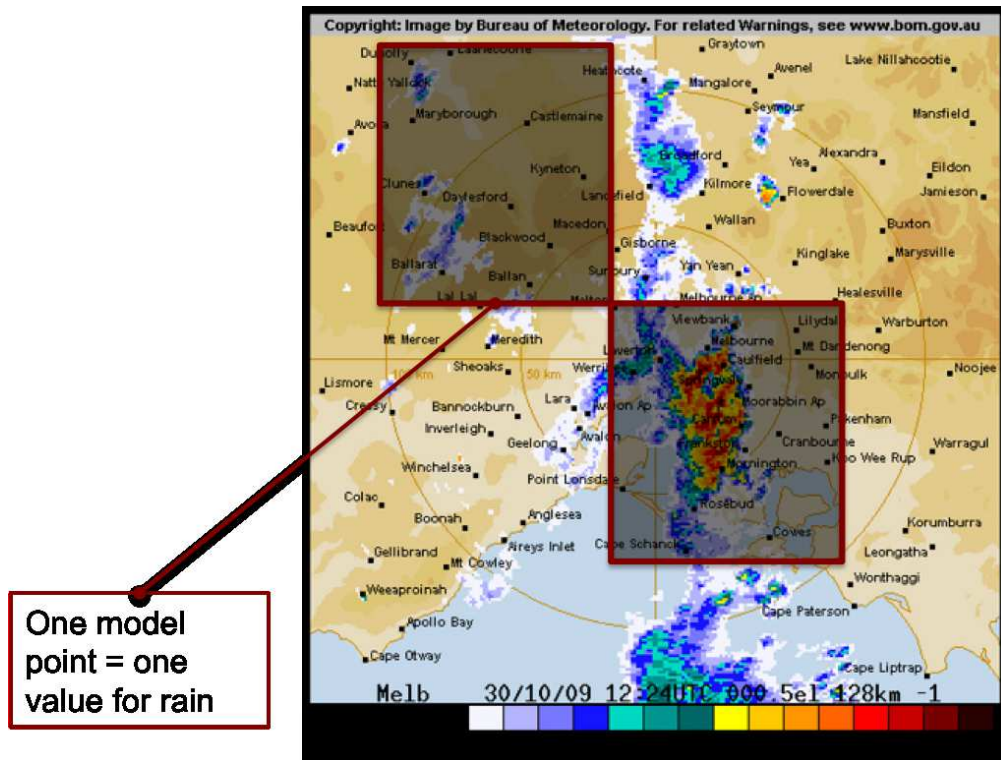


Figure 4.53: Rain radar view of Melbourne area

4.3.4 Cloud model

Clouds are a very complex system; it involves the simulation of water vapour and its condensation and evaporation, small changes in vertical motion of the atmosphere, formation of droplets or ice crystals, their interaction with particles in the atmosphere (called aerosols) and their movement in the air. Clouds form on very small scales, too small to be resolved by climate models. Models have to find smart simplifications (parameterizations). Models must be able to simulate different kinds of clouds.

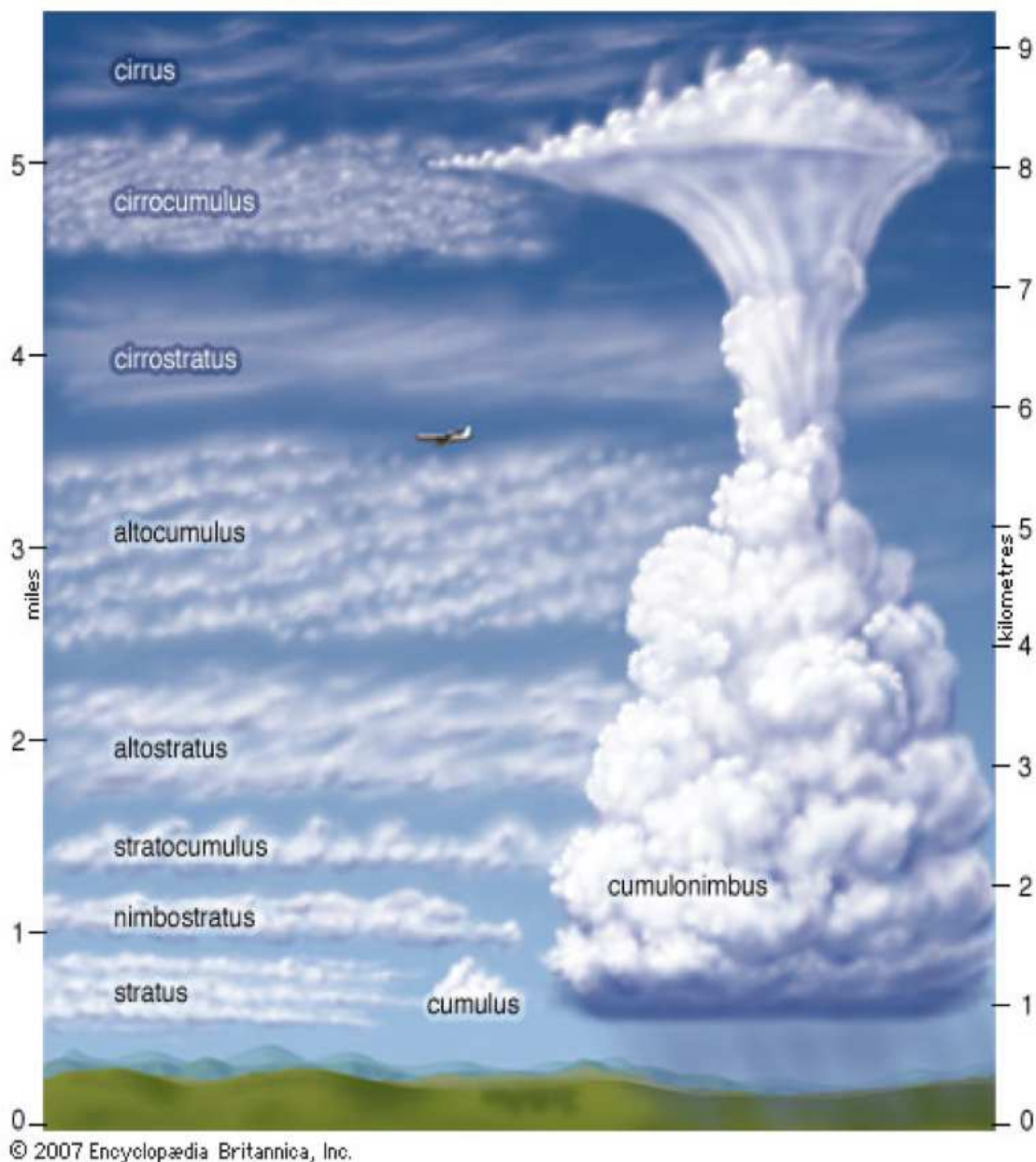


Figure 4.54

4.3.5 Land/Surface model

The land/surface model must simulate the surface conditions, which are influencing the atmosphere. Simulates surface temperatures, river run off, soil moisture and albedo. It may include a soil, vegetation, snow and river run off model.

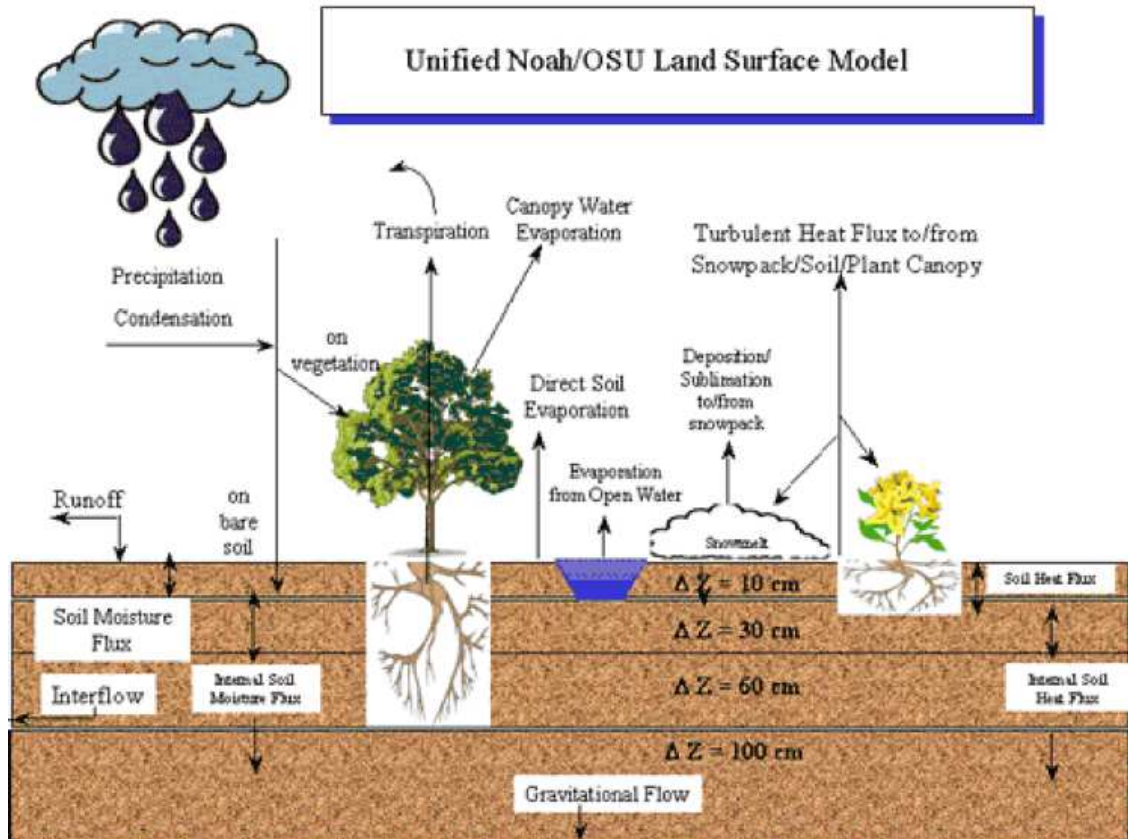


Figure 4.55: A sketch of a land surface model

4.3.6 Carbon cycle model

To predict future climate change we need to know the emissions of CO_2 and the resulting atmospheric concentrations.

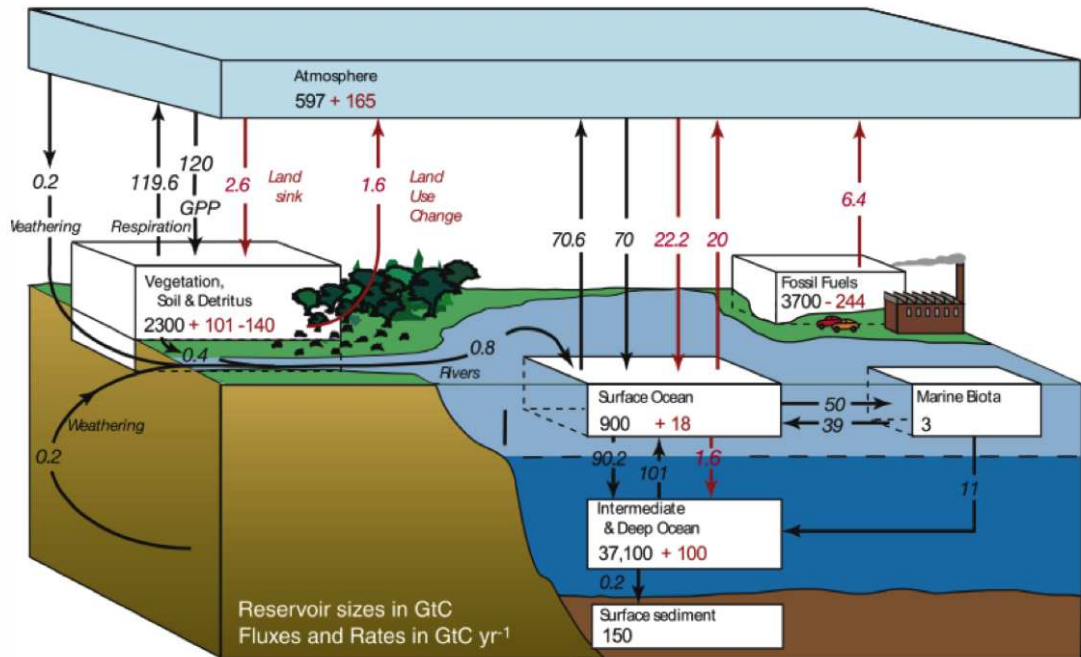


Figure 4.56: Carbon cycle model

- The sediments, oceans and vegetation are very large reservoirs of carbon (source for CO_2), which constantly exchange masses with the atmosphere.
- Anthropogenic emissions are to about 50% absorbed by land and ocean reservoirs.
- The amount of carbon uptake in the reservoirs depends on the atmospheric CO_2 concentrations, not on the emissions.
- Under current conditions atmospheric CO_2 concentrations would roughly stay constant if anthropogenic emissions are reduced by about 50%.
- Important sinks of carbon are in the biosphere over land and ocean, thus potential for taking up carbon is dependant on the climate itself.
- IPCC 2007 predictions have prescribed CO_2 concentrations, not emissions, as one would need a carbon model to compute atmospheric CO_2 concentrations from anthropogenic emissions.

4.3.7 Numerical realisations of GCMs

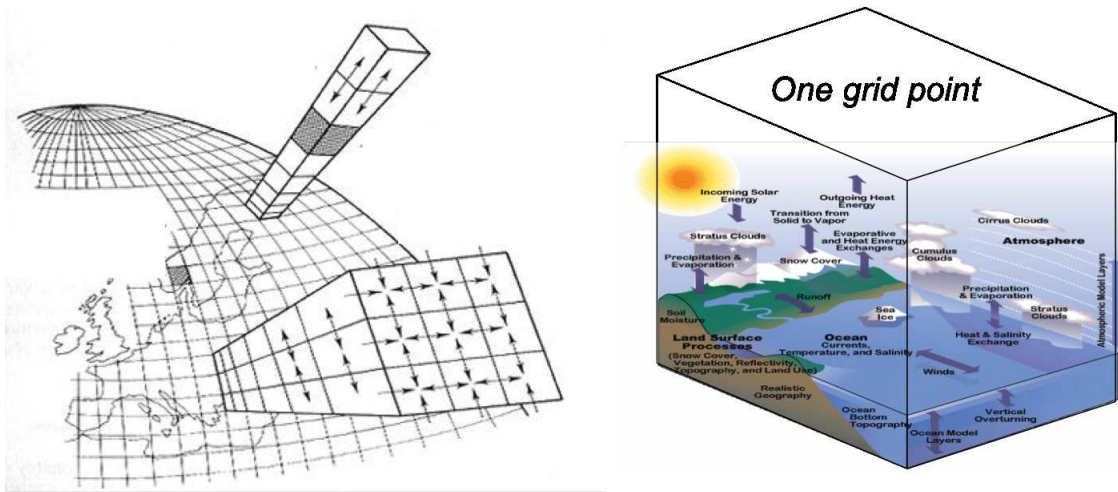


Figure 4.57

*Resolution:*Longitude: $1^\circ = 360$ pointsLatitude: $1^\circ = 180$ points

Vertical levels: 30 points

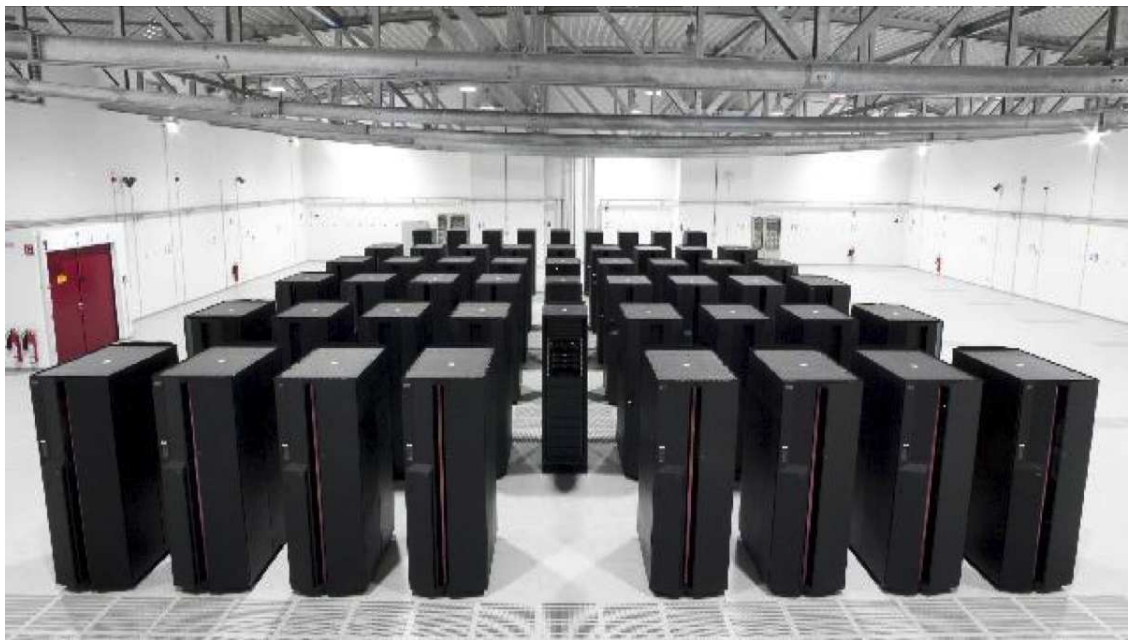
Total (ocean and atmosphere) $\approx 4,000,000$ pointsTime step = 20 min $\rightarrow 4,000,000$ computation of all equations to simulate 200 years

Figure 4.58: Computer for climate models

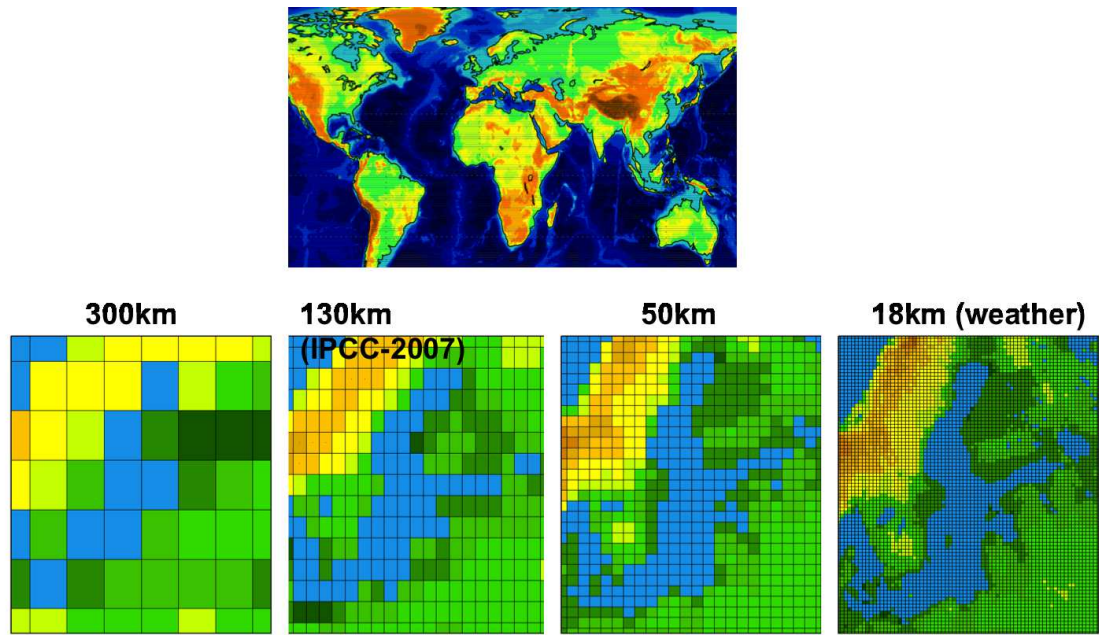


Figure 4.59: Resolution of GCMs

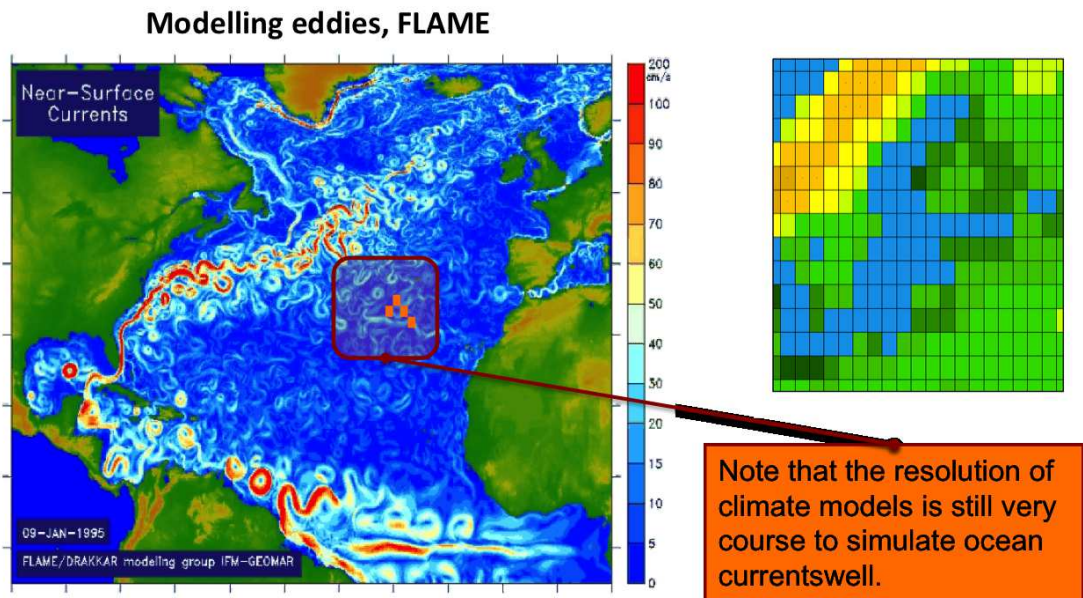


Figure 4.60: Resolution of GCMs

Chapter 5

Climate Change

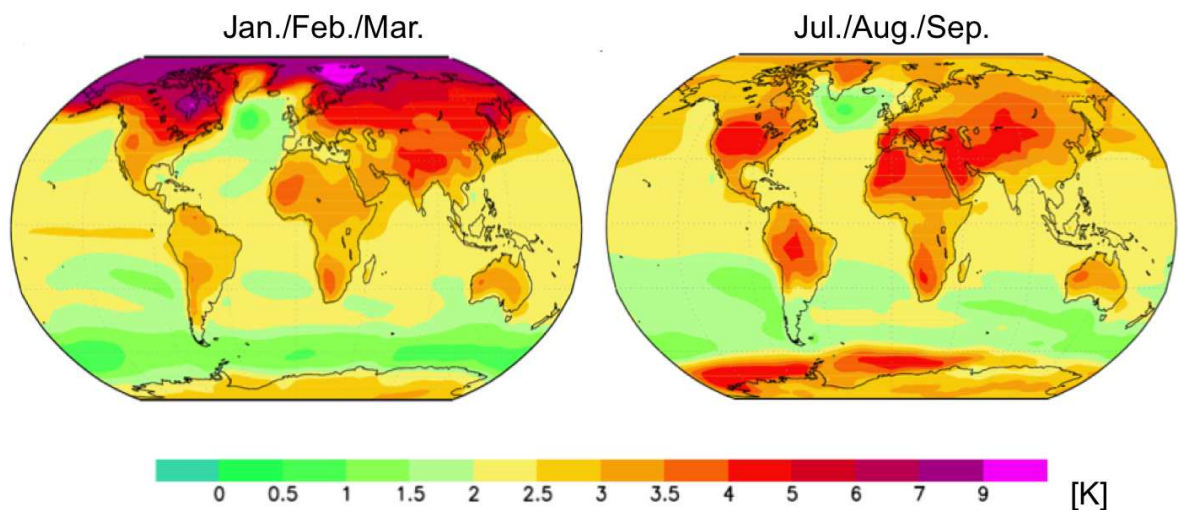


Figure 5.1: T_{surf} response to CO_2 forcing scenario IPCC A1B: Mean of 24 IPCC models (time intervals: [2070-2100] - [1970-2000])

The anthropogenic climate change is arguably the most important aspect of climate dynamics today. It is therefore the central aspect of this course. Before we go into any details it is helpful to have a look at the main feature of the anthropogenic climate change: The surface temperature, T_{surf} warming over the 21st century, see Fig. 5.1. Some main features of the global T_{surf} response to CO_2 forcing:

- Global mean warming by the end of the 21st century is about 2.6K.
- There are strong regional differences, although CO_2 concentration is the same everywhere.
- Land warms more than the ocean.
- The Arctic has the strongest warming.
- The Northern Hemisphere warms more than the Southern.
- The winter (cold) season warms more than the summer (warm) season.

The main aim of the next section is to understand what physical processes are involved in this global warming and how they cause these structures. We then discuss the IPCC-type GCM predictions. To understand the significance of the anthropogenic climate change we have to put it into the context of natural current and past climate variability. Finally we will have a look at the discussion of anthropogenic climate change in the media.

5.1 Conceptual deconstruction of climate change

In the following we will use the GREB model to deconstruct the surface temperature response to increases in CO_2 concentrations. This will help us to understand how the different processes interact to cause the main structures of the surface temperature response.

We do this by sensitivity experiments with the GREB model in which we turn some processes of the model "off". We will discuss 10 experiments that start with the simplest sensitivity experiments and ends with the complete GREB model. The experiments [1] to [4] focus on the local response to the direct CO_2 forcing without any climate feedbacks. Before we start the discussion of the feedbacks we discuss the role of heat advection in Exp. [5]. In the experiments [6] we address the ice/albedo and sea ice feedbacks and in the Exps. [7] to [9] we discuss the most important water vapor feedback. Finally we will discuss the ocean heat up take in Exp. [10].

5.1.1 The GREB model response to CO_2 forcing

Before start discussing the details of the GREB model simulation of CO_2 forcing we need to illustrate that the GREB model simulates a similar response to CO_2 forcing than current state of the art GCM simulations do. Fig. 5.2 show the response to CO_2 -forcing in GCM models and the GREB model. We can see that the GREB model is able to simulate the main IPCC T_{surf} response structures.

Climate response to CO_2 forcing scenario IPCC A1B:

time intervals: [2070-2100] - [1970-2000]

	IPCC	GREB	Comment
Global mean	2.6K	2.7K	This is somewhat expected as we have fitted our emissivity function by the IPCC results
Land warms more than oceans	60% more	30% more	GREB is not warming enough over land
Polar amplification	By factor 2	By factor 1.3	GREB is not warming enough over Arctic sea
Northern Hemisphere warms more than the Southern	Yes	Yes	GREB inter-hemispheric contrast is weaker
Cold season warms more	Yes	Yes	-

If we look at the difference between the IPCC models and GREB model response we can note a few aspects:

- Southern ocean warms too much: IPCC models show strong heat uptake in the Southern Ocean. Unclear if this is the problem in GREB.

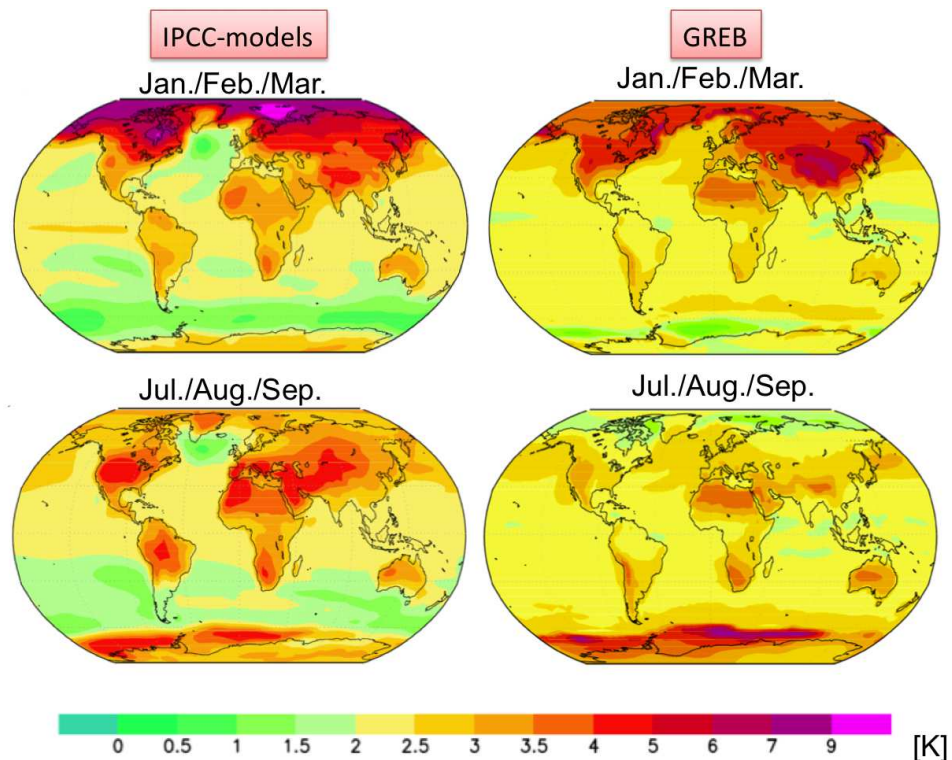


Figure 5.2: Comparison of the surface temperature response to CO_2 -forcing IPCC models vs. GREB. The main features are well simulated by the GREB model. Note, that we do not know what the 'real' response is, yet.

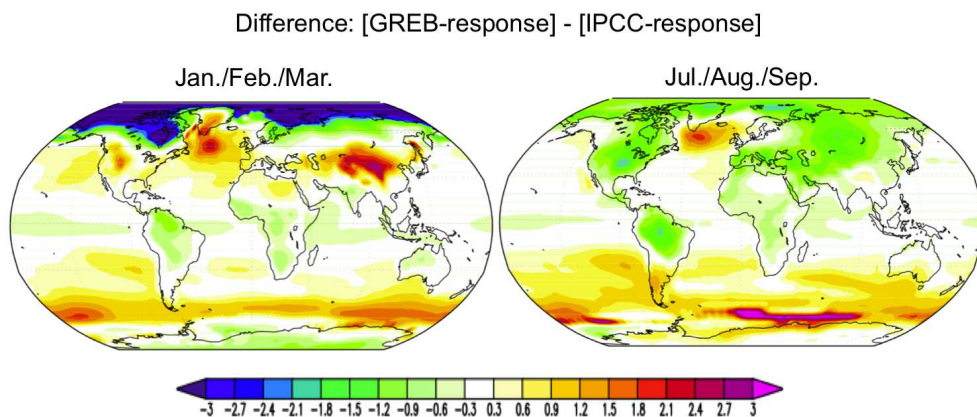


Figure 5.3: Difference in the surface temperature response to CO_2 -forcing IPCC models vs. GREB.

- Northern North Atlantic warms too much : IPCC models show a significant reduction of ocean transport (Gulf Stream), which is generally assumed to cause the weak warming in the North Atlantic.

Not that the GREB model deviations from the IPCC-models ensemble mean response is not s=much stronger than that of state of the art GCMs. Figure 5.4 shows the response of four different GCM simulations. We can see that the regional structures in the different model are quite different. It illustrates the current uncertainties in the climate response to CO_2 -forcing.

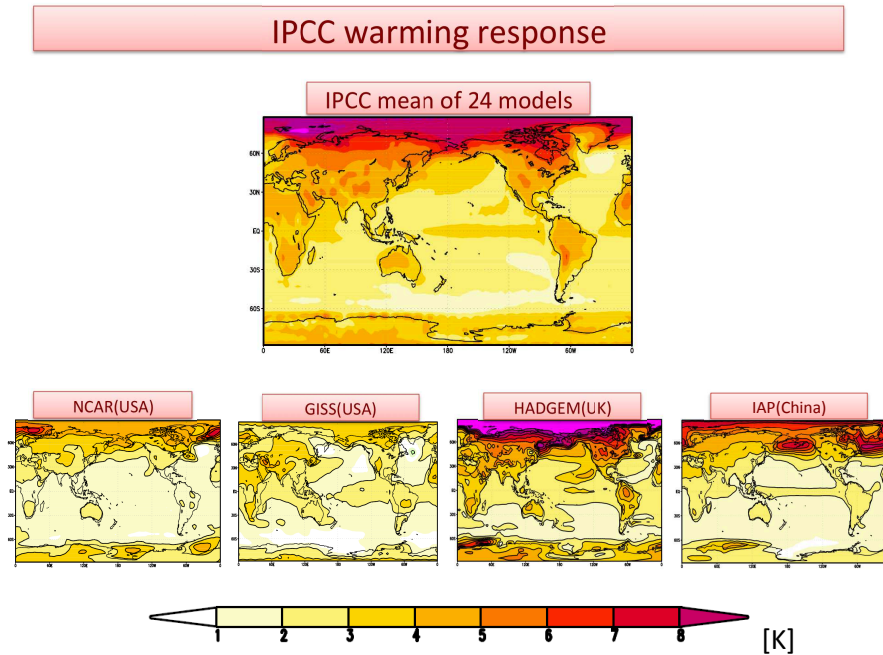


Figure 5.4: Upper: IPCC ensemble mmean response to CO_2 -forcing of 24 IPCC models. Lower: 4 example models. We can see that different models predict quite different warming patterns and global mean amplitudes.

GREB response ‘skill’: To understand how good or bad the model simulation is we would need to know what the climate response to CO_2 -forcing is. How, this is currently not known. In about a hundred years for now we will know, but for now we can only compare to other models. One way of estimating the skill in the GREB simulation is to see how much it deviates from the IPCC-models ensemble mean response, see Fig. 5.5. The GREB T_{surf} response is within the uncertainty of the 24 IPCC model predictions. Note, nothing is said about whether or not this response is similar to what the real world is doing.

GREB response in other variables

Response in relative humidity:

Mean values range from 20-80%

- mostly $\pm 3\%$, which is basically no change
- drying over land
- more humid over oceans

IPCC models: Similar, with mostly no significant change in humidity.

Response in precipitation:

- increasing everywhere by 10-20%

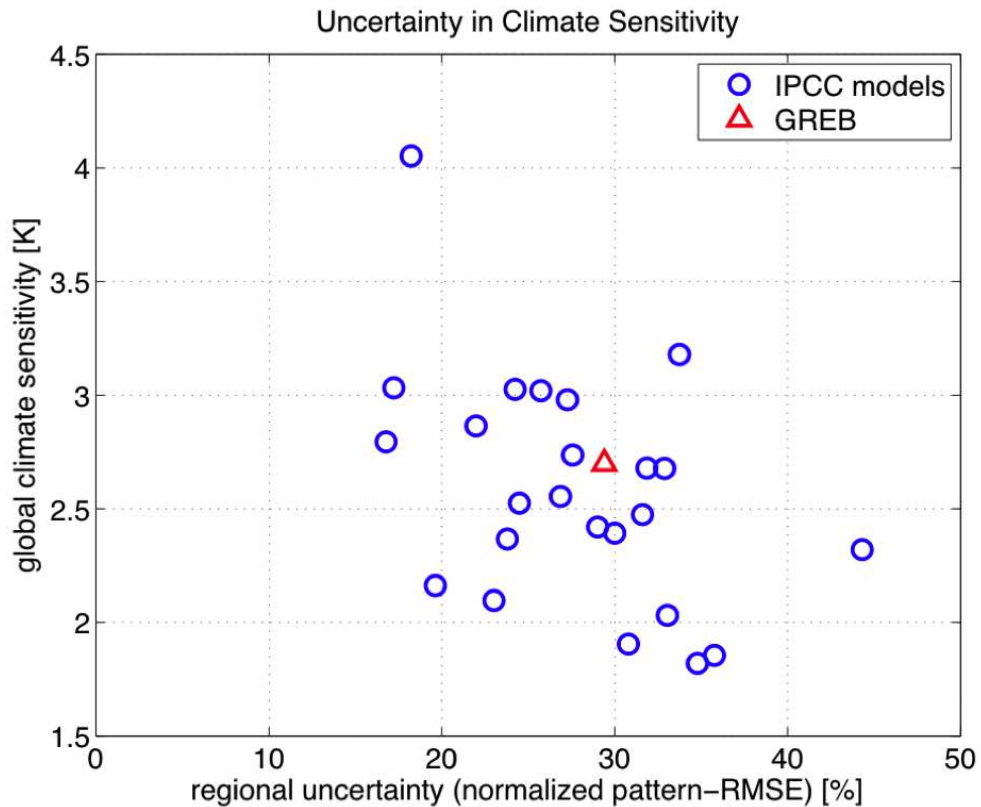


Figure 5.5: Spread in the model response. y-axis: The global mean warming. x-axis: similarity to the IPCC ensemble mean warming. 0 means the same warming pattern and 50% means in average a 50% different response amplitude.

- more strongly over dry regions
- GREB can only have increase in rain if q_{surf} increases - precipitation : $\Delta Q_{precip} = 0.1 \frac{1}{day} q_{surf}$

IPCC models: Mostly increasing by about 5-10%, but dry regions will mostly have a decrease in precipitation. Some models have quite significant decrease in precipitation.

GREB response in other variables

Response in T_{atmos} :

- T_{atmos} warms more than T_{surf}
- most strongly in the warm and wet regions
- this is caused by increased precipitation and the associated latent warming in the atmosphere and latent cooling at the surface

IPCC models: Similar, but more vertical structure of cause.

Response in ocean heat uptake:

- mostly in high latitudes - Southern Ocean, Atlantic and Pacific
- caused by deeper mixed layer depth in these regions

IPCC models: Similar in pattern and strength, but stronger over Southern Ocean.

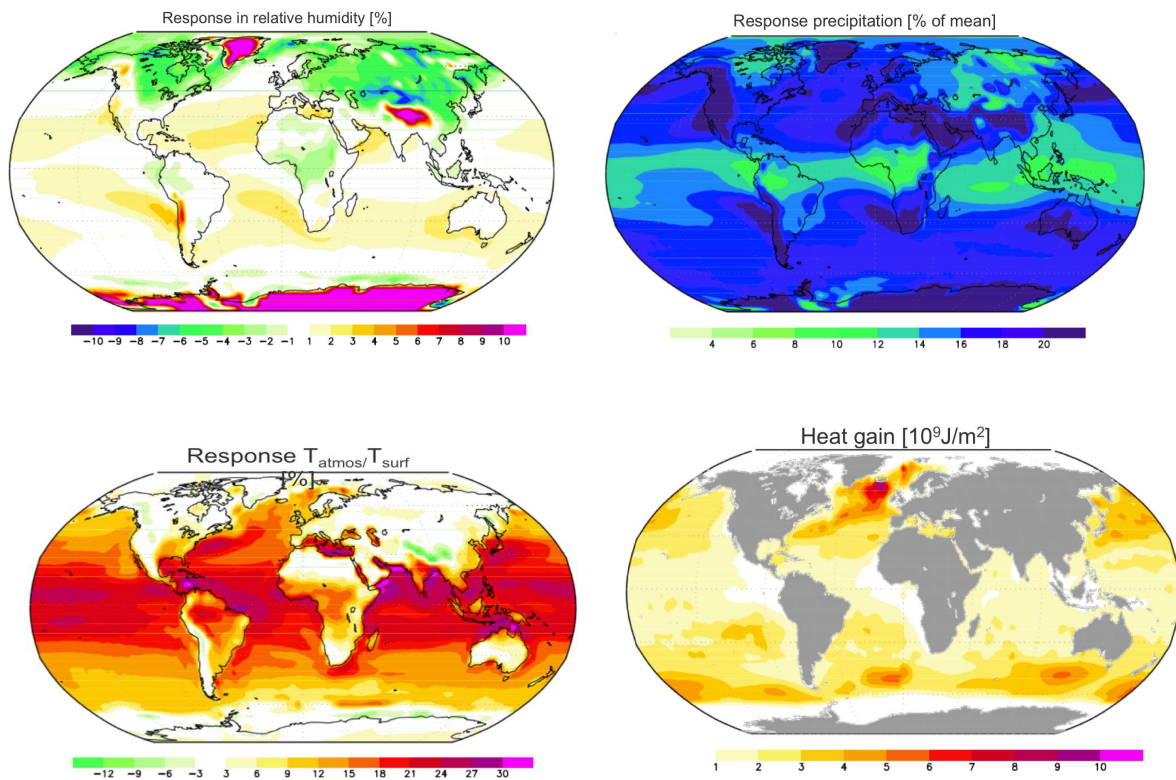


Figure 5.6: GREB response in other variables: Upper left: relative humidity in [%]. Upper right: precipitation in percentage of the mean precipitation. Lower left: Ratio of $\Delta T_{atmos}/\Delta T_{surf}$. Lower right: Oceans heat up take in [$10^9 J/m^2$].

GREB response precipitation:

Response precipitation [% of mean]

5.1.2 The Direct Local Forcing Effect - No Feedbacks (Exp. [1] to [4])

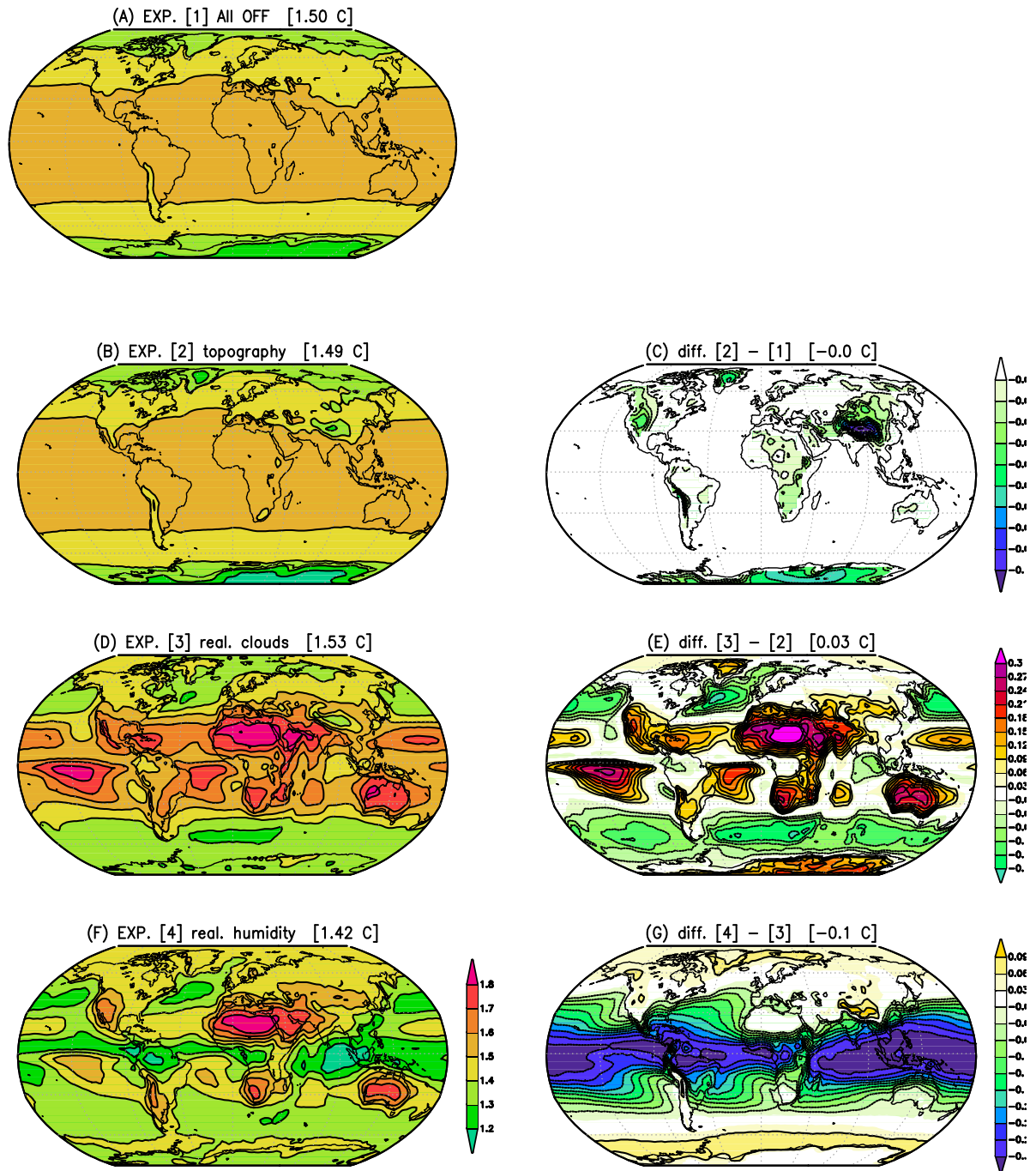


Figure 5.7: GREB model response to a doubling of the CO_2 concentration in four different sensitivity experiments. In each of the four experiments a number of processes and boundary conditions are changed. See text four details. The left column shows the annual mean response in T_{surf} and the right column show the difference in the response between two experiments. The color bar for the left column is the same in all panels and in the right column the color bars are different. The numbers in the heading mark the global mean values.

We start the series of experiments with 4 experiments where most processes are 'turned off'.

- No ocean heat uptake:
 - $\rightarrow F_{ocean} = 0$
 - $\rightarrow T_{ocean} = \text{fixed}$
- No feedbacks:
 - $\rightarrow \text{albedo} = \text{fixed}$
 - $\rightarrow q_{surf} = \text{fixed}$
 - $\rightarrow \text{No latent heating}$
- No circulation:
 - $\rightarrow \text{advection} = 0$
 - $\rightarrow \text{diffusion} = 0$

With the circulation turned 'off' we can discuss the response at each location independent of each other. Thus, effectively, each grid point of the GREB model is now responding independent of the others.

The four GREB Model tendencies equations are:

$$\gamma_{atmos} \frac{dT_{atmos}}{dt} = F_{thermal} + F_{atmos-latent} - F_{sense} + \gamma_{atmos} (\kappa \cdot \nabla^2 T - \tilde{u} \cdot \tilde{\nabla} T)$$

$$\gamma_{surf} \frac{dT_{surf}}{dt} = F_{solar} + F_{thermal} + F_{latent} + F_{sense} + F_{ocean} + F_{correct}$$

$$\gamma_{ocean} \frac{dT_{ocean}}{dt} = \Delta T_{O_{entrain}} - F_{O_{sense}} - F_{O_{correct}}$$

$$\frac{dq_{surf}}{dt} = \Delta q_{eva} + \Delta q_{precip} + (\kappa \cdot \nabla^2 q_{surf} - \tilde{u} \cdot \tilde{\nabla} q_{surf}) + \Delta q_{correct}$$

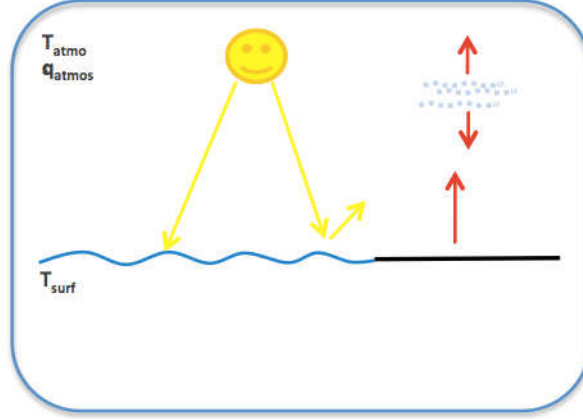
With the processes turned 'off' these equations reduce substantially:

$$\gamma_{atmos} \frac{dT_{atmos}}{dt} = F_{thermal} - F_{sense} \quad (5.1)$$

$$\gamma_{surf} \frac{dT_{surf}}{dt} = F_{solar} + F_{thermal} + F_{sense} + F_{correct} \quad (5.2)$$

To maintain the same reference mean T_{surf} we replace missing processes by additional flux corrections ($F_{correct}$).

Experiment [1]: The Pure Radiation Balance - No Regional Difference in Greenhouse Effect, Fig. 5.7a



For Exp. [1] we further set all boundary conditions that affect the thermal radiation to be globally uniform:

- No topography
- globally uniform clouds ($a_{cloud} = 0.7$)
- globally uniform water vapour ($q_{surf} = 0.0052$ and thus $H_2O = 14Kg/m^2$)

Most terms in the surface temperature tendencies equation are now constant (not changing over time other than the seasonal cycle). We can therefore now simplify our surface temperature tendencies equation:

$$\gamma_{surf} \frac{dT_{surf}}{dt} \approx F_{thermal} + F_{constant} \quad (5.3)$$

So only the $F_{thermal}$ term is depending on the climate and therefore changing over time. This strong simplification of the GREB model allows us to estimate the surface temperature response to increases in CO_2 concentrations analytically.

We can approximate the $F_{thermal}$ term by a linearisation:

$$F_{thermal} \approx C_{thermal} \cdot T_{surf} + Q_{CO_2} \quad (5.4)$$

with $C_{thermal} = \frac{dF_{thermal}}{dT_{surf}}$ the linear feedback parameter as defined in eq.[2.71]. The CO_2 forcing is now only included in the forcing Q_{CO_2} .

In equilibrium, we have now:

$$C_{thermal} \cdot T_{surf} + Q_{CO_2} + F_{constant} = 0 \quad (5.5)$$

The equilibrium response in the surface temperature to increases in CO_2 concentrations, ΔT_{surf} , is the difference in this equation between $Q_{CO_2}(2xCO_2)$ and $Q_{CO_2}(control)$, ΔQ_{CO_2} :

$$C_{thermal} \cdot \Delta T_{surf} + \Delta Q_{CO_2} = 0 \quad (5.6)$$

with $\Delta T_{surf} = T_{surf}(2xCO_2) - T_{surf}(control)$ and $\Delta Q_{CO_2} = Q_{CO_2}(2xCO_2) - Q_{CO_2}(control)$. Thus the equilibrium response is

$$\Delta T_{surf} = \frac{-\Delta Q_{CO_2}}{C_{thermal}} \quad (5.7)$$

We can estimate the linear feedback parameter $C_{thermal}$ by the thermal radiation term:

$$F_{thermal} = -\sigma T_{surf}^4 + \epsilon \sigma T_{atmos}^4 \quad (5.8)$$

The atmospheric temperature $T_{atmos} \approx 0.84 * T_{surf}$. We can therefore replace T_{atmos}

$$F_{thermal} \approx -\sigma T_{surf}^4 + \epsilon \sigma 0.84^4 T_{surf}^4 \quad (5.9)$$

Thus

$$F_{thermal} \approx (0.5\epsilon - 1)\sigma T_{surf}^4 \quad (5.10)$$

So we get

$$C_{thermal} \approx 4(0.5\epsilon - 1)\sigma T_{surf}^3 \quad (5.11)$$

Note, that the negative feedback of the thermal radiation is stronger (more negative) if ϵ is smaller. From the emissivity function we can estimate the mean $\epsilon \approx 0.8$ for the given cloud cover and mean water vapour, see Fig. 4.17.

So for a mean $T_{surf} = 288^\circ K$ we get

$$C_{thermal} \approx -3.3 \frac{W}{m^2 K} \quad (5.12)$$

This is similar to the values we discussed in the energy balance sections of the Budyko and the zero order model.

Next we have can estimate the ΔQ_{CO_2} :

$$\Delta Q_{CO_2} = \Delta F_{thermal} = F_{thermal}(2xCO_2) - F_{thermal}(control) \quad (5.13)$$

Note that ΔQ_{CO_2} is the initial forcing from the $2xCO_2$ before the climate is responding. So it is the initial forcing then T_{surf} is at the control climate values. So we need to compare $F_{thermal}(2xCO_2)$ and $F_{thermal}(control)$ for the same T_{surf} . Using eq.[5.9] we get:

$$\Delta Q_{CO_2} \approx 0.5\Delta\epsilon\sigma T_{surf}^4 \quad (5.14)$$

with $\Delta\epsilon = \epsilon(2xCO_2) - \epsilon(control)$. We can again estimate this as $\Delta\epsilon \approx 0.025$ for the given cloud cover and mean water vapour, see Fig. 4.17. So for a mean $T_{surf} = 288^\circ K$ we get

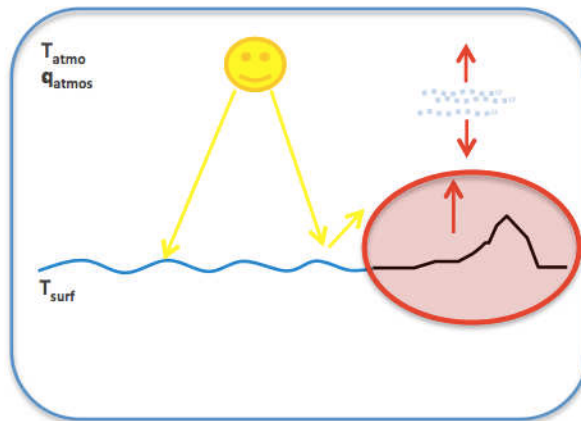
$$\Delta Q_{CO_2} \approx +4.8 \frac{W}{m^2} \quad (5.15)$$

So the doubling of the CO_2 concentration gives an initial forcing of $+4.8 \frac{W}{m^2}$. This value can be compare to those estimates from the IPCC report, see Fig. 2.1.

We can now use eq. [5.7] to get the equilibrium response

$$\Delta T_{surf} \approx \frac{-0.5\Delta\epsilon\sigma T_{surf}^4}{4(0.5\epsilon - 1)\sigma T_{surf}^3} = \frac{0.5\Delta\epsilon}{4(1 - 0.5\epsilon)} T_{surf} = 0.2 \cdot \Delta\epsilon \cdot T_{surf} \quad (5.16)$$

The direct response to doubling of the CO_2 concentration is a warming of about $+1.5$ degrees. It is proportional to the absolute temperature. So it is slightly larger in the tropics than in the polar regions, see Fig. 5.7a.

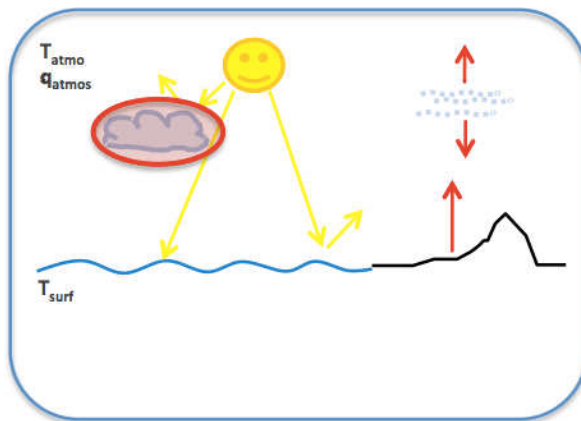
Experiment [2]: The Role of Altitude on CO_2 Forcing, Fig. 5.7b

- As [1] but with topography

In the emissivity function $\epsilon_{atmos} = F(CO_2^{topo}, H_2O, \text{cloud cover})$ the local CO_2 concentration, CO_2^{topo} , does depend on the topography:

$$CO_2^{topo} = CO_2 \cdot e^{\frac{z_{topo}}{h_{atmos}}} \quad (5.17)$$

Over high altitudes there is less atmosphere (lower pressure) and therefore less radiation effects. So the direct CO_2 effect is reduced.

Experiment [3]: Effect of the Mean Cloud Cover (No changes in clouds), Fig. 5.7d

- As [2] but with true cloud climatology

$$\epsilon_{atmos} = \frac{p_s - a_{cloud}}{p_9} (\epsilon_{clear-sky} - p_{10}) + p_{10}$$

- Cloud cover increases the mean ϵ
 - larger positive feedback by atmospheric thermal radiation (greenhouse effect)
 - more sensitive to external forcings

- Larger cloud cover dilutes the effect of the trace gasses ($\epsilon_{clear-sky}$) and therefore the CO_2 effect. So $\Delta\epsilon$ is smaller.

If we examine eq. [5.16] we see that a smaller $\Delta\epsilon$ would reduce the warming, but the larger mean ϵ would increase the warming. The later is less important for cloud cover. Overall cloudy regions will be less sensitive to CO_2 forcing than clear sky regions, but not as much as one may think from the change in sensitivity to CO_2 , because the increased mean ϵ is also increasing the positive feedback by *atmospheric thermal radiation*, see Fig. 5.8.

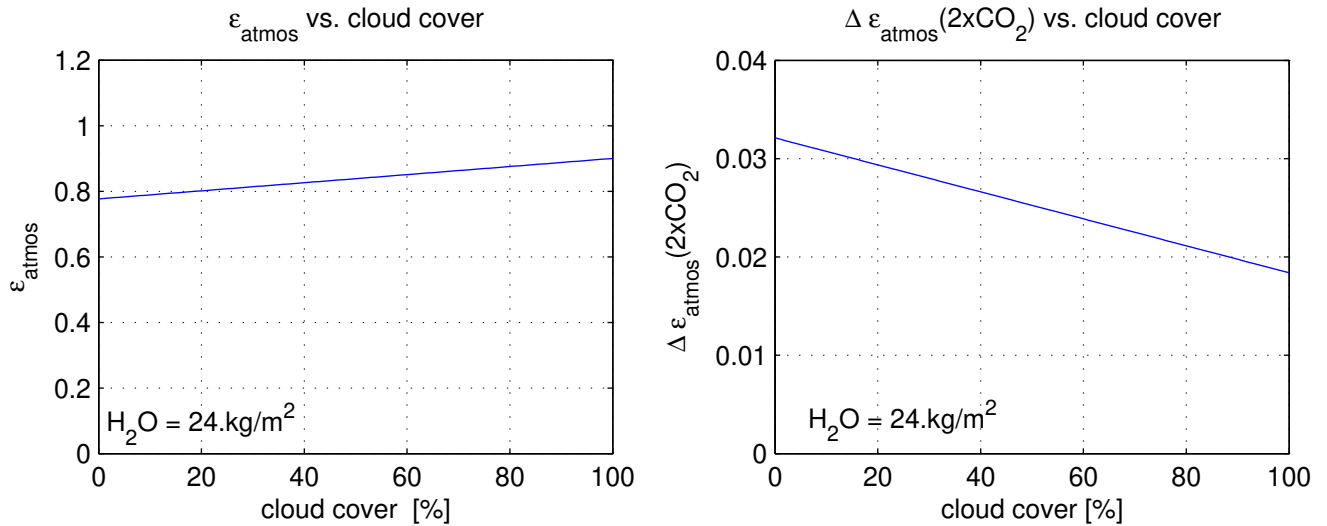
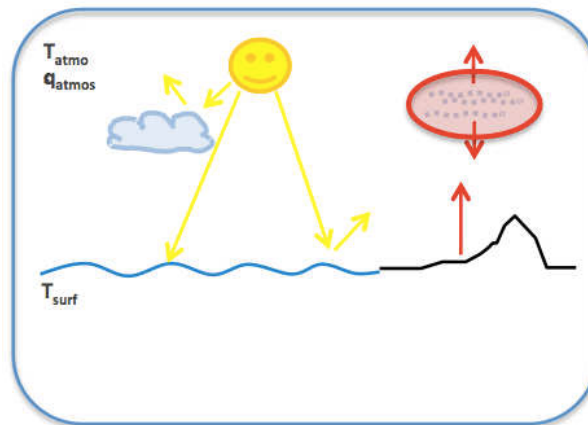


Figure 5.8: Sensitivity of the emissivity function to cloud cover.

Experiment [4]: *Effect of the mean atmospheric water vapour (no feedbacks)*, Fig. 5.7f



- As Exp. [3] but with true humidity climatology
- Humid regions are less sensitive to CO_2 forcing due to the spectral absorption band overlap:

The first term RHS is the log-function with both CO_2 and H_2O . If H_2O is low the CO_2 term has a bigger impact on the log-function and therefore on the emissivity. So a change in CO_2 leads to a

$$\epsilon_{clear-sky} = p_4 \cdot \log[p_1 \cdot CO_2^{topo} + p_2 \cdot H_2O_{vapor} + p_3] + p_5 \cdot \log[p_1 \cdot CO_2^{topo} + p_3] + p_6 \cdot \log[p_2 \cdot H_2O_{vapor} + p_3] + p_7$$

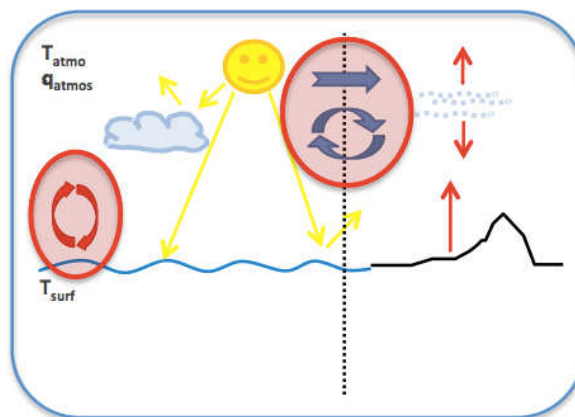
CO₂ and H₂O absorb
only CO₂ absorbs
only H₂O absorbs

bigger $\Delta\epsilon$. Further, if H_2O is low the overall emissivity ϵ is also low. If we examine eq. [5.16] we see that a smaller ϵ would increase the sensitivity and thus increase the warming. So lower H_2O increases the sensitivity by both the bigger $\Delta\epsilon$ and the smaller mean ϵ , see Fig.5.7f. In turn large H_2O concentrations decrease the CO_2 forcing.

Summary of the direct local CO_2 forcing

- differences in cloud cover, humidity and topography cause difference in the local response to CO_2 forcing
- the strongest response is over the warm dry deserts
- the weakest response is over the warm humid oceans
- the global mean response is 1.5 ° C

Experiment [5]: *Effect of atmospheric heat transport (no feedbacks)*, Fig. 5.9a

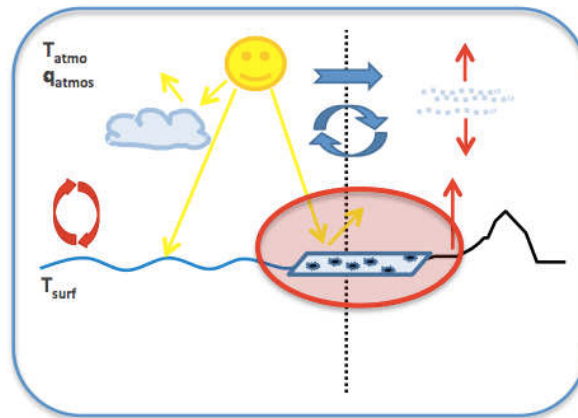


- As [4] but with atmospheric circulation of heat
- No ocean heat uptake
 - $\rightarrow F_{ocean} = 0$
 - $\rightarrow T_{ocean} = \text{fixed}$
- No feedbacks
 - $\rightarrow \text{albedo} = \text{fixed}$
 - $\rightarrow q_{surf} = \text{fixed}$
 - $\rightarrow \text{No latent heating}$

The atmospheric heat transport by mean advection and diffusion reduces temperature gradients and extremes. The differences in the local sensitivities are smoothed out.

5.1.3 Ice/Snow-Albedo and Sea Ice Feedback

Experiment [6]: *Ice/Snow-Albedo and Sea Ice Feedback*, Fig. 5.9c



- As [5] but with the ice-albedo and sea ice feedback.

- No ocean heat up take

In Sect. 4.1.2 we discussed the ice-albedo feedback. In Fig. 4.10 we illustrated that the ice-albedo feedback parameter is strongest in the midlatitudes of the northern hemisphere continents and around Australia. So the response to CO_2 forcing is amplified in these regions by the ice-albedo feedback to the warming T_{surf} .

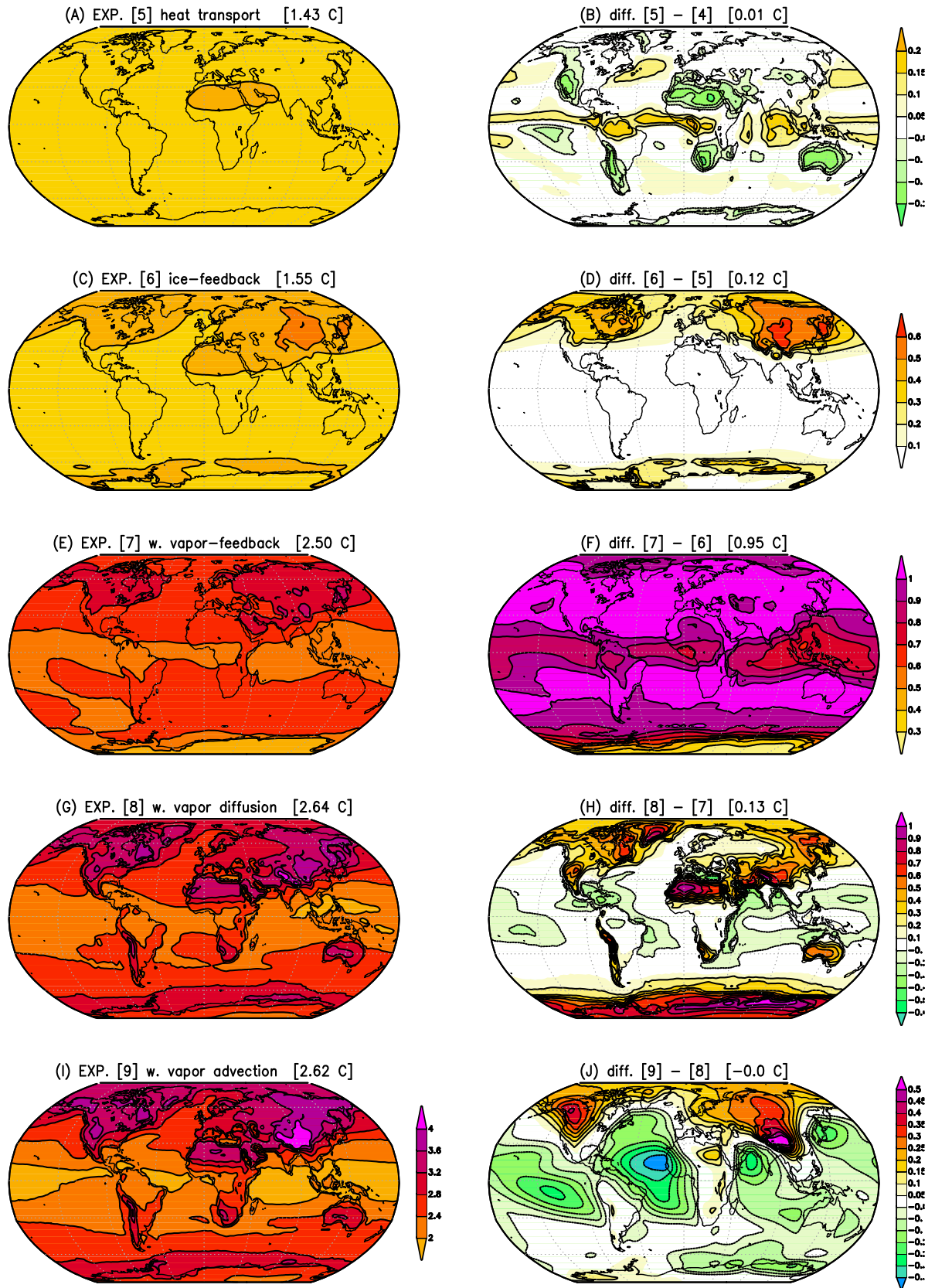
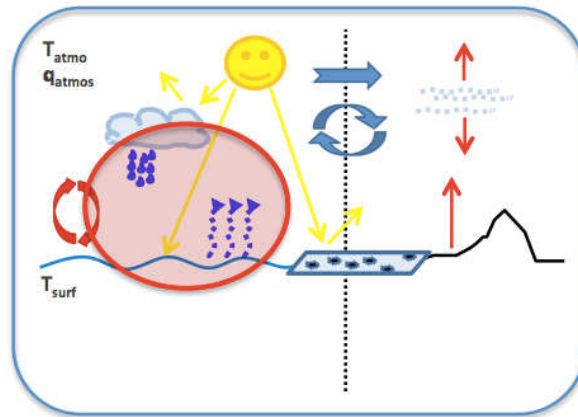


Figure 5.9: GREB model response to a doubling of the CO_2 concentration as in Fig. 5.7, but for the sensitivity experiments [5]-[9]

5.1.4 The Water Vapour Feedback

Experiment [7]: *Local Water Vapour Feedback*, Fig. 5.9e



- As [6] but with local water vapour response and latent heat release
- No ocean heat up take

The water vapour response to the warming is the most important feedback in the GREB model that amplifies the climate response to CO_2 forcing. The amount of water vapour in the atmosphere is strongly related to the temperature by the Clausius-Clapeyron equation (see eq. [4.15] and Fig. 4.21). A $3^\circ C$ warming will increase the amount of water vapour in the atmosphere by 20% if the relative humidity is not changing. A 20% increase in the water vapour in the atmosphere changes the emissivity by about 0.02, see Fig. 5.10. This is as strong as the initial CO_2 effect and thus it basically doubles the climate response globally.

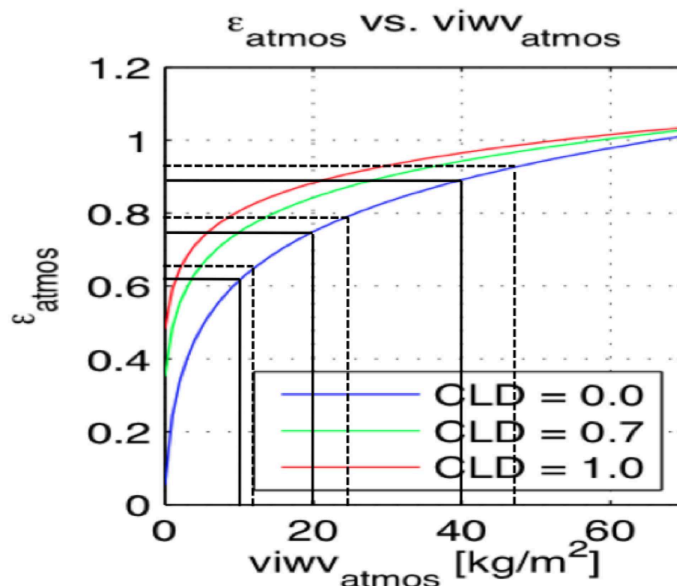
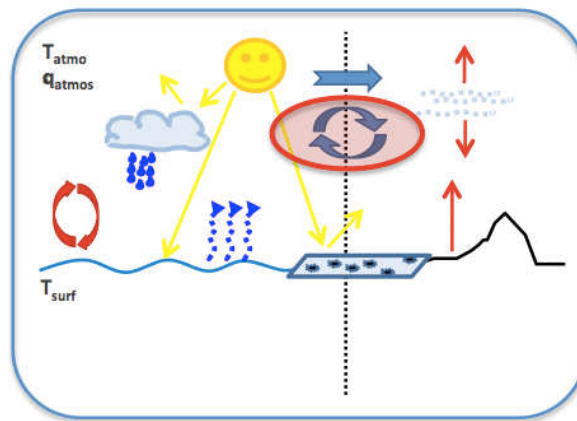


Figure 5.10: The sensitivity of the emissivity to changes in the total amount of water vapor in the atmosphere ($VIWV_{atmos}$). A 20% change in $VIWV_{atmos}$ will always lead to the same change in the emissivity.

Exp. [8] Effect of Turbulent Atmospheric Water Vapour Transport, Fig. 5.9g

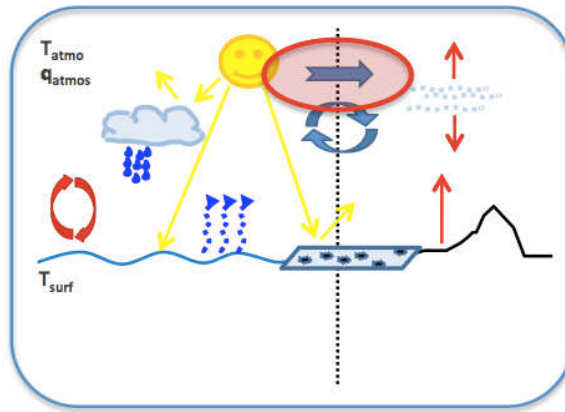


- As [7] but with turbulent (isotropic diffusion) water vapour transport
- No ocean heat up take
- Regions where water vapour increases a lot are now exporting additional water vapour to regions where water vapour increases less
- Warm and moist regions lose H₂O
- Cold and dry regions gain H₂O
- Dry and cold regions get additional warming by thermal radiation due to additional H₂O
- Warm and wet regions do the opposite
- There is also a minor effect of additional latent heating in the atmosphere by condensation of the additional H₂O

The local increase in the water vapour in the atmosphere is not uniform, warmer regions will have stronger increases in the water vapour. The atmospheric circulation will transport water vapour from regions with stronger local increase (warm and moist regions) to regions with smaller local increase (cold and dry).

The effect of the Turbulent Atmospheric Water Vapour Transport is therefore an additional warming in relatively dry and cold regions, see Fig. ???. These are in particular the land and polar regions. Thus the Turbulent Atmospheric Water Vapour Transport contributes to the land-sea warming contrast: the land warms more than the oceans.

Exp. [9] Effect of Water Vapour Transport by the Mean Advection, Fig. 5.9i

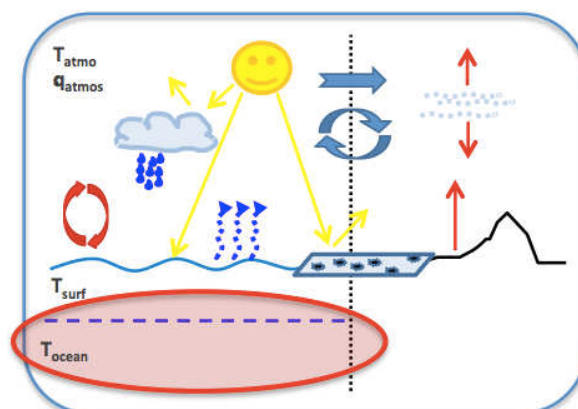


- As [8] but with mean advection transport of water vapour
- No ocean heat up take

The effect is similar to the turbulent atmospheric water vapour transport, but it is more focused on the northern hemisphere, because the mean winds blow more strongly across temperature and therefore water vapor gradients. In the southern hemisphere the more zonal wind do not blow across gradients in water vapor.

5.1.5 The Oceans Heat Up Take

Experiment [10]: Effect of deep ocean heat up take



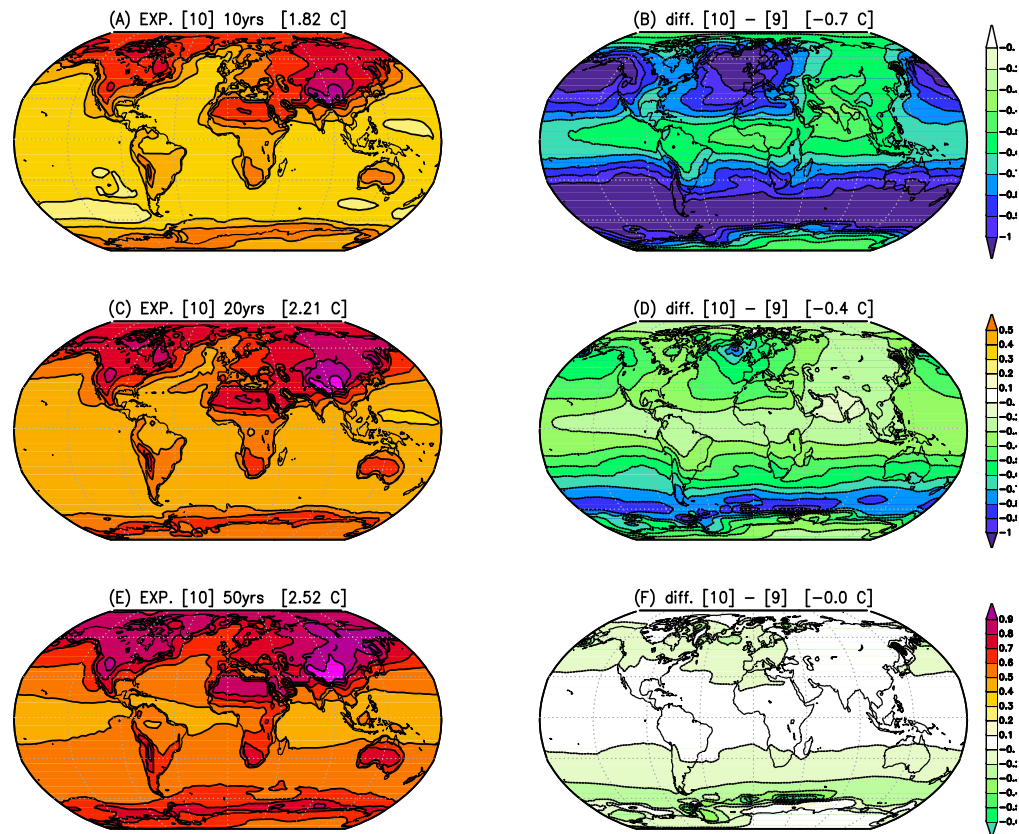


Figure 5.11: GREB model response to a doubling of the CO_2 concentration as in Fig. 5.7, but for the complete GREB model including all processes (Exp. [10]). the different panles show the response after 10yrs (upper), 20yrs (middle) and after 50yrs (lower).

- As [9] but with deep ocean interaction
- The complete GREB model
- Ocean heat up take slows down the warming over oceans.
- The land feels the ocean response by atmospheric circulation of heat and moisture and therefore also slows down.
- How much the ocean slows down the warming depends on how fast the CO_2 concentration is changing.
- Ocean damping is a transient effect. In equilibrium the global mean is mainly not effected.
- The strongest effects are over the southern and northern North Atlantic Ocean, but in general the effect is global.
- The land vs. ocean warming ratio is a function of response time, but will always stay larger than 1.0, due to other feedbacks.
- the global mean resonse to $2xCO_2$ forcing is $2.5^\circ C$ after 50 years. In equilibrium it is $2.6^\circ C$, as in experiment [9].
- Note the regions of small increases in warming at the sea ice boundaries are due to changes of mixed layer depth in the ocean, which is an artifact of the GREB model experiments design.

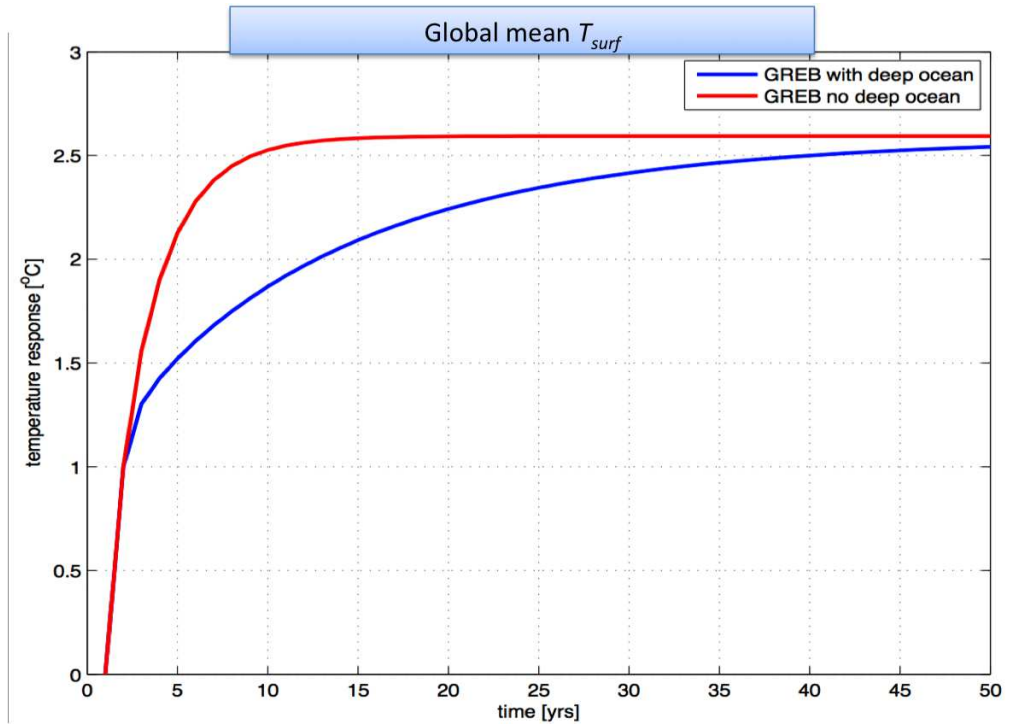


Figure 5.12: Effect of deep ocean heat up take - global mean surface temperature

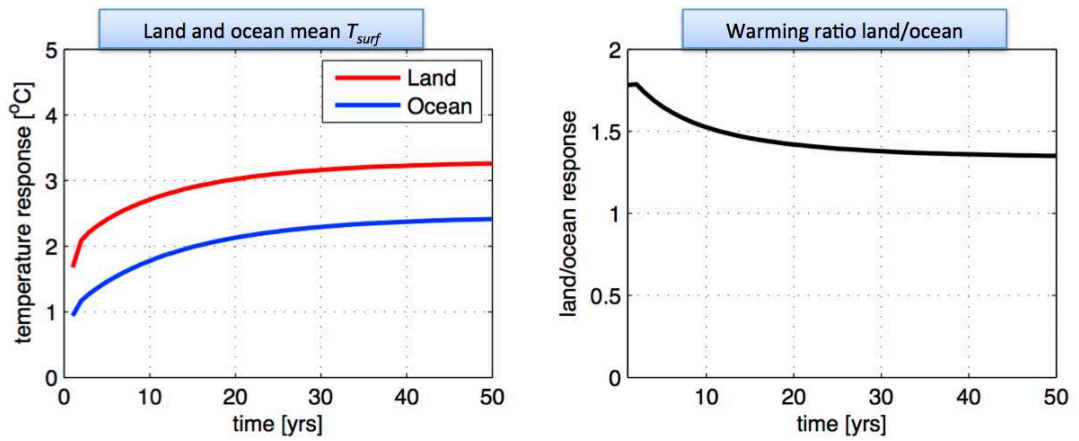


Figure 5.13: Effect of deep ocean heat up take - land vs. ocean

5.1.6 Cautionary Note on the GREB model global warming

- This is only a model, not the real world.
- The GREB is a very simple, uncertain and highly tuned (to IPCC models, not observed) model.
- IPCC model will in many regions or seasons have different responses for different reasons.
- The GREB model cannot say anything about how the circulation in the atmosphere or ocean responds. And it is likely that such responses will exist on the small scale (turbulence) and large scale (mean).
- GREB models cannot say anything about how cloud cover or soil moisture repond. Again this can be important.

5.2 Anthropogenic climate change predictions

In the following we take a closer look at the Anthropogenic climate change predictions. Our main source for this discussion is the summary provided by the IPCC report from 2007. We start the discussion with a short overview on the history on Anthropogenic climate change predictions. We then shortly describe the IPCC CO₂ scenarios and the most important climate responses. These include the response in precipitation and the sea level. To understand the significance of the Anthropogenic climate change we will put the predicted +3°K global warming into context of natural climate variability. Finally we take a look at the discussion of climate change in the media.

5.2.1 History of climate change predictions

- ~1900: First ideas about CO₂ thermal radiation could control climate over ice age cycles, see Fig. 5.14.
- ~1950: After World War II it became clear that human CO₂ emissions could potentially be large enough to change the atmospheric CO₂ concentration.
- At that point not much was known about CO₂ concentrations at present or in the past, nor were global mean surface temperatures at present or in the past known. So nobody knew if CO₂ concentrations or global mean surface temperatures were rising.
- ~1956: Measurements of atmospheric CO₂ concentrations on Hawaii (far away from any industry) started, see Fig. 5.15. The direct measurements of the CO₂ concentrations in Hawaii from 1958 onwards are later complimented with proxy estimations of pasted CO₂ concentrations from various data sources, see Fig.5.16.
- ~1970: First predictions of anthropogenic climate change estimated a warming of about 3°C at the end of 2100.
- 1990: First IPCC report. An IPCC report assesses all research regarding climate change and summarizes the results. It does **not** do research.



Svante August Arrhenius
(1859-1927, Nobel Preis in
Chemie 1903)

THE
LONDON, EDINBURGH, AND DUBLIN
PHILOSOPHICAL MAGAZINE
AND
JOURNAL OF SCIENCE.
[FIFTH SERIES.]
APRIL 1896.

XXXI. *On the Influence of Carbonic Acid in the Air upon the Temperature of the Ground.* By Prof. SVANTE ARRHENIUS *.

I. Introduction: *Observations of Langley on Atmospheric Absorption.*

A GREAT deal has been written on the influence of the absorption of the atmosphere upon the climate. Tyndall † in particular has pointed out the enormous importance of this question. To him it was chiefly the diurnal and annual variations of the temperature that were lessened by this circumstance. Another side of the question, that has long attracted the attention of physicists, is this: Is the mean temperature of the ground in any way influenced by the presence of heat-absorbing gases in the atmosphere? Fourier ‡ maintained that the atmosphere acts like the glass of a hot-house, because it lets through the light rays of the sun but retains the dark rays from the ground. This idea was elaborated by Pouillet §; and Langley was by some of his researches led to the view, that "the temperature of the earth under direct sunshine, even though our atmosphere were present as now, would probably fall to -200° C., if that atmosphere did not possess the quality of selective

* Extract from a paper presented to the Royal Swedish Academy of Sciences, 11th December, 1895. Communicated by the Author.

† 'Heat a Mode of Motion,' 2nd ed. p. 495 (Lond., 1865).

‡ *Mém. de l'Ac. R. d. Sci. de l'Inst. de France*, t. vii. 1827.

§ *Comptes rendus*, t. vii. p. 41 (1838).

Phil. Mag. S. 5. Vol. 41. No. 251. April 1896.

S

Figure 5.14: One of the first discussions of climate change due to change in the CO_2 concentrations: Article from 1896 by Sante August Arrrhenius discussing the role of CO_2 concentrations as cause of ice ages. Result: about +5 degrees global warming. Later discussions about a possible anthropogenic doubling of CO_2 concentrations: This would take about 3000 years if caused by human emissions(Not anticipating the future size of anthropogenic emissions; at this time human emissions were quite low.

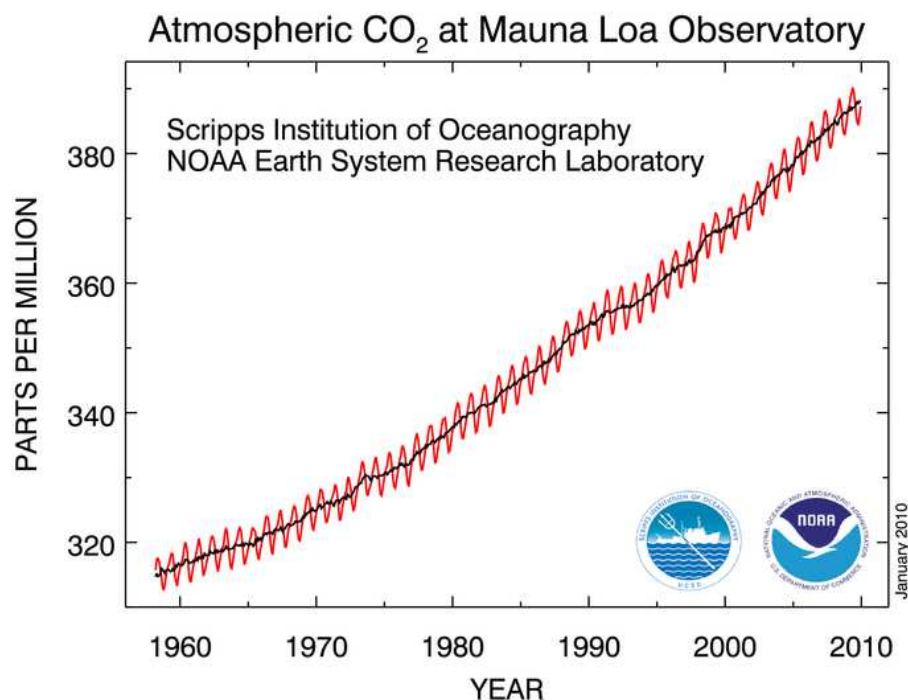


Figure 5.15: Atmospheric CO_2 concentrations from 1958 to 2008 as measured at Hawaii. The oscillations mark the natural annual cycle. The trend is caused by the anthropogenic emissions. It is about half the amount of anthropogenic emissions. The other half of anthropogenic emissions is taken up by natural reservoirs (e.g. oceans, or land biosphere.)

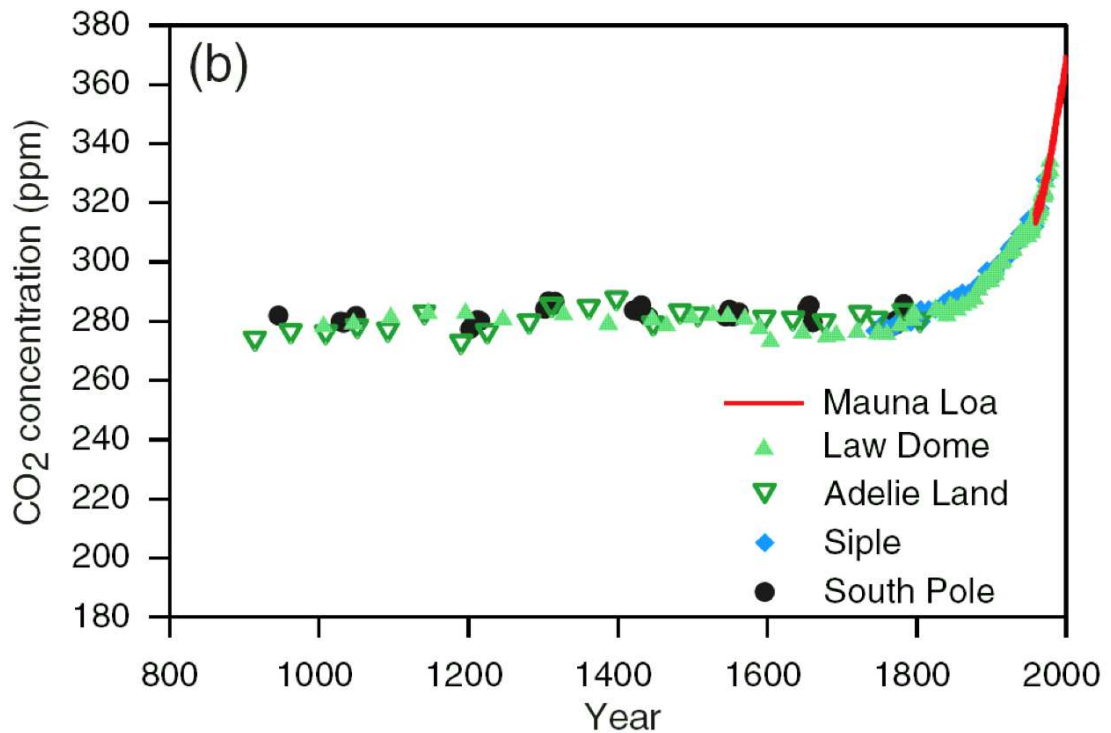


Figure 5.16: Atmospheric CO₂ concentrations from 800 to 2000 as estimated from various different proxy data.

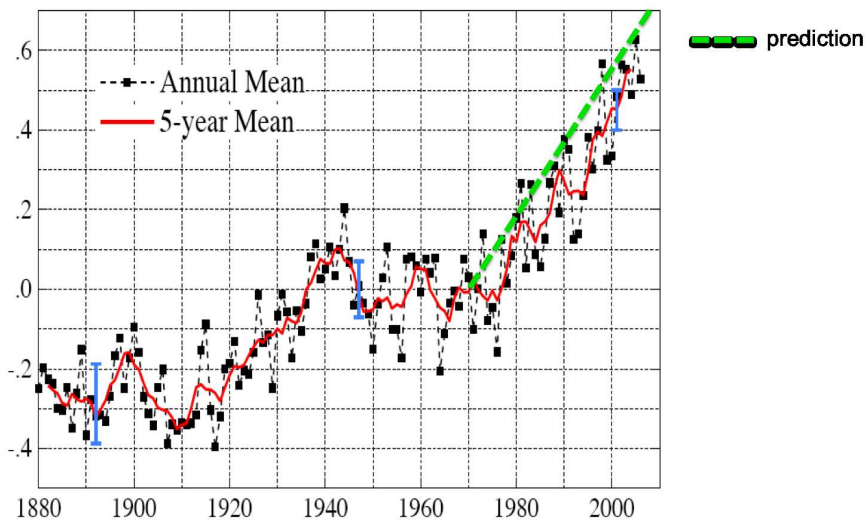


Figure 5.17: Observed global mean temperature versus a prediction from 1970. Note that the time the prediction was made the global mean temperatures variability over the past decades were virtually unknown and clearly the temperature trend from the 970s onward was not known. This is a remarkable good prediction, considering that these were made without the use of supercomputers.

5.2.2 IPCC CO₂ scenarios

- IPCC scenarios of CO₂ emissions are based on economical models

- Note, we simplify all forcings of CO₂. Keep in mind there are other anthropogenic forcings (e.g. methane or aerosols)
- Note, climate models need concentrations not emissions. So a carbon cycle model will provide estimates of CO₂ concentrations for the given CO₂ emissions
- **A2-scenario**: Roughly a business as usual scenario. Population is growing, economies are growing, in particular in the developing world. Not much change in fossil fuels consumption
- **A1B-scenario**: The most cited scenario. As A2, but more green technology development over the next decades. Reduced use of fossil fuels
- **B1-scenario**: Political goal of warming less than 2 degrees in global mean. Active reduction in fossil fuel consumption should have been started about 10 years ago

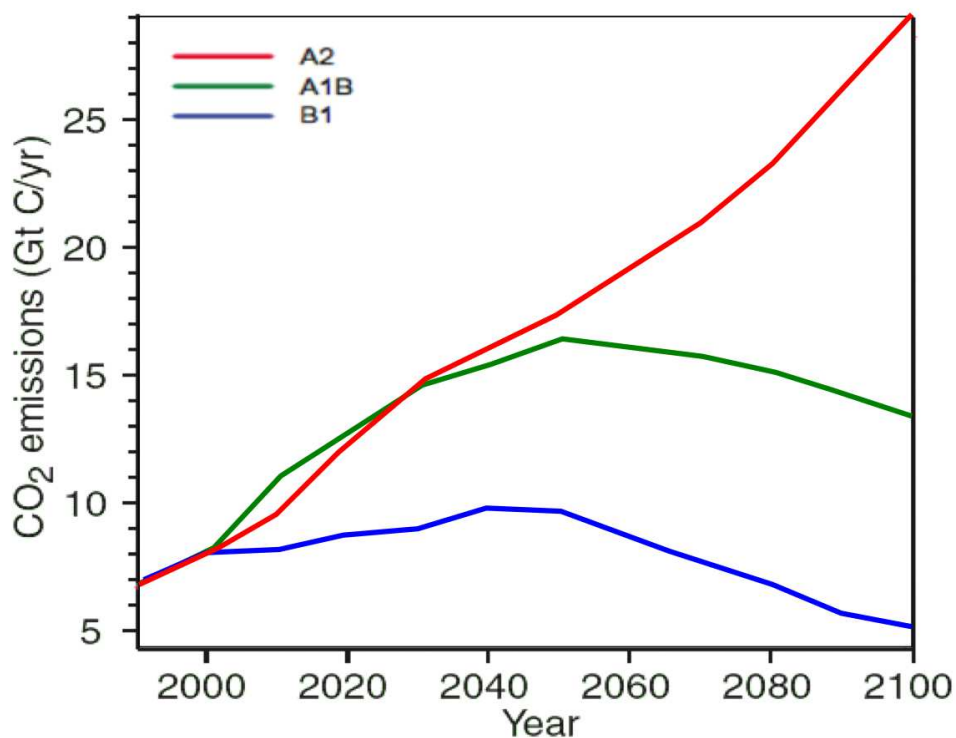


Figure 5.18: CO₂ emission scenarios from the IPCC report 2007.

IPCC global mean response

- Global mean response is more than 3°C at the end of 2100 if business as usual (A2-scenario), tendency of significant continued warming
- Global mean is mostly ocean warming. Land will warm by about 50% more than the oceans → 5°C
- Scenario B1 is history as emissions have not been reduced over the last decade
- All three scenarios are about the same for the next 50 years, they only differ significantly after about 80-100 years

- Even if emissions were zero (since 2000) climate continues to warm, due to the large inertia (heat capacity) of the climate system
- The predictions for each scenario have some uncertainty, because the models are not perfect. Different models give different global mean response

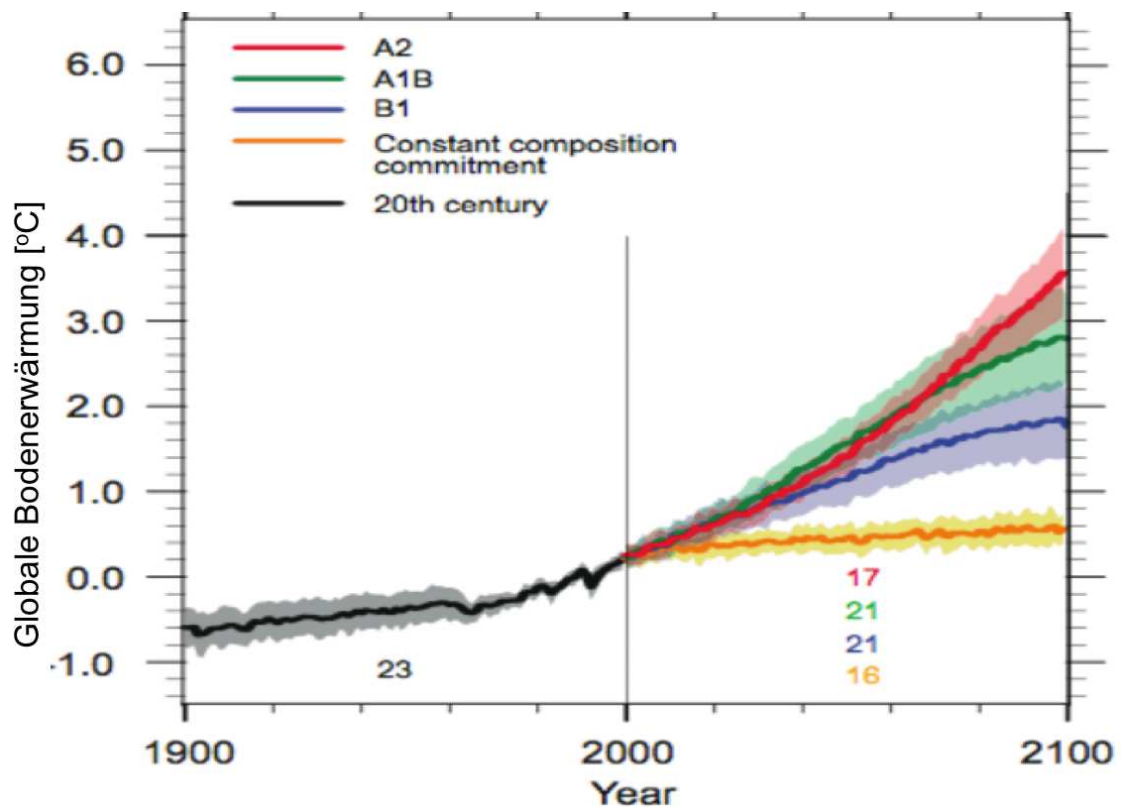


Figure 5.19: Global mean temperature change in the different CO_2 emission scenarios from the IPCC report 2007. The 20th century simulations are forced with observer passed CO_2 , solar radiation changes and volcanic emissions. the numbers in the lower right mark the number of models summarised in each scenario.

5.2.3 Prediction vs. Reality

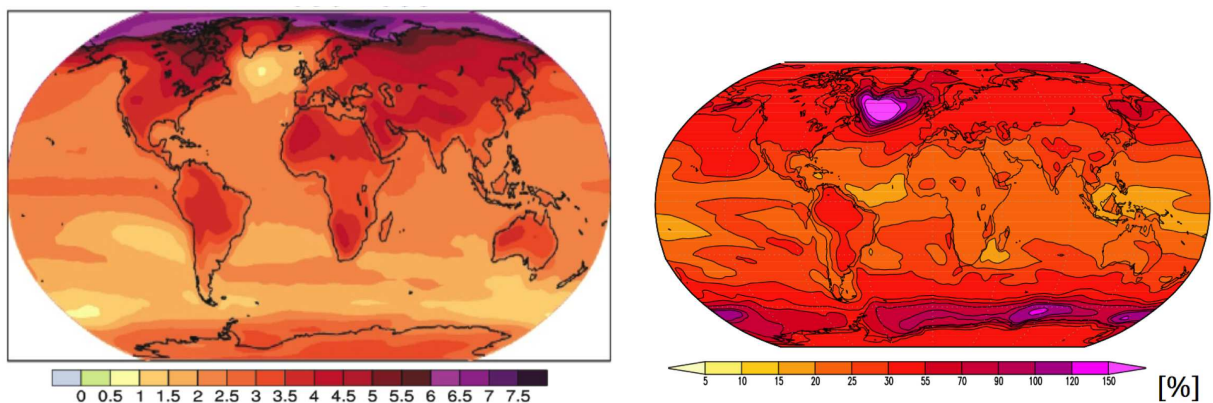


Figure 5.20: Left: Temperature change until 2100 (Scenario A1B) as the ensemble mean of 24 model simulations. Right: the relative spread within the 24 model simulations.

Climate models are not perfect. Different models predict different warming patterns. In some regions the uncertainties are quite large, see Fig. 5.20. Note most other climate changes (e.g. precipitation) are even more uncertain.

Observed warming

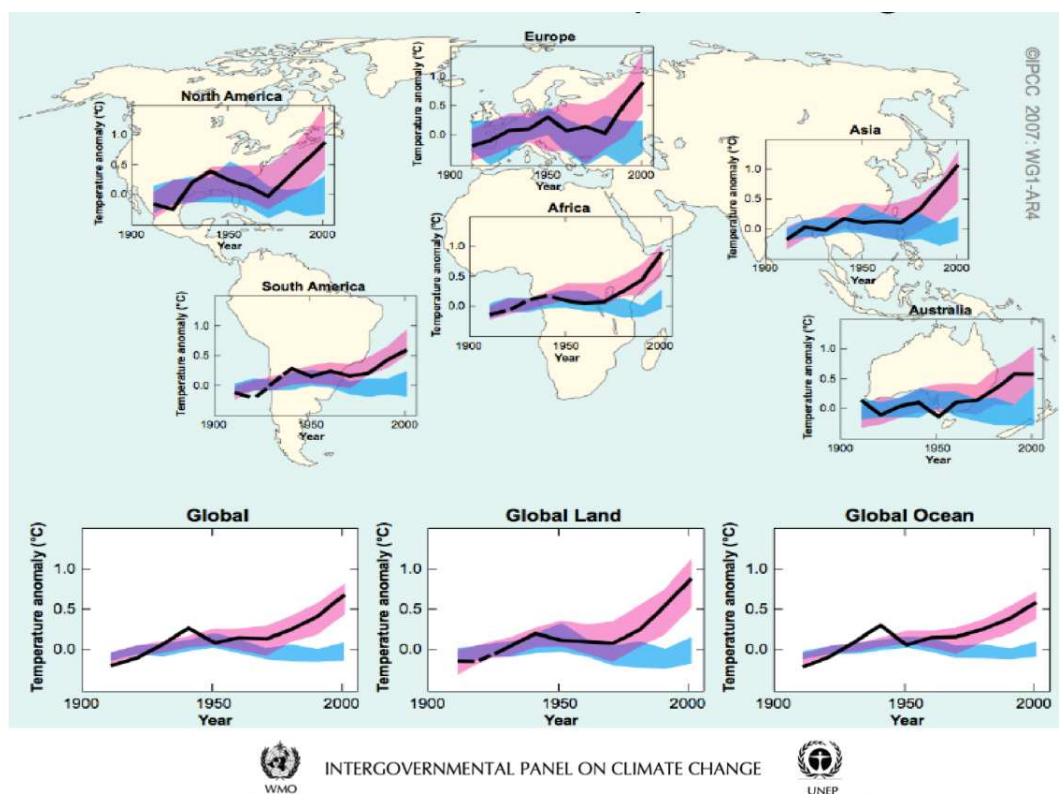


Figure 5.21: Global mean surface temperature change [K] for all continents and the oceans in comparison with simulations with anthropogenic and natural forcings (pink shading) and in comparison with simulations with natural forcings only (blue shading). Natural forcings are variations in the solar radiation and volcanic emissions.

The best explanation for 20th century warming is anthropogenic forcing. Natural forcing (e.g. solar radiation) cannot explain the warming trend, see fig. 5.21.

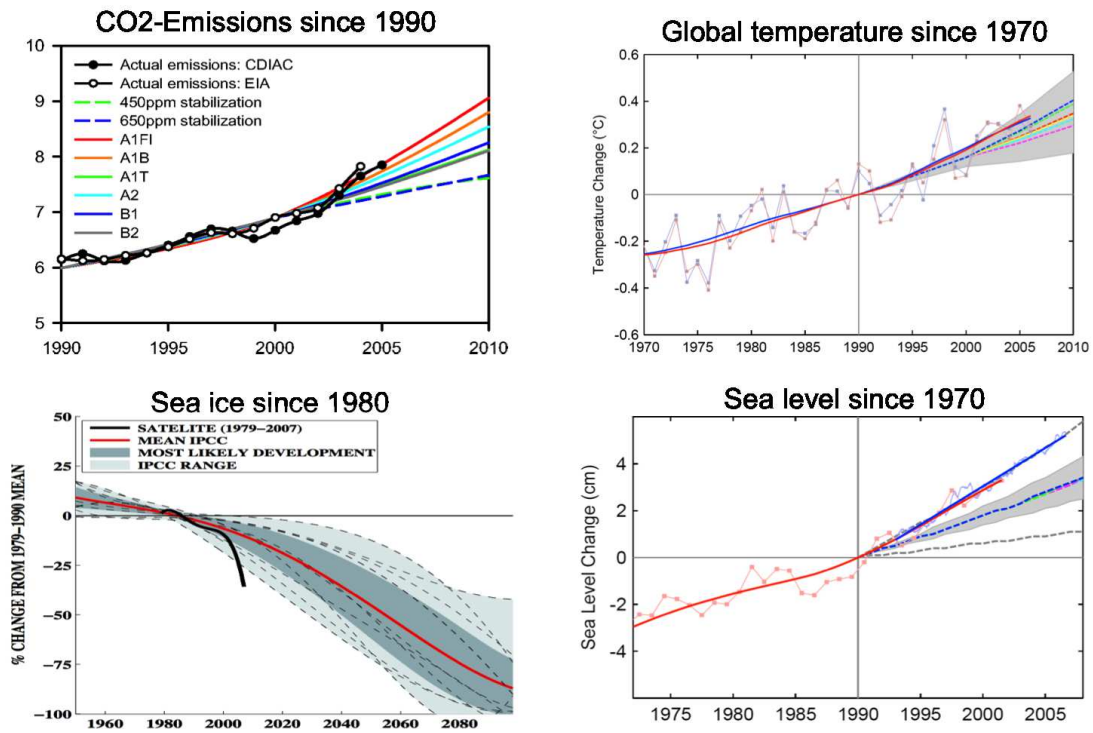


Figure 5.22: Prediction vs. Reality: Upper Left: observed (black lines and dots) CO_2 concentrations vs. simulated (coloured lines). Upper right: observed (blue and red lines and dots) global mean temperature changes vs. predicted by simulations (coloured lines and grey shaded area). Lower left: observed (black solid line) global sea ice cover changes vs. predicted by simulations (red line and grey shaded areas). Lower right: observed (red and blue lines and dots) global sea level changes vs. predicted by simulations (blue dashed lines and grey shaded area).

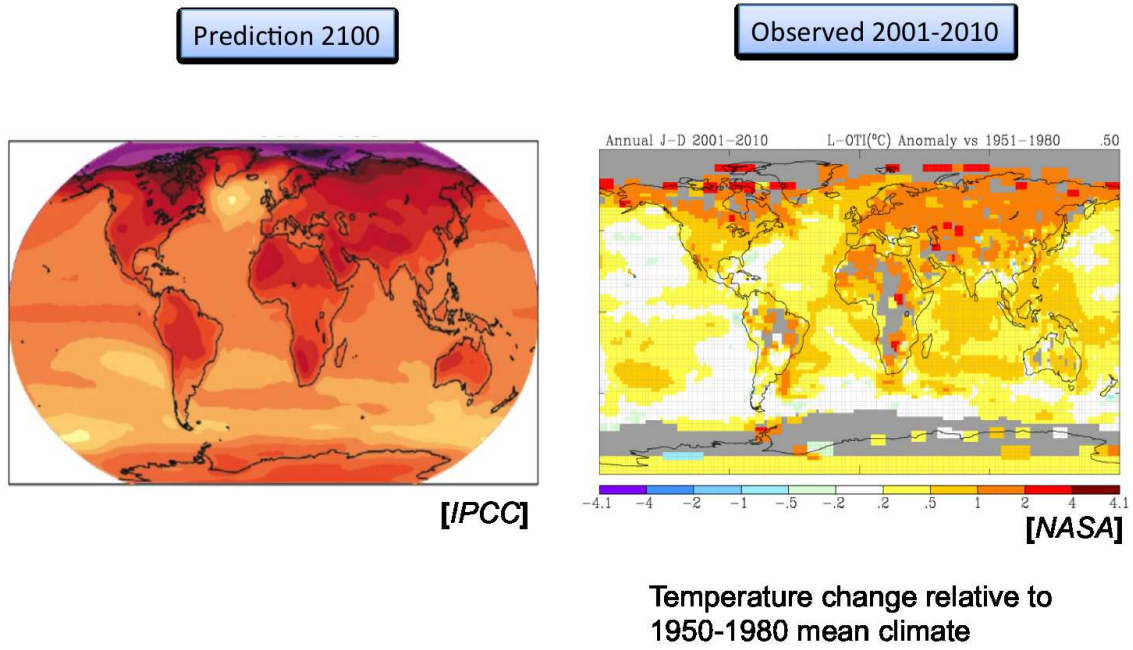


Figure 5.23: Predicted global warming pattern (left) vs. the observed warming in the last 10 years relative to the 1950 to 1980 period.

5.2.4 Precipitation

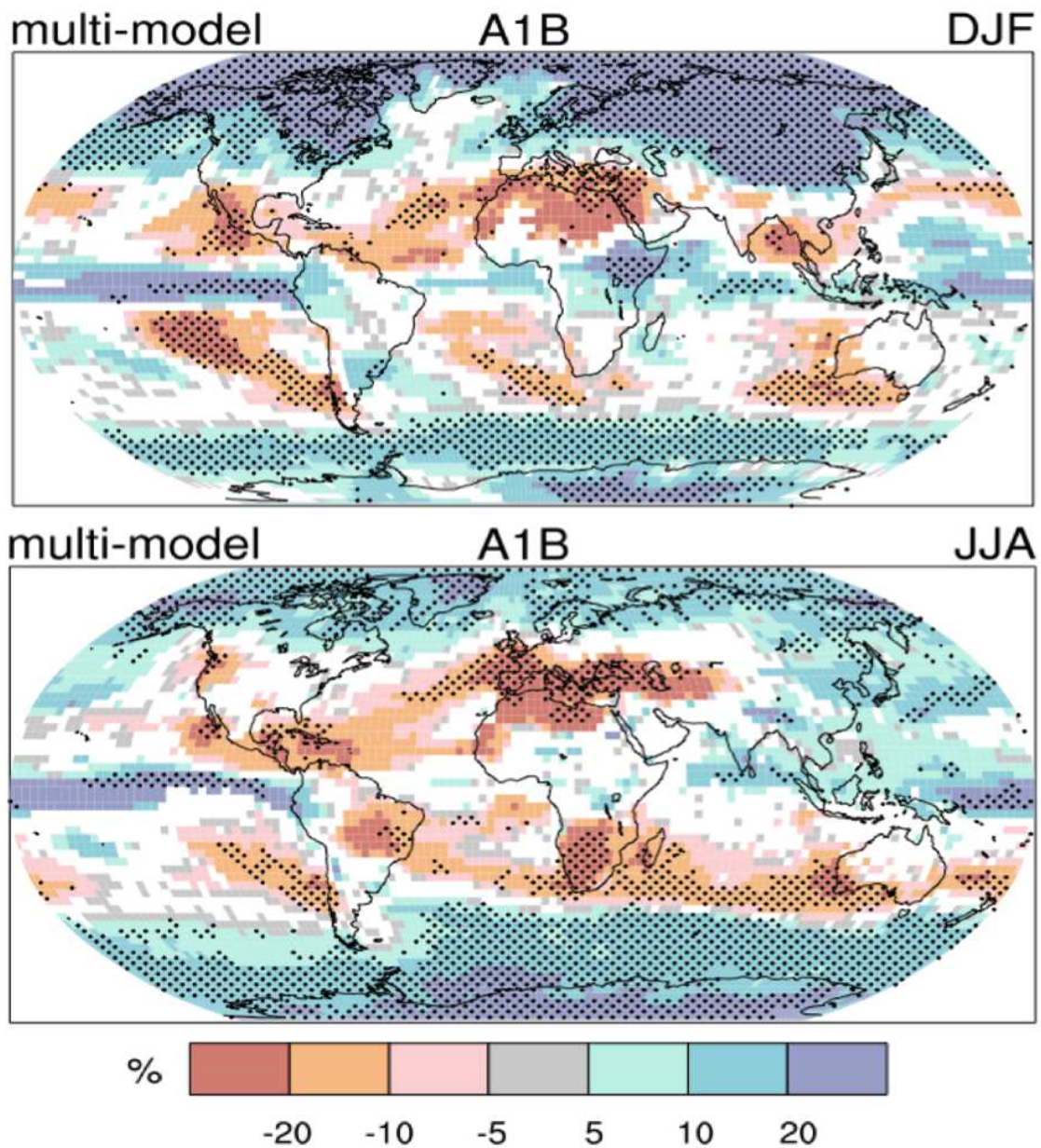


Figure 5.24: Relative changes in precipitation (in %) for the period 2090-2099, relative to 1980-1999. Dotted areas mark regions where the model predictions agree relatively well.

- For most regions precipitation is increasing, as humidity is also increasing.
- Precipitation does not increase as much as humidity.
- Dry regions tend to have decreasing precipitation.
- wet regions have increasing precipitation.
- There is no simple explanation of why that is, as small scale circulation changes may be important as well as large scale circulation changes.

- The response in precipitation is highly uncertain, see Fig. 5.24. Stippled areas are where more than 90% of the models agree in the sign (not the amount) of the change. White regions are where the models do not agree on the sign of the change at all.
- Rain response over Australia is highly uncertain, as models mostly do not even agree on the sign of the change.
- If the mean response is 10% less, that could mean that some models have 20% increase and others have 30% decrease. So it is highly uncertain.

5.2.5 Sea level

- In the past 2000-5000 years the sea level was relatively stable.
- Since the last ice age (about 18,000 years ago) the sea level has risen by about 120m, with a speed of about 1m/100 years.
- At present the sea level changes at a rate of about 0.3m/100 years (3mm/year).
- This is due to thermal expansion and melting of glaciers, but a large part of it is unexplained.
- The current sea level rise is not uniform, it has strong regional differences.
- Local coastal sea level changes can be quite different from this IPCC picture, as other local effects may dominate the sea level changes (e.g. local geological effects as rebound from last ice age, etc.).
- IPCC climate models do not predict glacier melting of Greenland or Antarctica, as they do not include an ice sheet model (ice sheets are the ice in glaciers, in contrast to seasonal snow or floating sea ice).
- Assuming increased CO₂ emissions to concentrations of about 700ppm it is very likely that Greenland will melt for the largest part, which will cause a sea level rise of about 5m in the next 1000 to 2000 years.

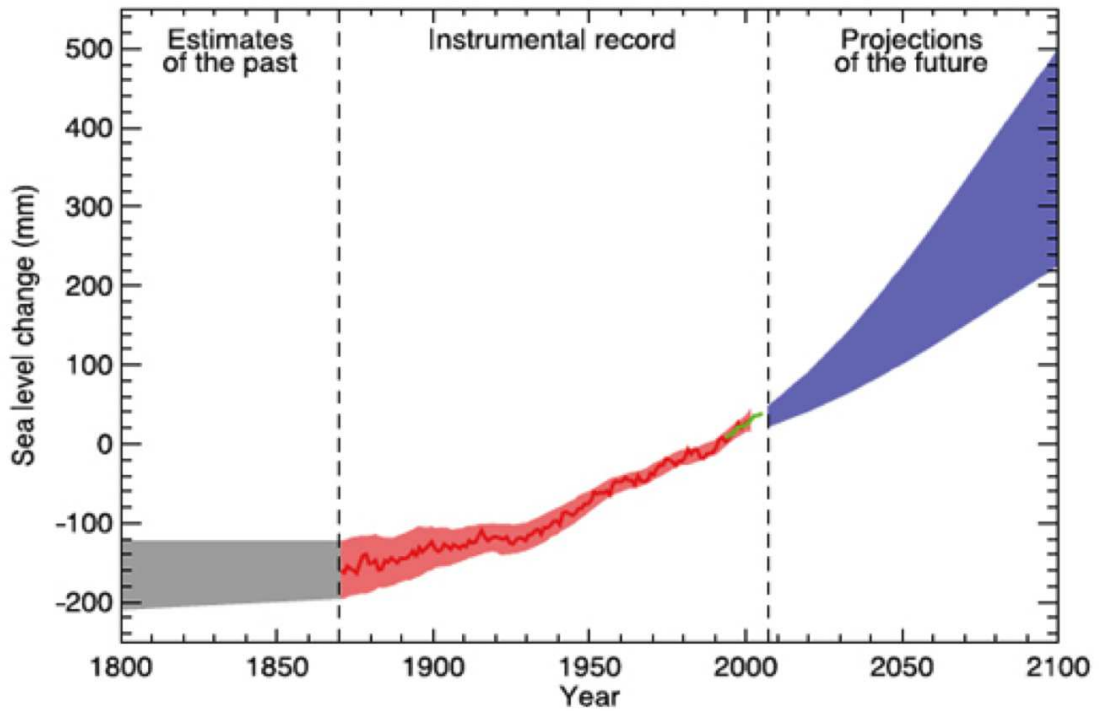


Figure 5.25: Global mean sea level change in the past (grey shaded area), the present observed (red and green) and the the predicted (blue). Source: IPCC report 2007.

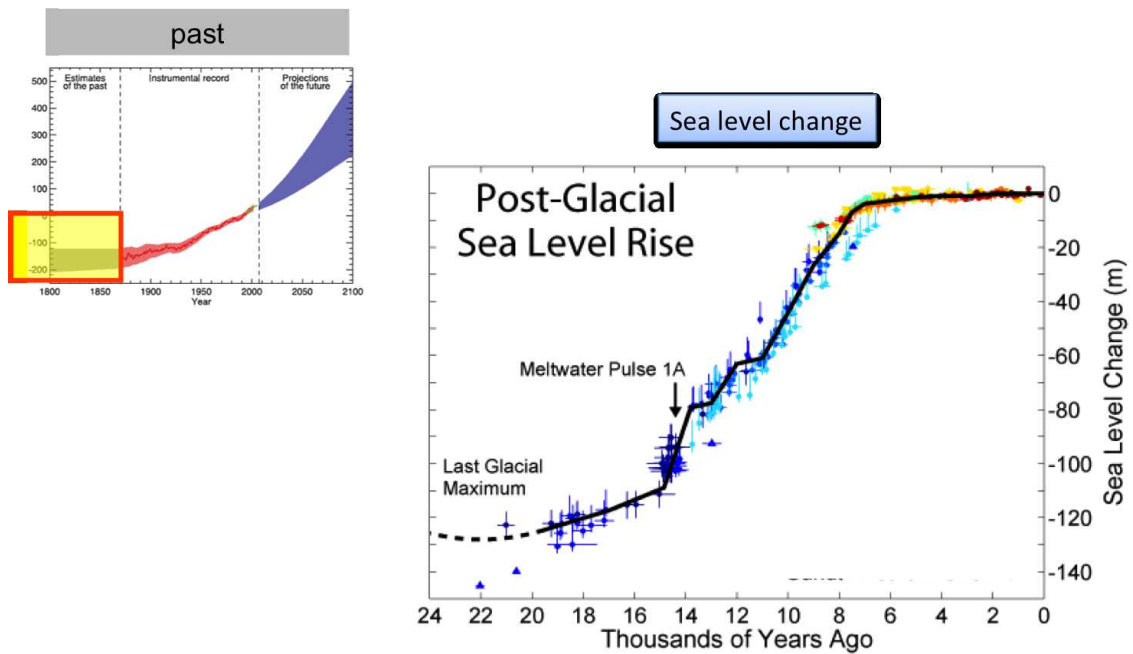


Figure 5.26: Past global mean sea level changes since the last glacial maximum (ice age). The changed by more than 100m in the global mean.

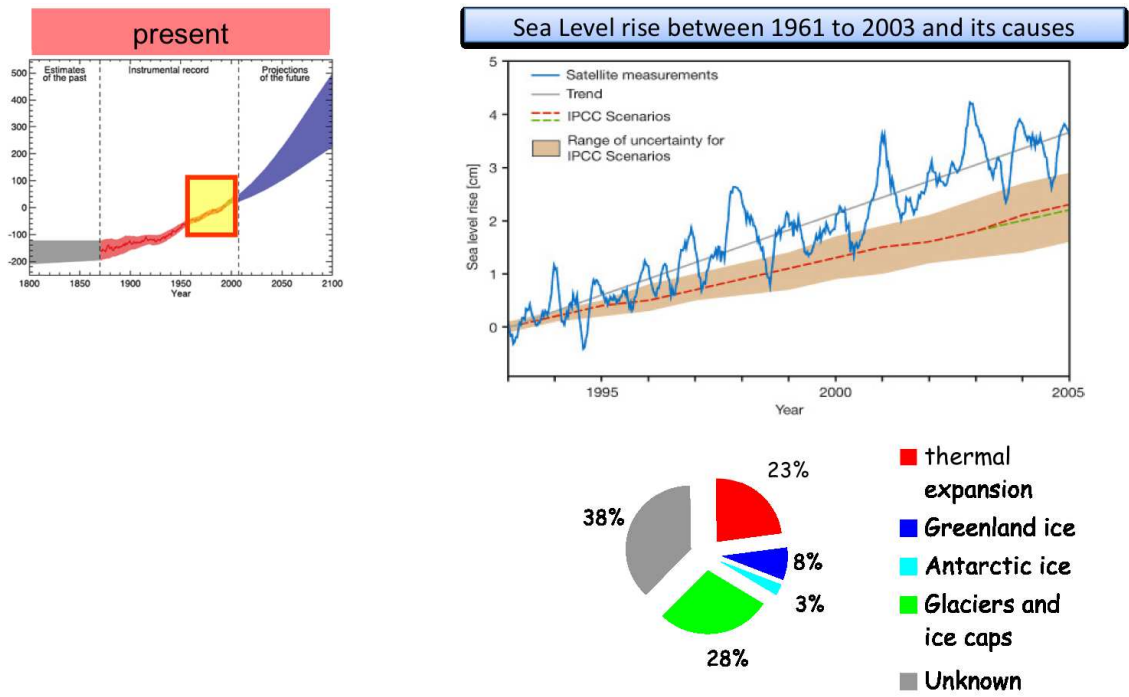


Figure 5.27: Present sea level changes: 38% of the changes have unknown causes.

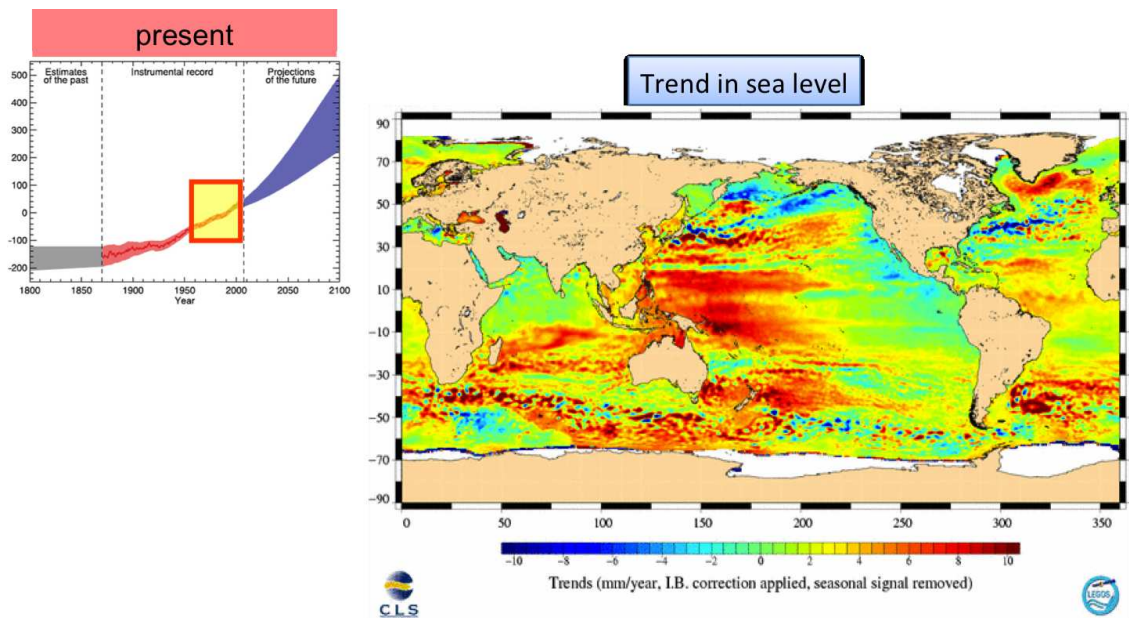


Figure 5.28: Present sea level trends. Note, that there are strong regional differences, with some regions having decreasing sea levels (e.g. northern North Pacific).

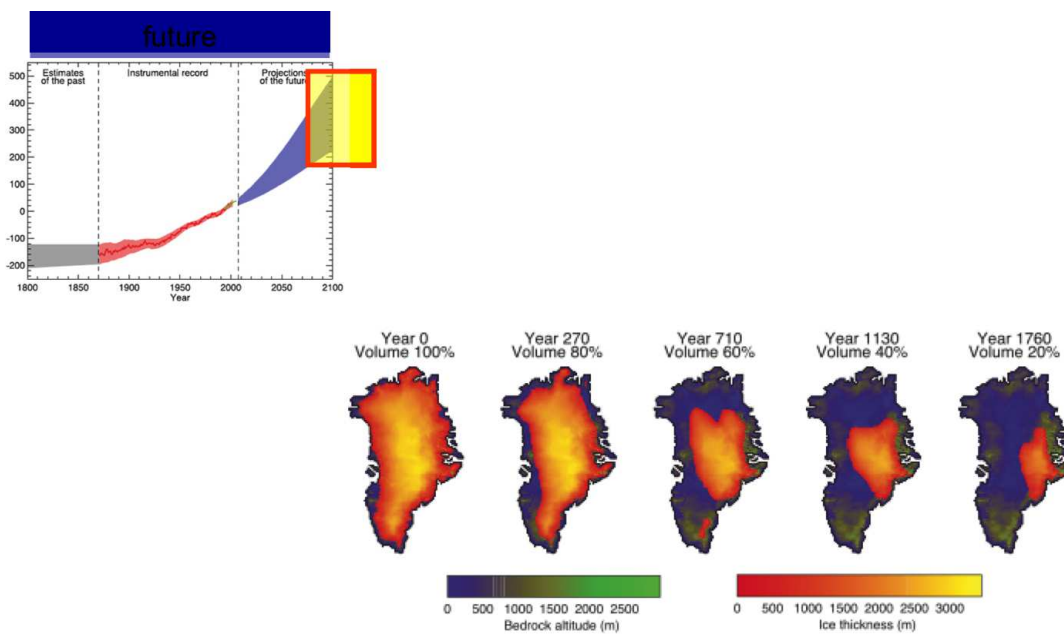


Figure 5.29: Changes in Greenland ice sheet for a hypothetical $4xCO_2$ concentrations over the next 2000yrs.

5.2.6 Extreme events



Figure 5.30: Heavy rainfall



Figure 5.31: Droughts

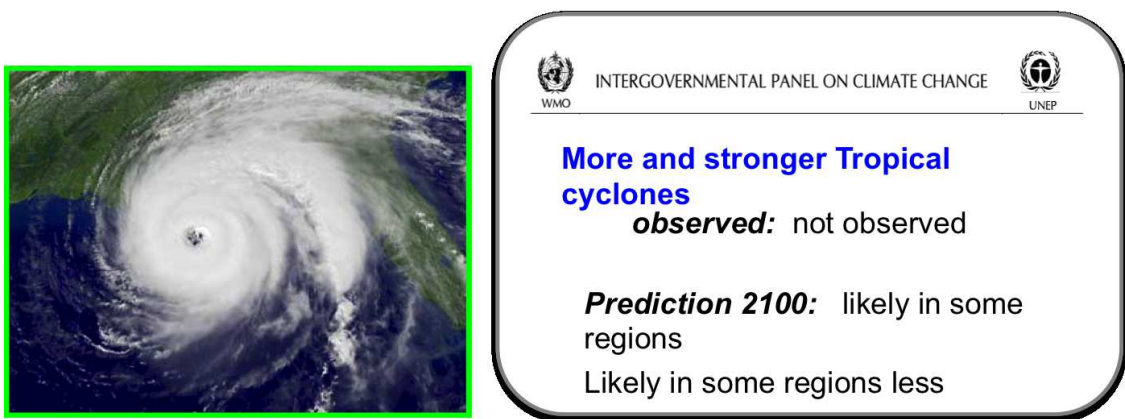


Figure 5.32: Tropical cyclones

5.2.7 How significant is a 3°C global warming?



It is difficult to understand how significant is a 3°C global warming is, as we have no intuition for global mean climate. Our personal experience about climate is based on local natural fluctuations

of the climate, which we call weather. The weather changes from day to day by 3°C on a regular basis, but the global mean climate does not. Thus, it is important to get a good reference frame to understand the significance of a 3°C global warming. We will base this on three different references:

- Natural climate variability: A comparison with the recent (thousand to million years) past of global or near global mean climate.
- Regional climate differences: A comparison of local climate changes due to global warming against today's regional climate differences.
- Seasonal climate differences: A comparison of a 3°C global climate shift against a local seasonal cycle.

5.2.7.1 A comparison against natural climate variability

The significance of a 3°C global warming very much depends on how it relates to natural global mean and regional climate variability. If, for instance, a 3°C global warming is a quite normal thing that happens on a natural basis all the time, then clearly a 3°C global warming is unlikely to have a major impact on the ecosystems or the humans.

Our starting point here is the local climate variability (weather) as we recognise it as a normal human being living, for instance, in Melbourne, Australia. In Figure 5.33 Melbourne daily temperature variations over 60 years (roughly the life time of a normal human being) is compared against the global warming trend. One thing we can notice here is that the global warming trend of the past 100 years is tiny compared to the daily temperature variations in Melbourne. Thus a normal human being will most likely not have noticed or experienced a significant climate change in his life at his home place. This may to some extent explain why many people still think that the man-made climate change is not happening.

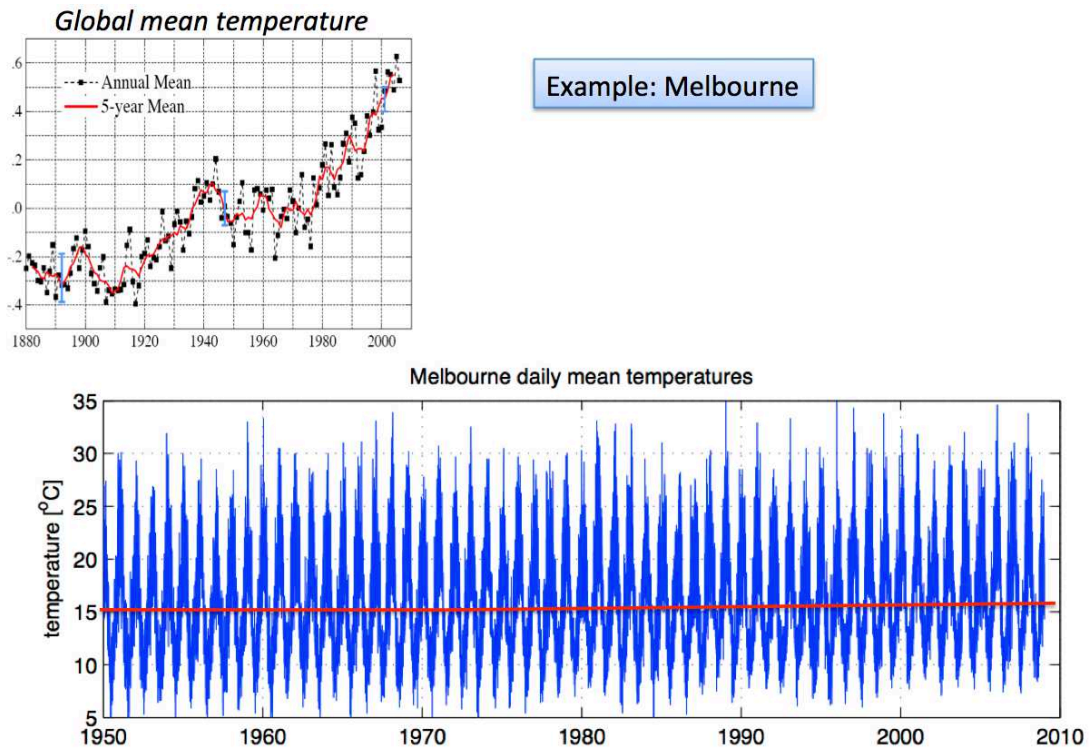


Figure 5.33: Example: Melbourne daily temperature variations against global warming trend. The global trend of the past 100yrs (red line in upper and lower panel) is tiny compared to the daily temperature variations Melbourne (blue in lower panel).

However, to get realistic understanding of the significant is a 3°C global warming we have to look at climate variability on a large scale and longer time scales. We therefore discuss a number of examples large scale and on longer time scales now.

Fig. 5.34 shows the result of a global warming scenario for the european mean surface temperature. This is different from the warm curves that we have seen previously (e.g. 5.19) in two ways: First of all it shows a continental mean instead of a global mean. Secondly, and more importantly, it shows the warming trend together with natural internal variability. In Fig. 5.19 the warming trend is shown as the average of many simulations (about 16 to 21) on the global mean. This does not allow us to compare it with natural internal variability, as the averaging of many simulations will reduce the amplitude of natural internal variability since the natural internal variability is random and therefore different in each simulation (see also sections 6 and 6.3).

If we look at the single realisation of a 21th century simulation for Europe (Fig. 5.34) we see how the large-scale and longer time scales relate to the warming trend. The warming trend is now clearly visible and on the longer time scales it is much stronger than any natural internal variability (the fluctuations in the time series). But we can also recognise that over several years or even a decade the warming trend is counter acted by fluctuations natural internal variability. Thus despite the overall clear and strong warming we can find decades which cool relative to the previous decade (e.g. the period around 2030 relative to the decade before that in Fig. 5.34).

The relation between natural internal variability on large-scale and longer time scales and the overall warming trend is quantified with the help probability distributions in Fig. 5.35. We find that on the global scale almost all decadal trends are positive. However, even here the longest period of decreasing temperatures was 18yrs. The distribution of decadal trends becomes wider if the region of interests becomes smaller, but the mean trends remain the same. On the spatial

scale of about 1000km (the size of the UK) the warming trends become much less obvious with 1/3 decades showing a cooling trend and a period of over 60yrs with cooling, despite the overall warming trend. This comparison illustrates the high significance of the global warming trend on the larger scales, but also highlights that on the smaller scales it is less significant.

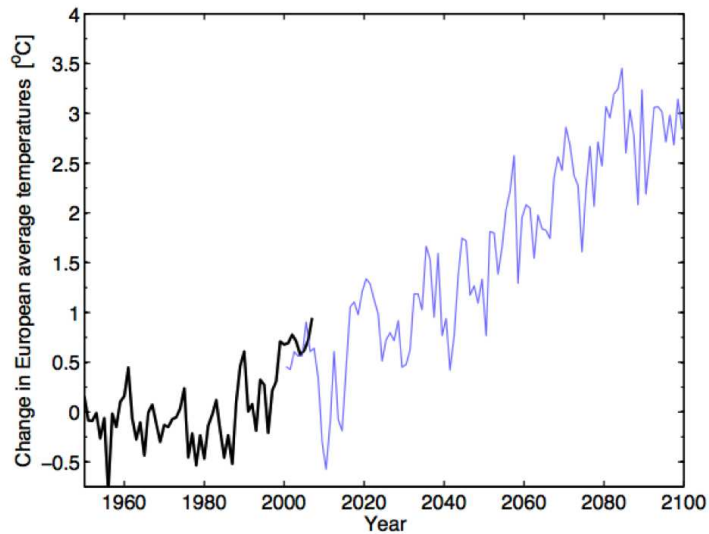


Figure 5.34: A single simulation of future European temperatures: Note that climate simulations of anthropogenic climate change also simulate natural, chaotic, internal variability. The warming trend will fluctuate, due to the natural variability. In this example you can see that between the years 2020 to 2030 Europe has a decade of cooling despite the overall anthropogenic global warming, due to natural variability. These fluctuations are random and mostly unpredictable.

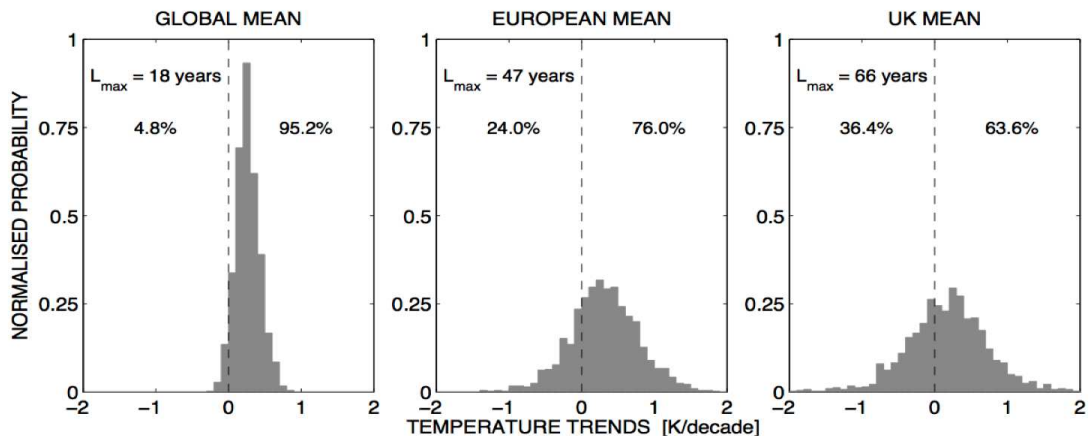


Figure 5.35: Distributions of decadal trends during global warming: This figure illustrates how natural, chaotic, internal variability leads to decadal (10yrs) trends despite the overall anthropogenic global warming. Left: distribution of decadal trends of the global mean temperature during a global warming scenario of the 21th cnetury. 5% of all decades will have a cooling trend and a period of $L_{max} = 18yrs$ is seen over which the global mean temperature has cooling trend despite the overall long time anthropogenic global warming. Middle: as the left panel, but for Europe mean temperature. Right as the left panel, but for UK mean temperature.

Another way of looking at the relation between natural internal variability and the global warming shift is to compare the present day distribution of the climate with future distribution, see Fig. 5.36. In this example the distribution of the summer seasonal mean temperatures for Germany in the 20th and 21th century for a global warming scenario are shown. The record hottest summer of 2003 is still cooler than the mean (!) of the predicted climate in 2100. This indicates that the future climate in Germany is very different from it is today. Similarly the example from Indian, see Fig. 5.37.

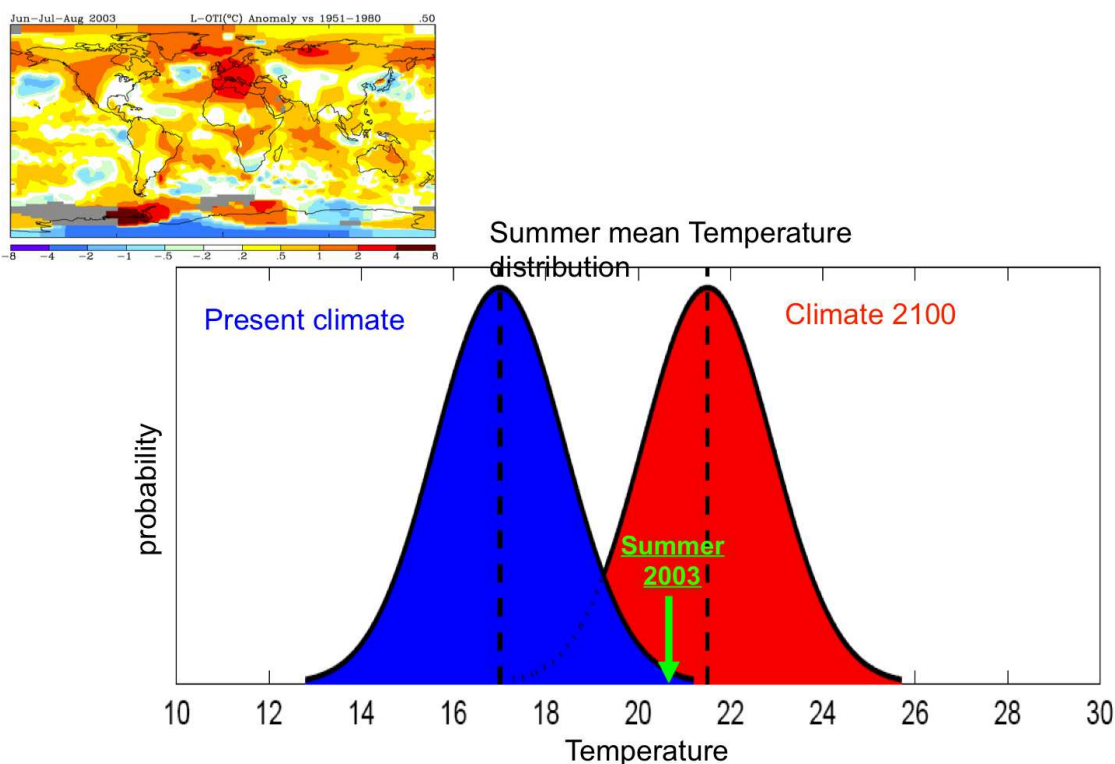


Figure 5.36: Example: Extreme seasonal heat wave in Germany in 2003. Upper: the temperature deviations from normal for the Northern hemispheric summer of 2003. You can see that central Europe has a 2-4 degrees warmer than normal temperature, which is the hottest ever (about 100yrs) recorded summer for this region. Lower: distribution of the summer seasonal mean temperatures for Germany in the 20th and 21th century for a global warming scenario. The record hot summer of 2003 is a relatively cool summer compared to the predicted 2100 climate.

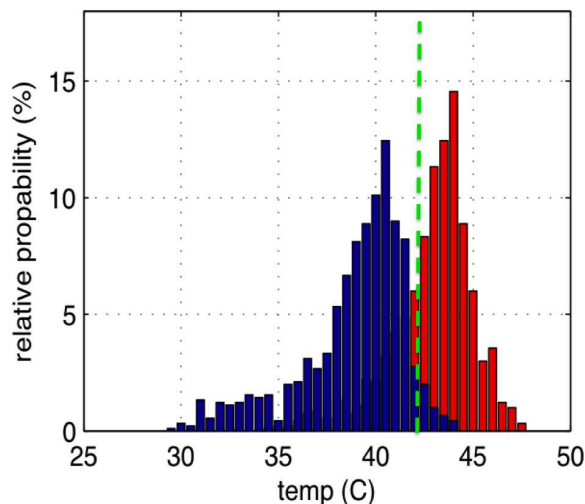


Figure 5.37: Example: Central India distribution of daily temperatures in May for the 20th and 21th century for a global warming scenario.

In the above examples we compared the global warming trend with current climate variability on time scales of years to decades. To understand the significance of this warming shift it is also important to compare the warming shift with a longer time record of the climate, because many of the ecosystems and the human society have adapted to the environment over time scales of 100yrs to 10,000yrs. Unfortunately we have no direct observations of the climate more than 100yrs ago. We therefore need to look at climate proxy data (see section 6.8 for more details). In Fig. 5.38 we see a number of estimates of the climate variability of the northern hemisphere for the last 2000yrs in comparison with observations of the last 100yrs and the projection of the next 100yrs. This graph is also known as the 'hockey stick' curve, as it (without the future projections) look a bit like a hockey stick. The figure illustrates that nothing in the past 2000yrs of natural climate variability is of the magnitude and speed in climate change as the current and project future climate change. In Section 6.8 we will go further back in time and will see that even the ice ages cycle of the 1-5 mill. years do not have global climate changes in a 100 years time interval of the magnitude as the anthropogenic climate change in the 21th century. This suggest that on the global-scale the anthropogenic climate change over next 100yrs is very likely to be stronger than any climate change that mankind has experienced every before.

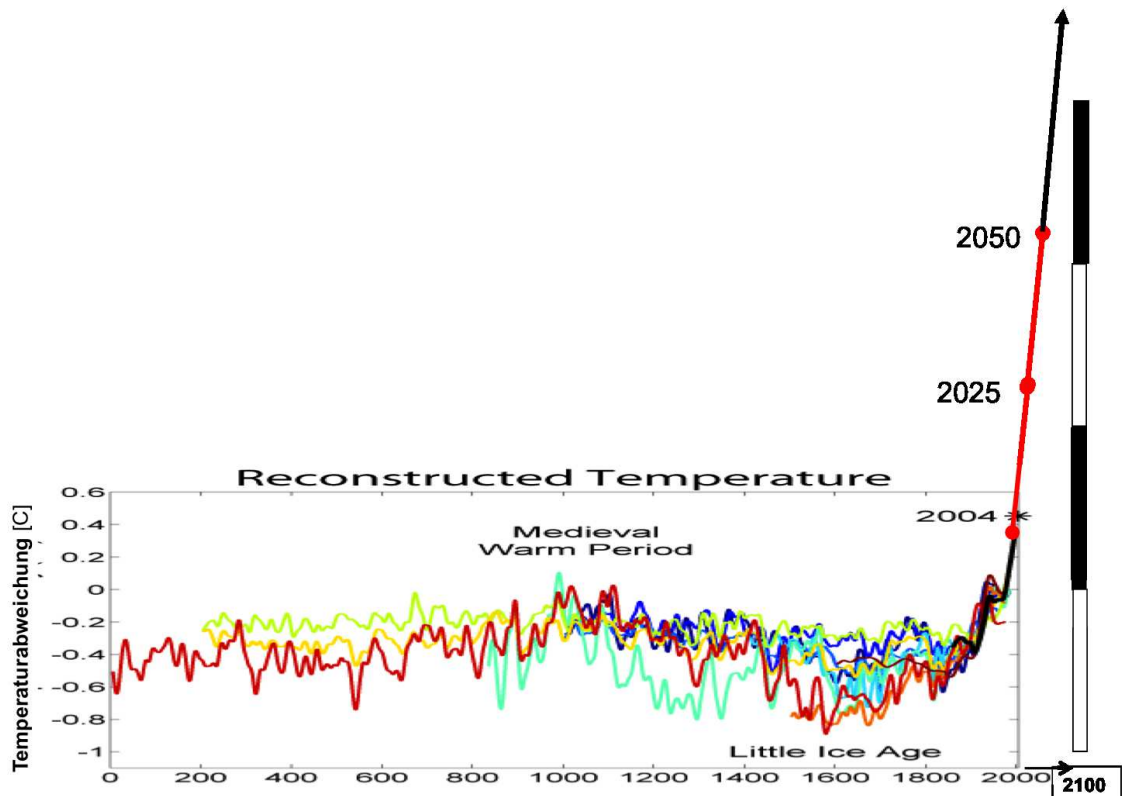


Figure 5.38: Reconstructed temperatures of the last 2000yrs for the Northern Hemisphere (coloured lines) compared against the predicted anthropogenic climate change over the next 100years. The anthropogenic climate change is high and fast compared to last 2000yrs of natural climate variability.

5.2.7.2 A comparison against regional climate differences

An alternative view is to compare the warming shift with a regional shift in climate. Therefore fig. 5.39 shows maps with cities shifted to new location according to a 3 degrees global warming. The new locations best match the future climate of these cities with today's climate at these locations. For example, the climate of Melbourne in 2100 most closely matches the climate at the gold coast in Queensland today. It illustrates that a global warming of 3 degrees (which is about 4 degrees over land, because the land warms more than the oceans) is roughly equivalent to more than a 1000km shift towards the equator.

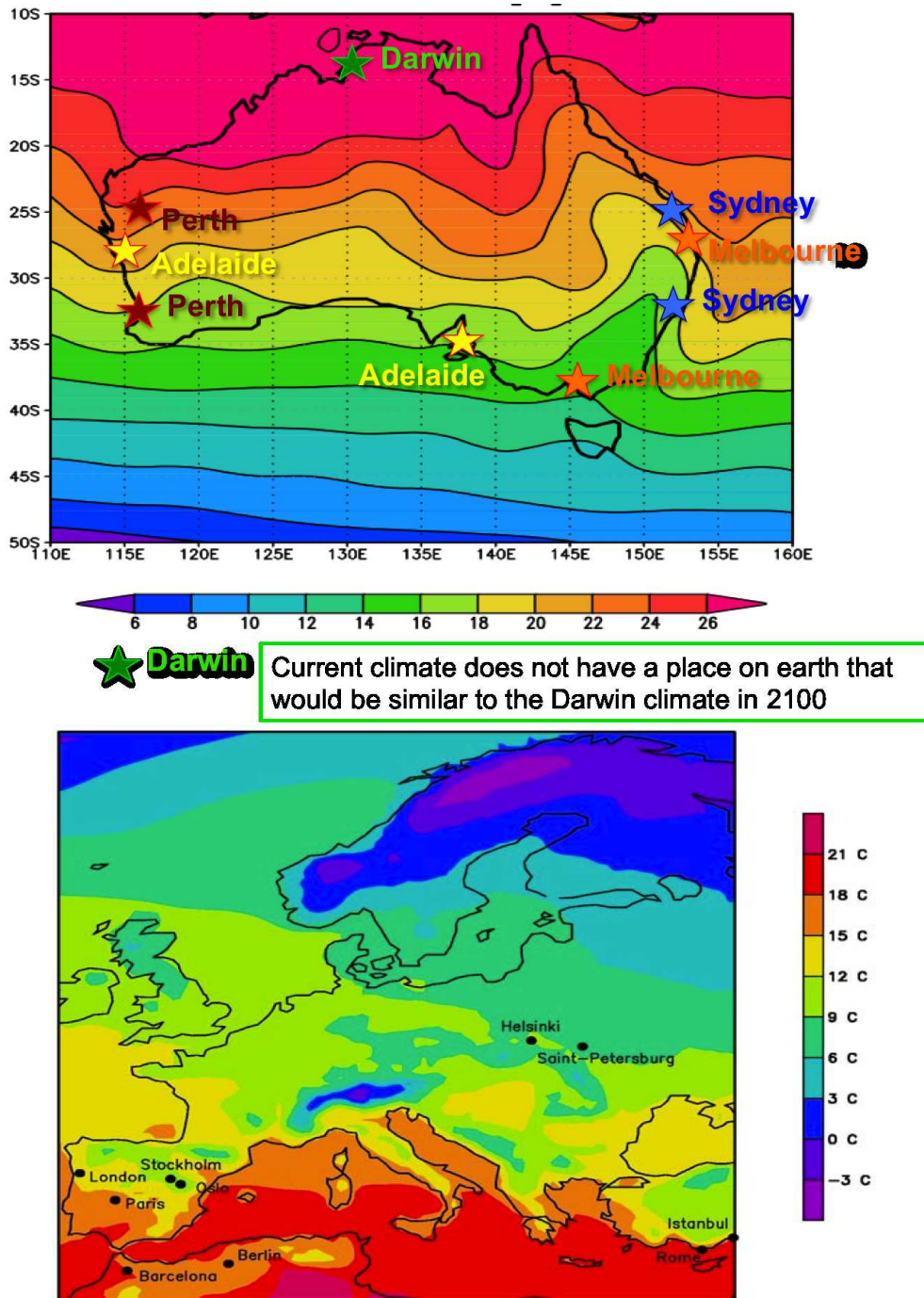


Figure 5.39: left: Australia climate map 2100: Regional shift of the major cities of Australia according to the climate shift predicted towards 2100. Right: Climate map for Europe 2071: Regional shift of the major cities of Europe according to the climate shift predicted towards 2071. This "map" shows the equivalent climate cities can expect in the future: for example, London of 2071 most closely matches the climate of the west coast of Portugal today.

5.2.7.3 A comparison against seasonal climate differences

Similarly we can consider the seasonal shifts, see Fig. 5.40. A 3 degrees global warming is about 4 degrees warming over land. For a place like Melbourne this roughly shifts each season to be one

season warmer.

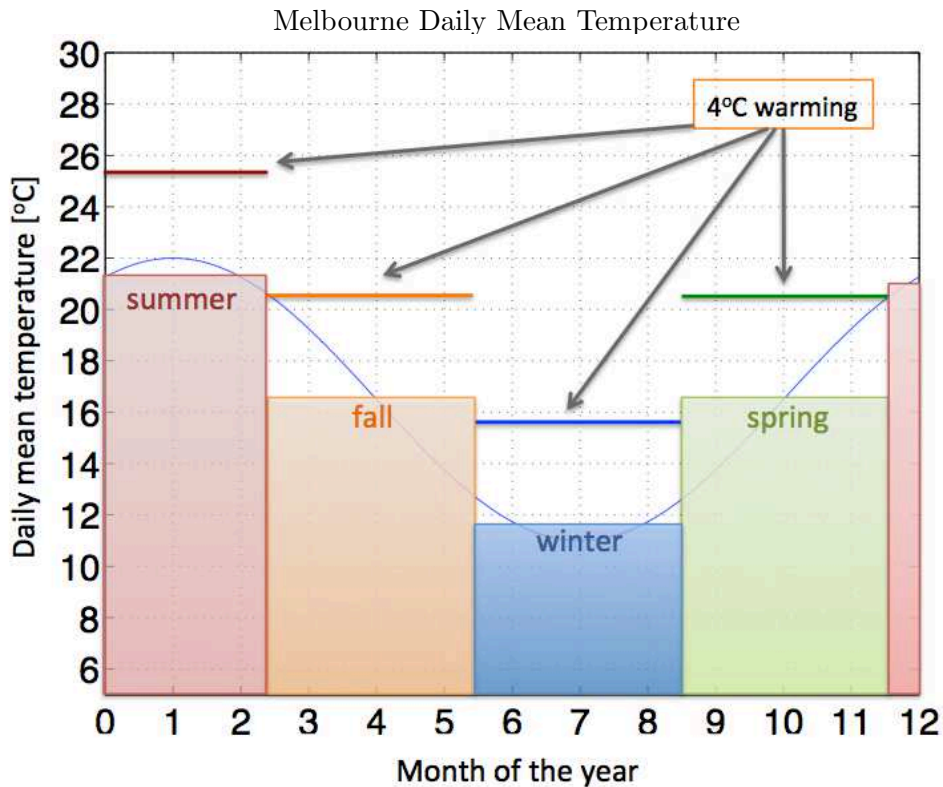


Figure 5.40: Example: Melbourne seasonal cycle. The coloured lines indicate the warming shift of each season for a 3°C global warming (roughly a 4°C warming for Melbourne).

5.2.7.4 Summary of the significance of climate change

- Note, that a 3°C global warming is roughly a 4°C warming for continental area where people live, because the land area tend to more than the oceans.
- Current climate change is weak compared to what there is to come.
- On local scales (personal experience) this will currently mostly not be recognizable. However, for someone born at the beginning of the 21th century, the changes will in most places be noticeable over the personal life time (e.g. you may have been used to go skiing in the Australian Alps as a kid on regular basis, but as a senior you will not be skiing there any more.).
- IPCC predictions are a smooth mean of many possible evolutions. The true future climate evolution will fluctuate, with regional decades of no warming at all, due to internal natural climate variability
- Seasonal climate shift will be quite substantial by 2100. The current extreme hot temperatures become the normal or cool season.
- The climate shift can be understood as a relocation of regions by several 1000km towards warmer climates

- Compared to the last 2000 years of natural global climate variability the next 100 years will see an extremely sharp rise in temperature which is unprecedented in recent history (2 million years) in amplitude and speed
- Going back in time by more than 100,000 years (ice age cycles) warmer climates than predicted have existed, but the rate of change has been much slower. This will be discussed later in the lecture when we discuss ice ages

5.3 Climate change in the media

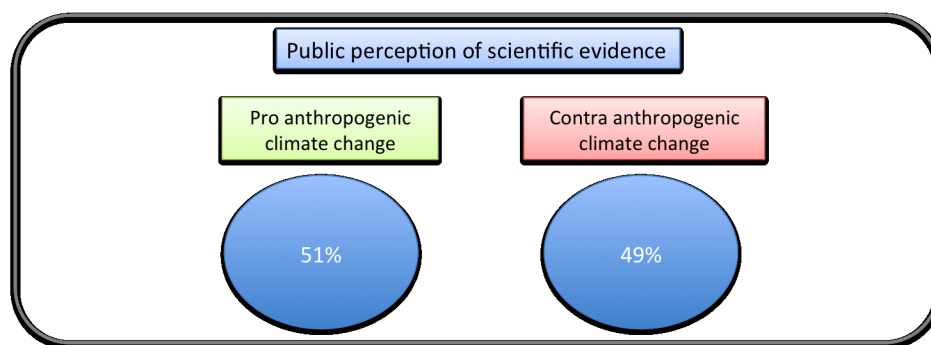


Figure 5.41: Public perception of scientific evidence

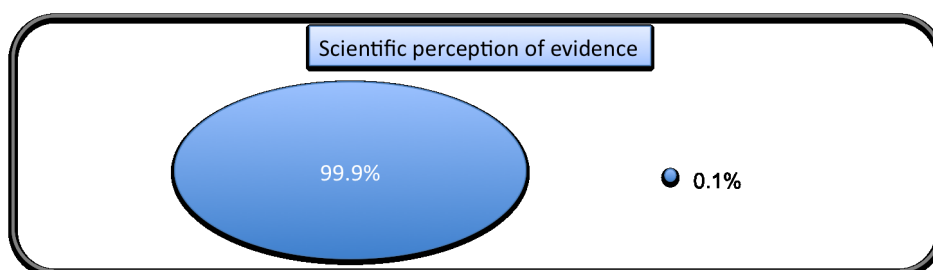


Figure 5.42: Scientific perception of evidence

In the Australian (it is quite different in Germany) media the debate on anthropogenic climate change seems about balanced between pro and cons for evidence of it, while in the scientific debate that is clearly not the case, as there is overwhelming evidence for the anthropogenic climate change. Media often cite climate change ‘experts’ that really are not experts in the scientific field of climate change. In most cases these ‘experts’ have never ever published a single scientific work on climate change in a scientific journal of climate science. These wannabe climate change experts dominate the discussion in the media. In public/political debate the extreme points of view get the most attention. The environmentalists will tell us that we should in principle be dead already, but if not most certainly tomorrow; while the economists/conservatives will tell us that it is ridiculous to assume that humans could influence the climate in any way: the Earth is essentially indestructible.

The main IPCC statement of a global mean surface temperature change of about 2-3° by 2100 for a doubling of the CO_2 concentration and that this is much stronger than any change of the last 2000 years is not seriously scientifically challenged. That means, there are no scientific studies that show evidence contrary to this statement. However, many details, such as how fast ice sheets melt, how sensitively precipitation or the ecosystem react to it, is much more controversial and is still a scientific debate. Always be very critical of any statements about climate change. The best source for climate change science is the IPCC report (available for free from the web).

Climate change propaganda

Some examples of how both sides manipulate and spread false ideas.



Figure 5.43: Examples of propaganda

These two documentaries are very good examples of how convincingly both sides can present false ideas. Even climate science experts will have problems telling right from wrong. Take a look at both, they are available on *Youtube*.

Example 1: CO₂ and Ice ages



Figure 5.44: Example 1

Al Gore indicates: over the last 500,000 years the CO₂ concentrations are causing ice ages. A change from 220 ppm (ice age) to 280 ppm (warm age) leads to a warming of 10°C.

First: Ice ages are mainly caused by changes in the incoming solar radiation, not by changes in CO₂ concentrations. Indeed the change in temperatures leads that of the CO₂ concentrations by a few thousand years.

Second (more importantly): Calculating his statement:

240 ppm to 300 ppm $\rightarrow \Delta T = 10^\circ\text{C}$

$\Rightarrow \Delta\text{CO}_2 = 60\text{ppm} \rightarrow \Delta T = 10^\circ\text{C}$

Linear interpolation:

$\Rightarrow \Delta\text{CO}_2(2 \times \text{CO}_2) = 280\text{ppm} \rightarrow 4.67 \times \Delta T = 47^\circ\text{C}$

He is suggesting doubling of CO_2 causes about 50°C of global warming, which is highly exaggerated. This is not science!!

Example 2: Melting of Greenland

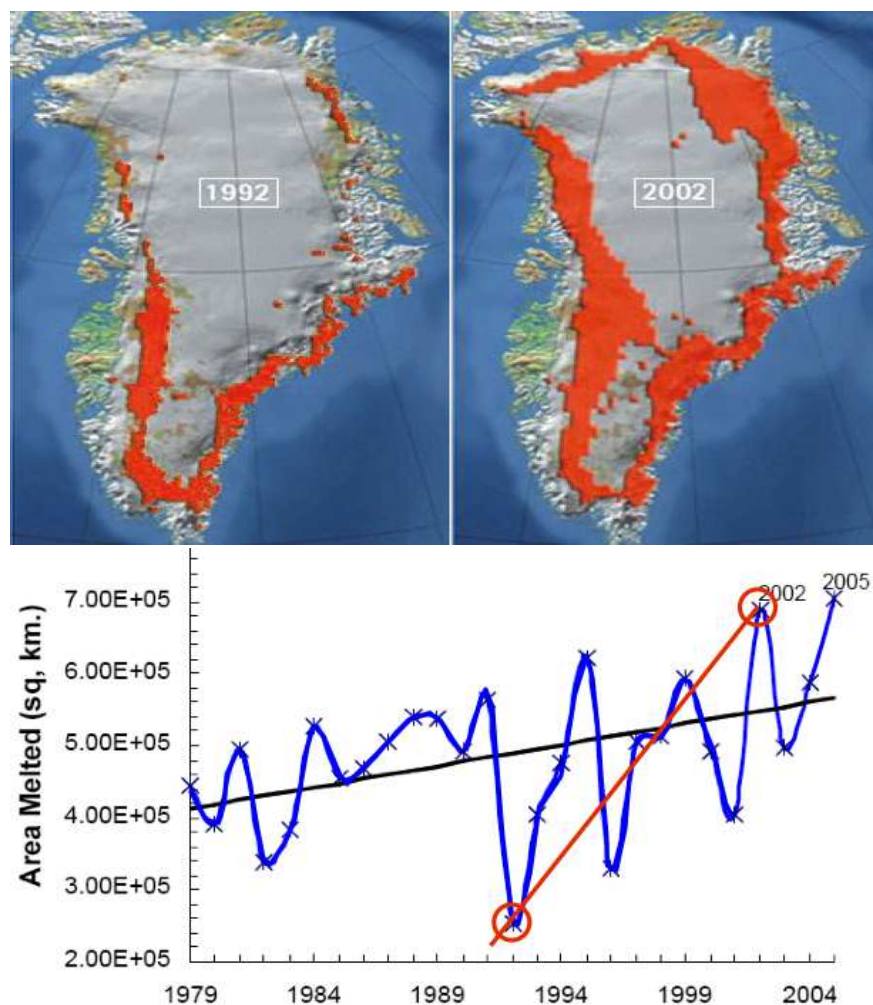


Figure 5.45: Example 2: Greenland melting. Upper: areas with at least one day of melting in the years 1992 and 2002. Lower: the time series of the area with at least one day of melting per year. The upper two maps are taken from this time series. Note, that if we pick the years 1991 and 2003 the trend would be reversed!!

From a newspaper arguing for dramatic melting of Greenland ice sheets, see Fig. 5.45. This just tells

you that there is at least one day of melting per year, nothing is said about the other potentially 364 days of the year, which may have heavy snow accumulation.

Glacier mass balance:

$$\Delta M = +\Delta_{\text{snow}} - \Delta_{\text{icebergs}} - \Delta_{\text{melting}}$$

Melting alone does not tell you if the glacier is decreasing. Warmer climate also causes more snow accumulation.

Example 3: Sun causes climate change

Climate swindle: The sun is the cause of climate change.

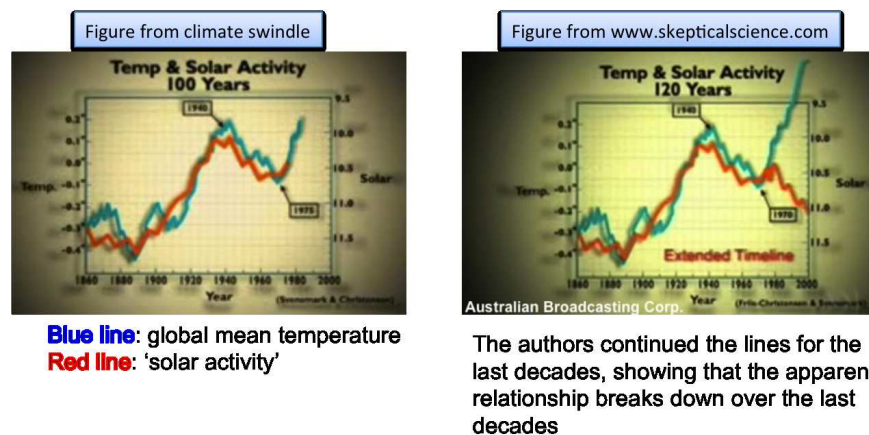


Figure 5.46

- The climate swindle documentation talks about solar 'activity', which is not solar radiation as we know it in terms of visible sunlight in W/m^2 .
- It is a complex index that tries to quantify some kind of solar activity that in a magical way may influence the climate by changing the number of clouds.
- No quantifiable equations based on physical understanding exist to explain how exactly this works. No climate model can produce this effect.
- It is entirely a speculation based on some statistical relationships some scientist found in the past.
- Solar radiation is not constant, but varies for different reasons. In the 20th century variations in the number of solar spots are the main reason for variability of the incoming solar radiation of about $\pm 1 \text{ W}/\text{m}^2$.
- $\Delta S_0 = 1\text{W}/\text{m}^2 \rightarrow \frac{1}{4}(1 - 0.3) \times 1\text{W}/\text{m}^2 = 0.175\text{W}/\text{m}^2$
- The solar forcing is a tiny little forcing with no obvious positive trend compared to the 20th century CO_2 forcing of $1.6 \text{ W}/\text{m}^2$ with a clear positive trend. There are thousands of scientific studies of the solar influence on the 20th century climate and the consensus is that it cannot

explain the warming trend observed over the past 40 years. This is very well summarised in the IPCC report.

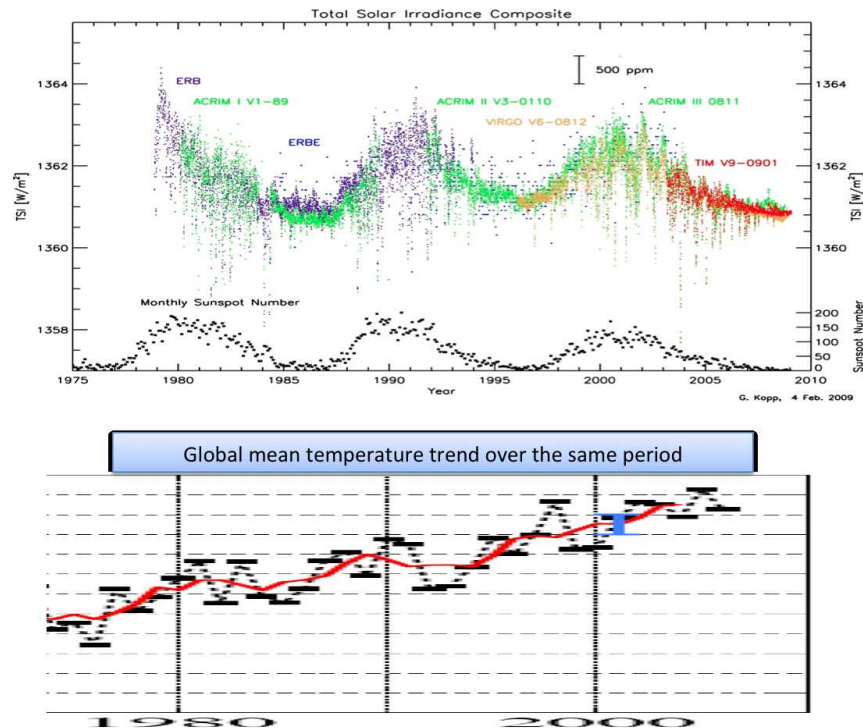


Figure 5.47: Observed solar radiation variability

Theoretical understanding vs. Statistical speculation

Example: Einstein's $E = mc^2$

This is based on the relativity theory. Einstein did not come to this equation by knowing a statistical relationship between mass and energy. Actually this was absolutely unknown before Einstein. The theory was very nicely demonstrated by the Manhattan Project and the first explosion of a nuclear bomb.

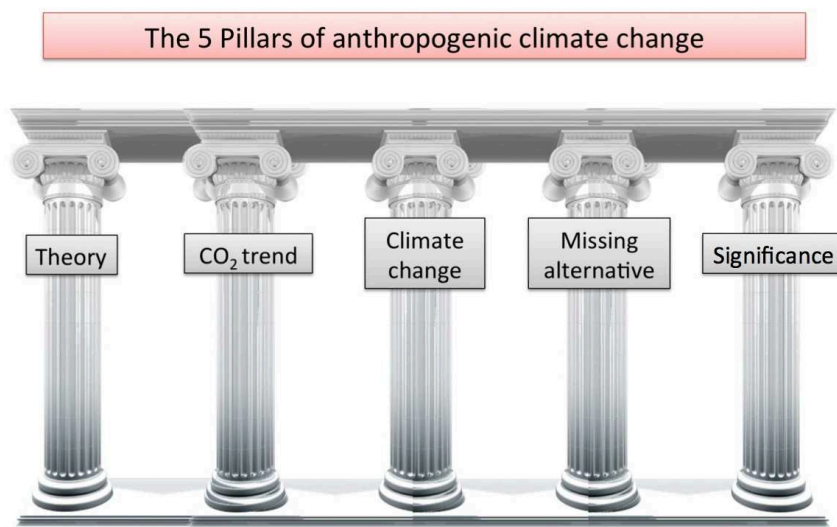
Example: Anthropogenic climate change

This is based on the radiation theory and energy balances in the climate system. Climate researchers did not come to this by knowing a statistical relationship between CO_2 and climate. Actually this was absolutely unknown. The theory is currently (since the 1970s) very nicely demonstrated by a world community working heavily to increase global mean temperatures.

Example: Other climate theories

Are mostly based on a statistical relationship between some index and climate in the past. The only thing they describe is the past but they never make any predictions that turn out to be skillful. They have NO quantifiable theory (no model with equations based on well known physical principles).

5.4 Summary: Evidence of anthropogenic climate change



Chapter 6

Natural Climate Variability

In this chapter we want to take a closer look at natural climate variability. We will in this context focus mostly on climate variability of the physical climate system of the atmosphere and oceans including some aspects of the land, sea ice and land ice sheets (Glaciers) on time scales from month to centuries. We will, however, also discuss climate variability on longer time-scales up to the age of the earth to get a complete picture of the natural climate variability.

In the discussion of climate variability we will try to understand why does the climate vary, what are the main characteristics in climate variability and what are the main drivers. We start the discussion with some simple characteristics of the climate variability and explore the dynamical cause for the chaotic unpredictable nature of internal climate variability in the subsequent section focussing on the Butterfly Effect (Lorenz model). The internal climate variability is mostly stochastic climate variability, which we will discuss in some details. This is then followed by two examples of important specific climate variability phenomena: El Nino and the Stommel model of the variability of the deep ocean circulation. We finish this chapter with a look at Ice Ages and long time scales climate variability.

6.1 Characteristics of climate variability

In this first section about climate variability we want to get a first impression on what the characteristics of climate variability are and how we can describe them. We define some simple statistics, look at some examples and point out some main characteristics. In the first subsection we will introduce some basic statistics that help us to describe variability in general. We will then discuss some characteristics of the climate variability of Melbourne, as this is the type of climate variability that we are most familiar with. It provides us a starting or reference point to look at the time scales and spatial characteristics of climate variability on global domains. Finally we will look at the different causes of climate variability and put this into the two categories of internal and external causes.

6.1.1 Some statistics background

In order to describe variability we need to have some understanding of statistics and need a set of statistical parameters and tools. Here we just want define a few parameters and later we will introduce a few more:

Mean: The mean or average of a variable is the center of mass of the distribution of this variable. For instance, the mean of the distribution shown in Fig. 6.1 is zero. In climate we often refer to the mean as the seasonal or the daily cycle. So the mean is different for each day of the calendar

year or for different times of the day.

Variability: Is what is different from the long time mean (e.g. not the seasonal or daily cycle). We therefore define **anomalies** as the values different from the mean (different from the normal seasonal or daily cycle).

Standard deviation, σ : In statistics the width or spread of a distribution is often described by the standard deviation. It gives the strength of the variability. In a *normal* distribution 68% (2/3) of all values are within $\pm\sigma$, 95% are within $\pm 2\sigma$, and 99.9% are within $\pm 3\sigma$ from the mean value.

Correlation: Correlation describes how much two variables vary in concert. Thus how much they tend to have the same anomalies at the same time. This varies between -1 (the two variable do exactly the opposite) and +1 (they do exactly the same). A zero correlation indicates that the variability of the two variables is entirely unrelated. The more similar they are to each other the closer the absolute value will go to unity. The more unrelated (independent) the two variables are from each other the closer the value will be to zero.

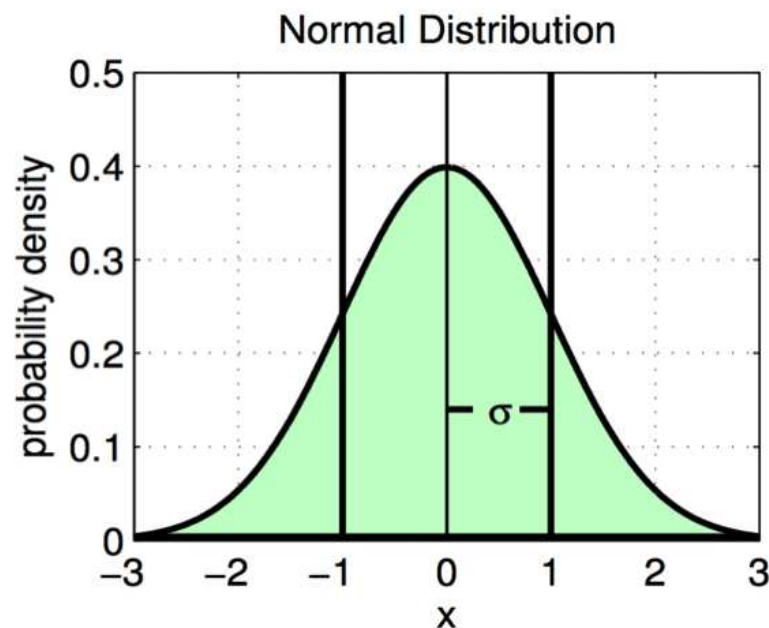


Figure 6.1: A theoretical Normal (Gaussian) distribution, with a mean of zero and a standard deviation (spread) of one. The shape of this distribution is very similar to most distributions of observed climate variables that can take any real value. Variables, such as rainfall or wind speed, that are often zero or can only take positive values, often have distribution quite different from the Normal distribution.

Some more complex statistics we will introduce and discuss in the following sections when we apply them.

6.1.2 Melbourne Temperature Variability

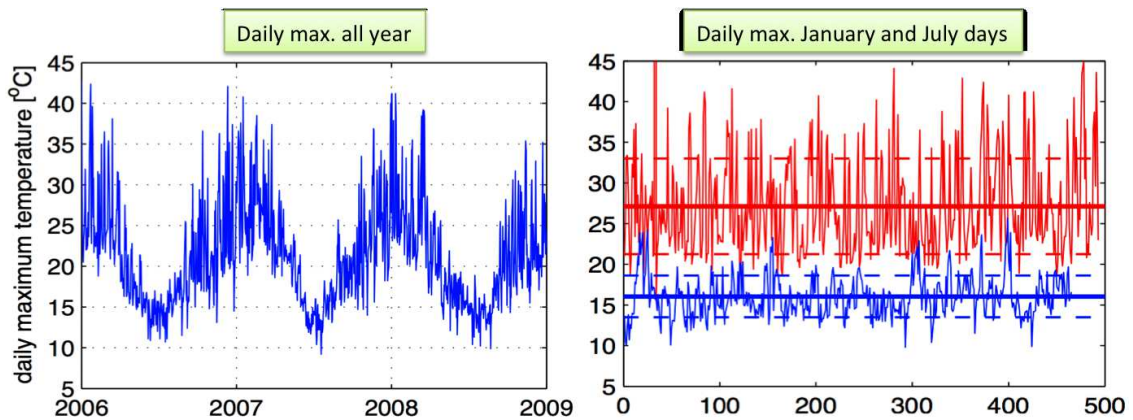


Figure 6.2: Left: Daily maximum temperatures in Melbourne for all days in 2006 to 2009. Right: Daily maximum temperatures in January (red) and July (blue) over the last 20 years (roughly).

The Melbourne climate variability is a good starting point for understanding the characteristics of climate variability, as we have good understanding of it by personal experience. In contrast climate variability on continental or global scale is nothing that we can relate to by personal experience. The characteristics of global or continental scale climate variability are fairly complex, and our personal experience of climate variability may not give us much indication of the nature these types of climate variability. However, we will use the Melbourne climate (here we use temperature) variability to build up a reference point from our personal experience against which we can put global or continental scale climate variability in relation to.

Figure 6.2a shows three years of daily maximum surface (2 meter) temperature in one location in Melbourne. We can clearly see the seasonal cycle and the daily variability. The variability is much stronger in summer than in winter, clearly indicating seasonal differences in the weather characteristics. The strong variability in summer comes from the strong temperature difference between the continent and the southern ocean. To highlight the difference in variability Figure 6.2b shows daily variability of maximum temperatures in January and July over the last 20 years. These daily weather fluctuations are something that we have quite good personal experience about. However, in climate variability we are interested in variability on longer time scales and on larger spatial scales. Longer time scales we can simply get by averaging the temperature over longer time intervals. Figure 6.3 shows the Melbourne temperature records average over different time intervals. In the first step we average over the whole day (24hrs mean in Fig. 6.3b). The 24hrs mean is much lower than the daily maximum temperature (compare Fig. 6.3a and b), as we now consider the mean of day and night. More interestingly the variability has also decreased. This is a general feature of random variability: if you average many random fluctuations (averager over a longer time interval), then the variability of these averages will become smaller than the variability of the individual random fluctuations. In statistics, this is known as the *central limite theorem*, which also explains the bell shape normal distribution (Fig. 6.1).

A 24hrs average is typically much longer than the fluctuations that lead to the daily maximum temperature, which are typically only a few hours (or less) long. Subsequently, the 24hrs average variability is smaller than the daily maximum temperature. This reduction in the variability continues over all time scales. The January monthly mean values have the same mean as the daily means of January, as they are just the average of them, but the variability is strongly reduced (Fig. 6.3c). Thus daily fluctuations mostly average out over the whole month. This is also the

case if we look at the annual mean values (Fig. 6.3d). First we can note that the annual means are smaller than the January means, which is due to the inclusion of all the other calendar month, which tend to be colder than the January month in Melbourne. The variability of annual mean values in Melbourne are now just several tenth of a degree, which is much smaller than the daily weather fluctuations that we are used to from personal experience.

The annual mean time series is better highlighted in Fig. 6.4. We can now clearly see the year to year fluctuations and more interestingly we can see a clear linear warming trend on top of the year to year fluctuations. This warming trend is related to the global warming trend, which we discussed in the earlier sections above. It is again interesting to note here that compared to the daily weather fluctuations or even relative to the monthly mean fluctuation the global warming trend seems tiny. It is not easily noticeable in Fig. 6.3a, b or c. Thus on the local scale of a single station (like Melbourne) the global warming trend is yet still very small. It is however, clear in the annual mean time series.

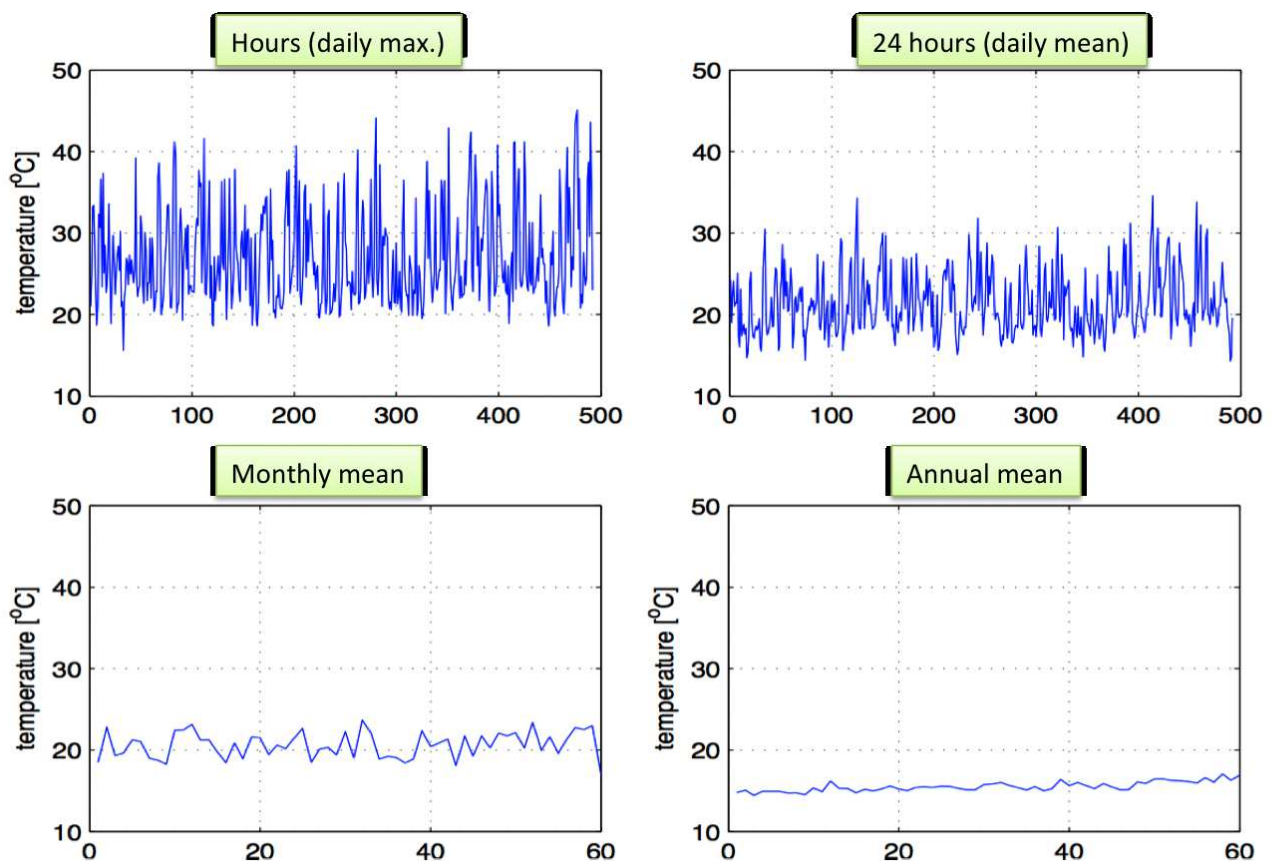


Figure 6.3: Different time scales: Melbourne temperatures for daily maximum in January (upper left), 24hrs mean in January (upper right), the January monthly mean (lower left) and the annual means (lower right) of the last 60yrs.

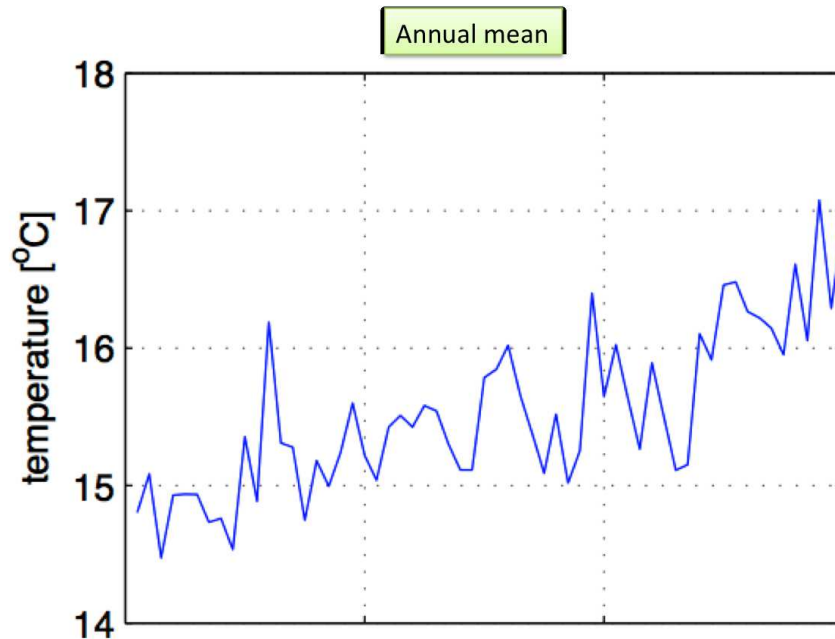


Figure 6.4: Melbourne temperature trend. The same as in Fig. 6.3, but with a different scaling on the y-axis to highlight the warming trend over the last decades.

Time scale dependence of variability:

We can try to summarise the changes in the strength of variability by plotting the standard deviation of each time series in Fig. 6.3 against the time scale, see Fig. ???. We see that with increasing time scale the variability is decreasing. For a better understanding of the time scale dependence of variability we will later define the *power spectrum* of climate variability in the context of the stochastic climate variability, see section 6.3.1. The power spectrum will help us to quantify the time scale behaviour of variability more precisely than we just discussed here.

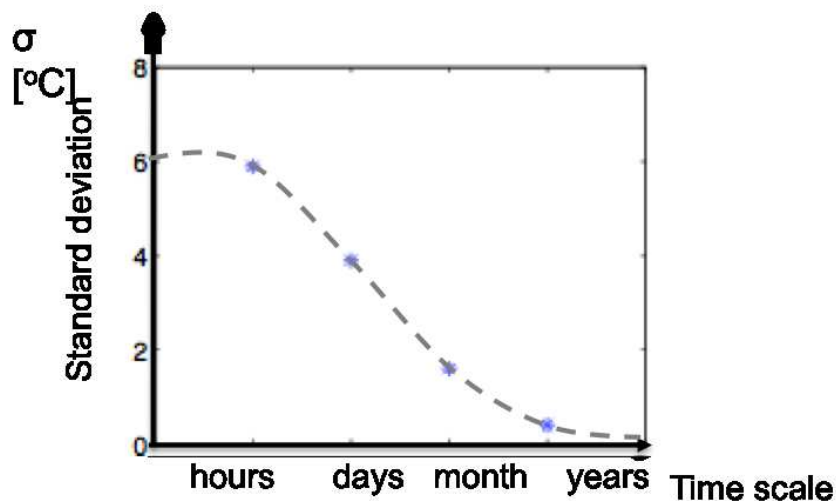


Figure 6.5: Standard deviation of Melbourne temperature as a function of time scale: The standard deviation of the four time series shown in Fig. 6.3. The annual mean time series has been detrended. It illustrates the different strength of variability on different time scales.

6.1.3 Observed global climate variability

We now take a look at some global maps of climate (again surface temperature) variability. Note, that surface temperature over land is in general at 2 meter height above the ground. Over oceans, it is usually called sea surface temperature (SST) and refers to the temperature at about 1m depth within the ocean.

Figure 6.6 shows the annual mean anomaly of 2007 relative to the mean of the period 1951-1980. The first thing we can not here is that this plot is dominated by the global mean warming. To better highlight the natural variability the data is often 'detrended'. This can be done by subtracting a linear trend or simply by subtracting the mean climate from a reference period closer to the actual date of the map, as shown in the right plot of Fig. 6.6.

Figure 6.7 shows another annual mean surface temperature anomaly from 1986. The figures illustrate quite a few characteristics of global climate variability. First we note some areas where no data is available to compute the surface temperature anomaly. In particular over the polar regions and over large parts of Africa. The amplitude of the anomalies is in the order of $0.2^{\circ}C$ to $2^{\circ}C$, which is similar to what we have seen for the annual mean of the Melbourne temperature record. The spatial scale of variability can be roughly estimated by the spatial extend of anomalies of the same sign. We can note that these tend to be several thousand kilometers or several 10 degrees in longitude or latitude. Quite often we may notice that the zonal extend of anomalies is larger than the meridional extend, reflecting the somewhat zonal organization of the climate system.

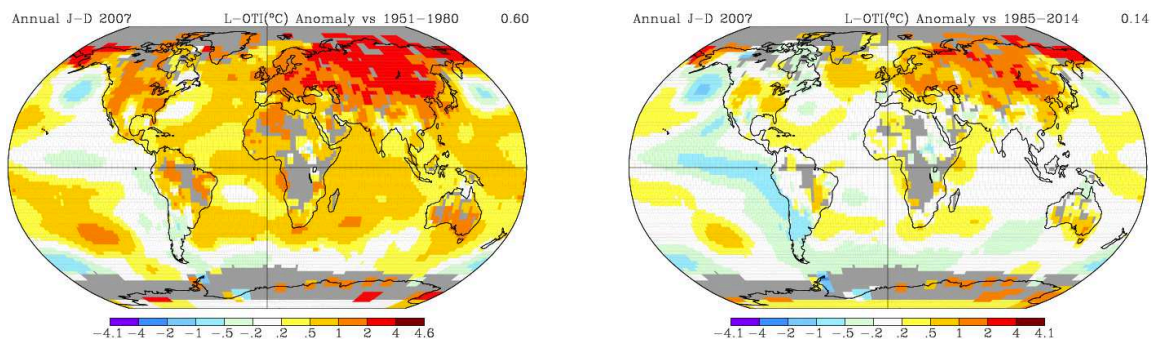


Figure 6.6: Examples of global surface temperature variability: Left: The annual mean anomaly of 2007 relative to the mean of the period 1951-1980. The structure is dominated by the global mean warming. For studying natural internal variability it is better to subtract the global warming trend. This can be done by computing the anomalies relative to more recent period such as 1985 to 2014 as shown in right plot. The grey areas mark regions where no data is available. Note that the colorbar is non-linear, which highlights smaller amplitudes of anomalies.

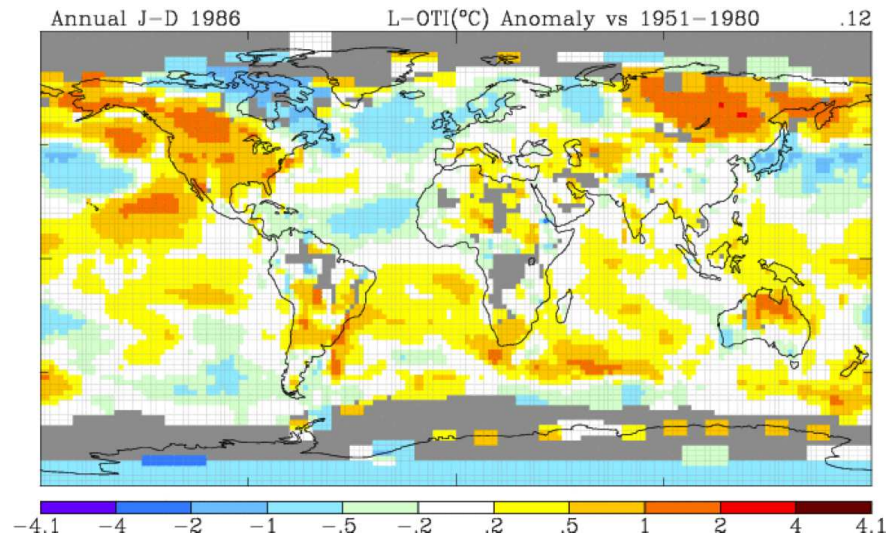


Figure 6.7: Observed annual mean surface temperature anomalies from 1986 relative to the mean from 1951-1980. The grey areas mark regions where no data is available. Note that the colorbar is non-linear, which highlights smaller amplitudes of anomalies.

Figure 6.8 shows a comparison of monthly (August 1986) and annual mean anomalies from the same year. It illustrates some differences in the anomalies spatial structure and amplitude for the different time scales. The monthly anomalies are typically of larger amplitude, in particular over land. The spatial scales are not that different from those of the annual means. The August anomalies are very similar to the annual mean anomalies for most of the ocean regions, but not over land. We can notice that over land some regions have substantially different anomalies on the the annual mean (e.g. the northeast of Europe and Asia in Fig. 6.8). The differences in the persistence of climate variability is highlighted in Fig. 6.9 by showing the temperature anomalies of two consecutive month. You can notice very little change over most ocean regions, but substantial changes over many land regions.

Figure 6.10 shows the temperature variability of two consecutive years. We can notice that not only are amplitudes smaller than for the monthly means, but also that most ocean regions now show changes in the anomalies from one year to the next. Further, we find that the spatial extent of the annual mean anomalies tend to be larger than those of the monthly mean anomalies. This indicates that variability on longer time scales is of also on large spatial scale.

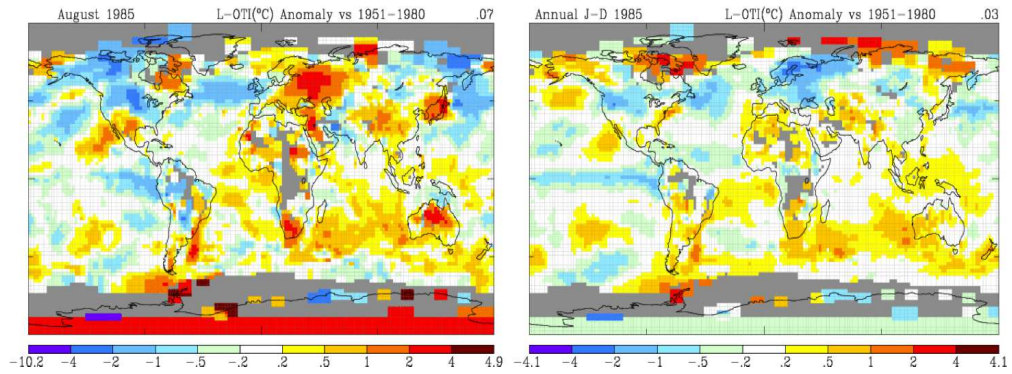


Figure 6.8: Monthly vs. annual mean: Observed monthly mean surface temperature anomalies from August 1986 (left) and annual mean relative to the mean from 1951-1980. The grey areas mark regions where no data is available. Note that the colorbar is non-linear, which highlights smaller amplitudes of anomalies.

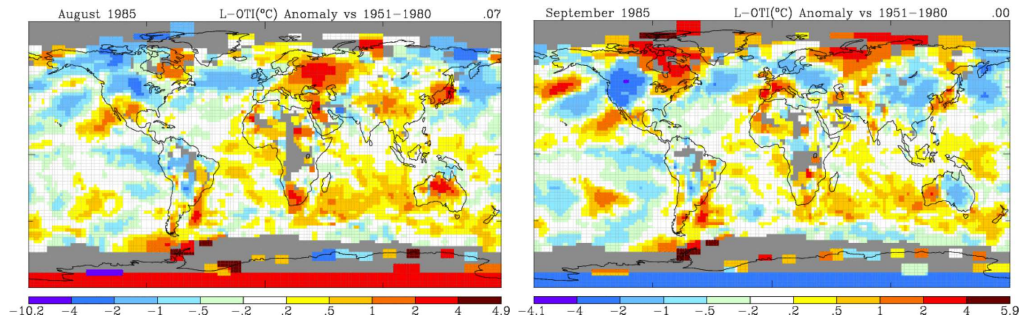


Figure 6.9: Variability of two consecutive month: August and September of 1985. The grey areas mark regions where no data is available. Note that the colorbar is non-linear, which highlights smaller amplitudes of anomalies.

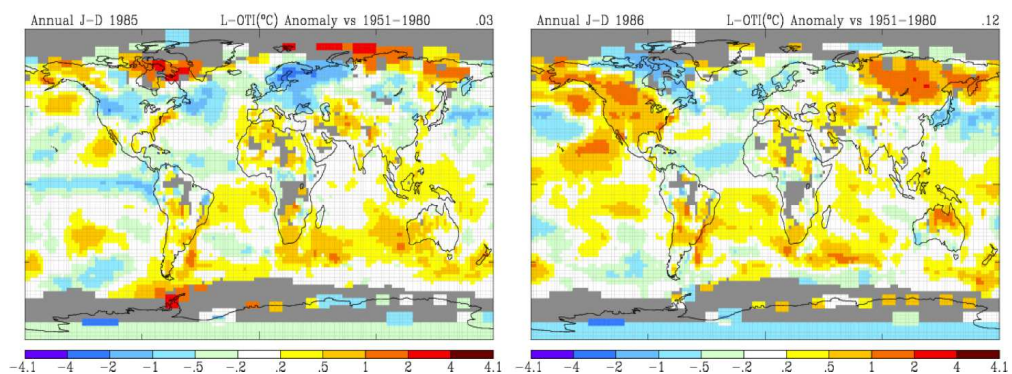


Figure 6.10: Variability of two consecutive years: Observed annual mean surface temperature anomalies for two consecutive years 1985 and 1986. The grey areas mark regions where no data is available. Note that the colorbar is non-linear, which highlights smaller amplitudes of anomalies.

6.1.4 Climate Variability Characteristics

The discussion of the Melbourne and global temperature variability gave us a number of characteristics that we could point out. The three main characteristics of climate variability that we will first of all discuss are:

1. Strength
2. Time scales
3. Spatial scales

In the following we go through each of the three characteristics and discuss them in some more details. Finally we will see how the time and spatial scales interact with each other.

Strength

We already noted that the strength of temperature variability on monthly mean time scales is different over land compared to oceans. In Figure 6.11 we quantify the strength of the monthly mean temperature variability by the standard deviation. We can clearly note a land-sea contrast, with much more variability over land. This is mostly related to the differences in the heat capacities, but is also related to the different feedbacks, as discussed in the previous sections of this course. Natural seasonal to interannual climate variability over land is in the order of 1°C . Over oceans it is weaker $\sim 0.5^{\circ}\text{C}$. We also note that, in general variability increase with higher latitudes. This is partly related to the stronger variability over partially ice covered regions. The 'movement' of ice edges or the fluctuations in ice and snow cover strongly increase the variability, which is related to the ice/snow feedbacks discussed in the earlier sections of this course. In particular, the strongest variability is at the edge of sea ice regions, where the shift of ice covered and ice-free regions lead to very large changes in the heat exchange between the surface and the ocean, and therefore to very large temperature variability. Away from ice cover regions, we also see very strong variability where strong temperature gradients between ocean and land exist (e.g. Melbourne in summer).

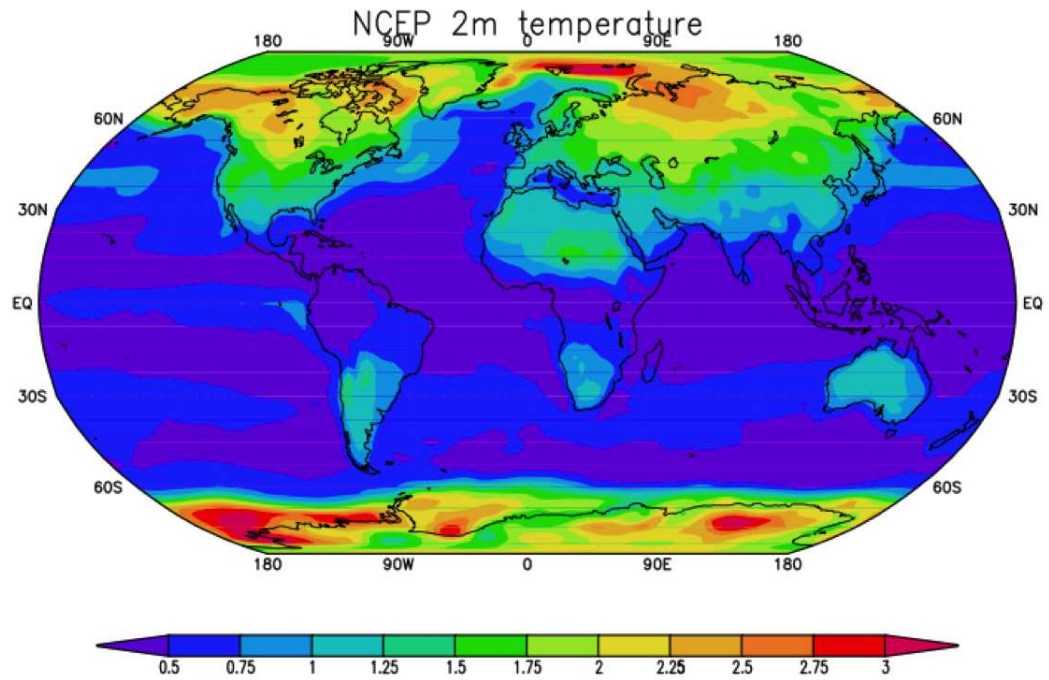


Figure 6.11: Surface temperature monthly mean standard deviation.

Time scales

The Melbourne temperature record and the global temperature anomaly maps showed some clear time scale dependence of the variability, with the longer time scales having in general less variability (e.g. Figs. ?? and 6.8). We will discuss this time scale dependent strength of variability more later when we discuss the stochastic climate variability, see section 6.3.

Figure 6.12 illustrate the different time scale behaviour of the atmosphere, ocean surface (SST) at two different locations and the deeper subsurface ocean. All four time series show the time evolution from 1950 to 2000. The atmospheric temperature over central Asia looks almost perfectly random. We don't see any long time fluctuations or anomalies of one sign persisting for more than a year. Thus the atmospheric temperature over central Asia is dominated by month-to-month variability. The SST in the North Pacific is also quite chaotic, but we can see now some anomalies that persist from several years (e.g. 1956-57). The SST in the tropical Pacific, which is a good indicator for the El Niño variability, appears less chaotic. The variability is not only stronger than in the North Pacific, but is also has less of the month-to-month variability and more pronounced interannual variability. Some of these variations over time look similar to regular oscillations (e.g. around 1965, 1977 or 1987). Finally the subsurface ocean temperature has almost no month-to-month variability and pronounced low-frequency (decadal) variability, with anomalies that persist more than a whole decade (e.g. 1960s).

In summary, the time scales of variability can be very different for different regions. Over land it fluctuates faster than over oceans. Land variability changes mostly from month to month and over oceans variability changes over several months or years and sometimes even decades. In the deeper ocean it takes 10 to 10,000 years.

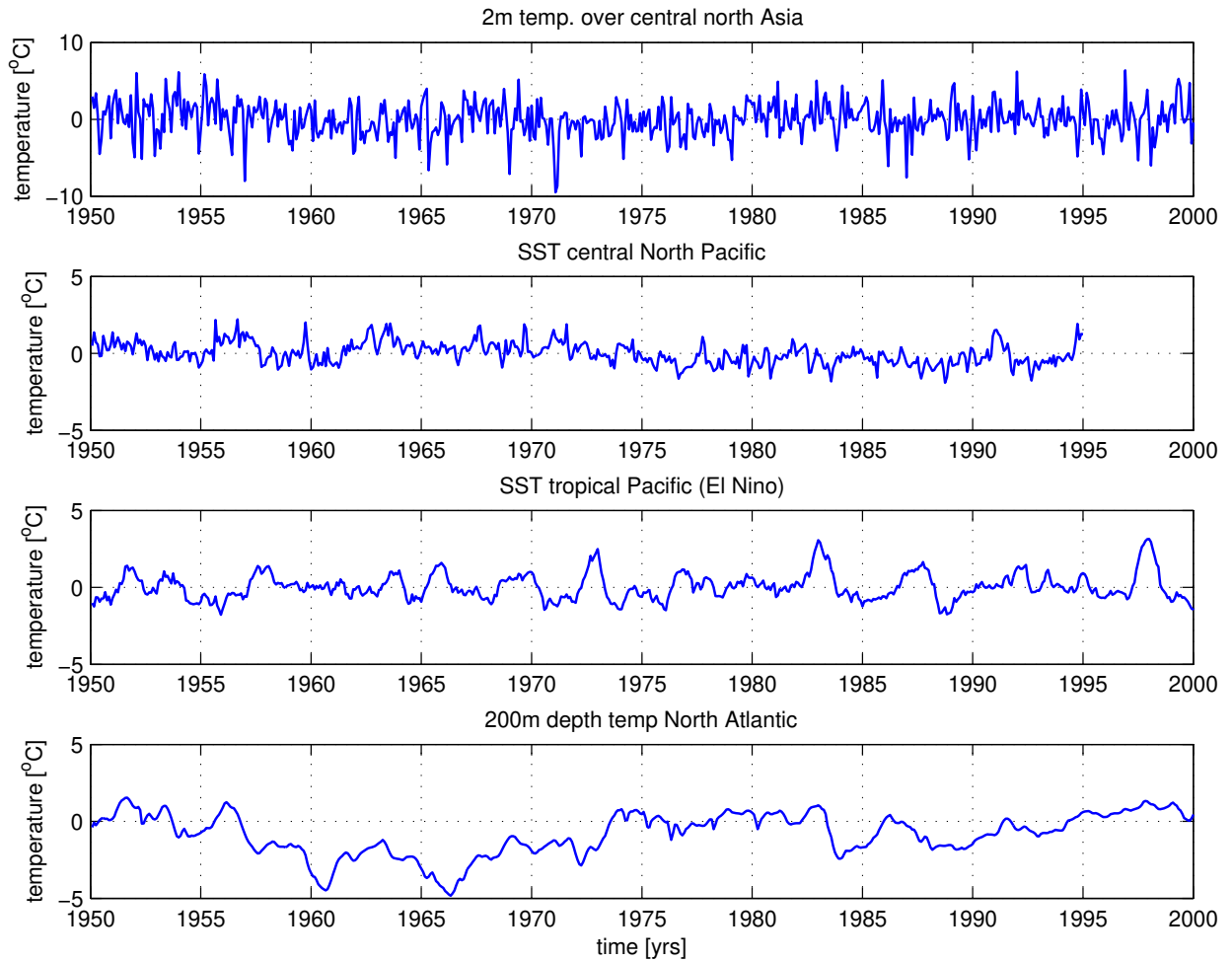


Figure 6.12: Four examples of monthly mean variability time scales: 2 meter over land (central northern Asia) (upper), sea surface temperature (SST) in the north Atlantic, ocean temperature at 200 meter depth and for the tropical Pacific El Nino SST variability. It illustrates the different time scales of variability. Amplitudes of the different time series

The characteristics of the time evolution of variability can be roughly put into the following characteristics:

1. *Oscillation*: Positive and negative anomalies taking turns on regular time intervals (periods). The time series of the tropical Pacific SST (El Nino) showed some indication of oscillations (Figure 6.12).
2. *Chaotic*: Positive and negative anomalies taking turns on irregular time intervals. Best described by the *persistence* of the anomalies. The time series of the 2m temperature over central north Asia was essentially purely chaotic without any persistence (Figure 6.12). The SST in the North Pacific showed some persistence, but was mostly chaotic too.
3. *Trend*: The climate drifts in one direction over time. This may actually in many cases just be a very slow version of (1) or (2), but can indicate a change in the climate system as a whole, such as global warming. The Melbourne annual mean temperature showed a clear trend (Fig. 6.4).

Spatial scales

In most regions the spatial extent of anomalies of the same sign is about several thousand kilometers. This is essentially a reflection of the spatial size of atmospheric weather patterns (not shown), which are one of the main drivers of these temperature variations, as we will discuss further in the following sections. The spatial scales of variability can be very different at different regions. Over land fluctuations are sometimes on smaller spatial scales than over most open oceans, which is often related to barriers such as mountain ranges.

In general variability in nearby regions will be related to each other, reflecting the turbulent diffusive character of the climate. Remote regions, in turn, will tend to be unrelated to each other. However, the patterns of how regions relate to each other can be quite complex and sometimes they can reveal connections between remote regions that are somewhat unexpected. These remote connections are called '*teleconnections*' or modes of climate variability. To get some idea of how regions relate to each other we take a look at the correlation of a few locations with the rest of the world, see Fig. 6.13. The SST in the northern North Atlantic (upper left in Fig. 6.13) has a strong positive correlation to nearby regions, which is what we would expect considering the diffusive nature of the atmosphere and ocean circulation. More interestingly it has negative correlations to the northeast and southwest further away from our reference point. Then even further away we see again increased positive correlations in the tropical North Atlantic. This is a quite distinct pattern of climate variability, which essentially is a quadrupole (two positive poles and two negative poles). It is fairly well known in the climate variability community of Europe and North America as it is related to the North Atlantic Oscillation, which is one of the dominant modes of atmospheric variability in this region (see also Section 6.4). Such distinct climate modes are an important characteristic of climate variability.

The other three ocean points all have different teleconnection patterns. Each of them is first of all highly correlated to nearby regions, but then have connections to more remote regions that are all somewhat different. These reflect how they relate to general circulation patterns in the atmosphere (e.g. connection to the Hadley or Ferrel cell) or oceans. Remarkable again is the point in the tropical Atlantic, which appears to have some teleconnection to the Indian and western tropical Pacific oceans, which is the other end of the world from the tropical Atlantic. Since there is no direct ocean circulation connection to these regions, it is quite clear that atmospheric teleconnections (circulation) must provide the link to these remote regions.

Even more interesting than the teleconnections between the SST at different ocean locations are the teleconnections within the atmospheric circulations. Two things we can point out here: First variability patterns in geopotential height level (or pressure) anomalies tend to be multipoles. This is due to the conservation of mass: If one location has positive geopotential height level (pressure) anomalies, then some other region has to have negative geopotential height level (pressure) anomalies to maintain the conservation of mass, since mass in the atmosphere does not disappear or appear. It can only be rearranged. This is quite clear in the points at higher latitudes in Fig. 6.13.

The second interesting point is that within the tropics the connections are essentially global. All of the tropics are strongly related to each other. This is due to the vanishing Coriolis force along the equator, which will allow anomalies to spread through the whole tropical atmosphere without being deflected into cyclones. We can see that this leads to very strong connections in the zonal directions and less strong connections in the meridional direction.

A particularly interesting pattern is related to El Niño, see Fig. 6.14. The El Niño variability is a phenomenon of the tropical eastern Pacific SST variability. The SST variability in this region has a pronounced pattern with near global teleconnections on interannual time scales. Most of the western and high latitudes Pacific is negatively correlated to El Niño (its colder than usual when El Niño index is positive; warm). Even the Indian Ocean, which is at the other end of the world from the eastern Pacific is strongly positively correlated. This marks the most dominant mode of

natural global climate variability on time scales from month to several years. We will focus more on this mode of climate variability later in Sec. 6.6.

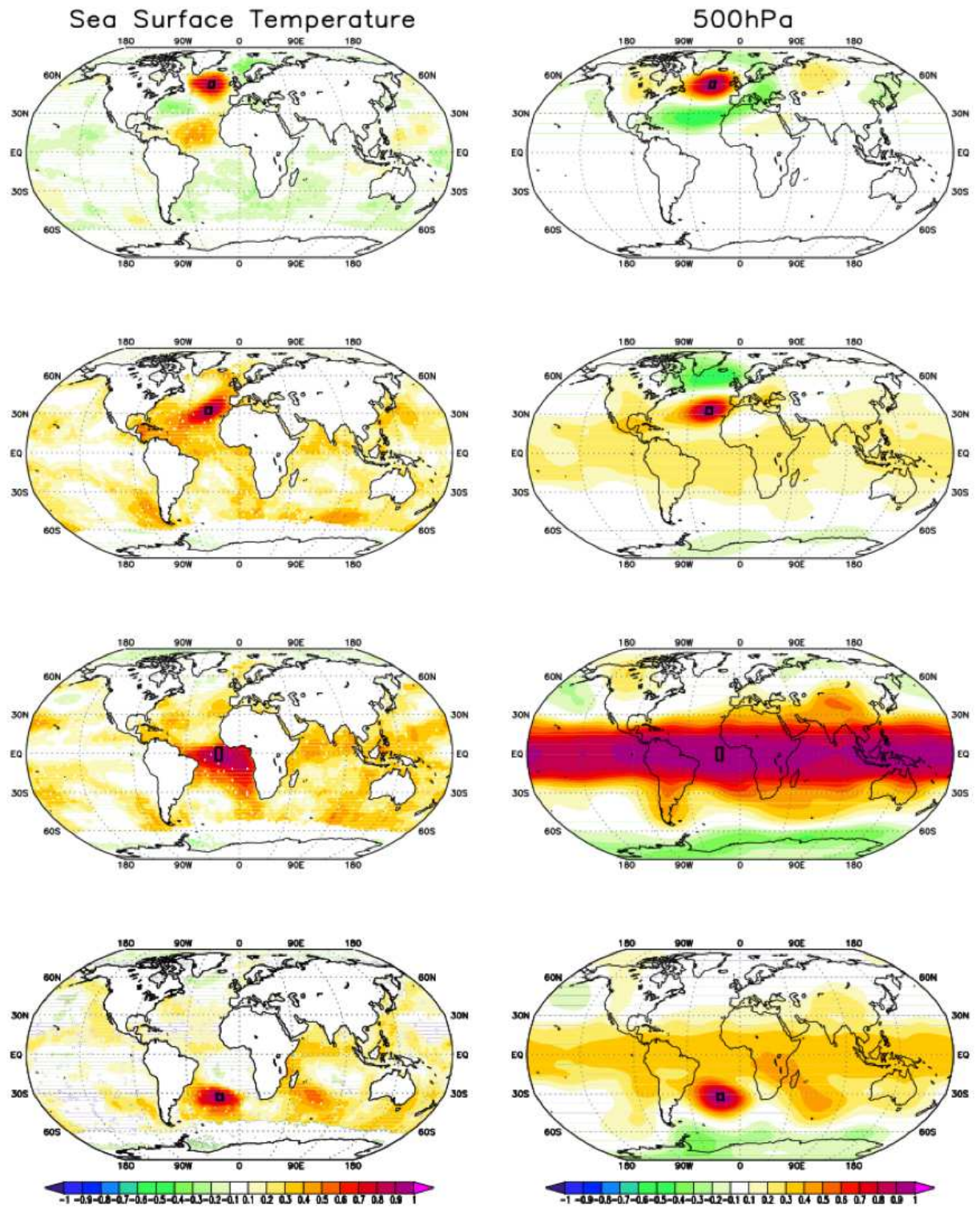


Figure 6.13: Correlation of climate variability: The correlation of the monthly mean SST anomalies at four different ocean points with the rest of worlds ocean (left). The correlation of the monthly mean 500hPa geopotential height level anomalies at four different points with the rest of world (right).

Another interesting aspect of the spatial climate variability is the spatial propagation of anomalies

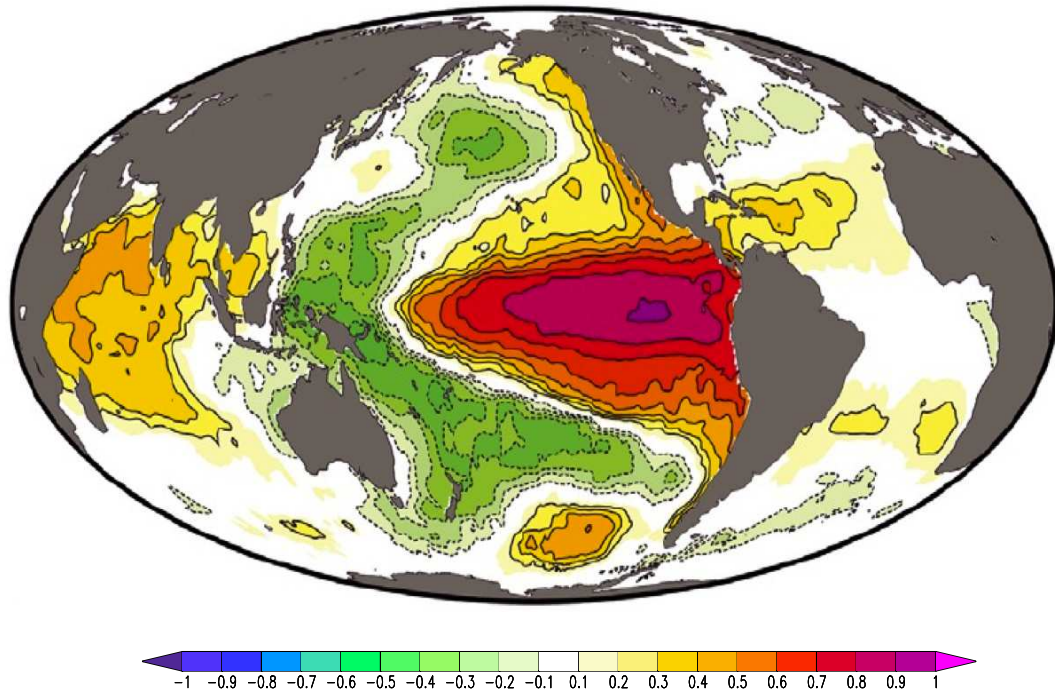


Figure 6.14: El Nino teleconnections: Correlation of the monthly mean SST anomalies in the central to eastern equatorial Pacific with the SST of the global oceans.

over time. Sometimes a climate anomalies starts at one location and than propagates over time to another region. A good example for such a propagation is the Madden-Julian Oscillation shown in Fig. 6.15. The rainfall patterns from the Indian Ocean propagate along the equator into the Pacific within a few weeks. Propagation from one region to another, over time, is often best presented in a so called *Hoevmoeller diagram* (Fig. 6.15 right). A Hoevmoeller diagram presents the variability of a climate variable as a function of a spatial direction (here the equator) versus the time dimension. Propagating climate variability will show up in a Hoevmoeller diagram as diagonal (neither horizontal nor vertical) structures. In the example shown in Fig. 6.15 we can clearly see diagonal features in the outgoing long wave radiation of the top of the atmosphere (OLR) along the equator of the Indian and Pacific oceans. It suggests a propagation time for the ORL anomalies from $40^{\circ}E$ to $160^{\circ}E$ in about 50 days.

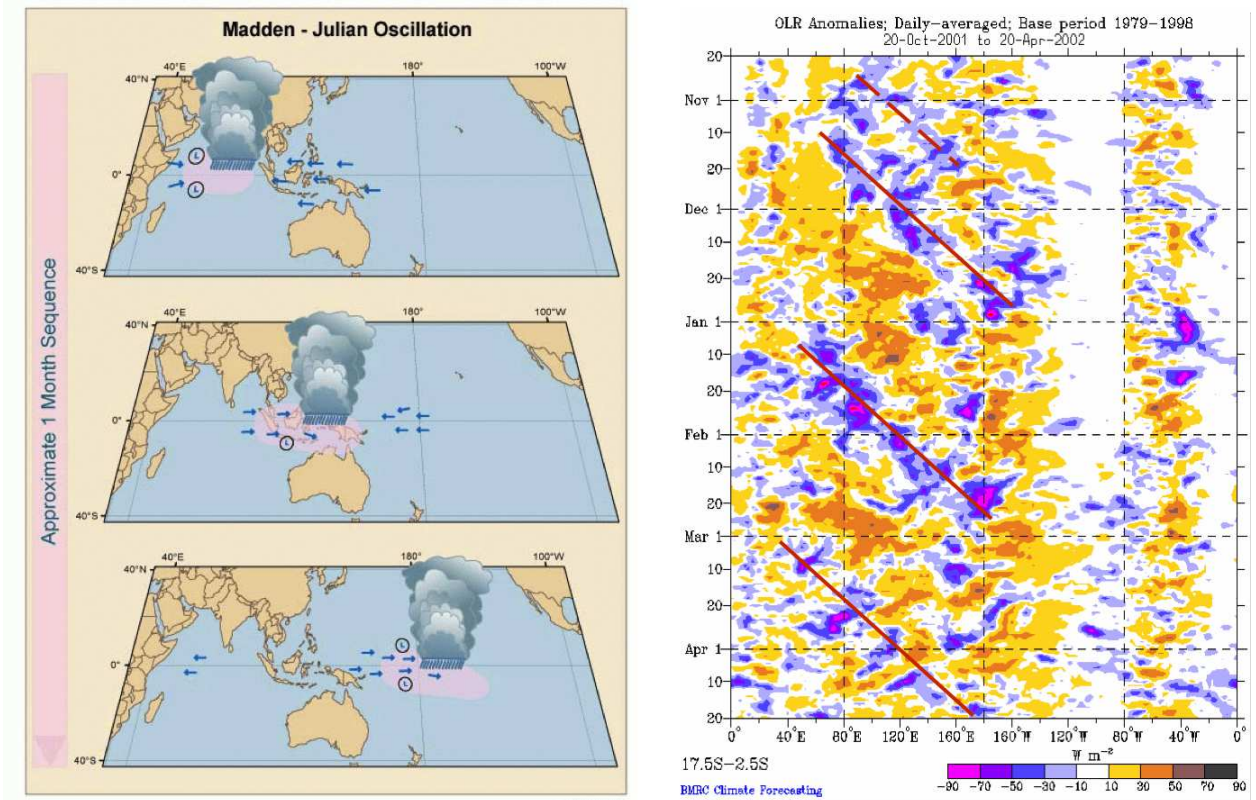


Figure 6.15: Madden-Julian Oscillation: Left: a sketch of the propagation of rainfall patterns from the Indian Ocean into the Pacific, which describes the Madden-Julian Oscillation phenomenon. Right: a Hovmöller diagram of the propagation outgoing long wave radiation of the top of the atmosphere (OLR) along the equator of the Indian and Pacific oceans for time period from Oct. 2001 to Apr. 2002. OLR is a good proxy for rainfall: below normal OLR indicates high clouds and therefore more rainfall. Diagonal structure in a Hovmöller diagram suggest propagation from one location to another over time. Here we see diagonals from upper left (east and earlier in time) to lower right (west and later in time), indicating propagation from east to west.

A further interesting aspect of natural climate variability is the co-variability between land and ocean on global scales, see Figure 6.16. The figure shows the global mean land and ocean temperatures from 1950 to 2010 with the linear warming trend removed. The two curves have a strong correlation (0.8) and the amplitude of the fluctuations over land are about 53% larger over land than over oceans in average. From the observed relation we cannot easily know if the land is responding to the ocean variability or the oceans to land variability or both to some third element. However, in model simulations in which the ocean SST variability is prescribed and the atmosphere and land can respond to it (not shown), we see a similar relation between T_{land} and T_{ocean} . We do not see this relation if we let the ocean respond to land temperature changes, suggesting that the land is indeed responding mostly to the oceans and not vice versa.

This effect is similar to the one we discussed previously in the context of global warming and the land-sea warming contrast (see section 5.1). It reflects the different climate feedbacks over land and ocean, which lets the land respond more strongly to external forcing than the oceans. In this context we can consider the ocean variability as an external forcing for the land climate. We also mentioned above that climate variability in the oceans is more persistent. This leads to the interesting effect that the land responses to variability over the oceans with an amplitude that is larger than the actual ocean forcing.

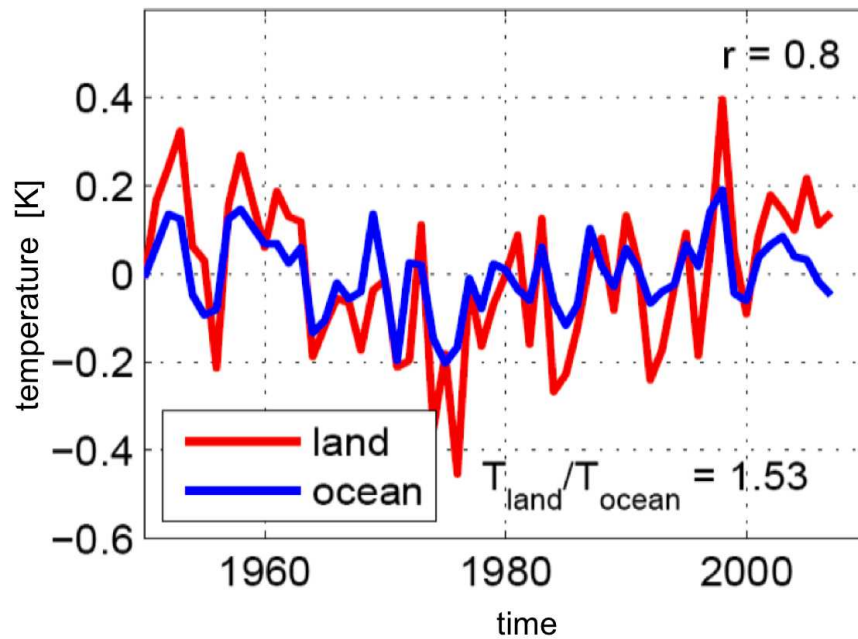


Figure 6.16: The global mean land and ocean temperatures from 1950 to 2010 with the linear warming trend removed. The correlation between the two curves $r = 0.8$ and the mean ratio in amplitudes is $T_{land}/T_{ocean} = 1.53$

We can note for the above examples that the teleconnections in the atmosphere and ocean can be fairly complex and unexpected. Some of the teleconnection patterns have names and are studied quite in detail (e.g. El Nino, Southern Annular mode (SAM), Southern Oscillation Index, etc.). They are known to have significant impacts on our local weather patterns. We will discuss the spatial patterns of climate modes in some more detail in the context of stochastic climate variability further below in section 6.4.

Climate variability characteristics: time vs. spatial scales

The time and spatial scale of variability are related to each other. The maps of global temperature variability showed that the spatial structure of variability changed from monthly to annual means. Shorter time scales variability tends to be on smaller spatial scales and longer time scale climate variability tend to on larger spatial scales. Figure 6.17 illustrates this relation between time and spatial scales. This follows from a simple idea, related to diffusion in the atmospheric and oceanic circulations: short-lived climate variations do not have enough time to influence remote regions. In turn, long-lived climate variability will have enough time to influence the whole global and get into balance with the global climate system. Therefore, climate variability on time scales longer than 100yrs tend to be on near global or at least hemispheric scale.

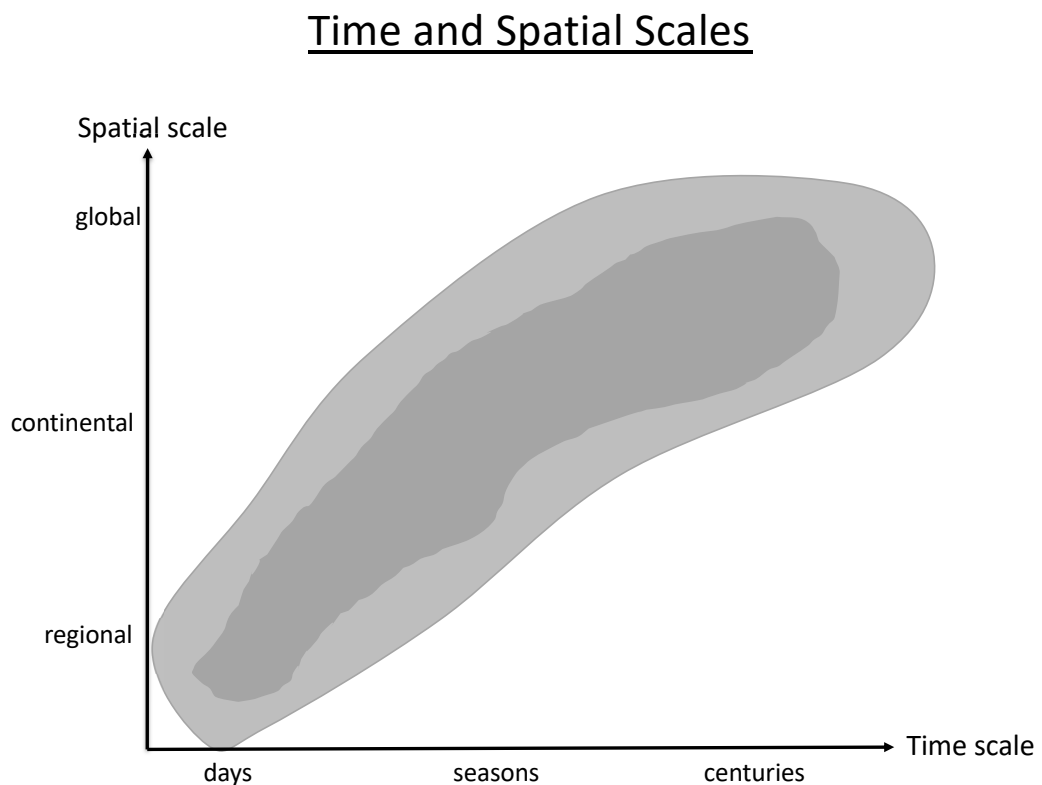


Figure 6.17: Idealised probability distribution of climate variability as function of time and spatial scales

6.1.5 Sources of climate variability

The causes or sources of climate variability can be categorised into: External and Internal.

External:

External influences on the climate are influences on which the climate system can not feedback. These are, for instance. changes in the incoming solar radiation, volcanic eruptions, anthropogenic forcing like CO₂ or meteorites. One may argue that the climate can feedback onto volcanoes or anthropogenic forcing, but to first order we can assume that the climate system does not influence (feedback) onto them. On longer time scales (million years and longer) plate tectonic movements, Biogeochemical reactions between the sediments ocean and atmosphere and Meteorites are important external forcings.

Figure 6.18 shows an example of externally forced climate variability over the last few hundred years. We can see that every time a strong volcanic eruption happens, the global mean temperature drops a bit over the next few years and then goes back to normal.

Internal:

Internal variability arises from the dynamics of the climate systems within itself given all external boundary conditions being constant (e.g. solar radiation). Non-linear, complex dynamics of the climate system cause the internal variability. Interactions of climate subsystems can lead to variability (e.g. interaction between ocean and atmosphere) on all time and spatial scales. The primary source of this kind of climate variability is the weather variability of the atmosphere, which we will discuss in more details in the next section.

In Figures 6.19 and 6.20 we can compare the observed temperatures of the Northern Hemisphere against the global mean temperatures from a model simulations with fixed boundary conditions (no external forcings). The model simulations gives us some idea of the amount of internal variability, assuming that the model simulations is realistic. It is fairly clear from this model simulation, that the internal climate variability is on all time scales, and it is similar in amplitude to the observed one. The observed variability seem to have some long time variations and a warming trend at the end that is missing in the internal natural variability simulation. In summary, this comparison indicates that much of the last 2000yrs variability (excluding the obvious anthropogenic warming at the end) is internal and not forced by any external forcings.

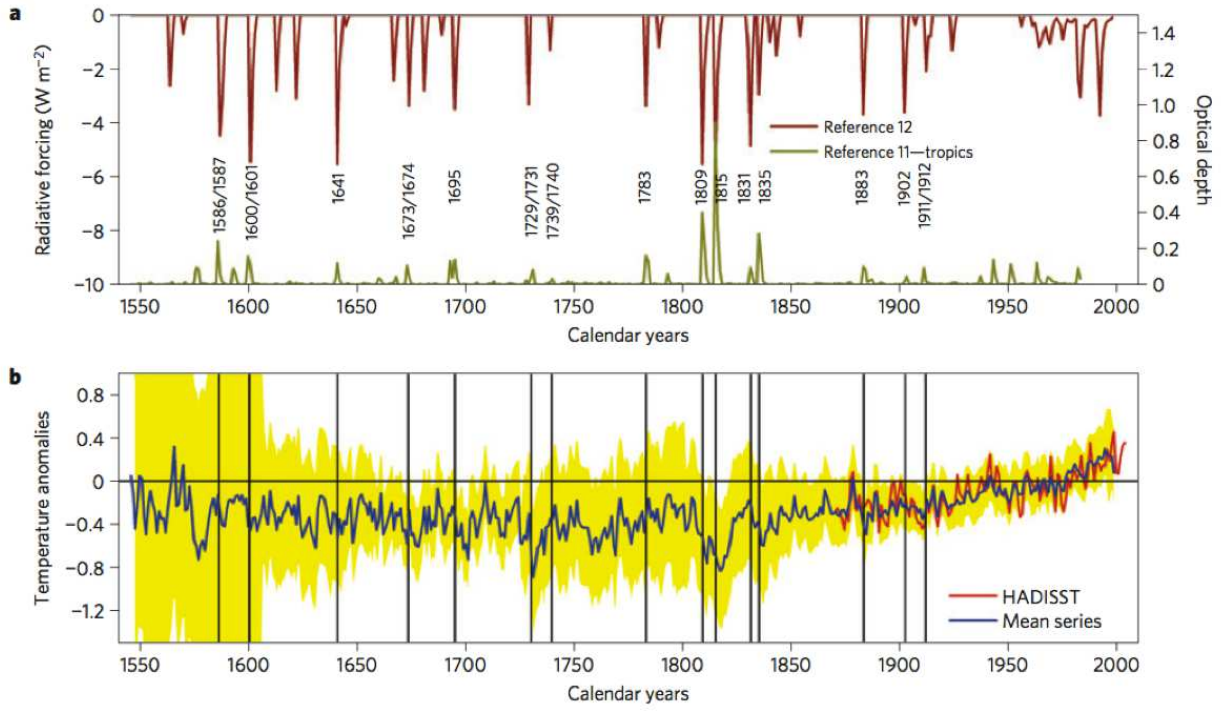


Figure 6.18: Volcanic forcing and surface temperature variability

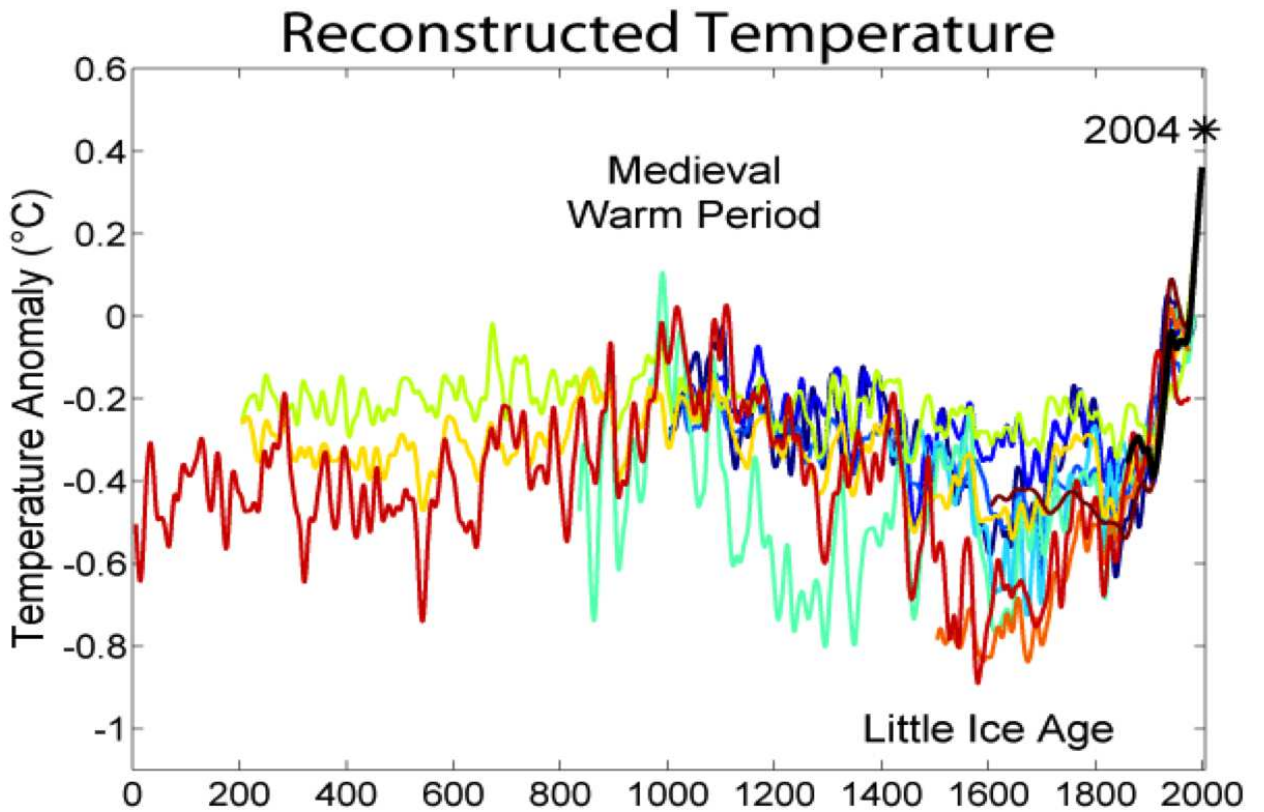


Figure 6.19: Reconstructed surface temperature in the northern hemisphere. Each curve is from a different study.

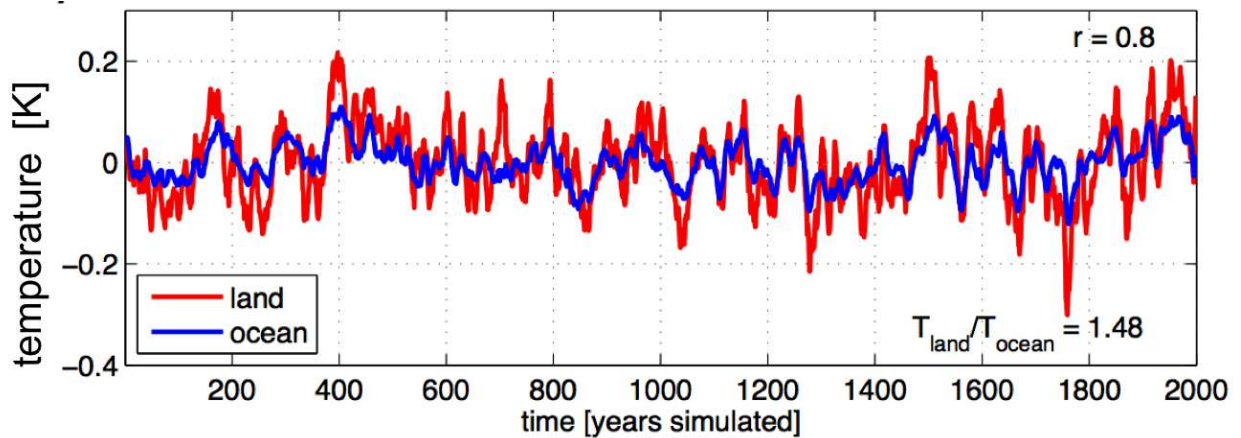


Figure 6.20: Simulated surface temperature global anomalies (no external forcings; decadal smoothed).

6.2 Chaos (The butterfly effect; The Lorenz Model (1963))

Why does the weather or climate vary at all when all external boundary conditions are fixed? Thinking about this, it seems very strange. Consider an indoor swimming pool and all boundary condition fixed. Some energy is coming in (e.g. sun light) and some is going out, but lets assume this is fixed, thus always the same. If you would measure the pool temperature or the room temperature, then you would always get the same result within less than $\pm 1/100^\circ C$. This is not the case for our weather or climate. The weather in Melbourne on January 15. at 3pm, for instance, can be hugely different from one year to the next. Even though we can assume that the boundary conditions are essentially the same. The temperature difference can be more than $25^\circ C$, which is almost as different as any two locations on earth on the same day, and theses different locations would have quite different boundary conditions (e.g. incoming sun light). The weather fluctuation and the related internal climate variability in the absence of any external boundary condition changes are a really interesting phenomenon.

Types of variability

To understand this better consider the different types of dynamical systems:

1. **A Stable equilibrium system**, $\lim_{t \rightarrow \infty} \Phi = \Phi_{eq}$: A dynamical system, such as the zero order energy balance model (eq. [2.10]) or the GREB model, starting from any initial condition would asymptotically converge towards an equilibrium point after some time and would than not vary anymore, if all boundary conditions are fixed. There is no internal variability in such a system other than the convergence from the initial condition towards an equilibrium point. Here it also does not matter whether or not the system would have many or just one equilibrium point.
2. **Oscillating system** $\vec{\Phi}(t+m) = \vec{\Phi}(t)$ with $m =$ phase of cycle (waves; orbit of the earth): An oscillating system, such as the earth's orbit around the sun, does have internal variability, but this is of a fairly trivial nature. It is a repeating cycle that is highly predictable and has no randomness like our weather fluctuations.

3. **Deterministic chaotic system** $\vec{\Phi}(t_1) \neq \vec{\Phi}(t_2)$. The climate variability is chaotic and unpredictable. The system is never in the same state again, thus no January 15. at 3pm in Melbourne in any year will ever be the same as in a previous year. This kind of a system is like our earth's climate.

The Deterministic chaotic system is a fairly new kind of system that people were not aware of before the formulation of the Chaos theory by Lorenz-Salzman model (1963). Here the system has no stable equilibria and it varies around the equilibria points in a non-periodic, chaotic and unpredictable way. It does so despite the fact that the tendency equations of the system are exactly known (deterministic). We will take a closer look at such a system in the next sections.

6.2.1 The Lorenz-Salzman model

The Chaos theory goes back to the Lorenz-Salzman model (1963). It is a discussion of simplified convection dynamics which illustrates some important characteristics of chaotic weather dynamics that are fundamental to weather and climate. The chaotic, always varying, weather dynamics are the primary source of all natural internal climate variability on all time scales (from days to 100,000yrs).

This Lorenz-Salman system is the first system in which *deterministic chaos* has been observed and described. It is the basis for *Chaos theory*. We will start with roughly sketching the derivation of the three tendency equations that make up the Lorenz-Salzman model. We will then study some important characteristics of this set equations, mostly focusing on its time evolution behaviour and its variability.

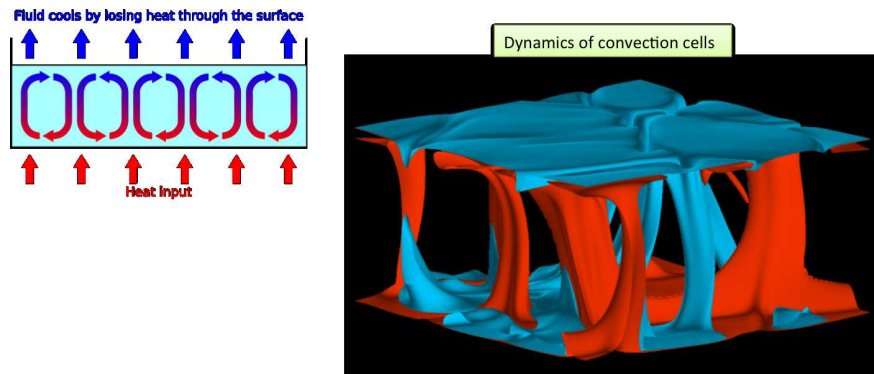


Figure 6.21: Illustration of the basic setup: We have volume of a fluid that is heated from below and cooled from above. This setup can be in a convective regime (as shown in the figures), in which the fluid builds up convection cells.

The Lorenz model discusses a simple set up of a volume of a fluid that is heated from below and cooled from above, see Fig. 6.21. It should simplify our weather system to the essential minimum system that behaves in a similar way. Here an essential aspect is that we have a fluid that is heated from below and then develops into chaotic convection cells. A very simple very day realisation that is similar to such a system is a lava lamp.

The following detailed set up is considered:

- We have an incompressible fluid (e.g. water) in a fixed domain. Thus density is not a function of pressure.

- Boundaries are closed. So mass is conserved.
- The fluid is heated from below and cold at the top.
- No rotation \rightarrow no Coriolis forcing.

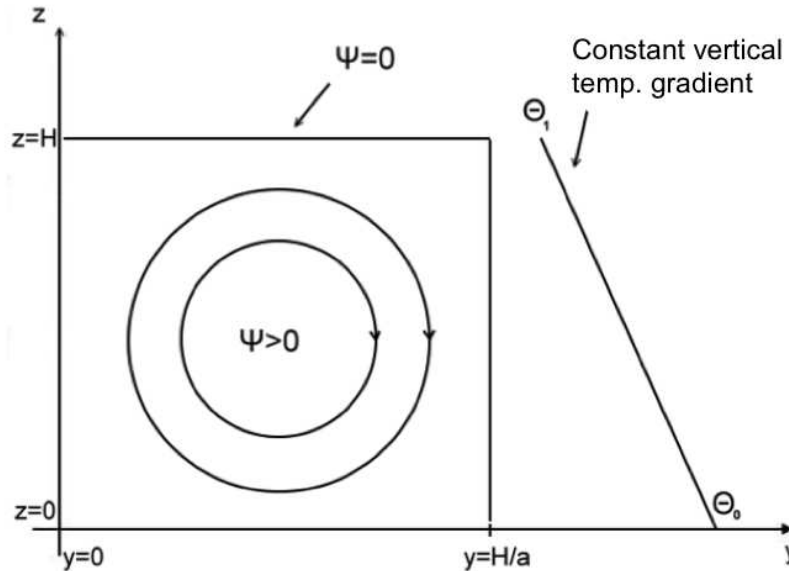


Figure 6.22: Sketch of the Lorenz-Salzman system setup: We have a box of length H/a and height H . The third dimension is neglected. The circulation of the fluid in the box is described by the stream function Ψ and the vertical temperature gradient is related to the constant temperature at the bottom, Θ_0 , and at the top, Θ_1 .

The situation relevant to the Lorenz-Salzman model is sketch in Fig. 6.22. The following assumptions and simplifications are given:

1. Boundary conditions:

$$T(z=0) = \Theta_0 = \text{constant}$$

$$T(z=H) = \Theta_1 = \text{constant}$$

$$u(\text{boundaries}) = 0$$

2. 2-dimensional problems:

$$\rightarrow d/dx = 0 \text{ (symmetric in } x)$$

3. Mass conservation (incompressible flow):

$$\text{div}(\vec{u}) = \nabla \cdot \vec{u} = 0 \implies \text{stream function } \Psi$$

The conservation of mass implies closed circles of flow, which allows us to define stream lines. In contrast divergent flow has streamlines crossing (e.g. at sinks or sources of mass). Thus we can simplify the two dimensional flow by a one dimensional stream function, Ψ .

4. Energy conservation

$$\frac{D\Theta}{Dt} = \kappa \cdot \nabla^2 \Theta$$

Heat is only diffused but does not go in or out of the domain (no radiation).

5. Gravity:

$$\frac{Dw}{Dt} \propto g \frac{\bar{\rho}}{\rho_0}$$

Vertical motion is caused by buoyancy with small deviations in density, ρ' , from the mean density ρ_0 .

6. Diffusivity:

$$\kappa \cdot \nabla^2 \Phi$$

Momentum and heat is diffused with a fluid constant κ_u (momentum) and κ (heat). The diffusivity of momentum is essentially due to the friction force within the fluid, related to the viscosity of the fluid.

The above assumptions and simplifications lead to strong simplification of the general dynamics. The dynamics in general are given by the momentum, density and temperature tendency equations:

Momentum:

$$\rho \frac{D\vec{u}}{Dt} = -2\rho \cdot \Omega \times \vec{u} - \vec{\nabla} p + \rho \vec{\nabla} \Phi + F$$

Density:

$$\frac{D\rho}{Dt} = -\rho \vec{\nabla} \cdot \vec{u}$$

Temperature:

$$\rho \frac{D\Theta}{Dt} = -\vec{\nabla} \cdot J_{\Theta}^{turb} - \vec{\nabla} \cdot \frac{J_{rad}}{c_p}$$

The general equations strongly simplify for the Lorenz-Salzman model due to the above assumptions and simplifications:

$$\frac{Dv}{Dt} = -\frac{1}{\rho_0} \frac{\partial p}{\partial y} + \kappa_u \cdot \nabla^2 v$$

$$\frac{Dw}{Dt} = -\frac{1}{\rho_0} \frac{\partial p}{\partial z} + \kappa_u \cdot \nabla^2 w - \frac{g}{\rho_0} \rho'$$

$$\implies \frac{d\Psi}{dt} = \dots$$

$$\frac{D\Theta}{Dt} = \kappa \cdot \nabla^2 \Theta$$

The mass conservation, incompressibility, neglecting Coriolis force and the 2dim-approach allows us to simplify the three dimensional momentum tendency equations and to reduce it to one single stream function tendency equation. The density can be diagnosed by the temperature and the tendency of temperature (recall: material derivative includes local and advective changes) is only

due to diffusion, since no radiation fluxes exist in the Lorenz-Salzman Model.

We can further simplify the model by some approximations and normalisations:

- We approximate solutions of this model only for the largest scale motions.
- We simplify temperature deviations from the mean vertical temperature gradient:

$$\Theta(y, z, t) = \Theta_0 - \frac{\Delta T}{H} z + \Theta'(y, z, t)$$

- Deviations from the mean are:
 - variations of the vertical gradient
 - differences in the upward vs downward flow
- Normalisation of all parameters/variables to simplify the equations

After some calculations we get to the set of three non-dimensional tendency equations that make up the Lorenz-Salzman model:

$$\frac{dX}{dt} = \sigma(Y - X)$$

$$\frac{dY}{dt} = -XZ + rX - Y$$

$$\frac{dZ}{dt} = XY - bZ$$

X : convective intensity; related to the stream function; a change in sign presents a change in the circulation direction (clockwise vs. counter clockwise).

Y : horizontal temperature difference (descending vs. ascending currents)

Z : difference in vertical temperature profile from reference gradient

The Lorenz Model has the following parameters:

σ : The Prandtl number $\sigma = \frac{\nu}{\kappa}$ $\nu = \kappa_u$. It describes the characteristic of the fluid's viscosity of the motion and diffusivity of heat.

$r = \frac{g \cdot \alpha \cdot H^3 \cdot \Delta t}{\nu \cdot \kappa} \cdot \frac{a^2}{\pi^4} \cdot (1 + a^2)^2$: The Rayleigh number, r , depends on a numbers of fluid and geometry characteristics (see Fig. 6.22 for H and a). The number describes the circulation characteristic. For turbulent convective flow we have $r > 1$ and for conductive flow (no convection cells) we have $r < 1$.

$b = \frac{4}{1+a^2}$: Domain geometry.

Note that all three parameters are positive. We can now take a closer look at the three tendency equations: the tendencies in X (convective intensity) is forced by two terms. The second term is a damping that reduces the circulation the stronger the circulation is. The first term is proportional to horizontal temperature gradient Y . Thus the circulation is strengthened by horizontal temperature gradients. Overall the tendencies of X are fairly simple and linear, as they do not involve products of the three dynamical variables X, Y and Z .

The other two tendency equations are more complex as they involve non-linear terms (terms with products of the three dynamical variables). Both again have a linear damping term contributing to the tendencies. The non-linear terms are the ones that make this system very complex and unstable.

The 3 dimensional Lorenz-Salzman system has three equilibria:

$$X_{eq} = (0, X1, X2)$$

$$Y_{eq} = (0, Y1, Y2)$$

$$Z_{eq} = (0, Z1, Z2)$$

One equilibrium point is at (0,0,0). Thus, no circulation and no temperature gradient in the horizontal and no vertical temperature difference from the reference temperature gradient. The other two equilibrium points are (X1,Y1,Z1) and (X2,Y2,Z2) with the X,Y and Z different from zero. We will see in the following that these two equilibria points are the ones around which the systems varies. They are often referred to as the two *attractors* for the two *regimes* of the system.

6.2.2 Characteristics of the Lorenz-Salzman model

In the following we will discuss an example with the following parameter:

$$\begin{aligned}\sigma &= 10 \\ b &= 8/3 \\ r &= 28\end{aligned}$$

The parameters are chosen in a way that we are clearly in a convective and chaotic regime. With $r \gg 1$ we are clearly in the convective regime. The following characteristics of the chaos regimes are the main aspects of the Lorenz-Salzman model in respect to this lecture and natural internal climate variability:

1. No stable equilibria:



The system has no stable equilibrium point and it never reaches an equilibrium point. Thus it always varies. It therefore has no valleys in the climate potential point of view, which is impossible to visualize. This non-linear behaviour is the reason why we have constantly changing weather variations.

2. Regime behaviour:

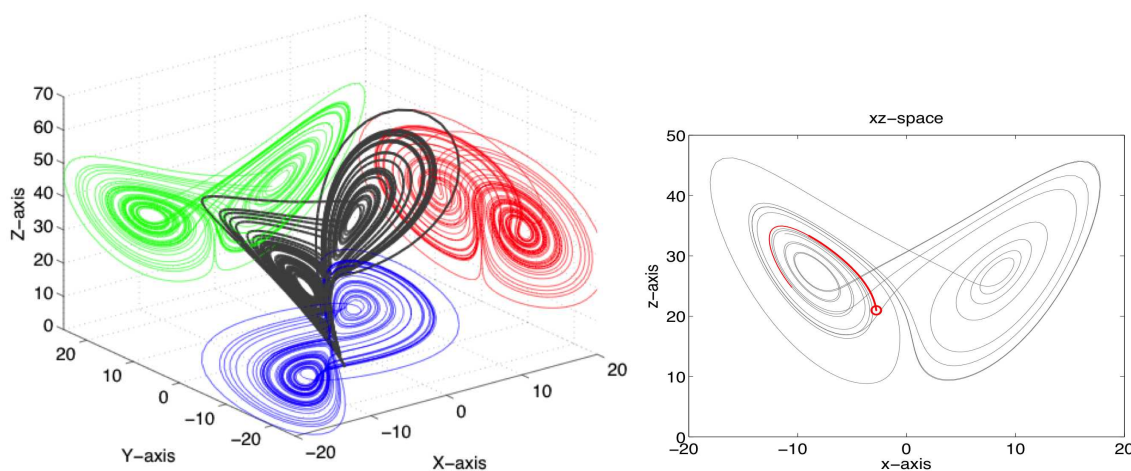


Figure 6.23: Tracks of the Lorenz-Salzman model in the dynamical space of the system: Left: 3D-view with projections on the three 2D planes. Right: projections on the three XZ-plane. The tracks around these two attractors look a bit like the wings of a butterfly, which may be one of the reasons why the chaos theory is often referred to as the Butterfly effect.

The time evolution of the Lorenz-Salzman shows oscillations around the two non-zero equilibrium points (attractors; regimes) with transitions between the two regimes, see Fig. 6.23. Thus like weather variations the system remains in one regime for a while until it transitions into the other regime. How long it remains in one regime and how close it is to the attractors varies from time to time.

The probability distribution shows that the most likely location in the dynamical space is near the two equilibrium points (attractors), Fig. 6.23.

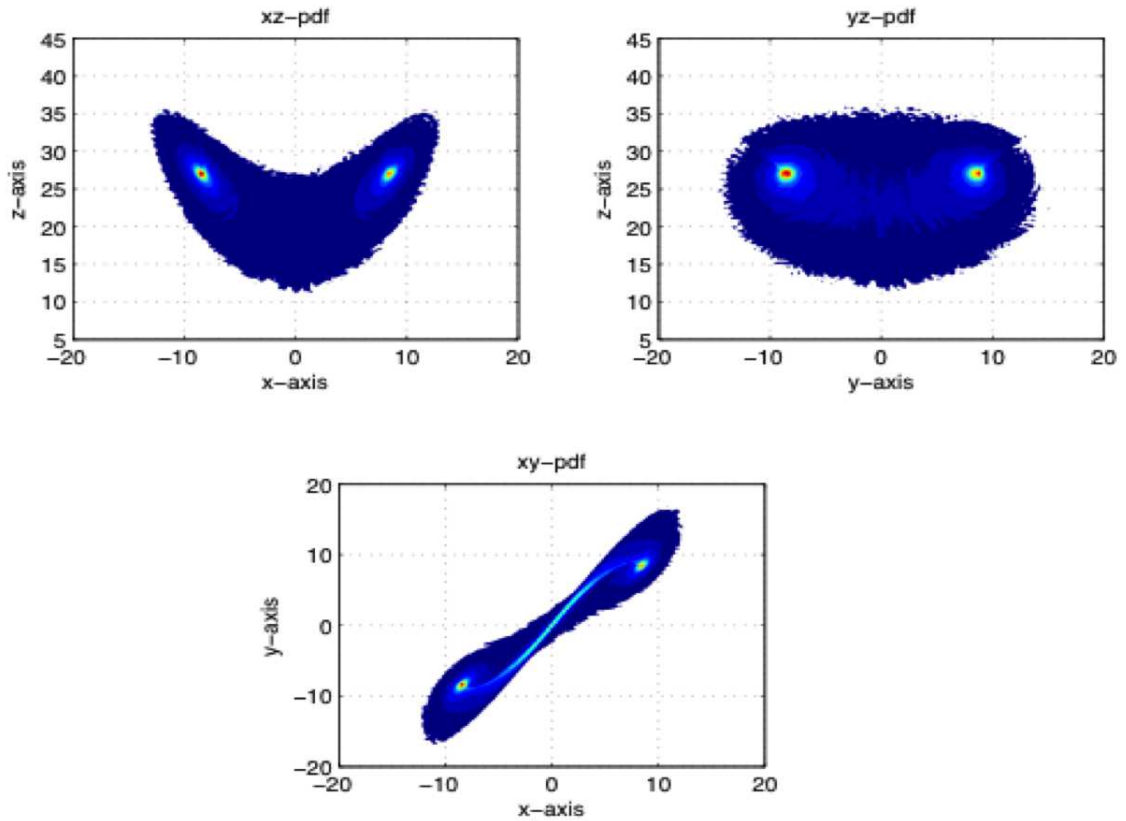


Figure 6.24: Probability density distributions for the Lorenz-Salzman model for the three different 2D-planes. Red colors mark high probability densities.

3. Non-periodic flow:

The time evolution of the system is non-periodic, which means:

$$\vec{X}(t_1) \neq \vec{X}(t_2) \quad \forall t_1 \neq t_2$$

This implies the system never reaches the same point twice. To understand the implications, consider that it would reach the some point twice:

$$\vec{X}(t_1) = \vec{X}(t_2) \quad t_1 \neq t_2$$

From this it follows that the tendencies at the two points in time are the same too:

$$\implies \frac{d}{dt} \vec{X}(t_1) = \frac{d}{dt} \vec{X}(t_2)$$

If $t_1 < t_2$ and $\Delta t = t_2 - t_1$ then the system will reach point t_1 again after Δt , because the tendencies are exactly the same for t_1 and t_2 :

$$\implies \vec{X}(t_2 + \Delta t) = \vec{X}(t_1)$$

Thus the system would be periodic. So the fact that the system never reaches the same dynamical point twice implies that the system is non-periodic and thus it is chaotic.

Deterministic chaos: The system is called Deterministic chaos, because it is both deterministic and chaotic.

Deterministic: The tendency equations are exactly defined if the state of the system is known.

Chaos: The time evolution beyond a given time interval cannot be predicted, no matter how well the initial state of the system is known.

4. Chaotic time evolution:

The non-periodic time evolution is only predictable up to a certain time period into the future, depending on how precisely the initial condition is known and how precisely the tendencies can be numerically estimated.

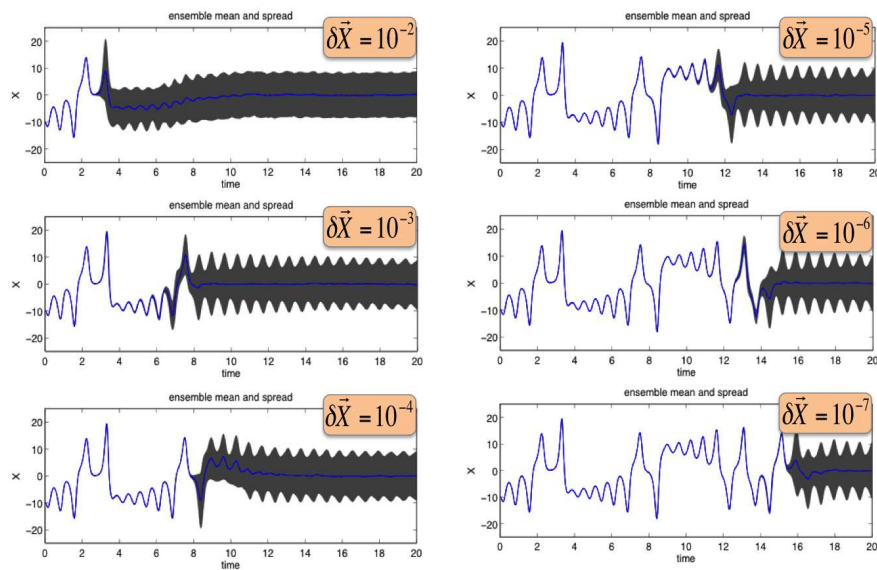


Figure 6.25: Forecast initial state uncertainty: In all six panels a very large ensemble or simulations are started at time zero with each have slightly different initial conditions for the Lorenz model. The spread in the initial conditions are given in each panel by the δX values. The ensemble mean is shown by the blue line and the spread is marked by the gray shaded area. In the first part of each time series the gray shaded area is not visible as the spread is smaller than the width of the blue line.

The best way to illustrate this is by example: Let assume we follow the time evolution of a large ensemble of slightly different initial states of the system, see Fig. 6.25. at the beginning the ensemble will follow the same time evolution, until a point in time from which they spread out and follow different time evolutions. How long the ensemble of slightly different initial conditions stays

together depends on how close to each other they are at the initial state. Thus it depends on how well we did know the initial state, see Fig. 6.25. No matter how well we know the initial state, there will always be a time from which the ensemble spreads out and basically fills out all likely points in the dynamical space. When the spread is as big as the probability distribution, then we have essentially no prediction skill any more. We can see in Fig. 6.25 that we can decrease the initial spread by a factor of 10,000 (from 10^{-3} to 10^{-7}), but the time period over which the system stays predictable (the ensemble shows no spread) only increases by a factor of 2. The prediction reaches a very hard to pass threshold. The system is essentially (in all practical real world situation) unpredictable beyond a certain point no matter how well you observe it or how well your weather forecasting model is.

This has also some practical real world implications: If you, for instance, change the temperature at one point (out of 1 million points) for a global numerical weather prediction model from $T = 15.35296826^{\circ}\text{C}$ to $T = 15.35296825^{\circ}\text{C}$, then the simulated weather will be completely different within 10 days everywhere in the world. This is also often described by: the Butterfly in New York that make a different turn, which changes the weather everywhere in the world within two weeks.

This characteristic of the climate is used to generate ‘ensemble’ forecasts. The ensemble forecasts are used to give a distribution of the predicted weather evolution, from which often only the mean evolution is used as the best forecast. The spread of the distribution gives some information of how reliable the forecast is.

How fast the ensemble spreads and how fast the system becomes unpredictable also depends on the initial condition itself, see Figs. 6.26 and 6.27. Here we have three different starting point for the ensembles. We can see that the ensemble spreads quit fast in the starting point between the two attractors, but stays much longer together for the other two starting points. This is similar to real world weather forecasts, some weather situations are more predictable, some are changing faster and some are more stable.

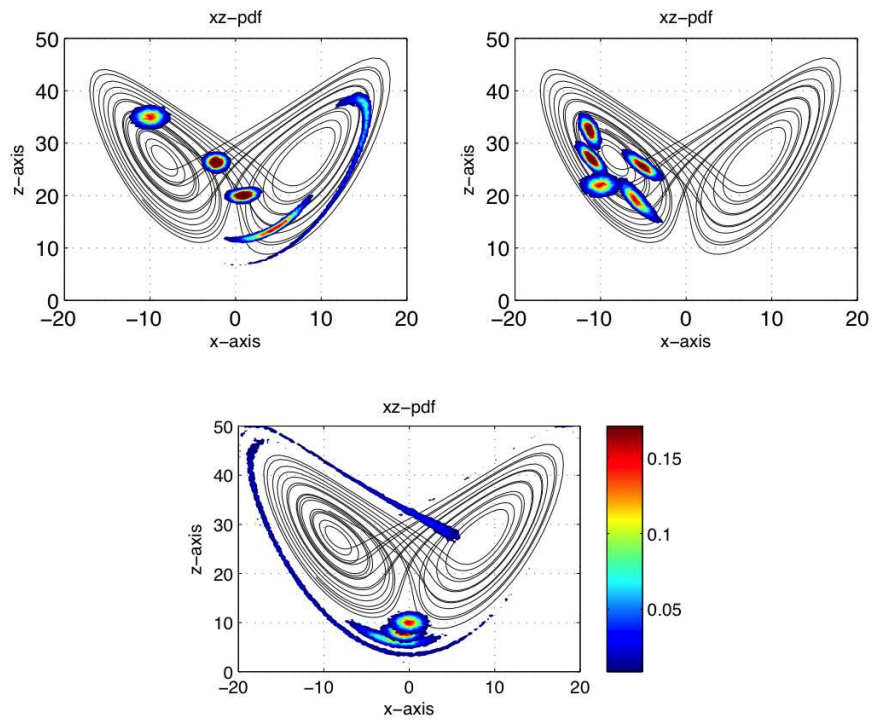


Figure 6.26: Forecast ensembles

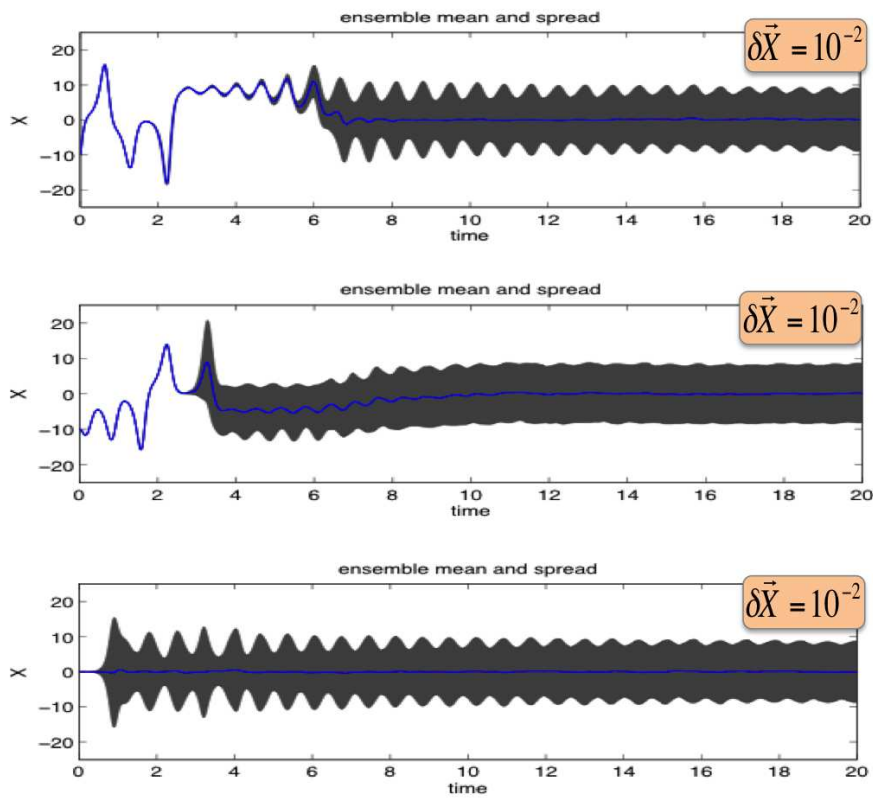


Figure 6.27: Forecast: Different initial states

5. Numerical uncertainty:

- The Lorenz system of differential equations has no general analytical solution, it must be estimated with numerical approximations.
- $\frac{dX}{dT} \sim \frac{\Delta X}{\Delta t}$
- Predictability limited by numerical precision of the computers.
- Given perfect initial state information, different computers of the exact same model will produce different time evolutions of the system, in the same way as small differences in the initial conditions would cause them.

5. Non-linear response to forcing:

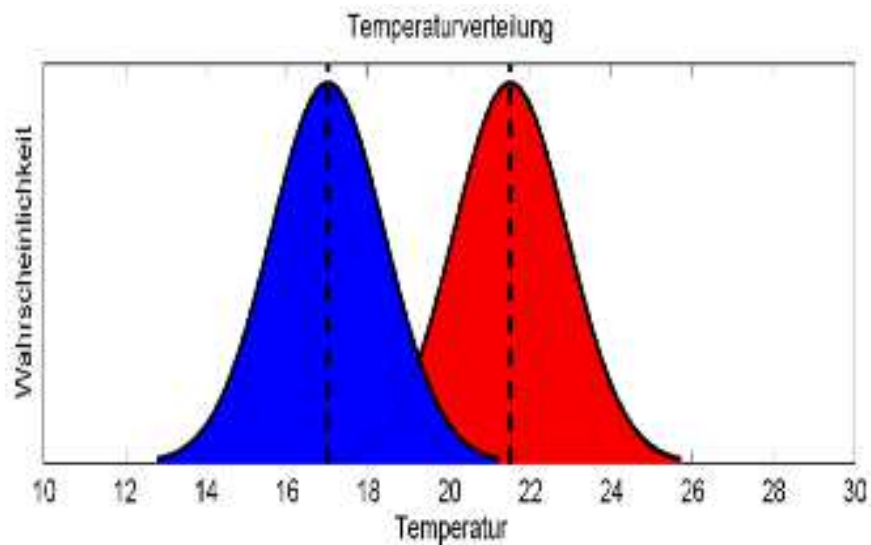


Figure 6.28: Simple linear model: distribution shifts, but does not change shape

If we warm the climate we would to first order assume that the probability distribution of temperature would just shift to higher values without changing its shape, as sketched in Fig. 5.36. However, complicated non-linear systems can respond quite differently to warming forcing. Fig. 6.29 shows the non-linear response of the Lorenz model to external forcing in X . We can see that the distribution shifts to higher values, as expect if a positive forcing in X , Fx , is added to the tendency equation of X . But most importantly it also changes its shape, which counter acts the overall shift. The distribution shifts overall to the right, but the left peak gets stronger and the right peak gets weaker. Thus while shifting to higher values the regime of the lower values become more likely, which is counterintuitive.

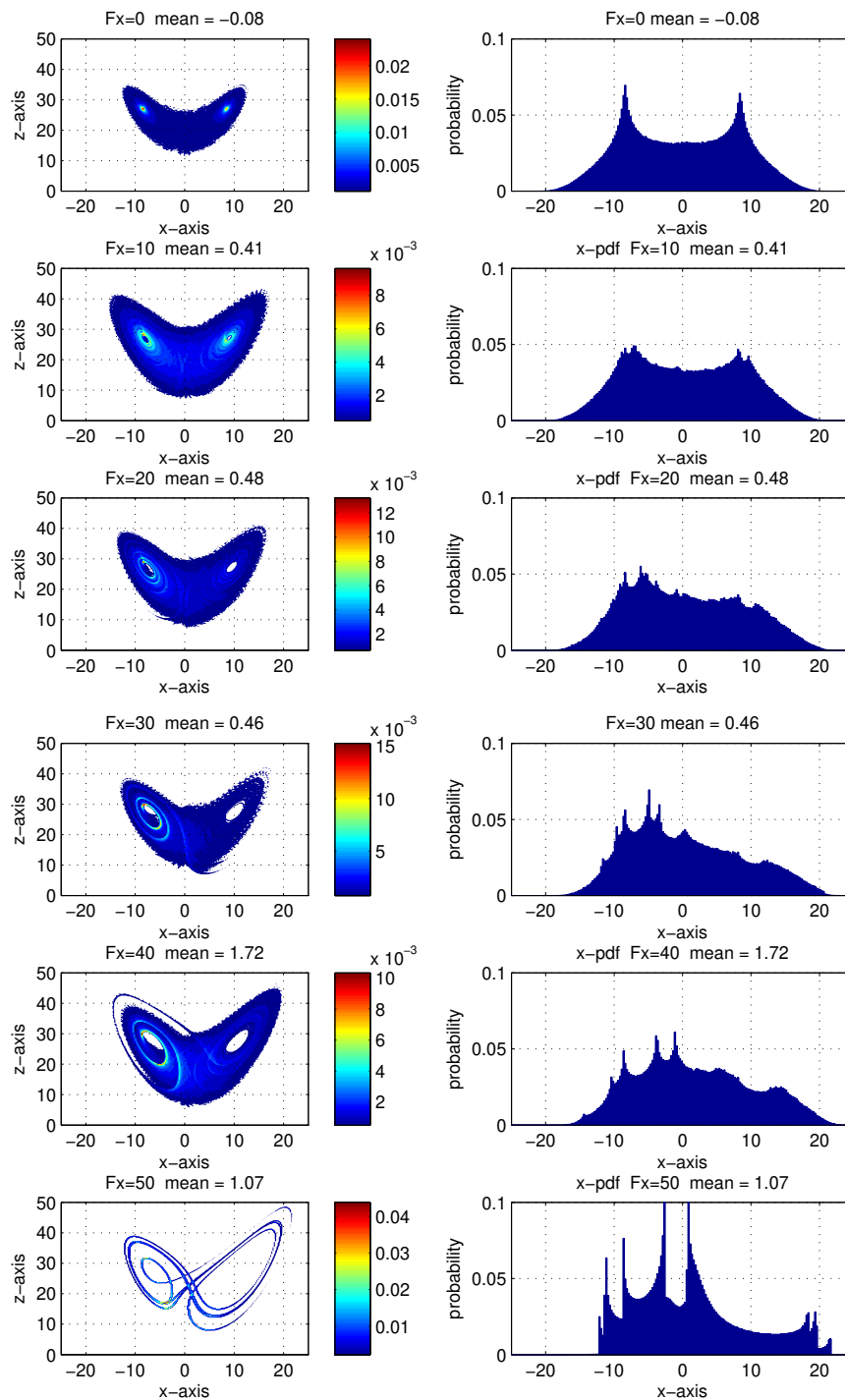


Figure 6.29: Non-linear response to external forcing: In each row we added a different positive forcing Fx to the tendency equation of X in the Lorenz model. We can see that the distribution shifts to higher values, but most importantly also changes its shape, which counteracts the overall shift. Note that the distribution shifts overall to the right, but the left peak gets stronger and the right peak gets weaker.

Lorenz model conclusions

- Non-linear dynamics of convection, cause convective systems to be chaotic.
- They never reach an equilibrium and therefore always vary.
- This is basically describing the variability of weather.
- The weather variability is the primary source of natural internal climate variability.
- This small spatial scale and short time scale variability is a forcing for large-scale and long time scale variability.

6.3 The Stochastic Climate Variability

Natural internal climate variability that does not result from any particular external forcings can in general be described as stochastic climate variability, where stochastic here means it involves randomness. The randomness of climate variability on the large scale and the longer time scales ultimately results from the weather dynamics on the shorter time and smaller spatial scales. The inherent chaotic behaviour of the weather dynamics, as discussed in the Lorenz model are the primary source of natural internal climate variability.

We will start our discussion of the stochastic climate variability by defining the power spectrum. The power spectrum of climate variability will help us to understand the time scale behaviour of climate variability. This helps us to define some specific time scale behaviours such as pure random noise, which is often called white noise. We will then define some simple stochastic climate models, including the red noise climate model. This is in particular relevant for the climate variability in the extra-tropical regions on time scales from months to about a thousand years. We will discuss some specific characteristics of the extra-tropical time scales behaviour. Finally, we will have some discussion of the spatial organisation of climate variability. Here we will first discuss how we can describe spatial patterns of variability and then we will define some simple null hypothesis for the spatial structure of stochastic climate variability.

6.3.1 The Power Spectrum

In section 6.1 we have seen that the amount and spatial structure of variability is different at different time scales. In Fig. ?? we tried to quantify this by plotting the standard deviation of different time series as a function of time scale. We will now discuss how this is done in a more quantitative way. The most commonly used approach to quantify the amount of variability as a function of time scale is the *Power Spectrum*.

We don't want to go into the mathematical details of how the power spectrum is defined or how it is estimated. Here we just define it as:

Power Spectrum, $\Gamma(\omega)$, of a time series: Variance (squared amplitude or standard deviation) per frequency, ω :

$$\Gamma(\omega) = \frac{\text{Var}(\omega)}{\omega} = \frac{\sigma^2}{\omega}$$

The total variance of the time series is the integral of the power spectrum over all frequencies:

$$\text{Var}(\text{timeseries}) = \int \Gamma(\omega) d\omega$$

So the area underneath the power spectrum curve can be interpreted as the total variance over the range of frequencies (note: only in linear plotting). Thus, a power spectrum is estimating how much each frequency contributes to the variability (variance) of the time series. This concept is used in many fields of research. For instance, in physics we know this for estimating the power (or variance) of electromagnetic or acoustic waves. If we have a time series of the electromagnetic field (e.g. waves of light) or pressure in the atmosphere (e.g. acoustic waves) we can compute the power spectrum of it, which tells us at which frequencies or wave lengths the electromagnetic field (e.g. waves of light) or pressure in the atmosphere (e.g. acoustic waves) have the strongest amplitudes (power or variance). In climate variability we may be interested in the frequencies or periods at which climate (e.g. temperature) varies.

Time Scales / Power Spectrum

The power spectrum is a very useful concept for understanding the time scale behaviour of climate variability. However, it needs to be noted that reading or interpreting the power spectrum is often not as simple as it may seem. It requires some experience to understand how to read the power spectrum. The best way to understand the power spectrum is to discuss some examples.

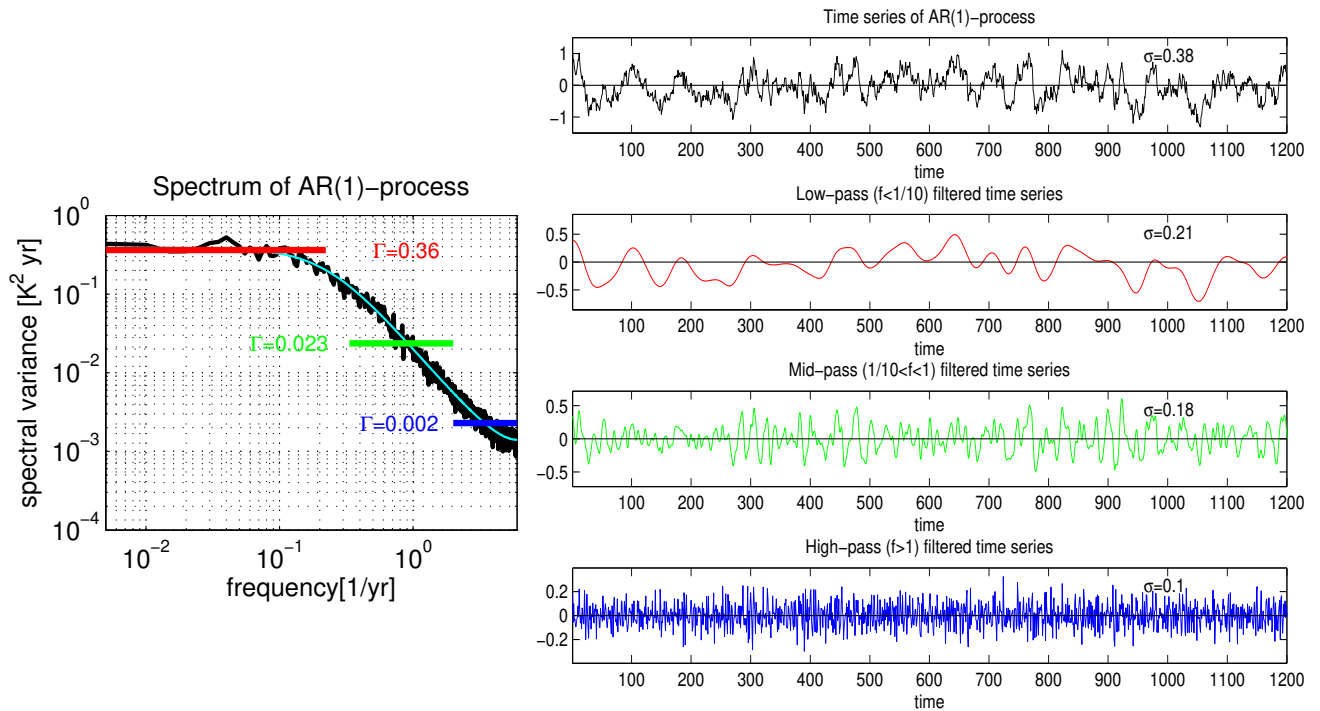


Figure 6.30: Time series vs. spectrum: This figure illustrates how the power spectrum, $\Gamma(\omega)$, as a function of frequency, ω , (left) of a time series relates to the time series itself (upper right). In the right column the three time series below the original time series are frequency band-pass filtered time series of the original time series. The three added together build to original time series. The frequency band that each of the three filtered time series represent are marked by the matching coloured lines in the power spectrum. Note, that the y-axis range on the right column are different for different time series. The average of $\sqrt{\Gamma(\omega) \cdot \omega}$ for each of the three frequency bands equates the standard deviation (σ) of each band-pass filter time series.

In Fig. 6.30 we illustrate how to read a power spectrum of a time series of climate variability. The time series (upper right panel) was created by a stochastic process called auto-regressive process of first order (AR-1 process; also called red noise). The details of this process are not important for now, but are discussed more in detail in subsection 6.3.3. The advantage to using a well defined theoretical process like the AR-1 process is that we know the theoretical power spectrum, which is shown in Fig. 6.30 together with the estimate based on the time series shown.

An important first characteristic that we can note is that the estimated power spectrum of the time series fluctuates around the theoretical one. This looks similar to how the time series fluctuates around zero. However, this is a very common point of confusion when reading the power spectrum. The fluctuations in the estimated power spectrum are of a different nature than those in the

time series. Figure 6.31 tries to illustrate this by showing the power spectrum estimate from the same time series, but with different length. The estimated power spectrum fluctuates around the theoretical expectation, because we have not used enough data to estimate the power spectrum (our time series is too short). If we would have an infinitely long time series to estimate the power spectrum then the uncertainties in it would disappear and it would converge towards the theoretical power spectrum. In contrast, the time series fluctuations around zero are our signal of interest. The fluctuations would not change its amplitude or 'noisiness' when we increase the length of the time series. They are inherent to the stochastic process. In summary, we need to understand what is the signal in the estimated power spectrum, which would be the underlying theoretical curve and what is the noise due to a limited amount of data. If we understand what the uncertainty level is, then we need to only read the smooth evolution of the estimated power spectrum that is not effected by the noise level. Thus we should not read every limit bump (peak) in it, which are just 'random' uncertainties.

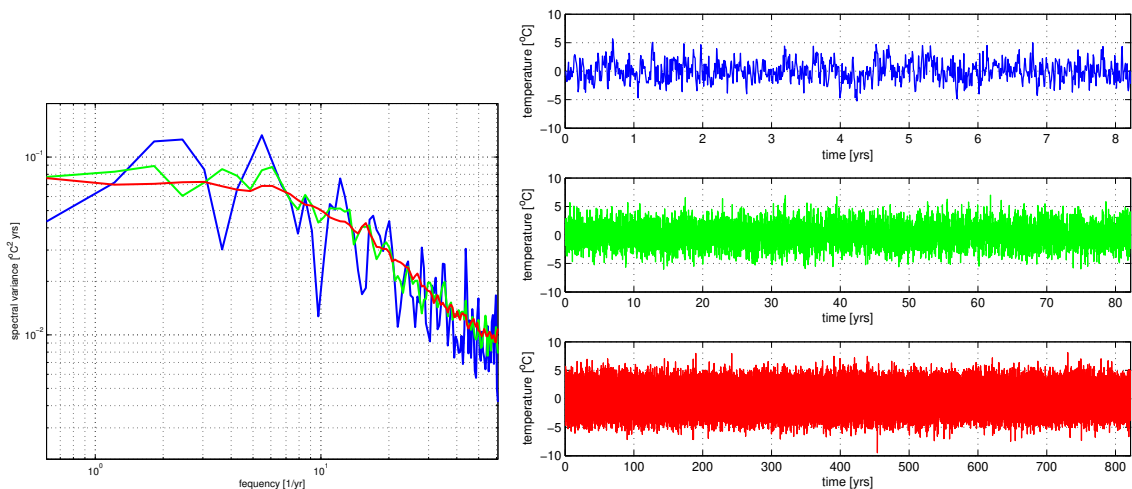


Figure 6.31: Noise level in spectrum: Power spectra of the same time series using three different length of the time series to estimate it (left). The different sections of the time series used are shown in matching colours (right). Note, that in the time series the level of noise is always the same, as the 'noise' is what we are interested in. In the power spectrum the level of 'noise' is a function of the length of the time series used to estimate it. The noise in the power spectrum is not what we are interested in and it is an uncertainty or error.

Coming back to Fig. 6.30 we can see how to read the power spectrum. We can note that the time series shown (upper right in Fig. 6.30) has variations of all kind of different periods or frequencies. It is chaotic, but we also note that maybe some of the longer period (about 50 to 100 time units) variations have larger amplitudes than the shorter period variations (2 to 10 time units). This is captured by the power spectrum by showing that it is larger for small frequencies (which is equivalent to saying longer periods) and smaller for larger frequencies (shorter periods). If we are interested of the standard deviation (amount of variability) in a certain frequency or period band interval, we can just integrate the power spectrum over this interval. For instance, the variability for frequencies lower than 0.1 (thus periods longer than 10; the area marked by the red line in power spectrum of fig. 6.30) has a standard deviation of:

$$\sigma \approx \sqrt{\Gamma(\omega) \cdot \omega} = \sqrt{0.36 \cdot 0.1} \approx 0.2$$

which is roughly the standard deviation for the low-pass filtered time series shown in Fig. 6.30

(red line; second time series from above). Similar calculations lead to the standard deviation of the other two filtered time series.

We now want to look at a few more examples of how the power spectrum describes the time scale behaviour of time series of climate variability. We started the introduction to climate variability with time series of Melbourne temperature variability (Fig. 6.3) and tried to quantify strength of the variability at different time scales by plotting the standard deviation as function of the period length (Fig. 6.5).

In Fig. 6.32 we compare our first guess approach against the now defined power spectrum. Note, the power spectrum has the x-axis flip relative to our first guess estimate of time scale behaviour (left in Fig. 6.32), since the power spectrum is a function of frequency, while our first guess was a function of period length. Further we can also note, that the y-axis values are flip too. The large values on short time scales in our first guess are now small values on large (high) frequencies. This is because the power spectrum is variance per frequency. So it appears smaller is frequencies are high.

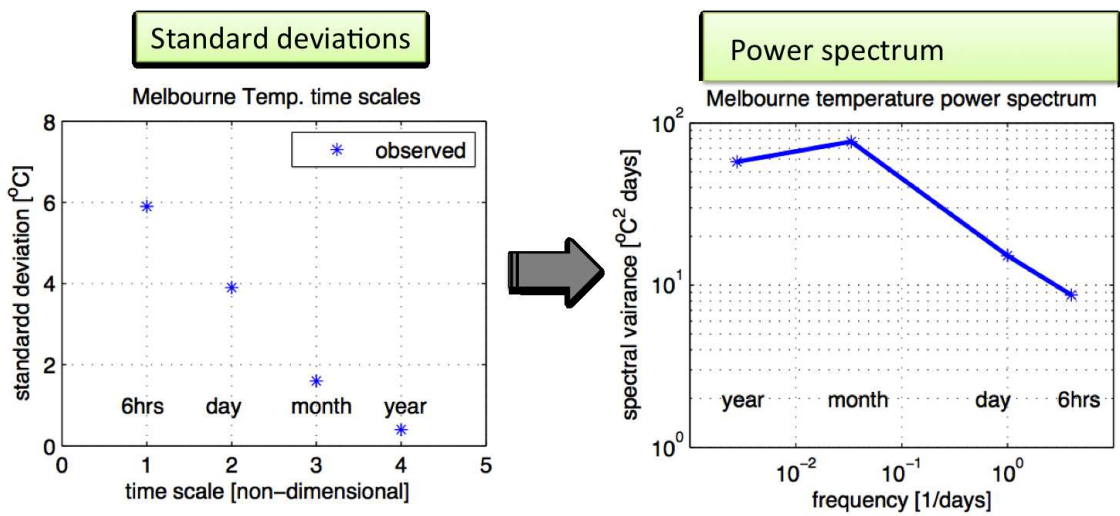


Figure 6.32: Comparison of our first guess estimate of time scale behaviour (left) from Fig. 6.3 and 6.5 against a power spectrum (right). Note the x-axes are reversed and the power spectrum has the largest variance on the long periods (years) where the standard deviation of mean time series is smallest.

In Figure 6.33 we show the time series and power spectrum of daily mean surface temperature variability in Melbourne, including the seasonal cycle. We can clearly see the peaks of the seasonal cycle. There are actually two peaks: One at $1/365$ days and one at $2/365$ days. This reflects the fact that the seasonal cycle in Melbourne is not a perfect harmonic oscillation (e.g. sine or cosine function). It could indicate, for instance, that either winter or summer are longer. This would be reflected in the power spectrum by the enhanced power at sub-harmonic variations of the main (annual) cycle. In this case it is the second peak at $2/365$ days.

In addition to the two peaks of the seasonal cycle, we can see continuous background power spectrum. This is a bit noisy, due to the limited length of the time series to estimate the power spectrum, but if we eyeball the smooth version of this background power spectrum, then we see a more or less constant power spectrum from low frequencies to about $1/10$ days and then a decrease to lower values for higher frequencies. This background power spectrum marks the natural variability in the data unrelated to the seasonal cycle. It is the power spectrum of weather variability in Melbourne. The increase in power from $1/2$ days to $1/10$ days suggests that the weather time scales is longer

than 2 days, as there is more power on longer time scales. At about five days periods is where the power spectrum becomes flat, and this period (or frequency) indicates the dominant time scale of weather variability in Melbourne.

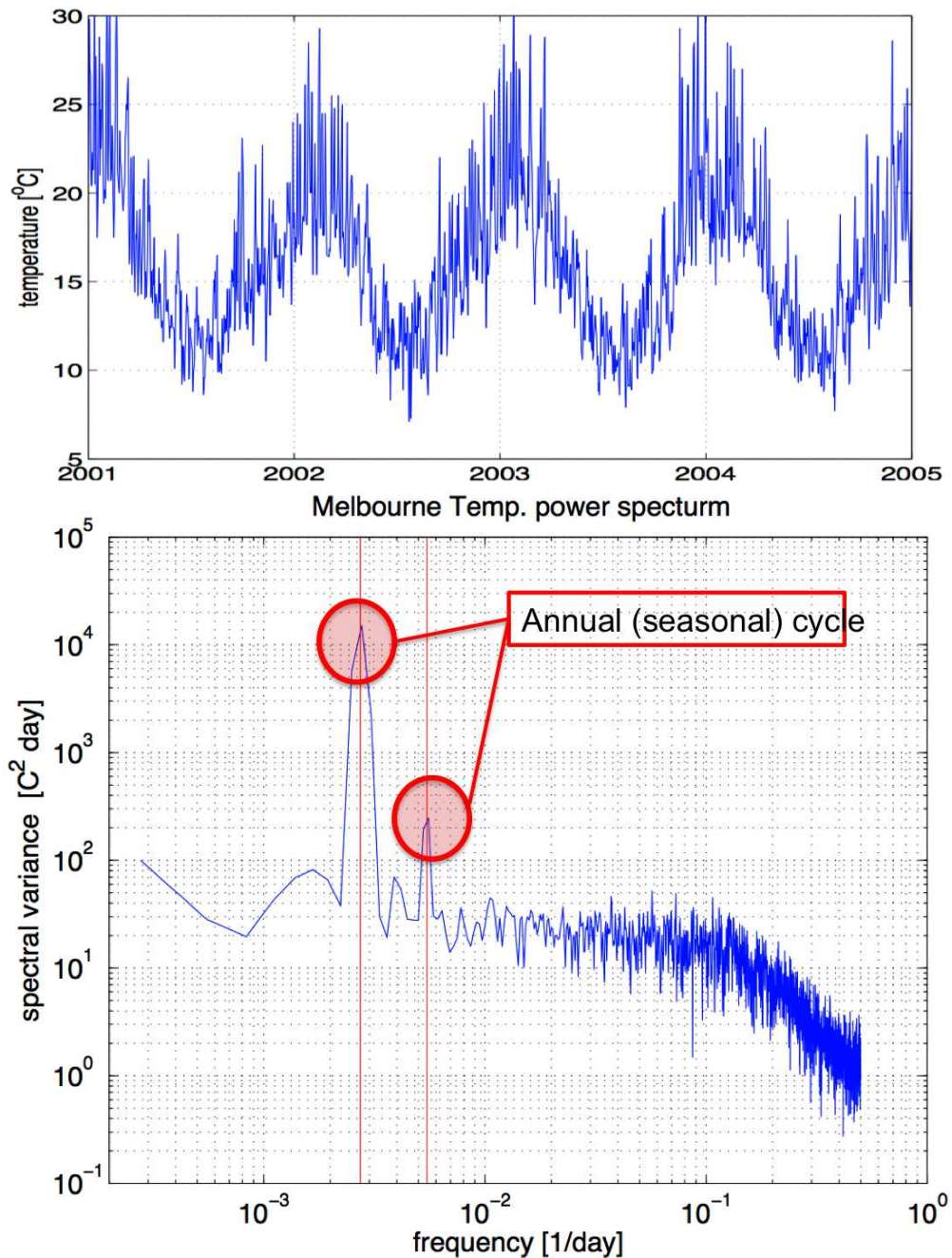


Figure 6.33: Melbourne spectrum: Time series of daily mean surface temperature variability, including the seasonal cycle, for four years (upper) and the power spectrum estimated from this time (lower). the vertical red lines mark the annual cycle ($1/365$ days) and semi-annual cycle ($2/365$ days).

So far we have presented the power spectrum in log-log scale. In Figure 6.34 we show the spectrum of monthly mean equatorial east Pacific (El Nino) SST in log-log scale and linear-log scale. There are few differences that we can notice in the two presentations of the same power spectrum: First of all we should recall that the area underneath the curve of the power spectrum is the variance.

However, this only holds for a linear presentation, not for the log-log presentation. Though, it does hold for the log-linear presentation (right in Fig. 6.34), because we scaled the power spectrum by multiplying it with the frequency. This 'trick' allows us to interpret the area underneath the curve as variance in this log-linear presentation.

Here we can clearly note that most of the variance of the equatorial east Pacific (El Nino) SST is in the interannual time scales (between 1/10yrs to 1yrs). This is not clear in the loglog-scale presentation, as this presentation seem to suggest that there is a lot of variance on low frequencies (long periods: $< 1/10$ yrs) and high frequencies (short periods; > 1 yrs). This marks a disadvantage of the log-log-scale presentation.

The power spectrum of the SST time series is also compared against a theoretical 'red noise' power spectrum with an uncertainty range. The uncertainty range is constant (not a function of frequency) in the loglog-scale, but changes proportional to the value of the theoretical 'red noise' power spectrum in the log-linear presentation. This marks a disadvantage of the log-linear presentation. When the power spectrum values are larger, than the uncertainties are larger too. This often leads to the problem that one may over interpret 'peaks' in the power spectrum that are actually only noisy fluctuations due to the limited amount of data used to compute the power spectrum. So, we see that in order to read the power spectrum properly one may need to be aware of some characteristics of it and some times it may help to plot the power spectrum in different ways.

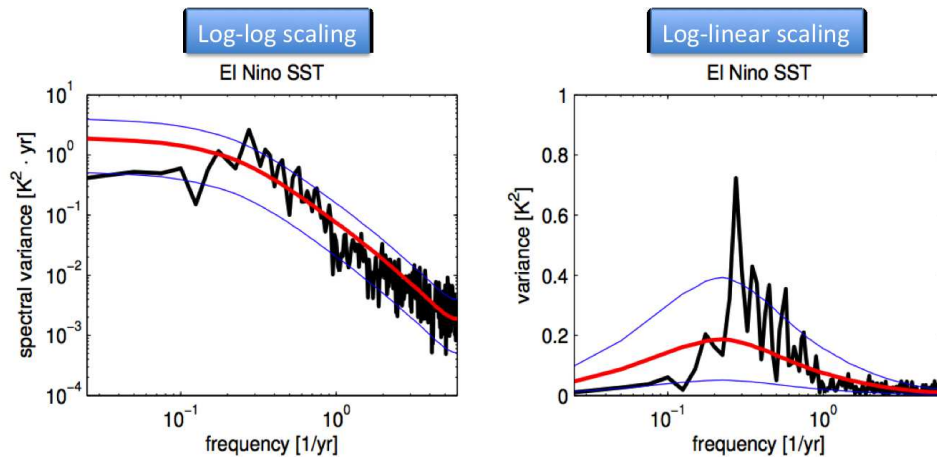


Figure 6.34: Power spectrum of monthly mean equatorial east Pacific (El Nino) SST (black lines): in log-log scale (left) and linear-log scale (right), with the power spectrum multiplied by frequency on the y-axis in linear scale. For comparison a theoretical 'red noise' power spectrum is fitted to the data (red lines) and the 90% confidence intervals for the statistical uncertainties are shown (blue lines).

Figure 6.35 show the time series and corresponding spectra for observed monthly mean temperatures in the atmosphere and ocean. The power spectrum show some interesting aspects. The atmospheric power spectrum is mostly flat, indicating that the variance on all frequencies is the same. This is also called white noise, see discussion further below. It is also much stronger on higher frequencies than the SST or subsurface ocean temperatures.

The SST and the subsurface ocean temperature variability increase from high frequencies towards lower frequencies. This is in particular true for the subsurface ocean temperatures. The variance of the subsurface ocean temperatures at high frequencies (1/2month) is several orders of magnitude smaller than the variance at low frequencies (1/10yrs). Interestingly, the variance of all three time series is about the same for all at frequencies of 1/5yrs or lower (longer periods). This indicates

that these three time series are actually interacting and that the variability in each other is related to each other. If that is true, one would expect that on the longer time scales (frequencies $\leq 1/10$ yrs) the atmospheric temperature variance should increase by the same amount as the subsurface ocean temperature variance does.

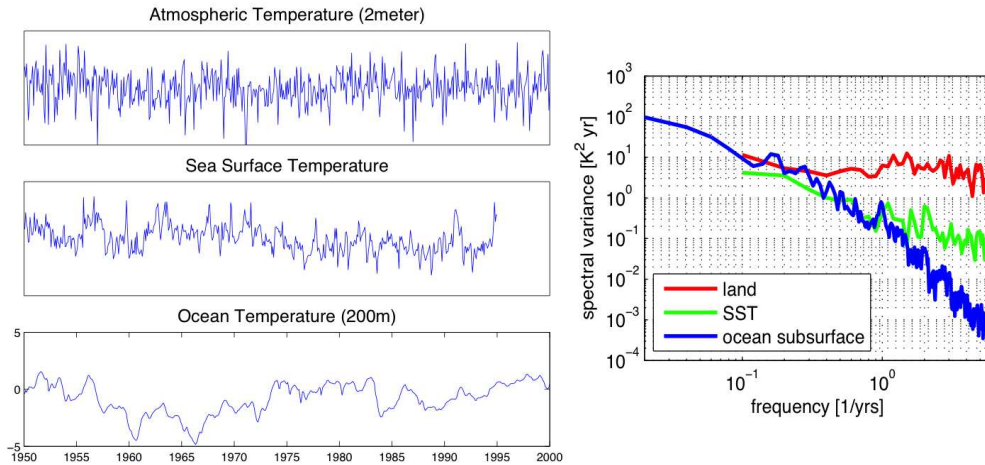


Figure 6.35: Time series (left) and corresponding spectra (right) of observed monthly mean temperature anomalies from 1950 to 2000 for atmospheric 2m temperatures in central Asia (upper left; red right), SST in the North Atlantic (middle left; green right) and the 200m depth ocean temperature in the North Atlantic (lower left; blue right).

6.3.2 White Noise

A power spectrum that is constant (flat) has the same amount of variance for all frequencies (see right Fig. 6.36). This power spectrum is called *white*, in reference to the power spectrum of visible light (time series of the electromagnetic field) where all wave length (different colors; frequencies) are about equally strong. Light with all colors equally strong is called white light.

A time series of pure random numbers has a white power spectrum. That is, each value of your time series is a random number unrelated to any of the previous values of the time series. Since a white power spectrum is the result of a time series of purely random numbers, we call it a *white noise* power spectrum. In turn, a time series of purely random, unrelated numbers is called a white noise time series.

Obviously a time series of purely random numbers does not have any predictable part in it. So a white noise power spectrum is an indication of climate variability that has no predictable variability in it. In turn, a power spectrum of climate variability that is not simply white noise (not just flat) could indicate some interesting or predictable part of the climate variability.

If we transfer white power spectrum back to our first guess approach, where we plot the standard deviation of time mean time series vs. the time scales of the averaging interval (Fig. 6.36) we can see that a time series of a white power spectrum has larger amplitudes for shorter time means (days) and smaller amplitudes for longer time means (annual). This may seem a bit counter-intuitive, but it is related to the nature of averaging random numbers. This is, in statistics, also known as the central limit theorem, which states that the mean of N random events has a spread of $\sigma_{mean}^2 = \frac{\sigma^2}{N}$, where σ is the spread of the individual random numbers.

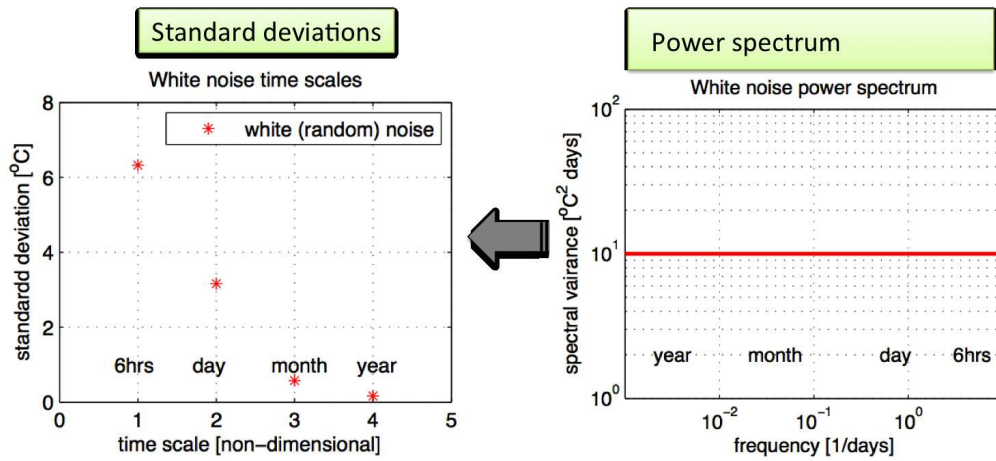


Figure 6.36: White noise. Note the x-axes are reversed and the white noise power spectrum has the largest standard deviation for time series with the shortest sampling period.

Integrated weather variability

Is the long time average variability of Melbourne temperatures just the sum of many random weather events? Thus is the variability of Melbourne temperatures just white noise?

- Thus we expect the long time mean of random weather events to have decreasing variability (standard deviations) proportional to $\sqrt{\frac{1}{N}}$
- We can roughly assume that weather events last for about 3 days $\rightarrow N = 10$ for a monthly time series and $N = 120$ for annual mean time series.
- Melbourne temperature variability is mostly the sum of random weather events (not explaining the linear warming trend).
- The sum of random weather events is a decent first order assumption for climate variability on land, but some additional variability unexplained by random weather events exists.

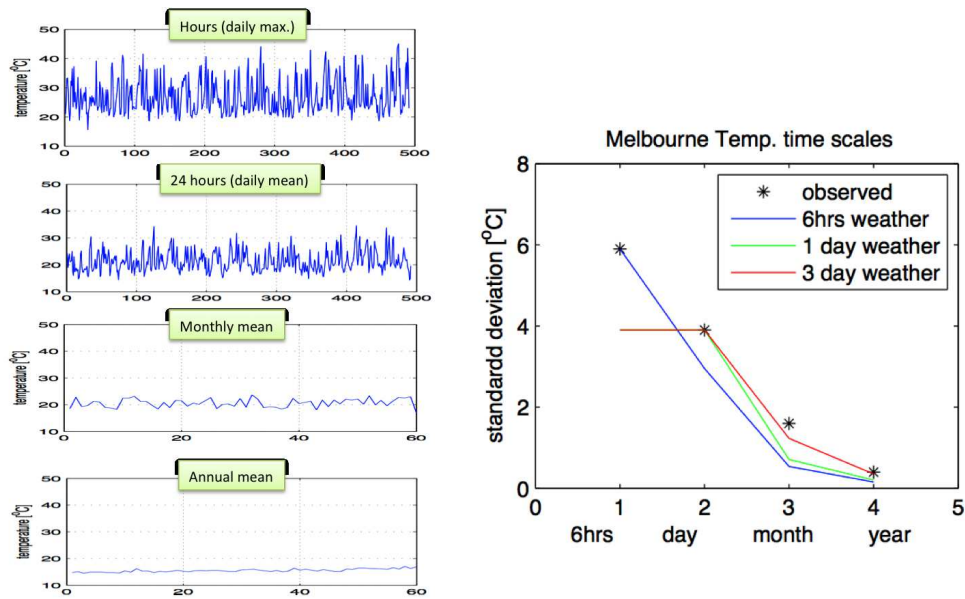


Figure 6.37: Melbourne climate variability

6.3.3 The Stochastic Climate Model (Red Noise)

Stochastic = random

Stochastic model = A model that involves random values.

Climate variability is, in general, not purely random (white noise). We have already looked at a few power spectra and most of them were not white noise (e.g. Figs. 6.33 and 6.35). We now like to take a closer look at stochastic climate variability and develop a first guess idea of how most of the long term climate variability can be explained.

Figure 6.38 shows three examples of climate variability time series. Each of the time series is an anomaly time series with each value presenting an annual or seasonal mean of a climate variable. If the data were pure white noise we would expect the values to fluctuate around zero with changing signs often. However, in each of these time series we can notice that there are periods of ten or more years where the climate anomalies stay on the same sign (e.g. AMO index from 1930 to 1960 is nearly always positive). This is extremely unlikely to happen by chance for a white noise process. Thus, it indicates that these variations are not purely random in time.

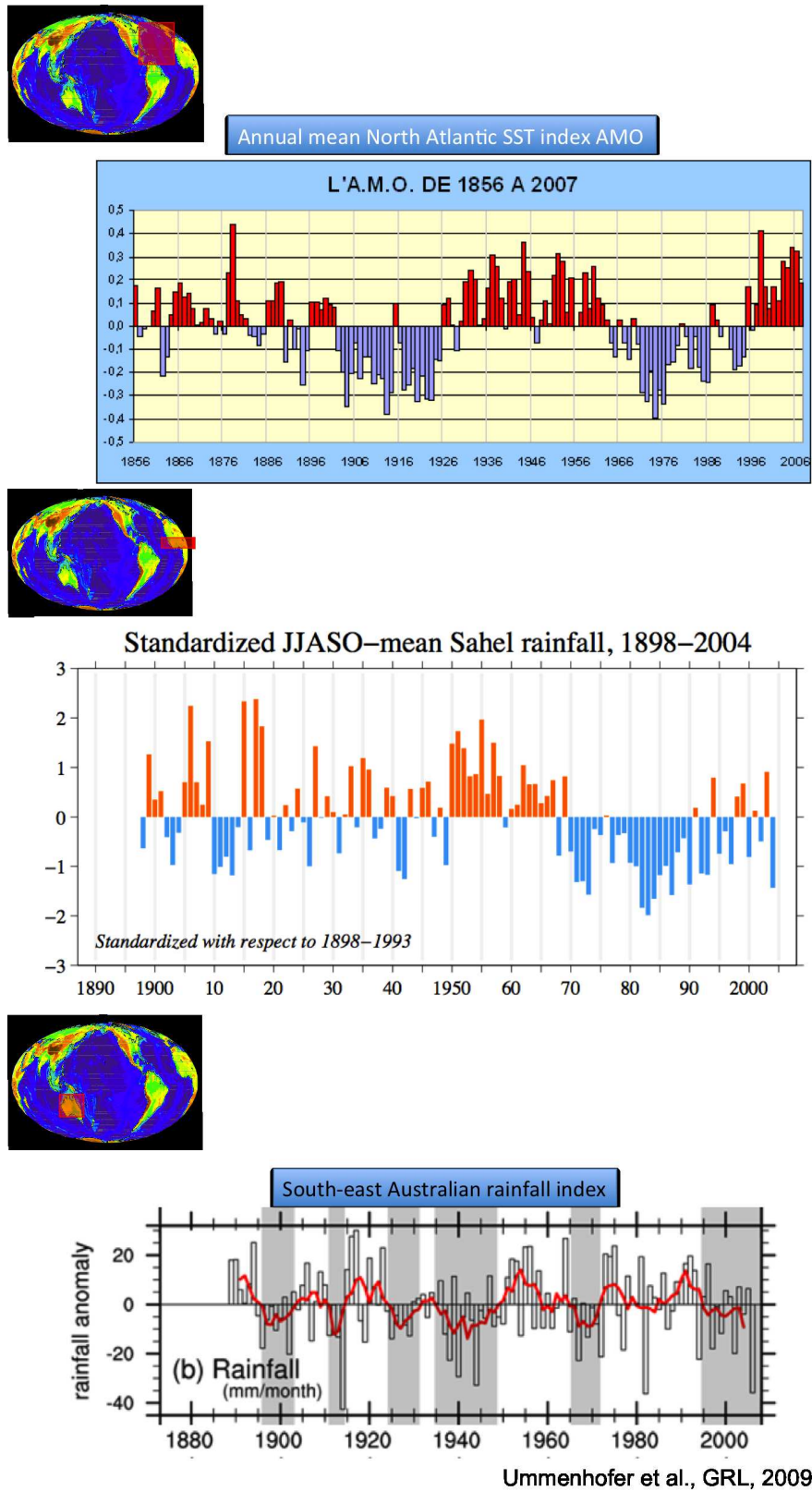


Figure 6.38: examples of climate variability time series that are not just white noise (purely random in time). Upper: Annual mean North Atlantic SST also known as the Atlantic Multi-decadal Oscillation (AMO) index from 1856 to 2006. Middle: Standardised JJASO-mean Sahel rainfall, 1898-2004. Lower: South-east Australian rainfall index from 1890 to 2005.

So, if the variability is not white noise (just random weather events averaged) then where does these long time variations come from? A good first order explanation for these long term variations are given by Hasselmann's stochastic climate model idea (1976). Also known as *Red Noise*.

Idea: The *fast* dynamics, such as atmospheric weather dynamics as describe in the Lorenz model, can force variability in the *slow* dynamics on longer time scales. The slow systems of the climate are the oceans, glaciers, biosphere, biogeochemistry or any subsystem those time scales are longer than months. The variability of the fast dynamics are, on the time scales of the slow system (month or longer), random fluctuations (white noise). So, the short time weather can cause long time climate variations in the slow systems of the climate. These long time variations in the slow systems of the climate can then feedback onto the fast systems (e.g. the atmosphere or land surface climate) and cause long time variations in the fast systems too.

Important conclusion: Climate can vary on long time scales without a cause (external forcing), simply due to the weather variability that exist on the shorter time scales. It notes the importance of internal climate variability.

Alternative idea (before Hasselmann): Every variation in a slow system has an external cause. For instance, if a glacier grows or melts, then this must be forced by some changes in the external boundary conditions (e.g. changes in solar radiation).

The climate models (equations) that we have worked with so far are deterministic models, which do not involve random numbers, but only involve exact values for all variables. In general our models look like this:

$$\frac{dX(t)}{dt} = A(X(t), Y_i(t)) + F(t) \quad (6.1)$$

with

$X(t)$ = time evolving climate variable (e.g. T_{surf})

$Y_i(t)$ = other time evolving climate variables (e.g. humidity, T_{atmos})

$A(.)$ = some kind of function

$F(t)$ = some kind of external forcing (e.g. sun light)

The tendency equations are exactly defined by the current state of the system.

In stochastic models the tendency equations involve random values that are purely chaotic (following some distribution) and which are not defined by the current state of the system.

Often the AR(1)-rocess is used as the simplest stochastic model null hypothesis for the climate variability: *Red Noise null hypothesis*.

In the Red Noise null hypothesis the system is linearly damped and forced by white noise (random weather).

By comparing the observed climate variability with a fitted red noise procedure one can get a good first idea about the dynamics of the system.

In general:

$$\frac{dX(t)}{dt} = f_m(t) * A(X(t), Y_i(t)) + f_a(t) \quad (6.2)$$

$A(.)$ = slow dynamics relative to Δt

f_m, f_a = fast dynamics relative to Δt

f_m = multiplicative noise

f_a = additive noise

Simple red noise null hypothesis:

$$\frac{dX}{dt} = -c * X + f \quad (6.3)$$

- A red noise system integrates the white noise forcing and thereby produces low-frequency variability.
- *Note:* Forcing and the climate variable have different units in the red noise model. Therefore a red noise model could be interpreted in two ways, depending on the interpretation of the forcing.
- *Integrator:* The climate system integrates the random forcing to produce much larger low-frequency variability than the forcing would suggest (e.g. glaciers or river run-off).
- *Damping/Inertia:* The climate system damps the random forcing by its large inertia, thereby leading to less high-frequency variability than suggested by the forcing. But on longer time scales (low-frequency) forcing and climate system are varying equally strongly and in phase (e.g. oceans or slab ocean model).

Red noise:

- The time scales of a red noise process are defined by the damping parameter c .
- The time scale of a red noise process basically describes how long the variability will be of one sign; how long the variability will be on one side of the zero line.
- For a red noise process this describes the *persistence* of the variability. The frequency at which the power spectrum gets flat, roughly sets the persistence time scale.
- For periods much longer than the persistence time scale the time series can be considered white noise.

Examples:

Weather persists for about 3 days. On time scales of months, weather can be considered white noise.

Sea surface temperatures persist for months to years. On time scales of 1000 years can be considered as white noise.

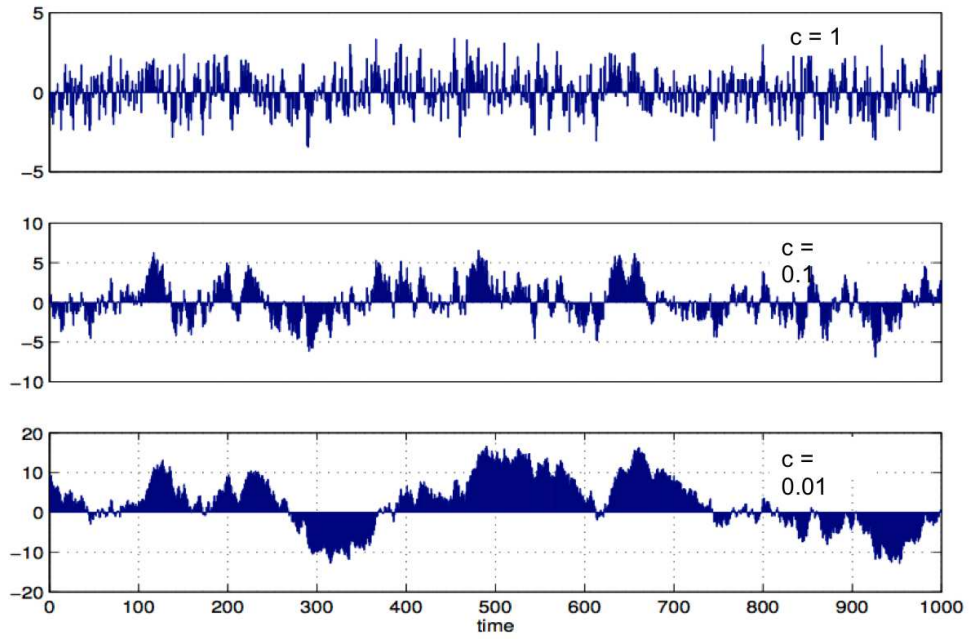


Figure 6.39: Red noise time series

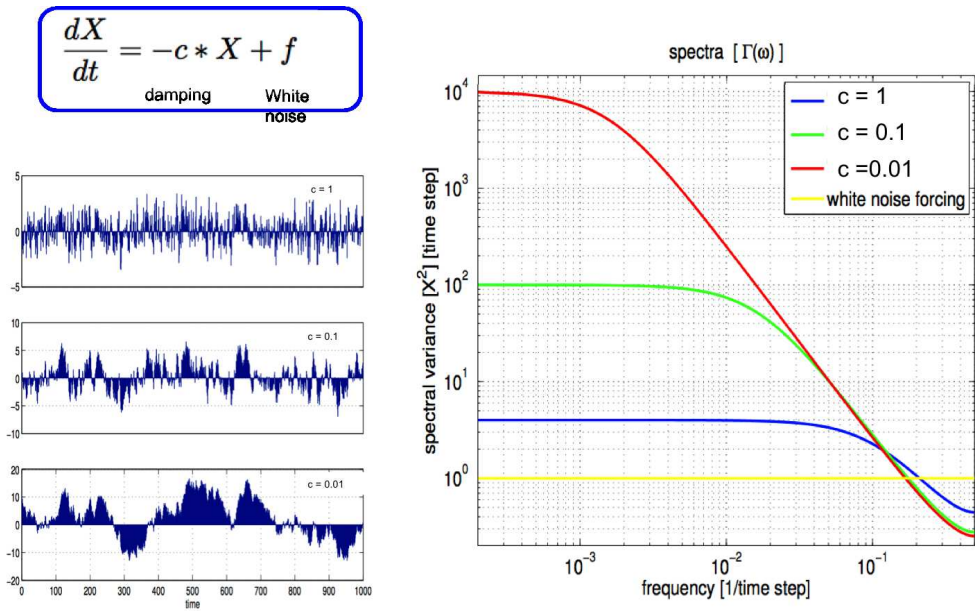


Figure 6.40: Red noise spectrum

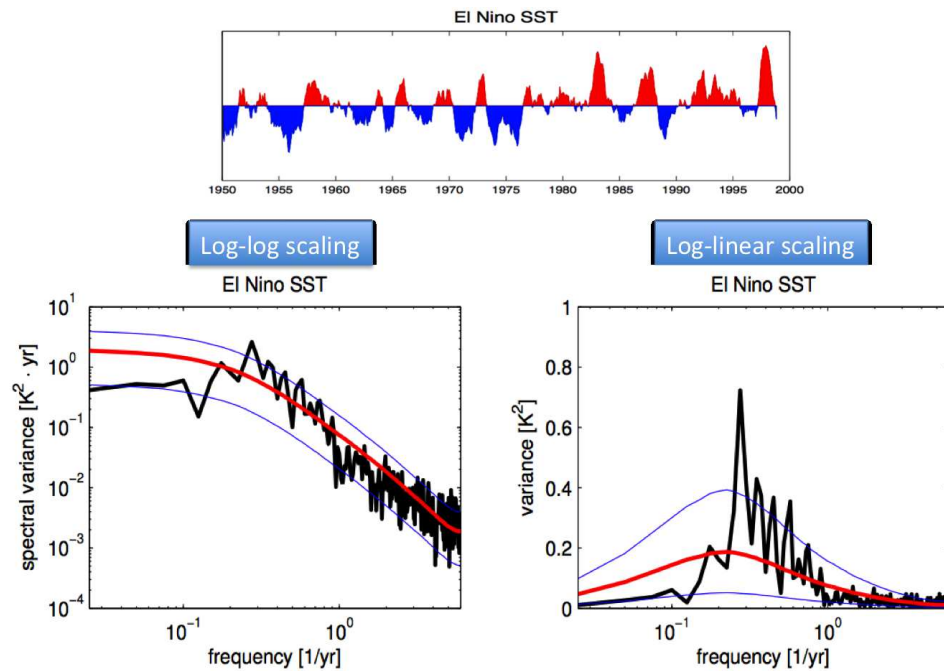


Figure 6.41: El Nino SST

Slab ocean model

An example of a red noise process.

Idea: The ocean is just a heat capacity, c_p , that integrates atmospheric sensible heat fluxes.

Assumptions:

- The upper layer of the ocean does not interact with the subsurface ocean.
- All changes in the sea surface temperature (SST) are caused by atmospheric forcing; all ocean currents or mixing are neglected.
- Damping of SST is caused by a linear coupling to atmospheric temperatures.

Characteristics:

- The SST follows the variability of the atmosphere on the long time scales exactly.
- On shorter time scales the variability of the SST is strongly damped by the large inertia of the system.
- This red noise process can be understood as a damped linear system.
- This model describes the large-scale SST variability from seasons to decades in the extra-tropics relatively well.

$$\frac{dSST}{dt} = \frac{1}{c_p h} F_{atmos} \quad (6.4)$$

$$c_p = 4 * 10^6 \text{ J/Km}^3$$

$$f_{atmos} = c_A (T_{atmos} - SST) \quad (6.5)$$

$$c_A = \frac{50W}{m^2K}$$

$$\implies \frac{dSST}{dt} = -cSST + cT_{atmos} \quad (6.6)$$

$$c = \frac{c_A}{c_p h}$$

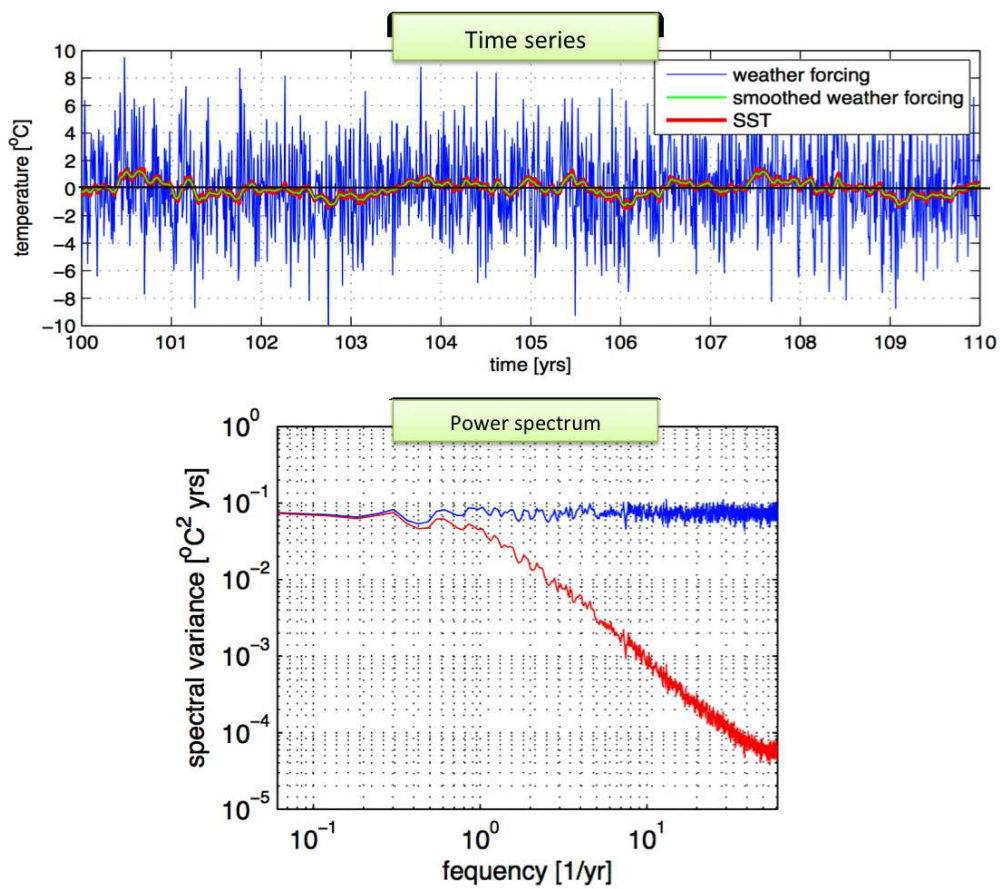


Figure 6.42: Slab ocean model

Glacier red noise model

An example of a red noise process

Idea: The glaciers mass is controlled by random weather events of snow accumulation and melting.

Assumptions :

- The glacier mass balance is forced by random weather events of snow accumulation and melting of ice.
- The glacier mass is linearly damped. While we do not know how strong the damping is, we can estimate it inversely by knowing the standard deviation of the weather forcing and the glacier mass.

Characteristics:

- The glacier mass varies much more strongly than the weather forcing.
- The very weak damping of the glaciers leads to very strong variability and very large time scales.
- This red noise process can be understood as an integrator of weather noise.
- The model does not quite fit to the observed glacier mass behaviour, as the time scales are a bit too long. This indicates that there could be another stronger forcing on longer time scales.

$$\frac{dM}{dt} = -c \cdot M + F_{weather} \quad (6.7)$$

$$\sigma(F_{weather}) \approx 1m$$

$$\sigma(M_{glacier}) \approx 200m \implies c = 0.0013 \cdot \frac{1}{yr}$$

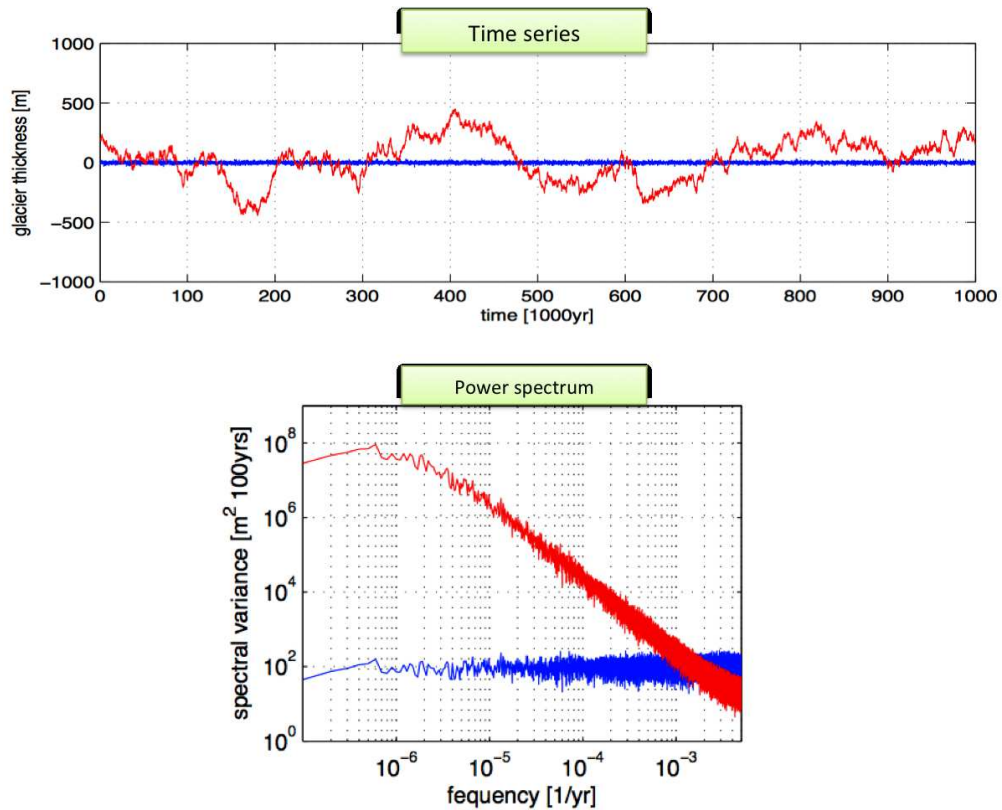


Figure 6.43: Glacier red noise model

SST standard deviation

- SST variability is the primary climate variable we study if we want to understand climate variability from seasons to decades.
- SST variability is in the order of 0.5°C .
- We can basically see several main features in the global distribution of SST standard deviation (stdv):
- *Tropical*: The strongest scale stdv is along the equatorial Pacific, marking the region of the El Niño mode of variability.
- *Extra-tropical*: The bands around 30° - 50° show strong variability that is related to atmospheric weather variability, but also to some ocean dynamics.
- *Sea ice regions*: Strong variability in the polar regions is related to the variability of sea ice.
- *Coastal upwelling*: Along the western coasts of the big continents we see strong variability due to coastal upwelling.

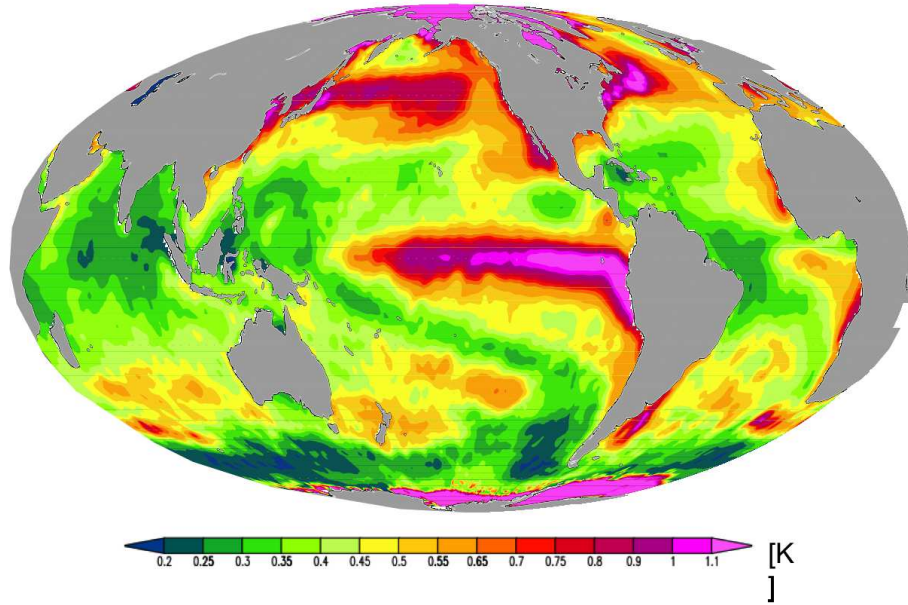


Figure 6.44: SST standard deviation

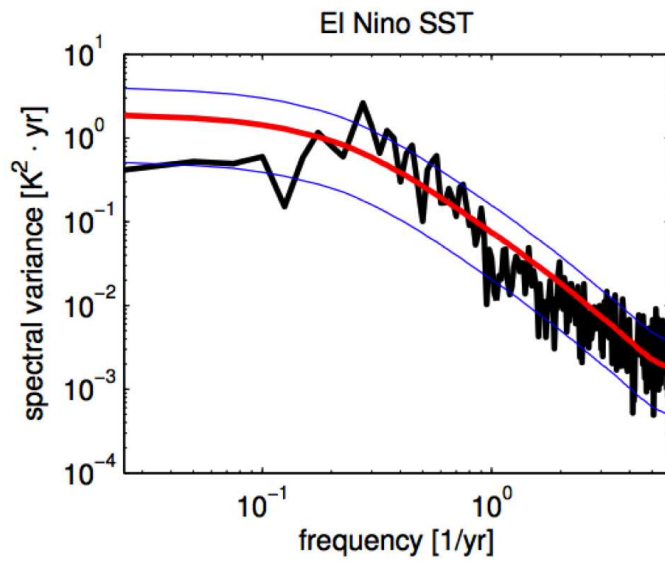
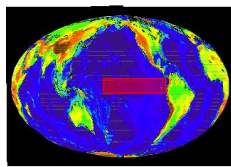


Figure 6.45: El Niño SST

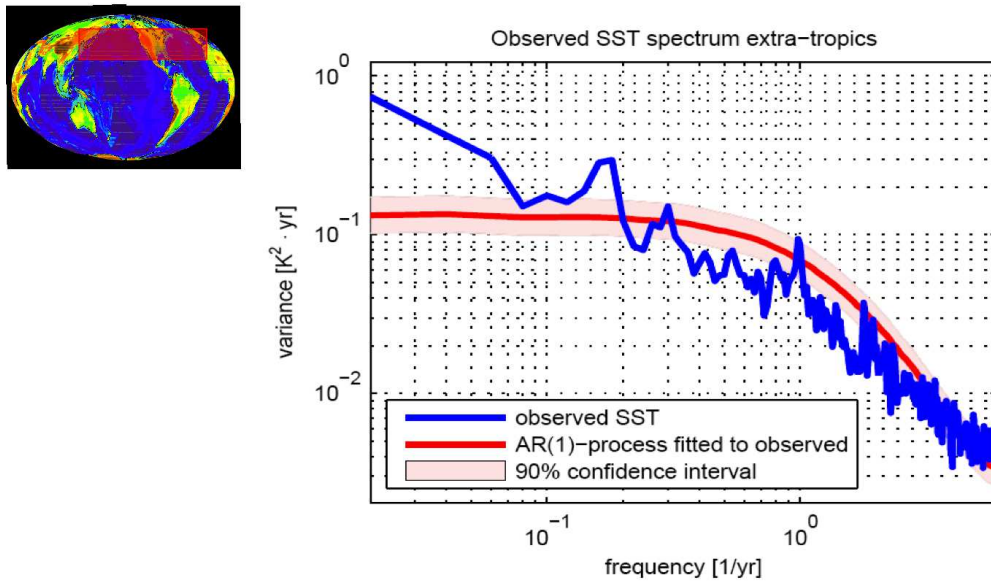


Figure 6.46: Extra-tropical SST

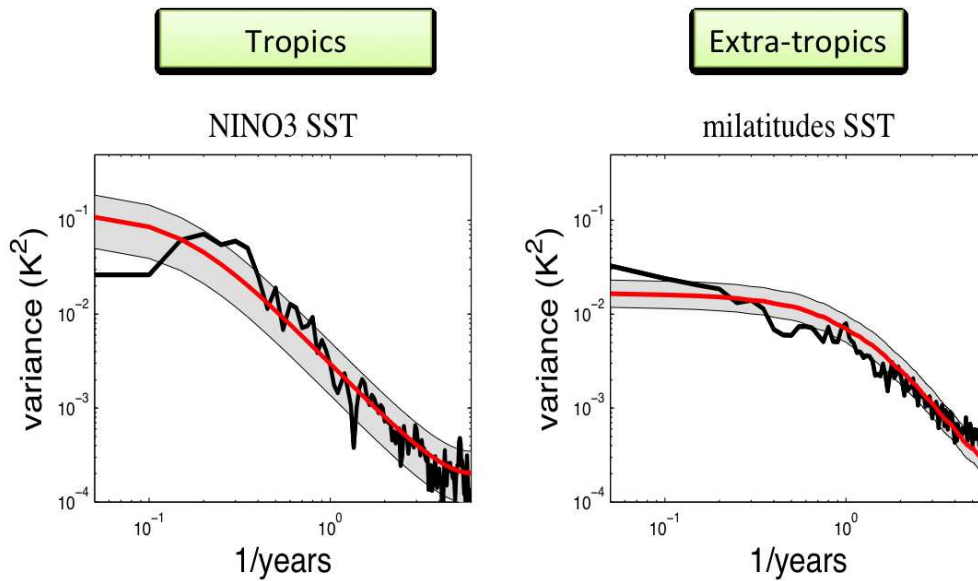


Figure 6.47: Tropical vs extra-tropical SST

Tropics: damped oscillation; El Nino

Extra-tropics: continuous time scale behaviour, different from red noise

6.3.4 Extra-tropical time scales

- Extra-tropical / midlatitudes SST variability on the larger scales is mostly forced by atmospheric weather fluctuations.
- The time scale behaviour (spectrum) is different from that of the slab ocean, because interaction with the subsurface ocean layers influences the SST as well.
- The spectrum increases over time scales longer than 100 years, but no observations exist to study these longer time scales.
- Climate models suggest it may continue to increase until about 1000 to 10,000 years periods.
- The time scale behaviour of the SST is controlled by the heat capacity of the well mixed upper layer, the strength of the coupling to the atmospheric variability, and the strength of mixing into the deeper ocean.

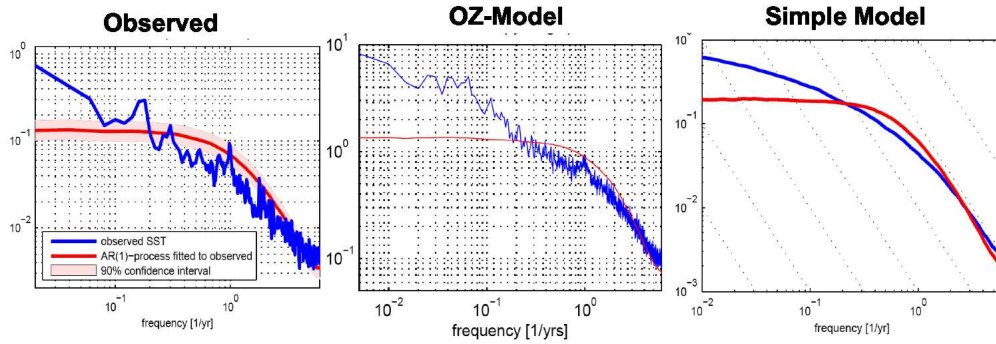


Figure 6.48: Observed annual mean surface temperature anomalies

No vertical diffusion: (slab ocean)

$$\gamma_{surf} \frac{dT_{surf}}{dt} = -cT_{surf} + \xi_{surf} \quad (6.8)$$

$$\xi_{surf} \propto T_{atmos}$$

With vertical diffusion:

$$\gamma_{surf} \frac{dT_{surf}}{dt} = -cT_{surf} + \kappa_z \nabla_z^2 T_{ocean} + \xi_{surf} \quad (6.9)$$

γ_{surf} = surface layer heat capacity

T_{surf} = surface layer temperature

c = damping by interaction with atmosphere

κ_z = vertical diffusivity coefficient

T_{ocean} = temperature of ocean

ξ_{surf} = surface forcing

$$\gamma_{surf} = H \cdot c_p$$

H = surface layer thickness

c_p = heat capacity of layer per m^3

$$\gamma_{surf} \frac{dT_{surf}}{dt} = -cT_{surf} + \kappa_z \nabla_z^2 T_{ocean} + \xi_{surf}$$

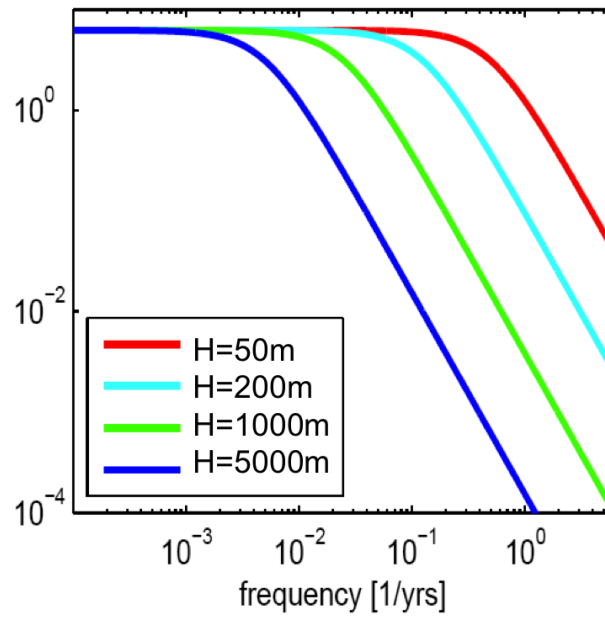


Figure 6.49

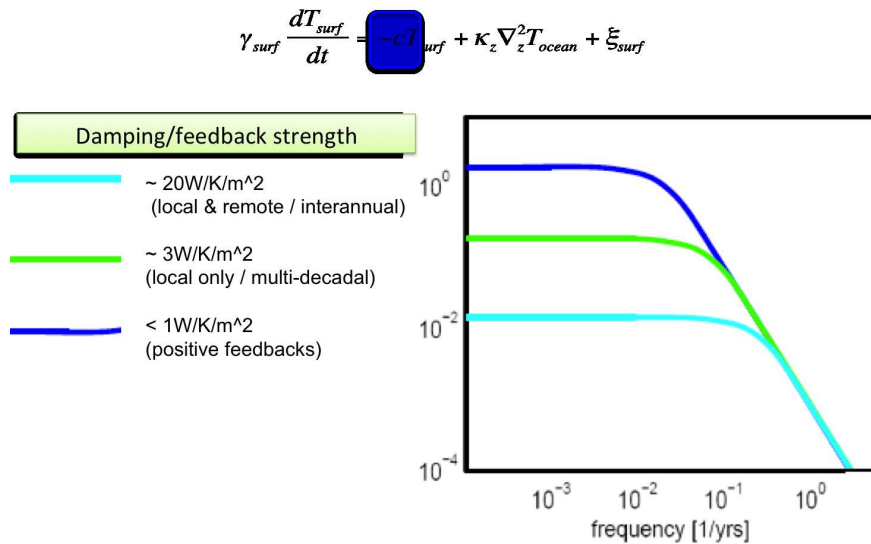


Figure 6.50

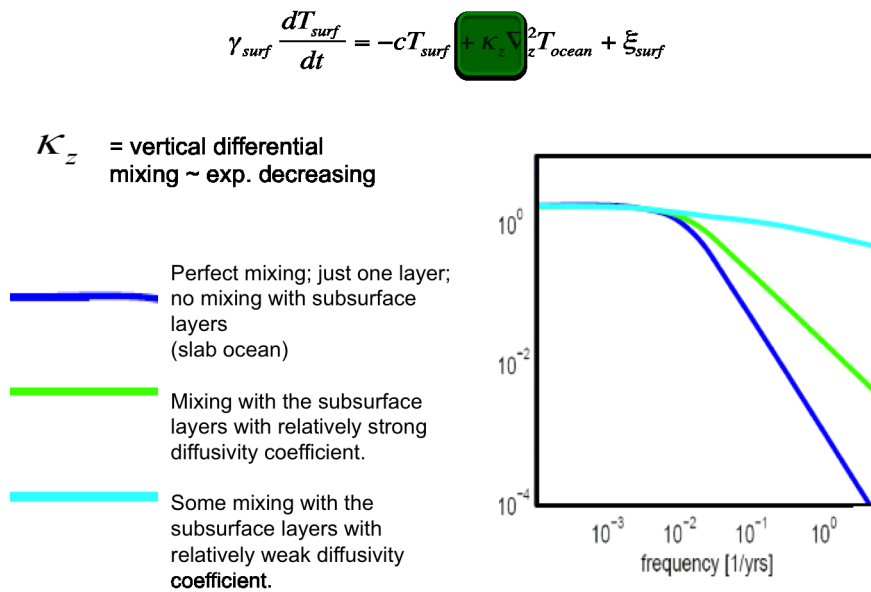


Figure 6.51

6.4 Spatial patterns of climate variability

- The stochastic climate model by Hasselmann describes the time scale behaviour of climate variability but does not make any statements about the spatial organisation of climate variability.
- The analysis of spatial structure is much more difficult than analysing the time scales, because the spatial domain has more dimensions and is more complex.

- Some elements of the spatial complexity:
 - domain boundaries (e.g. coastlines or mountains)
 - different mean states (e.g. wind directions, temperature)
 - different dynamics (e.g. Coriolis force or water vapour saturation pressure)
- The analysis of the spatial structure of climate variability relies heavily on relatively complex statistical methods, which produce a lot of complex patterns of climate variability, which are very difficult to understand.

6.4.1 Statistical patterns of climate variability

- Many different statistical methods are being used to define patterns of climate variability. No matter which method is used to define the patterns of variability, one has to be very careful in the interpretation of these statistical patterns.
- One of the most popular methods is the *principal component analysis*, also known as *Empirical Orthogonal Functions (EOFs)*. It is based on a data reduction approach similar to MP3 music or JPEG pictures.
- Note, that statistical methods will always find patterns of variability even if there are none. Further, most statistical methods like to present the variability in terms of multi-poles, even if the data is purely chaotic.

Statistical modes EOFs

Data fields: 1 pattern for each time step (measurement)

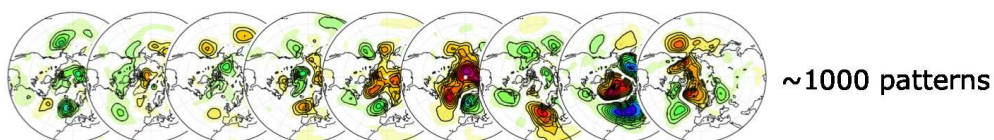


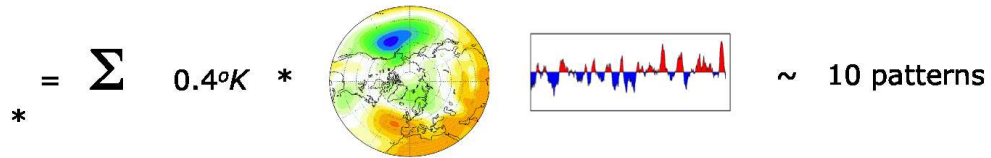
Figure 6.52

Statistical modes (Empirical Orthogonal Functions)

The idea of the EOF-analysis is to present your data as a superposition of modes, where each mode has three elements: (1) a fixed pattern, (2) a time series that varies around zero, and (3) a mean amplitude. The superposition of these three elements describes the data:

Data = Amplitude * EOF pattern * time series

So the climate variability of the domain at any given time is the sum of all the modes with the pattern times the amplitudes time the current value of the time series:

$$* = \sum 0.4^{\circ}K * \text{[Map]} \text{ [Time Series]} \sim 10 \text{ patterns}$$


The EOF-analysis has a number of important characteristics:

- Mode hierarchy: The Modes are order by how much they can explain of the data (e.g., explained variance of EOF-1 > EOF-2 > EOF-3 ...).
- Maximise variance: EOF-1 mode explains the most variance. No other mode explains more. The EOF-analysis is the optimal approach to maximise the explained variance in one mode. EOF-2 explains the large amount of variance that is not explained by EOF-1, and so on for all higher EOF-modes.
- Orthogonal: The EOF-modes are not similar to each other. They are orthogonal, which means the time series of two modes is uncorrelated with each other and the patterns of the modes are also different from each other (uncorrelated in their spatial structure).
- Multipoles: The orthogonality constrain of EOF-analysis leads in partise to a series of multipole like patterns that cover the whole domain. This is essentially irrespective of what the underlying variability structure is.

Examples of Patterns of variability (EOF-modes):

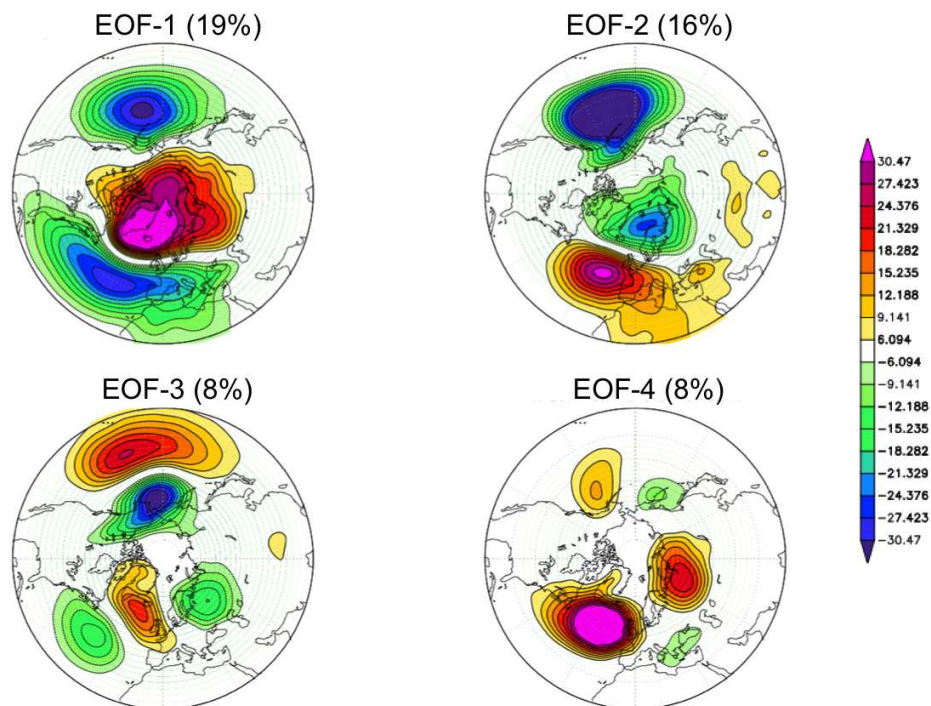


Figure 6.53: EOF modes 1000 hPa winter monthly mean

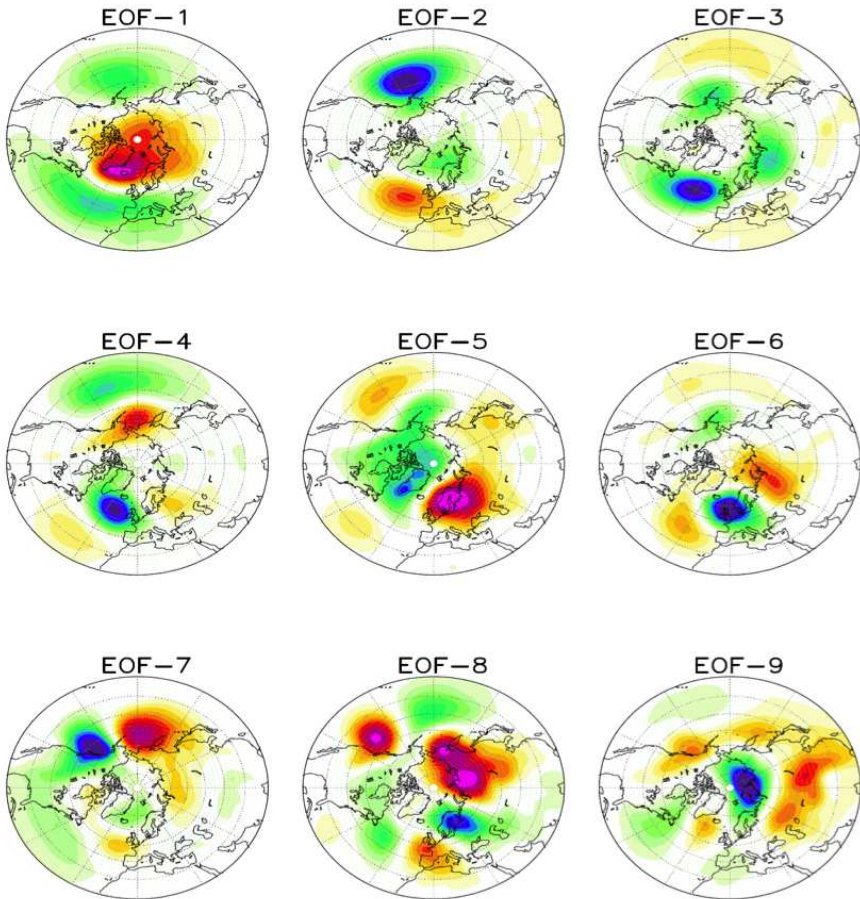


Figure 6.54: EOF modes 1000 hPa winter monthly mean

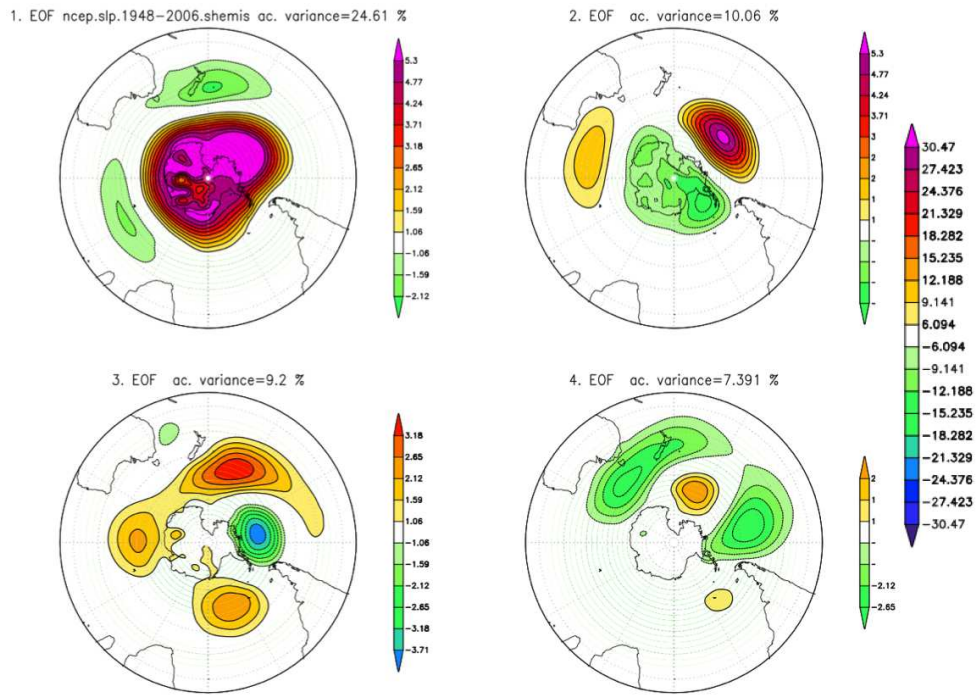


Figure 6.55: EOF modes 1000 hPa winter monthly mean

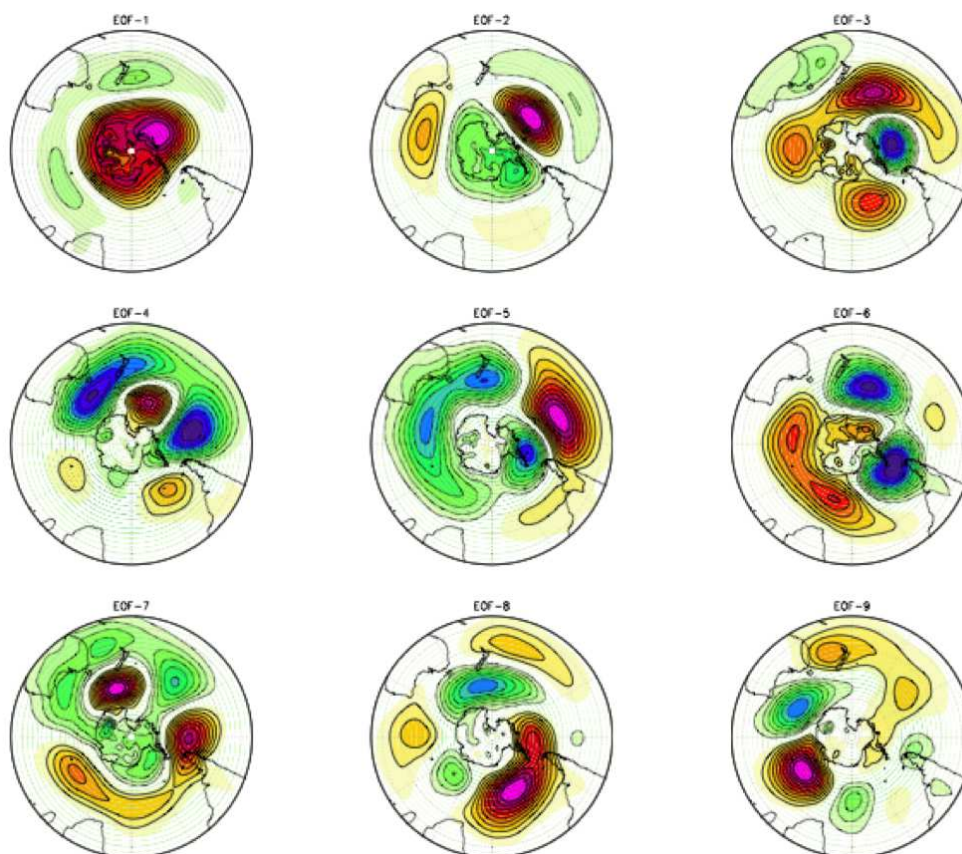


Figure 6.56: Observed EOF modes monthly mean sea level pressure

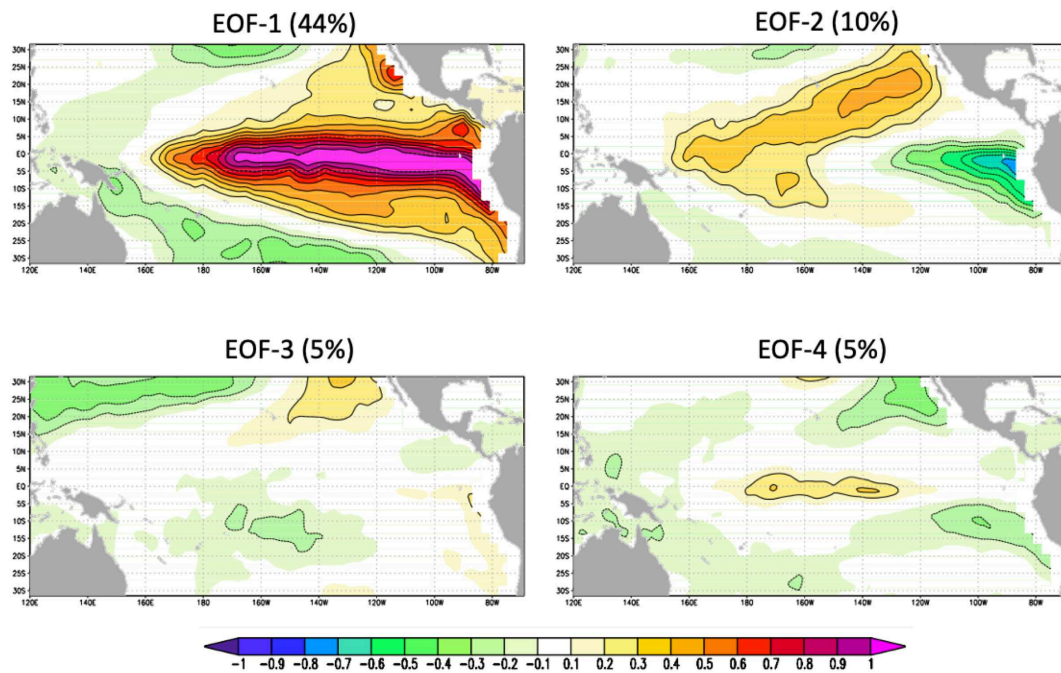


Figure 6.57: Observed EOF modes of tropical Pacific monthly mean SST anomalies with linear trend removed.

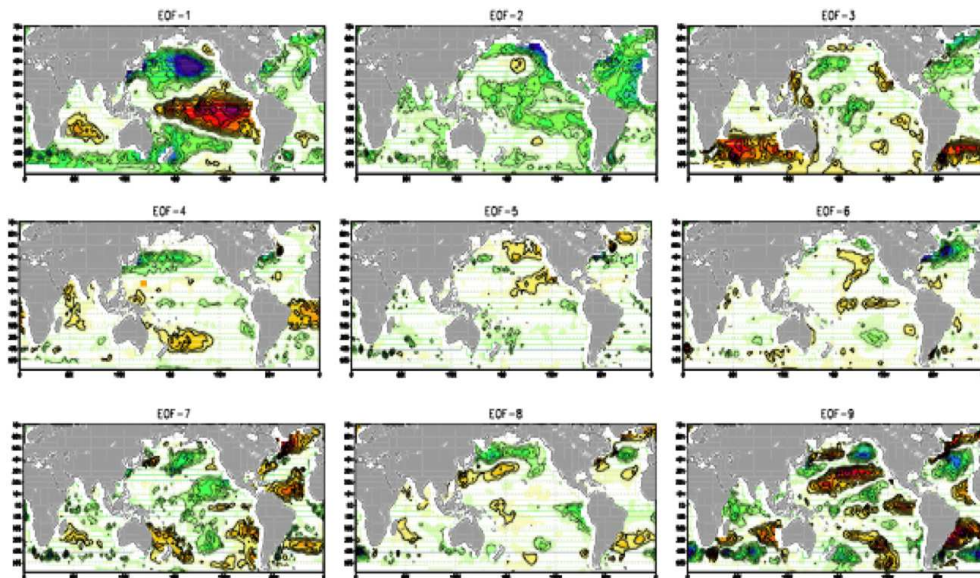


Figure 6.58: Observed EOF modes annual mean SST detrended, 5 yrs running mean

6.4.2 A Null hypothesis for the spatial structure

- The general idea in the literature is that there are patterns of climate variability.

- Alternatively, one could formulate a null hypothesis of what the structure of climate variability would look like if there are no patterns of variability. This could be in analogy to the time scales analysis with Hasselmann's null hypothesis.
- A simple null hypothesis could be based on the fact that nearby regions will influence each other to behave similarly over time.
- This basically describes the physical process of *isotropic diffusion*.
- The statistics of isotropic diffusion are similar to that of a *red noise* process but on the *spatial dimensions*.
- The only spatial structure that exists is an exponentially decreasing correlation between two points. So nearby regions show similar variability and remote regions are mostly unrelated, but show some weak similarity in variability.
- Large scale variability will be stronger than small scale climate variability → red noise.

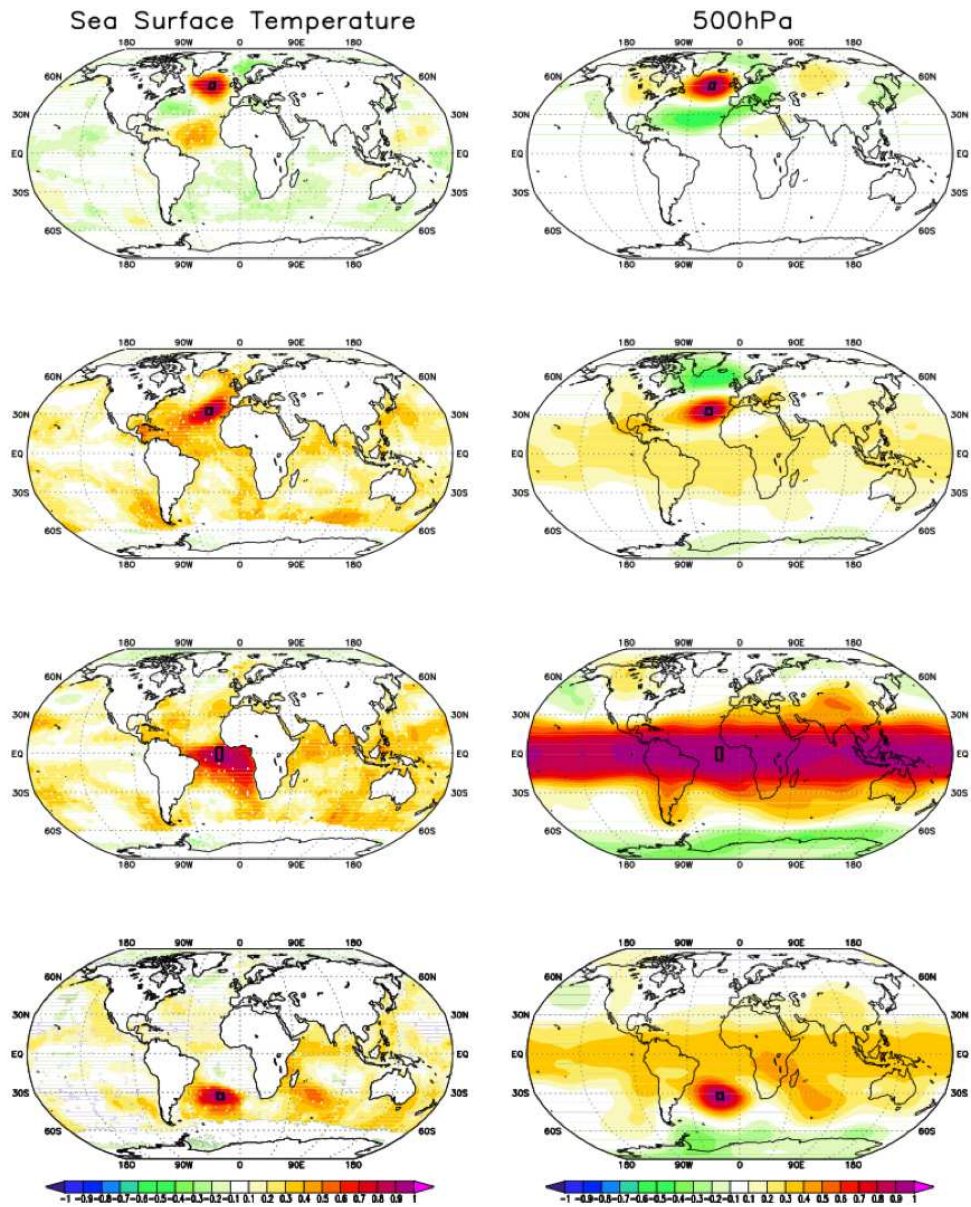


Figure 6.59: Correlation of climate variability

Isotropic diffusion

$$\frac{d}{dt}\Phi = c_{damp} \cdot \Phi + c_{diffuse} \nabla^2 \Phi + f \quad (6.10)$$

\Rightarrow spatial correlation: $\rho(d) = e^{-\frac{d}{d_0}}$

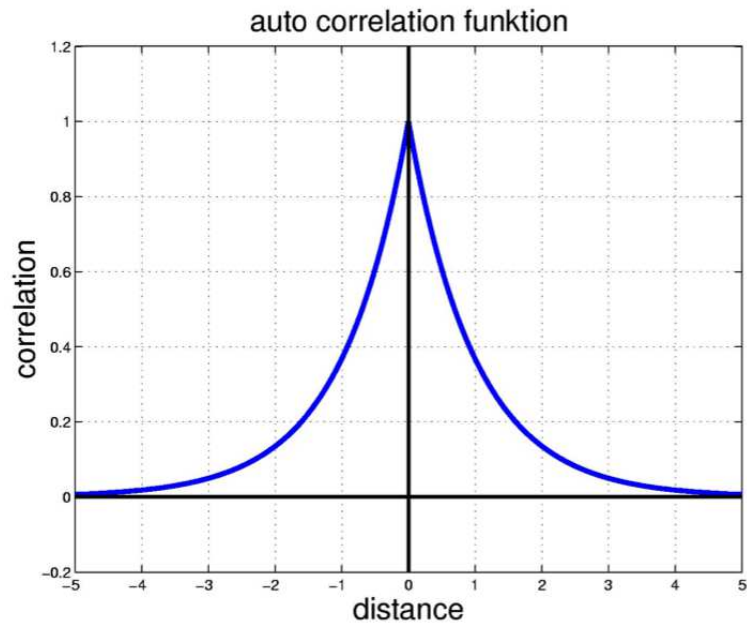


Figure 6.60

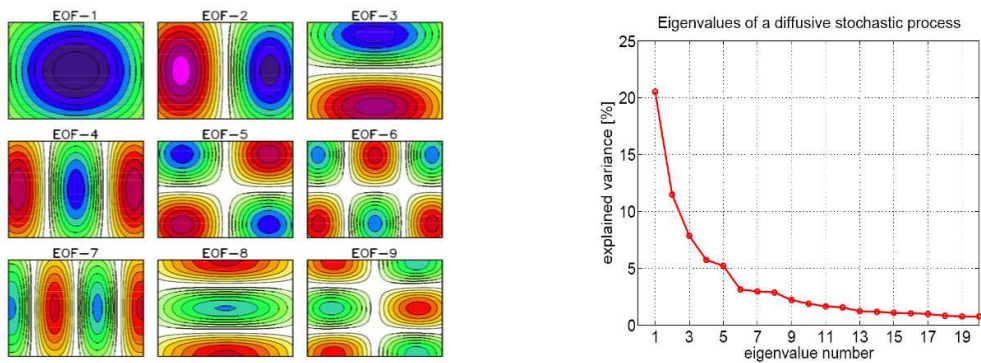


Figure 6.61: EOFs of isotropic diffusion / spatial red noise

- The EOF-1 peaks in the centre of the domain.
- The EOFs are a hierarchy of multi-poles, with increasing complexity with increasing mode number.
- None of the EOFs represent teleconnections. Note that all points have a positive correlation with all other points, despite the fact that the EOFs modes have negative teleconnections.
- EOF modes represent different spatial scales (similar to the continuous spectrum of red noise).

Time series		Patterns
	spectrum	
harmonics		empirical patterns (EOFs)
	hypothesis	
harmonic oscillation		coherent pattern teleconnections
	null hypothesis	
red noise AR(1)		red noise AR(1)
linear damped		isotropic diffusion
persistence		persistence
continuous spectrum		continuous spectrum of patterns
no preferred period		no preferred patterns

6.5 Climate Modes

The discussion of the stochastic nature of climate variability in the previous section gives the overall impression that climate variability is chaotic and unpredictable. It presents climate variability characterised by noise (e.g. white noise or red noise). This overall first impression is mostly correct and it is an important aspect of climate variability that need to be considered. However, this picture is not complete.

The stochastic climate model already indicated that the primary source for climate variability is the chaotic weather dynamics. Weather dynamics are dominated by spatial patterns of variability, often related to low and high pressure systems varying over time and space. The global distribution of these weather systems is not uniform and is one of the primary causes for different patterns in climate variability. Since weather has relative well defined patterns of variability, it makes sense to assume that climate variability would also have well defined patterns of variability.

The discussion of the spatial structure of climate variability in the previous section introduced the idea of '**Modes**'. While these modes are just a statistical presentation of the data, they are often a basis on which '**Climate Modes**' are defined. In the following we want to explore the idea of a Climate Mode in more detail and discuss how this relates to the stochastic climate model and what a climate mode implies.

A Climate Mode: The idea of a 'mode' in variability, is to highlight a reappearing pattern in space or time that is of importance and is potentially predictable beyond what we would expect from the stochastic red noise idea.

Some Examples of named climate modes are:

- Atlantic Multidecadal Oscillation (AMO)
- El Niño-Southern Oscillation (ENSO)
- Indian Ocean Dipole (IOD)
- Interdecadal Pacific Oscillation (IPO)
- Pacific North American pattern (PNA)
- Pacific Decadal Oscillation (PDO)
- Northern Annular Mode (NAM; aka Arctic Oscillation, AO)
- Southern Annular Mode (SAM; aka Antarctic Oscillation, AAO)

Most of these modes are strongly related or are identical by definition to the statistical modes that we defined in Section 6.4. For instance, ENSO is very well captured by the EOF-1 mode of SST in Fig. ?? and the SAM mode is essentially defined as the EOF-1 mode of Southern Hemispheric monthly mean pressure variability (Fig. 6.55), which is very similar to the definition of the NAM for the Northern Hemisphere (Fig. 6.53).

There are many more named climate modes than those listed here. We can note, that most of these have the word **oscillation** in it. This already indicates that the assumption is that such modes would oscillate in a predictable manner, similar to how a pendulum would oscillate at a specific period. The questions arise: How do researchers define such Climate Modes? What is a Climate Mode? Or what is not a Climate Mode? It is beyond the scope of this section to explore all the elements involved in this, but we like to give some discussion on it. We can basically note two elements that guide what a climate mode could be:

- **Deviation from Chaos:** A mode implies that the climate variability is not pure chaos. It suggests that the climate variability is not just white or red noise. There is structure in the variability beyond the simple stochastic climate model.
- **A Physical Mode:** The idea of a physical mode is that of an oscillator (e.g., a swing or pendulum). It implies predictability, as you can predict the next phase of the oscillator by knowing the current state of the system.

The idea of a climate mode is clearly in contrast to the idea of chaos or the stochastic climate model. A climate mode suggests that a part of the climate variability is following a somewhat predictable or deterministic evolution, unlike the chaos or red noise that is essentially not predictable beyond damped persistence (e.g., anomalies will stay as they are and go slowly back to normal).

6.5.1 A Physical Climate Mode

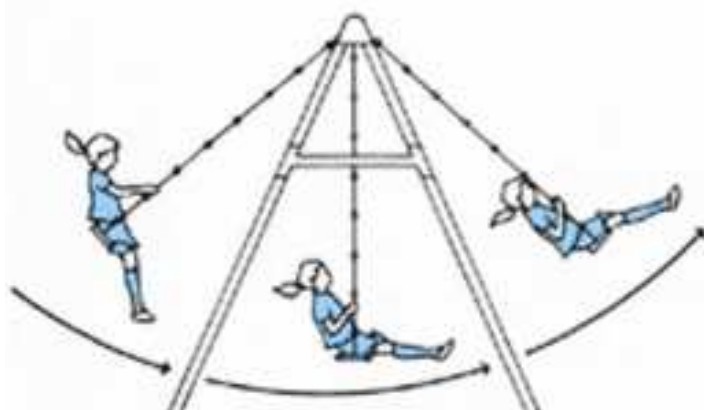


Figure 6.62: A swing or pendulum is an idealised oscillation, similar to what climate modes aim to represent

An idealised physical climate mode is like a swing or pendulum. It has clear physical dynamics that control its evolution in time and it is highly predictable. So, a look at the dynamics of a swing can help to understand what a climate mode should look like. In this swing, the system is controlled by an oscillation between potential energy from the gravity which is high when the swing is lifted to the right or left, and the kinetic energy when the swing is moving.

An important characteristic of a swing (pendulum) is that it has a clear cycle in which the system evolves. This cycle of the swing can be presented in a **Phase Space**. The physical phase space is an idea to present the cycling nature of a system, in which the system moves from one phase to the next in a highly predictable manner.

Figure 6.63 shows the phase space of a swing. The horizontal position of the swing is shown on the x-axis and the velocity of the swing is shown on the y-axis. In this diagram the swing evolves along a perfect cycle marked by the dashed line and following the direction marked by the arrows. Due to this cyclic nature we can think of each part of the cycle as a different phase of the cycle. Each phase of the cycle will lead to the next phase due to the dynamics of the system that make the system follow the direction of the arrows.

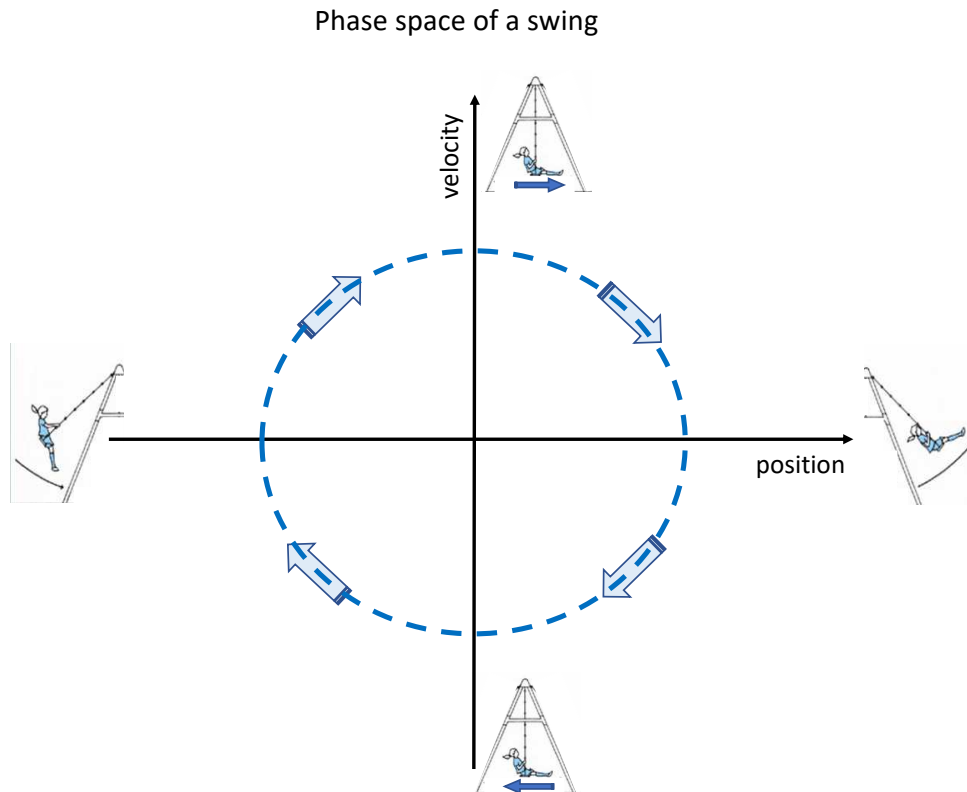


Figure 6.63: The phase space of a swing. The horizontal position of the swing is shown on the x-axis and the velocity of the swing is shown on the y-axis. The dashed line marks the line on which the swing would propagate if it maintains a constant oscillation amplitude. The arrows mark in which direction the swing system would propagate through the different phase over time.

For instance, if the swing is at the phase on the left of the diagram, the swing is not moving (velocity = 0), but the potential energy is high. This will lead to an acceleration of the swing to the right (velocity > 0) and at the same time the swing moves to the right. It will follow the dashed line in the direction of the arrows. Similarly, if the swing reaches the upper point in the diagram, the velocity has reached its maximum and the position is in the middle of the swing (position = 0). Now the swing will move further to the right, lift the swing (position > 0) and thereby slow down the swing. It will again follow the dashed line in the direction of the arrows.

This idea of the swing can be generalised to illustrate any kind of oscillating system. The important aspect of this phase space diagram is that we have two variables that we can measure (position and velocity) that have an out-of-phase relation. That is, when one of them reaches its maximum the other variable is zero and vice versa. Further, a large absolute value in one of the two variables help you to predict the evolution of the other variable (e.g., large velocity will lead to a large value in the position some time later), see Fig. 6.64.

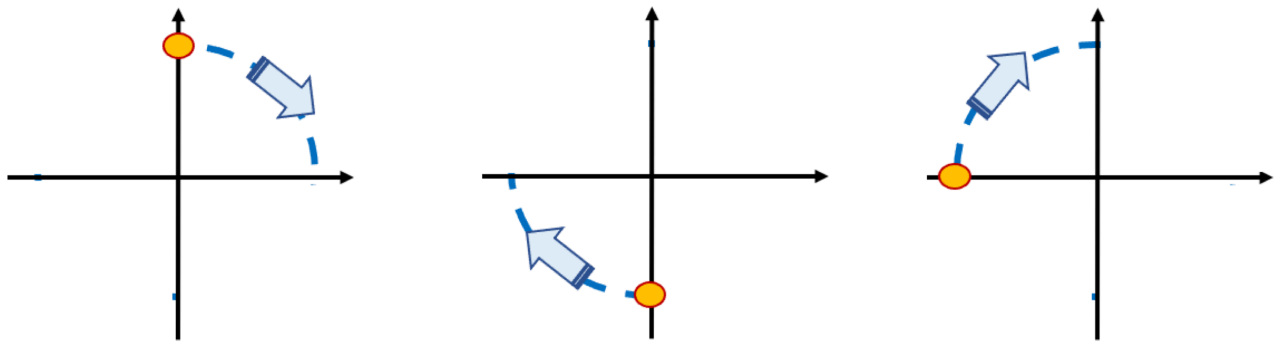


Figure 6.64: Illustration of predictability in an idealised phase space. The orange points mark a starting point and the dash lines and arrow mark how the system would evolve if it follows an idealised oscillator.

Definition of a physical Climate Mode:

This idea of an idealised oscillator with a phase space can be used to define what a physical climate is. A Physical climate mode has a phase space with two variables x and y with an out-of-phase relationship. The mode has clear propagation through all phase of the cycle in clockwise direction. This is the essence of a predictable oscillator.

In section 6.6 will discuss a real world example of such an oscillator for ENSO. We will illustrate a similar phase space diagram as it is describing the core dynamics of ENSO.

6.5.2 The problem with defining climate modes based on statistical modes

Climate Modes are often defined, or initially proposed, based on statistical analysis of the data. Often using methods such as the EOF-analysis as discussed in Section 6.4. In turn, they are usually not based on the above described idea of a physical model. Thus, they are not based on describing a physical process that would lead to a predictable oscillation.

EOF-2

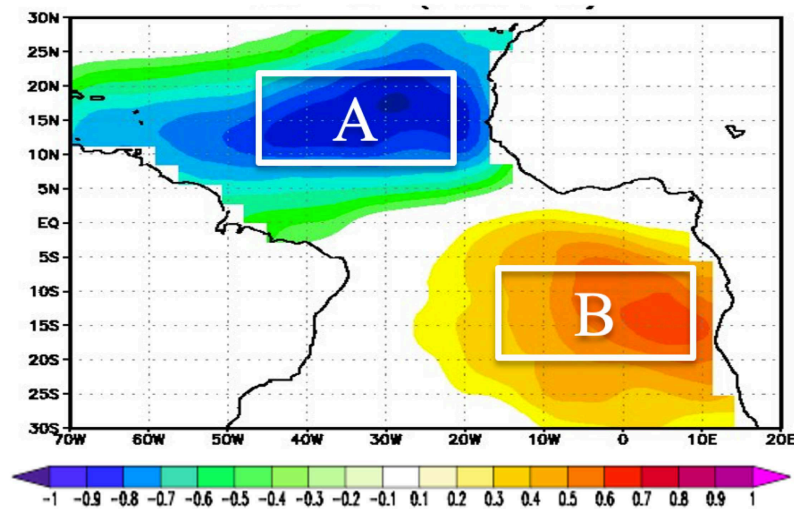


Figure 6.65: An Example of an EOF-2 mode with a dipole structure. The values of the EOF-pattern around region A are negative and positive around region B.

This statistical approach of defining what a climate mode is, has substantial problems. The problem may best be illustrated by an example: The EOF-2 mode shown in Fig. 6.65 shows a dipole pattern with negative values around region A and positive values around region B. The following two statements we may consider as an interpretation of this EOF-mode:

- (A) Anomalies in region A will have a negative correlation with those in region B.
- (B) Anomalies in region A will be mostly independent of those in region B, but may have a weak positive correlation.

Statement (A) seem to be a straight forward interpretation of the EOF-2 mode, as we can clearly see that according to this pattern values in region A and B have opposite signs and therefore would represent anti-correlation between the two regions in terms of the variability of this variable in this domain. However, this statements is unlikely to be true for the dataset on which this EOF-mode is based on. Indeed, statement (B) is more likely to be correct, although this is not apparent from looking at this EOF-2 alone.

So, why is statement (B) more likely to be true than statemnet (A)? Here we need to consider two things:

- **Consider all modes:** To understand how regions A and B in this example relate to each other we have to consider, in principle, all EOF-modes, since the data is described by the sum of all the modes. While EOF-2 mode suggests region A will have a negative correlation with those in region B, it is not the only mode in this domain. In particular, we have to consider what would EOF-1 mode look like? Since EOF-1 mode is more important than EOF-2 mode, it does not make much sense to discuss EOF-2 mode without knowing the EOF-1 mode. We also know that the EOF-1 is orthogonal to the EOF-2 mode. A monopole mode, for instance, would be possible for the EOF-1 mode. A monopole mode would suggest that regions A and B have a positive correlation.

- **Consider the null hypothesis of red noise:** If we do not know anything about our climate variability data, we should always assume that our data is at least partly related to red noise. Following from Section 6.4.2 spatial red noise has the following characteristics: (i) EOF-2 mode is a dipole similar to what we observed in this example, (ii) EOF-1 mode is a monopole that explains more variance than the EOF-2 mode, (iii) all regions are positively related to each other due to the diffusion process and (iv) the further away two regions are from each other the less related to each they are. In this example the regions A and B are relatively far away from each other in this domain. So they should have a weak positive correlation if the data results from a red noise process.

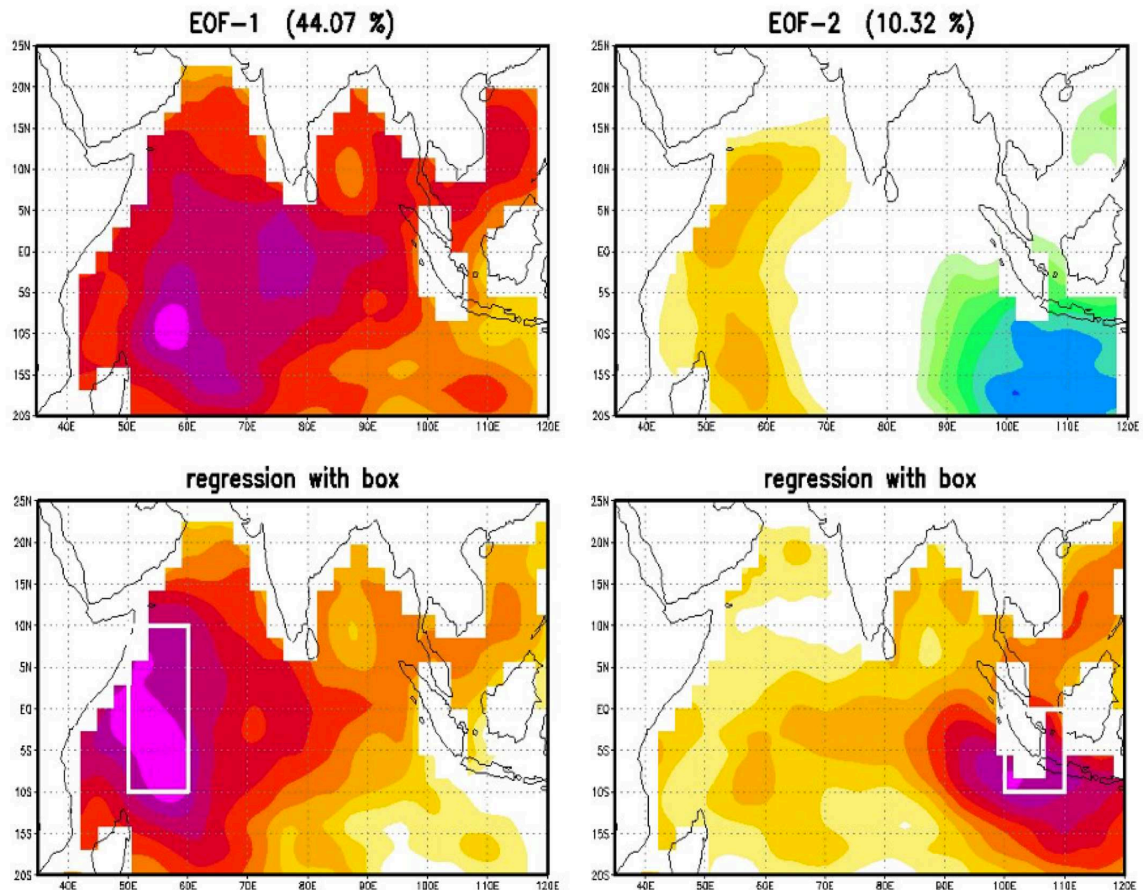


Figure 6.66: Tropical Indian Ocean SST modes. Upper: EOF modes 1 and 2 for monthly mean SST anomalies. Lower: correlation of the SST in the white framed regions with the SST in the domain.

Figure 6.66 illustrates this problem on the basis of tropical Indian Ocean SST variability. We can note that EOF-2 is a dipole like structure that explains about 10% of the total variance. Again we may think that EOF-2 mode suggests that the two regions with large amplitudes in this mode (to the west and east of the domain) would be anti-correlated. However, the two regions are clearly positively related to each other. This is related to the fact that the EOF-1 mode that explains about 44% of the total variance, and therefore is much more dominant than the EOF-2 mode.

The EOF-1 mode is essentially a monopole like structure that suggest that all regions are positively correlated to each other. Since it is by far the most dominant mode in the domain as tt explains 44% of the total variance, which is much more than EOF-2 with only 10% and all higher modes < 10%). It is therefore likely that the SST variability will mostly follow this mode and therefore has all regions being positively correlated to each other.

This example illustrate the complexity when interpreting climate modes. This can be further illustrated by contrasting two apparently contradicting hypothesis, see Fig. 6.67. In this example we have formulated two different hypothesis to explain what is causing the observed variability of a climate variable in a domain that has essentially three subregion: a western, central and eastern region. This example is motivated by the tropical Indian Ocean SST variability. So we can think of this domain as the tropical Indian Ocean SST.

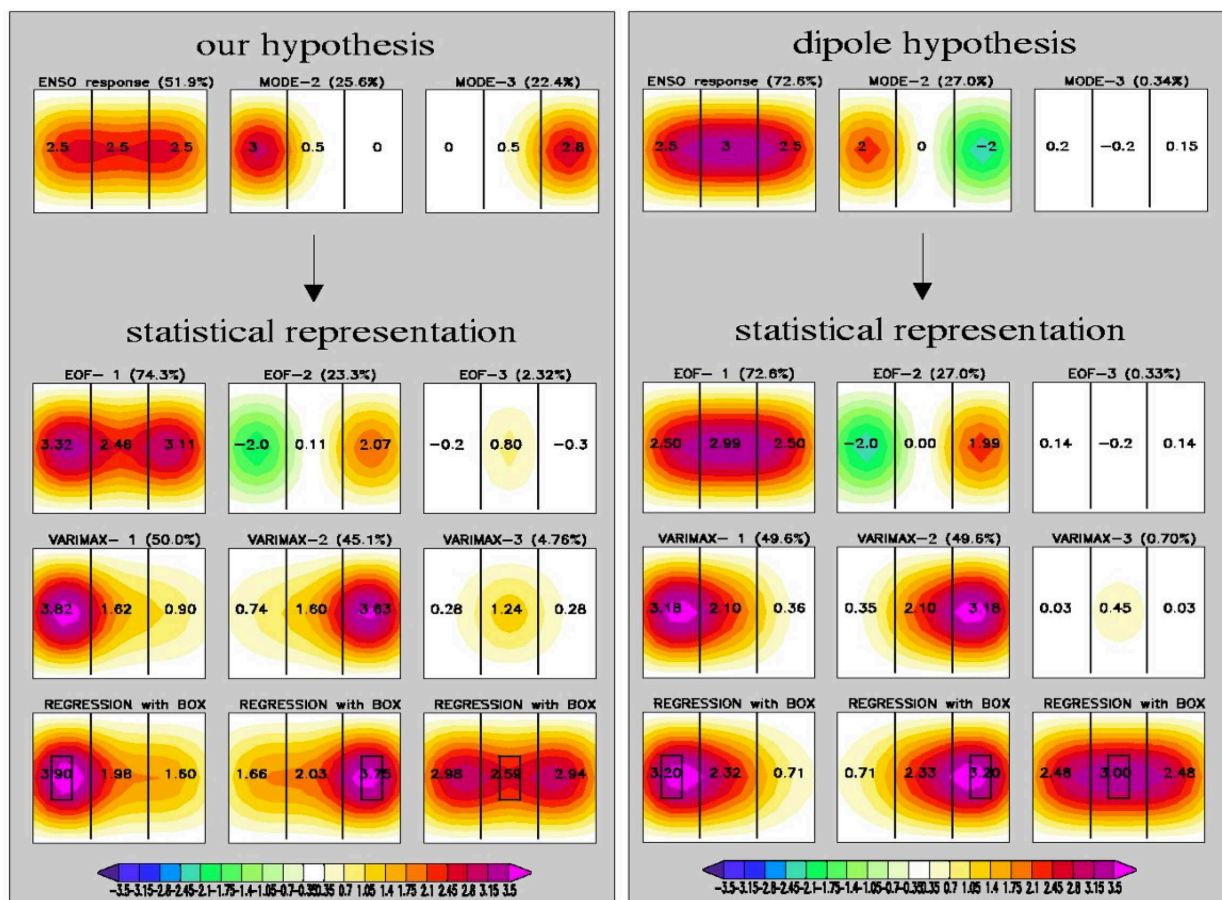


Figure 6.67: Discussion of two hypothesis of SST modes in the tropical Indian Ocean. Left: Hypothesis assumes EOF-1 mode is dominated by ENSO and modes 2 and 3 are regional monopoles in the western and eastern parts of the domain. Right: The Dipole hypothesis assumes that EOF-1 mode is dominated by ENSO, the second mode is a dipole and the third mode is small and unimportant. The three lower rows illustrate three different statistical representations of the two hypotheses: the first row shows the EOF-modes, the second the VARIAMX modes and the third row shows who each of the three regions of the domain regresses (correlates) with the other regions in the domain.

In the "Dipole" hypothesis (Fig. 6.67 on the right) we may assume that the leading mode is a monopole pattern covering the whole domain. In the tropical Indian Ocean SST this could be the influence of ENSO on this region. The second mode is a dipole structure with opposing (anti-correlated) variability in the western and eastern regions of the domain. The remaining third mode is small and not relevant.

As an alternative, and apparently contradicting, hypothesis (Fig. 6.67 on the left), we could assume that the leading mode is also a monopole pattern covering the whole domain, but the second and third modes are two fairly equally stronger local modes in the western and eastern regions that are unrelated to each other.

These two hypotheses are clearly different in terms of how we assume the physical processes interact in this domain. The "Dipole" hypothesis assumes that there is a physical process that leads to opposing (anti-correlated) variability in the western and eastern regions of the domain, while the other hypothesis does not. However, if we look at how different statistical methods would represent this variability in the domain (Fig. 6.67), we would recognise, that they are actually identical (mostly). Thus, two different ideas about the underlying physical modes can lead to the same observed statistics. This illustrates that the interpretation of Climate Modes can be fairly complex if we deal with variability that has more than one dominating mode. This is in general often the case for climate variability domains.

6.5.3 Levels of Climate Modes

Climate modes are often interpreted or discussed as if they are a physical mode (e.g., the QXZ oscillation). There is often no evidence for that. Indeed, Climate Modes are often not a physical mode, but are mostly a statistical mode. We can define different levels of modes to distinguish the nature of so called climate modes:

Level 1: subjective / impact focused

- Usually defined based on a statistical mode.
- It is subjective (e.g., depends on methods).
- Motivated by its impact on (remote) climate.
- No indication of deviations from pure noise (e.g., red noise).
- No indication of a physical oscillator.
- Not predictable beyond damped persistence.
- Is not level 2 or 3.

Level 2: structures different from noise

- Indication of deviations from pure noise (e.g., red noise). e.g., power spectrum is not just red noise. e.g., spatial EOF-modes are different from red noise
- Not clear if this is a physical mode.
- Could be chaotic, but different from red noise.

- Is not level 3.

Level 3: A physical mode / predictable oscillator

- A structure different from red noise
- A physical phase space with clear propagation in all phases.
- Predictable beyond damped persistence.

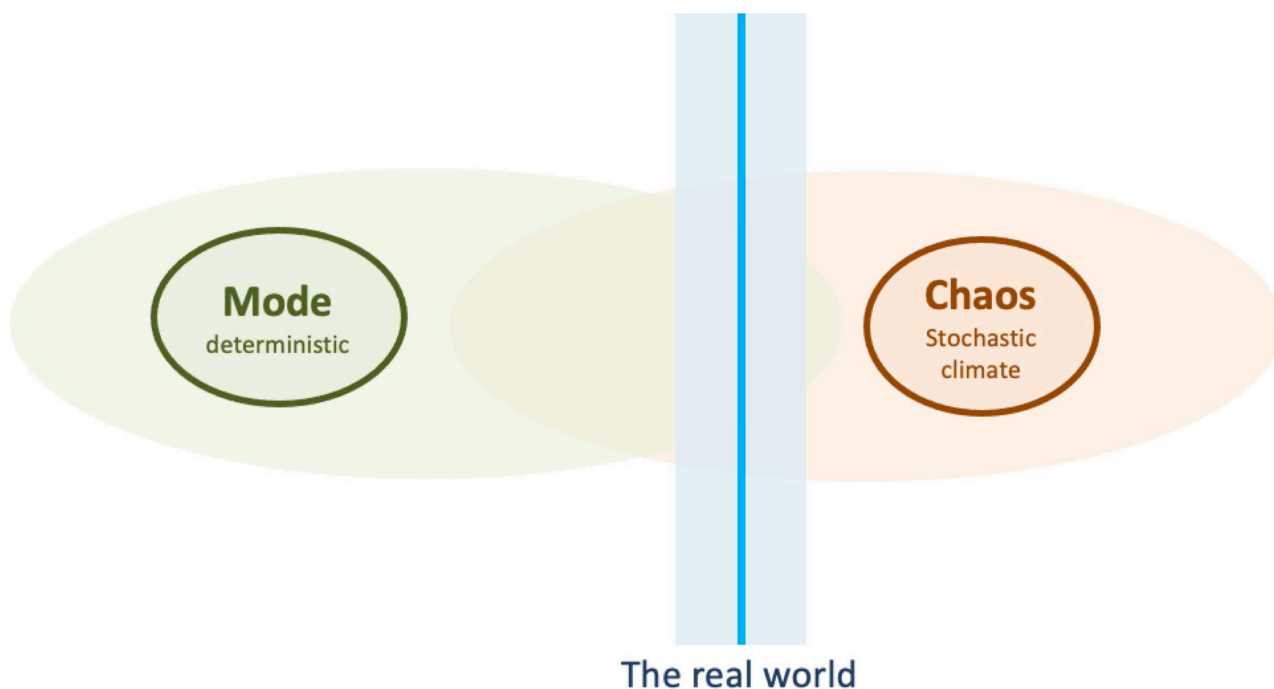


Figure 6.68: Sketch illustrating the contrast between deterministic climate modes and chaotic, stochastic climate variability.

In summary, the concept of a Climate Mode is an idea of a deterministic, predictable structure in the climate system that is distinguished from the background stochastic noise. In reality, though, Climate Modes are not that deterministic as one may hope, but are indeed often a reflection of the stochastic, chaotic climate variability. Indeed the concepts of Climate Modes and the stochastic climate model overlap, see Sketch 6.68. The real world is most likely dominated by the stochastic, chaotic nature and the deterministic Climate Modes are only a minor element of the climate variability.

6.6 El Nino / Southern Oscillation



The El Nino / Southern Oscillation (ENSO) is the most important phenomenon of natural internal climate variability on seasonal to decadal time scales. It originates in the tropical Pacific Ocean, but has near global teleconnections. It is a stochastically driven mode of climate variability that has some interesting aspects of predictable features, which give rise to possible seasonal climate variability forecasts. ENSO is essentially the main factor that would allow for some seasonal prediction of climate variability. It is also a very good example to discuss natural internal stochastic climate variability and its predictability.

We will introduce this section with the historical background and the description of the ENSO phenomenon. This will be followed by describing the global impact that ENSO has. The key dynamics that control ENSO are then explained in some more details. The section will be closed with some discussion of the predictability of ENSO.

6.6.1 History

El Nino: was always known to fishers in South America. Coastal waters of the Pacific coast of South America had dramatic warming events every few years around Christmas time (that is why it is called *El Nino*) causing large-scale fish deaths or emigration to other regions.

Southern Oscillation: Sir Gilbert Thomas Walker \sim 1910. Walker was analysing the variability of Indian Monsoon variability and found it to be related to very large-scale atmospheric sea level pressure variability to the south of India, which he thus called the Southern Oscillation. But it actually is more or less right on the equator. The Southern Oscillation is the pressure difference between Tahiti (central, south near equator Pacific) and Darwin: Darwin minus Tahiti.

ENSO coupling: Bjerknes 1969, Bjerknes was one of the first researchers who understood that *El Nino* and the *Southern Oscillation* (ENSO) are not only related to each other, but that the interaction between the two may actually be the cause for the variability in both.

ENSO numerical model: Cane and Zebiak, *Science*, 1985. Cane and Zebiak were the first to demonstrate that a numerical model of the ocean and atmospheric dynamics in the tropical Pacific could reproduce the ENSO mode. Modern numerical climate models are used to predict the ENSO evolution for the next few months to one year. It is basically the only process that allows for seasonal weather forecasting in the tropical regions.

ENSO research today: The ENSO is still a subject of ongoing research. Many aspects of the ENSO mode and how the interaction/feedbacks work are still unclear. It is also currently researched how ENSO may change in the changing climate and how ENSO relates to interactions with the rest of the world.

6.6.2 Phenomenon

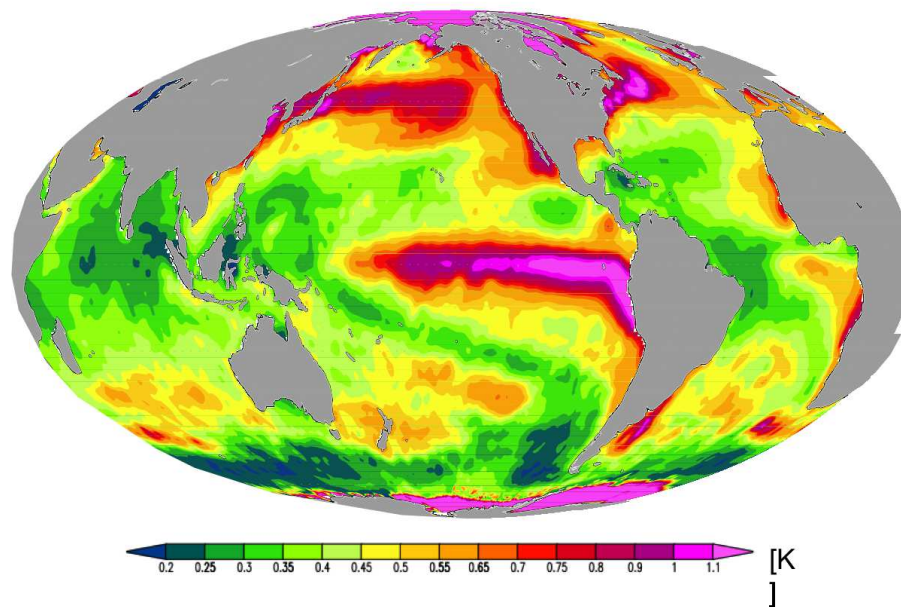


Figure 6.69: SST standard deviation

The El Nino variability:

- The global SST standard deviation already shows quite clearly that the equatorial region of the Pacific has a unique and globally dominating amount of variability.
- If we look at global SSST anomalies during ENSO events we quite clearly see how dominating the ENSO pattern of variability is compared to SST variability in the rest of the world.
- The ENSO events are marked by a very well defined SST pattern in the tropical Pacific.

- The warming events are called *El Nino* and tend to peak around November to January. They last less than a year. A strong event can warm by 4°C over most of the east equatorial Pacific.
- The cold events are called *La Nina* (the girl as in contrast to El Nino). They last longer and are usually not as strong as the positive events. They are basically an intensification of the mean state.
- The pattern of La Nina is slightly different from that of the El Nino events, The latter are narrower and have stronger amplitudes near the South American coast.
- ENSO is a quasi-periodic oscillation with a period of about 4 years (between 2-7 years). So warm and cold events follow each other.
- Strong ($\geq 2^{\circ}\text{C}$) El Nino events are rare and return every 10 to 20 years.
- Strong ENSO El Nino events have a significant global warming effect, that can be seen in the global mean surface temperatures.
- In response to the ENSO event, SST anomalies in the tropical Indian, North Pacific and the tropical Atlantic are forced. They tend to lag behind the time evolution of the ENSO event, as they need some time to respond to the ENSO forcing.

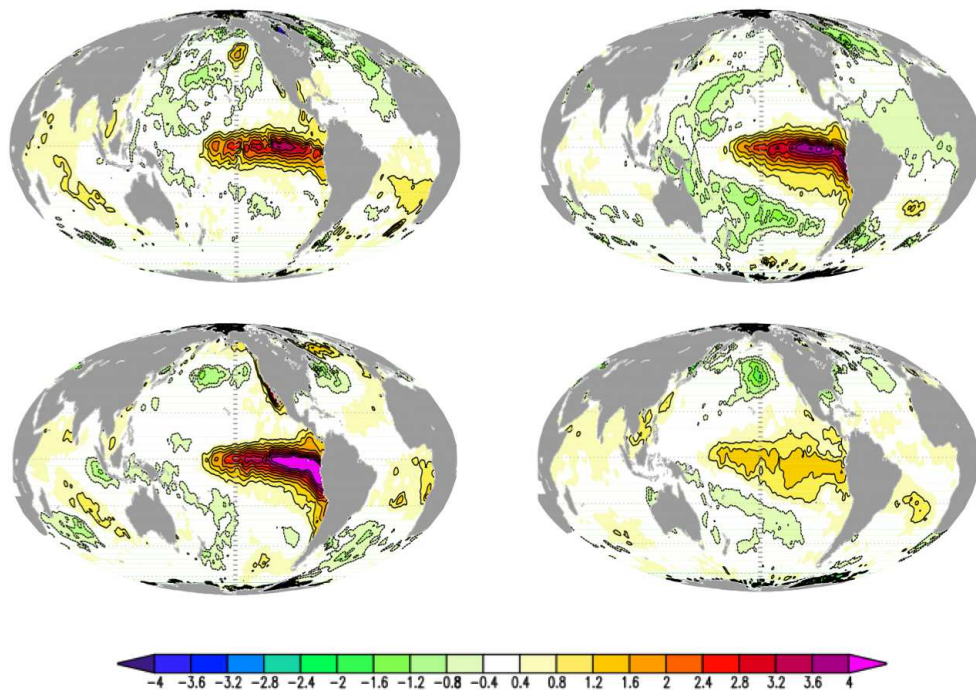


Figure 6.70: El Nino events: SST anomalies for four different Decembers of four different years with strong El Nino events; highlighting the global dominance of the El Nino pattern.

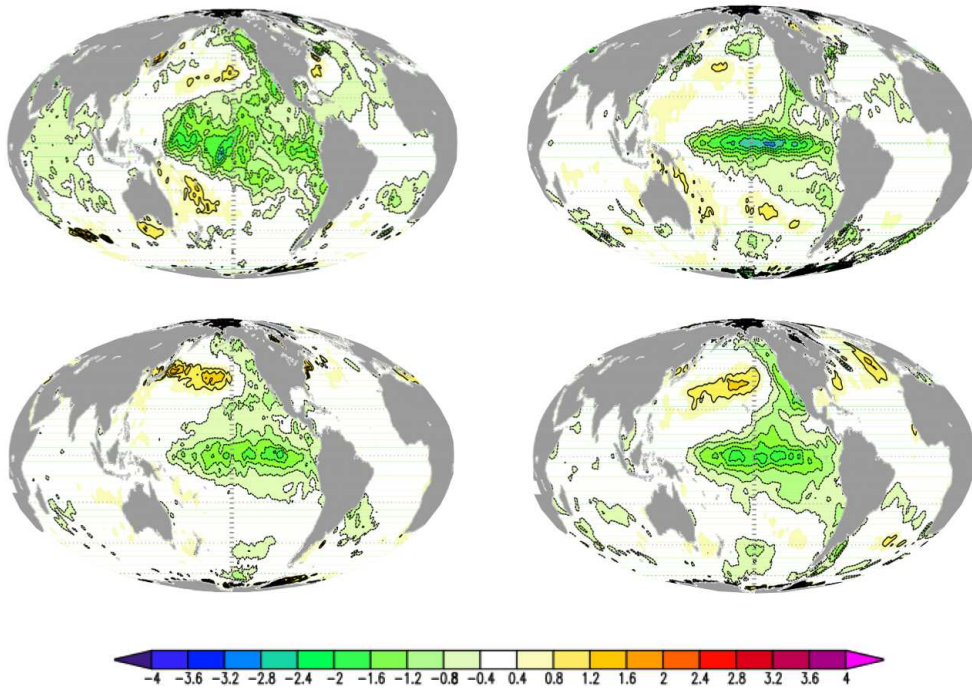


Figure 6.71: La Nina events: SST anomalies for four different Decembers of four different years with strong La Nina events.

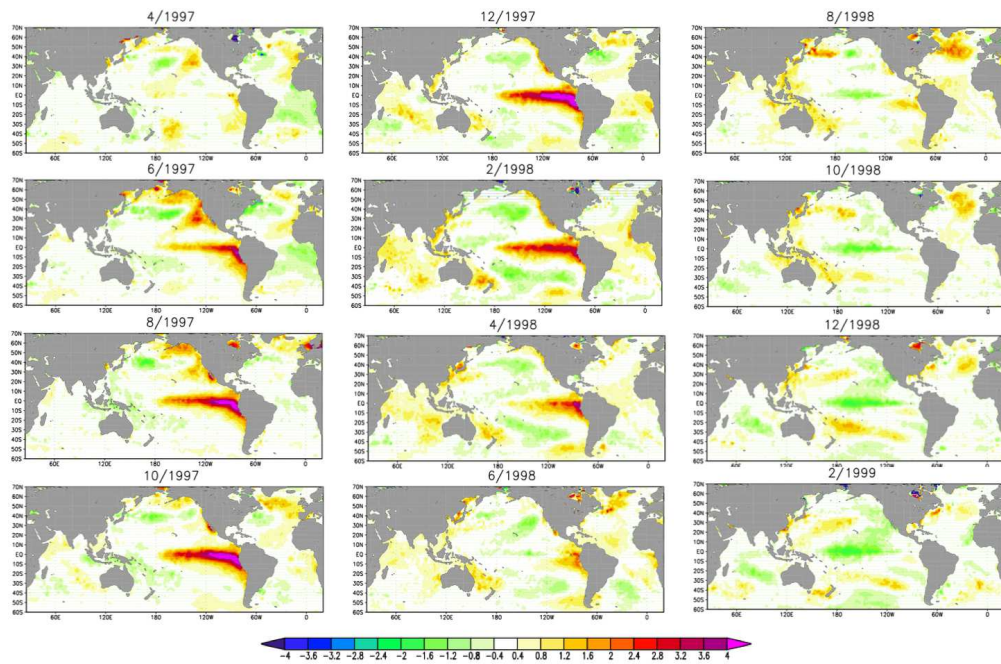


Figure 6.72: The time evolution of the strongest El Nino event in 1997.

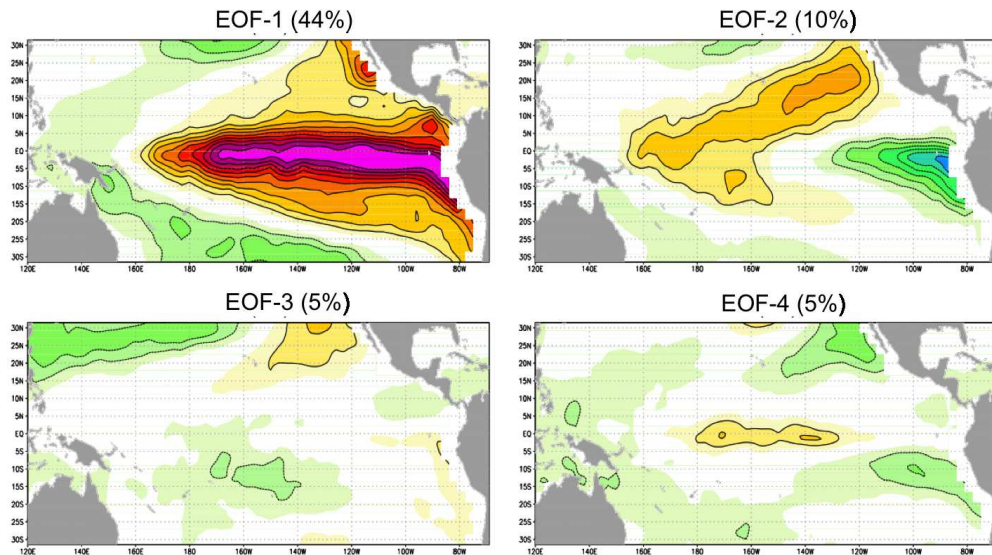


Figure 6.73: El Niño pattern (EOF): The EOF-1 mode explains 44% of the total variance, which indicates that it is really just one pattern that dominates the variability in the tropical Pacific. EOF-2 explains 10% of the variance and is dipole pattern along the equator. this in combination with the EOF-1 mode indicates some variations of the ENSO pattern along the equator.

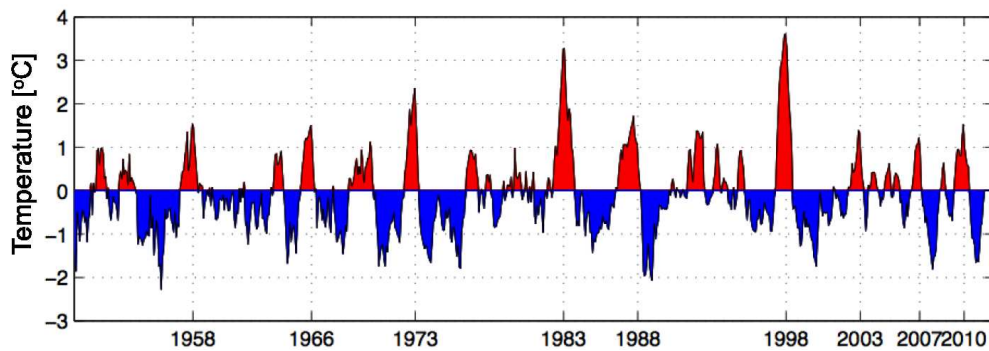


Figure 6.74: El Niño time series: the time series of the SST anomalies in the equatorial Pacific. The years mark the strongest El Niño events.

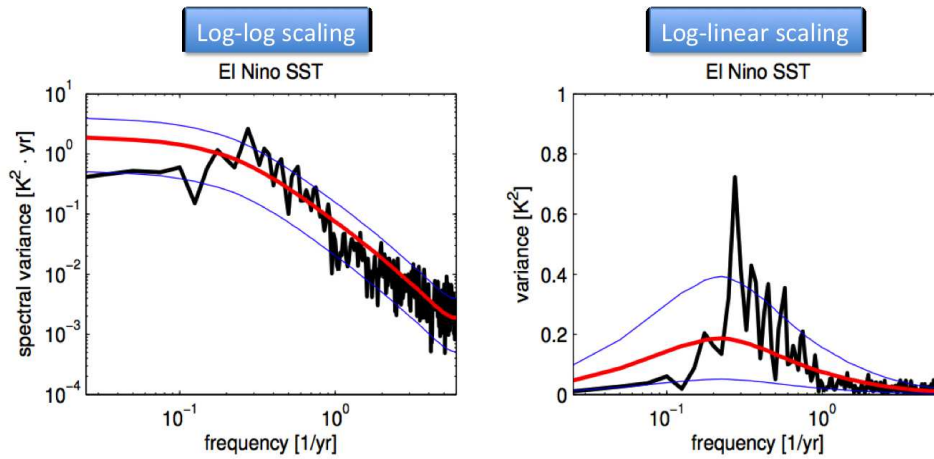


Figure 6.75: El Nino power spectrum: The right panel shows the spectrum multiplied by frequency in a log-linear plot, which allows to interpret the area underneath the curve as the total variance over the frequency band. It illustrates that most of the variance is at around 4 yrs periods.

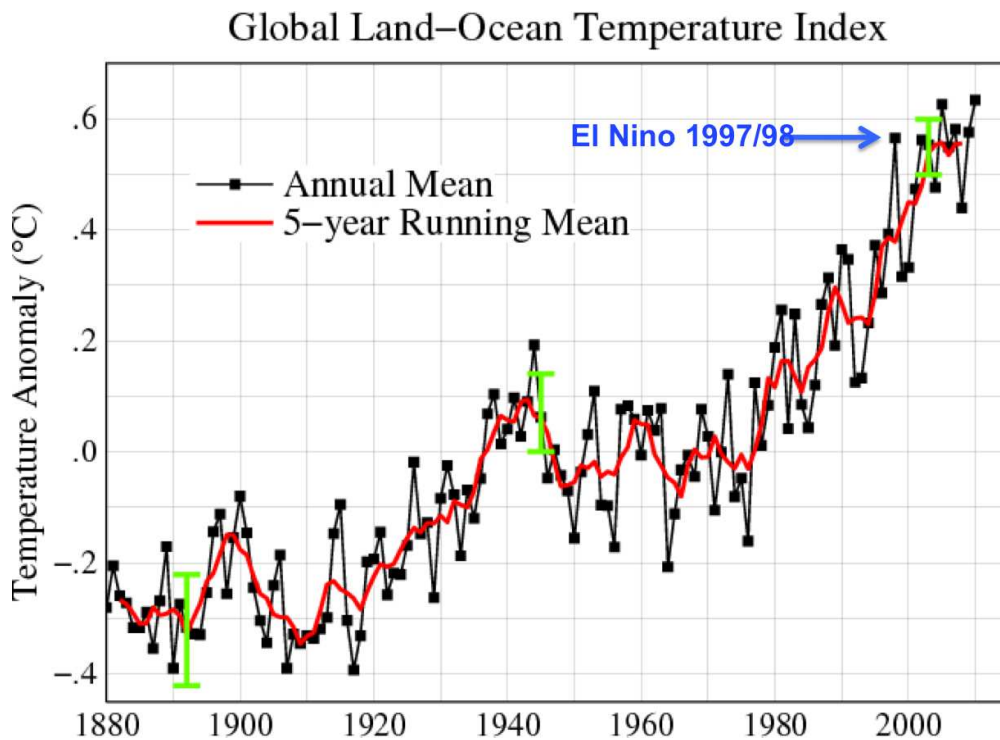


Figure 6.76: El Nino vs. global mean temperature: Strong El Nino events have an impact on the global mean temperature.

Some numbers for the El Nino heat release:

- El Nino heat release $\sim 10^{23} J$ in 6 months
- \rightarrow about 2 million 20GW power plants

- → about 500,000 hydrogen bombs
- → 10% of global annual Sun light

Some characteristics of the subsurface ENSO variability:

- ENSO dynamics are strongly controlled by dynamics in the upper ocean of the tropical Pacific.
- The strongest ENSO variability is not at the surface but in about a 100-200m depth in the *thermocline* of the ocean. The thermocline is the region of the upper ocean where the temperature decreases very quickly. It marks the change from light/warm surface water to dense/cold subsurface waters.
- New observation systems (local buoys or satellites) since the 1990s allow us to follow an ENSO event in the subsurface ocean, which very nicely demonstrates the dynamical evolution of an ENSO event.
- A deepening of the thermocline marks the increased heat content before an El Nino event in the western/central equatorial Pacific. This propagates to the east, which is followed by large scale warming of the surface.
- During the strong surface warming the western thermocline marks reduced heat content in the west, which starts to propagate to the east, introducing the end of the El Nino event and the change to a La Nina event.

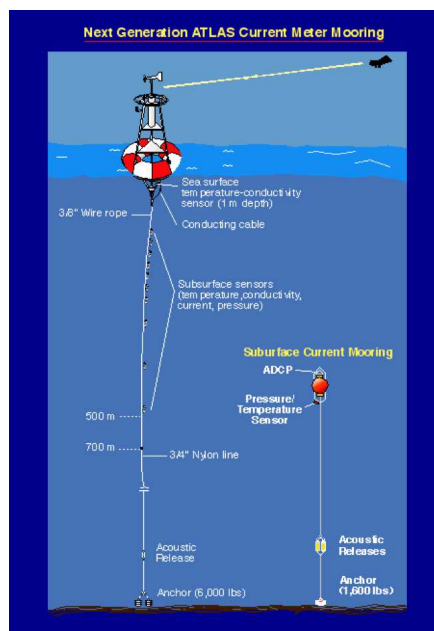


Figure 6.77: The tropical Pacific buoys observing system: The buoys are anchored on the seafloor and have measurement instruments (mostly in the upper 500m) for sea level, temperature, salinity and ocean current meters. Several of such buoys are distributed along and around the equator.

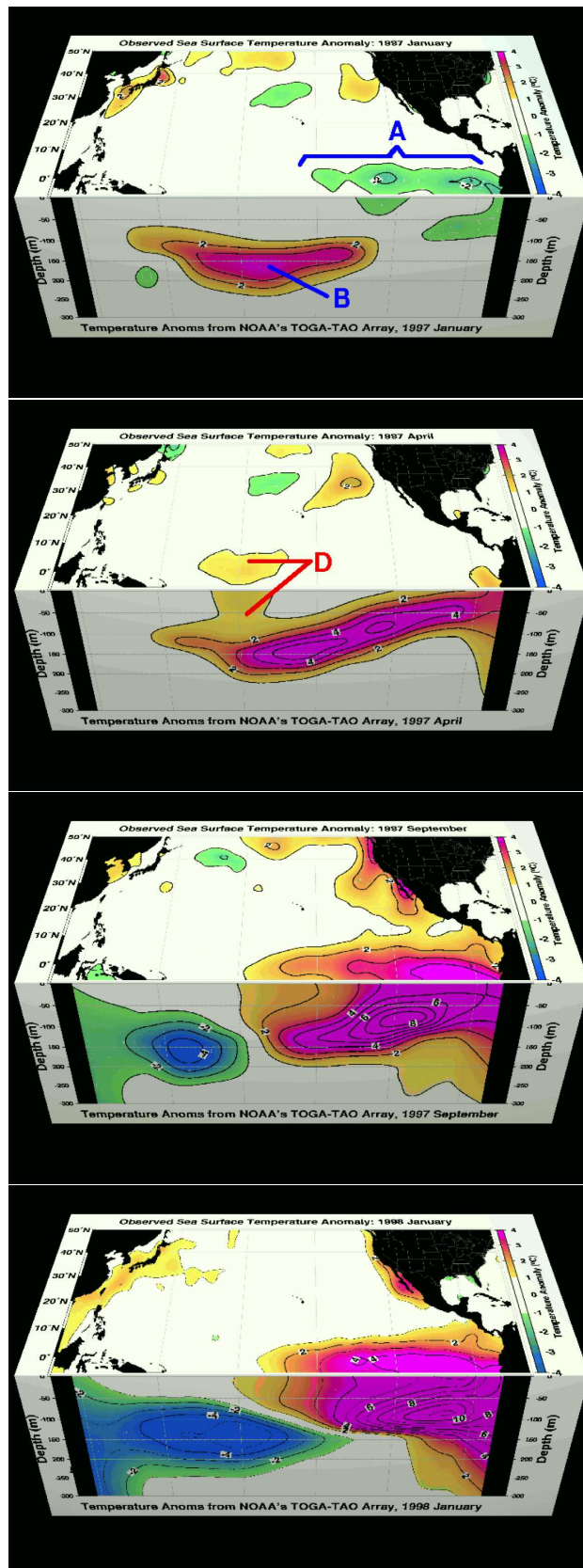


Figure 6.78: Subsurface view of on El Nino event time evolution:

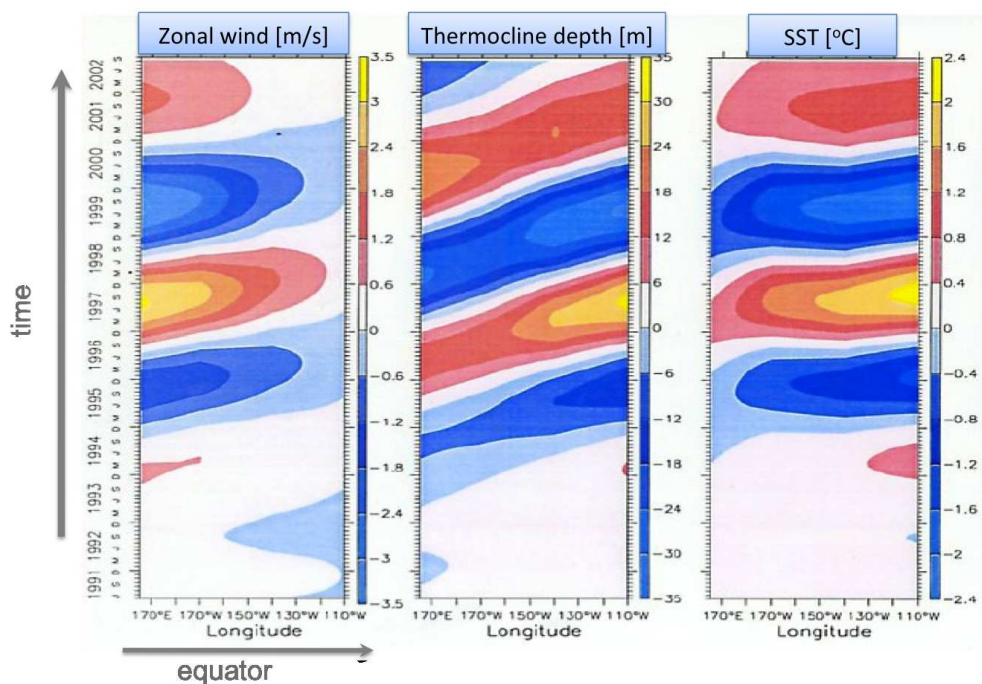


Figure 6.79: Idealised El Niño evolution: Hovmöller diagrams (spatial direction vs. time)

6.6.3 ENSO teleconnections

- ENSO has nearly global teleconnections. Which means that many regions have changes in the typical weather conditions.
- How ENSO changes the weather conditions strongly depends on the regions and season. Many teleconnections will be exactly the opposite in the opposing seasons.
- The most significant changes are related changes in the rainfall patterns of most of the tropical Indo-Pacific regions.
- Most famous teleconnections are the reduced Indian monsoon and the reduced number of hurricanes during El Niños.
- Australia tends to have significantly less rain during El Niño. Mostly in spring, but also throughout the year.
- The teleconnections roughly change sign for La Niña events.

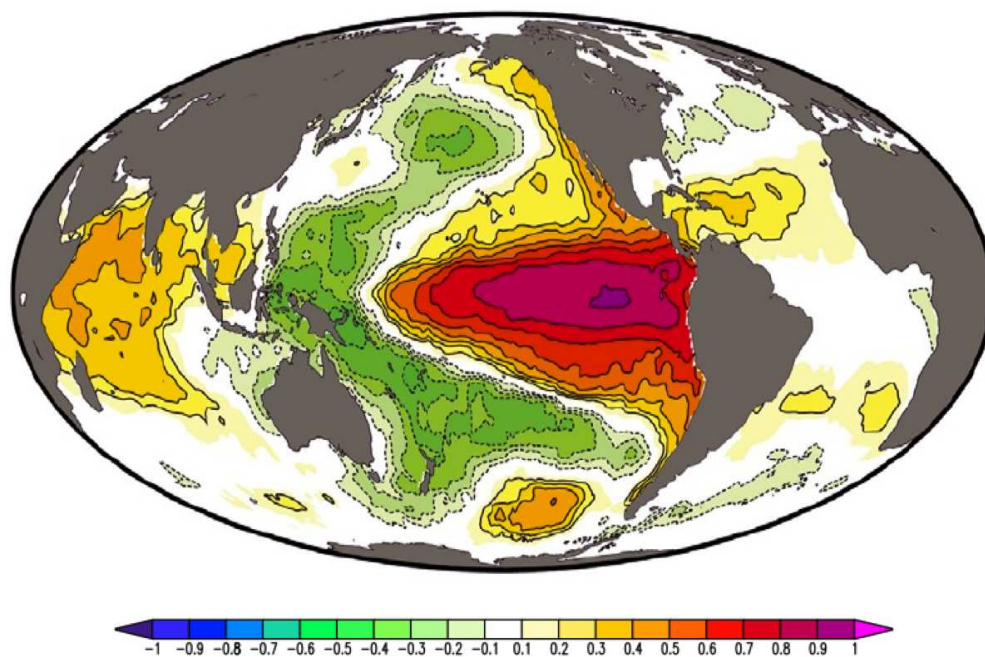


Figure 6.80: Typical El Nino pattern (correlation)

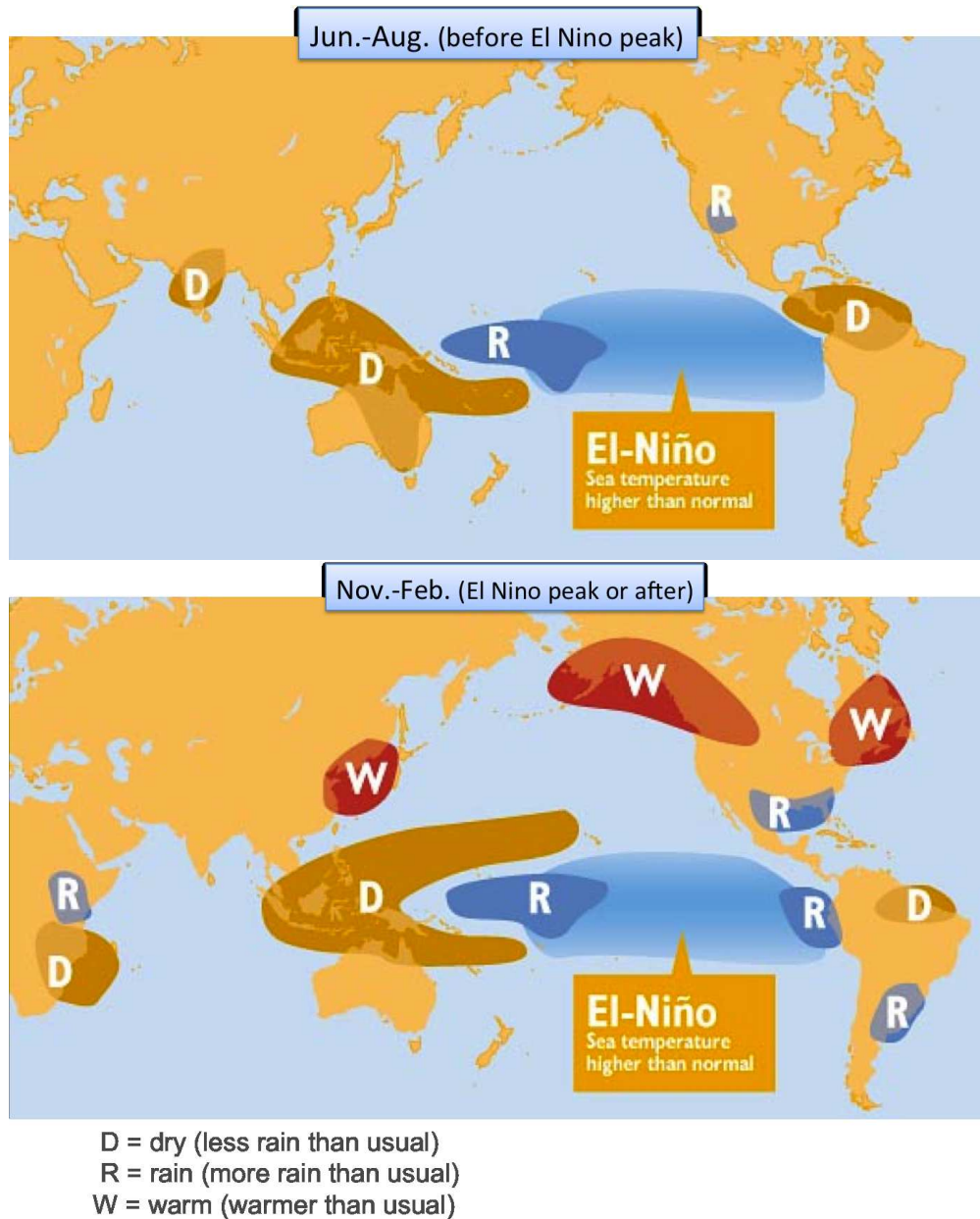


Figure 6.81: Simplified sketch of the strongest ENSO teleconnections: Upper: Jun-Aug (before El Niño peak) Lower: Nov-Feb (El Niño peak or after).

6.6.4 Dynamics

We now like to focus on the dynamics that cause the ENSO variability. For this we use what we have learned about the atmosphere and ocean dynamics in the previous sections (Chapter 3). Much of the dynamics that control the variability are strongly related to the dynamics of the mean state. So we first look at the mean state of the ocean and atmosphere in the tropical Pacific and try to understand what dynamics are causing it. We will then discuss the so called Bjerknes feedbacks, which are the main dynamical elements that cause ENSO variability. Finally, we will look at two simple conceptual toy models that describe the main features of the ENSO variability.

6.6.4.1 Mean State

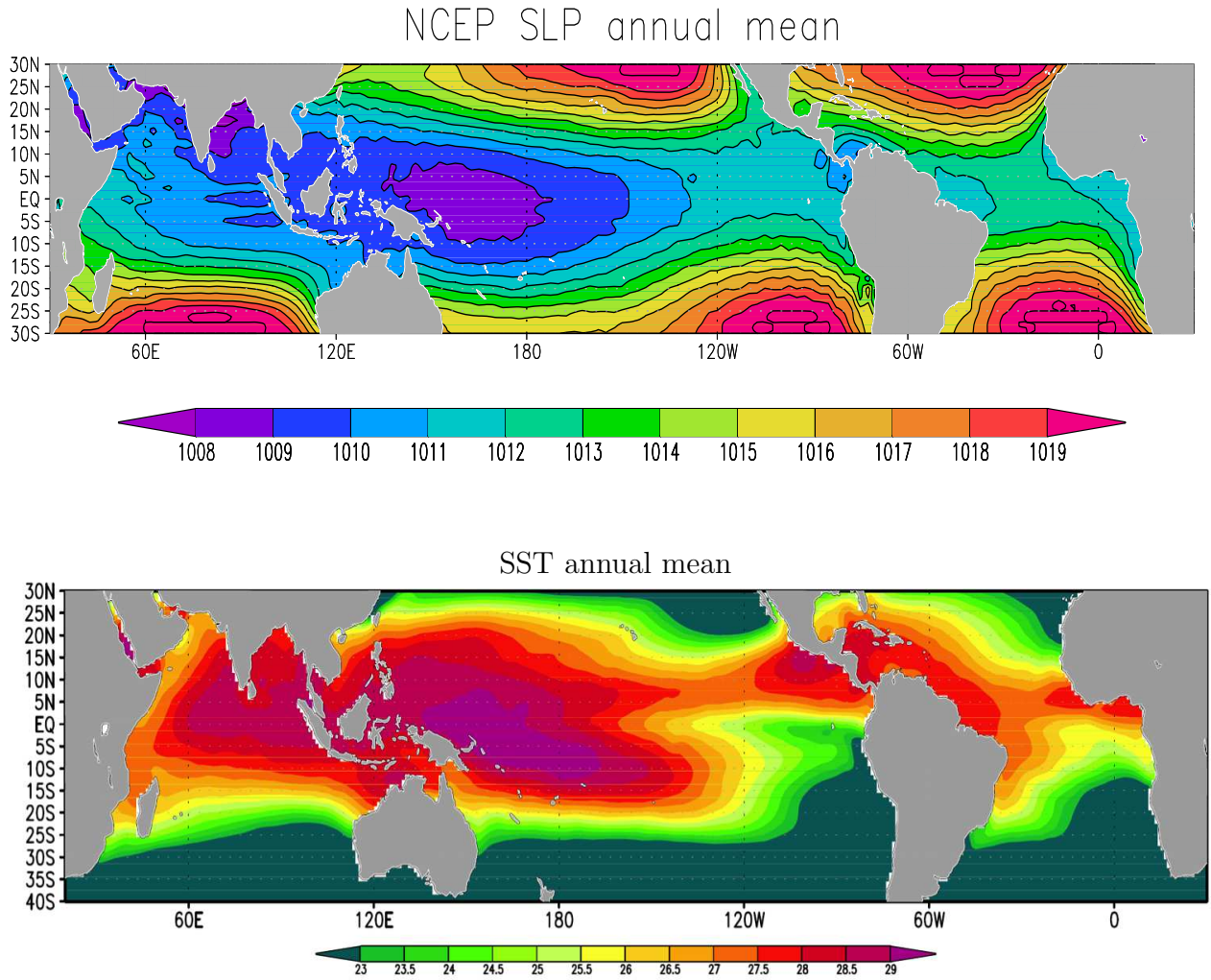


Figure 6.82: Mean state of the atmosphere and ocean: Upper: Atmospheric mean sea level pressure (SLP). Lower: mean SST.

The mean state of the tropical Pacific, and also the Atlantic and Indian Ocean has some interesting features. In Fig. 6.82 the mean atmospheric sea level pressure (SLP) and SST are shown for all tropical oceans. What is quite remarkable here is the cold eastern side of the Pacific and Atlantic and the relatively cold equatorial region along the equatorial Pacific and Atlantic ocean. Thus the tropical Pacific is marked by a strong temperature gradient from the east (cold) to the west (warm). Related to this we can not lower SLP in the western tropical Pacific and higher SLP in the eastern tropical Pacific. The tropical Pacific mean state in the ocean and atmosphere are very strongly linked. It is a quite unique situation, where you can not understand the state of one of the two systems without the state of the other. The most remarkable feature of the tropical Pacific mean state is the equatorial cold tongue. The fact that the equatorial SSTs are colder than the higher latitudes SSTs.

Important for understanding this picture is the mean wind field shown in Fig. 6.83. The near surface trade winds are primarily easterlies, which is related to the large-scale atmospheric Hadley circulation cell. Thus the zonal winds dominate.

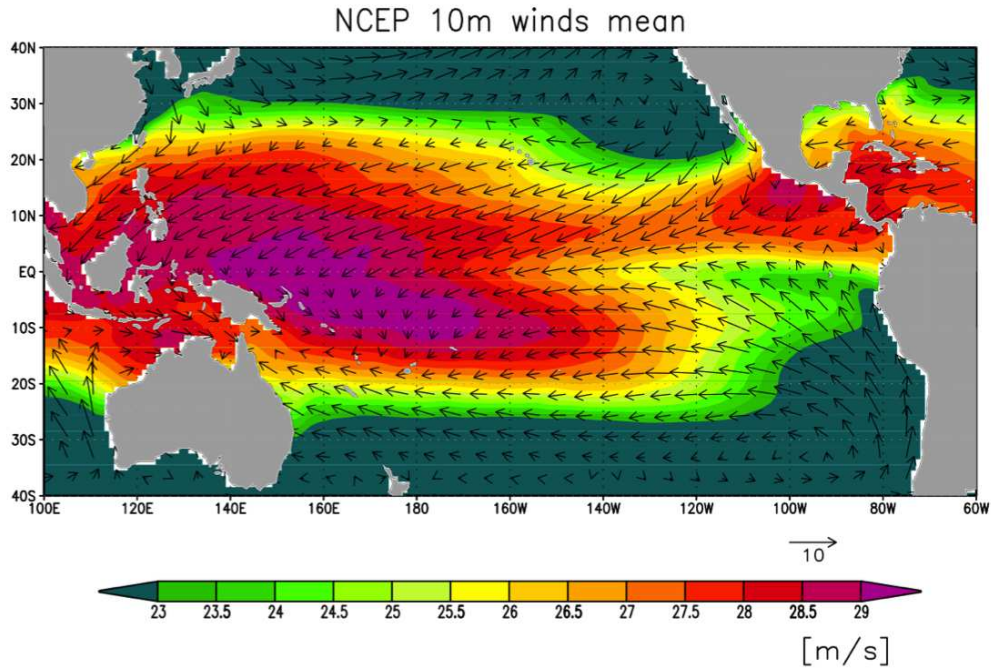


Figure 6.83: NCEP mean 10m winds and mean SST.

Ocean mean state dynamics

The most important feature of the equatorial cold tongue is a result of prevailing easterly trade winds and the Ekman ocean currents induced by the friction and Coriolis forcing. The easterly surface trade winds can be considered as a given boundary condition for the oceans, because they result from the large-scale direct heating Hadley cell circulation.

So we can start the discussion with considering what would happen to the equatorial ocean surface layer when prevailing easterly winds force it, see sketch Fig. 6.84. The warm surface waters will be pushed to the western side of the ocean basin. The warm water will pile up and lead to higher sea level on the western side and lower sea level on the eastern side of the basin. This will induce a vertical ocean circulation at the equator with downwelling on the western side and upwelling on the eastern side. We roughly have a counter-clockwise vertical overturning circulation along the equator. This whole circulation is entirely forced by the atmospheric winds. The upwelling in the east will lead to mean colder SSTs. It also causes the thermocline to have an east to west gradient. Note that the equator has the unique feature of no horizontal Coriolis forcing. Thus the induced circulation along the equator can be maintained without being deflected. This would not work at any other latitude, as the Coriolis forcing would lead to a deflection of the initially induced zonal circulation and eventually the circulation would break down into gyres (eddies).

The prevailing easterly trade winds also have strong effects on the surface current off the equator, see sketch Fig. 6.85. Off the equator the Coriolis forcing is not zero any more and is into opposite direction on the two hemispheres. This leads to diverging ocean current flow on the equator and therefore to upwelling of cold subsurface waters to maintain the mass balance. Again, this is a unique feature of the equator, as this is the only place where the Coriolis forcing can lead to diverging flows. The equatorial upwelling of cold subsurface waters induced by the winds and the Coriolis forcing lead to the remarkable equatorial cold tongue of the tropical Pacific. We can see some indication of this also in the tropical Atlantic, but not in the Indian Ocean. In the Indian Ocean the mean winds are dramatically changing directions during the seasons (monsoons) and the eastern boundary of the ocean basin is not closed, allowing warm Pacific ocean waters to flow in.

These two characteristics of the Indian ocean are likely to prevent the formation of an equatorial cold tongue here.

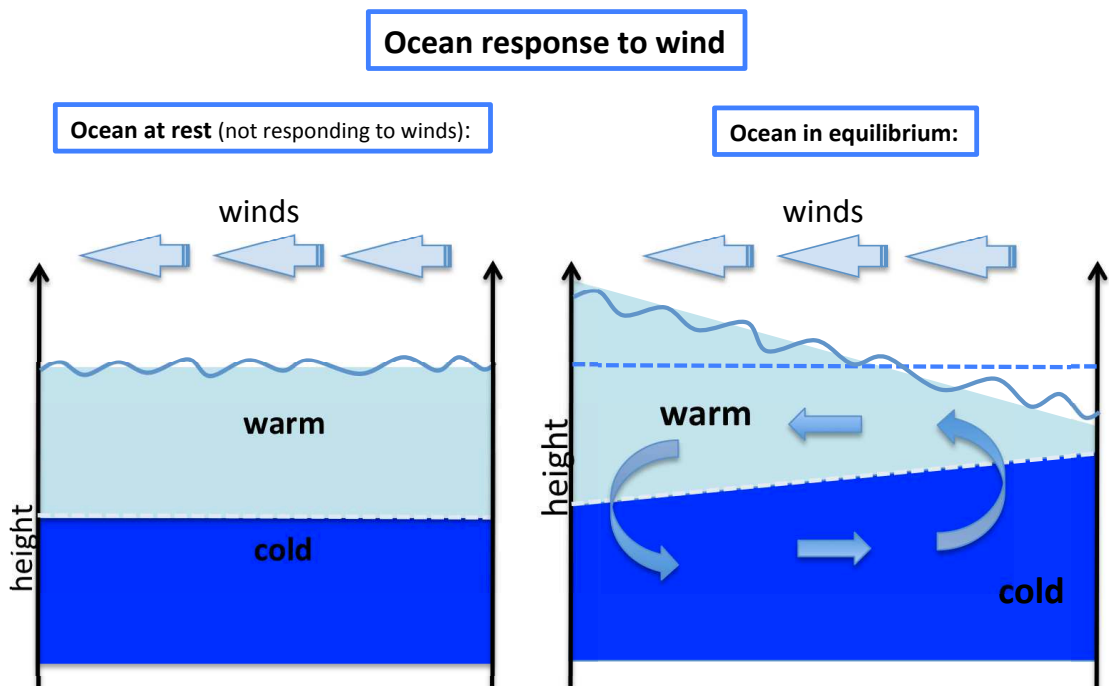


Figure 6.84: Sketch of ocean mean state. A vertical sketch of the ocean temperature and the surface winds above it along the equatorial Pacific. Left: assuming the SST along the equator is not responding to the winds. Right: the equilibrium state of the ocean in response to the surface easterly winds.

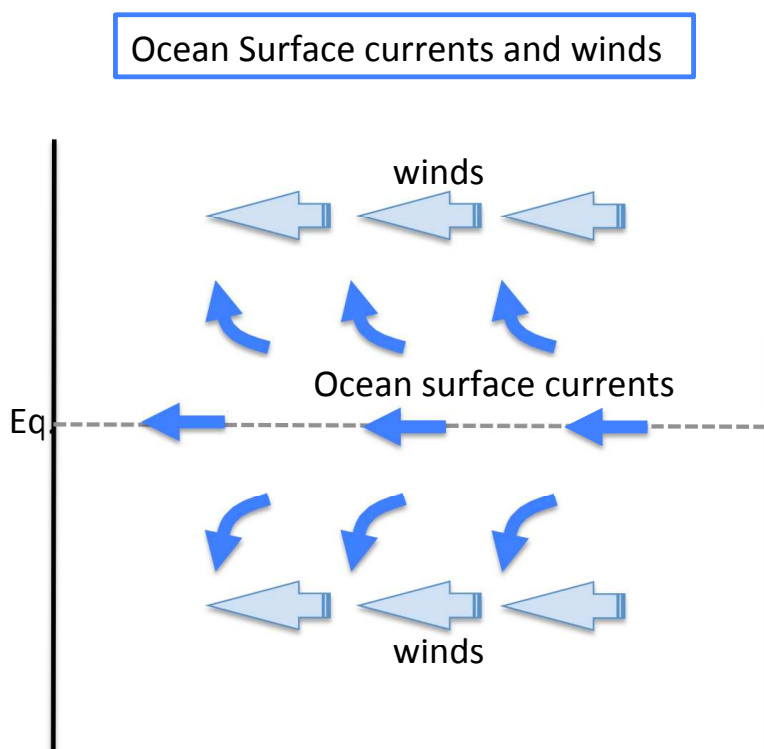


Figure 6.85: Sketch of ocean surface currents and winds. A view onto the Pacific ocean surface winds and resulting ocean currents. Off the equator the ocean currents are deflected away from the equator due to the Coriolis force.

Atmospheric mean state dynamics

The equatorial Pacific is marked by a strong surface temperature difference between the east (cold) and the west (warm), caused by ocean dynamics as described above. The atmospheric mean state dynamics are strongly affected by this SST gradient along the equator. The atmospheric circulation in general is mostly forced by surface temperature difference. It induces, for instance, the most dominant Hadley cell circulation in the tropics. With rising air over warmer regions and descending air over colder regions, forced by the buoyancy of the air masses. The Pacific temperature gradient induces a secondary tropical circulation, called the *Walker circulation*, with rising over the warm pool in the west and sinking over the cold east equatorial Pacific.

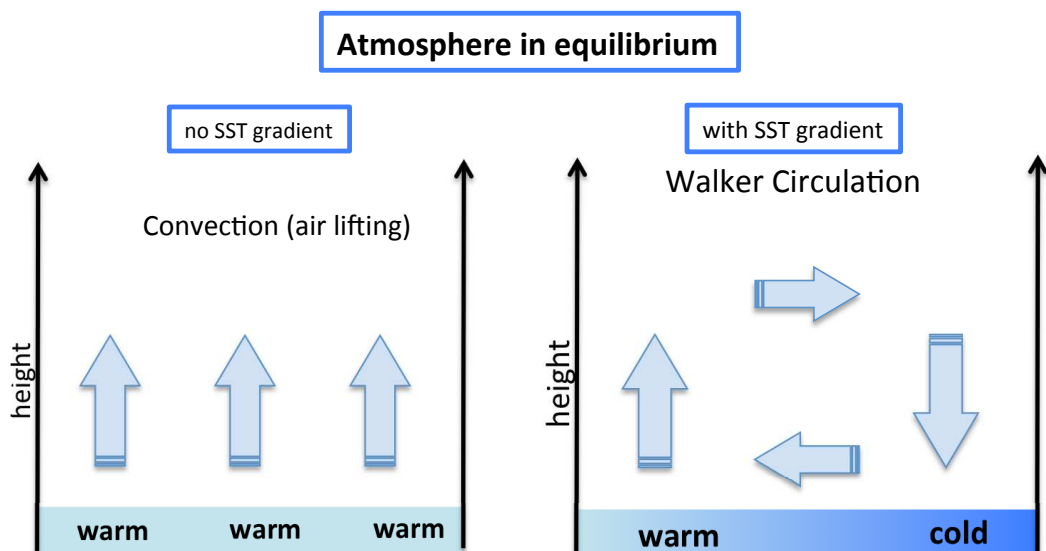


Figure 6.86: Sketch of atmospheric mean state. A vertical sketch of the SST and atmosphere above it along the equatorial Pacific. Left: assuming the SST along the equator is the same everywhere. Right: assuming it is warmer in the western and cooler in the east.

The sketch in Fig. 6.86 illustrates how the atmosphere response to the SST gradient along the equator. If we first of all assume no SST gradient, then the air would rise everywhere along the equator. This forms the upward branch of the primary large-scale meridional Hadley Cell circulation. Now with warmer SST in the west and colder in the east, the upward motion of the air is favoured over the warmer western Pacific and reduced over the colder eastern Pacific. Thus we will build up low surface pressure in the west and high surface pressure in the east, see Fig. 6.82. This induces a secondary zonal circulation along the equator with upward motion only in the western side and sinking on the eastern side. On higher levels in the atmosphere the winds will be westerlies to close the loop. At the surface the easterly trade winds are amplified by this secondary circulation. The secondary circulation cell is called the Walker circulation.

Again, the absence of the Coriolis force along the equator allows this secondary circulation to exist. Thus, the circulation induced by the surface temperature differences can be directly circulated from high surface pressure (cold SST) to low surface pressure (warm SST). This would not be possible at any other latitude, as the Coriolis force in balance with the pressure gradient force would lead to geostrophic balance, which would lead to circulations around the pressure extremes and not to a direct circulation between them.

Now with raising air in the west and sinking air in the east we have an influence on rainfall and clouds. Rising air favours convection, which favours precipitation. The opposite holds for sinking air. The Walker circulation causes the difference in the precipitation patterns, with very wet conditions in the western rising branch and very dry conditions in the eastern sinking branch. This is similar to the Hadley circulation pattern causing dry and wet regions at different latitudes (tropics and subtropics). We can see this effect in the mean rainfall along the equatorial regions, see Fig. 6.87.

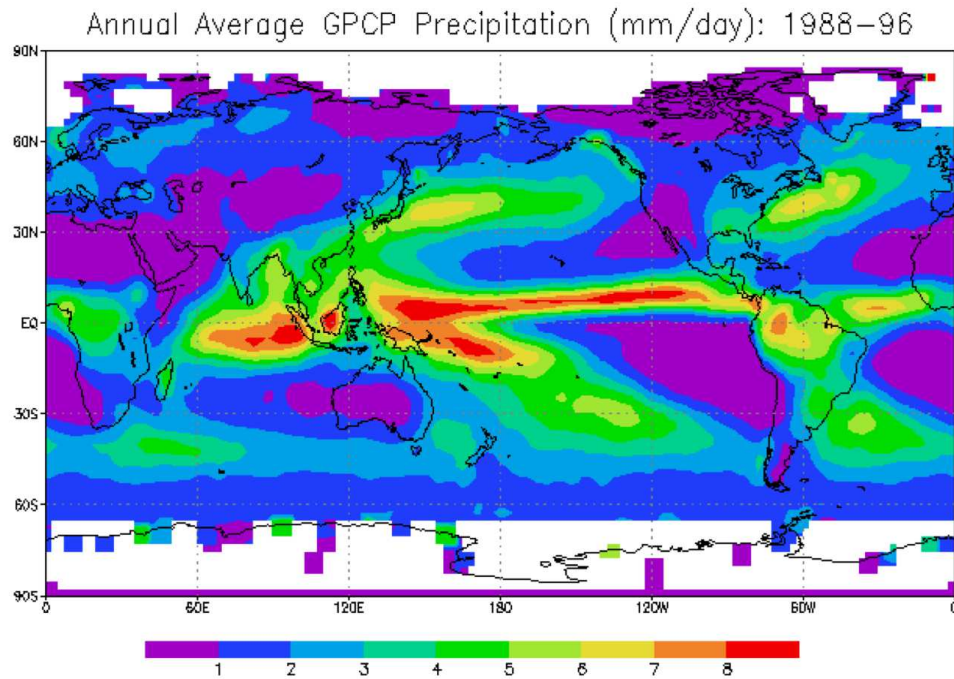


Figure 6.87: Annual average GPCP precipitation (mm/day): 1988 - 1996

Figure 6.88 illustrates both ocean and atmospheric mean circulations. The ocean forced by the surface easterly winds builds up warm water to the west and cold to the east. Along with this we have counter clockwise vertical circulation, which leads to shallow thermocline in the east and deep thermocline in the west. Thus we have a thermocline gradient along the equatorial Pacific.

The SST gradient along the equator induces the Walker Circulation, which leads to more rainfall in the warm pool of the western Pacific and less rainfall in the eastern Pacific. Both of these zonal circulation cells in the atmosphere and ocean strong depend on each other. Without the SST gradient there would be no Walker circulation and without the Walker circulation the surface easterly winds would be much weaker and the SST gradient would be strongly reduced.

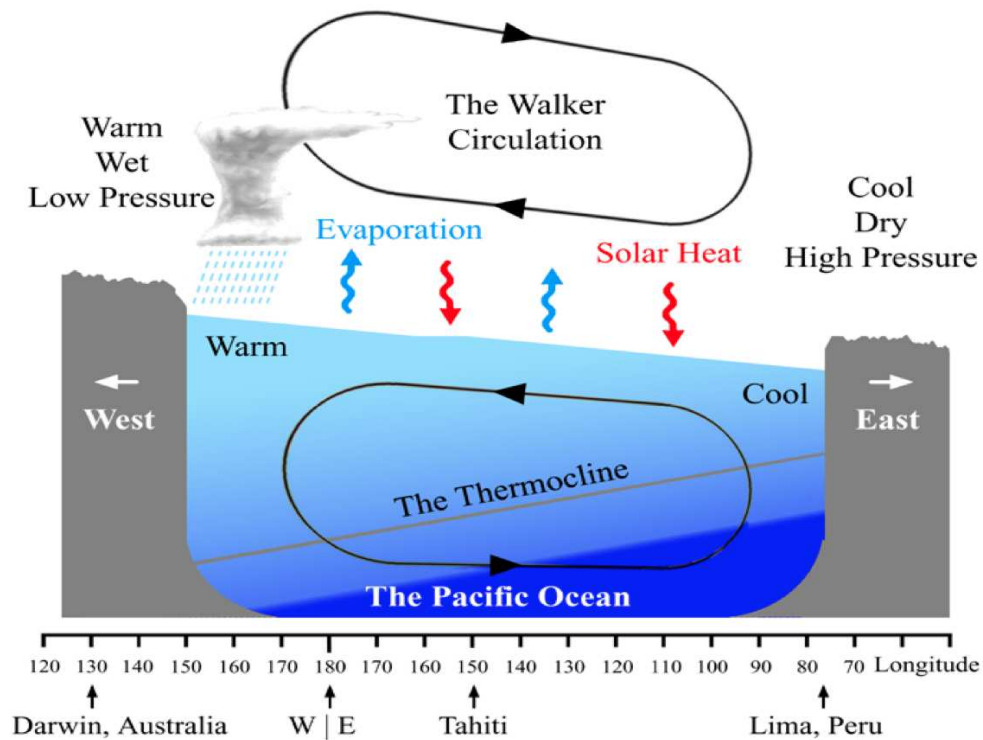


Figure 6.88: Sketch of the mean climatic state with the mean atmospheric and ocean circulation cells.

Variability of the Walker circulation is called the *Southern Oscillation* (for historical reasons). A strong Walker circulation means a positive *Southern Oscillation Index* (SOI). During El Nino the Walker circulation is weakened or even totally collapsed (negative SOI), because the SST gradient along the equator is reduced, see Figs. 6.89 and 6.90. During La Nina the opposite is true: the SST gradient is enhanced and the Walker circulation is enhanced.

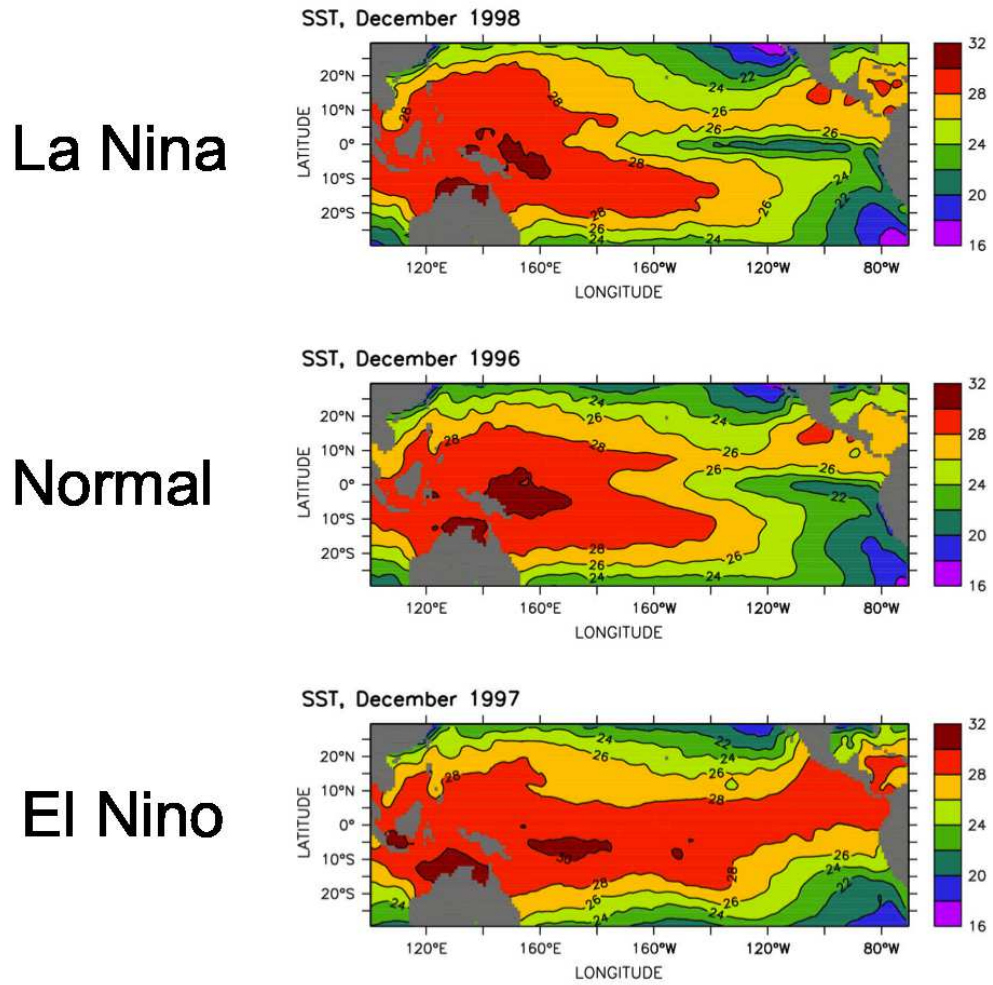


Figure 6.89: SST at different dates, illustrating El Nino, normal and La Nina conditions. La Nina is intensification of the mean cold tongue, whereas El Nino conditions have have no cold tongue.

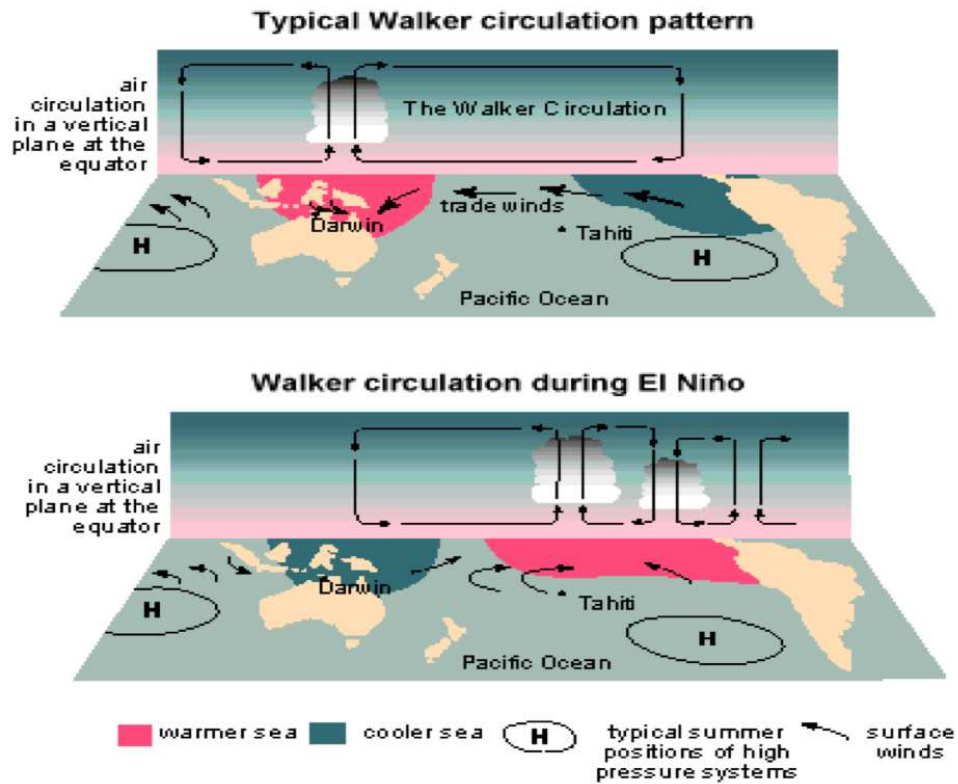


Figure 6.90: Walker circulation

This has consequences for the patterns of rainfall, see sketches in Fig. 6.91. During El Niño events the rainfall from the western Pacific follows the warm SST into the central to east Pacific. During La Niña the rainfall is pushed further to the west.

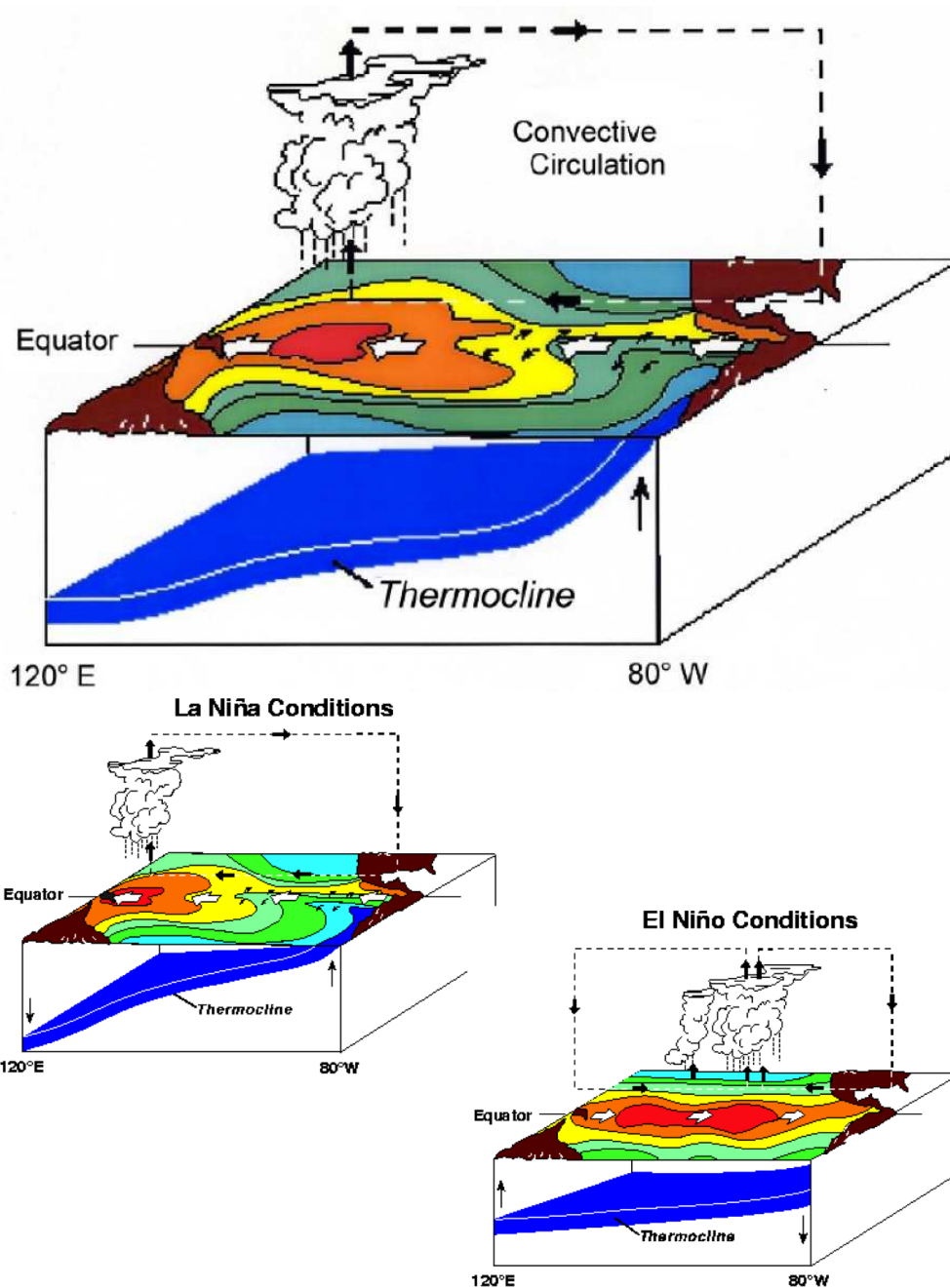


Figure 6.91: Sketch of the tropical Pacific conditions. Upper is average condition.

6.6.4.2 Bjerknes Feedbacks

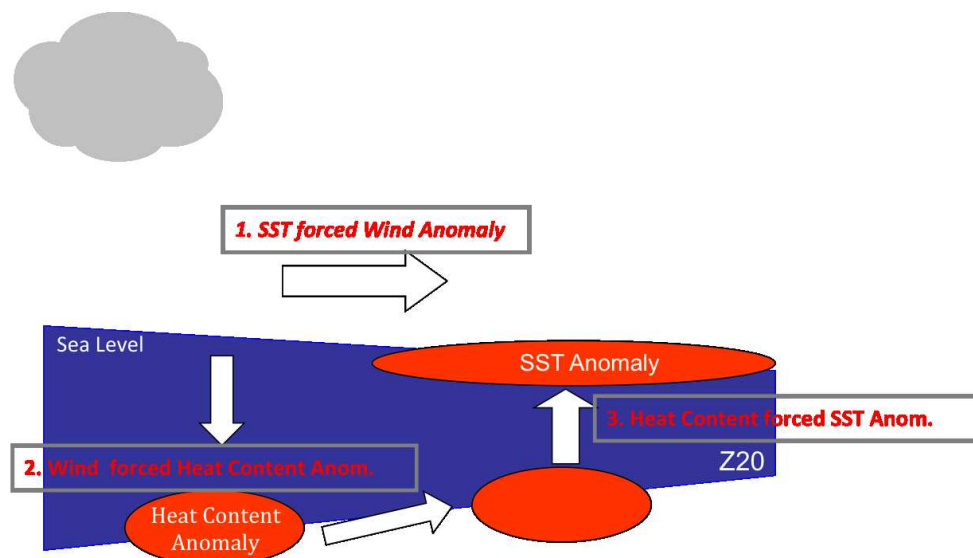


Figure 6.92: Bjerknes coupled feedbacks

The fact that both the atmospheric and the oceanic mean state and the associated zonal circulation patterns strongly depend on the other system's state, makes the ocean-atmosphere system in the tropical Pacific very sensitive and potentially unstable to small changes in one of the two systems. This is the main reason for the prominent climate variability in this region. No other large-scale region in the earth's climate system has any climate variability that strong on seasonal to decadal time scales. It makes the ENSO variability the most prominent element in natural climate variability on seasonal to decadal time scales.

The three main elements which are involved in these dynamics here are the *SST*, *zonal winds* and the *thermocline depth*, see sktech in Fig. 6.92. The interactions between these three elements are often described by the so-called *Bjerknes feedbacks*. They are:

- SST forces zonal wind
- Zonal wind forces thermocline
- Thermocline forces SST

As you can see these feedbacks define a feedback loop: the last element goes back to the first element of the feedbacks. Thus it builds a loop. It does not matter where we start the loop, but traditionally we can start the discussion with assuming some SST anomaly:

The *SST* forces *zonal wind*: A warm SST anomaly causes heating of the atmosphere, which leads to low surface pressure. The winds will blow towards the low pressure (no Coriolis deflection at the equator). This means reduced zonal easterly winds to the west (central Pacific). In Figure 6.93 this relation is estimated from observations in terms of a linear regression of the zonal near surface winds towards SST in different regions. In the Pacific we can see that when the SST anomalies in the eastern box are $+1^{\circ}\text{C}$ then in average we have positive zonal wind anomalies to the west of it. Positive zonal wind anomalies means reduced easterly winds or even stronger westerly winds. A similar effect we see in the Atlantic and Indian Ocean for the corresponding SST boxes in these ocean basins.

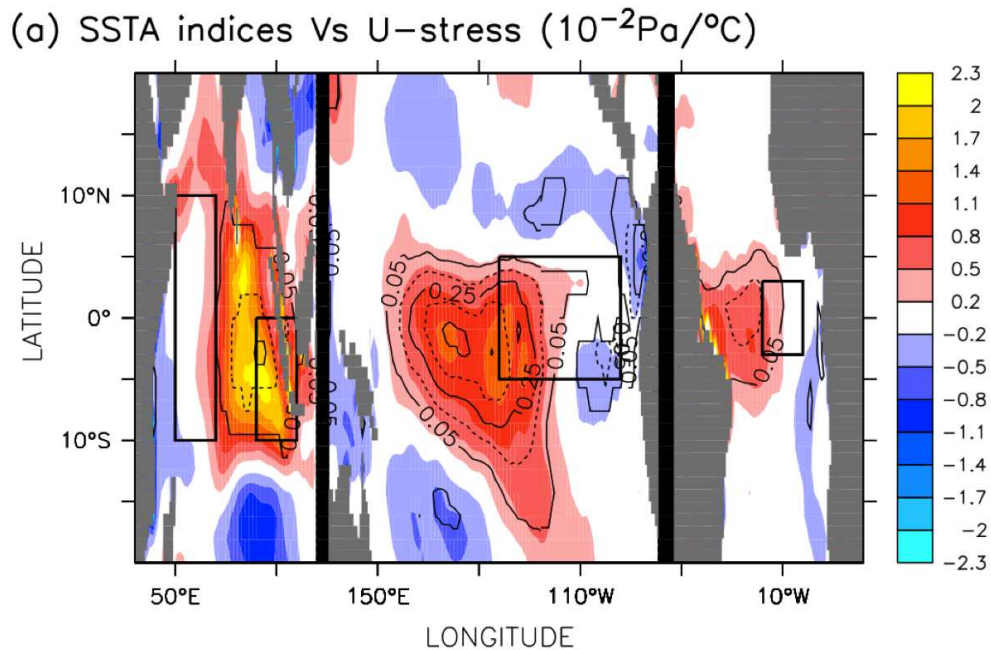


Figure 6.93: SST vs. zonal winds. Relation between the zonal wind field and the SST in the box. For the three tropical oceans separately. The linear regression estimates the mean wind stress anomaly (friction of the winds onto the ocean surface) (in units Pa) per SST anomaly of one degree celsius in the black box of each ocean basin. The analysis is done for each ocean basin independently. Note, that here zonal wind stress is related to SST, but not zonal wind itself. In the context of this analysis it does not matter whether it is wind or wind stress; both are strongly related to each other.

Zonal wind forces thermocline: The thermocline depth in the central and western Pacific is kept deeper than in the eastern Pacific by prevailing easterly zonal winds. Weaker than normal winds lead to a shallowing of the thermocline. Gravity waves will propagate the thermocline adjustment to the east leading to a deepening of the thermocline in the east (the bathtub effect). In Figure 6.94 this relation is estimated from observations in terms of a linear regression of the thermocline depth towards the zonal near surface winds in different regions. In the Pacific the winds in the central to western Pacific lead to a shallowing of the thermocline in the western side of the Pacific and, more importantly, a deepening of the thermocline in the eastern part of the Pacific. A similar structure can also be seen in the Atlantic and to a much lesser degree in the eastern Indian Ocean.

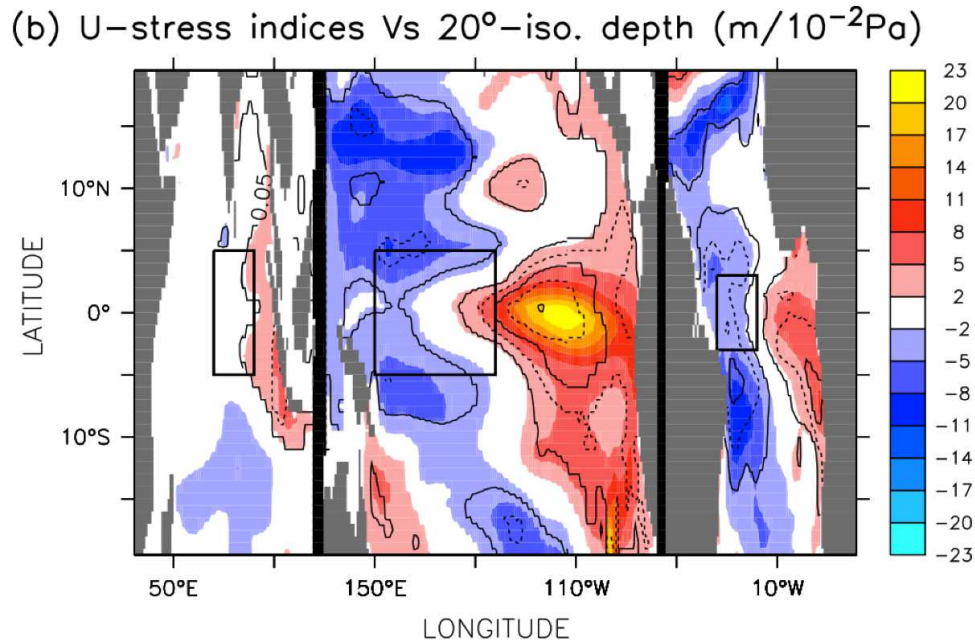


Figure 6.94: Zonal winds vs. heat content. Relation between the 20°C isotherm depth field (a good approximation of the depth of the thermocline) and the zonal wind in the box. For the three tropical oceans separately. Negative values indicate a shallower thermocline for westerly wind anomalies in the box of the corresponding ocean basin. In turn, positive values indicate a deeper thermocline for westerly wind anomalies. Vice versa for easterly wind anomalies.

Thermocline forces SST: A deeper thermocline in the east reduces the upwelling of cold subsurface waters along the equator and the South American coasts. This leads to warming of the SST, which closes the loop and re-enforces the initial SST anomaly. Thus, this is a positive feedback loop. In Figure 6.95 this relation is estimated from observations in terms of a linear regression of the SST at each point of the map towards the thermocline depth at the same location. In the eastern Pacific and Atlantic we can see a clear relation between thermocline and SST: In average we find that when the thermocline is deeper than normal, than the SST is also warmer than normal. This relationship is not found in the Indian Ocean.

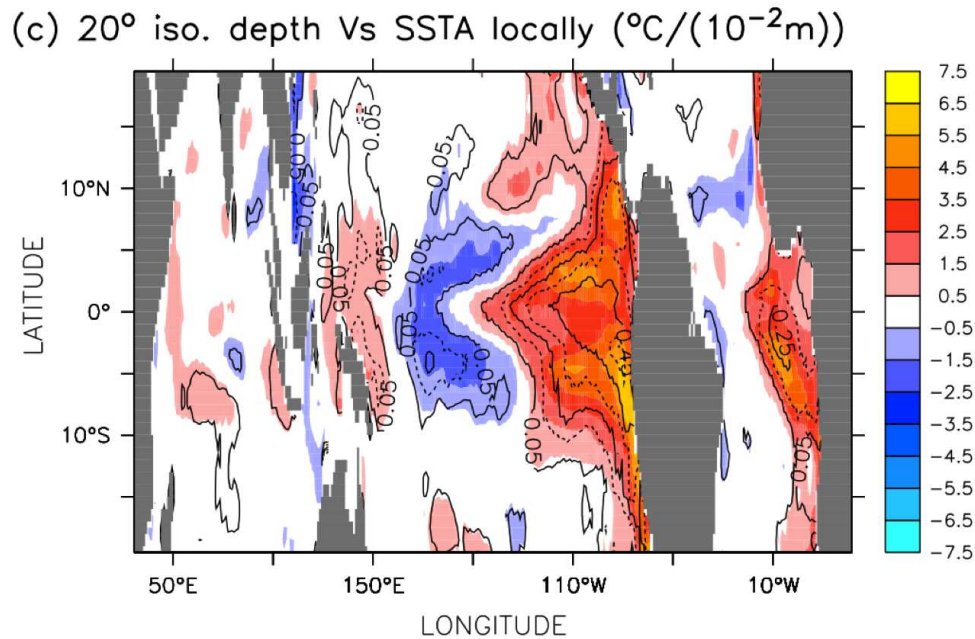


Figure 6.95: Heat content vs. SST. The local relation between the 20°C isotherm depth field and the SST field. Positive values indicate that in average deeper than normal thermocline at that location are associated with warmer than normal SST at the same location. Vice versa for negative values.

SST Feedbacks

Note that the strength of the SST response to changes in thermocline and zonal winds depend on many factors in the atmosphere and ocean. The atmospheric feedbacks depend on changes in cloud cover, which change the incoming solar radiation. It depends on the latent cooling by evaporation at the surface, which depends on the wind speed, humidity and SST. The oceanic feedbacks depend on the strength of the upwelling and the temperature difference between the surface, the subsurface ocean and off equatorial regions. This strongly depends on the sensitivity of the thermocline to zonal winds, which can be different at different regions. Overall these interactions are quite complex. State of the art IPCC climate models largely disagree in the characteristics of the SST Feedbacks with each other and with observations. Indicating that it is far from trivial to reproduce the ENSO SST Feedbacks correctly.

Wind Feedbacks

Similarly, the strength of the wind respond to changes in the SST depend on a number of processes in the atmosphere. The strength of the atmospheric circulation response in the tropics strongly depend on the moist convection, which is related to processes of evaporation, precipitation, cloud formation and also to the large-scale circulation patterns. Again, these interactions are quite complex and again state of the art IPCC climate models largely disagree in the characteristics of the wind feedbacks with each other and with observations. This is again indicating that it is far from trivial to reproduce the ENSO wind feedbacks correctly.

Thermocline Feedbacks

Finally, the thermocline feedbacks depends on a number of process within the ocean. How strong the thermocline responses to wind forcing is depending on the vertical and horizontal profiles of the

ocean temperatures and salinities, but also on mixing processes and other smaller scales dynamics. These interactions are also quite complex and yet again state of the art IPCC climate models largely disagree in the characteristics of the thermocline feedbacks with each other and with observations. Thus this process is also far from trivial to simulate correctly.

6.6.4.3 Delayed Action Oscillator

Delayed action oscillator model of ENSO

Schopf and Suarez 1988

- The fact that El Nino is just one large-scale fixed SST pattern changing over time supports the idea that El Nino can be described by just one value.
- The Schopf and Suarez model from 1988 is one of the first models that can describe the tendencies of El Nino over the next few months.
- It is based on the ad hoc assumption that the subsurface propagation of the signal influences the temperature tendencies with some delay.
- It is a very simple forecast model of El Nino with just knowing the current and past state of El Nino.

$$\frac{\partial T}{\partial t} = T - \gamma T(t - \Delta) = cT^3 \quad (6.11)$$

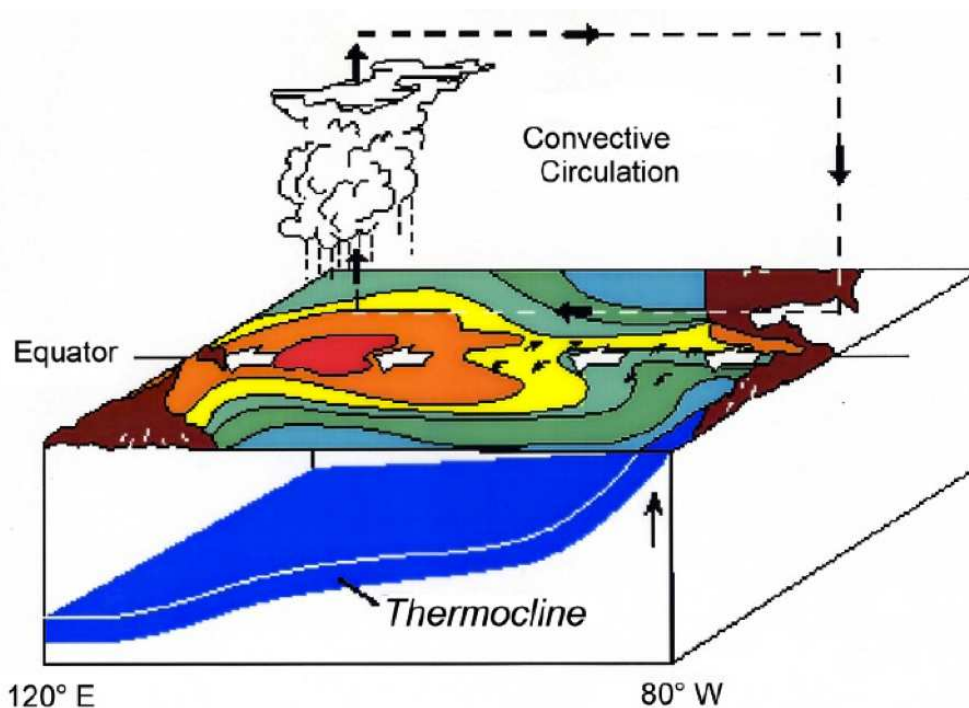


Figure 6.96

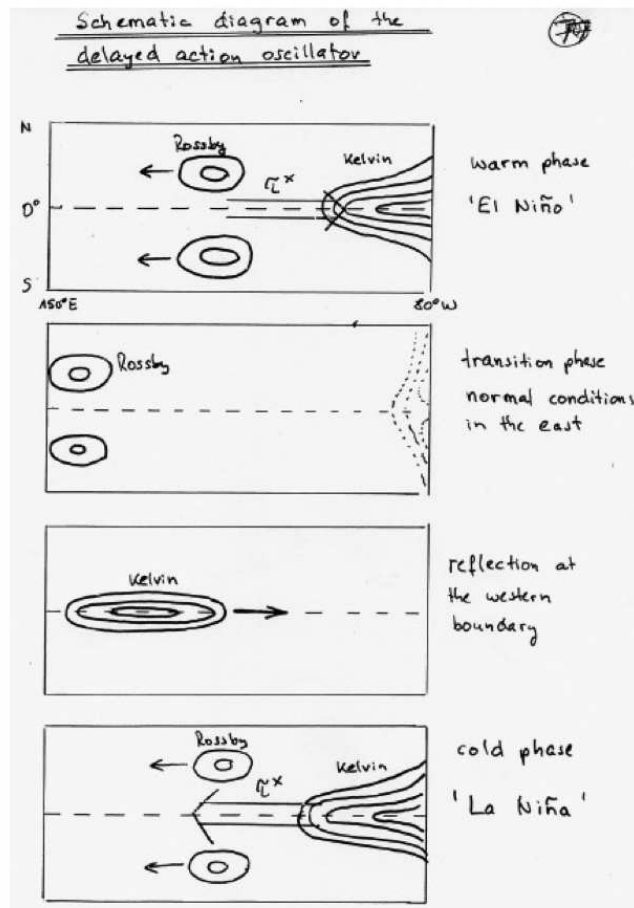


Figure 6.97: Schematic diagram of the delayed action oscillator

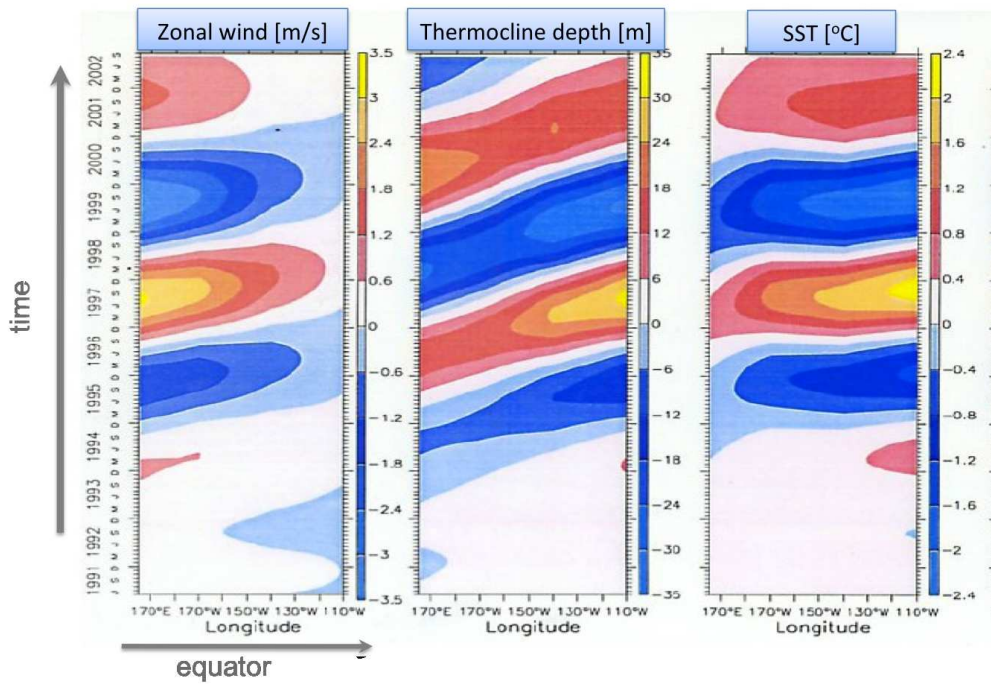


Figure 6.98: Heuristic derivation of the "delayed action oscillator"

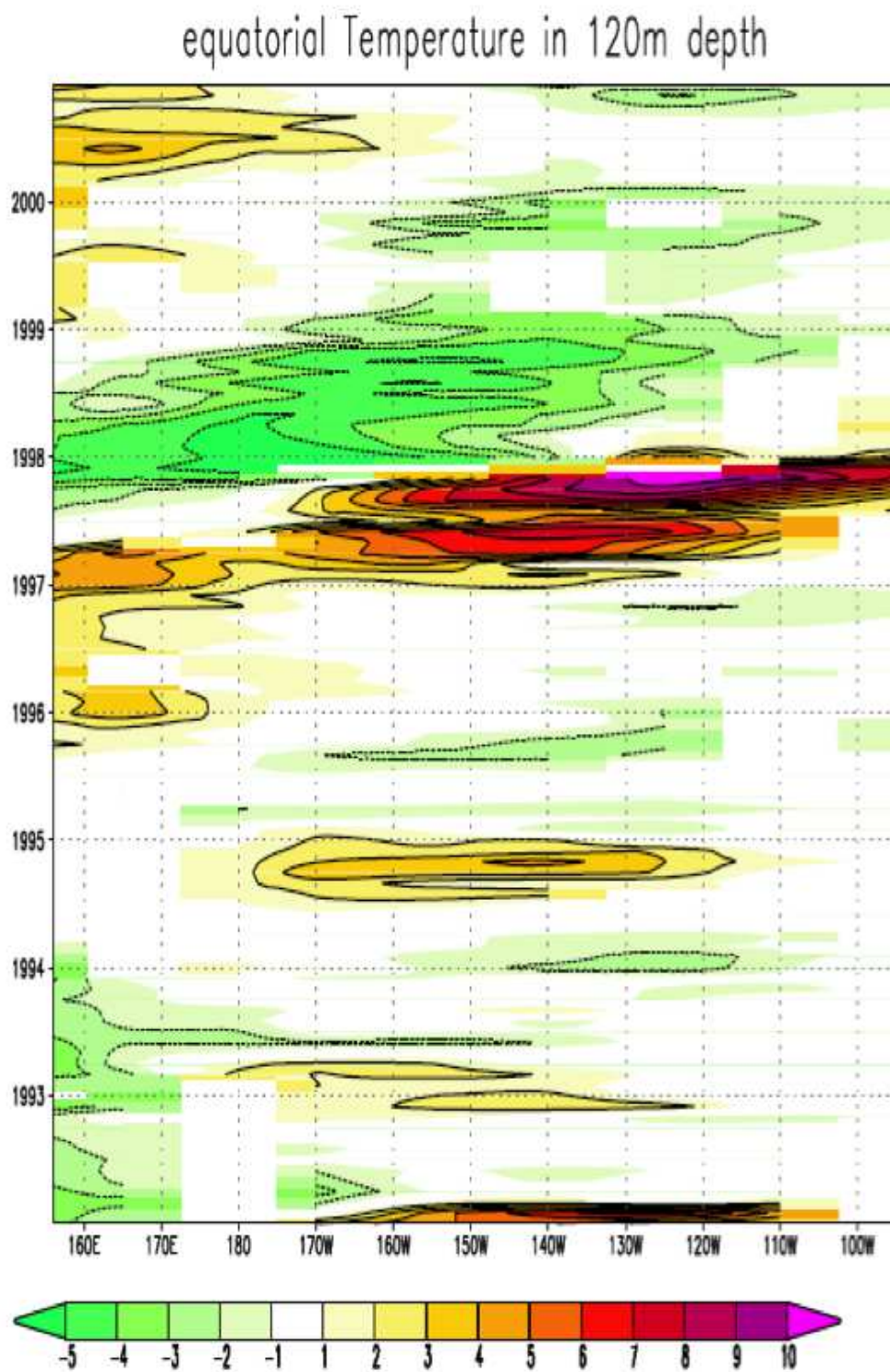


Figure 6.99: Heuristic derivation of the "delayed action oscillator"

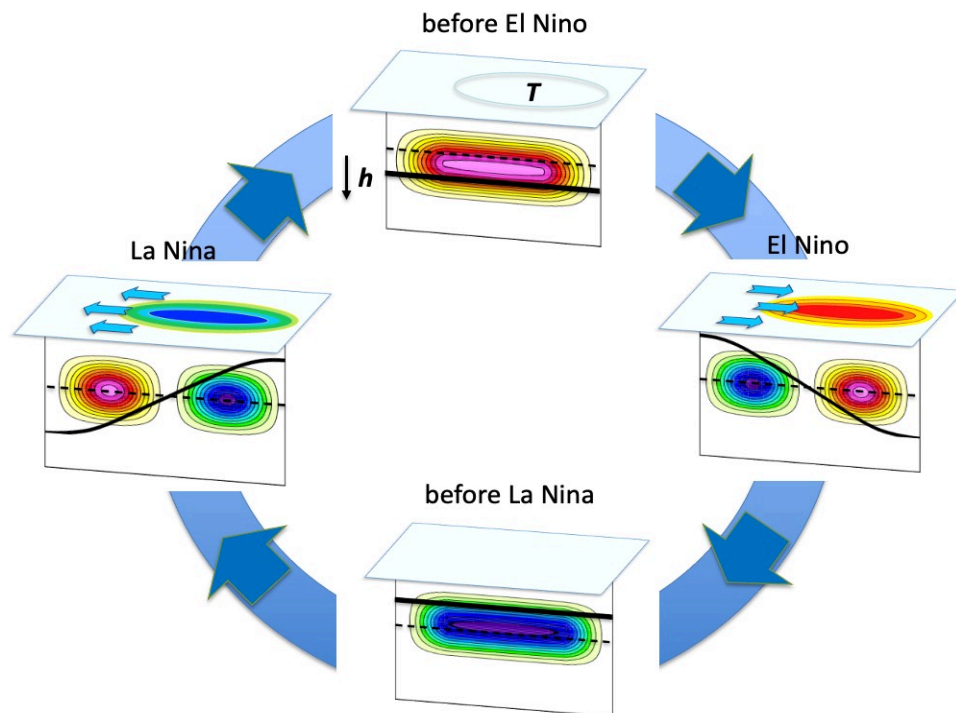


Figure 6.100: Sketch of the ENSO recharge oscillator model dynamics. The ENSO cycle is clockwise with the heat content (h) in the vertical direction and sea surface temperature anomalies (T) in the horizontal direction. The three blue arrows in the horizontal planes mark wind anomalies resulting from T .

6.6.4.4 The Recharge Oscillator Model

Jin 1997

- The recharge oscillator model of ENSO describes the dynamics of ENSO much better than previous conceptual models.
- It basically includes all the Bjerknes feedbacks in a consistent framework.
- ENSO can be understood as a coupling between thermocline depth over the whole Pacific, h , and the SST in the NINO3 region.
- Thermocline depth is basically a measure of heat content in the upper ocean. Large depth = large heat content.
- A large h forces positive SST tendencies, due to reduced cold water upwelling in the east eq. Pacific.

- A large SST reduces the thermocline depth, because warmer SST in the east eq. Pacific weakens the easterly winds, that normal push warmer waters to the west.
- The variability in thermocline depth and SST are 90° out of phase with the thermocline depth evolution leading the time evolution of the SST by a few months.
- This defines a 2-dimensional phase space of an oscillation cycle, see Fig. 6.100.
- The damping of the SST , a_{11} , is caused by atmospheric and oceanic feedbacks. The atmosphere has positive feedbacks dominating ($a_{A11} > 0$), and the ocean has negative feedbacks dominating ($a_{O11} < 0$).
- The model is a damped oscillation between heat content and SST with a period of about 4 years.
- Chaotic weather fluctuations in zonal winds and atmospheric heat fluxed force variability and oscillation in SST and h .
- Assuming the atmospheric forcing is white noise the predictability of this model is good until about 6 to 9 months lead time. State of the art seasonal forecast models of the big global weather forecasting centres are better, but not much.

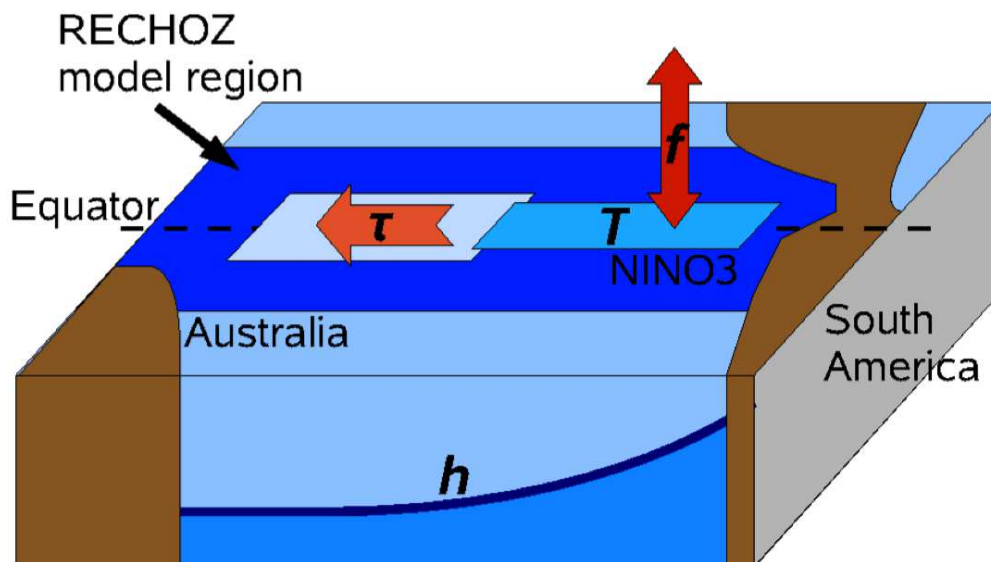


Figure 6.101: RECHOZ model

$$\frac{dT}{dt} = a_{11}T + a_{12}h + c_{T\tau}\tau^* + c_F F_{atmos}$$

$$\frac{dh}{dt} = a_{21}T + a_{22}h + c_{h\tau}\tau^*$$

Atmospheric weather noise

Coupling of T with h

Figure 6.102

$$a_{11} = -0.076 \frac{1}{month}$$

$$a_{12} = +0.021 \frac{1}{month}$$

$$a_{21} = -1.4 \frac{1}{month}$$

$$a_{22} = -0.008 \frac{1}{month}$$

τ^* = zonal winds (only the weather fluctuations)

$$a_{11} = aA_{11} + aO_{11}$$

$$aA_{11} = +0.41 \frac{1}{month}$$

$$aO_{11} = -0.49 \frac{1}{month}$$

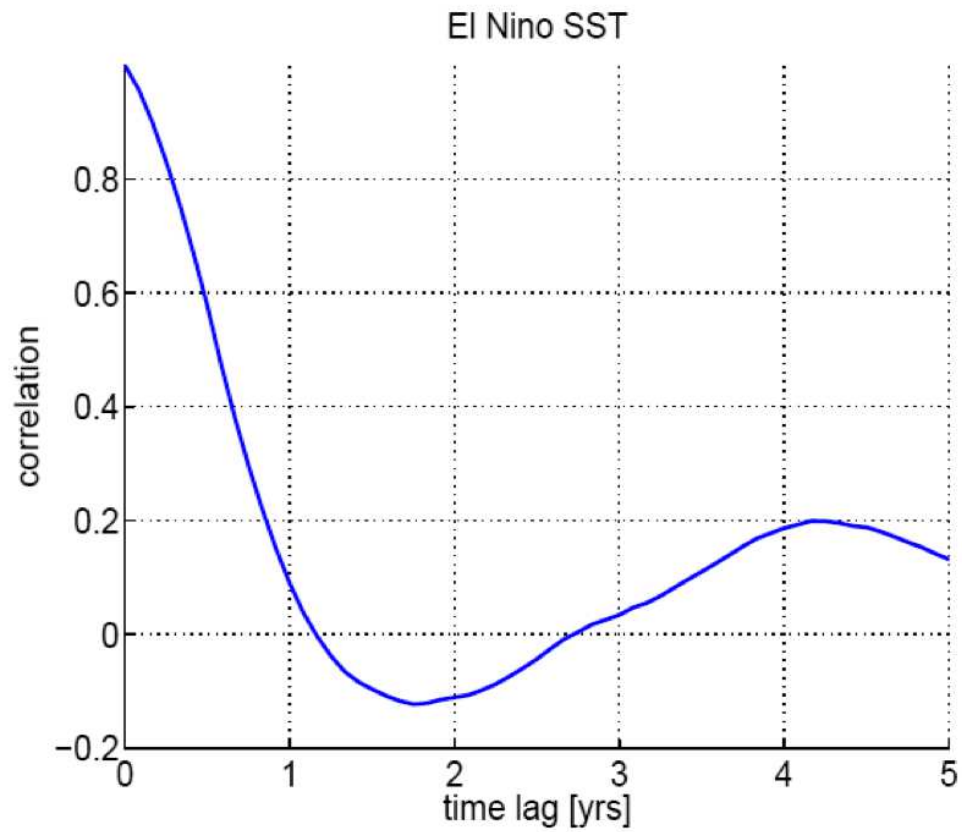


Figure 6.103: The auto-correlation function shows how the SST evolves over time in average, when you start with a value of 1.0

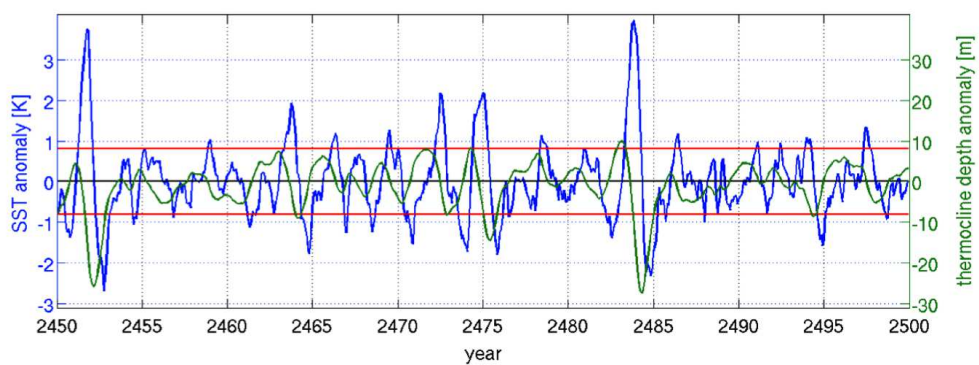


Figure 6.104

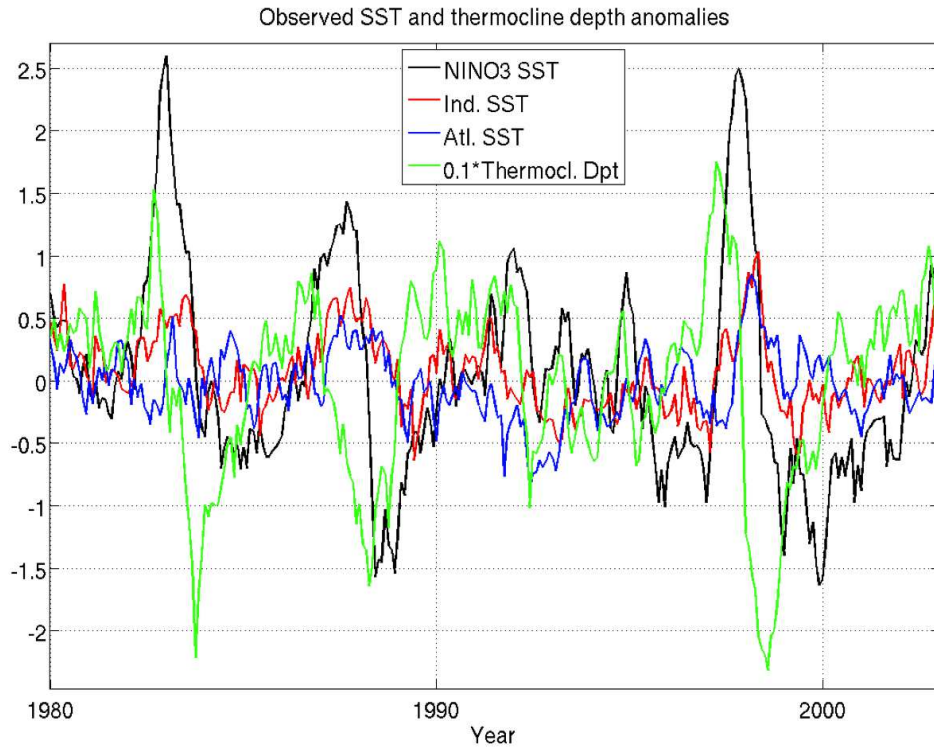


Figure 6.105: Observed SST and thermocline depth anomalies

6.6.5 Predictability of ENSO

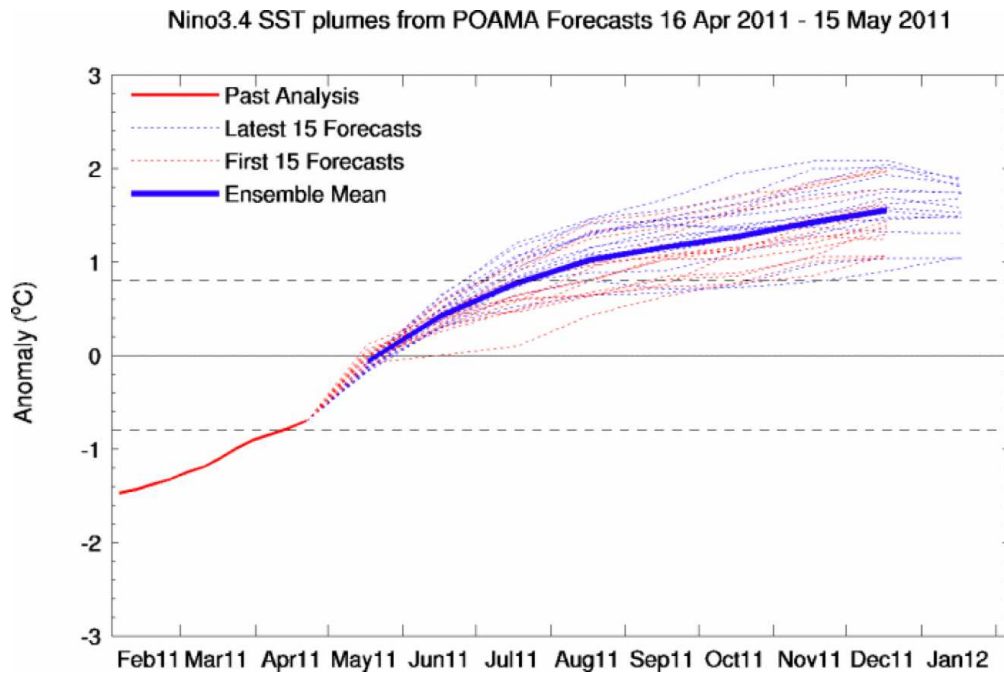


Figure 6.106: El Nino forecast

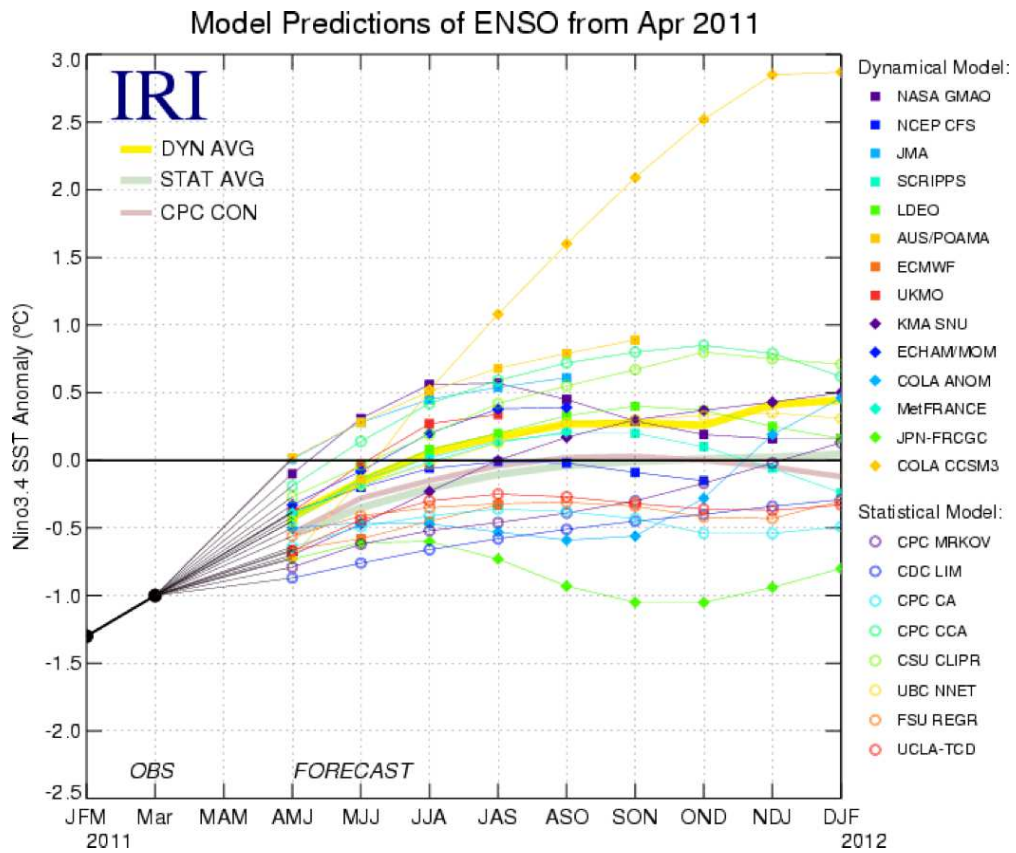


Figure 6.107: El Nino forecast

6.7 The Thermohaline Circulation (THC) Variability

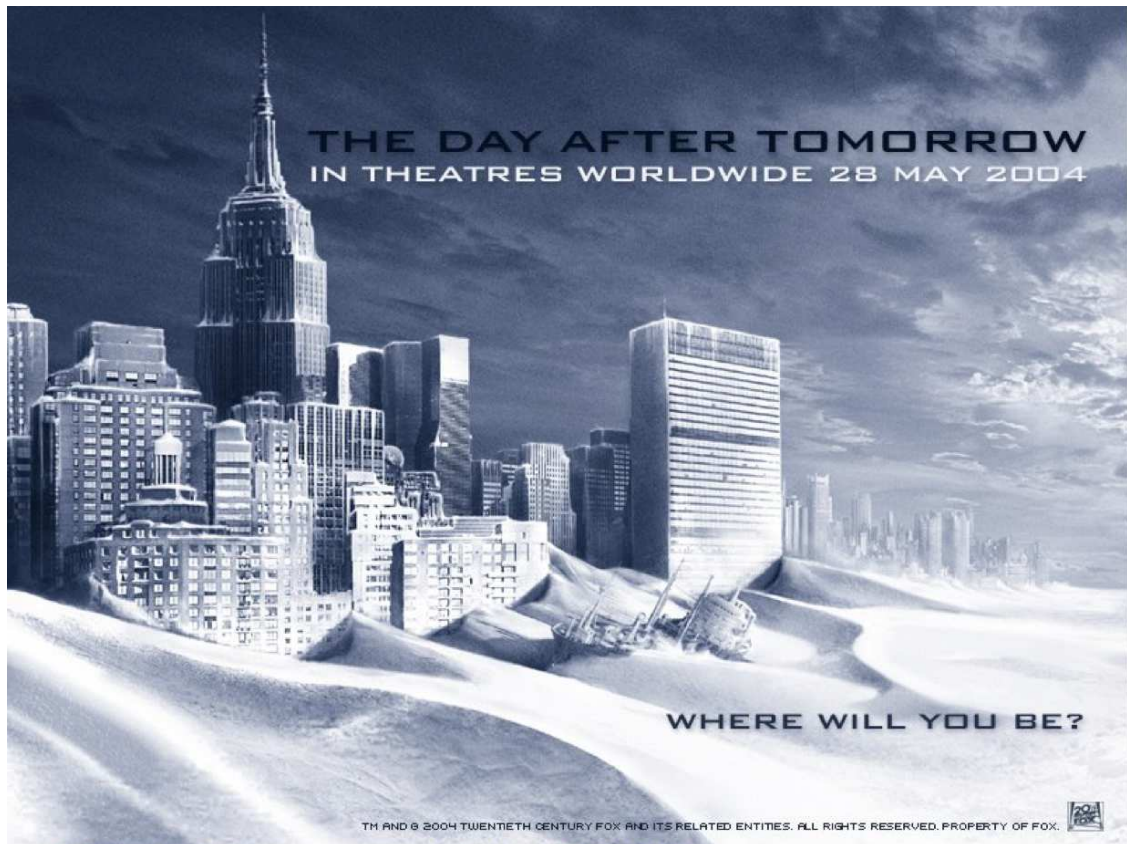


Figure 6.108: Hollywood blockbuster movie based (very very loosely; they screwed it up quite badly) on the theories of abrupt ocean circulation changes, as discussed in this section.

The Thermohaline Circulation (THC) is the deep ocean circulation that spans the global oceans, see sketch in Fig. 6.109. It connects the surface ocean with the deep ocean and therefore is capable of exchanging heat, trace gasses (CO_2 , oxygen, etc.) and nutrients with the deep ocean. In particular, in the North Atlantic it transports a large amount of heat, controlling to a large amount the climate in Northern Europe and North America.

This Thermohaline Circulation can have significant changes: Paleo studies show some remarkable temperature shifts during the ice age cycles that appear to be unrelated to solar radiation changes, but could potentially be caused by changes in the THC. In climate change simulations many models show a strong response in the meridional overturning circulation (MOC), leading to strong damping of the warming or even cooling in the North Atlantic.

The THC variability is another (the other was Budyko ice-albedo) good example of how, under present day climate conditions, the climate system could be in *two different equilibrium* climate states and how there could be a sudden transition from one state to the other (*bifurcation*). This is discussed in a simple two box ocean model by Stommel.

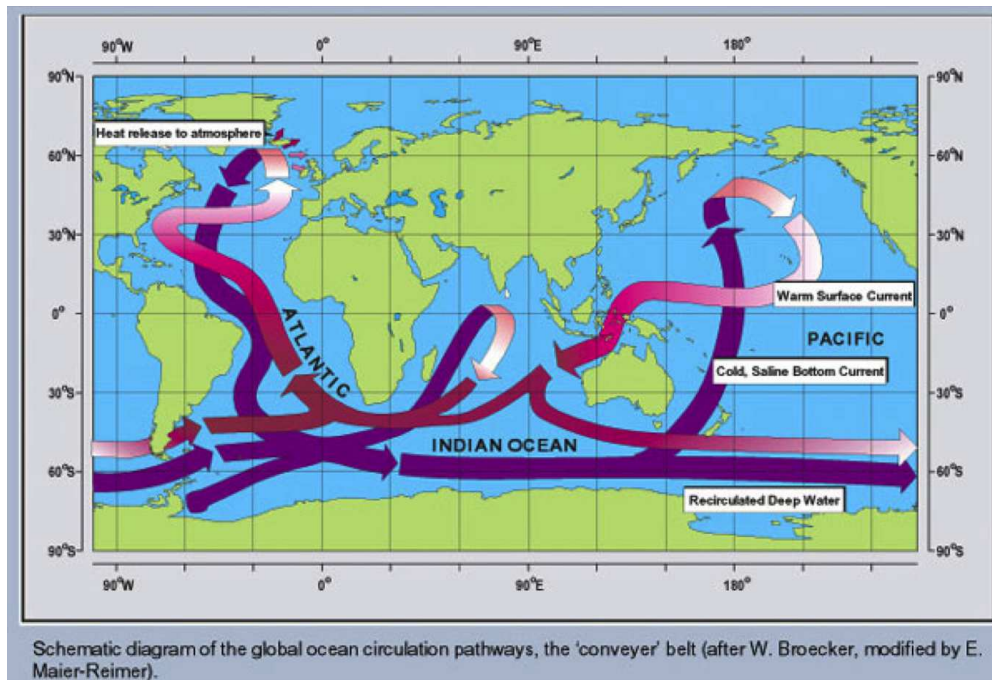


Figure 6.109: Schematic diagram of the global ocean circulation pathways

In the following we will take a short look at some paleo climate variability related to the THC variability and take a look at future climate change simulation that predict a breakdown in the North Atlantic MOC. We will then focus on the Stommel two box ocean model to understand the dynamics and characteristics of the THC variability.

6.7.1 Paleo climate variability of the THC

To understand the importance of the THC for Northern Hemisphere climate, it is first of all helpful to understand how important the oceanic heat transport in the North Atlantic is. Figure 6.110 shows the mean surface temperature in February. You can note, that the northern North Atlantic (around $60^{\circ}N$) is much warmer than all other regions on the same latitude. Now also considering that winds are mostly zonal and typically westerlies in these latitudes, then you can infer that this temperature gradient between the warm North Atlantic and the surrounding cold continents will lead to significant heat transport from the warm ocean to the cold continents. Also recall our discussion of the GREB model mean climate effect of mean heat advection in section 4.2 and in Fig. 4.42e. You can further note, that this does not exist in the North Pacific (at least not as strong) and nowhere in the Southern Hemisphere. Thus this is quite unique.

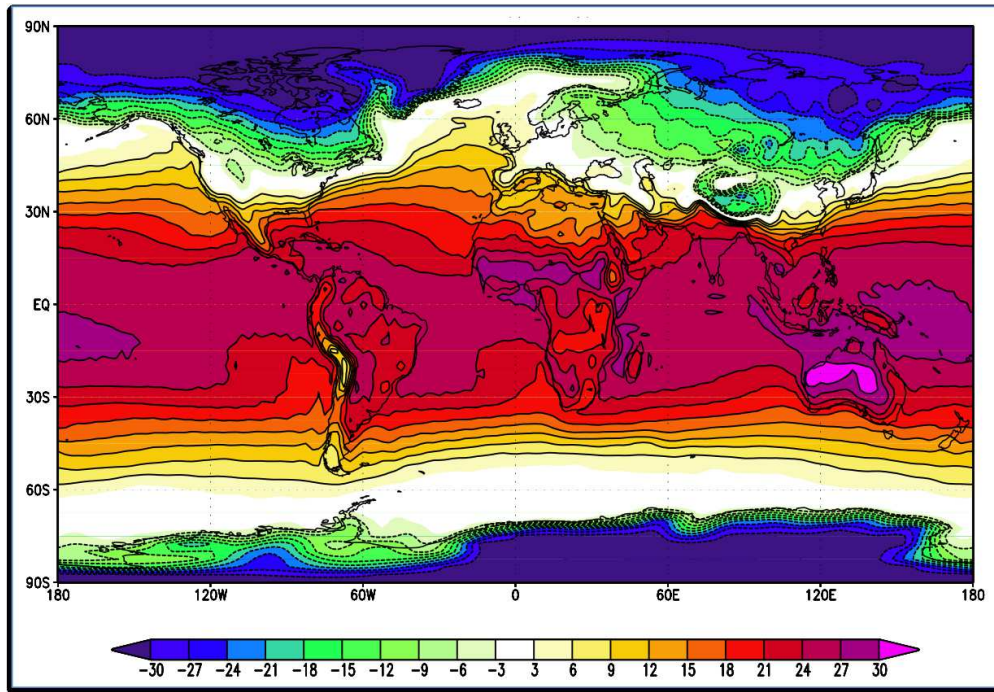


Figure 6.110: Surface temperature February: Note, that the northern North Atlantic (around $60^{\circ}N$) is much warmer than all other regions on the same latitude, which indicates that it is heating the other regions.

Studies of the past 100,000yrs climate variability have found some remarkable fast climate transitions in the North Atlantic region (more on paleo climate variability and ice ages follows in the section 6.8). In Figure 6.111 Greenland temperature during the last 100,000 years, as estimated from some climate prox data from Greenland ice cores, are shown. Quite remarkable are the fast (relatively speaking; note that the time scales are fairly long in this figure) and strong temperature changes that are marked with numbers. They indicate that during the last ice age (80 to 20 thousand years ago) there were sudden temperature increases, see also Fig. 6.112. The changes appear to happen without any external forcing (e.g. changes in solar radiation) and could thus result from internal climate dynamics. One idea to explain such internal climate dynamics are sudden changes in the THC in the North Atlantic induced by large land ice (glaciers) melting.

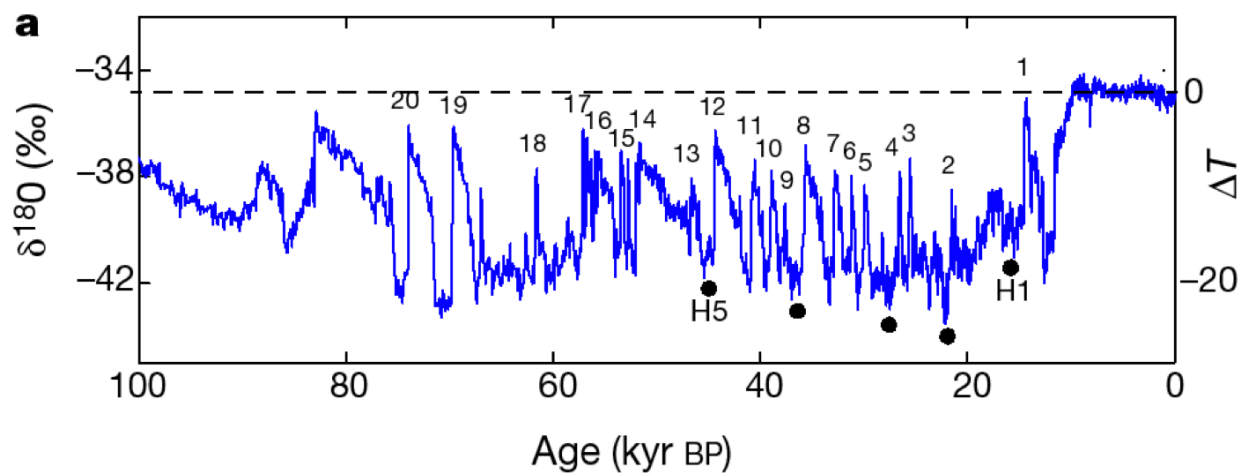


Figure 6.111: Greenland temperature during the last 100,000 years, as estimated from some climate prox data from Greenland ice cores. The strong fast Temperature changes are marker by numbers.

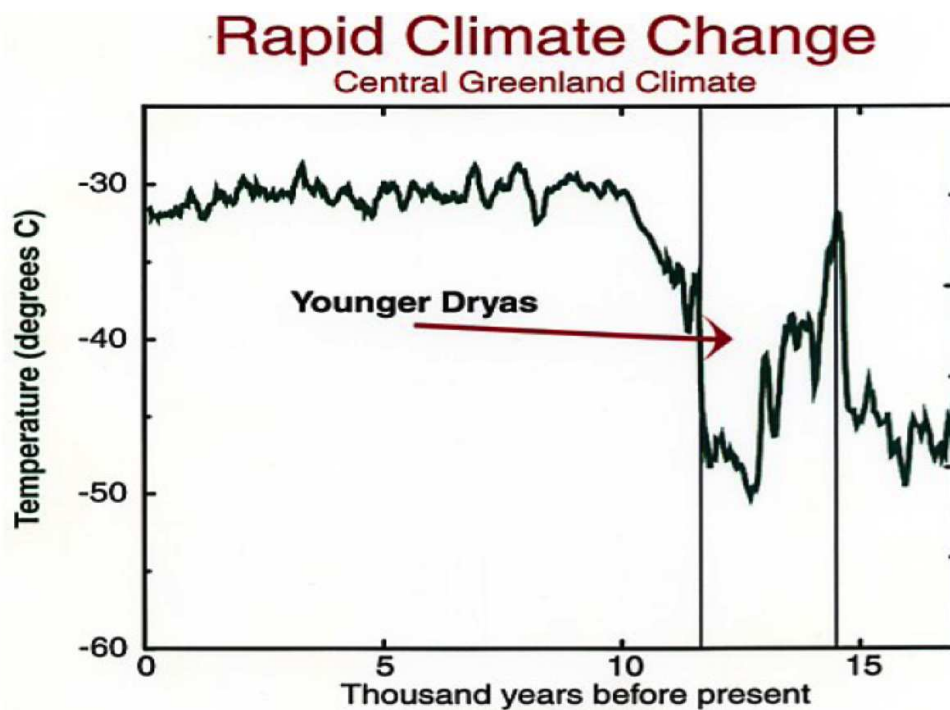


Figure 6.112: Last ice age fast temperature changes around Greenland named Younger Dryas: A section from the previous Fig. 6.111.

6.7.2 North Atlantic MOC circulation ”breakdown”

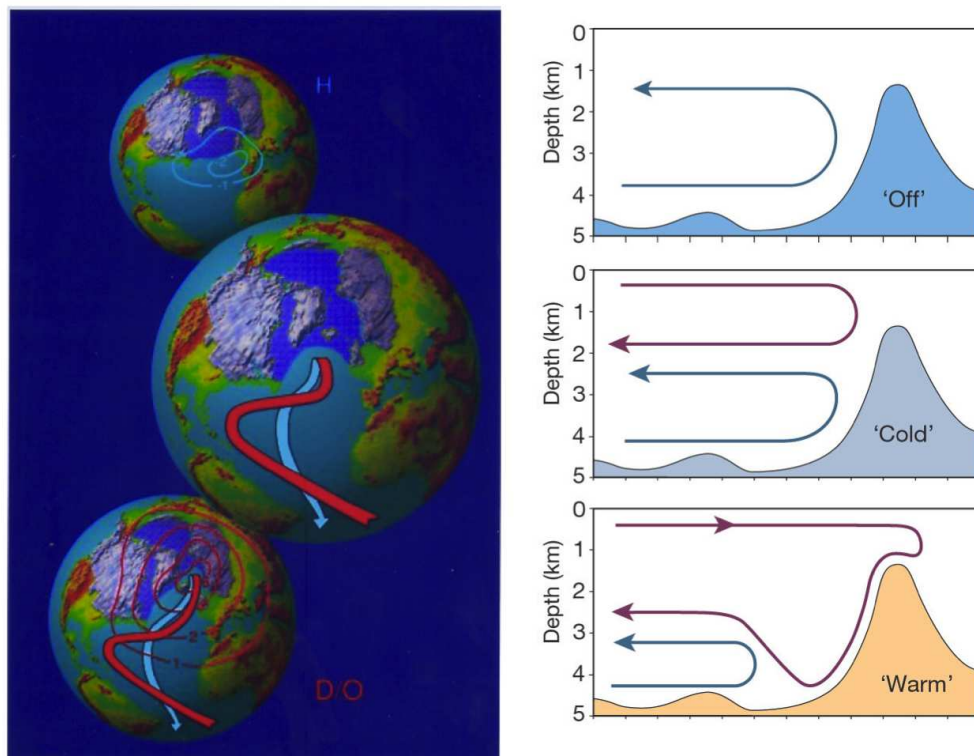


Figure 6.113: Meridional Overturning Circulation (MOC) in the North Atlantic at different circulation states.

The sketches in Fig. 6.113 illustrates different states of the THC in North Atlantic (North Atlantic MOC circulation) for present day conditions and past ice ages. The lower earth (left) and MOC circulation (right) depict a climate state as today or during one of the warming phases during the last ice ages as in Figs. 6.111 and 6.112. A strong MOC transports heat from the south to the north. Thus surface currents are from south to north. In the upper earth (left) and MOC circulation (right) a typical situation during ice ages is depicted. Large ice shelves (Glaciers) cover North America, Europe, Asia and large parts of the northern North Atlantic. In this case the MOC is weak or even reversed: with surface currents are from the north to the south. Meridional heat transport is weak or even reversed. The middle sketch depicts an in between state.

The different states of the THC in the North Atlantic are forced by the different climate conditions. In today's conditions the strong temperature difference between tropics and Polar regions drive the MOC in the North Atlantic. During ice ages large part of the northern North Atlantic is ice covered and does not allow for a strong MOC.

Changes in the THC did not only occur in the past ice ages or on time scales of ice ages, but are actually possible in today's climate and are likely to happen within the next hundred years. In our climate change discussion we noted that the northern North Atlantic is one of the regions on earth with the least amount of warming in response to CO_2 forcing, see Fig. 5.1 and discussion in chapter 5. This is due to a partial breakdown of the Meridional Overturning Circulation (MOC) in the North Atlantic, see Fig. 6.114. Most model simulation show a reduction in MOC transport. This is partly due to a reduction in meridional temperature gradients between tropics and Polar regions, since the polar regions warm more strongly. It is also partly due to increases in fresh water input into the northern North Atlantic by increased rainfall and by melting of glaciers (not simulated in

most CGCM simulations in Fig. 6.114).

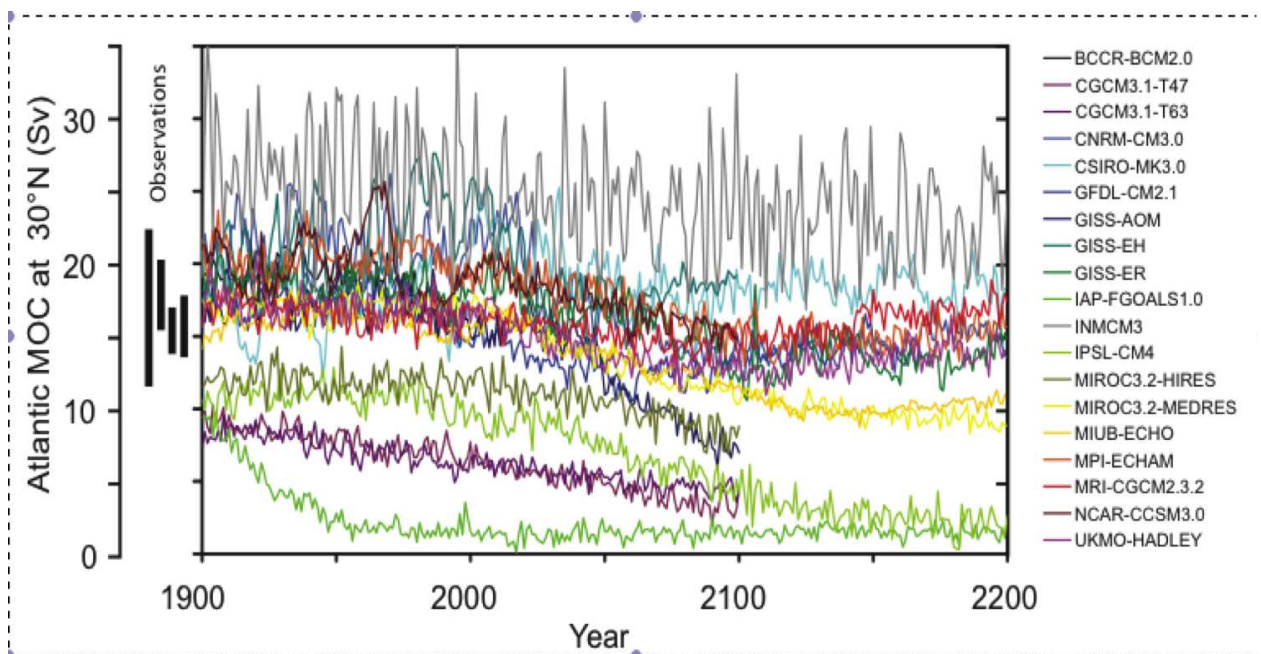


Figure 6.114: The Meridional Overturning Circulation (MOC) changes in the North Atlantic in different model simulations of future climate change scenarios.

6.7.3 The Stommel two box model

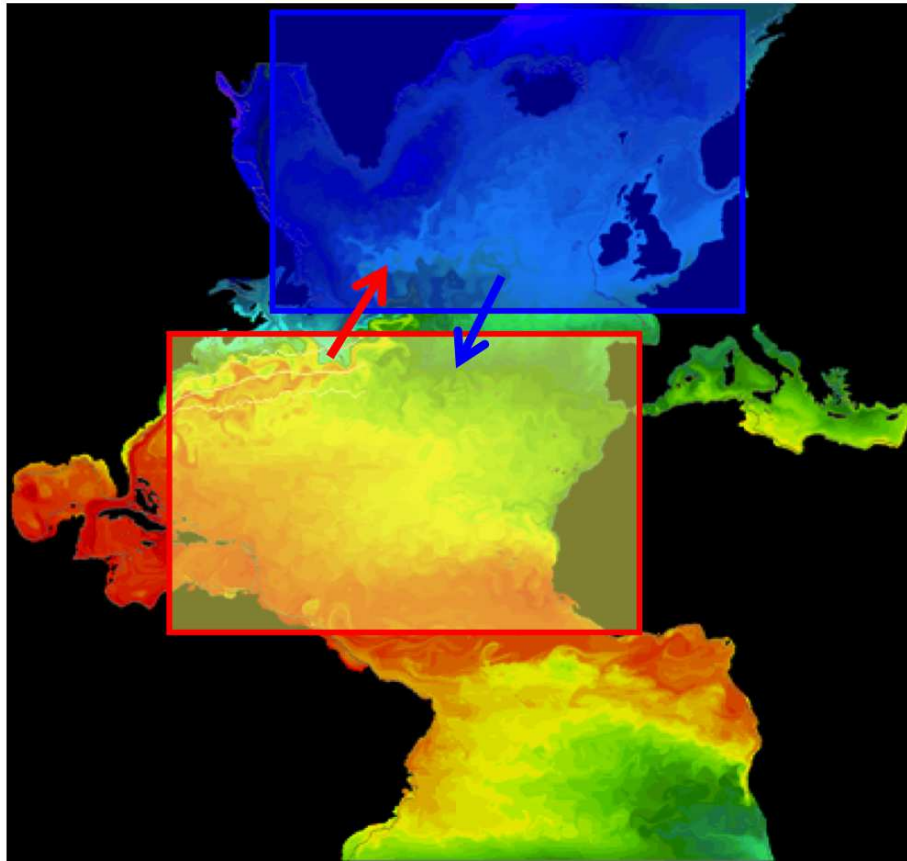


Figure 6.115: Stommel box model

The dynamics of THC changes or breakdowns are quite interesting. They involve change in heating or cooling and change in fresh water input or evaporation (which effectively is salt input). In the following we want to discuss these dynamics in more detail with the help of the simplified two box model from Stommel, 1961. We will first take a look at the climate state in the North Atlantic and will then formulate a simple two box model of the MOC in the North Atlantic. The characteristics of the two box model will then be discussed to highlight the interesting behaviour of the MOC. This includes tipping points and the associated reversal of the MOC.

6.7.3.1 The ocean state in the North Atlantic

To understand the dynamics of the North Atlantic we strongly simplify the North Atlantic (or any other ocean basin) into two boxes, an equatorial and a polar box, with some surface current and deep ocean return flow.

- Note sea water density is a non-linear function of temperature and salinity, which we simplify here to a linear function.
- Atmospheric heating is warming in the equatorial box and cooling in the polar box.
- Atmospheric evaporation and precipitation leads to a net salinity flux. If evaporation dominates over precipitation, then the salinity flux is positive.

- Atmospheric salinity flux is positive in the equatorial box due to large evaporation and weak precipitation and it is negative in the polar box due to weak evaporation and strong precipitation.

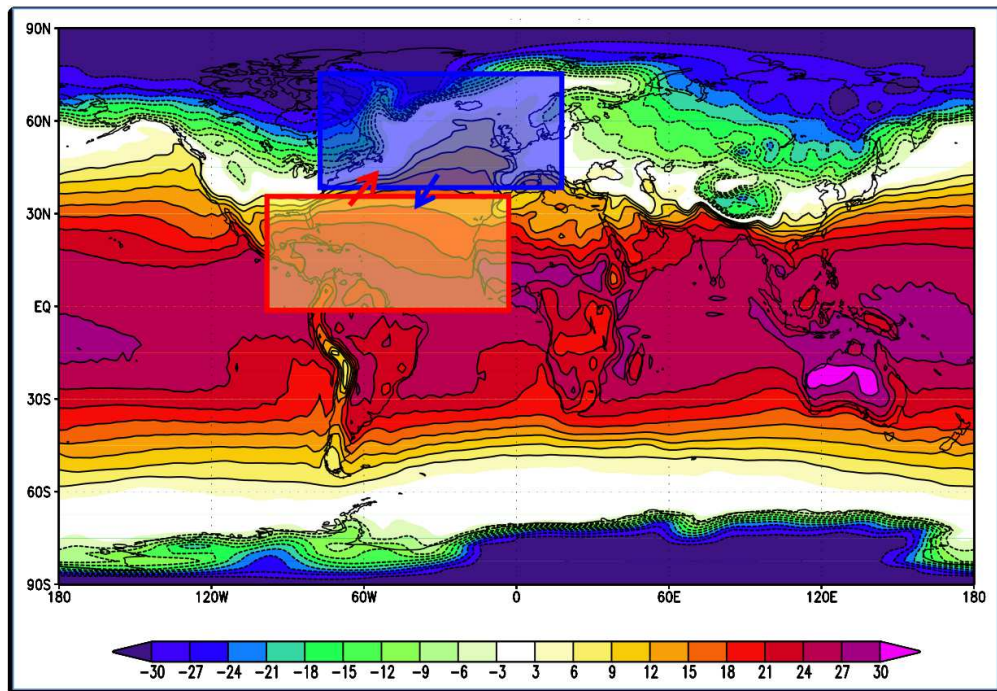


Figure 6.116: Surface temperature February

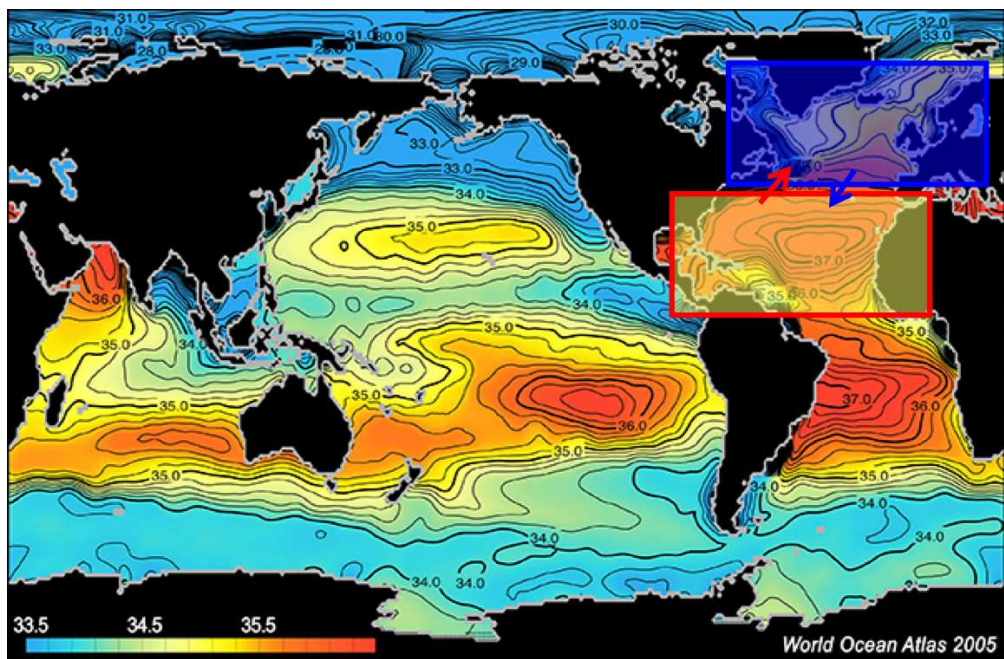
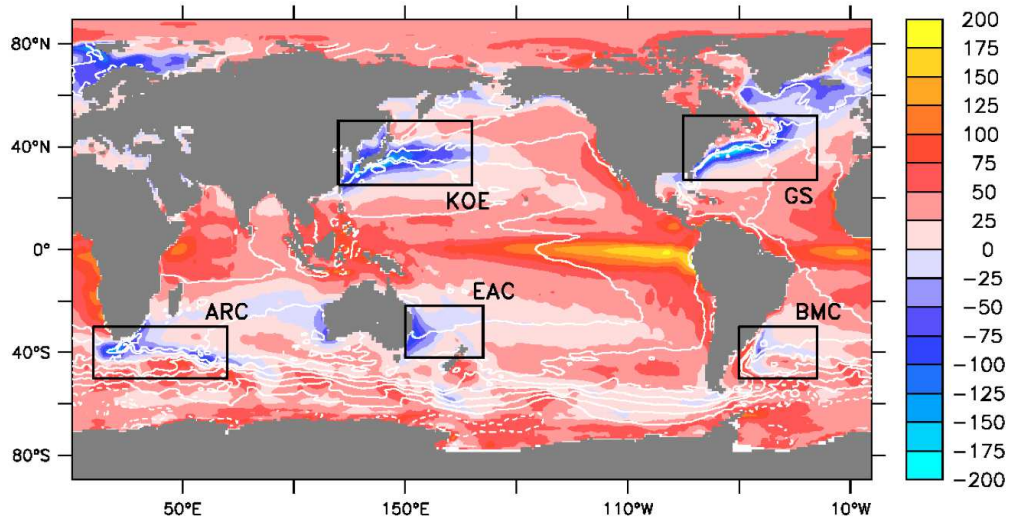


Figure 6.117



Mean Net Surface Heat Flux (Wm^{-2})

Figure 6.118: Net heat flux into the oceans

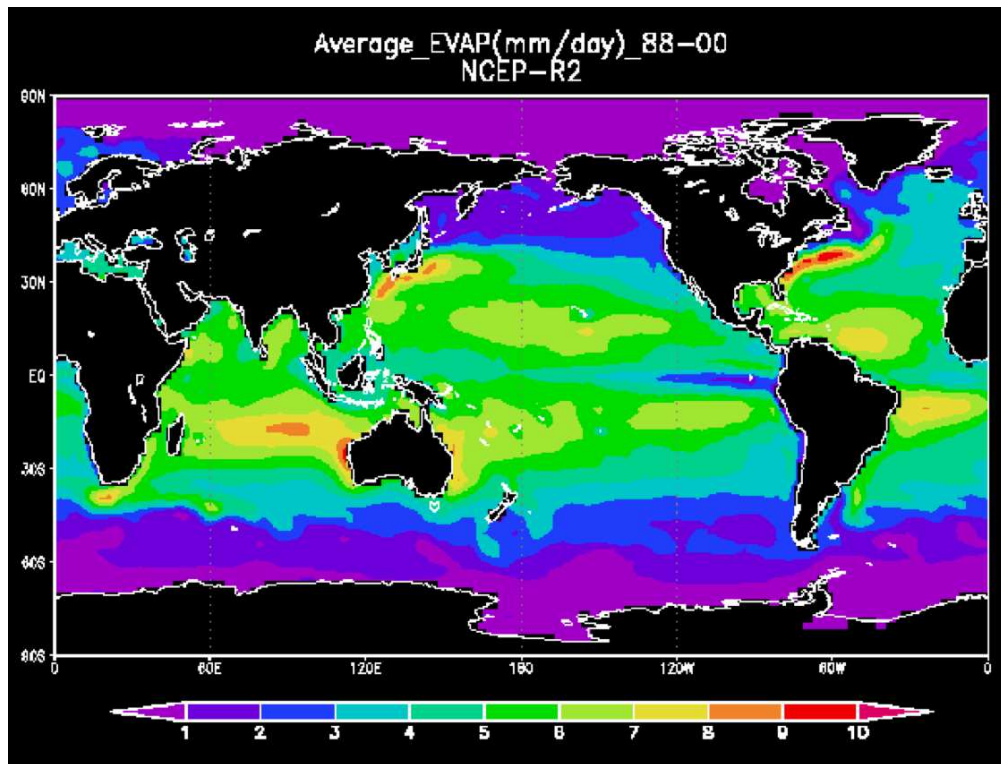


Figure 6.119: Net evaporation (mm/day)

- Circulation between the two boxes is driven by density differences between the two boxes.
- A lower density in the equatorial box, for instance, would either cause a larger volume and associated higher surface sea level, which pushes the surface waters to the lower sea level in the polar box; or the polar box would have a larger deep ocean bottom pressure, which would push the deep ocean polar box water into the equatorial box.
- This circulation is controlled by temperature and salinity differences between the two boxes.
- If temperature differences dominate (as in present climate) then the surface flow is from the equatorial box to the polar box; transporting heat to the polar box and reducing the temperature gradients.
- If the salinity differences dominate then the surface flow is from the polar box to the equatorial box, reducing the temperature in the equatorial box.

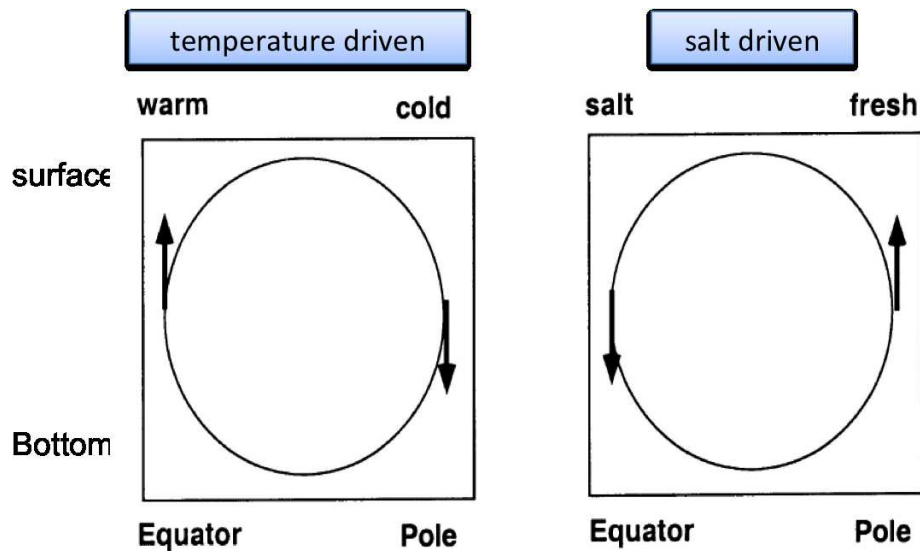


Figure 6.120: A two box THC model

- In the real world the temperature differences are dominated by the surface flow and not the deep ocean flow, as the deep ocean temperature gradients are much smaller than at the surface, due to the density stratification.
- So a surface poleward flow has a warmer climate than a surface flow towards the equator.
- Note also that the volumes of the two boxes are different, with the equatorial box being much bigger.
- The Stommel model T or S tendencies of each box depend on the differences in the atmospheric condition and on the transport by the ocean current.

6.7.3.2 The two box THC model set up

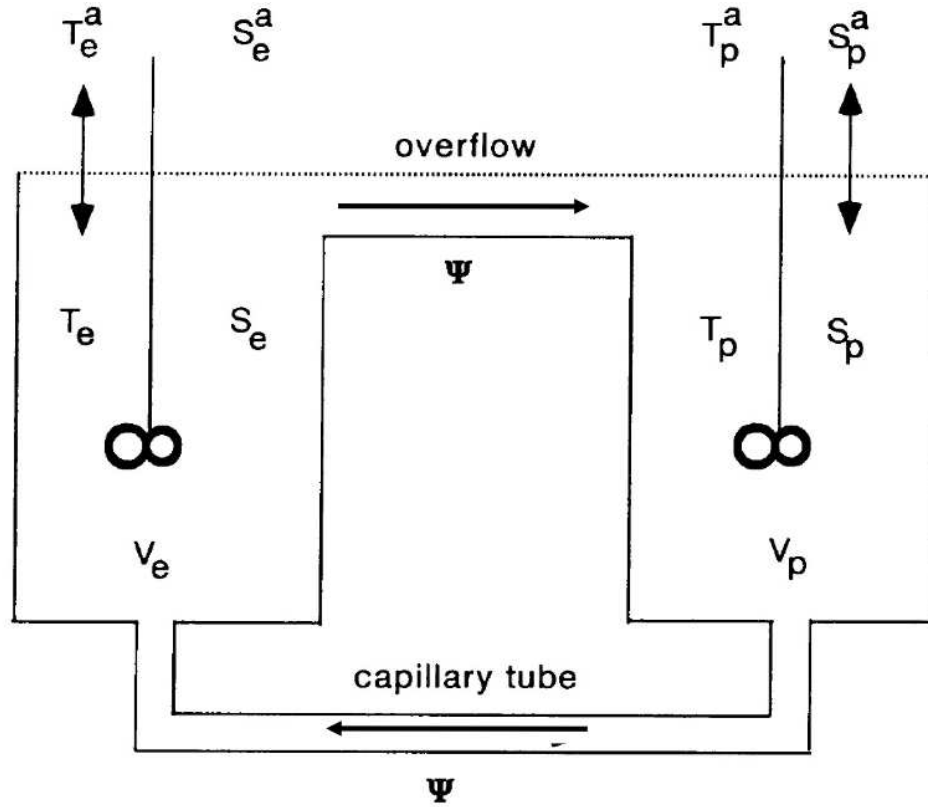


Figure 6.121: Two box Stommel model

T : Temperature

S : Salinity

V : Volume

Ψ : Current (positive if surface flow to North)

e: equator

p : polar

a : atmosphere

$\Psi \propto \rho_p - \rho_e$: Circulation is density driven

$\rho \propto \alpha_T T + \alpha_S S$: Density is function of Temperature and Salinity (assume linear function)

$$\Rightarrow V_e \frac{dT_e}{dt} = C_e^T (T_e^a - T_e) + |\Psi| (T_p - T_e) \quad (6.12)$$

$$V_p \frac{dT_p}{dt} = C_p^T (T_p^a - T_p) + |\Psi| (T_e - T_p) \quad (6.13)$$

$$V_e \frac{dS_e}{dt} = C_e^S (S_e^a - S_e) + |\Psi| (S_p - S_e) \quad (6.14)$$

$$V_p \frac{dS_p}{dt} = C_p^S (S_p^a - S_p) + |\Psi| (S_e - S_p) \quad (6.15)$$

- As we assume all density effects are linear, we can reduce the 4 tendency equations for each boxes t_i and S_i , to just two for the temperature and salinity differences, T and S .
- The transport between the two boxes can just be diagnosed by T and S .
- η_H is a heat forcing parameter depending on the atmospheric temperatures and the coupling parameters C_i^T . If it is strongly positive it means strong warming in the equatorial box and strong cooling in the polar box.
- η_S is a salinity forcing parameter depending on the atmospheric salinities and the coupling parameters C_i^S . If it is strongly positive it means strong salinity forcing in the equatorial box and strongly negative salinity forcing in the polar box.
- Differences in the coupling parameters C_i^S and C_i^T cause differences in the time scales of T and S .
- The current influences the T and S gradients only by its strength not by its sign, as there is always the same return flow in the deep ocean.

$$\text{Realistic case: } T_e^a - T_p^a > 0 \quad S_e^a - S_p^a > 0$$

Normalisation, scaling:

$$\Psi = T - S \quad (6.16)$$

$$\frac{dT}{dt} = \eta_H - T(1 + |T - S|) \quad (6.17)$$

$$\frac{dS}{dt} = \eta_S - S(\eta_{\frac{tT}{tS}} + |T - S|) \quad (6.18)$$

$$T = T_e - T_p$$

$$S = S_e - S_p$$

η_H : heat forcing parameter

η_S : salt forcing parameter

$\eta_{\frac{tT}{tS}}$: time scale ratio T/S

- For current climate conditions heat forcing is much bigger than salinity forcing (temperature differences dominate over salinity differences) $\implies \eta_H \gg \eta_S$
- Thus the time scale ratio $\frac{\eta_H}{\eta_S} < 1$.
- For these conditions we get the observed strong poleward transport and an equatorial box which is much warmer than the polar box $T > 0$.
- If we assume a *much stronger salinity forcing* (a much stronger fresh water input into the polar box, for instance), we get *two equilibria states*: one similar to our current state, but with weaker transport and another with a reversed but almost zero transport caused by the stronger salinity gradients.

- Note that the temperature and salinity gradients are both much stronger than in the present climate case, which is due to the almost zero transport.

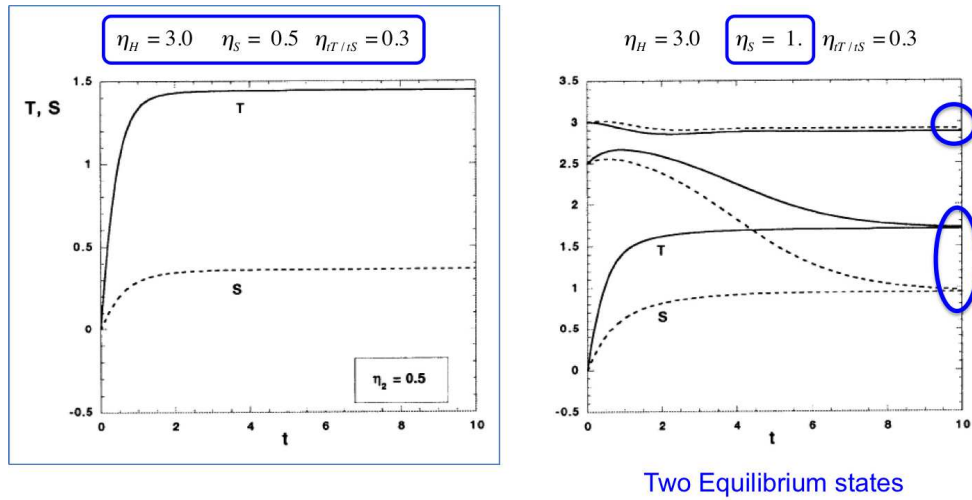


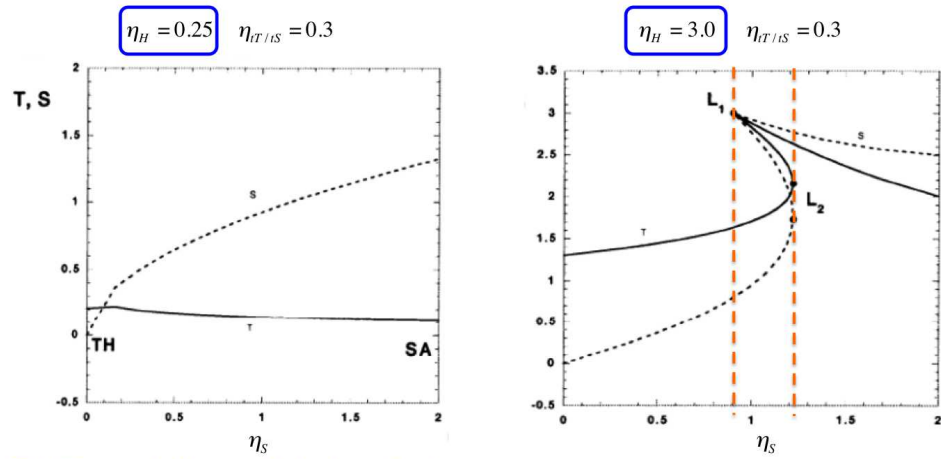
Figure 6.122: Two equilibrium states

$$\Psi_1 = T - S > 0 \text{ heat transport to the North}$$

$$\Psi_2 = T - S < 0 \text{ heat transport to the South}$$

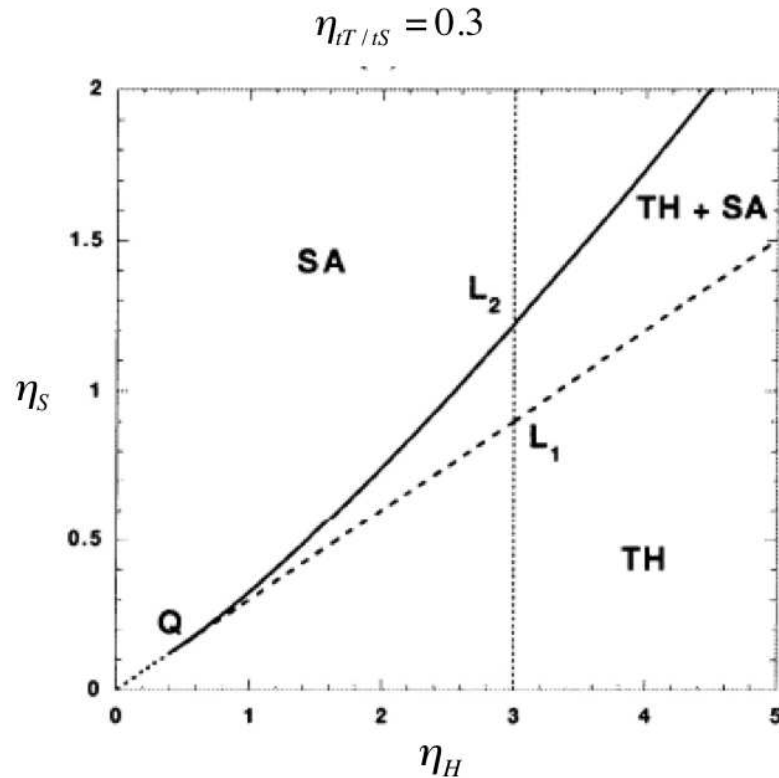
6.7.3.3 Characteristics, stability and tipping points of the two box model

- We can now study how the equilibrium T and S depend on the strength of η_H and η_S .
- We first consider a world with relatively weak heat forcing η_H and study variations of the salinity forcing η_S .
- For weak η_S the T is larger than S and the circulation is dominated by the temperature gradients, leading to the current poleward transport. If η_S gets larger the salinity gradient gets bigger and dominates the circulation, leading to the reversed transport.
- If we now consider the case with stronger heat forcing as of today, the situation gets more complicated. We find multiple equilibrium states for the same forcing conditions.
- We can now divide the η_S and η_H plane into different circulation regimes: TH regime, SA regime and a regime in which both circulations are possible.



TH: Thermal driven; sinking in polar box
 SA: Salt driven; sinking in polar box

Figure 6.123: Equilibrium states as function of salt forcing



TH: Thermal driven; sinking in polar box
 SA: Salt driven; sinking in polar box

Figure 6.124: Regime diagram

- In the regime where both circulation types are possible we need to ask the question, which of the equilibria are stable and if we are with the initial conditions within this regime, we need to know to which equilibrium the system will go.
- If we start with initial conditions at point *A* the system reaches the TH equilibrium at point *B*.
- We can study this for all possible initial conditions and find that for all points below the curved dashed line for point *L1* to *L2* the system will go to the SA equilibrium ($\Psi < 0$) and to the TH equilibrium ($\Psi > 0$) for all other initial conditions.
- So both TH and SA equilibria are stable.
- Some studies argue present day climate is in this regime where both circulation types could exist. However, we need to note that the real world is much more complex and it is unclear to what extent this discussion holds for the real world.

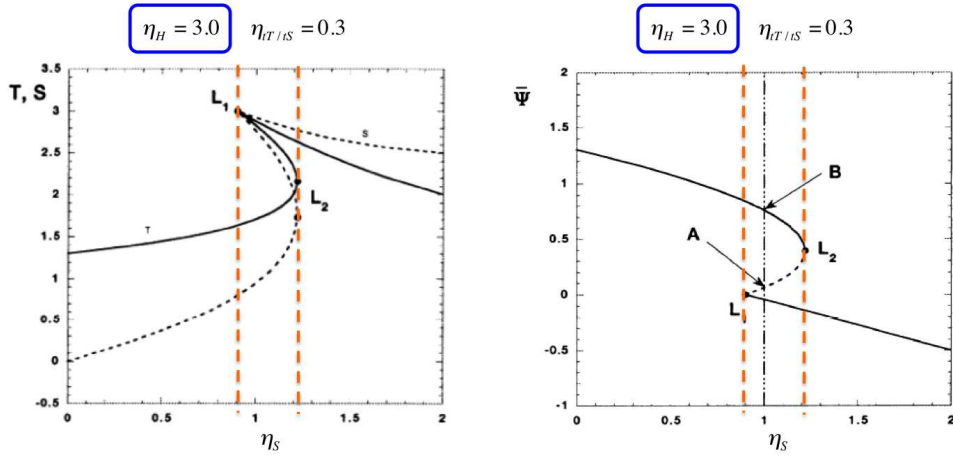


Figure 6.125: Equilibrium states as function of salt forcing

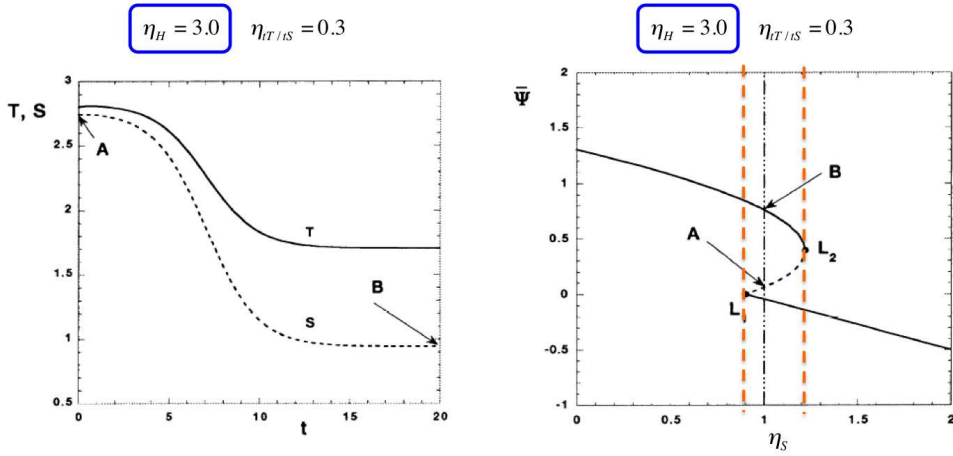


Figure 6.126: Equilibrium states as function of salt forcing

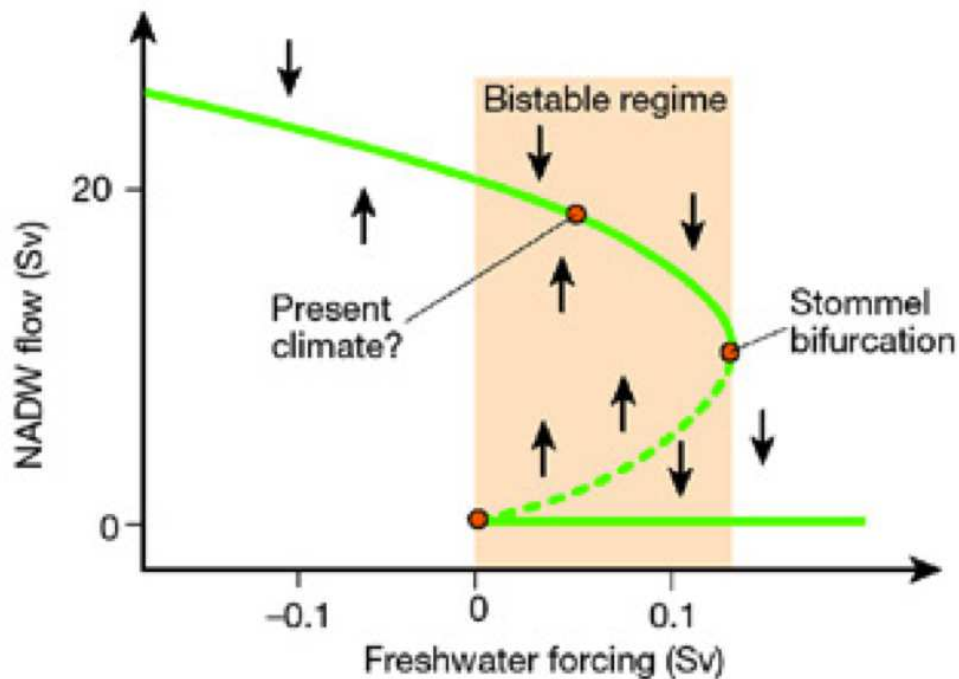


Figure 6.127: Equilibrium states as function of salt forcing

- Ocean-Atmosphere GCM simulations have been used to test the effect of a circulation breakdown in the North Atlantic. Therefore a very large amount of fresh water has been put into the North Atlantic ($\sim 2\text{Sv}$ - this is about twice all of the world's river run-off).
- In response the Meridional Overturning Circulation (MOC) in the North Atlantic collapsed and the climate in the North Atlantic but also in most of the Northern Hemisphere cooled down by quite a bit.
- The change in the MOC in the North Atlantic also leads to changes in the circulation in the Southern Atlantic, leading to an opposing but weaker effect on the climate in the Southern Hemisphere.
- During the end of the last ice age large glacier masses collapsed, leading to large fresh water flux into the North Atlantic (possibly through the St Lawrence stream in Canada), which could potentially cause the MOC to collapse causing a new cooling period, extending the ice age by several thousand years. This is the "Day After Tomorrow" scenario, only accelerated by a factor of about 100,000.

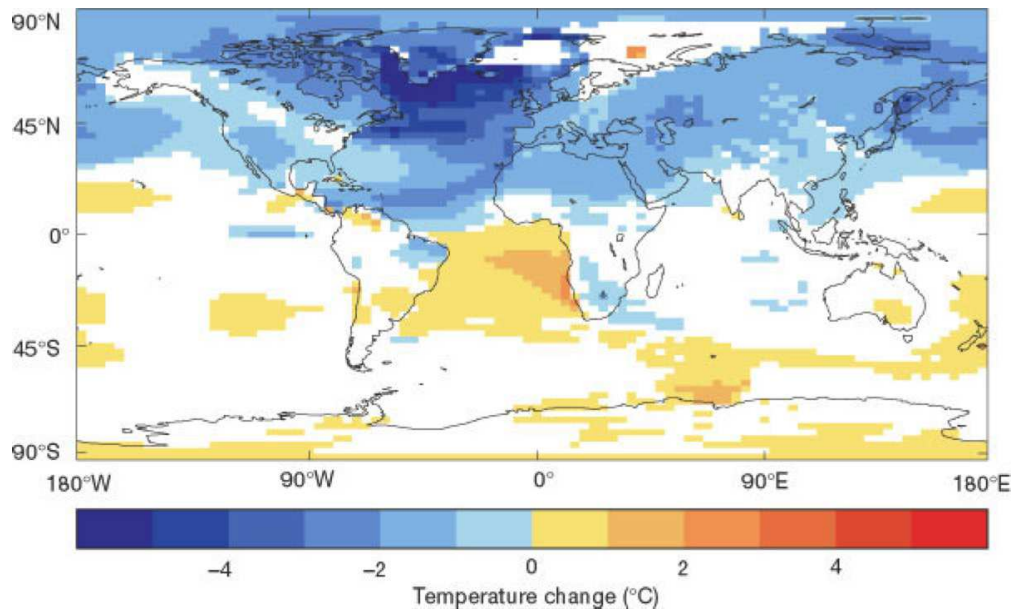


Figure 6.128: Response to MOC circulation shutdown

- During climate change two things can happen:
- *First the polar regions warm more* than the equatorial regions. This reduces the heat temperature gradient and therefore the heat forcing for the ocean circulation. The circulation should get weaker.
- *Second Greenland and other glaciers may melt*, leading to increased fresh water into the North Atlantic. This increases the salinity forcing of the circulation, causing the TH circulation to be reduced.
- The second effect may also be further supported by increased rainfall and decreased sea ice formation.
- Overall it should lead to a reduction of the MOC as simulated by most climate change GCM simulations.
- But keep in mind the real world is much more complex with lots of small scale eddies that may totally change the behaviour of the system.

6.8 Paleo Climate Variability (Ice Ages)



The paleo climate variations are the variations of the climate before the instrumental record periods began (roughly the 19th century). By looking back into the history of the earth climate we can learn a lot about the nature of climate variability both internally and externally forced. The biggest problem about the past climate variability is that we know very little about it and data about past climate is very difficult to get. Information of the variations of the climate before the instrumental record periods is based on so called Proxy data, which is data about the past climate which is not based on instrumental measurements.

In the following section we will have a look at the kind of Proxy data that we have for reconstructing past climate variability. We then discuss the climate variability of the past going back in time starting today and ending at about 500 millions before present. We will focus on the ice ages cycles and their feedbacks and forcings in some more details. We finish this section with summarising earth climate variability in a single power spectrum of climate variability from time scales from days to about a billion years.

6.8.1 Climate Proxy Data

Thermometer measurements

- Estimating the global mean surface temperature depends on measurements at many thousand locations.
- The regional coverage of these measurements is highly unequal, with large gaps on the Southern Hemisphere.
- This data coverage also decreases dramatically if we go back in time, with basically no measurements before 1900.

- Over time there were periods of little to no measurements (world wars).
- Over time the measurement techniques and locations of measurements have changed (e.g. trade routes of ships).
- Before the very recent years with satellites (roughly 1980s) all regional climate variability is highly uncertain.

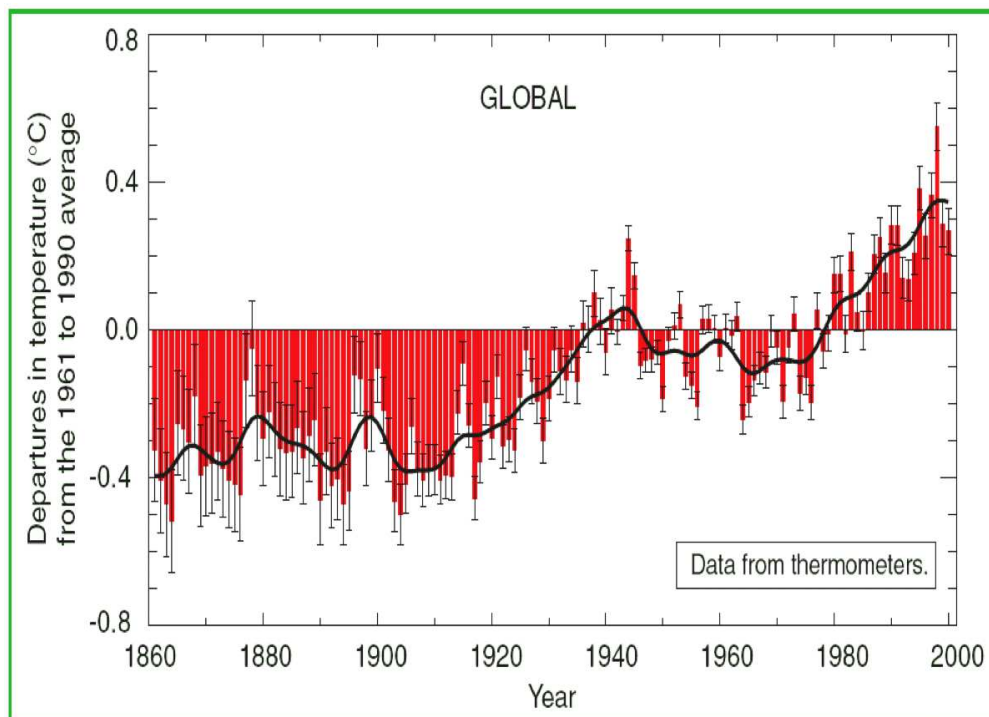


Figure 6.129: Global mean temperatures: Note how the error bars become larger further back in time. Not all of the fluctuation we see in this time series are "real" global mean temperature fluctuations, large uncertainties exist in this global mean temperature estimate.

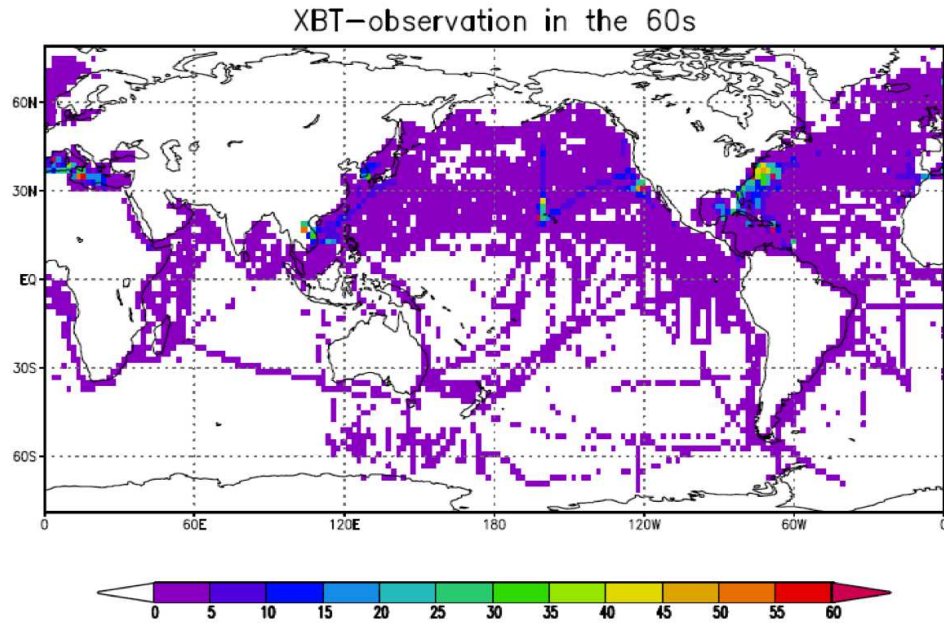


Figure 6.130: Data coverage: Upper ocean observations (XBTs) in the 1960s per grid box per month. Note, the lag of observation for most of the southern hemisphere. For most regions not a single observation has been made. It make you wonder how much we really know about the climate of the beginning of 20th century.

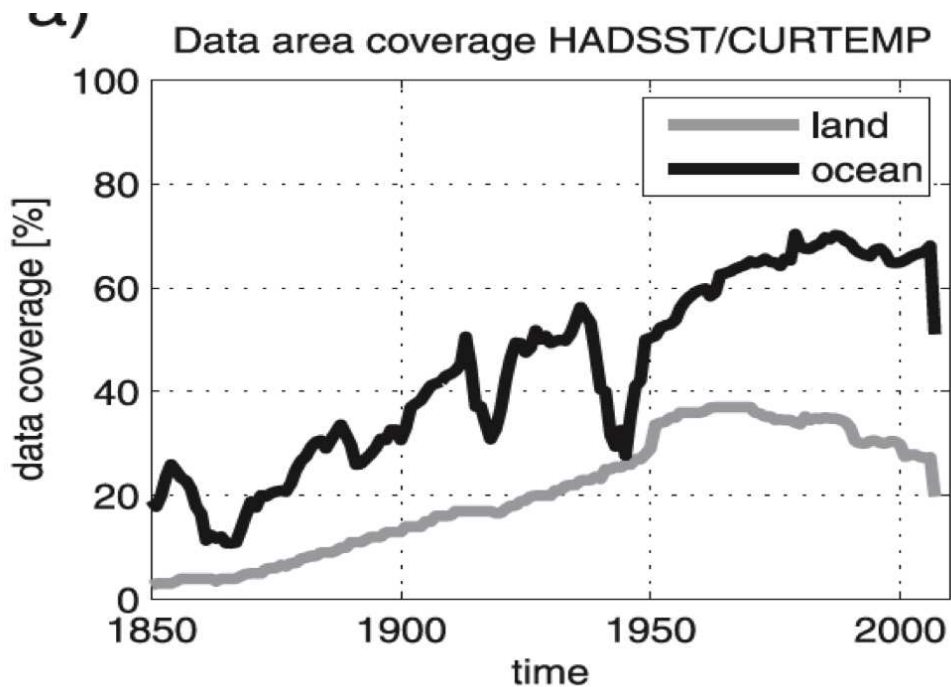


Figure 6.131: Data area coverage over land (CRUTEMP) and oceans (HADSST). Note the to drops in ocean observations over the periods of the two world wars.

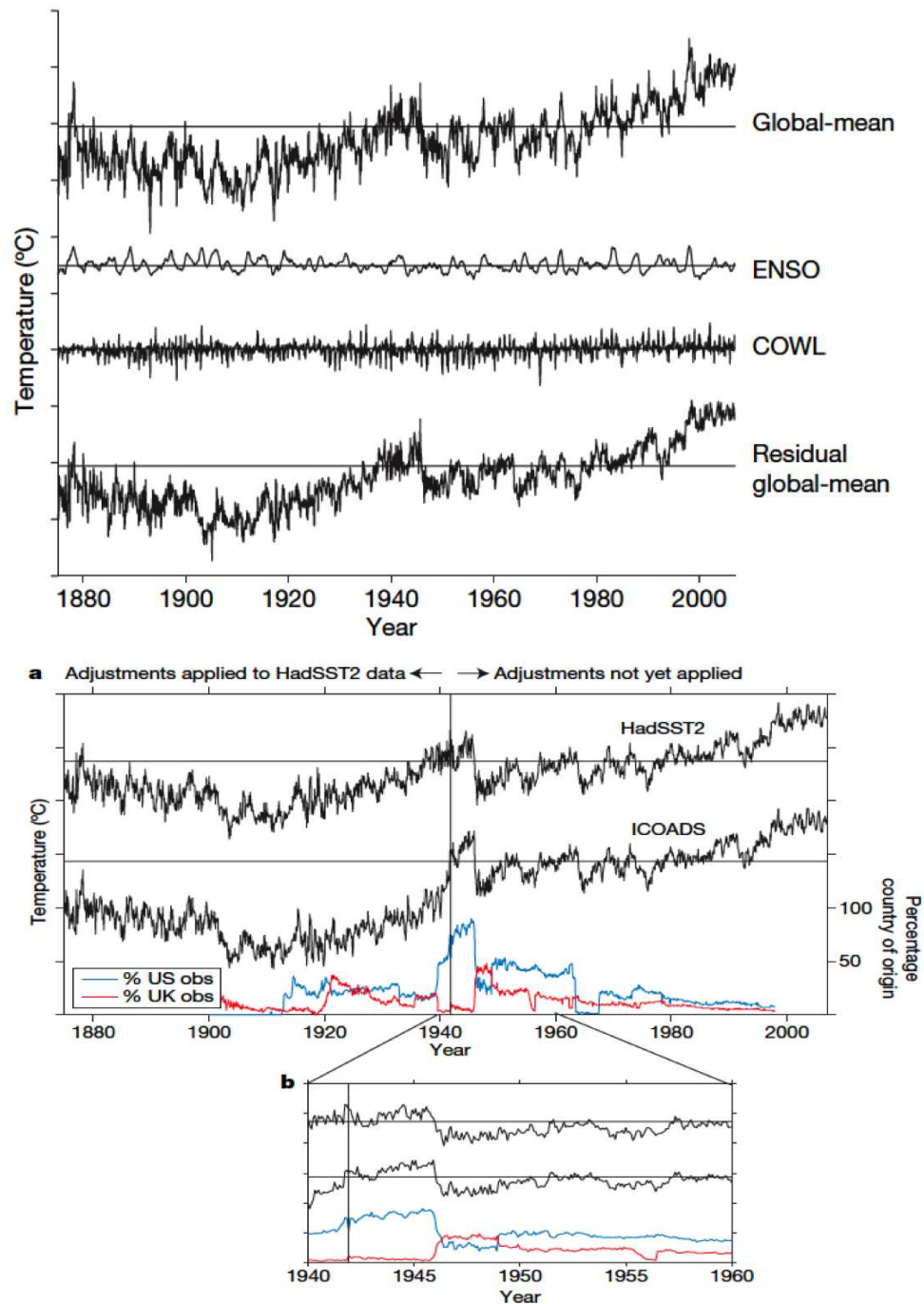


Figure 6.132: DATA PROBLEMS: Change in source/region of observations at the end of the second world war (August 1945) leads to an "apparent" temperature drop in the global mean temperature. It is very likely related to the fact that the UK ships measured in different regions of the earth (e.g. Atlantic) than the USA ships (e.g. Pacific).

Proxies

- Before the year 1900 temperature measurements by thermometers were largely non-existent for global climate measurements.

- To estimate the climate without thermometer measurements some *climate proxies* that record the climate history can be used to estimate the past climate.
- Note that none of these climate proxy estimates are anywhere near as precise as a thermometer measurement.
- The temperature information gained from the climate proxies are *very* rough estimates. In all proxies the information that is assumed to be a temperature signal is also caused by many other factors influencing the proxy, that have nothing to do with temperature (e.g. biosphere, chemistry, geology).
- For instance, think about Melbourne annual mean temperature change from one year to the next by about 0.1°C. A climate proxy by tree rings tries to extract this 0.1°C from the information in the yearly tree rings, which are also influenced by seasonal differences (seasonal cycle is 10°C!), by rainfall, extreme weather events, insects, the surrounding biotope, etc.



Figure 6.133: Climate Proxies: Tree rings.

- Trees have annual rings, match the growing seasons of the tree.
- The thickness of the annual rings and other information in the rings gives some information about the conditions for the tree in that year.
- As trees get a few hundred years all the climate of the past few hundred years can be studied by the tree rings.
- The information is always relative to the climate of the position of the tree. It does not give absolute values of temperature or any other values.

- Trees mostly grow in the warm season, so the tree ring proxy is mostly a proxy of the warm season, not the whole year.
- Some dead trees, which have been growing some 1000 years ago, have been preserved by natural processes. They allow us to study the climate of the past few 1000 years.

Proxies: Ice cores δO_{18}

- Glacier ice masses are very old. The snow flakes that form the bottom layer of the 4000m thick ice sheet in Antarctica are about 1 million years old. Studying these ice layers in the glaciers therefore allow us to go back in climate history by several 100,000 years.
- The water in the ice comes from precipitation, those *isotopic ratios* (δO_{18}) depend on the origin water masses and the atmospheric temperatures that produced the precipitation.
- This allows us to reconstruct a temperature of the past climate of those regions where the precipitation of the ice core came from. Thus the temperature signal reconstructed from ice cores does not relate to the temperature of the region of the ice core itself, but on the temperature of the water masses (mostly the nearby oceans) where the rain comes from.
- This temperature reconstruction has large uncertainties and may be uncertain by more than a factor of two.
- The ice cores also include little air bubbles, that preserved the atmospheric chemical composition of the past climates (e.g. CO_2).



Figure 6.134: Climate Proxies: Glacier Ice Cores.

- Just like trees, corals grow depending on the environmental conditions. So they keep a record of the past climate.
- This can go back in time by many thousand years, as dead corals have been preserved.
- Obviously corals are a proxy of ocean climate.
- They grow in shallow waters ($\sim 5\text{m}$) and are a proxy of SST, but may also track changes in salinity or ocean currents.

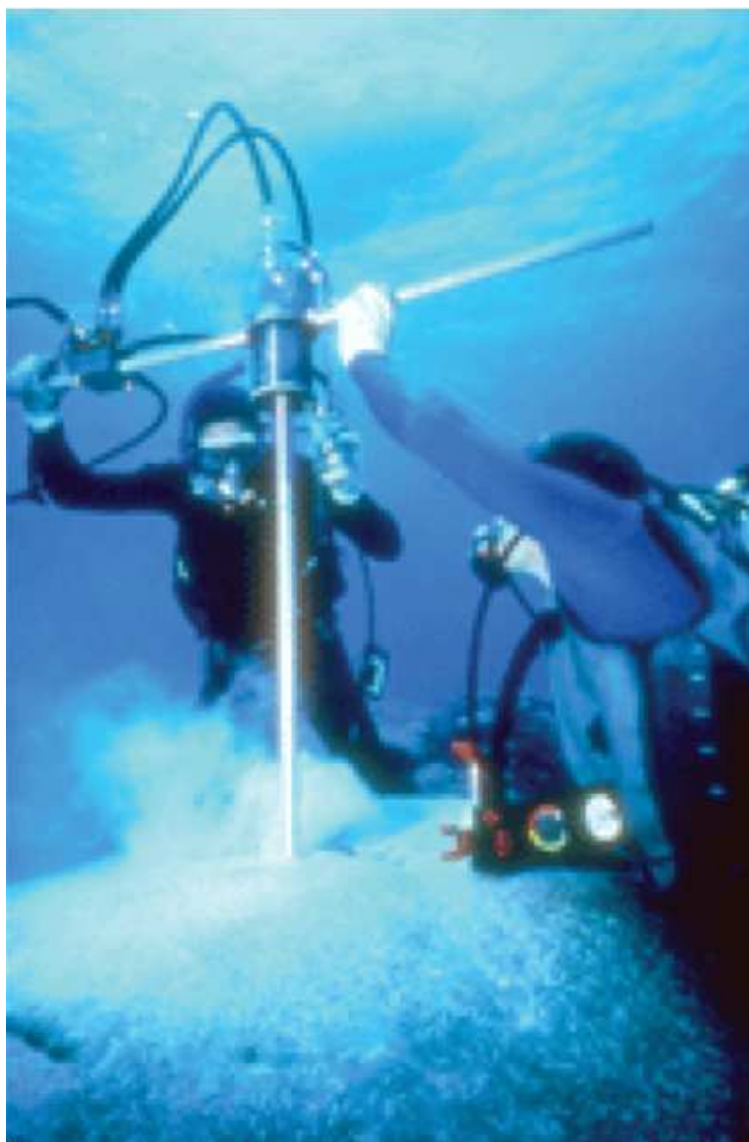


Figure 6.135: Climate Proxies: Corals.

Proxies: bore hole temperature

- Unbelievable, but true, the ice sheets keep their temperature from days that the layers were formed over many thousand years.

- This signal is of course somewhat smeared out by heat conduction, but it allows us to directly measure the temperature in the ice core bore hole at different depth, which correspond to different times of the past.
- They have been used to reconstruct the temperature up to 1000 years ago.



Figure 6.136: Climate Proxies: Ice Borehole temperatures. The temperatures in the bore hole at different depth is strongly related to the temperature that this ice layer had when it was formed (when it was a the surface).

Proxies: Sediments

- Sediments of lakes and oceans are a collection of a lot of climate indicators.
- This mostly tracks fossils, which give some indication of the past climate, as different species live under different climate conditions.
- They can be used to analyse the climate back many million years ago, as sediment formation of nearly all ages are preserved in some ways.



Figure 6.137: Climate Proxies: Sediments.

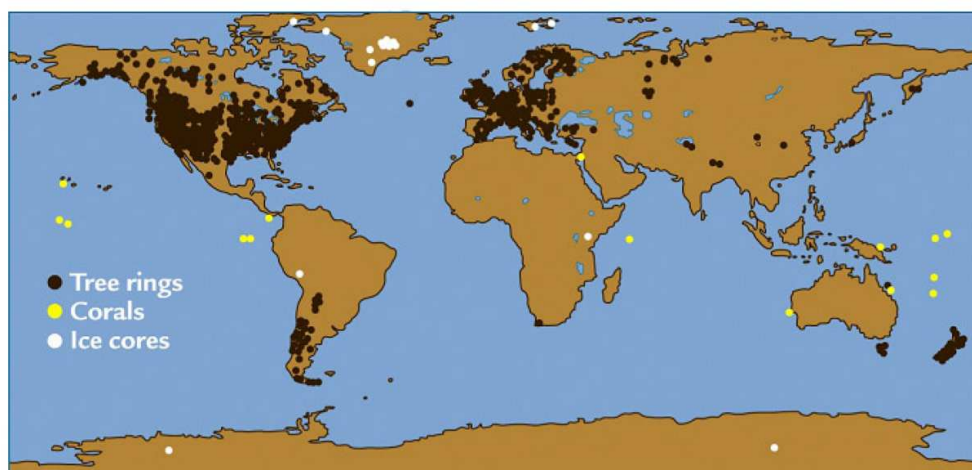


Figure 6.138: A global map of the distribution of climate proxy data.

6.8.2 The Climate History of the last 10,000 years

The last 2000 years:

- The climate of the past 2000 years was relatively stable.
- However, historical evidence from the development of civilizations around the world indicate that even in this globally stable climate, there seem to have been regional climate change with significant impact on the societies (.e.g. europe's medieval warm phase or little ice age).
- Most of this variability is probably internal climate variability, but fluctuation of the solar radiation (e.g. sun spots) and volcanic activity may have caused some of these fluctuations.
- On global or hemispheric scale the variability over the last 2000yrs was less than 0.2K stdv.
- Compared to the last hundred years the curve was basically flat and then strgonly increased; it looks like a hockey stick.
- Prediction of the future next 100yrs climate change compared to the last 2000yrs will be a very fast and very strong. IT is like nothing that mankind has experienced at least since the stone ages (5000yrs).

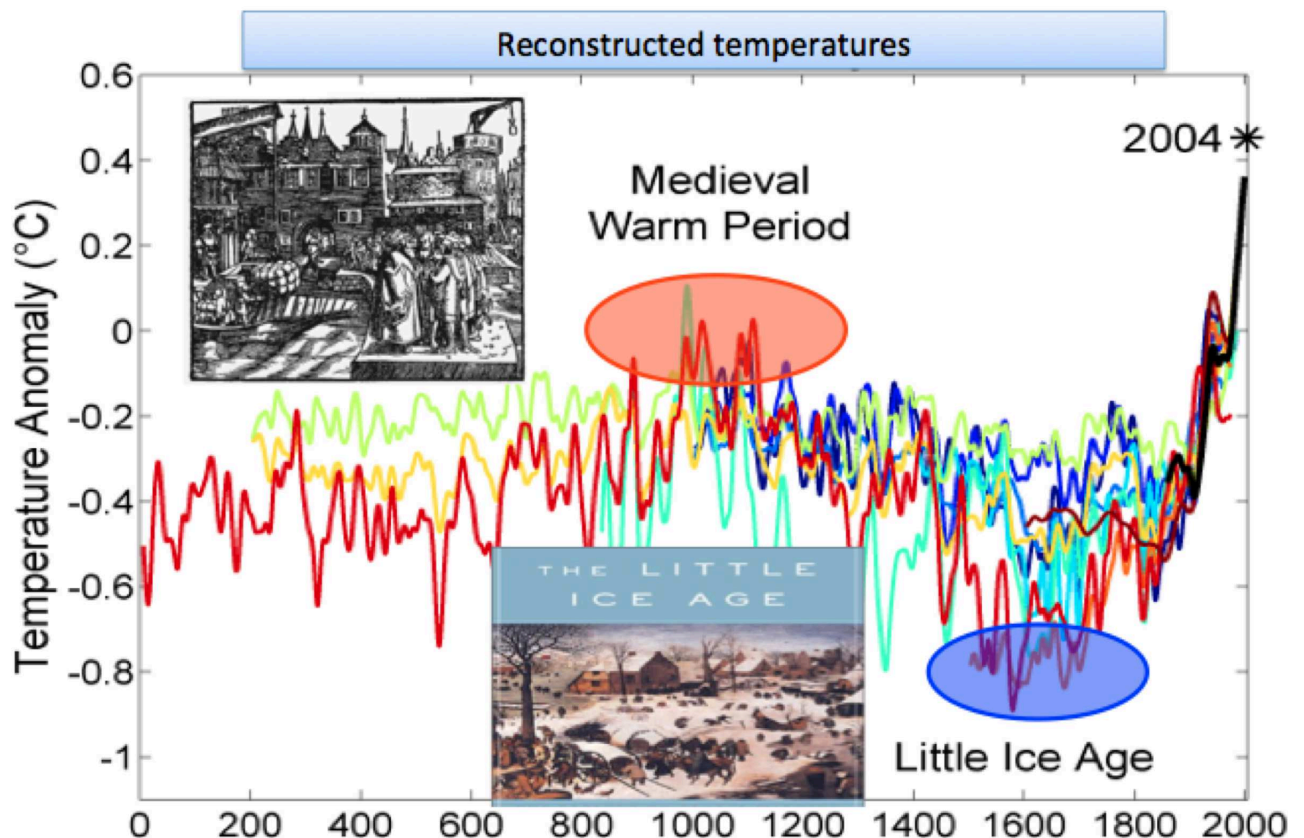


Figure 6.139: The reconstruction of the northern hemispheric temperatures over the past 2000 years based on different climate proxy estimations (coloured lines). The black line is the most recent instrumental record. this graph is also known as the "Hockeystick".

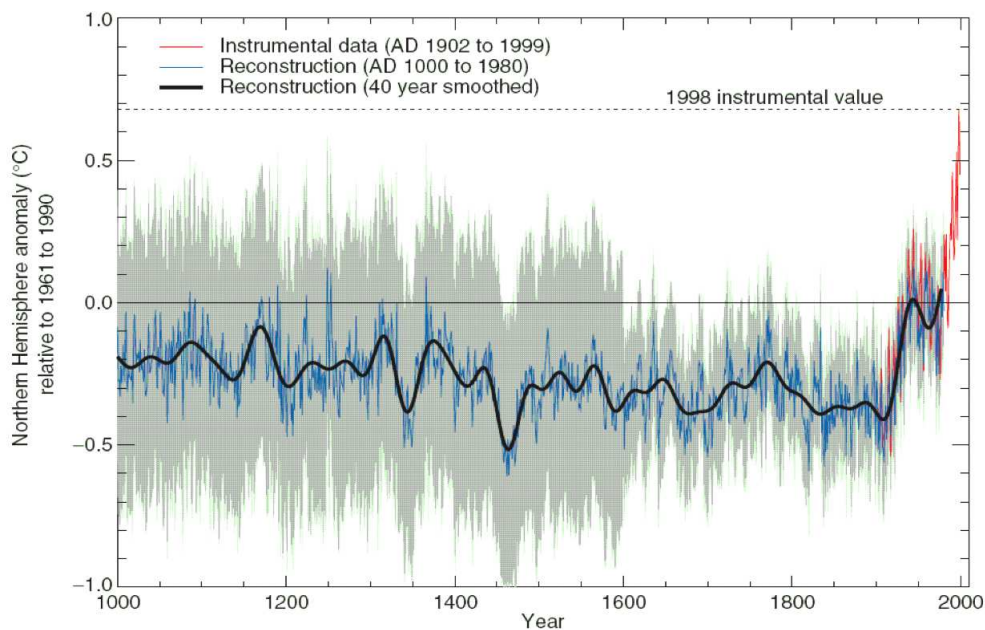


Figure 6.140: A reconstruction of the Northern Hemisphere surface temperature 1000-2000. Shaded area marks the estimated uncertainty in this temperature reconstruction.

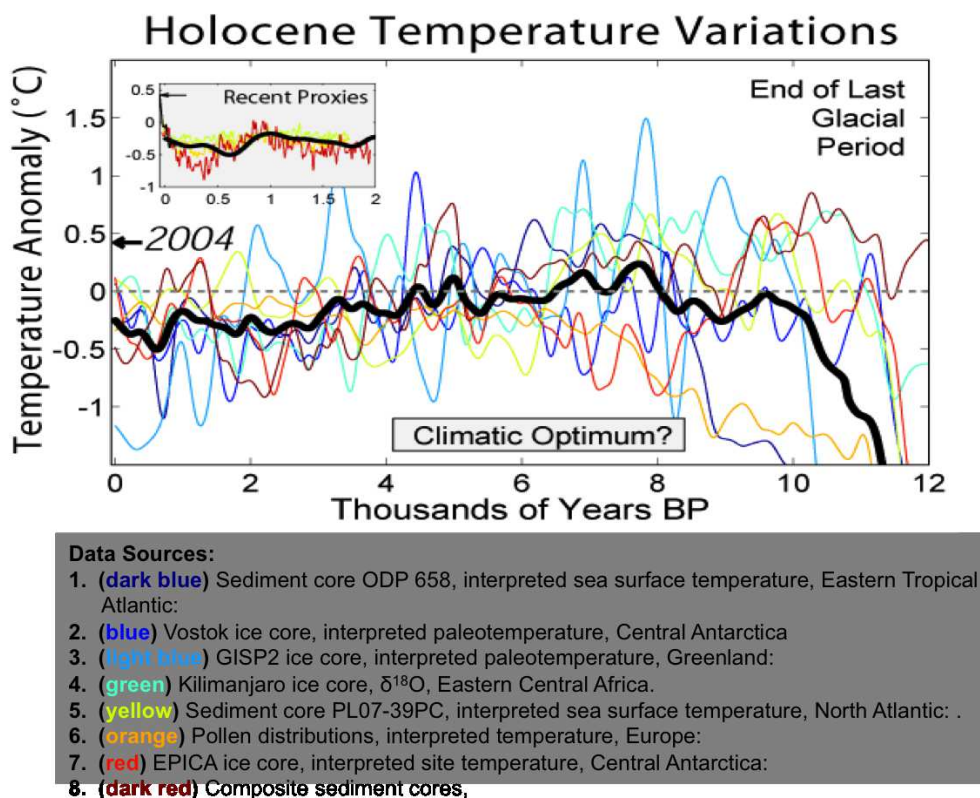


Figure 6.141: Holocene/last 10,000 years temperature variations using different proxy reconstructions. the black line is the average of the estimates. Note, the drop at the end indicating the end of the last ice age.

6.8.3 Ice Ages (The Milankovitch Cycles)

The last 500,000 years:

- The last 500,000 years of climate variability are dominated by the big ice age cycles.
- In roughly a 100,000 years time scales short warm phase (interglacials) and long ice ages (glacials).
- These events have been of nearly global extent, with synchronized variability at southern and northern latitudes.
- The transition from the last ice age at about 18,000 years ago to the current warm phase took about 5000 years.
- The global temperature different from an ice age to a warm phase is about $3^{\circ}C$, weak in the tropics but much larger in the polar regions.
- In the past 500,000 years there were phase warm than to day by about $1 - 2^{\circ}C$.
- Prediction of the future next 100yrs climate change compared to the ice age cycles will be similar in amplitude, but will be much faster (a factor about 50 times) and into a warmer climate than any of the previous 1 million years.

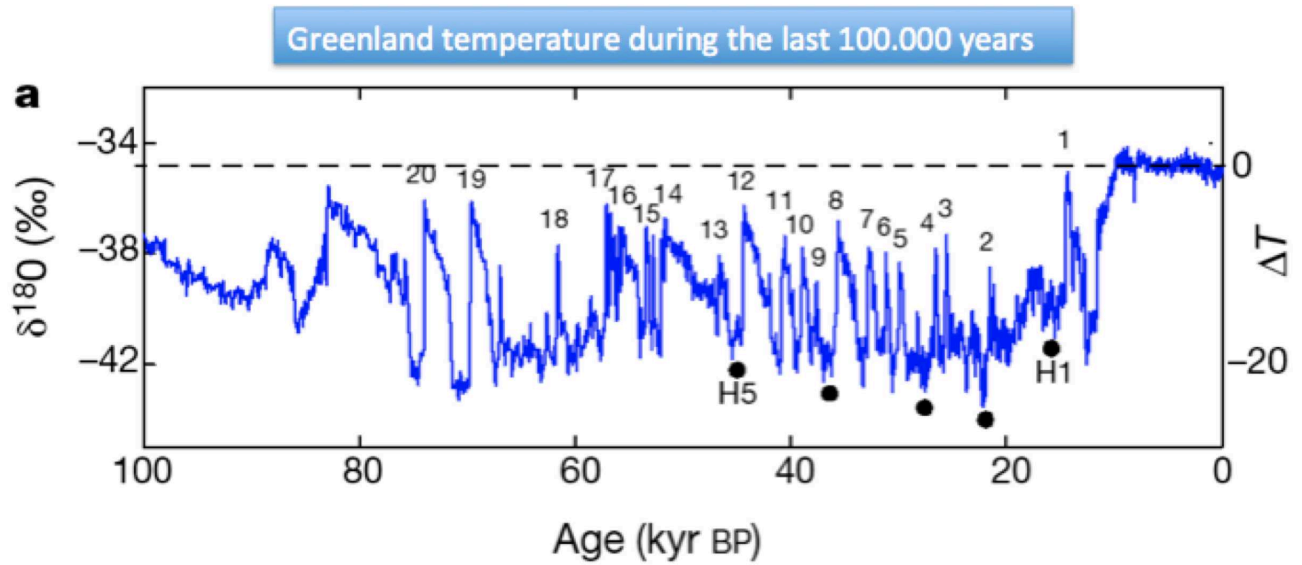


Figure 6.142: Temperature variations in greenland over the past 100,000 yrs as estimate from the $\delta^{18}O$ from Greenland ice cores. Remarkable are the the much colder temperatures compared to present indicating the existence of the last ice age and the strong and fast fluctuations within this period. The numbers and letters mark these climate events.

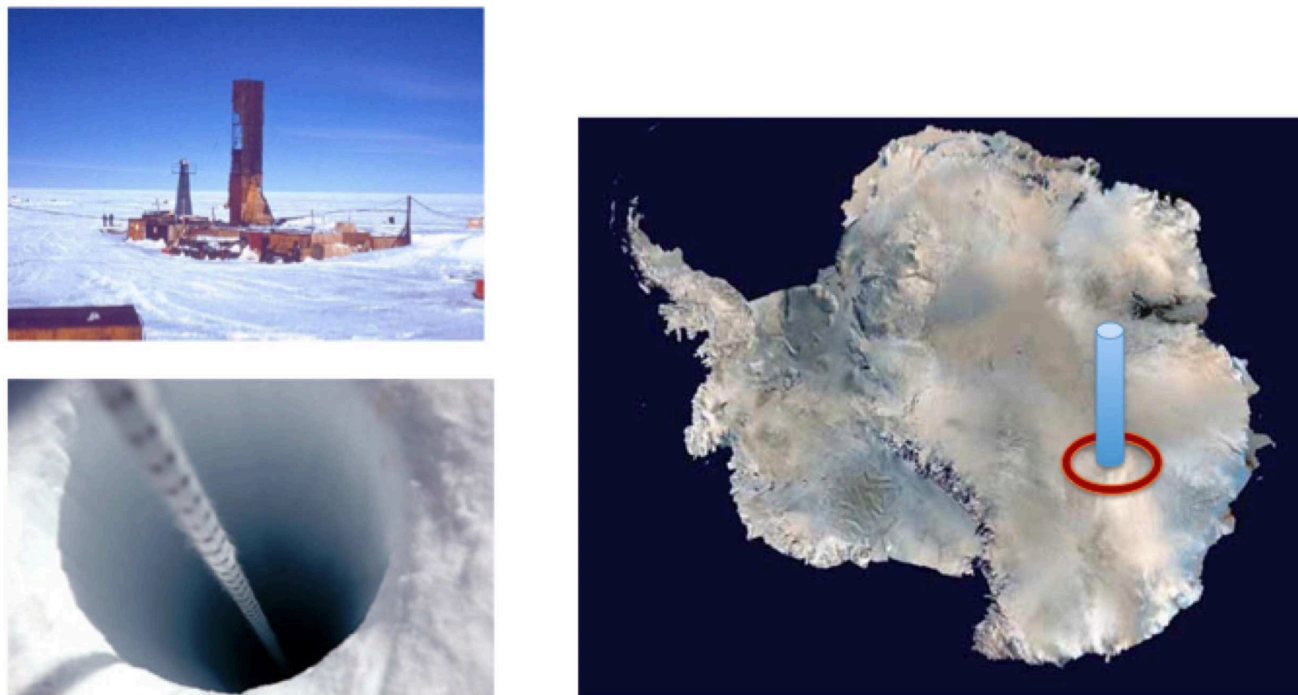


Figure 6.143: The Vostok ice core drilling site. It is the location in Antarctica which has the thickest Ice sheet, because it does not drift much from this point and it does not snow much (it is a desert). The ice here is the oldest on earth, which makes it the perfect place to gather information about the past climate.

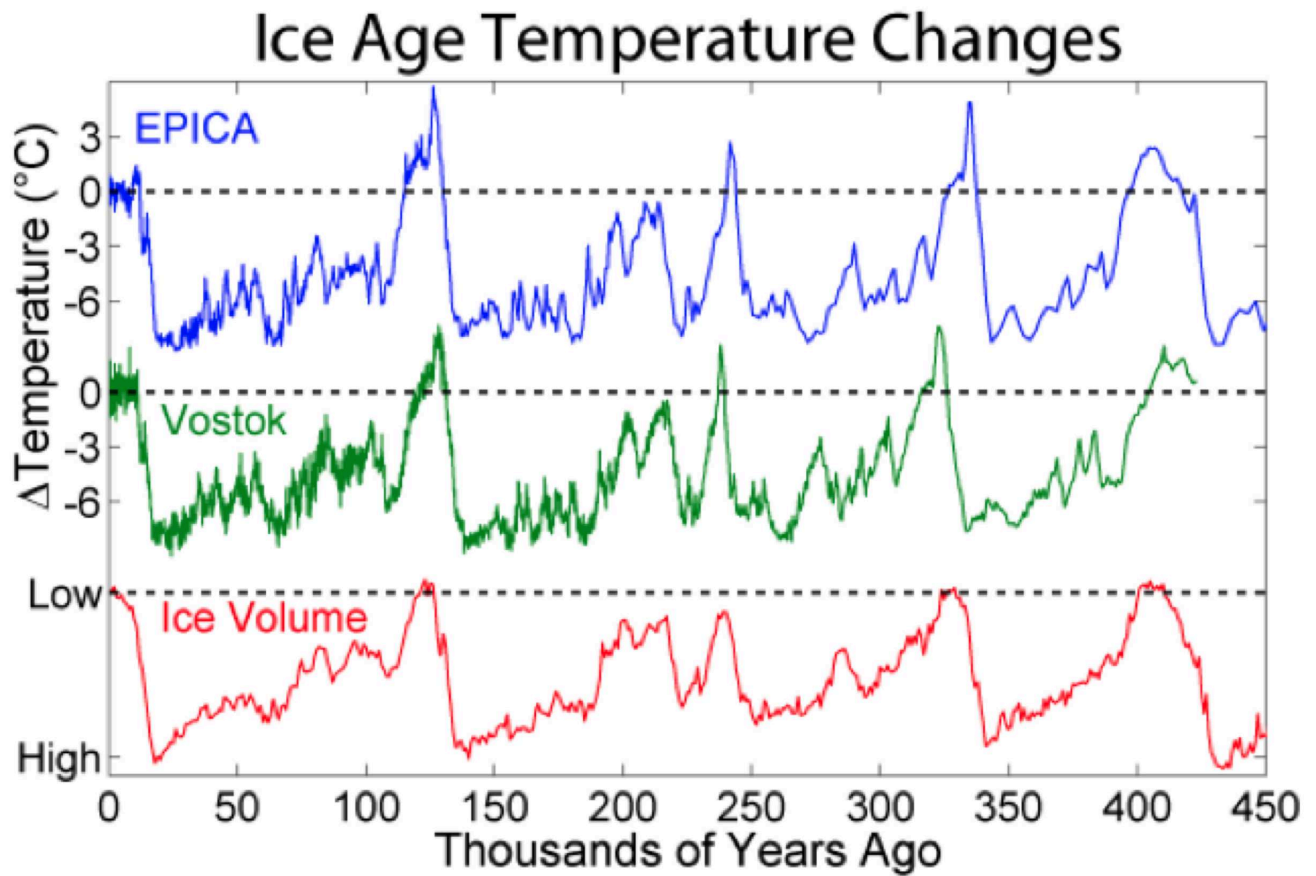


Figure 6.144: Temperature variations in antarctica over the past 450,000 yrs as estimate from the δO_{18} from antarctic ice cores. Also shown is the ice volume. We can note five warm interglacial periods between the five longer ice ages.

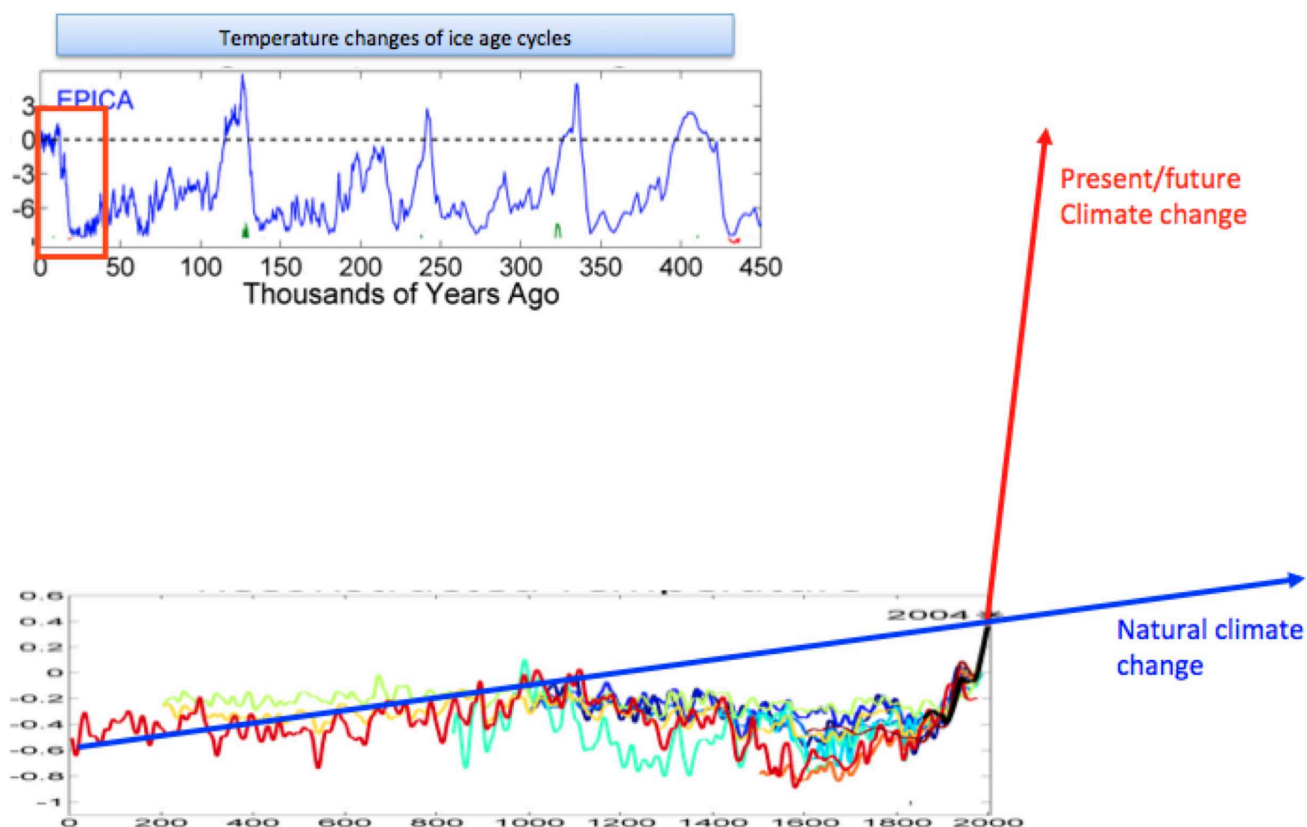


Figure 6.145: Comparison of the 'fast' warming at the end of the last ice age (blue line) with the predicted anthropogenic climate change in the 21st century (red line).

The causes of Ice Ages:

- The causes of Ice Ages are partly internal natural and external climate variability, and involve some important feedbacks in the climate system.
- The red noise stochastic climate model is in particular relevant for glacier mass balances.
- The biggest driver of ice ages cycles is most likely the variations of the earth orbit around the sun, cause by the other planets (Jupiter) and the moon. These variations are called Milankovitch cycles.
- Feedbacks in the climate system are central in the earth response to changes in the external forcings.
- Those are in principle the same feedbacks as in the current climate or future climate change caused by anthropogenic forcing, but there are also feedbacks that act only on the longer time scales.

Glacier feedbacks:

- Ice-albedo: the most obvious feedback of glaciers is not necessarily the most important one.

- Water vapor: The large cold and high altitude regions cover by glaciers will reduce the atmospheric water vapor and therefore cause reduced downward thermal radiation.
- Altitude cooling: When glaciers grow they build high mountains of ice. They reach up to 4000m high. The air pressure decrease with height leads to further cooling which is a positive feedback to the glaciers which further supports the glacier growth.
- Atmospheric circulation: Large glaciers such as Greenland change the atmospheric circulation significantly.

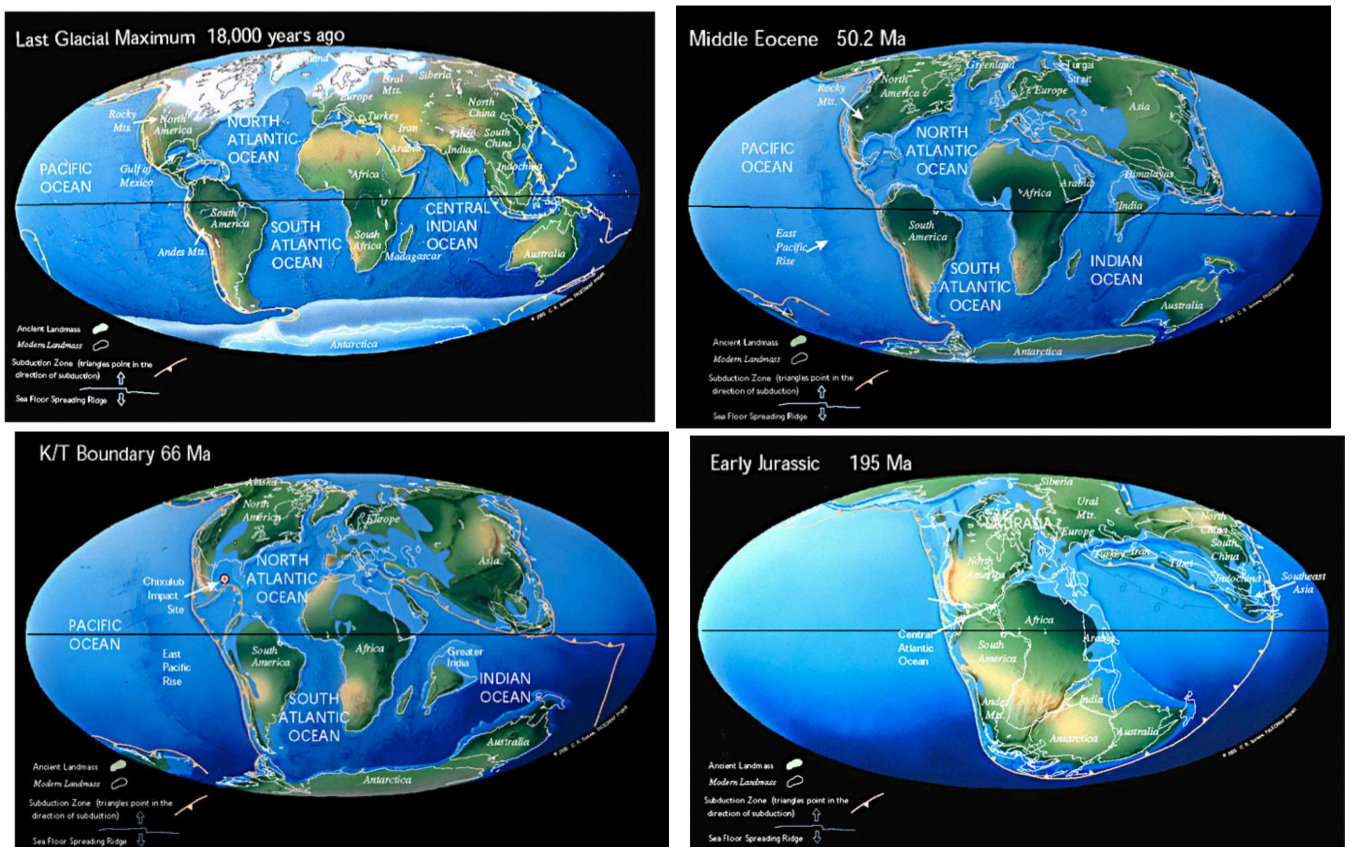


Figure 6.146: Changes in the topography, sea level and ice sheet cover over the past 200Ma.

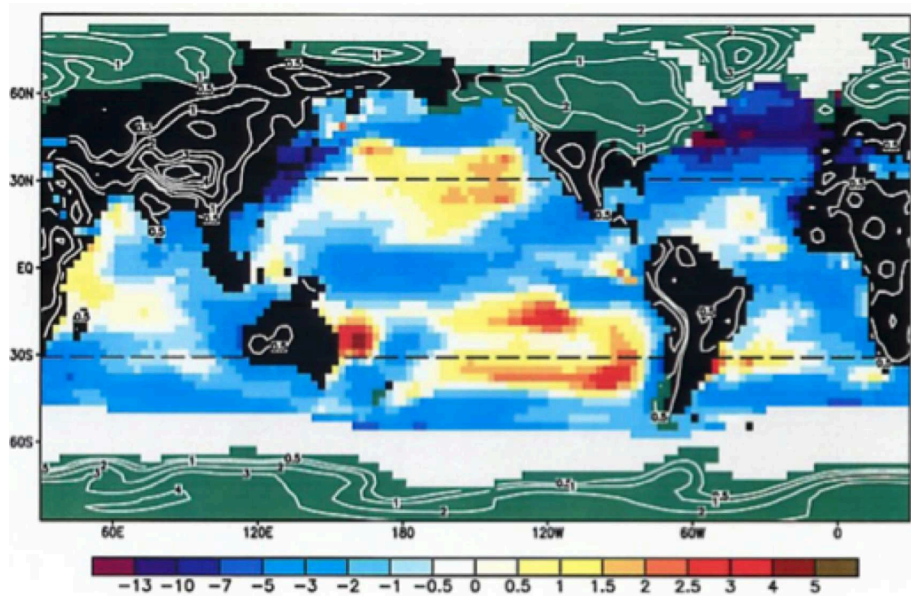


Figure 6.147: A reconstruction of the global temperatures during the last ice age maximum. Values are degrees different from present day climate. Note, some regions have even been warmer than present day.

Feedbacks on Ice Age cycles:

- In addition to the glacier feedbacks there may be other feedbacks:
- Ocean CO₂ up take: The oceans uptake of CO₂ depends on its temperature and the organisms leaving in the oceans. Cold oceans can take up more CO₂ than warm oceans. This leads to a positive feedback, with increased atmospheric CO₂ when its warm and reversed when its cold.
- Land vegetation: A similar effect may exist for the land vegetation. Glaciers will cover up large land regions and the remaining land may to a large part change its vegetations.

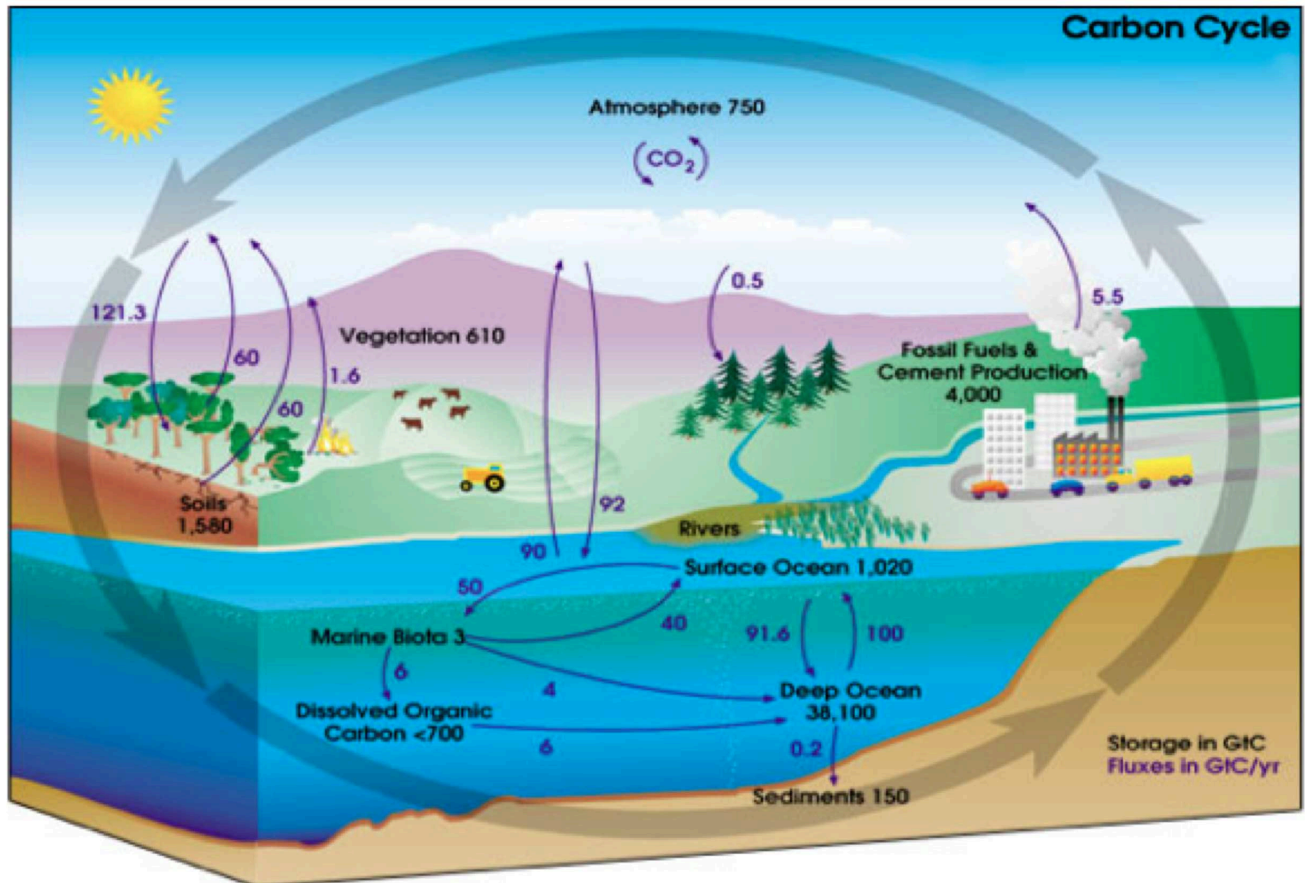


Figure 6.148: Sketch of the earth carbon cycle

6.8.4 Orbital forcings (The Milankovitch Cycles)

- The variation of the earth orbit caused by Jupiter and Moon have three elements:
- Exentricity: The shape of the earth orbit around the sun. Note, that the earth moves fast when it is closer to the sun. This can have a small impact on the global annual mean solar constant (S_0). The more the orbit is elliptic the smaller is the annual mean incoming solar radiation. But it only varies by a bout $0.7W/m^2$ in the annual mean. The orbit shape varies over a 100kyrs period.
- Precession: the position of the seasons within the orbit around the sun. This causes no changes in the global solar constant change (S_0) and varies with a period of about 20kyrs. How much the precession influences the incoming sun light also depends on the Exentricity and Obliquity. The Precession has no effect if there is no Exentricity or no Obliquity (no titled earth axis).
- Obliquity: The earth axis tilt towards the earth orbit around the sun varies between 22.16° to 24.5° . It has a period of about 40kyrs. It changes the strength and timing of the seasons, but has no effect onto the global annual mean incoming solar radiation.
- These cycles are predictable to a few million years.

- They cause mostly a redistribution of the incoming sun light between latitudes and seasons, but not much of a global solar constant change (S_0).
- Changes in solar constant change are less than $1W/m^2$ over 100,000 year, but regional changes in one seasons can be larger than $50W/m^2$ over 10,000 years.

Solar forcing vs. Climate Variability:

- Although the Milankovitch cycles of variations in the incoming solar radiation are the best explanation for the ice age cycles of the past 0.5 million years, they do not quite fit to the observations.
- Note that the data has to be shifted to fit to the Milankovitch cycles , also it seems that the δO_{18} fits better to the Milankovitch cycles than the temperature.
- Further it is unclear why the 100,000yrs cycle is so strong and other frequencies are not.
- Note also that the spectrum of temperature variability looks much more like red noise than the Milankovitch cycles, indicating that the Milankovitch cycles are not the whole story.

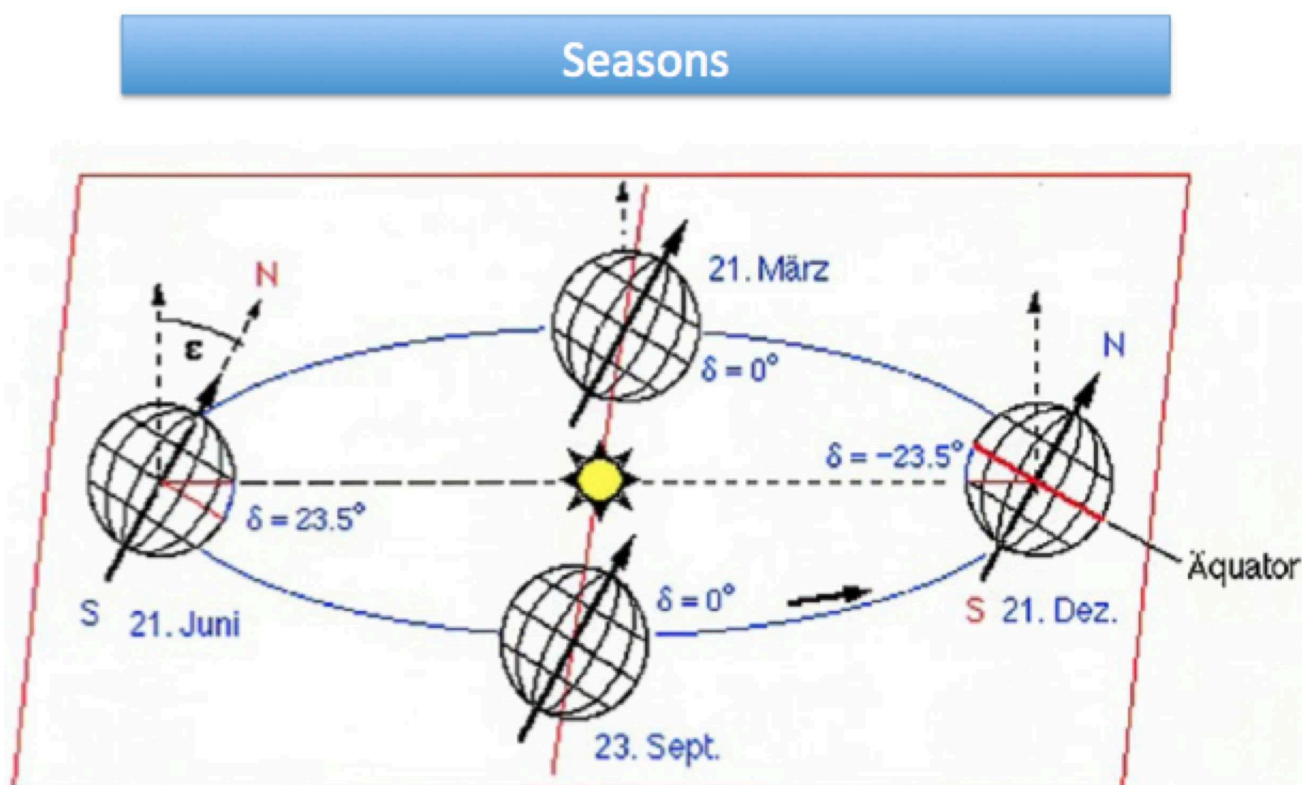


Figure 6.149: Sketch of the Earth orbit around the sun.

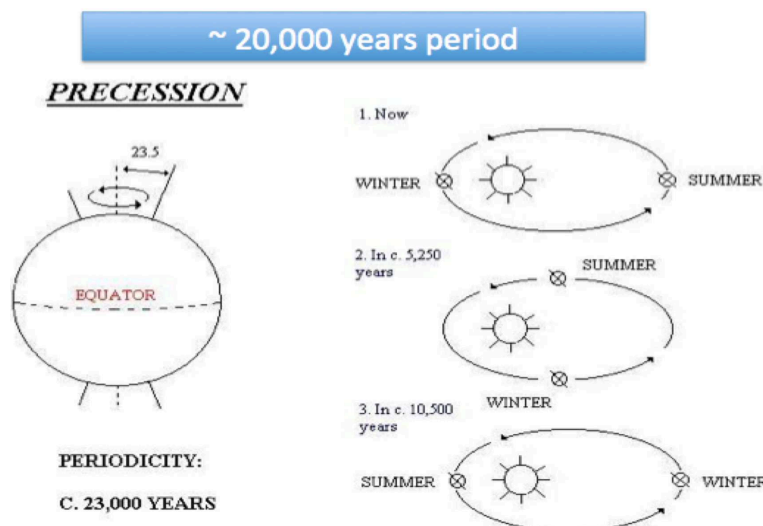
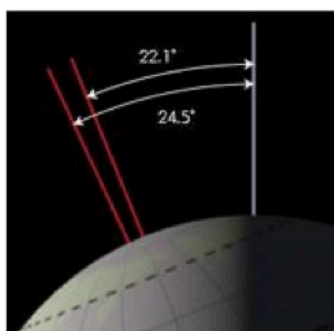
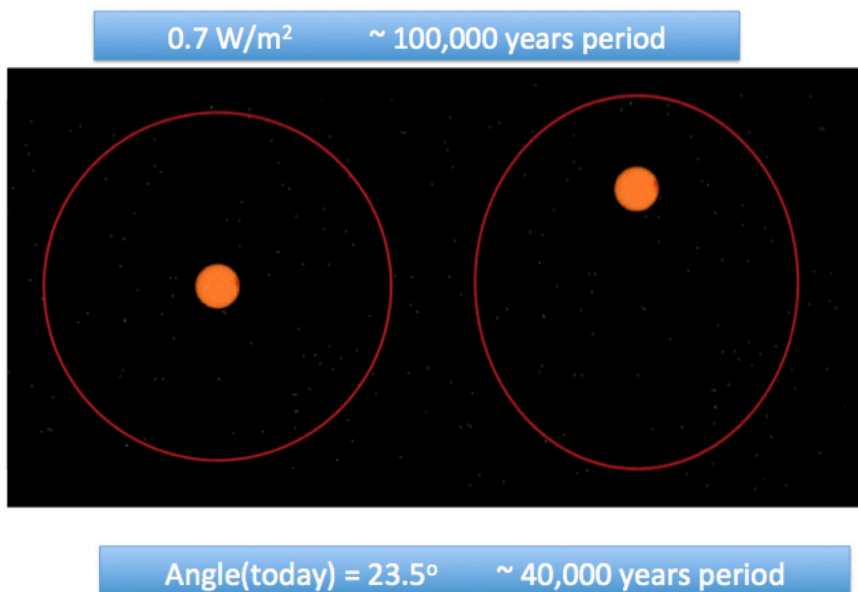


Figure 6.150: Upper: Eccentricity: The shape of the earth orbit around the sun. Note, that the earth moves fast when it is closer to the sun. Middle: Obliquity: The earth axis tilt towards the earth orbit around the sun varies between 22.16° to 24.5°. Lower: Precession: the position of the seasons within the orbit around the sun. This is in respect to the northern hemisphere seasons.

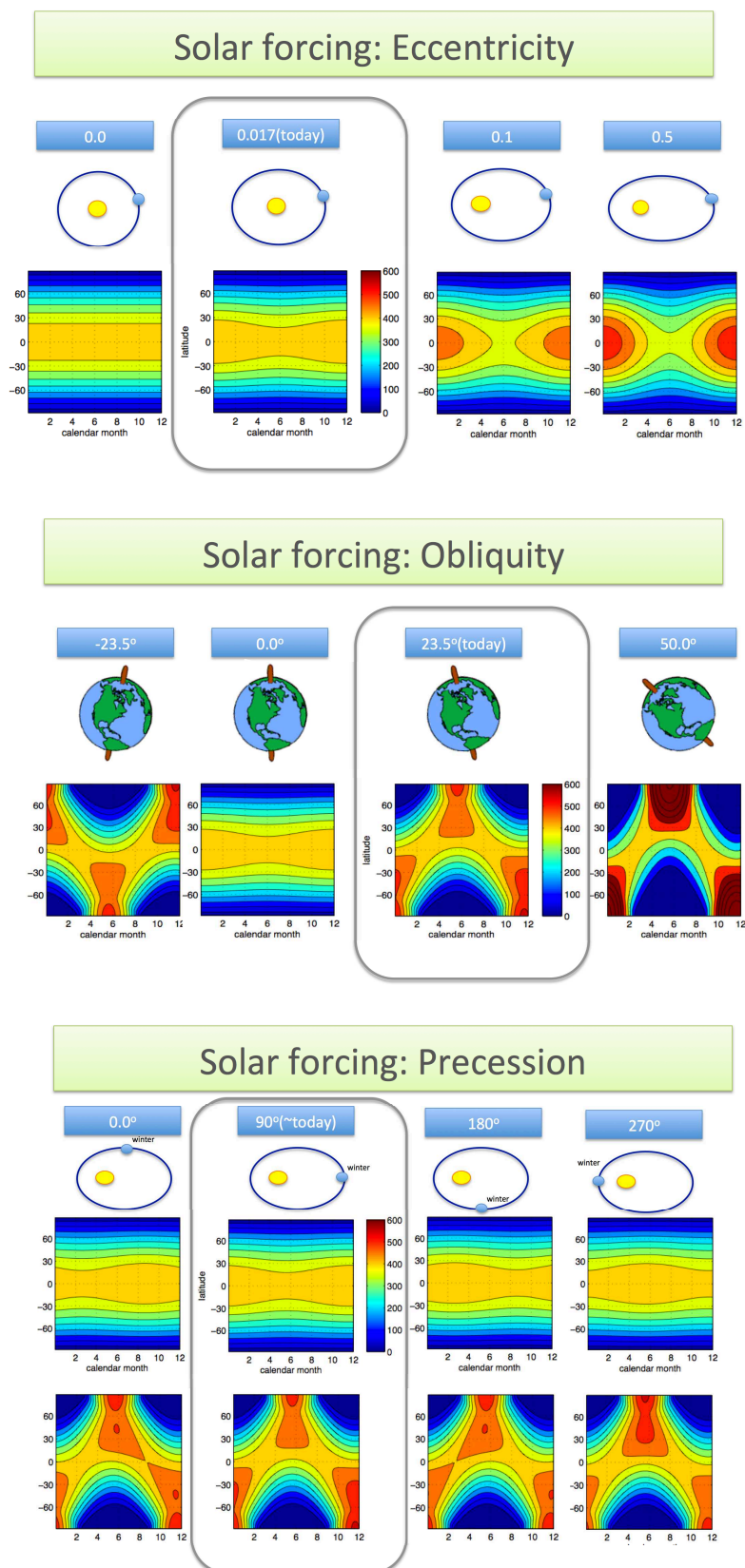


Figure 6.151: Upper: Eccentricity: changes in the incoming solar radiation due to changes in the eccentricity (orbit shape). Middle: Obliquity: changes in the incoming solar radiation due to changes in the obliquity (axis tilt). Lower: Precession: changes in the incoming solar radiation due to changes in the precession (orbit orientation relative to the seasons).

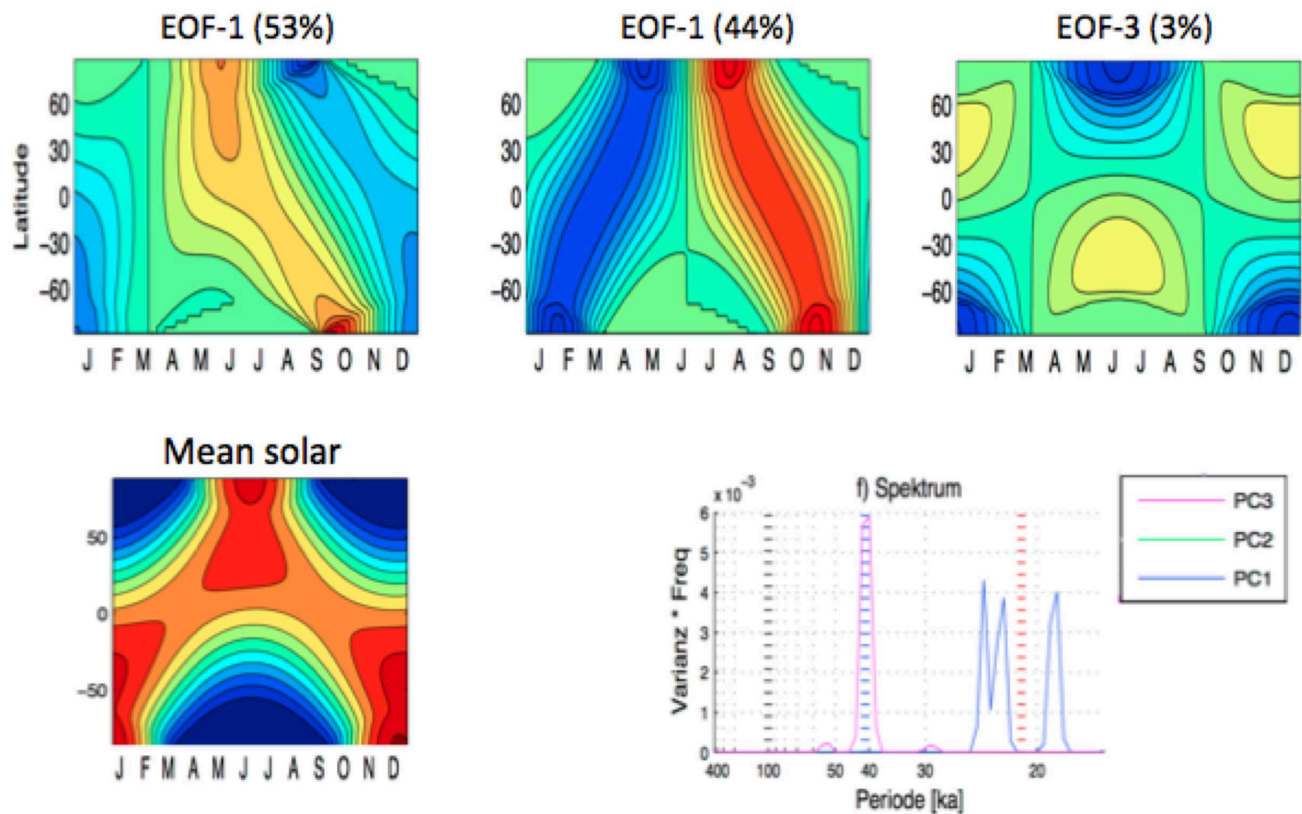


Figure 6.152: Upper: EOF patterns of the incoming solar radiation variability caused by the orbital changes as function of calendar month and latitude. The blue and green colours indicate negative and red and yellow indicate positive deviations from the normal incoming radiation (lower left). Note, that the first two pattern explain about 97% of the total variance and both represent only seasonal shifts with near zero global mean variability. Lower left: the mean incoming solar radiation. Lower right: the power spectrum of the time evolutions of the leading EOF patterns.

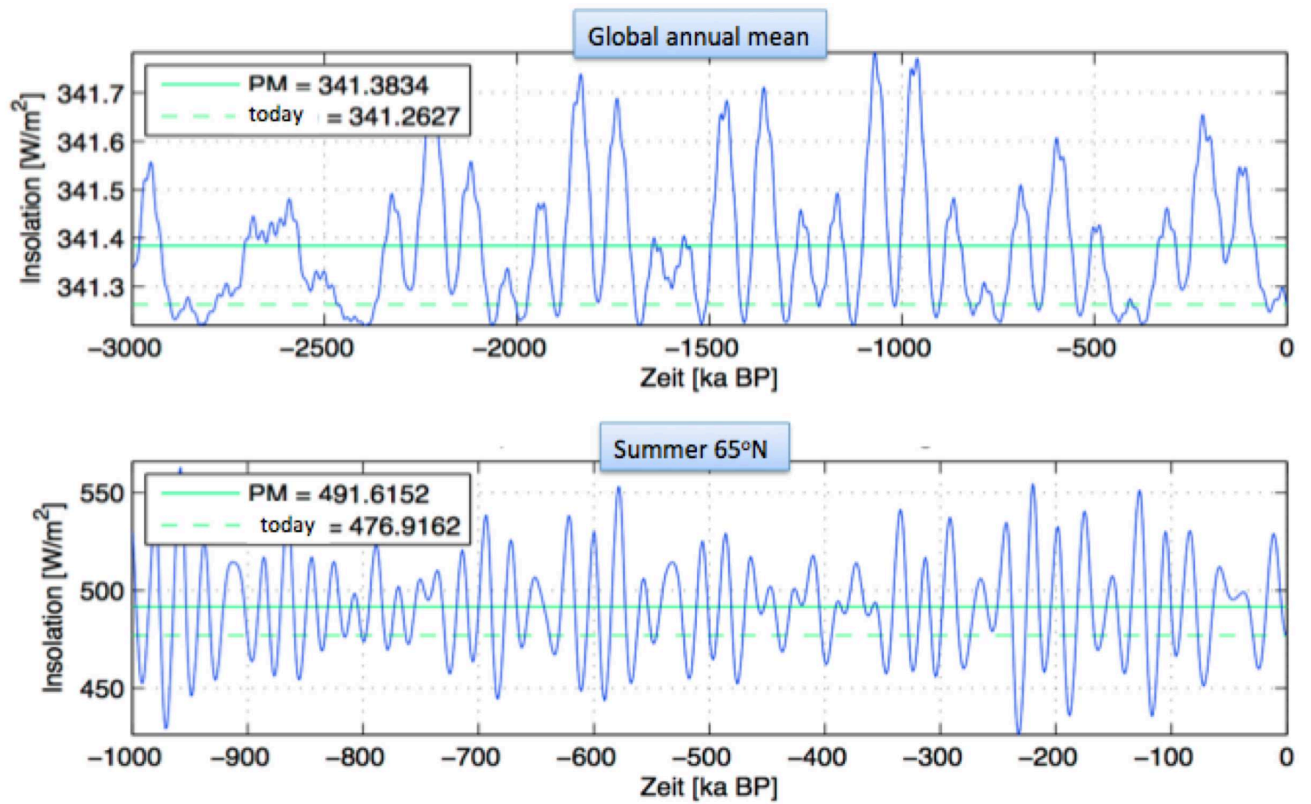


Figure 6.153: Upper: Time series of the global and annual mean incoming solar radiation over the last 3 million years. Lower: the same for the summer mean incoming solar radiation at 65°N latitudes. Note, the much smaller y-axis scaling in the upper plot.

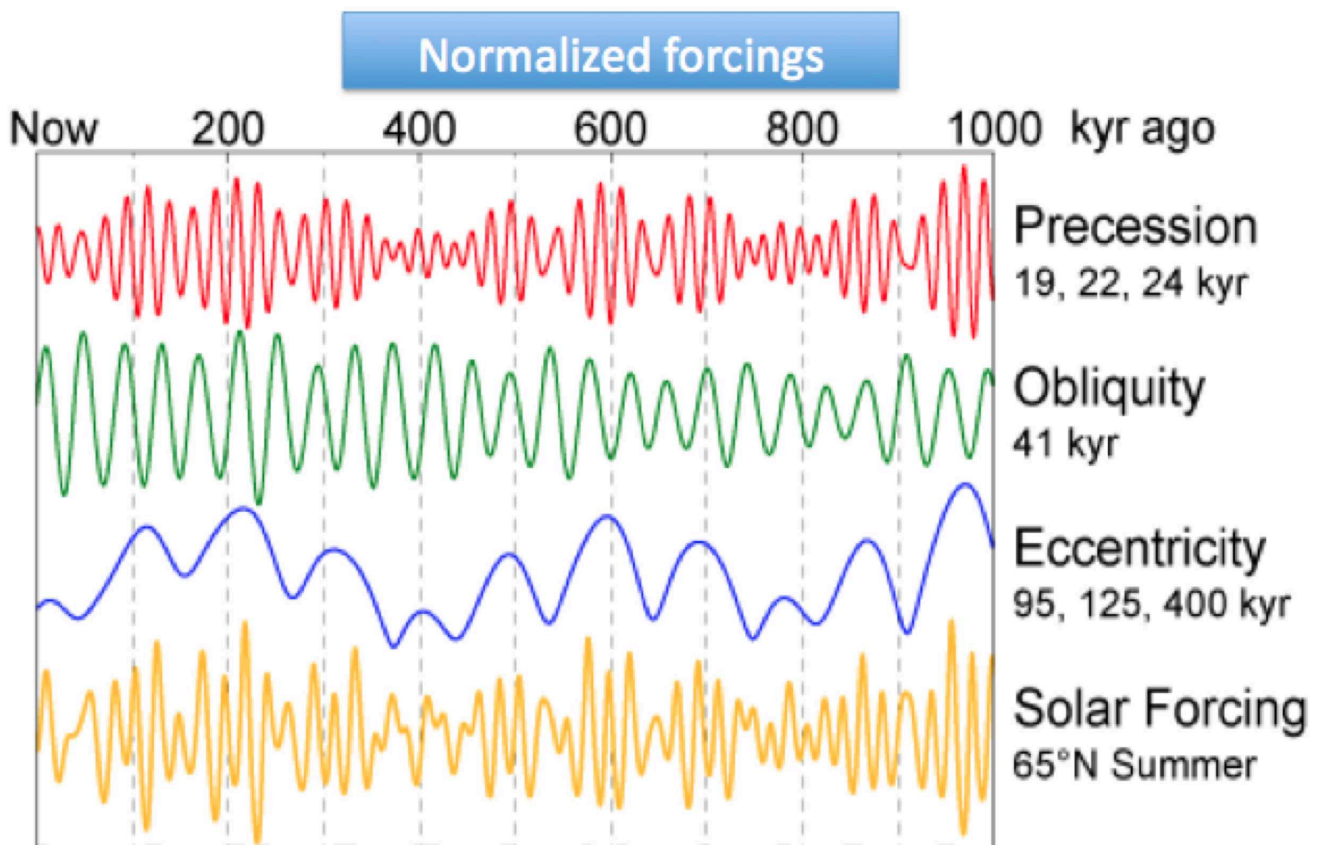


Figure 6.154: Time series of the different orbital forcings and the total for the summer mean incoming solar radiation at 65°N latitudes.

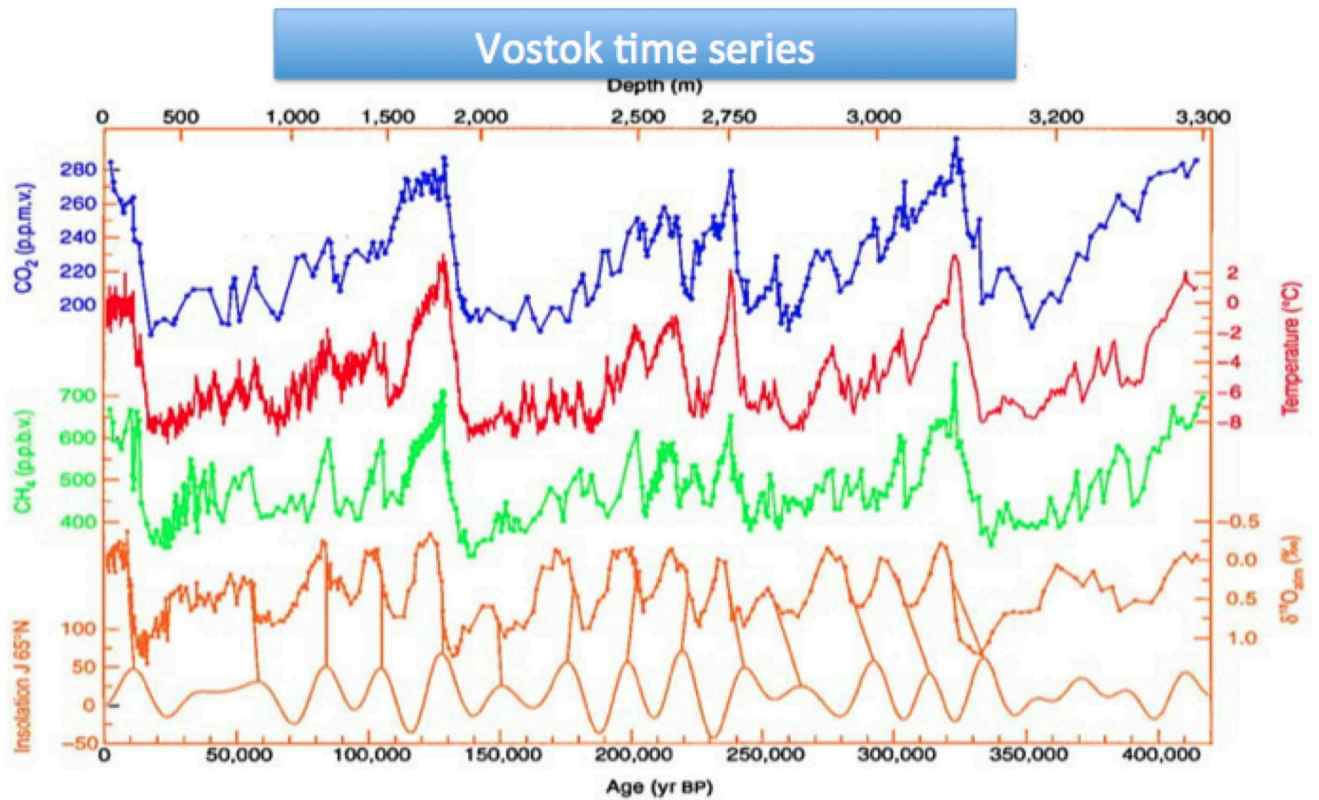


Figure 6.155: Different reconstructions of climate variables from Antarctic ice cores in comparison with the incoming solar radiation changes by orbital forcings. Note, that the time axis of the reconstructions need to slightly shifted to match the orbital forcing curve.

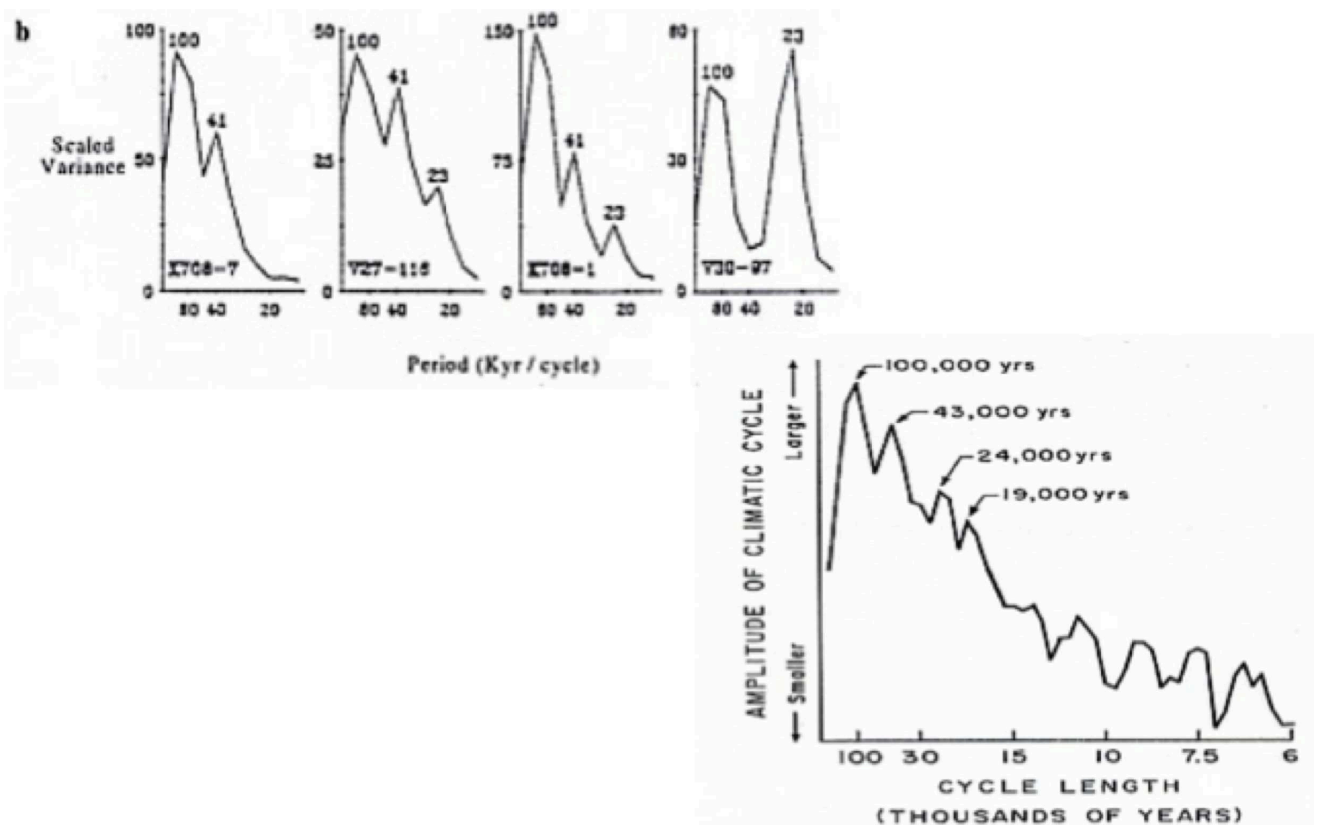


Figure 6.156: Power spectrum of different ice core records.

6.8.5 The Climate History of the Past 500 Mill. Years

Time scales longer than 1 million years:

- On time scales longer than a million year the geography of the earth is no more a external fixed boundary condition, but the geography starts to vary.
- The most recent event is the south polar position of Antarctica, which allows the creation of the ACC ocean current, which insulates Antarctica from the warm and humid tropics, that allows the glaciation of Antarctica. Leading most likely to a global cooling.
- About this time the human species develop, from the climate point of view caused by colder and harsher conditions, forcing the species to become smarter and more adaptive to find food (e.g. think about the difference between Jamaica and Germany).
- On even longer time scales the atmospheric chemistry also starts to vary significantly.

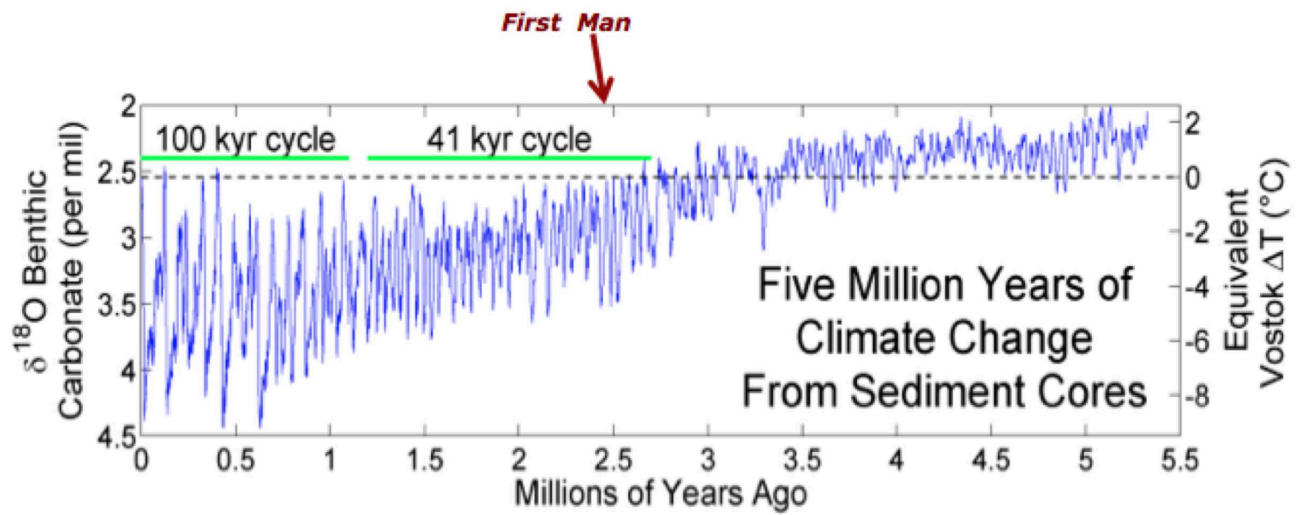


Figure 6.157: A climate proxy estimate of temperature change over the last 5.5 million years. Note, that the human race developed at around 2.5 Million year ago, a point in time when the climate did get colder.

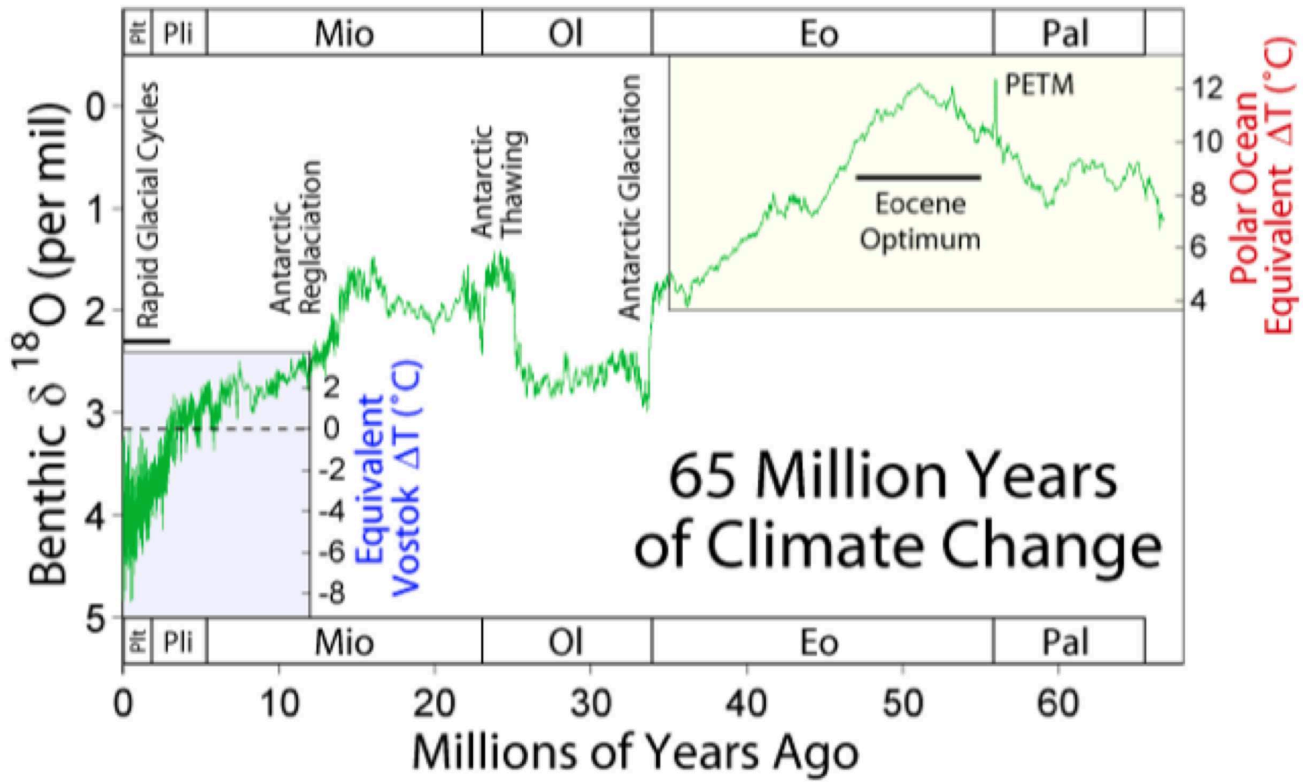


Figure 6.158: A climate proxy estimate of temperature change over the last 60 million years.

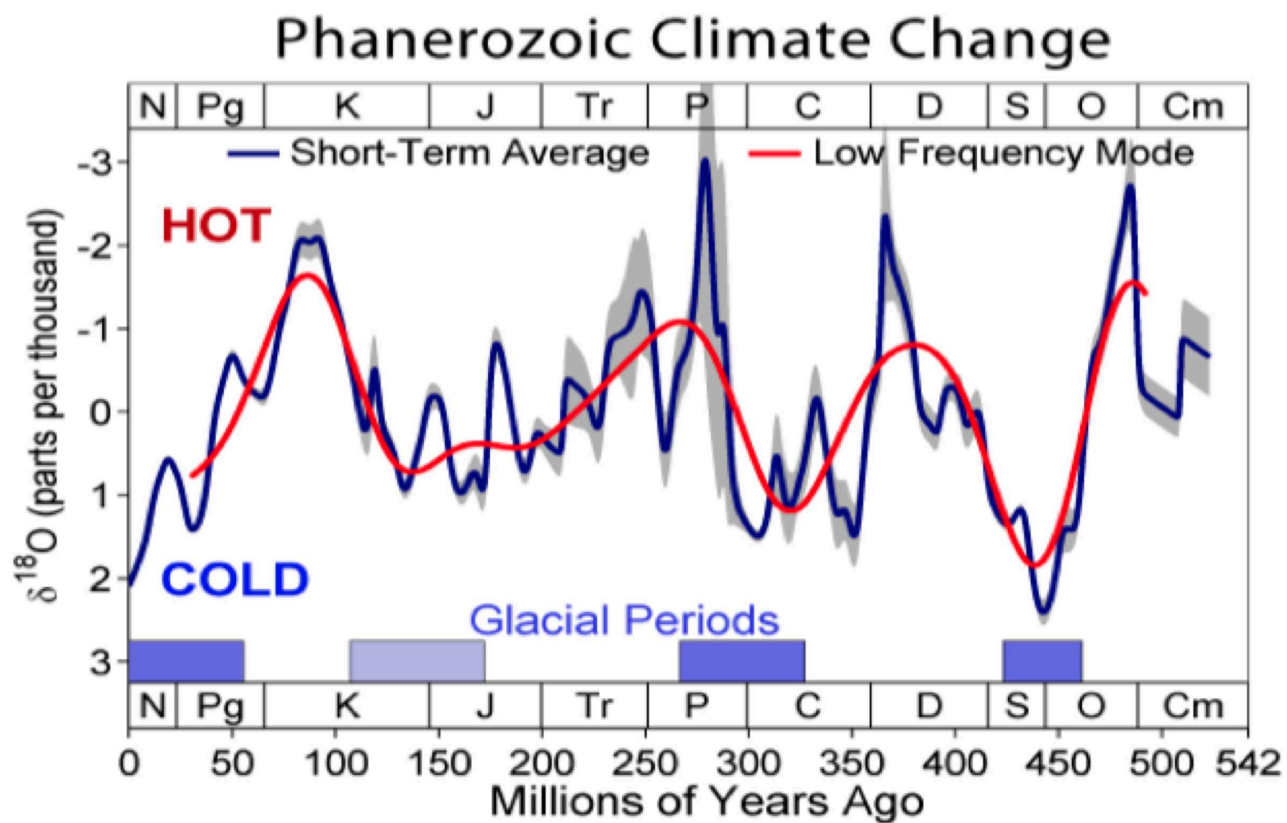


Figure 6.159: A climate proxy estimate of temperature change over the last 500 million years. Periods with glaciers are marked with blue shaded areas.

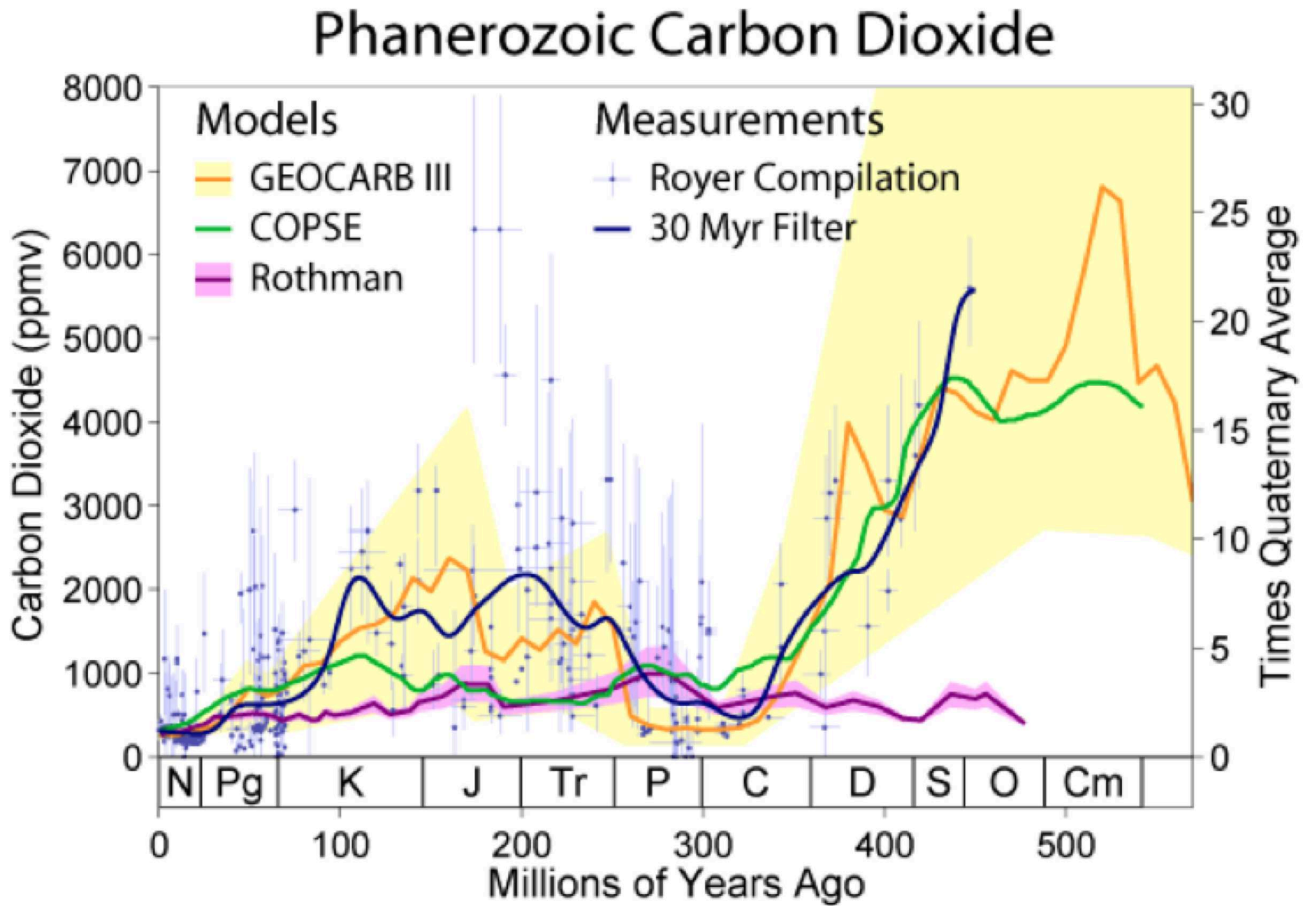


Figure 6.160: A climate proxy estimate of atmospheric CO_2 concentration changes over the last 500 million years. Note, that present day CO_2 concentration of 350ppm is very low compared to past values.

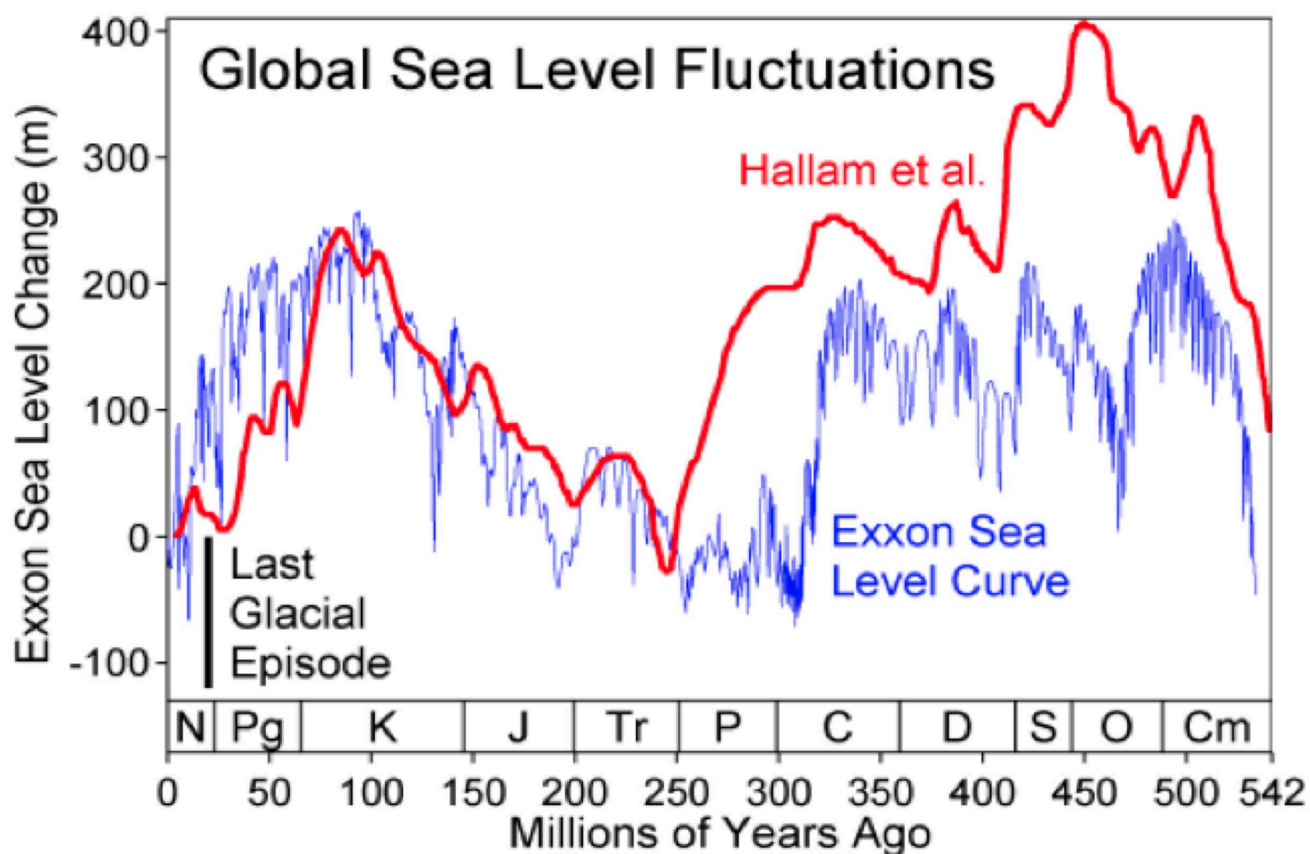


Figure 6.161: A climate proxy estimate of global sea level changes over the last 500 million years.

The Climate Power Spectrum

- We can summarize the climate variability from days to roughly the age of the earth by a power spectrum.
- The spectrum is mostly a continuous spectrum with variability on all time scales and no peaks or only weak peaks in the spectrum (except for the annual and daily cycles of cause).
- The overall power law of the spectrum roughly follows a $1/\text{frequency}$, even though the cause of climate variability are very different at different time scales. Thus if the frequency increase by 10 orders of magnitudes (from 10^{-8} to 10^2), than the spectral variance decrease by roughly the same orders of magnitudes (from 10^9 to 10^{-2}).
- The most important drivers or variations in the solar forcing, tectonic changes in the geography/atmospheric chemistry and internal climate dynamics (atmos, oceans and glaciers).

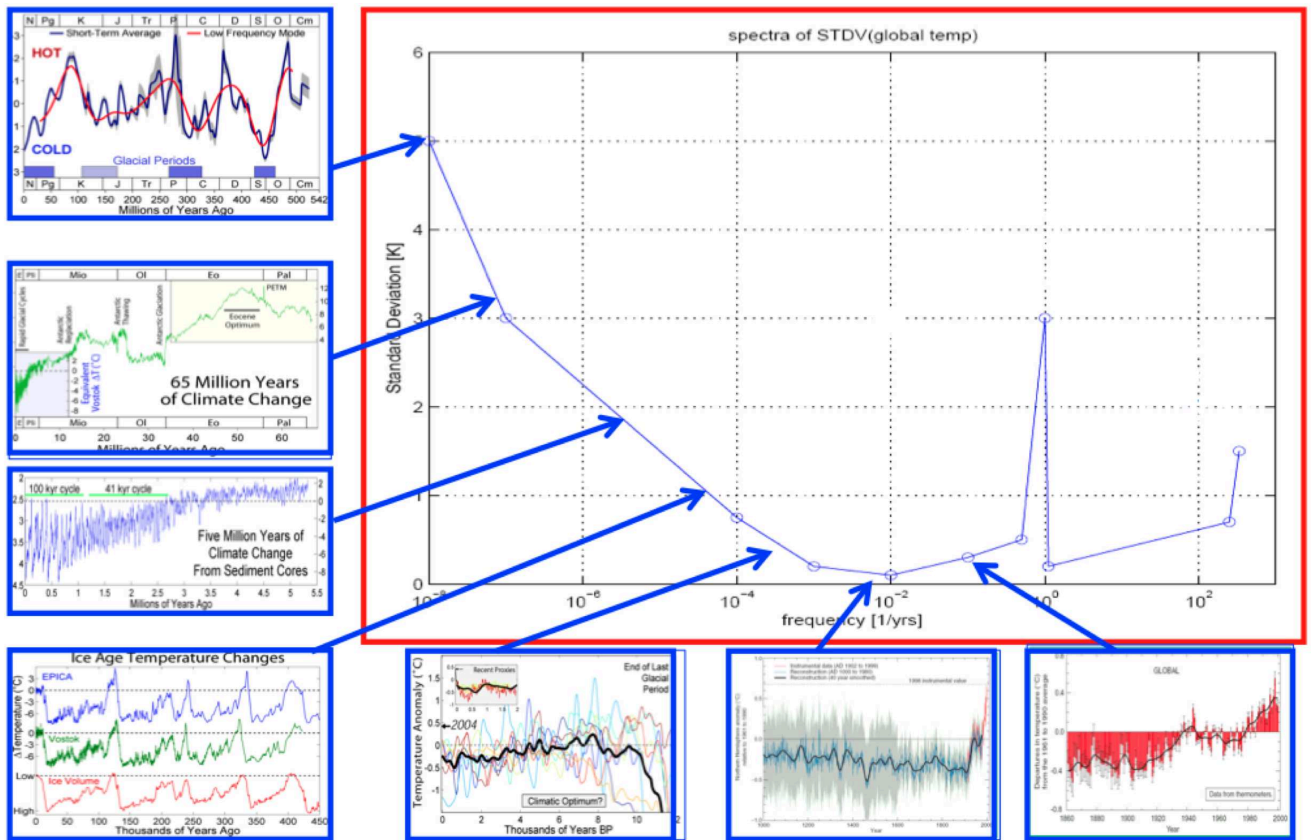


Figure 6.162: A summary of the climate variability on different time scales: the standard deviation of the different time series is plotted against the frequencies over which the time series are sampled. This is rough first estimate to create the power spectrum in the next figure.

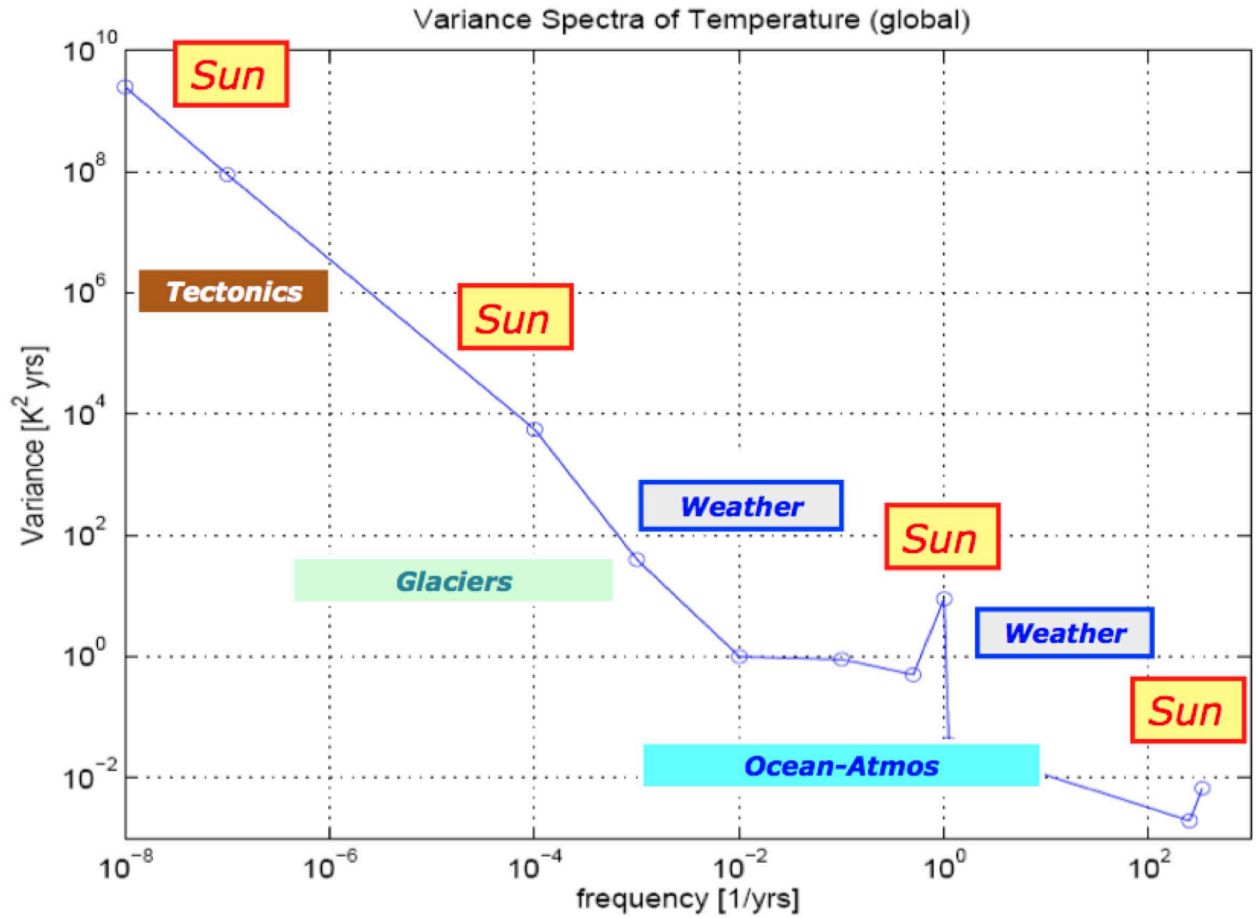


Figure 6.163: A summarising power spectrum of climate variability from periods of days to 500 million years. Based on the estimate in Fig. 6.162. The causes for the climate variability are noted for each time scales. The two peaks are the annual and daily cycle, both caused by the variations of the sun.